Dynamics of amorphous solids and viscous liquids

Dyre, Jeppe

Publication date:
1997

Document Version
Publisher's PDF, also known as Version of record

Citation for published version (APA):
Dyre, J. (1997). *Dynamics of amorphous solids and viscous liquids*. Roskilde Universitet. Tekster fra IMFUFA No. 335 http://milne.ruc.dk/ImfufaTekster/

TEKST NR 335 1997

Dynamics of Amorphous Solids and Viscous Liquids

Jeppe C. Dyre

TEKSTER fra

Abstract

This thesis was submitted for the Danish *doktorgrad* in December 1995. The defence is scheduled to take place March 14 1997 at 1 p.m. in the auditorium of building 46 of Roskilde University. The thesis consists of 15 publications and a summary. The publications are reprinted here after the summary. A three page abstract of the thesis is given on page 7-9; the Danish version of the abstract (required by the rules) is given on page 10-12.

Contents

4

Preface

This thesis was submitted for the Danish *doktorgrad* in December 1995 and will be defended March 14 1997 at 1 p.m. in the auditorium of building 46. The thesis consists of 15 publications and a summary. The publications are reprinted below after the summary. The summary states the main results, connects the publications, and gives some supplementary comments.

The thesis is the result of more than ten years of work in various directions in the field *Structure and Dynamics of Amorphous Solids*. My own employment at Roskilde University was part of an expansion of the research activities into this field at the Department of Mathematics and Physics. Throughout the years I have been given very good working conditions by the Department and have received generous grants from the Danish Natural Science Research Council. I would like to thank everyone in the Department for always being helpful and positive about the research carried out by the "glass" group.

On a more daily basis, I am indebted to Niels Boye Olsen and Tage Christensen for creating an inspiring research environment and always accepting interruptions for "urgent" physics discussions. The computer simulations would have been hard to carry out without help from Ib Høst Pedersen. In writing the summary, Tage Christensen have given a number of helpful comments and Jørgen Larsen have helped with LaTeX-technical problems. I would like to thank you all. At home, Pia and little Elisabeth Røsle have given moral support and been very patient during the writing of the thesis summary for which there - in the middle of moving into our new house - was little time.

Jeppe C. Dyre
Roskilde University
February 1997

List of publications

The 15 publications of the thesis are numbered from P1 to P15. P1-P7 are summarized in Chapter one, P8-P10 in Chapter two, and P11-P15 in Chapter three. The publications are reprinted after the summary.

P1 J. C. Dyre: *The Random Free-Energy Barrier Model for AC Conduction in Disordered Solids*, J. Appl. Phys. **64**, 2456-2468 (1988).

P2 J. C. Dyre: *Some Remarks on AC Conduction in Disordered Solids*, J. Non-Cryst. Solids **135**, 219-226 (1991).

P3 J. C. Dyre: *Universal AC Conductivity of Nonmetallic Disordered Solids at Low Temperatures*, Phys. Rev. B **47**, 9128-9131 (1993).

P4 J. C. Dyre: *Universal Low-Temperature AC Conductivity of Macroscopically Disordered Nonmetals*, Phys. Rev. B **48**, 12511-12526 (1993).

P5 J. C. Dyre: *Studies of AC Hopping Conduction at Low Temperatures*, Phys. Rev. B **49**, 11709-11720 (1994).

P6 J. C. Dyre and J. M. Jacobsen: *Universal Time Dependence of the Mean-Square Displacement in Extremely Rugged Energy Landscapes with Equal Minima*, Phys. Rev. E **52**, 2429-2433 (1995).

P7 J. C. Dyre and T. B. Schrøder: *Effective One-Dimensionality of Universal AC Hopping Conduction in the Extreme Disorder Limit*, Phys. Rev. B **54**, 14884-14887 (1996).

P8 J. C. Dyre: *Master-Equation Approach to the Glass Transition*, Phys. Rev. Lett. **58**, 792-795 (1987).

P9 J. C. Dyre: *Energy Master Equation: A Low-Temperature Approximation to Bässler's Random-Walk Model*, Phys. Rev. B **51**, 12276-12294 (1995).

P10 J. C. Dyre, N. B. Olsen, and T. Christensen: *Local Elastic Expansion Model for Viscous-Flow Activation Energies of Glass-Forming Molecular Liquids*, Phys. Rev. B **53**, 2171-2174 (1996).

P11 J. C. Dyre: *Unified Formalism for Excess Current Noise in Random-Walk Models*, Phys. Rev. B **37**, 10143-10149 (1988).

P12 J. C. Dyre: *Maximum Entropy Ansatz for Nonlinear Response Theory*, Phys. Rev. A **40**, 2207-2210 (1989).

P13 J. C. Dyre: *A 'Zero-Parameter' Constitutive Relation for Pure Shear Viscoelasticity*, Rheol. Acta **29**, 145-151 (1990).

P14 J. C. Dyre: *Langevin Models for Shear-Stress Fluctuations in Flows of Viscoelastic Liquids*, Phys. Rev. E **48**, 400-407 (1993).

P15 J. C. Dyre: *A Statistical Mechanical Approximation for the Calculation of Time Autocorrelation Functions* (IMFUFA tekst nr 287, Roskilde, 1994).

Abstract

This thesis consists of fifteen publications (P1-P15) published between 1987 and 1996 and a summary. In this abstract an overview of the main results is given by following the summary's three Chapters.

The first Chapter with the title "AC Conduction in Disordered Solids" reviews and comments P1-P7. In P1 from 1988 a phenomenological model for AC conduction in disordered solids is proposed. It is shown that the model explains the characteristic AC properties of disordered solids, summarized in 8 points. P3-P7 is an attempt to explain the success of the model of P1, which is based on a number of *ad hoc* hypotheses. In this line of reasoning, P2 from 1991 is a digression; in P2 - mainly for pedagogical reasons and with few original contributions - a number of common misunderstandings and misconceptions are cleared up. P3 and P4 from 1993 discuss a macroscopic model for AC conduction; P4 details the brief paper P3, that is included in the thesis mainly because its figures are more pedagogical than those of P4. By means of analytical approximations it is shown that at sufficiently low temperatures - corresponding to extreme disorder - all disordered solids with thermally activated conduction exhibit the same AC conductivity independent of the energy barrier probability distribution; the AC conductivity is "universal". This result is confirmed by computer simulations in two and three dimensions. The universal AC conductivity is very close to that of the phenomenological model studied in P1. P5 from 1994 derive universality for the microscopic so-called hopping model. The universality prediction is confirmed by computer simulations in two dimensions, but the quantitative agreement is not quite as good as for the macroscopic model. In P6 from 1995, the mean-square displacement as function of time for a charge carrier "hopping" in an extremely disordered solid is calculated from the expression for the universal AC conductivity derived in P5. P7 published in 1996 proposes a new expression for the universal AC conductivity in hopping models, derived by assuming that electrical conduction in extremely disordered solids is essentially a one-dimensional process. It is shown from computer simulations in two and three dimensions that the new expression is more realistic than that of P5. Still, the new expression is relatively close to that of the phenomenological model proposed in P1.

The second Chapter with the title "Viscous Liquids and the Glass Transition" reviews and comments P8-P10. In P8 from 1987 a simple model for the glass transition is proposed in which there is only one relevant degree of freedom, the potential energy of a region in the liquid. The model was originally constructed to explain the non-Arrhenius temperature-dependence of the average relaxation time in viscous liquids, an approach that is also fol-

lowed in Chapter 2. However, in P8 itself the focus was on the prediction that there are two different types of glass transitions. In P9 from 1995, Bässler's random walk model for viscous liquids is studied. It is argued that at low temperatures this model is well described by the simple model of P8. Thus, a clear physical picture of the low-temperature behavior of Bässler's random walk model is established. In P10 published in 1996, an alternative model for explaining the non-Arrhenius temperature-dependence of the average relaxation time in viscous liquids is proposed. In the new model, the short-time (or high-frequency) elastic properties of the liquid determine the activation energy for the average relaxation time. It is shown that the new model agrees well with experiment on a number of organic molecular liquids.

The third Chapter with the title "Extensions of Linear Response Theory" reviews and comments P11-P15. P11 from 1988 deals with electrical $1/f$ noise. This, in a sense, is a linear phenomenon, but as shown in P11 the magnitude of the noise is determined by *fourth order* cumulant averages of the equilibrium current fluctuations (while the ordinary linear response - the AC conductivity - is determined by the time autocorrelation function, a *second order* cumulant average). P12 from 1989 discusses a maximum entropy "ansatz" for nonlinear response theory. This "ansatz" makes it possible to predict the nonlinear response in a static external field from a complete knowledge of the equilibrium fluctuations of the quantity of interest. P13 and P14 both deal with nonlinear viscoelasticity. P13 from 1990 suggests a simple formula, a so-called "constitutive relation", for calculating the stress for an arbitrary shear flow. In P14 from 1993 it is shown that, if the equilibrium fluctuations of the stress are described by a Langevin equation, there is only one way to extend this equation to deal with stress fluctuations in a nonlinear flow. The extension is shown to be consistent with linear response theory, ensuring consistency. P15 from 1994 concerns the calculation of time autocorrelation functions (that via the fluctuation-dissipation theorem determine the linear response). An approximation is suggested, in which the calculation is reduced to calculating a "double" canonical average as well as the mean-square displacement as function of time.

The 15 publications are related to each other in the following way. P1-P7 is a continuously progressing attempt to explain the AC properties of extremely disordered solids (with P2 as a digression). P8 discusses a simple model for viscous liquids and the glass transition. In P9 it is shown that this model at low temperatures results from Bässler's random walk model, a model that is very similar to the hopping model studied in P1 and P5-P7. P10 discusses an alternative phenomenological model for viscous liquids. In many respects, the P10 model is complementary to the P8-P9 models. Thus, one may conjecture that these two models more or less span the "universe"

of possible phenomenological models. P11 concerns a frequency-dependent electrical property different from the conductivity, namely the electrical excess noise. P12 is related to P11, because the main result of P11 is a special case of the general formalism developed in P12. P13 and P14 both concern the same subject, nonlinear viscoelasticity. This subject is relevant for any viscous liquid close to the glass transition, where one expects the liquid to become nonlinear at shear rates larger than the inverse Maxwell relaxation time. In the linear limit, the constitutive relation suggested in P13 predicts a frequency-dependent viscosity that varies as one over the universal AC conductivity studied in Chapter 1. Thus, it is proposed that the atoms in a viscous liquid have the same mean-square displacement as function of time as that of charge carriers in an extremely disordered solid. P14, though only dealing with nonlinear viscoelasticity, is closely related to P12, because P14 gives an alternative recipe for estimating the nonlinear response from knowledge of the equilibrium fluctuations. In P15 the mean-square displacement as function of time is assumed known; this quantity is calculated in P6, if the liquid on the relevant time-scale may be regarded as a disordered solid, as suggested in P13. P15 is motivated by P8-P10: In these papers the focus is on the temperature-dependence of the mean relaxation time in a viscous liquid, and P15 starts from asking why quite different physical quantities in viscous liquids have roughly the same mean relaxation time.

Dansk resume

Denne afhandling består af 15 artikler (P1-P15) publicerede i perioden 1987-
1996 samt en resumering og kommentering af dem. Kommenteringen er delt
i tre kapitler vedrørende henholdsvis publikationerne P1-P7, P8-P10 og P11-
P15. Nedenfor gengives kort emnerne og hovedresultaterne af publikationerne
ved at tage udgangspunkt i kommenteringens strukturering i tre kapitler.

Det første kapitel med titlen "vekselstømsledningsevnen i uordnede fa-
ste stoffer" resumerer og kommenterer P1-P7. I P1 fra 1988 foreslås en fæ-
nomenologisk model for vekselstrømsledningsevnen i uordnede faste stoffer.
Det vises, at modellen forklarer en række karakteristiske egenskaber ved disse
stoffer opsummeret i 8 punkter. Publikationerne P3-P7 kan ses som et for-
søg på at forklare, hvorfor den ret primitive model fra P1, der er baseret på
en række "ad hoc" antagelser, virker så relativt godt, som den gør. I denne
argumentationsrække er P2 fra 1991 en digression, idet den - uden egent-
lige originale bidrag og i høj grad af pædagogiske grunde - opklarer en række
udbredte misforståelse og opsummerer væsentlige uløste problemer inden for
forskningsområdet. P3 og P4 fra 1993 diskuterer en makroskopisk model for
vekselstrømsledningsevnen. Det vises ud fra analytiske approksimationer, at
for ethvert uordnet stof, hvori ledningsevnen er termisk aktiveret, vil man
ved tilstrækkeligt lave temperaturer - svarende til ekstrem uorden - altid (dvs
uafhængigt af energibarriere-sandsynlighedsfordelingen) observere den samme
frekvensafhængighed af ledningsevnen: ledningsevnen bliver "universel". Dette
resultat underbygges af omfattende computersimuleringer i to og tre dimen-
sioner. Den universelle ledningsevne er meget lig den i P1 udledte. P5 fra
1994 viser det samme resultat for en mikroskopisk model for ledningsevnen,
den såkaldte hopmodel. Resultatet underbygges igen af computersimuleringer
i to dimensioner, men kvantitativt passer de knapt så pænt med teorien, som i
P3 og P4. P6 fra 1995 beregner den middel-kvadratiske forskydning som funk-
tion af tiden for en ladningsbærer i et uordnet stof, hvis frekvensafhængige
ledningsevne er givet ved det universelle udtryk udledt for hopmodellen i P5.
P7 publiceret i 1996 udleder et nyt udtryk for den universelle ledningsevne for
hopmodellen. Udtrykket udledes ud fra en antagelse om, at elektrisk ledning
i ekstremt uordnede faste stoffer essentielt er en én-dimensional proces. Det
vises ud fra computersimuleringer i to og tre dimensioner, at det ny udtryk
passer bedre end udtrykket fra P5; dog er det ny udtryk på mange måder ikke
væsensforskelligt fra det gamle, og det har de samme kvalitative egenskaber,
som udtrykket udledt i P5.

Det andet kapitel med titlen "seje væsker og glasovergangen" resumerer
og kommenterer P8-P10. I P8 fra 1987 fremsættes en simpel fænomenologisk
model for glasovergangen, en model der kun har én frihedsgrad, nemlig en

væskeregions potentielle energi. Modellen blev oprindeligt udviklet i et forsøg på at forklare temperaturafhængigheden af middelrelaksationstiden i seje væsker, men i publikationen P8 blev fokus i stedet sat på modellens forudsigelse, at der findes to forskellige slags glasovergange. I P9 fra 1995 studeres Bässlers hopmodel for seje væsker. Det vises, at ved lave temperaturer beskrives denne model godt af den simple model foreslået i P8. Herved opnås et klart fysisk billede af lavtemperaturopførslen af Bässlers model. I P10 publiceret i 1996 fremsættes en alternativ model til forklaring af middelrelaksationstidens temperaturafhængighed, baseret på helt andre mekanismer. I den ny model er det de elastiske egenskaber af væsken ved meget korte tider (svarende til høje frekvenser), der er den afgørende faktor. Det vises, at den ny model er i overensstemmelse med eksperimenter på en række organiske væsker, der danner glasser ved temperaturer betydeligt under stuetemperatur.

Det tredie kapitel med titlen "udvidelser af lineær responsteori" resumerer og kommenterer P11-P15. P11 fra 1988 handler om elektrisk 1/f støj. Dette fænomen er i en vis forstand lineært, men som vist er størrelsen af støjen bestemt af fjerde ordens kumulant-middelværdien af den fluktuerende strøm i termisk ligevægt, hvor det sædvanlige lineære respons (ledningsevnen) jo er bestemt af anden ordens kumulant-middelværdien (tidsautokorrelationsfunktionen). I P12 fra 1989 diskuteres en maximum entropy "ansatz" for ikkelineær responsteori. Ved hjælp af denne er det muligt at forudsige det ulineære respons i et statisk ydre felt på basis af et totalt kendskab til ligevægtsfluktuationerne af størrelsen, der studeres. P13 og P14 handler om ikke-lineær viskoelasticitet. I P13 fra 1990 foreslås en simpel formel til beregning af flydeegenskaber. I P14 fra 1993 vises det, at hvis stress-ligevægtsfluktuationerne er beskrevet ved en Langevin-ligning, er der netop én måde at udvide beskrivelsen på til at gælde stress-fluktuationer i en ulineær flydesituation. Det vises, at denne udvidelse reproducerer lineær responsteori, hvilket er nødvendigt for at undgå inkonsistenser. P15 fra 1994 vedrører beregning af tidsautokorrelationsfunktioner, der jo via fluktuations-dissipations teoremet bestemmer det lineære respons. Der foreslås en approksimation i følge hvilken, problemet reduceres til to elementer: dels en ny slags kanonisk middelværdiberegning og dels en beregning af den middel-kvadratiske forskydning som funktion af tiden.

De 15 publikationer er relateret til hinanden på følgende måde. P1-P7 udgør et jævnt fremadskridende forløb med bidrag til forståelsen af ekstremt uordnede faste stoffers vekselstrømsledningsevne (en undtagelse er P2, der diskuterer en række mere eller mindre løsrevne problemer inden for forskningsområdet). P8 vedrører en simpel fænomenonologisk model for seje væsker og glasovergangen. I P9 vises det, at denne model fås som lavtemperaturgrænsen af Bässlers hopmodel, en model der minder meget om hopmodellen for

vekselstrømsledningsevnen studeret i P1 og P5-P7. P10 vedrører en alternativ model for seje væsker og glasovergangen. Det vises i slutningen af kapitel 2, at P8-P9-modellerne på den ene side og P10-modellen på den anden er komplementære på en række punkter. Disse må derfor til en vis grad forventes at udspænde udfaldsrummet af mulige modeller. P11 vedrører en anden frekvensafhængig elektrisk egenskab end ledningsevenen, nemlig 1/f støj. P11 udgør dermed en modpol til P1-P7, også fordi det i P11 antages, at ledningevnen er helt frekvensuafhængig. P12 er relateret til P11, fordi hovedresultatet fra P11 i P12 fremkommer som et specialtilfælde. P13 og P14 vedrører samme emne, nemlig ulineær viskoelasticitet. Dette emne er relevant for enhver sej væske ved temperaturer tæt på glasovergangen, idet man forventer, at enhver sådan væske udviser ikke-lineære flydeegenskaber ved forskydningshastigheder, der overstiger den inverse Maxwell relaksationstid. Den konstitutive relation fremsat i P13 er i den lineære grænse ækvivalent med, hvad der gælder for de tids- og frekvensafhængige elektriske egenskaber i uordnede faste stoffer, hvorfor P13 er direkte relateret til P1-P7. Eksempelvis er et af resultaterne fra P6 den lineære grænse af krybefunktionen beregnet i P13. P14 er, skønt den ikke er formuleret generelt men kun med reference til ulineær viskoelasticitet, tæt relateret til P12, fordi disse begge søger at besvare spørgsmålet, hvorledes det ulineære respons kan estimeres ud fra kendskab til ligevægtsfluktuationer. P15 er relateret til P6, fordi der i P15 antages kendskab til den middel-kvadratiske forskydning som funktion af tiden; dette problem løses i P6 under antagelse af, at væsken på den relevante tidsskala kan betragtes som et ekstremt uordnet fast stof. Endvidere er P15 relateret til P8-P10. Disse diskuterer middelrelaksationstiden for en sej væske, og P15 tager, som den præsenteres i kapitel 3, sit udgangspunkt i spørgsmålet om, hvorfor der i seje væsker overhovedet er en fælles middelrelaksationstid for de fleste fysiske størrelser.

Chapter 1

AC CONDUCTION IN DISORDERED SOLIDS

1.1 Introduction

Any solid has an electrical conductivity, σ. If $\mathbf{J}$ is the current density and $\mathbf{E}$ the electric field, σ is defined by

$$\mathbf{J} = \sigma \, \mathbf{E} \,. \tag{1.1}$$

In general, the conductivity may be frequency-dependent: Writing $\mathbf{E}(t) = \mathrm{Re}(\mathbf{E}_0 e^{i\omega t})$ and similarly for $\mathbf{J}(t)$, $\sigma(\omega)$ is the complex number defined by

$$\mathbf{J}_0 = \sigma(\omega) \, \mathbf{E}_0 \,. \tag{1.2}$$

A non-zero imaginary part of $\sigma(\omega)$ signals a phase difference between the electric field and the current density.

For disordered solids at frequencies below phonon frequencies - the frequency range of interest in the present work - whenever there is a non-trivial frequency-dependence of the conductivity, the displacement of the charge carriers lags behind the electric field. This time-lag is at most that corresponding to one quarter period. Thus, the current reaches its maximum in time *earlier* than the electric field, causing a positive imaginary part of the conductivity in disordered solids. The requirement of a positive dissipation implies, of course, that the real part is also positive.

The frequency-dependent dielectric constant, $\epsilon(\omega)$, is defined by

$$\mathbf{D}_0 = \epsilon(\omega) \, \mathbf{E}_0 \,, \tag{1.3}$$

where $\mathbf{D}_0$ is the complex amplitude of the displacement vector $\mathbf{D} = \epsilon_0 \mathbf{E} + \mathbf{P}$

(ϵ_0 is the vacuum permittivity and $\mathbf{P}$ the dipole density). Since $\dot{\mathbf{P}} = \mathbf{J}$, the following relation exists between the conductivity and the dielectric constant:

$$\sigma(\omega) = i\omega \ [\epsilon(\omega) - \epsilon_0] . \tag{1.4}$$

Any solid with a non-zero DC conductivity has a dielectric constant that diverges as the frequency goes to zero. To avoid this, $\sigma(0)$ is often subtracted from $\sigma(\omega)$ in Eq. (1.4) as the definition of the frequency-dependent dielectric constant, as we will also do below whenever the term 'dielectric' loss is used:

$$\sigma(\omega) - \sigma(0) \ = \ i\omega \ [\epsilon(\omega) - \epsilon_0] . \tag{1.5}$$

The dielectric constant is usually thought of as referring to bound charges only, but experimentally bound charges cannot be distinguished from free charges and the only measurable quantity is the "total" dielectric constant of Eq. (1.4), which has contributions from bound as well as from free charges.

The *fluctuation-dissipation (FD) theorem* expresses any linear-response function in terms of equilibrium fluctuations. This theorem is fundamental to solid state physics. The earliest indication of the FD-theorem is probably Einstein's expression for the specific heat, which he showed is proportional to the variance of the energy in the canonical ensemble. In another precursor of the FD-theorem Einstein noted that the diffusion constant, D, by definition referring to the non-equilibrium situation of a concentration gradient, is related to the equilibrium mean-square displacement of a particle in time, t, by the following expression,

$$\left\langle \Delta x^2(t) \right\rangle \ = \ 2 \, D \, t . \tag{1.6}$$

Good discussions of the FD-theorem have been given by Voetmann Christiansen[1] and by Doi and Edwards.[2] The electrical version of the FD-theorem goes back to Nyquist's famous paper from 1928;[3] Kubo generalized the result and obtained the following expression[4] for the frequency-dependent conductivity

$$\sigma(\omega) \ = \ \frac{1}{3k_B T} \int_0^\infty \langle \mathbf{J}(0) \cdot \mathbf{J}(t) \rangle \ e^{-i\omega t} \, dt , \tag{1.7}$$

where the autocorrelation function on the right hand side refers to equilibrium fluctuations.

For a system of non-interacting particles the Kubo formula may be rewritten by performing two partial integrations.[5] Thereby, one arrives at the following frequency-dependent generalization of the Nernst-Einstein relation (where n is the charge carrier density and q is their charge),

$$\sigma(\omega) \;=\; \frac{n\,q^2}{k_B\,T}\,D(\omega)\,, \tag{1.8}$$

where the frequency-dependent diffusion constant is defined by

$$D(\omega) \;=\; -\frac{\omega^2}{2}\int_0^\infty \left\langle \Delta x^2(t)\right\rangle\, e^{-i\omega t}\,dt\,. \tag{1.9}$$

In Eq. (1.9) it is understood that there is a convergence factor $\lim_{\epsilon\to 0}\exp(-\epsilon t)$ in the integration. Note that for ordinary diffusion Eqs. (1.6) and (1.9) imply $D(\omega) = D$.

Solids can be classified into conductors and "insulators". By conductors we here mean metals; these are characterized by a large DC conductivity with a weak temperature-dependence. "Insulators" may have a zero or extremely small DC conductivity, or a somewhat larger DC conductivity. In the latter case they are conventionally referred to as semiconductors if the conduction is electronic, and superionic conductors if the conduction is ionic. Below, metals are not considered at all and by a solid is henceforth meant an "insulator".

Most solids in the real world are inhomogeneous. All inhomogeneous solids, whether inhomogeneous on a macroscopic or a microscopic scale, show pronounced frequency-dependence of the conductivity at frequencies below phonon frequencies. Examples of disordered solids are amorphous semiconductors, ionic conductive glasses, non-stoichiometric or polycrystals, ionic or electronically conducting polymers, organic semiconductors, polaronically conducting transition-metal oxides, or doped single crystal semiconductors at helium temperatures (where the disorder due to the random positions of the dopant atoms becomes important). Today, it is generally recognized that disordered solids exhibit common features for the temperature- and frequency-dependence of their conductivity (listed below in 8 points). However, until relatively recently this fact was only appreciated by a small number of experts in the field,[6–9] and there is still not general agreement as to how significant these common features are.[10]

Historically, the field developed in independent directions. Quite early (i.e., in the 1950's), measurements were made of the frequency-dependent dielectric constant of ionic conductive glasses. This work was motivated by technological requirements for a better understanding of glasses applied to X-ray tubes, transmitting valves, etc. The early measurements on ionic glasses[11,12] revealed a correlation between the DC conductivity, the dielectric loss peak frequency, ω_m, and the dielectric loss strength, $\Delta\epsilon = \epsilon(0) - \epsilon(\infty)$. The relation between these quantities, below termed the "BNN-relation" (a name introduced in 1986[13] to credit the contributions of Barton, Nakajima, and Namikawa[14–16]), is

$$\sigma(0) \;=\; p\,\Delta\epsilon\,\omega_{\mathrm{m}}, \tag{1.10}$$

where p is a numerical constant of order one.

Another direction of research into the AC properties of disordered solids was opened by Pollak and Geballe, when they in 1961 published their famous paper reporting AC hopping conduction in doped n-type semiconductors at helium temperatures.[17] The data were presented in terms of the real part of the conductivity, $\sigma'(\omega)$. This quantity was shown to follow an approximate power-law,

$$\sigma'(\omega) \;\propto\; \omega^{s}, \tag{1.11}$$

with an exponent s around 0.8. This means that the negative imaginary part of the dielectric constant, $\epsilon''(\omega)$, has a rather weak frequency-dependence. This was known previously for ionic glasses, which were found to exhibit extraordinarily broad dielectric loss peaks. However, as mentioned already, few noted the similarity between electronically and ionically conducting disordered solids until several years later.

It is convenient to focus on the real part of the conductivity, because the observed conductivity has the uninteresting purely imaginary contribution from electronic polarization, $i\omega(\epsilon(\infty) - \epsilon_0)$. It is usually the contribution to the conductivity from the mobile charge carriers that is of interest. This quantity is below denoted by $\sigma(\omega)$, thereby redefining this quantity: Where $\sigma(\omega)$ in Eq. (1.4) was the total observable conductivity, we now for this quantity write

$$\sigma_{\mathrm{obs}}(\omega) \;=\; \sigma(\omega) \;+\; i\omega(\epsilon(\infty) - \epsilon_0). \tag{1.12}$$

During the last 30 years enormous amounts of data for the frequency-dependent conductivity in disordered solids have been published. The measurements were fairly easy with classical bridges ; today they are even easier with modern frequency-analyzers. No detailed review of the literature will be given here. Instead we list in 8 Points (P1) the common features observed almost universally for disordered solids:

Point 1 For $\sigma'(\omega)$ one observes at high frequencies an approximate power-law (Eq. (1.11)) with an exponent s obeying $0.7 < s < 1.0$. If any deviation from a power-law is discernible, it corresponds to a weakly increasing exponent, $s(\omega)$.

Point 2 At lower frequencies there is a gradual transition to a frequency-independent conductivity (depending on temperature, the transition may take place at unobservably low frequencies).

Point 3 Whenever there is a measurable DC conductivity there is always a dielectric loss peak; the transition between DC and AC conductivity takes place around the dielectric loss peak frequency. The loss peak frequency satisfies the BNN-relation (Eq. (1.10)). When there is no measurable DC conductivity the exponent s of Eq. (1.11) is very close to one.

Point 4 As regards their temperature-dependence, $\sigma(0)$ and ω_m are roughly proportional and usually Arrhenius (thus, with the same activation energy), although more complicated temperature-dependencies are occasionally observed, e.g., in group-IV amorphous semiconductors.

Point 5 The shape of the dielectric loss peak (or equivalently of the real part of the conductivity) is temperature-independent in a log-log plot, i.e., it obeys the *time-temperature superposition principle (TTSP)*. The shape of this curve is roughly the same for all disordered solids.

Point 6 In a log-log plot the AC conductivity is much less temperature-dependent than the DC conductivity. For exponents s close to one the AC conductivity is almost temperature-independent.

Point 7 The exponent s increases as the temperature decreases, and for $T \to 0$ one finds $s \to 1$. In particular (compare Point 6) the AC conductivity becomes almost temperature-independent as $T \to 0$.

Point 8 While $\sigma(0)$ may vary several orders of magnitude, the AC conductivity - for different solids at different temperatures - varies only relatively little at frequencies safely above the loss peak frequency. In this regime, the AC conductivity is *very* roughly given by

$$\sigma'(\omega) \sim \epsilon_0 \, \omega \, . \tag{1.13}$$

After reviewing the experimental facts regarding ionic and electronic conduction in glasses Owen wrote in 1977:[7] *A unified theory for the loss or AC conductivity spectrum which accounted for the close correlation between the DC conductivity and the low-frequency loss peak, and the much weaker temperature-dependence of the $\sigma(\omega) \propto \omega^1$ region at higher frequencies, would certainly be physically appealing.* This quote may be regarded as the starting point for P1, the first publication to be reviewed below.

Many models for the AC conductivity of disordered solids have been proposed throughout the years. Most models (but not all) assume that the disorder is an essential ingredient. Few models address the surprising similarity between the AC properties of quite different disordered solids. In P1, this similarity is the starting point. In the subsequent papers the effect of disorder is studied in detail. It is found that in the extreme disorder limit a universality exists. A comparison of the universal AC conductivity to experiment is not given in P3-P7; however, the universal AC conductivity studied

in these papers is close to the predictions of the simple model of P1, that compares well to experiment.

1.2 Paper 1: Random Free Energy Barrier Model

Problem

1. Why are the AC conductivities of quite different disordered solids so similar?

2. Is it possible to construct a simple phenomenological model based on physically reasonable inputs, that is able to reproduce the 8 Points listed above?

Solution

The common feature of all solids obeying the 8 Points is their *disorder*, and more or less all disordered solids obey the 8 Points. Following what has become a standard approach, disorder is modelled by *randomness* of some parameters. A model that has been studied extensively in the literature is the so-called hopping model.[18-20] In a hopping model one sometimes assumes that charge carriers move on a simple cubic lattice; this is also done in P1. The jump rates vary randomly according to some probability distribution. For simplicity it is assumed that the charge carriers are non-interacting and that only nearest neighbor jumps are allowed. Not only are the long range Coulomb repulsions thus ignored, but so is the short range "self-exclusion" at any charge carrier site.

To guess at a realistic "ansatz" for the jump rate probability distribution, we refer to the observed AC conductivities and to the ion-electron analogy. In terms of the dielectric loss, the power-law of Eq. (1.11) implies a loss peak that is much broader than usually seen, e.g., in liquids. In the language of Debye processes, to describe extremely broad loss peaks one needs a super-position of processes that involves very many decades of relaxation times. This indicates a more or less uniform distribution of relaxation times, τ, on the logarithmic axis, leading to $p(\tau) \propto 1/\tau$. This conjecture is confirmed by considering the analogy between electronically and ionically conducting disordered solids: For amorphous semiconductors the jump is a quantum mechanical tunneling process, where the jump rate, Γ, depends exponentially on the tunneling distance r: $\Gamma \propto \exp(-\alpha r)$. For ionically conducting disordered solids the jump is a classical thermally activated process and the jump rate is given by Eyring's rate theory, according to which $\Gamma \propto \exp[-\Delta E/(k_B T)]$

where ΔE is the energy barrier. The simplest way to understand the ion-electron analogy is to assume that the jump distances resp. the activation energies vary randomly (i.e., according to a "Box" distribution). To adopt a uniform language covering both tunneling and barrier hopping, we write $\Gamma \propto \exp[-\Delta F/(k_B T)]$, where $\Delta F = \Delta E - T\Delta S$ is the free energy barrier. The tunneling case is then regarded as a case of entropy barrier dominated hopping.

For the jump rate probability distribution, the Box distribution of activation free energies implies

$$p(\Gamma) \ \propto \ \frac{1}{\Gamma}, \tag{1.14}$$

which is equivalent to $p(\tau) \propto 1/\tau$ where $\tau = 1/\Gamma$. This distribution is not normalizable, so both high- and low-frequency cut-off's must be introduced by assuming that only a finite range of jump frequencies are allowed: $\Gamma_{\min} < \Gamma < \Gamma_{\max}$. In order to reproduce the fact that the conductivity continues to increase with frequency up to phonon frequencies, the high-frequency cut-off must be chosen close to phonon frequencies. The low-frequency cut-off is much lower. To simplify things we therefore only investigate the limit $\Gamma_{\max}/\Gamma_{\min} \to \infty$. In this limit the DC conductivity itself diverges, but it is easy to remove this divergence by a "renormalization".[21]

The model has now been completely specified. Unfortunately, it is impossible to solve a hopping model analytically, even in one dimension. Either one has to study the model by computer simulations (which in the limit of many decades of jump frequencies requires considerable computer capacity and development of new algorithms, see P5), or one must solve the model by analytical approximations. The latter approximate solutions give an estimate of the average Green's function (i.e., averaged over all realizations of the jump frequencies). From this quantity it is straightforward to calculate the frequency-dependent conductivity.

The simplest approximation is the continuous time random walk (CTRW) approximation of Scher and Lax.[5] When the random free energy barrier model is solved in this approximation one finds (where $\tau = 1/\Gamma_{\min}$)

$$\sigma(\omega) \ = \ \sigma(0) \, \frac{i\omega\tau}{\ln(1 + i\omega\tau)}. \tag{1.15}$$

In terms of the dimensionless "reduced" conductivity $\tilde{\sigma} = \sigma/\sigma(0)$ and the dimensionless imaginary ("Laplace") frequency $\tilde{s} = i\omega\tau$, the CTRW solution of the random free energy barrier model is

$$\tilde{\sigma} = \frac{\tilde{s}}{\ln(1 + \tilde{s})}.\qquad(1.16)$$

A more reliable approximation than the CTRW is the effective medium approximation (EMA),[18,19] that was introduced around 1980 simultaneously by several groups (building on the coherent potential approximation[22] - the standard approximation for dealing with systems with a disordered Hamiltonian). The EMA does not lead to an explicit expression for the conductivity, but to a transcendental equation. For the random free energy barrier model the EMA leads (P1) to

$$\tilde{\sigma} \ln \tilde{\sigma} = \tilde{s}.\qquad(1.17)$$

As shown in Fig. 7 of P1 the CTRW and the EMA approximate solutions of the random free energy barrier model are almost indistinguishable. In particular, all qualitative features are the same for the two solutions. We therefore only discuss the CTRW solution below, where each of the 8 Points are considered.

Point 1: The real part of the conductivity is given by (with $\tilde{\omega} = \omega\tau$)

$$\tilde{\sigma}'(\tilde{\omega}) = \frac{\tilde{\omega}\ \arctan(\tilde{\omega})}{\ln^2(1 + \tilde{\omega}^2)/4\ +\ \arctan^2(\tilde{\omega})}.\qquad(1.18)$$

Considerably above the loss peak frequency (marking the onset of AC conduction) one has $\tilde{\omega} \gg 1$ and consequently

$$\tilde{\sigma}'(\tilde{\omega}) \simeq \frac{\pi}{2}\frac{\tilde{\omega}}{\ln^2(\tilde{\omega})}.\qquad(1.19)$$

This implies an approximate power-law where the exponent s of Eq. (1.11) is given by

$$s \equiv \frac{d\ln\tilde{\sigma}'}{d\ln\tilde{\omega}} = 1 - \frac{2}{\ln(\tilde{\omega})}.\qquad(1.20)$$

At frequencies high enough for the term an "approximate power-law" to make sense, Eq. (1.20) implies $0.7 < s < 1.0$. The function $s(\tilde{\omega})$ is weakly increasing and goes to one as the frequency goes to infinity. Note that the conductivity curve in a log-log plot (Fig. 7 of P1) is very close to a straight line just a few decades above the onset of AC conduction.

Point 2: At lower frequencies there is a gradual transition to frequency-independent conductivity, the DC conductivity. The transition takes place around the dielectric loss peak frequency; in dimensionless units the loss peak frequency is given by

$$\tilde{\omega}_m = 4.71. \tag{1.21}$$

Point 3: The dielectric loss peak is shown in Fig. 4 of P1. This loss peak is very broad compared to typical dielectric loss peaks in viscous liquids. In real units the loss strength is given by

$$\Delta\epsilon = \frac{1}{2}\,\sigma(0)\,\tau. \tag{1.22}$$

From Eqs. (1.21) and (1.22) we find that the BNN p-parameter of Eq. (1.10) is given by

$$p = 0.42. \tag{1.23}$$

The EMA leads to $p = 0.59$, which is somewhat closer to the experimentally reported $p \simeq 1$.[16] When there is no measurable loss peak, the time τ corresponds to frequencies lower than those accessible by experiment. In this case, measurements take place in the regime where $\tilde{\omega} >> 1$, and thus the exponent s is close to one (Eq. (1.20)).

Point 4: Experimentally, the dielectric loss strength is only weakly temperature-dependent compared to the DC conductivity or the loss peak frequency. The latter two quantities are usually Arrhenius; because of the BNN-relation, their activation energies are equal.

Point 5: The shape of the dielectric loss peak or of the conductivity curve is temperature-independent, because in reduced units the same function applies at all temperatures. Thus, the model obeys the TTSP. The function given in Eq. (1.18) gives a rather good fit to experiments for quite different solids, as is clear from Fig. 3 of P1.

Point 6 : As the temperature is lowered, the whole conductivity curve is displaced in a direction 45 degrees to the x- and y- axis of the standard log-log plot (compare Fig.1 of P1). Clearly, the AC conductivity is less temperature-dependent than the DC conductivity, and if the exponent s is very close to one, the AC conductivity is almost temperature-independent.

Point 7: From Fig.1 or Fig. 6 of P1 it is clear that, if the temperature is decreased, one effectively in a fixed frequency range measures further and further out on the same conductivity curve. Consequently, the model predicts that $s \to 1$ for $T \to 0$. In particular, according to Point 6 the AC conductivity becomes almost temperature-independent at low temperatures.

Point 8: Experimentally, the dielectric loss strength is usually of the same order of magnitude as ϵ_0. At high frequencies one finds from Eqs. (1.19) and (1.22) the following *very* rough order of magnitude estimate

$$\sigma'(\omega) \sim \frac{\Delta\epsilon}{\ln^2(\omega\tau)} \omega \sim \epsilon_0\,\omega\,, \qquad\qquad (1.24)$$

which is Eq. (1.13).

In conclusion, in P1 a simple phenomenological model was constructed that is able to explain the 8 Points. The model is also able to explain the so-called "Summerfield-scaling",[23] according to which the reduced conductivity, $\tilde{\sigma}$, is a function of a single variable:

$$\tilde{\sigma} \;=\; F\left(\frac{\omega}{\sigma(0)\,T}\right). \qquad\qquad (1.25)$$

Because of Eq. (1.22), if one assumes the Debye law for the dielectric loss strength, $\Delta\epsilon \propto T^{-1}$, Summerfield scaling follows from the fact that the reduced conductivity is a function of $\tilde{\omega}$.

The model of P1 is based on the assumption of randomly varying energy barriers. Ideas in this direction were discussed early in the history of the field. Thus, Stevels and Taylor[11] already in the 1950's - justified from Zachariasen's random network model for oxide glasses - discussed the possibility of having random barriers for jumps in ionic conductive glasses. The idea was that AC conduction takes place over limited ranges and involves the smaller energy barriers, while DC conduction extends to infinity and thus involves the largest barriers. These authors erroneously concluded that such a model is inconsistent with experiment. This was based on two arguments. First, they argued that any distribution of energy barriers must lead to a temperature-dependent shape of the loss peak (increasing in width as the temperature is lowered). Secondly, they argued that the BNN-relation cannot be explained in this approach, because the activation energy of the loss peak frequency, by referring to AC conduction, must be lower than that of the DC conductivity. Both things are wrong. The Box distribution implies Eq. (1.14) at any temperature (Stevels and Taylor may have known this, but were probably looking at superpositions of Debye processes for which the Box distribution of energy barriers leads to a completely frequency-independent dielectric loss). And the loss peak frequency of the random free energy barrier model is the lowest effective jump rate and therefore its activation energy is the same as that of the DC conduction. When the present author briefly met Stevels in 1985 and told him that their old idea works much better than they themselves expected, he looked quite pleased.

Outlook

The random free energy barrier model involves a number of simplifying assumptions: a) The distribution of energy barriers is a Box distribution; b) there is a sharp activation energy cut-off; c) the charge carriers are non-interacting; and d) the charge carriers jump on a cubic lattice. Given these rather restrictive assumptions, the obvious question is: *Why does the model work well?* Most of the contents of P3-P7 may be regarded as an attempt to answer this question. In this connection it should be noted that in arriving at Eqs. (1.16) and (1.17) a further assumption is made by using the approximate CTRW or EMA. These are both mean-field theories, and *a priori* it is far from obvious that either are realistic in the extreme disorder limit. This question is also addressed below by reference to computer simulations.

Another problem is to explain the AC response of macroscopically inhomogeneous solids, where one also finds that Eq. (1.16) works well. Why is this, when Eq. (1.16) was derived assuming microscopic disorder? A hint to understanding this is provided by the one-dimensional electrical impedance network consisting of a series of RC-elements as shown in Fig. 8a of P1. If one assumes that all capacitances, C, are equal while the resistances, R, are distributed uniformly on a logarithmic scale (corresponding to a Box distribution of energy barriers, compare Eq. (1.14)), the characteristic time $t = RC$ is distributed according to $p(t) \propto 1/t$ and the impedance of the circuit is given by (where K is a normalization constant and τ is the maximum characteristic time)

$$
\begin{aligned}
Z(\omega) &= \left\langle \frac{1}{R^{-1} + i\omega C} \right\rangle = \frac{K}{C} \int_0^\tau \frac{1}{t^{-1} + i\omega} \frac{dt}{t} \\
&= \frac{K}{C} \int_0^\tau \frac{1}{1 + i\omega t} dt \, .
\end{aligned}
\tag{1.26}
$$

When the constant K is determined self-consistently and expressed in terms of the DC conductivity, this expression leads to Eq. (1.16). The circuit has been used by many authors, including Macedo, Moynihan and Bose in their famous paper introducing the modulus formalism.[24] But how is the circuit justified?

A final question that arises on the basis of the success of the random free energy barrier model is: What can be learnt at all from measuring the AC conductivity? The model predicts that all solids have the same AC conductivity. This is not quite the case experimentally,[10] although the AC conductivities of quite different solids are surprisingly similar. Some time ago Pollak and Pike[25] suggested that $\sigma(\omega) \propto \omega$ is the "natural" low-temperature

(i.e., extreme disorder) limit of the conductivity of disordered solids, and that information about the solid under study is provided by *deviations* from this. While our expression Eq. (1.16) in a sense also gives the Pollak-Pike high-frequency limit, the random free energy barrier model suggests a more subtle result: Detailed information about a solid is provided by *deviations from Eq. (1.16)*, that itself is non-trivial.

1.3 Paper 2: Comments on AC Conduction

Paper 2 is pedagogical in the sense that most of the results discussed are not new, but more or less buried in the literature. P2 discusses a number of controversial issues and some workers in the field would undoubtedly say that the paper presents a rather personal point of view. A number of unrelated comments are made, and below we consider these comments one by one, following the numbering used in P2.

2.1 The observed power-law frequency-dependence of the conductivity is hardly fundamental.

For many years the results of AC measurements were reported in terms of the exponent s of Eq. (1.11). This is an obvious thing to do, because to plot the data meaningfully log-log plots must be used, and in these plots almost straight lines do emerge. However, and this is a point to be emphasized, almost anything is a straight line in a log-log plot.

The problem is not that data are reported in terms of exponents, but that these exponents subsequently by theorists are often regarded as rigorously established experimental facts. The reason for this is probably that power-laws in the 1970's became a new paradigm for solid state physics inspired by the renormalization group theory of second order phase transitions.[26] Before Widom's paper from 1965[27] power-laws were virtually unknown in solid state physics, but after about 1980 they seemed to show up everywhere. Once power-laws were regarded as fundamental even for the understanding of AC transport in disordered solids, many more or less esoteric explanations were proposed, often assuming some kind of spatially fractal structure of the solid.[28-32] Thus, the observation of what should rightly be termed "approximate power-laws" were taken as direct experimental evidence for the existence of fractals in disordered solids. The purpose of 2.1 was simply to warn against this "over"interpretation of experiment.

2.2 The Ngai relation is a consequence of the BNN relation and the time-temperature superposition principle.

As mentioned on page 21 of this summary, the BNN-relation implies that upon lowering the temperature the conductivity curve is displaced in a

direction 45 degrees to the x- and y-axis of the log-log plot (ignoring the weak temperature-dependence of $\Delta\epsilon$). As is easy to show, this implies that for a power-law frequency-dependent conductivity with exponent s, the activation energy for AC conductivity (found as the usual derivative of the logarithm of the conductivity) is related to that of the DC conductivity by

$$\Delta E_{AC} = (1 - s)\, \Delta E_{DC}. \tag{1.27}$$

Experiments confirm this relation which is quoted by Ngai as evidence in favor of the coupling model.[33] However, Eq. (1.27) is model independent and a mathematical consequence of other well-established experimental facts.

2.3 The shape of the modulus peak has no fundamental significance.

The electric modulus, $M(\omega)$, is defined by analogy with the ordinary mechanical modulus[24] as force over displacement; thus

$$M(\omega) = \frac{i\,\omega}{\sigma_{obs}(\omega)}. \tag{1.28}$$

This quantity was introduced in connection with modeling a disordered solid via the one-dimensional circuit of Fig. 8a in P1. The basic idea of the circuit is to emphasize that the same mechanism is responsible for both DC and AC conduction.[34] The concept of "electric field relaxation" was also discussed in the original paper by Macedo et al.[24] By this is meant the relaxation of the electric field towards zero for a suddenly imposed constant displacement, **D**. The modulus is the Laplace transform of the electric field relaxation function. There are two practical arguments for the use of electric modulus. First, the electrodes often give serious problems for accurate conductivity measurements. The simplest model is to regard the electrodes as pure capacitances in series with the sample; in this case the electrodes only contribute to the real part of the electric modulus and by focusing just on the imaginary part, electrode effects are eliminated. Secondly, the imaginary part of $M(\omega)$ shows a "loss peak", while the imaginary part of the dielectric constant only shows a loss peak if the DC conductivity is subtracted from $\sigma(\omega)$ (and because of electrode effects $\sigma(0)$ is often difficult to measure accurately).

Since its introduction, the electric modulus has become a popular means of data representation. From the modulus loss peak frequency a characteristic time is deduced, which may be compared to other characteristic times. Another application of the electric modulus formalism is a deduction regarding the conduction mechanism in ionic conductive glasses. It is usually observed that upon dilution of ion concentration the modulus loss peak in these systems narrows and and approaches a Debye peak. This is "explained" as being due to the fact that the Coulomb interactions between the mobile

ions become less and less significant upon dilution.[34,35]

Both these applications of the modulus formalism are flawed as will be explained now, the point being that "the shape of the modulus peak has no fundamental significance" as regards the conduction mechanism. One might add: The modulus loss peak frequency also has no significance. In fact, already in 1983 did Almond and West point out the limited usefulness of the modulus formalism.[36] In P2 this was reinforced and illustrated by a figure (Fig. 2). Since then the point has also been made by Elliott,[37] who emphasizes that there is a modulus peak even when there is no non-trivial frequency-dependence of the conductivity, i.e., when $\sigma_{obs}(\omega) = \sigma(0) + i\omega(\epsilon_\infty - \epsilon_0)$ (here and henceforth $\epsilon(\infty)$ is denoted by ϵ_∞).

In P2 it is noted that the observed conductivity is additive: When there are two different and unrelated conduction mechanisms, the observed conductivity is the sum of the two conductivities. There is always the purely imaginary contribution $i\omega(\epsilon_\infty - \epsilon_0)$ to the observed conductivity (Eq. (1.12)). Because the conductivity goes into the denominator in the definition of $M(\omega)$, the entire modulus loss peak thus depends on the value of ϵ_∞. This is illustrated in Fig. 2 of P2 from which it is clear that, when ϵ_∞ is changed for a fixed mobile charge carrier contribution to the conductivity, not only does the shape of the loss peak change, but so does the value of the loss peak maximum. The figure furthermore shows that the peak narrows when $\sigma(0)\tau/\epsilon_\infty \to 0$, which is precisely what is observed in experiment. This mathematical fact carries no information about the conduction mechanism. In conclusion, the modulus representation is misleading and should be avoided.

2.4 There are close mechanical analogies to the observed AC behavior.

One of the signals of ionic motion is the existence of a mechanical loss peak at the dielectric loss peak frequency. Another mechanical "signal" is seen in viscous ionic liquids, where one finds that the frequency-dependent viscosity behaves much like $1/\sigma(\omega)$ for a typical disordered solid. This is easy to understand from the FD-theorem applied to a hydrodynamic model for ionic motion, and it is one of the starting points for P13 reviewed in Chapter 3.

3.1 Three common arguments against hopping models are all incorrect.

As mentioned already, two early arguments against Stevels' and Taylor's model (that the loss peak frequency should have a lower activation energy than the DC conductivity and that the loss peak cannot have a temperature-independent shape) are wrong. A third argument against hopping models based on distributions of activation energies is also wrong: In these models the DC conductivity does not have to be non-Arrhenius as is sometimes claimed; in fact, at low temperatures $\sigma(0)$ is always Arrhenius due to the importance of percolation (P3-P7).

3.2 The conductivity is frequency-dependent only if there are correlations between the directions of charge carrier jumps.

Several models discussed in the literature, including the CTRW model,[5] are inconsistent. In order to have a non-trivial AC conductivity there must be correlations in the directions of subsequent charge carrier jumps. The mere existence of a distribution of waiting times or a non-exponential decay of the probability to be at one site (a non-Markovian dynamics) does not give rise to frequency-dispersion. For the CTRW model this was pointed out by Tunaley already in 1974,[38] but was subsequently almost forgotten. (While the CTRW *model* is inconsistent, the CTRW *formula* for the conductivity derived by Scher and Lax[5] is mathematically equivalent to the Hartree approximation, the simplest possible mean-field approximation,[39] thus justifying the use of the CTRW in P1.)

4.1 Are reported data always reliable and not due to contact effects?

Contact effects at the electrodes cause serious problems for accurate AC conductivity measurements, in particular below the loss peak. Due to contact effects, sometimes one cannot see the low-frequency leveling-off of the conductivity as function of frequency; instead the conductivity is observed to continue to decrease when the frequency is decreased. This is due to the blocking effect of the contacts, which is particularly serious for ionic conduction. In principle one could vary the sample dimensions to eliminate this problem. However, it is often difficult to prepare identical samples: since the conductivity is thermally activated, a slight change in the activation energy causes a considerable change in the conductivity. In some cases, varying sample size does indeed work.[40] The contacts may even influence the frequency-dependence of the conductivity, leading to a spurious $\omega^{1/2}$-frequency-dependence.[41] In conclusion, it seems that reported data are not always reliable.

4.2 Are DC and AC conduction always due to the same mechanism?

A BNN-like relationship between the DC conductivity and the frequency marking the onset of AC conduction does not necessarily imply that DC and AC conductivity are due to the same mechanism. A nice illustration of this fact was provided recently by Moynihan, discussing old measurements on a dilute solution of Li in glycerol.[34]

4.3 There are theoretical reasons to expect $\epsilon''(\omega)$ is proportional to $\omega^{1/2}$ on the low-frequency side of the dielectric loss peak.

In hopping models the long-time tails well-known from liquid state physics manifest themselves in the above fashion for the AC conductivity:[18] If $s = i\omega$ one has for $s \to 0$ the following expansion: $\sigma(s) = \sigma(0) + As + Bs^{3/2} + ...$ (in Paper 2 the second term is missing). As is easy to show this expansion leads to the prediction that the dielectric loss varies

as the squareroot of the frequency at low frequencies compared to the loss peak frequency.

4.4 Does any solid exist which has $\sigma'(\omega) \ll \epsilon_0 \, \omega$?

The answer to this question is, in fact, yes. A more relevant question was recently posed by Angell.[42] We know that the conductivity in the infrared region (i.e., at phonon frequencies) is of the order 1 $(\Omega\text{cm})^{-1}$ (this also follows from the sum rule for the real part of the conductivity[4]). If there is nothing going on at lower frequencies (i.e., if the charge carriers are permanently localized) the real part of the conductivity decreases as ω^2 below phonon frequencies. The question is: Is it possible to come arbitrarily close to this lower limit of the AC conductivity? Unfortunately, experiments are here extremely difficult because of the dominance of the imaginary contribution to the conductivity from the ϵ_∞-polarizations.

4.5 What kind of measurements could supplement the measurements of $\sigma(\omega)$?

Several quantities could supplement conductivity measurements. For ionic conduction, NMR has recently been shown to give valuable extra information about the conduction process.[35,43]

4.6 Is the observed AC behavior due to microscopic or macroscopic inhomogeneities?

This question inspired to the work behind the publications P3 and P4.

4.7 How accurate are the presently available approximate analytical solutions of hopping models, and what is the cause of the quasi-universality among different models?

This question is dealt with in P5-P7.

4.8 Are hopping models the correct framework for describing experiments?

This question is addressed in P3-P7, albeit indirectly.

1.4   Paper 3 and 4: Macroscopic Model

Hopping models are the most popular models for AC conduction in disordered solids, and extensive work has gone into developing theories for hopping.[18-20] However, only hopping of non-interacting charge carriers may be treated analytically with reasonable reliability. It may well be questioned whether it is realistic to completely ignore Coulomb repulsion between charge carriers. In any case, the assumption of non-interacting charge carriers is certainly inconsistent with Maxwell's equations; a particle can only feel an electric field if it has a charge, and if it has a charge it must interact with other charged particles. In view of this one may ask:

Problem

What is the simplest possible realistic model for AC conduction in disordered solids that does take into account Coulomb interactions?

Solution

The hopping of interacting charge carriers may be studied in computer simulations,[44] but as mentioned there is no reliable approximate analytical treatment of such models.[45] Instead, one may take a macroscopic approach and consider the AC conductivity of disordered solids in light of Maxwell's equations for an inhomogeneous conductor. The study of inhomogeneous conductors goes back to Maxwell himself. In P4 some care was taken in deriving the model from basic principles, because the resulting electrical circuit is usually incorrectly interpreted. For this part of P4 there is, of course, no claim of originality.

Consider a solid with bound charges described by the frequency-independent dielectric constant, ϵ_∞, and free charges described by a spatially varying frequency-independent conductivity, $g(\mathbf{r})$. It is assumed that all charge is either free or bound. The free charge carrier density is denoted by ρ and the free charge current density by $\mathbf{J}$. The relevant Maxwell equations are $\nabla \cdot \mathbf{D} = \rho$ and $\nabla \times \mathbf{E} = -\partial \mathbf{B}/\partial t$. In our frequency range the magnetic field is practically zero so the latter equation implies that an electrostatic potential may be defined, $\mathbf{E} = -\nabla \phi$. There is free charge conservation, of course, $\dot{\rho} + \nabla \cdot \mathbf{J} = 0$. Combining these equations in periodic fields with $\mathbf{D} = \epsilon_\infty \mathbf{E}$ and $\mathbf{J} = g(\mathbf{r})\mathbf{E}$ yields for the electrostatic potential where $s = i\omega\epsilon_\infty$ is the "Laplace frequency"

$$\nabla \cdot \Big([s + g(\mathbf{r})]\nabla \phi(\mathbf{r}, s)\Big) = 0. \tag{1.29}$$

When this equation is discretized one arrives at the electrical circuit shown in Fig. 1 of P4 where, if a is the lattice constant and d the dimension, each capacitor has the value $a^{d-2}\epsilon_\infty$ and each resistance has the value $a^{d-2}/g(\mathbf{r})$.

The interpretation of the circuit is the following. When the circuit is subjected to an external potential drop, the solution to Kirchhoff's equations gives the corresponding potential inside the solid. Converted to a current density, in the circuit the current is locally equal to $\mathbf{J} + \mathbf{J}_D$, where $\mathbf{J} = g(\mathbf{r})\mathbf{E}$ is the free charge current density and $\mathbf{J}_D = s\mathbf{E}$ is Maxwell's displacement current density: $\mathbf{J}_D = \dot{\mathbf{D}} = i\omega\epsilon_\infty\mathbf{E}$. The Kirchhoff law expressing current conservation at each site allows for no charge accumulation at any site. This law is an expression of the identity $\nabla \cdot (\mathbf{J} + \mathbf{J}_D) = 0$, that follows from Maxwell's equations and charge conservation:

$$\nabla \cdot \mathbf{J}_D \;=\; \nabla \cdot \dot{\mathbf{D}} \;=\; \dot{\rho} \;=\; -\nabla \cdot \mathbf{J}. \tag{1.30}$$

The current flowing in the circuit has *three* contributions: Free charge, bound charge and "ghost" charge, the latter being the non-physical part of the charge in Maxwell's displacement current. Thus, while the circuit allows no charge accumulation at any site, the real free+bound charge may very well accumulate here and there in the solid. We have gone through this rather trivial point in some detail, because the circuit has often been discussed in the literature as a phenomenological model for AC conduction in inhomogeneous solids[24,46-51] etc, without proper physical interpretation. In particular, the capacitor currents are often erroneously identified with the bound charge currents. The correct interpretation of the circuit may be found implicitly in the paper by Fishchuk from 1986[52] and probably many other places in the literature.

The actual spatial disorder of the solid, which must have some finite correlation length, ξ, is reflected in the value of the resistors of the circuit. It is convenient to choose the discretization length equal to ξ and ignore correlations beyond this length. This is of course an approximation. Making this assumption, however, the resistors are uncorrelated from link to link and the model is completely specified by the resistor probability distribution. Next, we assume that the free charge conductivity is thermally activated, i.e., that it is given by an activation energy: $g(\mathbf{r}) = g_0 \exp[-\beta E(\mathbf{r})]$. The model is completely specified by the activation energy probability distribution, $p(E)$. A "solution" of the model consists of calculating the overall free charge admittance. It is convenient to convert this quantity to a free charge conductivity, $\sigma(\omega)$. Clearly, the free charge conductivity is determined by the average resistor current (for a given external potential drop across the sample).

The model may be studied numerically by computer simulations or approximately analytically. The latter is done by using the effective medium approximation (EMA) for admittance circuits. This approximation, the mathematics of which is identical to the mathematics of finding the effective dielectric constant of a random mixture of dielectrica, is more than 50 years old.[53]

We first consider the dielectric version of the EMA. It is derived in the following way. Given a random mixture of materials with different dielectric constants, what is the "macroscopic" dielectric constant of the mixture, ϵ_m? If $\langle \rangle$ denotes a spatial average, ϵ_m is defined by

$$\langle \mathbf{D} \rangle \;=\; \epsilon_m \langle \mathbf{E} \rangle. \tag{1.31}$$

The fact that we are concerned with a mixture is expressed mathematically

in the equation

$$\mathbf{D(r)} = \epsilon(\mathbf{r})\mathbf{E(r)}\,, \tag{1.32}$$

where the dielectric constant in some sense depends randomly on the position. The problem is to calculate ϵ_m from a knowledge of $\epsilon(\mathbf{r})$: Consider a sphere of dielectric constant, ϵ, embedded in an effective medium. The effective medium represents the average surroundings of the sphere in the actual inhomogeneous medium; the effective medium is characterized by the "average" dielectric constant, ϵ_m. In an electric field, which far away from the sphere is equal to $\mathbf{E_0}$, the sphere becomes polarized whenever $\epsilon \neq \epsilon_m$. Consequently, the electric field inside the sphere is different from $\mathbf{E_0}$. It is straightforward to show[54] that the field inside the sphere, $\mathbf{E}$, is homogenous and given by

$$\mathbf{E} = \frac{3}{2 + \epsilon/\epsilon_m}\, \mathbf{E_0}\,. \tag{1.33}$$

The EMA equation is now derived by the "self-consistency" requirement that, on the average, $\mathbf{E}$ is equal to $\mathbf{E_0}$, i.e.,

$$\langle \mathbf{E} \rangle = \mathbf{E_0}\,. \tag{1.34}$$

This implies $\langle 3/(2 + \epsilon/\epsilon_m) \rangle = 1$, or

$$\left\langle \frac{\epsilon(\mathbf{r}) - \epsilon_m}{2\epsilon_m + \epsilon(\mathbf{r})} \right\rangle = 0\,. \tag{1.35}$$

Returning now to conduction in disordered solids, in the DC case Eq. (1.29) is mathematically equivalent to the basic equation for an inhomogeneous dielectric, $\nabla \cdot [\epsilon(\mathbf{r})\nabla\phi] = 0$. We thus immediately from Eq. (1.35) get an equation for the average DC conductivity, $\sigma(0)$,

$$\left\langle \frac{g(\mathbf{r}) - \sigma(0)}{2\sigma(0) + g(\mathbf{r})} \right\rangle = 0\,. \tag{1.36}$$

This expression is also valid for the complex average conductivity of an admittance circuit. For the circuit characterizing the macroscopic model, the capacitor currents are not of interest. When these are eliminated, the following EMA expression for the free charge conductivity, $\sigma(s)$, in d dimensions is arrived at[52]

$$\left\langle \frac{g - \sigma}{g + (d-1)\sigma + ds} \right\rangle = 0\,. \tag{1.37}$$

In P3 and P4 this equation is solved in the *extreme disorder limit*. By this we mean the limit $\beta \to \infty$, where the local conductivity varies more and more decades. In this limit Eq. (1.17), $\tilde{\sigma} \ln(\tilde{\sigma}) = \tilde{s}$, is arrived at independently of the activation energy probability distribution, where $\tilde{\sigma} = \sigma(\omega)/\sigma(0)$ and

$$\tilde{s} = \frac{\beta}{d\, p(E_c)\, \sigma(0)}\, s\,.\qquad(1.38)$$

Here, E_c is the percolation energy, the largest energy met on an optimal "percolating" path.

To test the EMA and in particular the universality prediction, extensive computer simulations of the macroscopic model were undertaken in P3 and P4. For simplicity the simulations were only carried out for *real* Laplace frequencies. There are two problems in simulating the model at low temperatures. First, using standard algorithms one encounters endless overflow problems when the local conductivity varies 100 or more decades. Secondly, very large lattices are needed to obtain reasonable reproducibility. The first problem was solved by referring to the star-mesh transformation well-known from electrical engineering.[55] The star-mesh transformation allows one to remove an internal point in a circuit without changing the "external" properties of the circuit. In two dimensions this was developed into a very efficient algorithm by Frank and Lobb;[56] earlier and more generally the star-mesh transformation was applied by Fogelholm to the study of percolating networks.[57] The advantage of the star-mesh transformation is that it involves no subtractions. To avoid the second problem with large lattices, most of the simulations were two-dimensional. However, the simulations of Fig. 5 in P4 were done in three dimensions; these results may be somewhat uncertain, but they were subsequently confirmed by a real-space renormalization numerical technique developed by Thomas Riedel in his master's thesis.[58,59]

In comparing the simulations to the EMA, we have considered only the EMA prediction for the *relative* conductivity, $\tilde{\sigma}$, and in the definition of $\tilde{s}$ (Eq. (1.38)), the correct percolation energy and the empirical $\sigma(0)$ were used and not those predicted by the EMA. This was done because the main focus is on the *shape* of the conductivity curve. In this approach, the simulations of P3 and P4 show that the EMA is a very good approximation at all frequencies and temperatures studied. This is rather surprising, because existing quasi-rigorous derivations of the EMA arrive at it from weak-disorder expansions.

The fact that percolation dominates DC conduction has been known for many years,[60,61] but a rigorous proof that the DC conductivity activation energy is the percolation energy was only given recently.[62] The crucial importance of percolation is the starting point for the phenomenological "percolation path approximation" (PPA). While the macroscopic model justifies

the use of the electrical circuit of Fig.1 in P4 as a model for conduction in disordered solids, the one-dimensional version of the circuit is arrived at as the percolation path approximation to the circuit, valid at extreme disorder. In this limit, conduction effectively becomes one-dimensional with a sharp activation energy cut-off, leading to the CTRW expression for the frequency-dependent conductivity Eq. (1.16). According to the PPA universality arises because at low temperatures only activation energies slightly below E_c are important for the frequency-dependence of the conductivity.

The naive approach behind the PPA ignores the fact that the percolation cluster is a fractal with dimension larger than one. However, only the so-called "backbone" part of the percolation cluster is important for conduction, and the backbone has a lower fractal dimension than the percolation cluster. On the backbone the so-called "red bonds" (defined as the bonds that stop the current if they are cut) are the main contributors to conduction; the set of red bonds has an even lower fractal dimension, not far from one.[63]

Outlook

The macroscopic model is conceptually very different from the hopping model: the first is macroscopic, the latter is microscopic; the first is deterministic, the latter is stochastic; for the macroscopic model the overall potential drop across the sample is controlled, for the hopping model the local (uniform) electric field is controlled. If one were free to choose, the macroscopic model is to be preferred for the following reasons: 1) It takes the effects of Coulomb interactions into account and is thus more realistic; 2) because one controls the overall potential drop, the field inside the sample varies and adjusts itself so that Gauss' law is obeyed; 3) when subjected to approximate analytical treatment, the macroscopic model is simpler than the hopping model; 4) the macroscopic model is easier to computer simulate. On the other hand, understanding the hopping model is important also for other fields where hopping is relevant (e.g., stochastic transport in multidimensional parameter spaces), while the macroscopic model specifically concerns electrical conduction.

Since hopping is quite different from the macroscopic model, it is surprising that both models lead to similar results for the AC conductivity. We have seen that the EMA for the macroscopic model leads to the expression Eq. (1.17) for the universal frequency-dependence of the conductivity in the extreme disorder limit. Also, the PPA leads to the CTRW expression for the random free energy barrier model (Eq. (1.16)). A closer investigation of hopping is needed including computer simulations, before the following questions that logically arise may be answered: 1) Is conduction in hopping

models also universal at low temperatures? If yes: 2) Does the EMA lead to Eq. (1.17) for hopping in the extreme disorder limit? If yes: 3) Do computer simulations confirm the EMA for hopping?

1.5   Paper 5 and 6: Hopping Model

After the results obtained for the macroscopic model in P3 and P4, the logical next step is to investigate hopping models from the same point of view. P5 and P6 present a study of hopping models, again emphasizing the extreme disorder limit.

Problem

1) Is AC hopping conduction universal in the extreme disorder limit?

2) If yes: Is the universality confirmed by computer simulations? How are these difficult simulations performed at extreme disorder?

Solution

The above questions are dealt with mainly in P5, while P6 evaluates an important consequence of the results obtained in P5. As in P1, only symmetric hopping of non-interacting charge carriers on a cubic lattice is studied. Symmetric hopping involves hopping between energetically equivalent sites. To look into the possible existence of universality we use the EMA approximation for hopping. This approximation is not identical to the EMA for the macroscopic model discussed above, but the two approximations have the same name because they are based on the same mean-field idea. For hopping one wants to calculate the Green's function averaged over all realizations of the disorder. The EMA considers one link of the lattice embedded in an "effective medium", which is homogeneous and described by the average Green's function. Selfconsistency is then required, i.e., that the Green's function for the effective medium plus the link on the average is equal to the average Green's function. Remembering that the frequency-dependent diffusion constant is proportional to the frequency-dependent conductivity (the Nernst-Einstein relation Eq. (1.8)), instead of following P5 we below give the EMA equation for the frequency-dependent diffusion constant, $D(s)$: In the unit system where the diffusion constant on a homogeneous lattice with jump rate Γ is given by $D = \Gamma$, if the dimension is d, if one defines $p(\mathbf{k}) = \frac{1}{d}\sum_{i=1}^{d}\cos(k_i)$ and if $s\tilde{G}$ is the following integral over the first Brillouin zone ($-\pi < k_i < \pi$),

$$s\tilde{G} = \int_{1-BZ} \frac{s}{s + 2\, d\, D[1 - p(\mathbf{k})]} \frac{d\mathbf{k}}{(2\pi)^d}, \qquad (1.39)$$

the EMA equation is given by the following average over the jump frequency probability distribution

$$\left\langle \frac{\Gamma - D}{d\, D + [1 - s\tilde{G}(\Gamma - D)]} \right\rangle = 0. \qquad (1.40)$$

For hopping with thermally activated jump rates, the EMA equation becomes *universal* in the extreme disorder limit (P5). In this limit, the EMA equation reduces to the diffusion constant analogy of Eq. (1.17),

$$\tilde{D} \ln \tilde{D} = \tilde{s}, \qquad (1.41)$$

where $\tilde{D} = D(s)/D(0)$ and $\tilde{s} = \text{Const.}s/D(0)$ (interestingly, the constant of proportionality has a different temperature-dependence in two dimensions and in more than two dimensions (P5)). In P1 Eq. (1.41) was derived for the special case of a Box distribution of energy barriers, where the average in Eq. (1.40) may be calculated explicitly. Equation (1.41) was first derived by Bryksin in 1980[18,64] for the specific hopping model with tunneling between random positions (so-called r-hopping). The derivation of Eq. (1.41) presented in P5 not only proves universality within EMA, but is also more transparent than Bryksin's derivation.

P6 presents a calculation of the mean-square displacement for diffusion in d dimensions when the frequency-dependent diffusion constant is given by Eq. (1.41). The derivation is complicated by the fact that the diffusion constant is only given indirectly as the solution of a transcendental equation. If the mean-square displacement in dimensionless units in some fixed axis direction is denoted by $\langle \Delta \tilde{x}^2(\tilde{t}) \rangle$, one finds from Eq. (1.41) after a Laplace inversion of Eq. (1.9)

$$\langle \Delta \tilde{x}^2(\tilde{t}) \rangle = 2\tilde{t} + \frac{2}{\pi} \int_0^\pi F(\theta) \left(1 - e^{-\tilde{t}E(\theta)}\right) d\theta, \qquad (1.42)$$

where $E(\theta) = \theta \exp(-\theta \cot \theta)/\sin \theta$ and $F(\theta) = (\cos \theta - \sin \theta/\theta)^2 + \sin^2 \theta$. At long times ($\tilde{t} \gg 1$) Eq. (1.42) gives ordinary diffusion with a mean-square displacement proportional to time. At short times ($\tilde{t} \ll 1$) the mean-square displacement is logarithmic in time: $\langle \Delta \tilde{x}^2(\tilde{t}) \rangle \cong 2/\ln(\tilde{t}^{-1})$. An expression that extrapolates between these two limits is the following

$$\langle \Delta \tilde{x}^2(\tilde{t}) \rangle \cong \frac{2}{\ln(1 + \tilde{t}^{-1})}. \qquad (1.43)$$

Note that by Laplace transforming Eq. (1.42) one obtains an explicit integral expression for the solution of Eq. (1.41):

$$\tilde{D}(\tilde{s}) = 1 + \frac{1}{\pi}\int_0^\pi F(\theta) \frac{\tilde{s}E(\theta)}{\tilde{s} + E(\theta)}\, d\theta. \qquad (1.44)$$

The numerical study of AC hopping may in principle be performed by Monte Carlo simulations. This method, however, is of little use when the focus is on the extreme disorder limit: At low temperatures, the particles jump back and forth billions and billions of times on links with small energy barriers. This behavior reflects the real physics of hopping and is the cause of the much larger AC conductivity than DC conductivity. But in a computer simulation it is clearly inefficient to waste time on monitoring these back and forth jumps.

Any stochastic process is in one to one correspondence with its Chapman-Kolmogorov equation or its differential form, the master equation.[65] In the numerical study of hopping it is an obvious idea to solve the master equation instead of actually following the motion of particles as done in Monte Carlo simulations. The master equation is a first-order linear differential equation in time. Upon Laplace transforming, the master equation for hopping results in a sparse linear system of equations, the solution of which gives the frequency-dependent diffusion constant or conductivity (P5). In order to go to low temperatures but still retain reasonable reproducibility, large lattices must be studied. The master equation is thus a large linear system of sparse equations with coefficients that - in the case of low temperature hopping - vary many orders of magnitude. Solving this system of equations is numerically very difficult. In P5 a new algorithm was developed to deal with this problem. The algorithm makes use of an electrical equivalent circuit of the hopping master equation, termed the "ACMA circuit" (AC Miller-Abrahams), proposed by Pollak in 1974.[66] In the DC limit the circuit reduces to an ordinary resistance circuit, just as in the macroscopic model. The algorithm of P5 was inspired by the Fogelholm algorithm for the macroscopic model (P4). It turns out that, by circuit reductions of the same type as used in P3 and P4 for simulating the macroscopic model (removing "internal" nodes without changing the "external" properties of the circuit), it is possible to evaluate a matrix from which the frequency-dependent conductivity is easily and accurately calculated. The algorithm is numerically stable even when hundreds of decades of jump frequencies are present. This is because the algorithm involves no subtractions. However, the algorithm is much more complex and slower than the Frank-Lobb algorithm used for the macroscopic model in P3 and P4.

Only simulations of hopping in two dimensions were carried out in P5.

The results show that the EMA works well at relatively high temperatures. When the temperature is lowered, there is a tendency for the data to deviate from the EMA (Fig. 4 of P5), shifting towards the low-frequency side of the plot. The data clearly show the existence of universality (Fig.5 of P5), but there is not a quantitative agreement with the EMA predictions: the data indicate a smoother onset of AC conduction than predicted by the EMA. This could be due to the fact that low enough temperatures were not reached (only 100×100 lattices were studied, in contrast to the 200×200 lattices of the macroscopic model, where thus lower temperatures are possible). However, this is not the whole explanation; a comparison of Fig. 4 of P5 with Fig. 3 of P4 shows that the EMA for hopping *is* less reliable than it is for the macroscopic model.

Outlook

According to the EMA, both the macroscopic model and the hopping model give identical predictions for the universal AC conductivity in the extreme disorder limit. However, while the simulations of P4 and P5 prove the existence of universality for both models, it is not quite clear whether the universal AC conductivity is the same for both models. The question is: Are the two models distinguishable as regards their frequency-dependent conductivity? If the answer is no, AC measurements are of little use for identifying the conduction mechanism. To settle this question more simulations of hopping are needed in two dimensions, and results for three dimensions are also very much needed.

Another question that naturally arises is whether asymmetric hopping models (involving hopping between energetically inequivalent sites) have the same properties as symmetric models. Do these models exhibit universality in the extreme disorder limit and, if yes, is the universal conductivity the same as for symmetric hopping?

The first question is addressed below, the second is not. For asymmetric hopping the simulations are even more demanding than for symmetric hopping, and sofar nobody has studied asymmetric hopping in the extreme disorder limit. We note in passing that there are several ways to choose the transition rates for asymmetric hopping, possibly leading to different results for $\sigma(\omega)$. A simple starting point would be to choose Metropolis jump rates, i.e., real Monte Carlo dynamics (as in P9). These dynamics are physically satisfactory because there is a maximum "down-hill" transition rate.

1.6 Paper 7: Hopping Model revisited

Problem

1) Are the AC properties of the macroscopic model and the hopping model identical in the low-temperature limit? If no:
2) Can a simple approximation be developed for hopping that is more accurate than the EMA?

Solution

The background for P7 is the following. P5 indicated that the EMA does not work as well for hopping as for the macroscopic model. Given that the EMA is a mean-field theory derived from a weak disorder expansion, it must be said to work rather well for hopping at extreme disorder. But there are systematic deviations from the EMA: The universal low-temperature AC hopping conductivity has a smoother onset than predicted by the EMA. Also, as the temperature is lowered, the curves systematically shift to the left compared to the EMA (Fig. 4 in P5).

In P7 the percolation path approximation (PPA), proposed in P4 for the macroscopic model, is developed for hopping. For both models the basis for the PPA is the long known fact that percolation is important for DC transport in severely disordered solids. Both models are described by electrical circuits. The PPA is based on assuming that not only for DC, but also for relatively low-frequency AC conduction does the current choose the easiest way through the circuit. On the lattice, links with high energy barriers (i.e., higher than the percolation energy) are avoided. The percolation cluster is a fractal, but a naive model for optimal paths on this cluster is to regard them as independent and one-dimensional; this ignores the fractal nature of the percolation cluster as well as the fact that paths may cross occasionally.

Based on this physical picture, the PPA models hopping in the extreme disorder limit as equivalent to a one-dimensional hopping with sharp activation energy cut-off. In contrast to what is the case for the macroscopic model, further approximations must be introduced to evaluate $\sigma(\omega)$ for the one-dimensional hopping model. The simplest approach is to use the EMA to arrive at an approximate analytical solution of the one-dimensional hopping model with an activation energy cut-off. One might ask how the use of the EMA is justified, when the purpose of the PPA is to arrive at a better approximation than the EMA. However, most likely the problem with the EMA in more than one dimension is that the one-dimensional nature of the conduction process at extreme disorder is eliminated by the homogeneous

effective medium; this problem does not arise when the EMA is used in one dimension.

The EMA solution of one-dimensional hopping with a sharp activation energy cut-off proceeds along the following lines. Whenever $s\tilde{G} \ll 1$ and $d = 1$, Eq. (1.40) (with σ now instead of D) implies (Eq. (46) of P5)

$$\frac{1}{\sigma} = \left\langle \frac{1}{\Gamma + s\tilde{G}\sigma} \right\rangle = \sum_{n=0}^{\infty} (-s\tilde{G}\sigma)^n \left\langle \Gamma^{-(n+1)} \right\rangle . \qquad (1.45)$$

As shown in P7, if the activation energy probability distribution, $p(E)$, has a sharp cut-off at E_c, Eq. (1.45) implies as $\beta \to \infty$

$$\sqrt{\tilde{\sigma}} \, \ln \left[1 + \sqrt{\tilde{s}\tilde{\sigma}} \right] = \sqrt{\tilde{s}} , \qquad (1.46)$$

where $\tilde{\beta} = \beta / p(E_c)$ and

$$\tilde{s} = \frac{\tilde{\beta}^2}{4 \, \sigma(0)} \, s . \qquad (1.47)$$

Equation (1.46) gives the universal low-temperature EMA solution of hopping in one dimension with a sharp activation energy cut-off. This result is referred to as PPA for hopping. Before comparing the PPA to results of simulations in two and three dimensions, the reliability of Eq. (1.46) must be checked by one-dimensional simulations of hopping with an activation energy cut-off. This is done in Fig. 2a of P7, plotting the approximate exponent as function of $\tilde{\sigma}$ (thereby avoiding empirical scalings of the frequency). Clearly, the EMA works very well in one dimension. The algorithm of P5 is extremely effective in one dimension, if one first removes every second point of the lattice, then every fourth point, etc. In contrast to in higher dimensions, there is no significant memory requirement for this simulation.

Once the reliability of Eq. (1.46) has been established, the PPA is compared to simulations in two and three dimensions in Figs. 1, 2b, and 2c of P7. In the simulations an algorithm developed by Thomas Schrøder, based on the circuit reduction method of P5, was used.[67] In Fig. 1 an empirical rescaling of the reduced Laplace frequency, $\tilde{s}$, was allowed to focus exclusively on the shape of the conductivity curve. The PPA works better than the EMA in two dimensions and much better than the EMA in three dimensions. A further indication of the reliability of the PPA (not discussed in P7) is given by studying the temperature-dependence of the reduced frequency: For a given distribution, if one empirically scales the conductivity curves at different temperatures to a master curve, the EMA predicts a factor of β between $\tilde{s}$ and $s/\sigma(0)$ (Eq. (56) resp. Eq. (59) of P5) while the PPA predicts a factor of β^2 (Eq. (1.47) above). The simulations give a scaling of $\beta^{2.5}$ in

two dimensions and $\beta^{1.5}$ in three dimensions. The different scalings of the EMA and the PPA explain the fact that the conductivity curves of Fig. 4 in P5 move to the left as the temperature is lowered, when compared to the EMA predictions. On the other hand, at higher temperatures the data of this figure agree well with the EMA. Thus, the EMA works well at high temperatures but not quite as well at low temperatures, where percolation becomes important. This is precisely what has been conjectured by Hunt.[68]

We are now in a position to answer the questions raised on page 38. P7 confirms that the AC properties of hopping models **are** different from those of the macroscopic model, though the difference is not large. The two models have in common that a universal frequency-dependence of the conductivity appears in the extreme disorder limit. For both models the universal conductivity exhibits an approximate power-law with an exponent less than but close to one, which goes to one as the frequency goes to infinity. While the approximate exponent for the real part of the universal conductivity of the macroscopic model is equal to $1 - 2/\ln(\tilde{\omega})$ (Eq. (1.20)), Eq. (1.46) implies the approximate exponent $1 - 3/\ln(\tilde{\omega})$. This means a somewhat slower approach to the high frequency behavior $\tilde{\sigma} \sim \tilde{s}$ for hopping than for the macroscopic model. There is also a smoother onset of AC conduction for hopping. Still, Eq. (1.46) reproduces all 8 Points mentioned in the Introduction, with one important exception (there has not been time to compare Eq. (1.46) to experiment, but the onset of AC conduction for most ionic glasses is often somewhat smoother than predicted by Eq. (1.17)): There is no BNN relation for Eq. (1.46). This is because Eq. (1.46) predicts that $\tilde{\sigma} = 1 + \sqrt{\tilde{s}}/2$ as $\tilde{s} \to 0$, which implies that the real part of the dielectric constant diverges as the frequency goes to zero and $\Delta\epsilon = \infty$. This is not as serious as it may sound, because the determination of $\Delta\epsilon$ is in fact experimentally difficult. Sometimes, the real part of the dielectric constant does not show signs of leveling off, but many workers regard this is a spurious effect due to contact problems.

Question 2) raised above is answered by the PPA. The PPA is not only a better approximation than the EMA for hopping in the extreme disorder limit, but it also gives a hint as to why the EMA works better for the macroscopic model than for hopping: The two models have in common that conduction becomes effectively one-dimensional in the limit of extreme disorder, and the PPA is a useful approximation for both models. However, hopping in one dimension with a sharp activation energy cut-off has *different* $\sigma(\omega)$ from the macroscopic model in one dimension with a cut-off. The PPA therefore gives *different* predictions for the two models. For the macroscopic model the EMA *happens to give* a prediction for the universal conductivity in more than one dimension that is very close to the PPA; for hopping this

is not the case. This is why the EMA works better for the macroscopic model than for hopping.

Outlook

P7 shows that hopping is different from the macroscopic model. This conclusion is not that given in P5, which was based on a conviction that the two models are more or less indistinguishable. If so, little is to be learnt from measuring the AC conductivity of a disordered solid. However, the conclusion is now that it *is* actually possible to determine whether Coulomb interactions are important or not, at least if the two simple models studied in P3-P7 are realistic.

Open questions that till today remain unanswered are:
1) Is asymmetric hopping identical to symmetric hopping as regards AC properties in the extreme disorder limit? Does asymmetric hopping exhibit universality at all?
2) How does the introduction of Coulomb interactions into a hopping model influence the AC conductivity in the extreme disorder limit?

1.7   Discussion of Paper 1-7

We finally give some overall comments to the 7 papers dealing with AC conduction in disordered solids. The comments relate to the *models* that have been discussed and to their relation to *reality*.
Models:

The publications P3-P7 give a systematic investigation of two models, emphasizing the extreme disorder limit. This limit has not previously been discussed in the literature, although the understanding of it must be important for understanding the behavior of these models at finite temperatures. The models were designed to be as simple as possible. They differ in a number of important respects, but also have common features. The differences refer to the physical assumptions involved. The macroscopic model and the hopping model are in many respects complementary, because the former is 1) macroscopic; 2) deterministic; 3) externally "controlled" by the overall potential drop; the latter is 1) microscopic; 2) stochastic; 3) externally "controlled" by the local homogeneous electric field. The similarities between the two models are of a mathematical nature. Both models lead to large sparse linear systems of equations with random coefficients that are thermally activated. A further and all important point is that the two models have quite

similar extreme disorder behavior.

The main result of P3-P7 is the proof of the existence of *universality in the extreme disorder limit* for both models. The physical background for the universality is the fact that, for both models, percolation is important for conduction in extremely disordered systems, as suggested more than 20 years ago.[60,61] The DC consequences of this fact are immediate and obvious: The activation energy of $\sigma(0)$ is equal to the percolation energy, E_c.[60-62] The AC consequences of the importance of percolation have been the subject of the present works. We find that, for both models, a simple pedestrian approach - the "percolation path approximation" (PPA) - gives a good description of the simulations and provides insight into the physics of AC conduction in extremely disordered solids. According to the PPA, conduction at extreme disorder is essentially a one-dimensional process, which involves only activation energies lower than E_c. In the PPA, universality arises at low temperatures because the details of the activation energy distribution are blurred and the distribution appears effectively as flat: For a given frequency range around the frequency marking the onset of AC conduction, as the temperature is lowered, a more and more narrow range of activation energies around E_c is involved.

The understanding provided by the PPA sheds light on the question raised on page 23 in the discussion of the random free energy barrier model. The question was: Why does Eq. (1.16) work so well, given that it is derived by a quite crude approximation (CTRW) to a model based on a number of rather restrictive assumptions (a sharp activation energy cut-off, a Box distribution, no Coulomb interactions, motion on a lattice). The answer to this question is the following: The Box distribution with its sharp cut-off is the effective distribution that appears due to the dominance of percolation at low temperatures. The inclusion of Coulomb interactions changes little; in fact, Eq. (1.16) is the PPA for the *macroscopic* model (thus, it is now clear that the CTRW solution of the random free energy barrier model is not quite realistic, since the PPA for *hopping* leads to Eq. (1.46)). The assumption of a regular lattice is not important at extreme disorder, since the main parameter is the enormous variation of the jump rates (random sites with nearest-neighbor hopping give only a factor of 2-3 variation in the jump distances).

We finally wish to stress once again the importance of the BNN-relation. The BNN-relation is Eq. (1.10), of course. However, in view of the non-existence of the BNN-relation for the PPA for hopping, by the BNN-relation we now just mean the rough proportionality of $\sigma(0)$ and the characteristic frequency marking the onset of AC conduction (the loss peak frequency). As discussed in P1, the BNN-relation - in conjunction with the existence

of a dielectric loss peak - implies that AC conduction is due to the same mechanism as DC conduction. For ionic glasses this was never questioned but, e.g., for amorphous semiconductors, AC conduction was traditionally thought to be due to jumping between isolated pairs of states[69] (giving no contribution to the DC conductivity). The BNN-relation tells us that the characteristic frequency marking the onset of AC conduction has the same activation energy as $\sigma(0)$. This fact points directly to the importance of percolation (the following argument refers to hopping, but may equally well be applied to the macroscopic model): For times longer than $1/\omega_m$ the solid "looks" homogeneous, for shorter times it "looks" inhomogeneous, giving rise to a frequency-dependence of the conductivity. This can be so only if ω_m is the lowest effective jump frequency on a typical DC conducting path. If the lowest effective jump frequency is to be roughly the one determining the DC conductivity activation energy, there must be a large spread in jump rates, and in this case percolation *is* important.

Reality:

The hopping model and the macroscopic model are typical examples of models discussed in theoretical physics, above all emphasizing simplicity. Only in P1 and P2 is the connection to experiment thoroughly discussed. In the spirit of the discussion in P2, one might conclude that the problem of describing AC conduction has been largely solved now. This is not the case. First of all, there is no conclusive evidence proving that the symmetric hopping model without interactions (or the macroscopic model), is the correct framework for describing the conduction process. Secondly, at low temperatures we know that other processes such as tunneling are important. Finally, despite the similarities between quite different solids, it is not certain that they should be described by the same type of models. The only thing that can be said at the present is that the universal AC conductivity of the extreme disorder limit gives a surprisingly good fit to many experiments (P1). Rather than being the last word to be said, the publications P1-P7 should be viewed as a first step towards a real understanding of AC conduction in disordered solids; much remains to be done in this field.

Chapter 2

VISCOUS LIQUIDS AND THE GLASS TRANSITION

2.1 Introduction

Glass formation is a universal property of supercooled liquids.[70–80] For simple liquids rapid cooling is required to avoid crystallization. For most complex liquids supercooling causes no problems. The glass transition takes place when the viscosity of the supercooled liquid becomes so large that molecular motion is arrested on the time-scale of the experiment. For cooling rates of order Kelvin per minute, the glass transition takes place when the viscosity, η, is around 10^{13} Poise (10^{12}Pa s).

The glass transition is still far from well-understood. At first sight, the transition looks like a second order phase transition, i.e., with continuity of free energy and its first derivatives and discontinuity of its second derivatives like specific heat, expansion coefficient, etc. However, it has been known for many years that the transition is of a kinetic nature. This is evidenced by several facts universally observed: The transition is not sharp, the transition temperature, T_g, depends on cooling rate, and the transition is irreversible and associated with various hysteresis phenomena (e.g., overshoot of the specific heat upon reheating, crossover effect, prepeak upon melting of a well-annealed glass). While the laboratory glass transition is a kinetic phenomenon, many workers in the field believe that the dramatic slowing down of molecular motion as the transition is approached is a manifestation of an underlying second order phase transition to a state of zero configurational entropy.[81,82]

The fascination of the glass transition lies in the fact that chemically very different liquids - involving ionic interactions, van der Waals forces,

hydrogen bonds, covalent bonds, or even metallic bonds - exhibit a number of common properties when cooled to become very viscous. Theoretical investigations of the glass transition should first attempt to understand the "equilibrium" viscous liquid ("equilibrium" in quotation marks because usually the crystal has the lowest free energy). There is no doubt that the last 20 years have brought a much better understanding of all types of viscous liquids. There has also been progress in theory, notably by the introduction of mode-coupling theories.[83,84] The most important question regarding viscous liquids has however, in the author's opinion, not yet been answered:

($\star$) *What is the cause of the non-Arrhenius average relaxation time?*

The publications P8-P10 are motivated mainly by this question. In formulating question ($\star$) it is implicitly assumed that an answer does exist which is common to all glass-forming liquids. This is far from certain, but at least it is a reasonable working hypothesis.

The average relaxation time, τ, may be determined, e.g., as the inverse dielectric, mechanical or specific heat loss peak frequency. Alternatively, it may be calculated from the viscosity, η, and the infinite frequency shear modulus, G_∞, by means of Maxwell's expression

$$\tau \ = \ \frac{\eta}{G_\infty} .\qquad (2.1)$$

These definitions do not give exactly identical τ's, but for our purpose the difference is insignificant. The important point is that, as the glass transition is approached, τ becomes longer and longer; for typical cooling rates τ is of order 10^3 s at T_g. This is to be compared to molecular vibration times of order 10^{-13} s.

From a general physical/chemical point of view, the temperature-dependence of τ is anomalous in the following sense. In only very few liquids is τ Arrhenius (examples are SiO_2, GeO_2, BeF_2 or albite $(NaAlSi_3O_8)$[72]). For all other glass-forming liquids is τ non-Arrhenius by exhibiting an apparent activation energy, which *increases* as the temperature *decreases* (the apparent activation energy is defined as $\partial \ln \tau / \partial (k_B T)^{-1}$). A measure of the departure from non-Arrhenius behavior is the fragility, m, defined as the apparent activation energy at $T = T_g$ in units of $k_B T_g \ln(10)$. This quantity was introduced by Angell in 1985.[85] For a simple Arrhenius liquid m is about 16; for most viscous liquids, m is between 50 and 150.

The fact that τ is non-Arrhenius is not itself surprising, given that a liquid is a disordered structure. However, for any simple model of disorder one

would expect the opposite non-Arrhenius temperature-dependence, namely a *decreasing* apparent activation energy as the temperature decreases. This is because one expects that the system at low temperatures searches thoroughly for the lowest energy barriers, while at higher temperatures the fact that there are many paths across somewhat higher barriers makes the average barrier to be overcome higher. Even in a severely disordered structure one expects at most simple Arrhenius behavior due to the importance of percolation (Chapter 1).

In view of the above, it is clear that the non-Arrhenius τ's must provide an important clue to the understanding of viscous liquids, and answering question ($\star$) should have a very high priority. This was also the case historically, but more recently the focus seems to have diffused away from question ($\star$).

There are two important phenomenological models for the non-Arrhenius average relaxation time. In the *entropy model* of Gibbs and coworkers[81,82] the decrease in configurational entropy S_c (the entropy in excess of that associated with harmonic vibrations) upon cooling is the cause of the non-Arrhenius behavior. Since at least two states must be involved in a "flow event", the fact that the configurational entropy decreases as temperature decreases implies that the average size of regions involved in a flow event increases. Assuming that the activation energy is proportional to the size of the region, Adam and Gibbs[82] arrived at the expression $\tau \propto \exp[C/(TS_c)]$, where C is a constant. S_c is known to extrapolate to zero at a finite temperature, the Kauzmann temperature. If the Kauzmann temperature is denoted by T_0, one finds from the Adam-Gibbs expression to lowest order in $(T-T_0)/T_0$ the Vogel-Fulcher-Tammann (VFT) formula, which expresses the non-Arrhenius temperature-dependence in the following way

$$\tau \ = \ \tau_0 \ \exp \left[\frac{A}{T - T_0} \right] . \tag{2.2}$$

We will not here comment on the verification of this picture from experiment but refer the reader to existing excellent reviews.[70-80]

The other "standard" answer to question ($\star$) is the *free volume model*,[86] which is particularly popular in polymer physics and chemistry. According to this model, the molecules take up most of the space in a viscous liquid; however, there is also some "free" volume. Upon cooling, the free volume decreases. In the simplest version, the free volume model results in the expression $\tau \propto \exp(C/V_f)$, where V_f is the free volume. If V_f extrapolates to zero at a finite temperature T_0, one again arrives at the VFT equation Eq. (2.2). This time, however, T_0 is not related to the Kauzmann temperature.

In the two above models the average relaxation time is controlled by *en-*

tropy resp. *volume*. A phenomenological model may also assume that *energy* is the variable controlling τ. In fact, the principle of detailed balance, which must be obeyed by any master equation,[65] implies a necessary correlation between energies and relaxation times. The relevance of potential energy was emphasized by Goldstein in a classic paper from 1969.[87] Later, Brawer proposed other models based on energy as the relevant thermodynamic quantity[72,88] where, incidentally, the energy is correlated to the volume.

The first two papers to be discussed below (P8 and P9) discuss models of "energy-controlled" type, the third paper (P10) discusses a model of "volume-controlled" type.

2.2 Paper 8: Simple Master Equation for Viscous Liquids

This paper discusses a very simple phenomenological model, focusing on different types of glass transitions. Below, we do not follow the paper but instead the line of reasoning that originally lead the author to the model.

Problem

1. What is the simplest possible model exhibiting non-Arrhenius behavior of the type observed in viscous liquids?
2. What happens at the glass transition according to this model?

Solution

For simplicity we do not distinguish between activation energy and activation free energy, and write for the temperature-dependence of τ

$$\tau = \tau_0 \exp\left[\frac{\Delta E(T)}{k_B T}\right] . \tag{2.3}$$

Note that $\Delta E(T)$ is different from the above defined "apparent activation energy"; however, their temperature-dependencies are qualitatively the same as is easy to show: $\Delta E(T)$ increases upon cooling if and only if the apparent activation energy does so. The observed non-Arrhenius behavior of τ implies that $\Delta E(T)$ increases as the temperature decreases. From an abstract point of view, the only thing we know *a priori* relating energies to temperatures is that the average energy, $\overline{E}(T)$, decreases with decreasing temperature. It is tempting to correlate this fact to the increase of the activation energy

upon cooling. If the barrier to be overcome, E_0, is assumed temperature-independent, the simple expression

$$\Delta E(T) \;=\; E_0 \;-\; \overline{E}(T) \tag{2.4}$$

would explain the non-Arrhenius behavior.

With this starting point, the problem is now to formulate an explicit model for viscous liquids. Here and henceforth by the term "energy" is meant the configurational part of the total energy. We assume a stochastic framework, i.e., that the dynamics are described by a master equation.[65] Whenever the focus is on the dynamics at long times compared to microscopic times, this is believed to be a realistic assumption. To simplify things, it is furthermore assumed that energy is the only relevant variable - a much more restrictive assumption.

The thermally activated process whose relaxation time is given by Eq. (2.3) is the "flow event", a sudden local rearrangement of molecules (the "flow event" mechanism of viscous flow is assumed by most authors[70,72,82,86–96]). In P8 it is assumed that the liquid is divided into non-interacting regions; the regions are assumed to relax independently, and there are no region-region interactions so the total energy is the sum of the region energies.

A region is characterized by its density of states, $n(E)$. In the present context a "state" is a potential energy minimum and the energy of a state is the potential energy at the minimum.

While Eq. (2.4) looks obvious, a little reflection shows that it doesn't have to be obeyed. For Eq. (2.4) to be valid it is necessary that the average energy is close to the most likely energy. For a constant density of states with a low-energy cut-off, the most likely energy is the ground state energy; the average energy lies $k_B T$ above this. Depending on the temperature and the value of E_0, Eq. (2.4) may or may not be valid in this case. To guarantee that Eq. (2.4) is obeyed, it is necessary to assume that a region has many degrees of freedom. In this case, by general principles of statistical mechanics, the energy probability distribution is an approximate Gaussian. For the Gaussian, of course, the average energy is equal to the most likely energy. In P8, as density of states was chosen $n(E) \propto E^{c-1}$, corresponding to a temperature-independent specific heat equal to ck_B. For this density of states, whenever $c \gg 1$, the average energy is close to the most likely energy.

The next problem is to formulate a master equation consistent with Eqs. (2.3) and (2.4). Inspired by Eq. (2.4) it is natural to assume that the relaxation time for jumps away from a state with energy E, $\tau(E)$, is given by (for $E < E_0$)

$$\tau(E) \;=\; \tau_0 \;\exp\left[\frac{E_0 - E}{k_B T}\right].\tag{2.5}$$

To avoid complications it is assumed that, once excited into the transition state, the state has forgotten where it came from and drops into a randomly chosen other state. These assumptions lead to the following master equation for the energy probability distribution as function of time, $P(E, t)$ (assuming henceforth that the density of states, $n(E)$, is normalized):

$$\frac{\partial P(E, t)}{\partial t} \;=\; -\frac{P(E, t)}{\tau(E)} \;+\; n(E) \int \frac{P(E', t)}{\tau(E')} dE'.\tag{2.6}$$

This equation is referred to as the energy master equation (EME).

The EME may be studied numerically for any arbitrarily varying temperature as function of time, for instance going through the glass transition. First, however, we briefly discuss how the EME is related to similar work. Equation (2.6) was originally proposed as a model for thermalization of photo-excited charge carriers in amorphous semiconductors.[97,98] Inspired by this work, the EME was arrived at as a phenomenological model for viscous liquids by the author along the lines sketched above. However, already three years before P8 appeared, Brawer arrived at a very similar, but somewhat more complicated equation.[72,88] P8 contains a reference to his very nice works, but unfortunately it is stated in P8 that the EME is "equivalent to Brawer's kinetic equation". This is inaccurate; rather, the EME is a particularly simple *special case* of Brawer's equation, which contains an additional entropy factor enumerating the number of paths across the barrier.

The EME may be regarded as a mathematical formulation of ideas discussed by Goldstein in a very nice, but seldom quoted paper from 1972.[91] In this paper it was suggested that the transition state for viscous flow is the "high-temperature, more-fluid, liquid usually studied by theorists". Once the region is excited into this transition state - being totally different from the potential energy minimum the region was excited from - the only reasonable assumption is that any other state can be reached. In the EME these states are all reached with equal probability.

The EME may be solved accurately utilizing a combination of analytical and numerical techniques (Appendix of P9). This makes it possible to study the EME at realistic laboratory times, despite the fact that the prefactor τ_0 realistically is of order a phonon time ($\simeq 10^{-13}$ s). In P8, however, the EME was studied numerically using a "pedestrian" algorithm, making it possible to step ahead only τ_0 in time. The EME was solved for different choices of the specific heat, c, for coolings at constant rate to zero temperature, starting from thermal equilibrium at high temperature. The calculations were carried

out on an Amstrad home computer. The simulations correspond to extremely rapid and therefore unrealistic cooling rates. However, a pattern appeared which it is possible to understand analytically:

For slow coolings, the frozen energy probability distribution, $P_0(E)$, is a Gaussian, corresponding to the equilibrium probability distribution at $T = T_g$. This is what is expected from the conventional picture of the glass transition, according to which the glass inherits the structure of the liquid at T_g. For fast coolings, however, the frozen energy probability distribution is *not* identical to that of the equilibrium liquid at T_g. What happens is that, during the freezing there is still some relaxation, resulting in a "deformed" $P_0(E)$ which is exponential rather than Gaussian on the low-energy side of the maximum. Thus, P8 proposes that there are two different types of glass transitions, "slow" and "fast" (in P9, for reasons to be detailed on page 55, new names are suggested: "simple freezing" contra "relaxational" glass transitions).

To understand the difference between a slow and a fast glass transition we consider the "demarcation energy" E_d originally introduced by Arkhipov and coworkers[97] for understanding relaxations at constant temperature of photo-excited charge carriers in amorphous semiconductors. If the cooling time is denoted by t_0, E_d is defined in P8 by

$$E_d = E_0 - k_B T \ln(t_0/\tau_0). \tag{2.7}$$

As is clear from Eq. (2.5), the demarcation energy (which depends on time via $T = T(t)$) separates states that have been frozen ($E < E_d$) from states which are not yet frozen ($E > E_d$). As the temperature is lowered, E_d moves towards higher energy while the distribution $P(E,t)$ moves towards lower energies. When E_d meets the distribution, energies are frozen, and when E_d has completely passed the distribution the glassy state has been reached. There are two limiting cases: A dimensionless number is arrived at, if one considers the ratio between the "velocity" with which E_d moves on the energy axis and the "velocity" with which $\overline{E}$ moves. If the former is much larger than the latter, the energy probability distribution is simply frozen at T_g; this is a "slow" glass transition since it requires long cooling times (P8). In the opposite limiting case, E_d almost does not move at all as the energy probability distribution "collides" with it, coming in from higher energies. To understand what happens in this case, it is convenient to consider the individual energy fluctuations of one region. The region jumps and jumps until it, at some point in time, jumps into a state with an energy below E_d. This last jump, like all others, ends up in a randomly chosen state, i.e., with probability proportional to the density of states. According to statistical

mechanics, for energies close to $\overline{E}(T_g)$ the density of states is approximately exponential: $n(E) \propto \exp[E/(k_B T_g)]$. Therefore, for a fast glass transition the frozen energy distribution $P_0(E)$ is approximately an exponential (with a cut-off, of course), as shown by Fig. 1d of P8. Supplementing this picture which is that given in P8, it should be noted that even in the case of a slow glass transition may one focus on the fluctuations of a particular region's energy. In that case, however, most regions do not have their final jump *into* a state with a frozen energy, but are instead frozen while *being* in some particular state.

P8 speculates briefly as to the experimental consequences of the possible existence of two different types of glass transitions. Around the time the paper was written, it became increasingly clear that in amorphous semiconductors exponential band tails of localized states - stretching into the band gap of the corresponding crystalline semiconductor - occur almost ubiquitously.[99–103] In P8 it was conjectured that these exponential band tails arise because amorphous semiconductors are prepared by the equivalent of a fast glass transition: If this is the case the exponential distribution of frozen energies translates into an exponential distribution of average transfer integrals, implying the existence of exponential band tails of localized states.[104]

Outlook

The model studied in P8 is certainly oversimplified. The assumption that the liquid may be divided into non-interacting regions is hard to justify. Why shouldn't a flow event be allowed involving molecules from more than one region[105]? Another serious problem[105,106] is the fact that, if correct non-Arrhenius τ's are to be arrived at, large region specific heats are implied, leading to too broad distributions of relaxation times for linear relaxations like those monitored by dielectric, mechanical or specific heat spectroscopy. On the other hand, the EME does exhibit a number of the interesting hysteresis phenomena observed close to the glass transition (unpublished), and there have recently been attempts to extend the EME to solve the problem with the prediction of too broad distributions of relaxation times.[107] Also, the EME is used in contexts different from that of viscous liquids (e.g., as a model for spin glasses or protein dynamics[108]). Thus, from a general point of view it does make sense to ask: Is it possible to justify the EME from some "natural" starting point? This question is addressed in P9.

2.3 Paper 9: Approximation to Bässler's Random Walk Model

The same issue of Physical Review Letters in which P8 appeared (23 February 1987) contains a paper by Bässler discussing a phenomenological random walk model for viscous liquids.[109] This model is based on a Gaussian distribution of energies and predicts the average relaxation time to have a temperature-dependence of the form

$$\tau = \tau_0 \, \exp\left[\frac{C}{T^2}\right] . \qquad (2.8)$$

This expression fits experiment well.[109] Equation (2.8), in fact, is partly a rediscovery,[110,111] and it has been known for some time[71] that a better fit is provided by $\tau \propto \exp(C/T^n)$. However, Bässler's random walk model is in some sense "natural" and has some very attractive properties, making it worthwhile to study further.

Usually, in a random walk model one would let the energy maxima vary randomly (as in the symmetric hopping model studied in P1 and P5-P7) or let the energy minima vary randomly (as in the standard model for trap limited charge carrier thermalization in amorphous semiconductors[97,98]). Bässler's model is elegant, because all states are equivalent and no states are maxima or minima. His model considers the motion of a "particle" (representing the state of a liquid region) on a cubic lattice in d dimensions. The model is defined in the following way. Only nearest neighbor jumps are allowed and the jumps take place with Metropolis jump rates: jumps to lower energy states take place with a jump rate of order a phonon frequency. Each site has an energy that is chosen randomly according to a Gaussian, and the site energies are uncorrelated. The model is completely specified by the dimension, d, the variance of the Gaussian, σ^2, and the "downhill" jump rate, Γ_0. Two of these parameters have a dimension, and there is only one dimensionless parameter in the model, namely d.

Problem

Is it possible to arrive at a simple picture of energy fluctuations at low temperatures in Bässler's random walk model?

Solution

As mentioned above, Bässler's random walk model is "natural" because no states at the outset are specified as maxima or minima. Effectively, however,

the low-energy states *are* minima, since all their surrounding states almost certainly have higher energy. Some of these surrounding states, as well as others further away, act as barriers: At low temperatures in thermal equilibrium the most likely energy is low and therefore far into the negative Gaussian tail. The low-energy states are extremely rare on the lattice; however, they are the important ones at low temperatures. Thus, effectively the dynamics may be viewed as consisting of transitions between these states. A transition between two low-energy states involves a complex sequence of steps. At low temperatures, the most likely sequences are those with the lowest maximum energy. This lowest maximum energy on a long path is estimated as the percolation energy, E_c, defined by (where $n(E)$ is the normalized Gaussian density of states)

$$\int_{-\infty}^{E_c} n(E)dE = p_c.$$ (2.9)

Here, p_c is the site percolation threshold, not to be confused with the bond percolation threshold appearing in Chapter 1. The effective transition rate for jumps between two low-energy sites starting at energy E is expected to be given by $\Gamma \propto \exp[-(E_c - E)/(k_BT)]$. Since this is independent of the energy of the final state, the total rate for jumps away from a low-energy state with energy E is given by the same expression (with a larger constant of proportionality, of course). In high dimensions there are many likely final states; it is reasonable to regard them all as equally likely, because the same barrier height has to be overcome to reach each of them. We thus end up with the EME as the effective equation describing energy fluctuations at low temperatures in high dimensions at long times. Note that the parameters of the EME are uniquely determined from the parameters of the random walk model (a simple argument detailed in P9 shows that the EME jump rate prefactor is equal to $2\Gamma_0$).

According to this picture, the average relaxation time is given by (compare Eq. (2.5)) (where $\tau_0 = 1/(2\Gamma_0)$)

$$\tau = \tau_0 \exp\left[\frac{E_c - \overline{E}(T)}{k_BT}\right].$$ (2.10)

Since $\overline{E}(T) = -\sigma^2/(k_BT)$ for the Gaussian density of states with width σ, to leading order in T^{-1} one thus arrives at Bässler's expression Eq. (2.8) with $C = \sigma^2/k_B^2$.

It is interesting to note that each low-energy state is the center of a complex "basin" including neighboring states with relatively low energy. The minima are thus rather complex,[74,112] despite the fact that the energies are uncorrelated from site to site.

In P9 the predictions of the EME are compared to computer simulations of Bässler's random walk model in two dimensions. The agreement is rather good. In particular, during a sudden heating from thermal equilibrium a two-bump distribution appears in the simulations of the random walk model (Fig. 5 of P9), a phenomenon that is reproduced by the EME. When inspecting Figs. 2-5 of P9 it should be remembered that all parameters of the EME are fixed. Also, the simulations could only be carried out at moderately low temperatures.

In P9 the glass transition was not studied by computer simulations. However, once the EME has been established as a reliable effective low-temperature description of Bässler's random walk model, the EME can be used as a guide for what to expect at the glass transition. In P8 it was argued that the character of the glass transition is determined by the ratio between the "velocities" on the energy axis of the demarcation energy and of the average energy. In P9 this is rationalized by defining the parameter ι by

$$\iota = \left| \frac{d\,\overline{E}}{dE_d} \right| (T_g) . \tag{2.11}$$

In the terminology of P8, $\iota \ll 1$ corresponds to a "slow" glass transition and $\iota \gg 1$ to a "fast" glass transition. A "slow" glass transition is characterized by a frozen energy probability distribution that is just the equilibrium distribution at $T = T_g$; a "fast" glass transition has a frozen distribution differing from the equilibrium distribution due to additional relaxations taking place right at the glass transition. The analysis of the effective EME for Bässler's random walk model, however, shows that these names are inconvenient: In all dimensions one thus finds $\iota \to 1$ as the cooling time goes to infinity; this signals a mixed situation at slow cooling rates. Furthermore, in two dimensions one finds $\iota \to 0$ as the cooling time goes to zero, signalling a "slow" glass transition in this case! (This is a consequence of the fact that in two dimensions the site percolation threshold is larger than 0.5.) To avoid the confusing names of P8, it was suggested in P9 to refer to "simple freezing glass transitions" (those with $\iota \ll 1$, previously "slow") contra "relaxational glass transitions" (those with $\iota \gg 1$, previously "fast").

Outlook

Bässler's random walk model is beautifully simple, but still has quite interesting properties. It has a non-Arrhenius average relaxation time of the right type (with apparent activation energy that increases upon cooling). Thus, if the cause of the non-Arrhenius average relaxation rate is the fact that the

average energy decreases upon cooling (compare Eq. (2.4)), Bässler's model is quite "natural".

Future work should focus on justifying how the fact that flow events are localized - which seems absolutely reasonable - translates into the postulate that the viscous liquid may be modelled as an ensemble of non-interacting regions - which seems less reasonable. (It is not possible just to describe the whole sample by the random walk model, because one elementary jump on the lattice would then change the energy by an extensive amount and the relaxation time would not be an intensive variable.)

2.4   Paper 10: Local Elastic Expansion Model

The models of P8 and P9 both assume that cooperatively rearranging regions relax independently. There are several problems with this assumption.[105] First, the very definition of a region involves assuming that it exists as a real entity with a well-defined border to its surroundings; is the liquid really divided into regions? Secondly, it is assumed that the border between a region and its surroundings cannot move with time, i.e., that a given molecule for all times - despite diffusion and possible flow - belongs to a certain region. Finally, because the border between region and surroundings is large (small spheres have a relatively large surface) it is not obvious that, even if regions do exist permanently, they may be regarded as independently relaxing. One would expect the surroundings to have at least some influence on the dynamics of one region. To closer look into the influence of the surroundings one may ask:

Problem

1. Is it possible to construct a realistic model for the temperature-dependence of the average relaxation time, where the surroundings of a relaxing region are the cause of the non-Arrhenius behavior?
2. How essential is the region assumption in such a model?

Solution

The model of P10 is restricted to molecular liquids, but possibly the model may be applied to other glass-forming liquids. Before proceeding, the author would like to acknowledge the contribution of Niels Boye Olsen. For several years he insisted that there must be a link between the non-Arrhenius average relaxation time and the temperature-dependence of the high frequency shear

or bulk moduli. He was thus the driving force behind P10. Furthermore he, in collaboration with Tage Christensen, through years of hard work developed the "piezo-electric shear gauge transducer (PSG)"[113] that made it possible to check this hypothesis (P10). The present author's contribution was to construct a specific model consistent with Boye's ideas.

The basic idea of the model of P10 is the same as the idea in the free volume model[86] or in Brawer's model,[72] namely that a flow event requires a local volume increase. The picture is the following. ·The molecules of a viscous liquid are closely packed. Therefore, a rearrangement cannot take place unless there is sufficient space available. In contrast to the free volume theory, we do not assume that a certain fraction of the volume is "free" and do not consider *diffusion* of free volume (the free volume model assumes conservation of free volume, which seems hard to justify).

The common starting point for these models is the assumption of a positive activation volume for flow events:

$$\Delta V > 0.$$
(2.12)

Why is it reasonable to assume that there is a positive activation volume? Of course, one could refer to high-pressure experiments that point in this direction (but as we will se later, according to the new model the activation volume cannot be directly deduced from these experiments). To answer this question we first note that, like any thermally activated process, a flow event is very fast, taking place probably within picoseconds. Secondly, we remind of the very basic characteristic of molecular forces, namely that the repulsive forces are harsh while the attractive forces are only weak. This fact is responsible for thermal expansion and a number of other common phenomena in liquids.[114] If a flow event were to take place at a constant volume, a considerable amount of energy would be required to overcome the strong repulsive forces. It is easier for the liquid to spend some energy on "shoving" aside the surrounding liquid, leading to Eq. (2.12).

In the above picture, there are two contributions to the activation energy: One from the "shoving" work and one from the increase of the region energy during the flow event. To consider the relative importance of these contributions, we note that for highly viscous liquids it is reasonable to assume that, on the rapid time scale where flow events take place, the liquid behaves like a solid. To simplify things, it is assumed that during a flow event the volume of the molecules involved is expanded from one sphere to a larger sphere, the latter being the transition state. Consider first the case of a perfectly harmonic solid. In such a solid, as is easy to show, the elastic energy of the "excited" sphere is comparable to the elastic energy of the surround-

ings that have been "shoved" aside. However, while the molecule movements in the surroundings are relatively small and thus within the harmonic approximation, the molecules of the region itself move much more than within the harmonic approximation. Because of the weak attractions, the harmonic approximation considerably overestimates the elastic energy of the "excited" sphere. For simplicity this contribution is ignored, and the activation energy is taken to be just the work done on the surrounding liquid.

On a fast time scale, the surrounding liquid behaves as an elastic isotropic solid characterized by the bulk modulus, K_∞, and the shear modulus, G_∞. Both these elastic constants are known to be much more temperature-dependent in viscous liquids than in simple liquids or ordinary solids (crystals or glasses). Both K_∞ and G_∞ increase as the temperature decreases. Since the work done on the surroundings during a flow event depends linearly on these constants, it is clear without further computation that according to the new model, the cause of non-Arrhenius behavior is the strong temperature-dependence of the high frequency elastic constants in supercooled liquids.

Actually, it is only the shear modulus that is important. To show this we refer to the theory of elasticity of isotropic media,[115] assuming that the activation volume is relatively small; if V is the volume of the cooperatively rearranging region it is assumed that $\Delta V << V$. We identify the activation energy with the elastic energy stored in the surroundings when the volume of the region has expanded to $V + \Delta V$ (the additional kinetic energy of the surroundings is ignored). Thus, on the one hand a flow event is assumed to be rapid enough for the surrounding liquid to behave as a solid, but on the other hand it is assumed to be slow enough for the kinetic energy associated with the expansion to be insignificant. Proceeding now to calculate the activation energy, we remind that elasticity theory[115] concerns the relation between the stress tensor, σ_{ij}, and the strain tensor, u_{ij}. The latter is defined by

$$u_{ij} = \frac{1}{2}\left(\partial_i u_j + \partial_j u_i\right), \qquad (2.13)$$

where $\partial_i \equiv \partial/\partial x_i$ and u_i is the i'th component of the elastic displacement vector $\mathbf{u}$. The trace of the strain tensor $u_{ll} = \partial_l u_l$ (using standard notation with sum over repeated indices) gives the relative volume change. For any isotropic solid, the bulk and shear moduli K and G are defined by[115]

$$\sigma_{ij} = K u_{ll}\delta_{ij} + 2G\left(u_{ij} - \frac{1}{3}\delta_{ij}u_{ll}\right). \qquad (2.14)$$

The equation for static equilibrium is

$$\partial_i \sigma_{ij} = 0. \tag{2.15}$$

Substituting Eq. (2.13) into Eq. (2.14) and subsequently Eq. (2.14) into Eq. (2.15) leads to

$$K\partial_j(\partial_l u_l) \ + \ G\left(\partial_i \partial_i u_j + \partial_j(\partial_i u_i) - \frac{2}{3}\partial_j(\partial_l u_l)\right) \ = \ 0. \tag{2.16}$$

In vector notation Eq. (2.16) is

$$\left(K + \frac{1}{3}G\right)\nabla(\nabla \cdot \mathbf{u}) \ + \ G\,\nabla^2\mathbf{u} \ = \ 0. \tag{2.17}$$

For a purely radial displacement $\nabla \times \mathbf{u} = \mathbf{0}$ and thus, via the well-known vector identity $\nabla \times (\nabla \times \mathbf{u}) = \nabla(\nabla \cdot \mathbf{u}) - \nabla^2\mathbf{u}$, we have $\nabla^2\mathbf{u} = \nabla(\nabla \cdot \mathbf{u})$. When this is substituted into Eq. (2.17) one finds simply

$$\nabla(\nabla \cdot \mathbf{u}) = 0. \tag{2.18}$$

Equation (2.18) implies that $\nabla \cdot \mathbf{u} = C_1$, where C_1 is a constant. The displacement (which is radial) is found by solving $\nabla \cdot \mathbf{u} = r^{-2}\partial_r(r^2 u_r) = C_1$, leading to $u_r = C_2 r^{-2} + C_1 r/3$. The latter term diverges as $r \to \infty$ and thus $C_1 = 0$. In conclusion $\nabla \cdot \mathbf{u} = 0$ and there is no compression of the surroundings during a flow event: The surroundings are subjected to the *pure shear* displacement $u_r = C_2 r^{-2}$ (note the analogy to the electric field from a point charge, which by Gauss' law has zero divergence).

If the radius of the region before the expansion is R and the change of radius is ΔR, we have (remember that $\Delta R << R$)

$$u_r \ = \ \Delta R\,\frac{R^2}{r^2}\,(r > R). \tag{2.19}$$

The energy density of an elastic solid is[115] $\frac{1}{2}K u_{ll}^2 + G\left(u_{ij} - \frac{1}{3}\delta_{ij}u_{ll}\right)^2$. Since $u_{ll} = 0$ the energy density is given by $G u_{ij} u_{ji} = G(u_{rr}^2 + u_{\phi\phi}^2 + u_{\theta\theta}^2)$ (all mixed terms like, e.g., $u_{r\phi}^2$ are zero because the displacement is purely radial). When Eq. (2.19) is used in the definition of the strain tensor in polar coordinates, we get for the energy density $6G(\Delta R)^2 R^4 r^{-6}$. Thus, the elastic energy is given by

$$\int_R^\infty 6G(\Delta R)^2 R^4 r^{-6}\,(4\pi r^2)dr \ = \ 8\pi G\,(\Delta R)^2\,R. \tag{2.20}$$

Substituting $V = 4\pi R^3/3$ and $\Delta V = 4\pi R^2 \Delta R$ into Eq. (2.20) we find, introducing the "characteristic volume"

$$V_c = \frac{2}{3}\frac{(\Delta V)^2}{V},\tag{2.21}$$

for the activation energy of the average relaxation time (with $G \equiv G_\infty(T)$)

$$\Delta E(T) = G_\infty(T)\, V_c.\tag{2.22}$$

Substituting Eq. (2.22) into Eq. (2.3) finally leads to

$$\tau = \tau_0\, \exp\left[\frac{G_\infty(T)\, V_c}{k_B T}\right].\tag{2.23}$$

The prediction of Eq. (2.23) was checked against experiment on a number of organic liquids in P10, using the following version of the "Angell plot": Instead of plotting the logarithm of the viscosity or any other average relaxation time (the temperature-dependence of G_∞ in Eq. (2.1) is not important in this context) as function of T^{-1}, we plot it as function of $G_\infty(T)/T$ normalized to one at T_g. In Fig. 1a of P10 results are shown for measurements covering the frequency range 1mHz-50kHz. All liquids studied follow the time-temperature superposition principle (TTSP) - an extremely interesting fact that we do not understand. Because of the TTSP, the value of the imaginary part of the shear modulus at the loss peak is proportional to G_∞ and there is no need to extrapolate the data to high frequencies (since the x-coordinate is normalized to one at T_g). For this procedure to work, it must be assumed that possible additional relaxations at higher frequencies are insignificant compared to the alpha relaxation. Figure 1a in P10 shows good agreement between theory and experiments, since the use of the new x-coordinate results in a straight line with a physically acceptable prefactor (10^{-4}P). Figure 1b shows the data of Barlow and coworkers from 1967 obtained by an ultrasonic standing wave technique operating in a rather narrow frequency range in the MHz region. Analytical approximations to the data were given in the original paper,[116] so it was easy to replot the data. Finally, Fig. 1c of P10 shows data for two liquids, where G_∞ was derived from transverse Brillouin scattering. Again we find good agreement with the theory. When P10 was written, Brillouin data for two non-organic liquids, B_2O_3 and $Ca_{0.4}K_{0.6}(NO_3)_{1.4}$ (CKN), were also looked at. For the first liquid G_∞ is much too temperature-dependent and for the second it is not quite enough temperature-dependent to fit the theory.

P10 gives a lengthy discussion of related work in the literature. This will not be repeated here; instead we would like to supplement with some new comments. First, however, we take the opportunity to quote the last part of the original version of P10, a part that was removed during the lengthy

process of "negotiations" with the referee via the editor before the paper was finally accepted for publication:

Many molecular liquids have additional relaxations above the dominant α-relaxation. These additional relaxations are Arrhenius and they are always less temperature-dependent than the α-relaxation. One may ask how these relaxations fit into the above model, which deals with the α-relaxation. At high temperature all relaxations are indistinguishable, they only separate upon cooling. According to our model, any relaxation process with a non-zero activation volume becomes non-Arrhenius in the highly viscous state. In view of this, we would like to suggest that the relaxations above the α-relaxation are those with a zero or very small activation volume. If this is correct, the additional relaxations should not be influenced by the glass transition (that freezes G_∞). Experimentally, this is the case for β-relaxation. Note also that β-relaxation is much less pressure-dependent than α-relaxation, indicating a much smaller activation volume for β-relaxation than for α-relaxation.

It is generally believed that the initial stages of glassy relaxation proceeds with a temperature-independent activation energy, which is a characteristic of the frozen structure. According to the present model, however, there is a slight temperature-dependence of the activation energy for glassy relaxation, deriving from the fact that G_∞ is not completely temperature-independent in the glassy phase. For long-time glassy relaxation there is the additional well-known effect that the activation energy increases due to the structural relaxation of the glass. The fact that G_∞ is measurable means that, if our model is valid, it is possible directly to monitor the activation energy for glassy relaxation. If one assumes Eq. (1) for the structural relaxation rate, the model gives definite predictions for the rate of relaxation of G_∞ itself.

In the new model the high frequency shear modulus determines the activation energy for the average relaxation time. Thus, G_∞ is a direct measure of the "fictive temperature". In contrast to what is the case for other phenomenological models, in the new model the fictive temperature is not an abstract concept but a physical quantity that can be measured at any time via a fast measurement. It may seem strange that a fast measurement allows one to predict the value of the very long average relaxation time, but this is not at all surprising: While the time *between* flow events may be extremely long, a flow event itself is a fast process. It "monitors" the elastic properties of the liquid on a short time scale, and this "monitoring" may of course be done by fast experiments like, e.g., Brillouin scattering.

According to the new model, G_∞ controls the temperature-dependence of the average relaxation time. If this idea is correct, G_∞ is central for understanding the dynamics of viscous liquids and glasses. A number of measurements of the temperature-dependence of G_∞ have previously been made with

the sole purpose of converting viscosity to the shear relaxation time[71] using Maxwell's Eq. (2.1). In view[71] of the relatively weak temperature-dependence of G_∞ and the fact that one may define several "relaxation times" that are not quite identical, it may seem strange that so much effort was put into measurements of G_∞. However, we now have a theory in which G_∞ is all important because it enters into an *exponential*, and it is fortunate that measurements of this quantity exist. Unfortunately, at present the most direct method of obtaining G_∞ - transverse Brillouin scattering - gives somewhat inaccurate data (because the peaks are broad and barely distinguishable from the background).

We end this Section by a few remarks and speculations. First, however, we reflect briefly on question 2 on page 56 concerning the region assumption. In P8 and P9 it was assumed that the liquid may be divided into non-interacting regions, a division that is not allowed to change with time. In the new model the situation is different. Any flow event is assumed to take place at a specific place in the liquid, a "region". However, there is no need to assume a permanent division of the liquid into regions; a flow event may very well involve some, but not all of the molecules of a previous flow event. In this sense, no "region assumption" is needed.

Here are the final remarks, numbered from 1 to 6:

1. In P10 the model was proposed for molecular liquids only. We found good agreement with experiment, but have only data for molecular liquids with a rather narrow range of fragilities. It cannot be excluded that the agreement between theory and experiment is a pure coincidence. On the other hand, it is possible - and in our opinion likely - that the new mechanism is valid also for glass-forming liquids with ionic, covalent, or metallic bonds. One may ask whether the model possibly may have an even further validity. It has often been discussed whether relaxation phenomena seen in orientational glasses, where non-Arrhenius behaviors are also observed,[117] may be due to a mechanism similar to that operative in ordinary viscous liquids. The present model is easily extended to orientational glasses, and actually these glasses do exhibit a large temperature-dependence of the high frequency shear modulus. We have not made a quantitative comparison. For spin glasses, on the other hand, the new model cannot apply. Thus, even in the "best of all worlds" for the new model, the non-Arrhenius behaviors observed in disordered systems have more than one origin. Clearly, further work is needed to test the model and determine the limits of its validity.

2. A well-known empiricism is the so-called "2/3 rule" relating glass transition temperature to melting temperature, T_m:

$$T_g \; \cong \; \frac{2}{3} T_m \,.$$

(2.24)

We will not attempt to explain the factor 2/3, but ask the more basic question: Why does T_g scale with T_m? In principle, a liquid could "glassify" long before it crystallizes ($T_g \gg T_m$) or this could happen close to zero temperature: $T_g \ll T_m$. The first possibility occurs in a few exotic liquids that are believed to be amorphous in their ground state[79] (implying $T_m = 0$), but in the overwhelming number of cases the scaling is obeyed. This is so, despite the fact that T_m may vary quite a lot for different liquids with different chemical bonds. The new model gives a hint as to what is the answer to this question: According to the Lindemann melting criterion,[118] melting takes place when the average vibrational displacement of the atoms in the crystal is about 10% of the lattice constant. We now "view the glass transition from the solid".[79] If the interatomic potential in the harmonic approximation is $\frac{1}{2} m \omega^2 u^2$, where u is the displacement from equilibrium in the glass, the equipartition principle implies $m \omega^2 \langle u^2 \rangle \propto T$. For simplicity we do not distinguish between shear and bulk high-frequency moduli and denote both by M_∞. Since the sound velocity is proportional to ω and to $M_\infty^{1/2}$ (implying $M_\infty \propto \omega^2$), one finds $M_\infty \langle u^2 \rangle \propto T$. This implies that, according to the new model, if the characteristic volume does not vary much from liquid to liquid, the glass transition takes place when $\langle u^2 \rangle$ has a definite value. This is a "Lindemann" melting criterion for glasses. Since $\langle u^2 \rangle$ is roughly proportional to the temperature, it follows that T_g scales with T_m. The argument may be reversed: Given the fact that T_g scales with and is relatively close to T_m, one concludes that the glass transition takes place when M_∞/T has a definite value. Since the glass transition takes place when the average relaxation time has a definite value, one is more or less lead to conjecture that the average relaxation time is a function of M_∞/T. Given this assumption, it is clear that in order to explain the only weak cooling rate dependence of T_g, M_∞/T must enter into an exponential. This almost brings us to the new model (where it is just furthermore specified, that the relevant elastic constant is the high frequency shear modulus). A weakness in the above argument is that, in the new model the characteristic volume is not fixed, while above V_c must be more or less the same for all glass-forming liquids. On the other hand, following a different line of reasoning, Nemilov has concluded that the region volume is almost constant for 90 quite different glass-forming liquids[119,120] and via Eq. (2.21) this leads to a constant characteristic volume if the activation volume is relatively constant.

3. The activation volume is usually deduced from high pressure experiments using the expression $\Delta V = (k_B T) \partial \ln \tau / \partial p$. In the new model,

however, τ depends on pressure according to

$$\tau = \tau_0 \exp\left[\frac{G_\infty(p,T) V_c + p\Delta V}{k_B T}\right] . \tag{2.25}$$

Since G_∞ depends on pressure, if our new model applies the activation volume found by the conventional method is incorrect. This is rather unfortunate, since it means that the activation volume is not directly measurable.

4. Based on the new model it is possible to argue that

$$G_\infty = \frac{3}{4} K_0 , \tag{2.26}$$

where K_0 is the isothermal zero-frequency bulk modulus. The argument goes as follows. Standard statistical mechanics implies that (where V is the volume of the entire macroscopic sample and $\langle V_0^2 \rangle$ its mean-square fluctuation in thermal equilibrium)

$$K_0 = \frac{V k_B T}{\langle V_0^2 \rangle} . \tag{2.27}$$

The average relaxation time is via Eqs. (2.21) and (2.23) given by

$$\tau = \tau_0 \exp\left[\frac{2G_\infty(\Delta V)^2}{3V_{reg} k_B T}\right] , \tag{2.28}$$

where V_{reg} is the region volume. Because the surroundings are only subjected to pure shear displacements during volume fluctuations of a region, it is consistent to assume that the density fluctuations are uncorrelated in space beyond the size of one region. Thus, if σ_V^2 is the mean-square fluctuation of the region volume, it is reasonable to assume that

$$\frac{\sigma_V^2}{V_{reg}} = \frac{\langle V_0^2 \rangle}{V} = \frac{k_B T}{K_0} . \tag{2.29}$$

The probability of a volume fluctuation equal to ΔV is approximately given by a Gaussian,

$$p \propto \exp\left[-\frac{(\Delta V)^2}{2\sigma_V^2}\right] = \exp\left[-\frac{(\Delta V)^2 K_0}{2V_{reg} k_B T}\right] . \tag{2.30}$$

Since the average relaxation time is one over this probability (times a microscopic time=inverse attempt frequency) comparing Eqs. (2.28) with (2.30) one arrives at Eq. (2.26). We have not checked this prediction against experiment.

5.   An interesting point to note is that the experiments of Olsen and Christensen show that the high-frequency *bulk* modulus is not sufficiently temperature-dependent to explain the non-Arrhenius average relaxation time. This supports the new model and goes against a number of related alternatives (briefly reviewed in P10) that focus on the temperature-dependence of the mean-square displacement at short times as the cause of the non-Arrhenius average relaxation time.

6.   It has been conjectured by Niels Boye Olsen that G_∞ is a function solely of volume:

$$G_\infty = G_\infty(V).$$ (2.31)

This is a rather natural guess, given that G_∞ is a thermal average of a quantity (essentially the shear stress squared) which depends on the atomic positions at any given instant (thus, involving no time autocorrelation functions). According to Boye's conjecture, the temperature-dependence of G_∞ is caused by thermal expansion, and therefore basically due to the anharmonic parts of the intermolecular interactions: When temperature is lowered the volume decreases and G_∞ increases. Equation (2.31) implies that the rate of structural relaxation for two different preparations of a glass is the same if just their volume and temperature is the same. Thus, under these conditions the annealing state does not matter at all! One might object that this is contradicted by experiment, using the standard criticism against the free volume theory. However, in the new model the *activation energy* for flow is a function of volume; the viscosity itself is a function of volume *and* temperature.

If Eq. (2.31) holds, the rate of structural relaxation of a glass can in principle be determined by "easy" and "fast" measurements of temperature and volume (the latter could perhaps be monitored via interference from reflections of a laser). We have not been able to formulate a more precise model for structural relaxations, mainly because of the well-known problem that a distribution of relaxation times is involved.

According to Eq. (2.31) the equation defining the glass transition temperature as function of pressure is

$$d\left(\frac{G_\infty(V)}{T}\right) = 0.$$ (2.32)

In terms of the thermal expansion coefficient, $\alpha = (1/V)(\partial V/\partial T)_p$, the compressibility $\kappa = -(1/V)(\partial V/\partial p)_T$ (equal to the inverse of the isothermal zero-frequency bulk modulus), and the following dimensionless measure of the volume-dependence of G_∞, $\lambda = -d\ln G_\infty/d\ln V > 0$, one easily finds

from Eq. (2.32)

$$\frac{dT_g}{dp} = \frac{\kappa\lambda T}{\alpha\lambda T - 1}.$$
(2.33)

Note that in contrast to the two "standard" expressions for this ratio (derived from continuity of volume resp. entropy across the glass transition), Eq. (2.33) does not involve differences between properties of glass and liquid; only the properties of the "equilibrium" liquid are involved.

Outlook

The mechanism for the non-Arrhenius average relaxation time of glass-forming liquids suggested in P10 deserves further work to establish in which cases it may apply. There are three problems that should be looked into.

1. At present the main problem with the model is the fact that no really good data exist for G_∞. The measurements of Niels Boye Olsen and Tage Christensen are quite accurate, but restricted to frequencies below 50 kHz. Possible secondary relaxations at higher frequencies cannot be detected by their method. The ultrasonic method may be promising, but the most direct method for measuring G_∞ is transverse Brillouin scattering. For the latter, unfortunately, it is hard to obtain accuracy. Attempts should be made to improve this technique, if possible.

2. Independent of the experimental situation, computer simulations of viscous liquids should be carried out; this is a good way to test any model. The evaluation of G_∞ causes no problem, but reaching thermal equilibrium and evaluating the average relaxation time in highly viscous liquids is a challenge to the computer hardware. We do have access to fast computers and plan to perform molecular dynamics simulations in the near future to test the new model.

3. Finally, in particular in relation to Boye's hypothesis Eq. (2.31), it is increasingly clear that high pressure experiments are relevant.

2.5   Discussion of Paper 8-10

The models (A) of P8 and P9 and the model (B) of P10 are complementary in several respects:

1. In (A) the average relaxation time is *energy controlled*, in (B) it is *volume controlled*.

2. In (A) the inner of a region determines the temperature-dependence of τ, in (B) it is the surroundings.

3. In (A) there is a distribution of relaxation times which is related to the non-Arrhenius τ, in (B) this is not the case.

4. In (A) one must assume the liquid is permanently divided into regions, in (B) this does not have to be assumed.

5. In (A) there is no reason to expect that the glass transition temperature scales with the melting temperature, in (B) this is the case.

There are indications that the more fragile liquids have broader spectra of relaxation times[85,121-123] (although there are exceptions to this general tendency[124]). This correlation is present in the P8-P9 models. For the 4 other above points, it seems that the model of P10 is to be preferred compared to those of P8 and P9.

Finally, we note that none of the discussed models can explain the experimental correlation between the Kauzmann temperature and T_0 of the VFT expression (Eq. (2.2)). Whether this is a serious problem or not is open to discussion.

Chapter 3

EXTENSIONS OF LINEAR RESPONSE THEORY

3.1 Introduction

This Chapter deals with five papers (P11-P15) that one way or the other extend or elaborate standard linear response theory and the fluctuation-dissipation (FD) theorem. It has been known for many years[125] that no simple generalization of the fluctuation-dissipation theorem exists which makes it possible to predict the nonlinear response from a knowledge of equilibrium fluctuations. Some general results are available though, relating different cumulant averages in an external field to each other. These results have been derived most generally by Bochkov and Kuzovlev from statistical mechanics and time-reversal invariance.[126] In any further development one has to consider approximations or special cases. Some examples of this are discussed in this Chapter.

The first paper (P11) deals with electrical 1/f noise. This - in a sense - is a linear phenomenon, but as shown in P11, the magnitude of the noise is determined by *fourth* order cumulant averages of the equilibrium current fluctuations. The FD-theorem only concerns time autocorrelation functions (i.e., second order cumulant averages). The next three papers (P12-P14) deal with genuine non-linear responses. P12 discusses a maximum entropy "ansatz" for the non-linear response of a time-independent external field. The formalism developed in P12 include the main result of P11 as a special case. P13 and P14 deal with nonlinear viscoelasticity. This subject is relevant for viscous liquids close to the glass transition, because one expects[127] any liquid to exhibit nonlinear flow properties whenever the shear rate exceeds the inverse Maxwell relaxation time (which is large close to T_g). P13

concerns a simple model for nonlinear shear viscoelasticity, where the linear frequency-dependent viscosity is the inverse of the universal AC conductivity for disordered solids (Chapter 1). P14 discusses how to couple a shear rate "field" to a Langevin equation for the shear stress fluctuations. Finally P15 proposes an approximation for the calculation of time autocorrelation functions. P15 is completely within standard linear response theory; however, while P15 is not an *extension* of linear response theory it presents an *elaboration*. The scheme proposed in P15 reduces the problem of finding a time autocorrelation function to calculating a "double" canonical average and the mean-square displacement as function of time.

3.2   Paper 11: Resistance Fluctuations

We first review the fundamental theorem for stochastic processes, the Wiener-Khinchin theorem connecting the time autocorrelation function with the noise spectrum. Consider a stationary stochastic process, $Y(t)$, with zero mean. In studies of electrical noise, $Y(t)$ is either the current or the voltage minus their average. In this research field the noise spectrum, $S_Y(\omega)$, is usually defined by

$$S_Y(\omega) \;=\; \lim_{T \to \infty} \frac{2}{T} \left\langle \left| \int_0^T Y(t) e^{i\omega t} dt \right|^2 \right\rangle. \qquad (3.1)$$

In this convention, $S_Y(\omega)$ is equal to $S_Y(f)$ in van Kampen's book.[65] Note that in Eq. (3.1) an ensemble average is needed besides taking the limit $T \to \infty$. The variance of $Y(t)$ may be calculated from the noise via

$$\left\langle Y^2 \right\rangle \;=\; \frac{1}{2\pi} \int_0^\infty S_Y(\omega) d\omega. \qquad (3.2)$$

The Wiener-Khinchin theorem (which is a straightforward consequence of the Fourier inversion theorem) states that the noise spectrum is the cosine transform of the time autocorrelation function:

$$S_Y(\omega) \;=\; 4 \int_0^\infty \langle Y(0)Y(t) \rangle \cos(\omega t) dt. \qquad (3.3)$$

The study of electrical noise spectra goes back to the works of Johnson and Nyquist.[3,128] They showed that in thermal equilibrium there are always current fluctuations (or voltage fluctuations, depending on the experimental setup). These fluctuations directly reflect the electrical resistance of the sample: The DC resistance is proportional to the zero frequency noise spectrum of the equilibrium voltage fluctuations. More generally, the real part

of the conductivity is proportional to the cosine transform of the equilibrium current autocorrelation function.[3,129] This result is simply the real part of the Kubo formula for electrical conduction,[4] a special case of the general FD-theorem. A simple proof of the FD-theorem has been given by Doi and Edwards.[2]

As is clear from the above, the equilibrium current or voltage fluctuations and their relation to the linear electrical properties have been fully understood for many years. However, it has been known also for several years that in non-zero electric fields there are additional current or voltage fluctuations ("excess noise"). The origin of excess noise is not well-understood. The fascination of the phenomenon comes from the fact that almost all solids have excess noise which increases as the frequency decreases, without any sign of leveling-off at low frequencies. The excess noise usually varies as an approximate inverse power-law - $S(\omega) \propto \omega^{-\alpha}$ - with α close to one ("1/f noise"). Thus, there are some very slow processes going on in solids and this is the surprising thing. It is also surprising that quite different solids have similar excess noise characteristics.

The excess current noise for a sample of volume V in an external electric field E is given by the approximate expression (where J is the average current)

$$S_J(\omega) \;=\; K \,\frac{\langle J \rangle_E^2}{V}\, \omega^{-\alpha}. \tag{3.4}$$

There are two things to be noted. First, the noise varies inversely with volume; this is what is expected if the noise is due to uncorrelated localized processes. Secondly, the noise varies as the average current squared. This is what to expect if it is the *resistance* that fluctuates. However, given the fact that the resistance itself is a measure of the Nyquist noise (a measure that by definition cannot fluctuate in time), it is not quite clear what it means that the resistance fluctuates. The purpose of P11 is to look into this question, building on earlier work.

Forgetting about the conceptual problem of "noise magnitude fluctuations", if the resistance somehow does fluctuate, one would expect fluctuations in the magnitude of the Nyquist noise in thermal equilibrium. In 1976 Voss and Clarke[130] showed that this is actually the case and that the equilibrium resistance fluctuations are precisely large enough to explain the excess current noise in external fields. Their experiment was a breakthrough, because it showed that the 1/f noise is present in thermal equilibrium (and not generated by the rather large electric fields usually applied to measure the noise). Still the theoretical dilemma remains: Precisely what does it mean that the resistance fluctuates?

Problem

How can resistance fluctuations be understood in the simplest possible terms?

Solution

The FD-theorem for electrical conduction implies in particular that the DC conductivity is proportional to the DC diffusion constant (the Nernst-Einstein relation). A simple way to understand this is to study random walk models. In random walk models the Nernst-Einstein relation basically comes about in the following way: The diffusion constant is proportional to the mean-square displacement per unit time, i.e., the average number of jumps per unit time. In an electric field, jumps in the field direction become more likely than opposite to it. The average current is proportional to the average number of jumps per unit time and therefore to the diffusion constant.

Inspired by the FD-theorem, it is an obvious idea to discuss resistance or conductivity fluctuations in terms of diffusion constant fluctuations. Before P11 was written several papers had been published addressing the question of what it means that the diffusion constant fluctuates.[131-134] The role of P11 was only to provide a simplification and clarification of already obtained results.

In 1983 Kuzovlev and Bochkov showed for "slowly fluctuating" $D(t)$ that[133] (where k is arbitrary and $\Delta x(t)$ is the displacement in time t)

$$\left\langle e^{ik\Delta x(t)} \right\rangle = \left\langle \exp\left[-k^2 \int_0^t D(t')dt'\right] \right\rangle . \tag{3.5}$$

Unfortunately, they gave no precise definition of $D(t)$. From Eq. (3.5) it is straightforward to prove that the fourth order cumulant average of the stochastic quantity $\Delta x(t)$, $\left\langle \Delta x^{(4)}(t) \right\rangle$, is related to the diffusion constant autocorrelation function, $C_D(t) \equiv \langle D(0)D(t) \rangle - D^2$ (where $D = \langle D(t) \rangle$ is the ordinary diffusion constant) by

$$C_D(t) = \frac{1}{24}\frac{d^2}{dt^2}\left\langle \Delta x^{(4)}(t) \right\rangle . \tag{3.6}$$

This result may be rewritten in terms of fourth order cumulant averages of the velocity (using the russian notation for cumulant averages)

$$C_D(t) = \int_0^t d\tau' \int_0^{\tau'} d\tau'' \left\langle v(t), v(\tau'), v(\tau''), v(0) \right\rangle . \tag{3.7}$$

Equation (3.7) was independently derived by Niewenhuizen and Ernst.[134] They define the "fluctuating diffusion coefficient", $D(t,\tau)$, by

$$D(t, \tau) = \frac{1}{2} \frac{\partial}{\partial t} [x(t) - x(\tau)]^2 , \tag{3.8}$$

and showed for the Markovian model under study that $C_D(t - t') \equiv \langle D(t, \tau) D(t', \tau') \rangle - D^2$ for "large values of t' and t" is in fact a function of $t - t'$ only which obeys Eq. (3.7).

In P11 we consider the motion of one particle on a one-dimensional lattice. It is assumed that the conductivity is frequency-independent. At certain times, τ_i, the particle jumps. We know from P2 that, since the conductivity is frequency-independent, each jump occurs in a random direction. If one were to associate with the particle a diffusion constant fluctuating in time, it is natural to assume that $D(t) = 0$ if the particle does not jump right at time t: then it does not move at all. Since the jumps are infinitely fast and the average of $D(t)$ must be the ordinary diffusion constant, this immediately leads to our definition of $D(t)$ (a is the lattice constant):

$$D(t) \equiv \frac{a^2}{2} \sum_i \delta(t - \tau_i) . \tag{3.9}$$

From this definition it is shown in P11 that the current autocorrelation function in weak external field is given by (where q is the charge)

$$\langle J(t) J(0) \rangle_E = \left(\frac{q^2 E}{k_B T} \right)^2 \langle D(t) D(0) \rangle_0 \quad (t > 0) . \tag{3.10}$$

The average on the right hand side refers to equilibrium (zero field) fluctuations. In deriving Eq. (3.10), the ensemble average is taken in two steps: The first step averages over all possible jump histories with the same jump times, τ_i, (the "restricted ensemble average") - the next step averages over all possible jump times.

Equation (3.10) is the main result of P11, showing that excess current noise probes equilibrium diffusion constant fluctuations. Combining Eqs. (3.7) (which is derived in P11 with the new exact definition of $D(t)$) with (3.10) leads to (for $t > 0$)

$$\langle J(t) J(0) \rangle_E = \langle J \rangle_E^2 + \left(\frac{E}{k_B T} \right)^2 \int_0^t d\tau' \int_0^{\tau'} d\tau'' \langle J(t), J(\tau'), J(\tau''), J(0) \rangle_0 . \tag{3.11}$$

We end by three remarks.

1. It is straightforward to show that our definition of $D(t)$ leads to the inverse volume-dependence of the noise observed in experiment (Eq. (3.4)).

2. Our definition of $D(t)$ is related to that by Niewenhuizen and Ernst (Eq. (3.8)) by

$$D(t) = \lim_{\epsilon \to 0} D(t - \epsilon, t + \epsilon).$$ (3.12)

Unfortunately, this simple fact was noted only after the publication of P11.

3. $D(t)$ is proportional to the *speed* of the particle at time t, the numerical value of the velocity. Thus, while the ordinary frequency-dependent conductivity probes the equilibrium *velocity* autocorrelation function, the excess current noise spectrum probes the equilibrium *speed* autocorrelation function.

Outlook

An obvious question to look into is how to generalize the results of P11 to the case of a frequency-dependent conductivity. This is done in P12. If possible, the results obtained should also be generalized to other conduction mechanisms than hopping. Those of the above formulas that explicitly contain the lattice constant clearly cannot be generalized but, e.g., the final result Eq. (3.11) is possibly generally valid.

3.3   Paper 12: Ansatz for Nonlinear Response Theory

It was already in the 1950's discussed how to generalize linear response theory.[4,135] In linear response theory the response is uniquely determined from equilibrium fluctuations. Unfortunately, this is not so in the nonlinear case, where the formal expansion in the external field leads to a little useful expression.[4] The problem is that, in the expansion of the response in terms of the external field, the coefficients cannot be expressed in terms of equilibrium fluctuations of the degree of freedom that couples to the field.[125] The best one can hope for is an approximate theory that *estimates* the nonlinear response from equilibrium fluctuations. There is another problem which must be faced. In a non-infinitesimal field, the dissipated heat cannot be ignored and the response depends on the way this heat is removed, i.e., the size of the sample, etc. A general formalism that estimates the response from equilibrium fluctuations cannot take this into account, and should be applied only at fields small enough that the temperature is almost constant throughout the sample. In many cases this condition is fulfilled for sufficiently small samples.

Some important nonlinear phenomena do take place at very small dissipation rate. An example is flow of a highly viscous liquid: It is an empirical fact[127] that this becomes nonlinear at shear rate of order $1/\tau_M$, where τ_M is the Maxwell relaxation time (Eq. (2.1)). Thus, if G_∞ is the infinite frequency shear modulus and η the (DC) viscosity, at the onset of nonlinearity the dissipation rate per unit volume is of the order G_∞^2/η. For large viscosities this quantity is very small and the temperature is almost constant throughout even a large sample.

Historically, due to the above mentioned problems, interest in the subject gradually diminished. When interest arouse again it was in connection with the problem of how to computer simulate systems subject to large fields, without having the temperature run away.[136] This problem is nowadays usually solved by introducing a thermostat modifying the equations of motion.[137] In P12 and below, by retaining the true Hamiltonian we follow Bochkov and Kuzovlev in their little known, but extremely interesting papers[126] . P12 extends one of their conjectures and relates it to other work, including P11.

Problem

What is the simplest "ansatz" for approximate calculation of the nonlinear response from equilibrium fluctuations?

Solution

All complications of quantum mechanics are ignored and it is assumed that the dynamics are described either by classical mechanics or by a master equation. The degree of freedom of interest is denoted by Q. It is assumed that Q is time-reversal invariant; we define $J = \dot{Q}$ and refer to J as a "current". The external field coupling to Q is denoted by E, giving rise to the extra term in the Hamiltonian, $-EQ$. Only the case of a constant time-independent field is discussed in P12. Following Bochkov and Kuzovlev[126] we focus on the path probability, $P_E[J(t)]$, i.e., the probability of the entire current "history", $J(t)$ $(-\infty < t < \infty)$ in the external field. A knowledge of $P_E[J(t)]$ allows a calculation of not only the average current in the external field, but also the current autocorrelation function and higher order cumulant averages.

The maximum entropy formalism[138,139] is a general method for estimating probabilities based on insufficient information. If the stochastic variables in question are denoted x_i and if it is known that $\langle f(x_i) \rangle = C$, the maximum entropy estimate of the probability of x_i is $P_i \propto \exp[-\lambda f(x_i)]$. The Lagrangian multiplier, λ, is adjusted to give the correct mean of $f(x)$. As

an example, consider throwing a dice. After many throws, a proper dice gives average 3.5 . Suppose a dice turns out to have average 4. Clearly, this fact does not give us enough information to determine the probabilities (i.e., frequencies) of having 1, 2, etc; there are many possible solution to this problem. According to the maximum entropy formalism, the best "unbiased" estimate of the probabilities is $P_i = N^{-1} \exp(-\lambda i)$, where N is a normalization constant and λ is chosen so that $\sum_{i=1}^{6} i P_i = 4$. A simple way to understand how the maximum entropy estimate is arrived at is to consider all possible outcomes of K throws, in the end letting $K \to \infty$. If all possible sequences of K throws with average 4 are considered, one finds by a simple calculation using the Stirling approximation for $n!$ precisely the maximum entropy estimates for the actual occurrences of 1, 2, etc. Thus, for a "typical" sequence with average 4, the frequencies of 1, 2, etc are those of the maximum entropy formalism.

Returning now to nonlinear response theory, we know that in an external field the energy dissipation is equal to $-E \int_{-\infty}^{\infty} J(t)dt$. We don't know *a priori* the value of the dissipation, but may still apply the maximum entropy formalism to estimate the path probabilities. In continuous problems like the present a complication arises, since a reference measure is needed. This is a serious problem if there is no obvious candidate for the reference measure. In the present case, however, to ensure a smooth transition to the zero field case, the reference measure must be $P_0[J(t)]$, the equilibrium path probability. Thus, the maximum entropy estimate of the external field path probability, based solely on knowledge of the fact that there is energy dissipation in an external field, is

$$P_E[J(t)] = N^{-1} P_0[J(t)] \exp\left[-\lambda E \int_{-\infty}^{\infty} J(t)dt\right] . \tag{3.13}$$

The time-reversal invariance of the classical equations of motion (or the principle of detailed balance if a master equation is assumed) implies[126] that the ratio between the probability for one current "history" and the time-reversed "history" is given (where $\beta = 1/(k_B T)$) by

$$\frac{P_E[J(t)]}{P_E[-J(-t)]} = \exp\left[\beta E \int_{-\infty}^{\infty} J(t)dt\right] . \tag{3.14}$$

Combining Eqs. (3.13) and (3.14) lead immediately to

$$P_E[J(t)] = N^{-1} P_0[J(t)] \exp\left[\frac{\beta}{2} E \int_{-\infty}^{\infty} J(t)dt\right] . \tag{3.15}$$

This "ansatz" allows a calculation of all cumulant averages of $J(t)$ in the external field from a knowledge of the equilibrium cumulants, since these

uniquely determine $P_0[J(t)]$. P12 gives a number of examples and remarks relating to the consequences of Eq. (3.15), summarized below.

1. For the average current in an external field one finds

$$\langle J \rangle_E = \sum_{n=0}^{\infty} \frac{1}{n!} \left(\frac{\beta E}{2} \right)^n \int_{-\infty}^{\infty} \langle J(0), J(t_1), \ldots, J(t_n) \rangle_0 \, dt_1 \ldots dt_n, \qquad (3.16)$$

where the subscript 0 denotes an equilibrium average. Clearly, the zero'th and first-order terms are those predicted by linear response theory.

2. For a random walk on a lattice one finds from Eq. (3.16) for the average velocity in an external field (where a is the lattice constant and Γ the jump rate)

$$\langle v \rangle_E = \Gamma a \sinh \left[\frac{\beta E a}{2} \right]. \qquad (3.17)$$

This is the correct result, if the random walk is realized as the low-temperature limit of a Langevin particle in a symmetric potential. Behind the maximum entropy ansatz somehow lies a postulate that the maxima generally are placed symmetrically between minima. Thus, an equivalent of Eq. (3.16) was first derived by Stratonovich[140] for stochastic systems from the assumption that the energy maximum to be overcome in the transition is placed midway (in the "direction" of Q) between the two minima.

3. For the current autocorrelation function in an external field, Eq. (3.15) for a system with frequency-independent conductivity implies Eq. (3.11) of the preceding Section on excess current noise. In contrast to what is the case in P11, in P12 the excess current noise is calculated without specific assumptions regarding the nature of the system, thus allowing for frequency-dependence of the conductivity.

4. Equation (3.15) implies

$$\frac{d}{dE} \langle J \rangle_E = \frac{\beta}{2} \int_{-\infty}^{\infty} \langle J(0), J(t) \rangle_E \, dt. \qquad (3.18)$$

This is a special case of an exact theorem from 1967 due to Peterson.[141]

5. It is possible to justify the maximum entropy ansatz by referring to a Langevin equation for Q, for which an exact expression for the path probability exists.[142] The maximum entropy ansatz corresponds to dropping one term from the exponential expression for the exact path probability (compare Eq. (14) of P12).

6. A further connection to previous works sheds light on the possible range of validity of the maximum entropy ansatz. In 1975 Furukawa noted

that for "slowly fluctuating" $J(t)$, the exact equations of motion imply for the path probability[143]

$$P_E[J(t)] \;=\; N^{-1}\, P_0[J(t)]\; \exp\left[\frac{\beta}{2}E \int_{-\infty}^{\infty} J(t)dt + O(E^2)\right]. \qquad (3.19)$$

The maximum entropy ansatz corresponds to ignoring the $O(E^2)$ terms. Equation (3.19) suggests that there are two different ways a system may become nonlinear: Either as an interplay between non-Gaussian equilibrium fluctuations and the first order term of the exponential, or as a result of the higher order terms becoming important. The first case may be referred to as a "simple" nonlinearity, since it results from the same term in the exponential of Eq. (3.19) that gives rise to the linear response. This is when the maximum entropy ansatz gives correct results. Upon increasing the field, a system may pass from linear via "simple" nonlinear response to finally the "complex" nonlinear response due to the higher order terms of the exponential of Eq. (3.19). In this case the maximum entropy ansatz gives correct results at intermediate field strengths. Alternatively, the system may go directly to the "complex" nonlinear response, in which case the maximum entropy ansatz is not valid beyond the linear regime.

Outlook

Nonlinear response theory is a subject that deserves further study. While the presently popular approach of thermostating is certainly important, there are cases with no need for thermostats because the nonlinearities occur in systems that have a well-defined temperature. These "simple" systems should be studied more. It is not clear whether a useful and general approximate nonlinear response theory may be constructed, for instance by somehow generalizing the above to time-dependent fields, or whether such a general theory does not exist. In an unpublished paper[144] five requirements were formulated that a general approximate nonlinear response theory should obey: 1. The theory should calculate the response from a knowledge of the equilibrium fluctuations; 2. it should satisfy causality; 3. it should reflect the time-reversal invariance of the microscopic equations of motion; 4. it should predict an exactly linear response whenever the equilibrium fluctuations of the degree of freedom of interest are exactly Gaussian; 5. if two degrees of freedom fluctuate independently in equilibrium, a field coupling to one should not result in a response for the other. It is possible to formulate a theory that satisfies all these requirements except, possibly, time-reversal invariance.[144] Unfortunately, this theory is inconsistent with

the maximum entropy ansatz of P13. For instance, for a random walk, the maximum entropy ansatz corresponds to having the barrier in middle between two minima, while the theory of Ref. 144 instead corresponds to Metropolis dynamics. There may not exist a general approximate time-dependent nonlinear response theory.

3.4 Paper 13: Simple Model of Nonlinear Viscoelasticity

One of the most thoroughly studied nonlinearities is viscoelasticity.[127,145,146] Viscous liquids usually become nonlinear at shear rates of order the inverse Maxwell relaxation time,[127] so nonlinearities at small shear rates are common to all glass-forming liquids close to the glass transition. Close to T_g, however, the viscosity is enormous and flow experiments not easily carried out. Therefore, nonlinear viscoelasticity is often studied in polymeric liquids that usually become nonlinear considerably above T_g.[145]

The single most important characteristic of nonlinear viscoelastic liquids is their shear rate dependent viscosity, usually decreasing with increasing shear rate. This is referred to as "shear-thinning" (there are a few examples of "shear-thickening" fluids, e.g., fairly concentrated suspensions of very small particles[145]). Another important characteristic of nonlinear viscoelasticity is the so-called "normal stress effect". This phenomenon, which disappears in the linear limit, gives rise to spectacular effects like "rod-climbing": When a rotating rod is inserted into a viscoelastic liquid, the liquid climbs up the rod.[145]

One of the objectives of viscoelastic theory is to set up so-called "constitutive relations" that predict the stress tensor based on the strain tensor history. The simplest constitutive relations are scalar and involve only shear strain and shear stress, ignoring the existence of normal stresses. The first constitutive relations considered were differential equations,[147] but it was soon realized that these are not able to reproduce linear frequency-dependent viscosity involving broad ranges of relaxation times. More successful are the so-called single integral constitutive relations,[145] that involve integration over the strain history. Many constitutive relations have already been proposed, so an obvious question to ask is:

Problem

What is the simplest possible realistic scalar constitutive relation?

Solution

Henceforth, by the term "stress" is meant shear stress, by "strain " is meant shear strain, and by "shear rate" is meant the time derivative of the strain. A constitutive relation involves at least two parameters with a dimension, a characteristic time and a characteristic stress; all other parameters are dimensionless. In the name of simplicity, in P13 we look for a constitutive relation with no dimensionless parameters.

Following the common terminology in the field[145] we denote the stress by τ and the strain by γ. Dimensionless units are used throughout P13. The basic postulate of linear response theory is that the shear rate history, $\dot{\gamma}(t)$, determines the stress via a convolution integral:

$$\tau(t) = \int_0^\infty G(t')\dot{\gamma}(t-t')dt'. \tag{3.20}$$

The function $G(t')$ is the stress relaxation modulus, the stress decay as function of time t' if a unit strain is suddenly applied to the equilibrium system at time zero. In the standard way Eq. (3.20) implies that the complex linear frequency-dependent viscosity, $\eta_0(\omega)$, is given by

$$\eta_0(\omega) = \int_0^\infty G(t')e^{-i\omega t'}dt'. \tag{3.21}$$

The problem is now to find a realistic stress relaxation modulus and subsequently to extend Eq. (3.20) to cover nonlinear situations. For the traditionally studied broad molecular weight polymeric liquids it turns out (Fig. 6 in P13) that the following function gives a good fit to data for $\eta_0(\omega)$:

$$\eta_0(\omega) = \frac{\ln(1+i\omega)}{i\omega}. \tag{3.22}$$

As function of $s = i\omega$, this is the Laplace transform of the so-called exponential integral, $E_1(t)$, defined by

$$E_1(t) = \int_t^\infty \frac{e^{-u}}{u}du. \tag{3.23}$$

Consequently, we choose $E_1(t)$ as stress relaxation modulus, $G(t)$. It is straightforward to show that, if the system is modelled as a number of Maxwell elements in parallel with thermally activated relaxation times, the stress relaxation modulus $E_1(t)$ corresponds to the Box distribution of energy barriers.

To generalize Eq. (3.20) to nonlinear situations we take as starting point the empirical Cox-Merz rule[148] obeyed by most broad molecular weight poly-

meric liquids. This rule states that the nonlinear steady state shear viscosity, $\eta(\dot{\gamma})$, is related to the complex linear frequency-dependent viscosity by

$$\eta(\dot{\gamma}) = |\eta_0(\omega = \dot{\gamma})| . \tag{3.24}$$

Comparing the Cox-Merz rule to Eq. (3.21) suggests that the nonlinear steady state viscosity is given by

$$\eta(\dot{\gamma}) = \int_0^\infty E_1(t')e^{-\dot{\gamma}t'} dt' \ (\dot{\gamma} > 0) . \tag{3.25}$$

In turn, this suggests the following generalization of Eq. (3.20)

$$\tau(t) = \int_0^\infty E_1(t')\dot{\gamma}(t - t') \exp\left[-\int_{t-t'}^t |\dot{\gamma}(t'')| \, dt''\right] dt' , \tag{3.26}$$

since Eq. (3.26) in the steady state case implies Eq. (3.25).

Most of P13 is concerned with evaluating the consequences of Eq. (3.26). On page 113 in the excellent book by Bird et al[145] seven typical shear flow experiments used in rheology are listed: 1. Steady flow; 2. small amplitude oscillatory flow; 3. stress growth upon inception of a steady flow; 4. stress relaxation after cessation of a steady flow; 5. stress relaxation after a sudden displacement; 6. creep after applying a constant stress; 7. constrained recoil after suddenly removing the stress for a steady flow. Each of these situations is solved analytically in P13 for the constitutive relation Eq. (3.26). It is shown that the model reproduces all qualitative features of experimental shear viscoelasticity, except the overshoot of the stress growth upon inception of a steady flow.

We now give four remarks to P13.

1. The linear frequency-dependent viscosity that fits experiment (Eq. (3.22)) is the inverse of the universal AC conductivity for extremely disordered solids (Chapter 1). This may be understood as follows: Consider a foreign microscopic particle introduced into the liquid. On a short time scale the particle "feels" the liquid as a disordered solid. It is thus reasonable to assume that the particle's frequency-dependent mobility is the universal function discussed in Chapter 1; assuming that a frequency-dependent generalization of Stoke's law is valid for the particle, the mobility is the inverse of the viscosity, leading to Eq. (3.22). On a longer time scale, the liquid structure is broken down and on this time scale the diffusion of the particle becomes linear in time. The characteristic time separating short and long times is the longest relaxation time of the liquid, approximately equal to the Maxwell relaxation time (Eq. (2.1)). If this time is identified with the longest

relaxation time of the universal AC conductivity, it makes good sense to use the universal expression at all frequencies.

2. The constitutive relation Eq. (3.26) allows an analytical calculation of the nonlinear creep function (Eq. (30) in P13). Since the frequency-dependent viscosity is the inverse of the universal AC mobility, the creep function reduces to Eq. (17) in P6 in the linear limit.

3. For the nonlinear steady state viscosity Eq. (3.26) implies

$$\eta(\dot{\gamma}) = \frac{\ln(1 + \dot{\gamma})}{\dot{\gamma}}. \tag{3.27}$$

For large shear rates $\eta(\dot{\gamma}) \simeq \ln(\dot{\gamma})/\dot{\gamma}$, which is the same asymptotic behavior as that predicted by Eyring's expression,[149]

$$\eta(\dot{\gamma}) = \frac{\sinh^{-1}(\dot{\gamma})}{\dot{\gamma}}. \tag{3.28}$$

This expression comes from $\dot{\gamma} = \sinh(\tau)$ which - incidently - is valid for the nonlinear velocity in random walk models (compare Eq. (3.17)).

4. Although stated in P13 that the constitutive relation, as regards the introduction of an exponential damping function, is "inspired by Wagner's[150] work" , the basic idea was in fact developed in ignorance about his closely related papers. Wagner did not refer to the Cox-Merz rule in his paper,[150] but showed the usefulness of an exponential damping function by direct comparison to experiment. The advantage of rediscovery is that a new angle to the subject is sometimes introduced. This is the case here, since Wagner assumed the damping to be a function of *strain* history and not of *shear rate* history: His damping term is $\exp\left[-\left|\int_{t-t'}^{t} \dot{\gamma}\right|\right]$, while our is $\exp\left[-\int_{t-t'}^{t} |\dot{\gamma}|\right]$. For any monotonously increasing or decreasing strain as function of time there is no difference between the two damping functions. In general, however, there is a significant difference. Thus, in Wagner's damping function, if the strain displacement between time $t - t'$ and time t is zero, there is no damping. Wagner noted that in this respect his damping function contradicts experiment[151] and suggested a rather complicated remedy (summing over all possible histories), whereby the simplicity is lost. The problem of how to introduce "irreversibility" into constitutive relations is still actively discussed.[152] By introducing an irreversibility closely related to the network rupture hypothesis of Tanner,[153] the damping function of Eq. (3.26) gives a possible solution to this problem. In fact, our damping function may be regarded as a continuous version of Tanner's idea, that entanglements are lost irreversibly in the process of deformation as soon as a limiting strain is exceeded.

Outlook

One obvious problem to consider in the future is how to extend the constitutive relation to deal with non-scalar viscoelasticity. Another problem that would be interesting to study is whether a simple microscopic model exists that follows the constitutive relation. One possibility is the one-dimensional symmetric hopping model with a Box distribution of energy barriers. This model may be coupled to an external stress in several ways. The two most obvious choices are Metropolis dynamics or the coupling corresponding to a barrier placed symmetrically between two minima (leading in the nonlinear steady state to Eq. (3.17) or Eq. (3.28)). The one-dimensional random walk model has been studied numerically by the author (unpublished). The model does follow the constitutive relation reasonably well, but there are some deviations, e.g., in the stress growth upon inception of a shear flow, where the model by exhibiting an overshoot behaves more like experiment than the constitutive relation does.

3.5   Paper 14: Shear Stress Fluctuations in a Flow

P12 considers the problem of estimating the nonlinear response from a knowledge of equilibrium fluctuations. P14 attacks this problem from a different perspective, restricting attention to the subject of P13 which is nonlinear shear viscoelasticity. In contrast to the approach of P12, in P14 we do not assume a knowledge of the entire equilibrium current history path probabilities. Only the equilibrium (static) probability distribution of the relevant variable is assumed known. This is because the standard Langevin approach is taken, the idea of which is briefly the following:

   Consider a variable, s. In thermal equilibrium the free energy as function of s, $F(s)$, is defined by (where Γ collectively denotes the complete set of microscopic degrees of freedom and $E(\Gamma)$ is the energy)

$$e^{-\beta F(s)} = \int \delta[s - s(\Gamma)]e^{-\beta E(\Gamma)}d\Gamma . \tag{3.29}$$

Clearly, the equilibrium probability distribution of s is proportional to $\exp[-\beta F(s)]$. If $\xi(t)$ is a Gaussian white noise term, the Langevin equation is

$$\dot{s} = -\mu \frac{dF}{ds} + \xi(t), \tag{3.30}$$

where

$$\langle \xi(t)\xi(t')\rangle \ = \ 2\mu k_B T\delta(t-t')\,. \tag{3.31}$$

The crucial fact about the Langevin equation is that the probability distribution, which develops in time according to the Smoluchowski equation,[2,65] after long time converges to the equilibrium distribution proportional to $\exp[-\beta F(s)]$.

In P14 s is the shear stress and the question that now obviously arises is:

Problem

How is the Langevin equation for s modified in a shear flow?

Solution

The liquid is assumed to be divided into regions whose stresses fluctuate independently ("region assumption", compare P9). We redefine viscosity, η, and stress, so that by the term "stress", s, is henceforth meant the shear stress *times* the region volume. Thus, s has dimension energy and is given[2] by (where x_i is the x-coordinate of the i'th atom, $F_{i,y}$ is the y'th component of the force on the i'th particle, and the sum is over all atoms of the region)

$$s \ = \ -\sum_i x_i F_{i,y}\,. \tag{3.32}$$

The FD-theorem states that in a small shear rate "field", $\dot{\gamma}(t)$, the average stress is given[2] by

$$\langle s(t)\rangle_{\dot{\gamma}} \ = \ \beta\int_0^\infty \langle s(0)s(\tau)\rangle_0\,\dot{\gamma}(t-\tau)d\tau\,, \tag{3.33}$$

where the autocorrelation function on the right hand side refers to equilibrium fluctuations.

To solve the problem of how Eq. (3.30) is modified in a shear flow, we refer to the "principle of virtual work".[2,154] If $P(s)$ is the probability distribution, one defines the "dynamical free energy", A, by[2,154]

$$A \ = \ \int_{-\infty}^\infty P(s)\big(F(s)+k_B T\ln[P(s)]\big)\,ds\,. \tag{3.34}$$

Except for a constant, the dynamical free energy is minus the generalized entropy defined for any master equation[65] (here the Smoluchowski equation). The generalized entropy increases monotonically in time until equilibrium is

reached. In the dynamical free energy, there is (as for the ordinary thermo-dynamic free energy) an energy term, $\langle F \rangle$, and an entropy term, $\langle -\ln P \rangle$. The principle of virtual work states that after a "virtual" (i.e., infinitely fast) infinitesimal displacement, $\delta\gamma$, A changes by

$$\delta A \ = \ \langle s \rangle \, \delta\gamma \,. \tag{3.35}$$

This equation states that work is equal to force times displacement.

For a system of interacting particles it is straightforward to show that the principle of virtual work leads to the correct expression for the stress tensor (Eq. (3.32)). Since the actual physical system that lies behind the Langevin equation for the stress fluctuations of one region (Eq. (3.30)) is a system of interacting particles, the principle of virtual work must be obeyed for the generalization of Eq. (3.30) that we are looking for. The main result of P14 is that the principle of virtual work uniquely determines the generalization:

First, it is noted that the shear rate "field" must enter linearly into the generalization of Eq. (3.30); otherwise, the expression for the change in probability during a virtual displacement, δP, depends not only on s but also on the shear rate. Thus, for a so far unknown function, $J(s)$, in a non-zero flow Eq. (3.30) is modified into

$$\dot{s} \ = \ -\mu\frac{dF}{ds} + \dot{\gamma}(t)J(s) + \xi(t) \,. \tag{3.36}$$

The main result of P14 is that the principle of virtual work implies that $J(s)$ must obey

$$\frac{dJ}{ds} \ = \ \beta\frac{dF}{ds}J - \beta s \,. \tag{3.37}$$

This first order differential equation has a unique solution, if it is required that s does not run off to infinity whenever the shear rate is different from zero. The next step in P14 is a consistency check: In the linear limit Eq. (3.36) should imply Eq. (3.33). This is shown to be the case (if this condition were not fulfilled, the whole thing would be meaningless).

Four examples of the formalism are worked out in P14. The first example is the "Gaussian" model, where $F(s) \propto s^2$. It is shown that viscoelasticity in this model is linear at all shear rates. The model has a simple exponential decay of the equilibrium stress autocorrelation function. This result is satisfactory for two reasons: 1. In equilibrium statistical mechanics exact linearity is always linked to an exactly Gaussian probability distribution (i.e., an exactly quadratic free energy); 2. for time-dependent nonlinear phenomena there is a tendency that wider distributions of relaxation times lead to

more severe nonlinearities. The Gaussian model corresponds to the opposite extreme; in this model there is exact linearity and a single relaxation time.

The second example studied in P14 is the "Box" model, where the stress in equilibrium is free to fluctuate without any free energy cost below a certain limit. This model, of course, leads to nonlinearities, since there is a maximum allowed stress independent of the shear rate. The model may be solved analytically for the nonlinear steady state viscosity and for the frequency-dependent viscosity. As shown in Fig. 1 of P14 the results show some resemblance to the Cox-Merz rule.[148]

The third example is a model based on a free energy that is a Cosine Hyperbolic function of the stress. This model was constructed to mimic the Eyring viscosity equation, as well as its generalization to deal with non-steady state stress relaxation[147,149,155]

$$\dot{\gamma} \;=\; A\dot{s} + B\sinh\left(\frac{s}{s_0}\right). \tag{3.38}$$

The Cosine Hyperbolic model is an attempt to incorporate these early ideas into a framework consistent with statistical mechanics. It turns out that Eq. (3.38) is *not* exactly reproduced in the zero noise limit. This is an illustration of the fact[65] that, by adding a noise term to an equation of the form $\dot{s} = f(s)$, if the equation is nonlinear, some of the properties of the equation are lost and the mean-value of s does not have to obey the equation.

The final model that was studied in P14 is that of a Power-law free energy as function of the stress, $F(s) \propto s^n$. For $n = 2$ this is the Gaussian model and for $n \to \infty$ it becomes the Box model. It is shown in P14 that the model makes sense only if $n > 3/2$. For $3/2 < n < 2$ the model exhibits shear-thickening, while for $2 < n$ the model exhibits shear-thinning. The Power-law model leads to an interesting correlation, which may inspire to new ideas about the origin of viscoelasticity. From Eq. (3.36) it is clear that $J(s)$ is nothing but the infinite frequency shear modulus as function of stress:

$$J(s) \;=\; G_\infty(s). \tag{3.39}$$

Since $J(s) \propto s^{2-n}$ in the Power-law model (P14) whenever $3/2 < n < 2$ one has $J(s) \to \infty$ as $|s| \to \infty$, and whenever $2 < n$ one has $J(s) \to 0$ as $|s| \to \infty$. Thus, shear-thickening is linked to $G_\infty(s)$ increasing with increasing s, while shear-thinning is linked to $G_\infty(s)$ decreasing with increasing s.

To investigate whether this result is valid more generally, we note that in the relaxational regime (i.e., when inertial forces are unimportant as is usually the case) any viscoelastic liquid has a stress-dependent characteristic relaxation time, $\tau_0(s)$, that obeys a generalized Maxwell relation: We define

$\tau_0(s)$ from the initial stress decay following the cessation of a steady shear flow with stress, s, according to the expression

$$\frac{ds}{dt}(t = 0^+) \;\; = \;\; -\frac{s}{\tau_0(s)}\,. \tag{3.40}$$

Because the flow is in the relaxational regime, instead of having a constant shear rate, $\dot\gamma$, the flow may be regarded as generated by many sudden very small infinitely fast displacements:

$$\dot\gamma(t) \;\; = \;\; \sum_{j=-\infty}^{\infty} \delta\gamma\,\delta(t - j\delta t)\,, \tag{3.41}$$

where $\delta\gamma/\delta t = \dot\gamma$. Immediately after one sudden displacement, the stress decays an amount δs during the time that passes until the next sudden displacement δt later, where the stress is increased the same amount; thus, $\delta s = G_\infty(s)\delta\gamma$. By combining these equations one finds that, since $\eta(s) = s/\dot\gamma$, $\tau_0(s)$ is given by the generalized Maxwell expression,

$$\tau_0(s) \;\; = \;\; \frac{s}{\delta s}\delta t \;\; = \;\; \frac{\eta(s)}{G_\infty(s)}\,. \tag{3.42}$$

Experimentally, one always finds[145,153] that $\tau_0(s) \to 0$ as $s \to \infty$: In a nonlinear flow, relaxation times larger than the inverse shear rate are removed from the relaxation time spectrum (this is the idea behind Tanner's network rupture hypotheses, and is also essentially what the constitutive relation Eq. (3.26) expresses). Thus, if $G_\infty(s) \to 0$ as $s \to \infty$, from Eq. (3.42) we expect shear thinning, as found above for the power-law model whenever $n > 2$. In general, however, the opposite implication is not valid.

In passing we note that the above way of regarding a flow as composed of sudden small fast displacements leads to the following expression for the initial shear decay upon cessation of an arbitrary flow at $t = t_0$[156] (where $\dot s$ is the time derivative of the stress of the uninterrupted flow),

$$\frac{ds}{dt}(t = t_0^+) \;\; = \;\; \dot s(t_0) \;\; + \;\; G_\infty(s)\dot\gamma(t_0)\,. \tag{3.43}$$

Finally, it should be noted that the formalism developed in P14 may be generalized. The stress is the transverse momentum current, and the formalism may be generalized to other thermodynamic "currents". In "extended irreversible thermodynamics"[157] one considers thermodynamic currents as independent degrees of freedom. The formalism developed in P14 may be regarded as a statistical mechanical counterpart of extended irreversible thermodynamics.

Outlook

P14 solves the theoretical problem of how to extend the Langevin equation for stress fluctuations to non-zero flows. The extension is unique and from a theoretical point of view there is nothing more to say. Things are worse when it comes to comparison to experiment: At least for the models studied in P14 there is only a very narrow distribution of relaxation times. These models are therefore unrealistic. Either one should look for other choices of $F(s)$, for instance involving energy barriers to be overcome, or a more general approach should be taken. One such approach could be to formulate a field theory for viscous liquids, where the field is the stress tensor (in such a model the region assumption is avoided). For instance, one could postulate that the free energy density, $\mathcal{F}$, is given by an expression of the form (where $I_n = \mathrm{Tr}(\sigma^n)$ for $n = 1, 2, 3$ and h_n is a possibly random function)

$$\mathcal{F} = (\partial_i \sigma_{ij})^2 + h_1(I_1) + h_2(I_2) + h_3(I_3). \qquad (3.44)$$

The first term, corresponding to the "kinetic energy" term of a field theory, ensures that states with mechanical equilibrium have minimum free energy. In the standard way the free energy density of Eq. (3.44) gives rise to a Langevin dynamics of the stress tensor at each point in space which, incidently, allows for a study of spatial stress correlations, reflected in the k-vector dependence of the frequency-dependent viscosity.

3.6 Paper 15: Approximation for Autocorrelation Functions

As discussed in Chapter 2, glass-forming liquids are characterized by a strongly temperature-dependent average relaxation time. This quantity may be deduced from measurements of a number of different physical quantities that have roughly the same average relaxation time. But one may very well ask:

Problem

1. Why do different physical quantities in viscous liquids have roughly equal average relaxation times?

2. Is it possible to develop an approximation for the calculation of time autocorrelation functions that rationalizes the insight gained from answering question 1?

Solution

The average relaxation time of a physical quantity, A, is usually determined from the linear response in the frequency domain, e.g., as the inverse of the loss peak frequency. If the response function is referred to as $\chi(\omega)$, the FD-theorem states that $\chi(\omega)$ is the Laplace transform of the equilibrium time autocorrelation function of A (below $s = i\omega$ is the imaginary "Laplace" frequency and it is assumed that $\langle A \rangle = 0$):

$$\chi(\omega) = \frac{1}{k_B T} \int_0^\infty \langle A(0)A(t) \rangle \, e^{-i\omega t} dt. \tag{3.45}$$

For instance, if the physical quantity A is the dipole moment, the average relaxation time is measured via the frequency-dependent dielectric relaxation; similarly, if A is the shear stress, $\chi(\omega)$ is the frequency-dependent shear viscosity. A final example: The average relaxation time of the energy is measured via the frequency-dependent specific heat.

Assuming that A is independent of momenta and thus a function only of the microscopic configurational degrees of freedom, $X = (X_1, ... X_n)$, the autocorrelation function $\langle A(0)A(t) \rangle$ is given by

$$\langle A(0)A(t) \rangle = \int dX dX' \, A(X)A(X')P(X, X'; t), \tag{3.46}$$

where $P(X, X'; t)$ is the joint probability of having "initial" point X and "final" point X' a time t later on the path in configuration space. If $U(X)$ is the potential energy, $Z(\beta)$ is the partition function for the potential energy, and $G(X \to X'; t)$ is the Green's function, $P(X, X'; t)$ is given by

$$P(X, X'; t) = \frac{e^{-\beta U(X)}}{Z(\beta)} \, G(X \to X'; t). \tag{3.47}$$

According to Eq. (3.46), the autocorrelation function becomes small whenever the initial point X and final point X' most probably are so far apart that $A(X)$ and $A(X')$ are almost uncorrelated. It is reasonable to assume, that this is the case whenever the distance between X and X' is larger than about one Ångstrom per molecular degree of freedom. This assumption immediately answers question 1 on the preceding page, since the average relaxation time in this picture is the time it takes for the molecules to move a certain distance away from each other which is, of course, independent of the physical quantity, A.

We now turn to the problem of developing an approximation for the evaluation of $\langle A(0)A(t) \rangle$ based on the above physical picture. In the course of time, the two points X and X' move further and further away from each

other. The correlation is gradually lost for any physical quantity and the time autocorrelation function decays to zero. The idea is now simply to estimate $\langle A(0)A(t)\rangle$ as the "spatial" correlation of A in configuration space, taken at the typical distance between X and X', $\sqrt{\langle \Delta X^2(t)\rangle}$, where the mean-square displacement in time t, $\langle \Delta X^2(t)\rangle$, is defined by

$$\left\langle \Delta X^2(t)\right\rangle \;=\; \left\langle (X - X')^2\right\rangle \;\equiv\; \left\langle \sum_{i=1}^{n}(X_i - X'_i)^2\right\rangle . \qquad (3.48)$$

For a given time, t, this distance scales proportionally to the number of degrees of freedom, n (this is not a problem, however). The important point is that the relative distance fluctuations are small when n is large.

The above physical picture indicates that non-Debye (i.e., non-exponential) relaxation may have two causes. To see this, note first that Debye relaxation corresponds to ordinary diffusion with a linear mean-square time-dependence in configuration space in conjunction with a Gaussian distance decay of the "spatial" correlation function. Non-Debye relaxation may be caused either by the "early" nonlinear time-dependence of the mean-square displacement (compare Eq. (1.43)), or from a non-Gaussian distance decay at long times corresponding to linear diffusion. Interestingly, a simple exponential distance decay of the "spatial" correlation function in the long-time linear diffusion regime gives rise to a stretched exponential time autocorrelation function with exponent 0.5. This function gives a good fit to many data.[158]

The conversion of the above idea into a practical calculational scheme is described in P15. The naive approach would be to estimate $\langle A(0)A(t)\rangle$ by taking an average over configurational space where the "beginning point", X, and the "end point", X', are both weighted by their canonical probabilities, $\propto \exp[-\beta U]$. However, this does not work for the following reason. At short times X and X' are close and weighting each point by a Boltzmann factor gives the wrong limit: $\lim_{t\to 0}\langle A(0)A(t)\rangle \neq \langle A^2\rangle$. The problem, of course, is that the energies of X and X' are correlated when the points are close. One might think that this problem is solved by using a $\exp[-(\beta/2)U]$ factor for each of the points X and X'. Then, however, the long times behavior is wrong, because in this limit each of the two points *should* be weighted by a Boltzmann factor. This problem delayed further progress by two years, before a solution was found. The solution is to utilize the general ideas of statistical mechanics in the following way:

Switching from the microcanonical ensemble to the canonical ensemble, it is shown in P15 that the time autocorrelation function may be estimated from the multidimensional integral

$$\langle A(0)A(t)\rangle \ = \ \int \frac{dXdX'}{D(a,b)}A(X)A(X')e^{-a(X-X')^2-b[U(X)+U(X')]} , \qquad (3.49)$$

where $D(a,b)$ is the "double" partition function defined as follows:

$$D(a,b) \ = \ \int dXdX'e^{-a(X-X')^2-b[U(X)+U(X')]} . \qquad (3.50)$$

Short times correspond to large a and long times to small a. The two Lagrangian multipliers a and b are determined in the following way. First, $b = b(a)$ is found from the condition that the average potential energy of initial point plus that of the final point is equal to twice the canonical average potential energy. With the boundary condition $b(0) = \beta$ (from requiring a canonical weighting of X and X' in the long time limit) this leads (P15) to the following ordinary differential equation for $b(a)$,

$$\frac{d}{da}\frac{\partial \ln D}{\partial b} \ = \ 0 . \qquad (3.51)$$

Once, $b(a)$ has been determined, $a = a(t)$ is determined from $\langle \Delta X^2(t)\rangle$ (which is assumed known) via the requirement that the double canonical average distance between initial and final point is correct, leading (P15) to

$$-\frac{\partial \ln D}{\partial a} \ = \ \langle \Delta X^2(t)\rangle . \qquad (3.52)$$

Two different dynamics may reasonably be assumed. One is Newton's classical equations of motion. The other is Langevin dynamics for the configurational degrees of freedom. As shown in P15, at short times both dynamics are explicitly consistent with the formalism proposed; however, they give different predictions for the function $a(t)$ (due to the importance/non-importance of inertial effects at short times).

We end by giving 5 remarks.

1. The use of Langevin dynamics for systems with relaxation times many orders of magnitude longer than 1 ps is motivated by the expectation that at these long times Langevin dynamics lead to more or less the same predictions as Newtonian dynamics (thus, the use of Langevin equations is standard in polymer physics[2]). The proposed approximation for $\langle A(0)A(t)\rangle$ implies that, if the two dynamics lead to the same prediction for $\langle \Delta X^2(t)\rangle$, *all* time autocorrelation function are identical for the two dynamics.

2. An interesting property of Langevin dynamics is that in this dynamics, the calculation of $\langle \Delta X^2(t)\rangle$ (and thus of $a(t)$) is reduced to a double canonical average (P15). This is because the second time derivative of the

mean-square displacement is proportional to the force time autocorrelation function, leading (P15) to the following equation for $a(t)$

$$\left(\frac{d^2}{dt^2} + 8\mu^2\frac{a^2}{b^2}\right)\frac{\partial \ln D}{\partial a} = 0. \tag{3.53}$$

3. In P15 the formalism was checked against computer simulations for a Langevin particle in a one-dimensional double-well potential, where, if the coordinate is denoted by X, the time autocorrelation function of X^3 was calculated by solving the Smoluchowski equation numerically, as well as according to the above approximation. Figure 2 of P15 shows a good agreement between approximation and exact calculation.

4. The validity of the time-temperature superposition principle (TTSP) in glass-forming liquids - stating that at different temperatures the time autocorrelation functions is just scaled by a temperature-dependent factor - is a matter of debate. Traditionally, the TTSP was often assumed to be valid without real justification, in order to be able to evaluate the response over many decades in time or frequency from measurements covering only few decades at each temperature. However, the TTSP cannot be assumed without further justification. There are many examples of breakdown of the TTSP and today the TTSP is not taken for granted; it is recognized that the TTSP must be checked carefully in each case. On the other hand, if the TTSP is indeed obeyed, this must provide an important clue to the dynamics. Recently, Niels Boye Olsen and Tage Christensen in their measurements of frequency-dependent shear modula observed that the TTSP is obeyed with great accuracy for the alpha relaxation in a number of molecular liquids. We do not understand why. However, the above proposed formalism gives a natural framework for understanding why the TTSP may be valid. The mean-square displacement acts as a "molecular clock", determining the time-scale. If, over a range of temperatures, the function $b(a)$ is the same and the mean-square displacement has the same time-dependence, just scaled, the time autocorrelation function of A is the same. A simple example of this is if the mean-square displacement is linear in time (this is probably unrealistic, but a good illustration of the point); another more realistic example is the case where the mean-square displacement as function of time is given by the universal expression calculated in P6.

5. P15 was submitted to Phys. Rev. B in the spring 1994, but the paper was not accepted for publication. The referee suggested that the approximation should be tested on more complex systems, because "the fluctuations in the Langevin model are Gaussian". While more extensive testing is definitely a good idea, there has not yet been time to do this and no second

version of the paper has been written yet. However, it should be noted that while the *noise* in any Langevin model is Gaussian, the fluctuations of $X(t)$ itself are not Gaussian in the model studied in Fig. 2. More usefully, the referee pointed out that Haan in 1979[159] (working in real space) proposed a related idea. Haan suggested that, by knowing the function defined by $C(|\mathbf{r} - \mathbf{r}'|) = \langle A(\mathbf{r})A(\mathbf{r}')\rangle$, one can approximate the time autocorrelation function from $\langle A(0)A(t)\rangle = C(\langle \Delta \mathbf{r}^2(t)\rangle^{1/2})$. Haan's work is based on the same idea as above, but valid only if A is a function of one spatial coordinate. The problem of weighting initial and final point was not discussed by him.

Outlook

An approximate scheme is only useful if it has been shown to work reasonably well. Most approximations used in physics are more or less uncontrolled in the sense that one cannot estimate the usefulness of the approximation *a priori*; the approximations are justified *a posteriori*. Today, computer simulations make testing possible in most cases. Further simulations should be undertaken to investigate whether the approximation proposed in P15 is reliable.

3.7   Discussion of Paper 11-15

Chapter 3 deals with extensions and elaborations of linear response theory. Due to the non-existence of a general nonlinear response theory, the work summarized in Chapter 3 is more fragmented than that of Chapter 1 and 2. Clearly, much remains to be done in this field, in particular in respect to testing the approximations that have been proposed. It is hoped that eventually the insights gained lead to, e.g., useful constitutive relations for viscoelastic liquids or for the thermal history dependence of structural relaxations in glass-forming liquids and glasses.

REFERENCES

[1] P. Voetmann Christiansen, "Dynamik og diagrammer. Introduktion til energi-bond-graph formalismen" (IMFUFA tekst nr 8, Roskilde, 1978) and "Semiotik og systemegenskaber" (IMFUFA tekst nr 22, Roskilde, 1979).

[2] M. Doi and S. F. Edwards, *The Theory of Polymer Dynamics* (Clarendon, Oxford, 1986).

[3] H. Nyquist, Phys. Rev. **32**, 110 (1928).

[4] R. Kubo, J. Phys. Soc. Japan **12**, 570 (1957).

[5] H. Scher and M. Lax, Phys. Rev. B **7**, 4491 and 4502 (1973).

[6] J. O. Isard, J. Non-Cryst. Solids **4**, 357 (1970).

[7] A. E. Owen, J. Non-Cryst. Solids **25**, 372 (1977).

[8] A. K. Jonscher, Nature **267**, 673 (1977).

[9] A. Mansingh, Bull. Mater. Sci. (India) **2**, 325 (1980).

[10] S. R. Elliott, Solid State Ionics **70/71**, 27 (1994).

[11] J. M. Stevels, in *Handbuch der Physik*, ed. S. Flügge (Springer, Berlin, 1957), Vol. 20, p. 350.

[12] A. E. Owen, in *Progress in Ceramic Science*, ed. J. E. Burke (Macmillan, New York, 1963), Vol.3, p. 77.

[13] J. C. Dyre, J. Non-Cryst. Solids **88**, 271 (1986).

[14] J. L. Barton, Verres Réfr. **20**, 328 (1966).

[15] T. Nakajima, in *1971 Annual Report, Conference on Electric Insulation and Dielectric Phenomena* (National Academy of Sciences, Washington, DC, 1972), p. 168.

[16] H. Namikawa, J. Non-Cryst. Solids **18**, 173 (1975).

[17] M. Pollak and T. H. Geballe, Phys. Rev. **122**, 1742 (1961).

[18] H. Böttger and V. V. Bryksin, *Hopping Conduction in Solids* (Akademie-Verlag, Berlin, 1985).

[19] J. W. Haus and K. W. Kehr, Phys. Rep. **195**, 263 (1987).

[20] J.-P. Bouchaud and A. Georges, Phys. Rep. **195**, 127 (1990).

[21] J. C. Dyre, Phys. Lett. A **108**, 457 (1985).

[22] F. Yonezawa, in *The Structure and Properties of Matter*, ed. T. Matsubara (Springer, Berlin, 1982), p. 383.

[23] S. Summerfield, Philos. Mag. B **52**, 9 (1985).

[24] P. B. Macedo, C. T. Moynihan, and R. Bose, Phys. Chem. Glasses **13**, 171 (1972).

[25] M. Pollak and G. E. Pike, Phys. Rev. Lett. **28**, 1449 (1972).

[26] N. Goldenfeld, *Lectures on Phase Transitions and the Renormalization Group* (Addison-Wesley, New York, 1992).

[27] B. Widom, J. Chem. Phys. **43**, 3892 and 3898 (1965).

[28] K. L. Ngai and C. T. White, Phys. Rev. B **20**, 2475 (1979).

[29] R. M. Hill and A. K. Jonscher, Cont. Phys. **24**, 75 (1983).

[30] G. A. Niklasson, J. Appl. Phys. **62**, R1 (1987).

[31] S. Havlin and D. Ben-Avraham, Adv. Phys. **36**, 695 (1988).

[32] J. P. Clerc, G. Giraud, and J. M. Langer, Adv. Phys. **39**, 191 (1990).

[33] K. L. Ngai, Solid State Ionics **5**, 27 (1982).

[34] C. T. Moynihan, J. Non-Cryst. Solids **172-174**, 1395 (1994).

[35] H. K. Patel and S. W. Martin, Phys. Rev. B **45**, 10292 (1992).

[36] D. P. Almond and A. R. West, Solid State Ionics **11**, 57 (1983).

[37] S. R. Elliott, J. Non-Cryst. Solids **170**, 97 (1994).

[38] J. K. E. Tunaley, Phys. Rev. Lett. **33**, 1037 (1974).

[39] T. Odagaki and M. Lax, Phys. Rev. B **24**, 5284 (1981).

[40] J. M. Hyde, M. Tomozawa, and M. Yoshiyagawa, Phys. Chem. Glasses **28**, 174 (1987).

[41] J. R. Macdonald, J. Chem. Phys. **61**, 3977 (1974).

[42] C. A. Angell, at *Workshop on non-equilibrium phenomena in super-cooled fluids, glasses and amorphous materials* (Pisa, 25-29 September, 1995).

[43] I. Svare, F. Borsa, and D. R. Torgeson, Phys. Rev. B **48**, 9336 (1993).

[44] P. Maass, J. Petersen, A. Bunde, W. Dieterich, and H. E. Roman, Phys. Rev. Lett. **66**, 52 (1991).

[45] S. Summerfield, talk given at the *Second Hopping Symposium* (Trieste, August, 1985).

[46] J. O. Isard, Philos. Mag. **62**, 139 (1990).

[47] L. A. Dissado and R. M. Hill, Phys. Rev. B **37**, 3434 (1988).

[48] I. M. Hodge, M. D. Ingram, and A. R. West, J. Electroanal. Chem. **74**, 125 (1976).

[49] J. R. Macdonald, J. Appl. Phys. **62**, R51 (1987).

[50] R. Stumpe, Phys. Status Solidi A **88**, 315 (1985).

[51] R. Blender and W. Dieterich, J. Phys. C **20**, 6113 (1987).

[52] I. I. Fishchuk, Phys. Status Solidi A **93**, 675 (1986).

[53] D. A. G. Brüggeman, Ann. Physik **24**, 636 (1935).

[54] J. R. Reitz, F. J. Milford, and R. W. Christy, *Foundations of Electromagnetic Theory*, 4th Ed. (Addison-Wesley, New York, 1993).

[55] N. M. Morris, *Electrical Circuit Analysis and Design* (Macmillan, London, 1993).

[56] D. J. Frank and C. J. Lobb, Phys. Rev. B **37**, 302 (1988).

[57] R. Fogelholm, J. Phys. C **13**, L571 (1980).

[58] Thomas Riedel, *System i Rodet? - Universalitet i den frekvens-afhængige ledningsevne af faste uordnede stoffer ved lave temperaturer*, master's thesis (Roskilde University, 1994).

[59] T. Riedel and J. C. Dyre, J. Non-Cryst. Solids **172-174**, 1419 (1994).

[60] V. Ambegaokar, B. I. Halperin, and J. S. Langer, Phys. Rev. B **4**, 2612 (1971).

[61] B. I. Shklovskii and A. L. Efros, Sov. Phys. JETP **33**, 468 (1971).

[62] S. Tyc and B. I. Halperin, Phys. Rev. B **39**, 877 (1989).

[63] M. B. Isichenko, Rev. Mod. Phys. **64**, 961 (1992).

[64] V. V. Bryksin, Sov. Phys. Solid State **22**, 1421 (1980).

[65] N. G. van Kampen, *Stochastic Processes in Physics and Chemistry* (North-Holland, Amsterdam, 1981).

[66] M. Pollak, in *Proceedings of the Fifth International Conference on Amorphous and Liquid Semiconductors*, Garmisch-Partenkirchen, 1973 (Taylor and Francis, London, 1974), Vol. 1, p. 127.

[67] T. Schrøder, *Den symmetriske hop-model for AC-ledning i uordnede faste stoffer*, master's thesis (Roskilde University, 1996).

[68] A. Hunt, J. Non-Cryst. Solids **183**, 109 (1995).

[69] N. F. Mott and E. A. Davis, *Electronic Processes in Non-Crystalline Materials* (Oxford University Press, Oxford, 1979).

[70] W. Kauzmann, Chem. Rev. **43**, 219 (1948).

[71] G. Harrison, *The Dynamic Properties of Supercooled Liquids* (Academic Press, New York, 1976).

[72] S. Brawer, *Relaxation in Viscous Liquids and Glasses* (American Ceramic Society, Columbus, Ohio, 1985).

[73] J. Jäckle, Rep. Progr. Phys. **49**, 171 (1986).

[74] C. A. Angell, J. Phys. Chem. Solids **49**, 863 (1988).

[75] G. W. Scherer, J. Non-Cryst. Solids **123**, 75 (1990).

[76] C. A. Angell, J. Non-Cryst. Solids **131-133**, 13 (1991).

[77] A. Hunt, J. Non-Cryst. Solids **160**, 183 (1993).

[78] I. M. Hodge, J. Non-Cryst. Solids **169**, 211 (1994).

[79] C. A. Angell, Science **267**, 1924 (1995).

[80] U. Mohanty, Adv. Chem. Phys. **89**, 89 (1995).

[81] J. H. Gibbs and E. A. DiMarzio, J. Chem. Phys. **28**, 373 (1958).

[82] G. Adam and J. H. Gibbs, J. Chem. Phys. **43**, 139 (1965).

[83] S. P. Das and G. F. Mazenko, Phys. Rev. A **34**, 2265 (1986).

[84] W. Götze and L. Sjögren, Rep. Progr. Phys. **55**, 241 (1992).

[85] C. A. Angell, in *Relaxations in Complex Systems*, Eds. K. L. Ngai and G. B. Wright (U. S. Government Printing Office, Washington, DC, 1985), p. 3.

[86] G. S. Grest and M. H. Cohen, Adv. Chem. Phys. **48**, 455 (1981).

[87] M. Goldstein, J. Chem. Phys. **51**, 3728 (1969).

[88] S. A. Brawer, J. Chem. Phys. **81**, 954 (1984).

[89] W. Kauzmann, Rev. Mod. Phys. **14**, 12 (1942).

[90] T. Alfrey, *Mechanical Properties of High Polymers* (Interscience Publishers, New York, 1948).

[91] M. Goldstein, Faraday Symp. Chem. Soc. **6**, 7 (1972).

[92] G. Williams, in: *Dielectric and Related Molecular Processes, Specialist Periodical Report, Vol. 2*, Ed. M. Davies (Chem. Soc., London, 1975), p. 151.

[93] E. Donth, *Glasübergang* (Akademie-Verlag, Berlin, 1981).

[94] E. Donth, J. Non-Cryst. Solids **53**, 325 (1982).

[95] F. H. Stillinger, J. Chem. Phys. **89**, 6461 (1988).

[96] R. V. Chamberlin, Phys. Rev. B **48**, 15638 (1993).

[97] V. I. Arkhipov, M. S. Iovu, A. I. Rudenko, and S. D. Shutov, Phys. Status Solidi (a) **54**, 67 (1979).

[98] J. Orenstein, M. A. Kastner, and V. Vaninov, Philos. Mag. **46**, 23 (1982).

[99] J. M. Hvam and M. H. Brodsky, Phys. Rev. Lett. **46**, 371 (1981).

[100] J. Orenstein and M. Kastner, Phys. Rev. Lett. **46**, 1421 (1981).

[101] J. C. Dyre, J. Phys. C **19**, 5655 (1986).

[102] D. J. Dunstan and F. Boulitrop, Phys. Rev. B **30**, 5945 (1984).

[103] N. Maloufi, A. Audouard, M. Piecuch, and G. Marchal, Phys. Rev. Lett. **56**, 2307 (1986).

[104] J. C. Dyre, Key Engineering Materials **13-15**, 501 (1987).

[105] Johannes Nielsen and Klaus Dahl Jensen, *Masterlignings-modeller af glasovergangen*, master's thesis (IMFUFA tekst nr 303, Roskilde, 1995).

[106] J. C. Dyre, *Master Equation Approach to Viscous Liquids and the Glass Transition* (IMFUFA tekst nr 154, Roskilde, 1988).

[107] V. I. Arkhipov and H. Bässler, Phys. Rev. E **52**, 1227 (1995).

[108] E. I. Shakhnovich and A. M. Gutin, Europhys. Lett. **9**, 569 (1989).

[109] H. Bässler, Phys. Rev. Lett. **58**, 767 (1987).

[110] J. H. Simmons and P. B. Macedo, J. Res. Nat. Bureau Stand. **75A**, 175 (1971).

[111] H. Tweer, J. H. Simmons, and P. B. Macedo, J. Chem. Phys. **54**, 1952 (1971).

[112] F. H. Stillinger, Phys. Rev. B **41**, 2409 (1990).

[113] T. Christensen and N. B. Olsen, Rev. Sci. Instrum. **66**, 5019 (1995).

[114] D. Chandler, J. D. Weeks, and H. C. Andersen, Science **220**, 787 (1983).

[115] L. D. Landau and E. M. Lifshitz, *Theory of Elasticity* (Pergamon Press, Oxford, 1970).

[116] A. J. Barlow, J. Lamb, A. J. Matheson, P. R. K. L. Padmini, and J. Richter, Proc. Roy. Soc. **A 298**, 467 (1967).

[117] U. T. Höchli, K. Knorr, and A. Loidl, Adv. Phys. **39**, 405 (1990).

[118] A. R. Ubbelohde, *Melting and Crystal Structure* (Oxford, Clarendon, 1965).

[119] S. V. Nemilov, Fiz. Khim. Stekla **2**, 193 (1976) [Sov. J. Glass Phys. Chem. **2**, 187 (1976)].

[120] S. V. Nemilov, Fiz. Khim. Stekla **4**, 129 (1978) [Sov. J. Glass Phys. Chem. **4**, 113 (1978)].

[121] L. Torell, J. Chem. Phys. **76**, 3467 (1982).

[122] T. A. Vilgis, Phys. Rev. B **47**, 2882 (1993).

[123] R. Böhmer, J. Non-Cryst. Solids **172-174**, 628 (1994).

[124] G. P. Johari, Ann. N. Y. Acad. Sci. **279**, 117 (1976).

[125] R. L. Stratonivich, Zh. Eksp. Teor. Fiz. **58**, 1612 (1970) [Sov. Phys.-JETP **31**, 864 (1970)].

[126] G. N. Bochkov and Yu. E. Kuzovlev, Physica **106A**, 443 and 480 (1981).

[127] W. W. Graessley, Adv. Polym. Sci **16**, 1 (1974).

[128] J. B. Johnson, Phys. Rev. **26**, 71 (1925).

[129] H. B. Callen and T. A. Welton, Phys. Rev. **83**, 34 (1951).

[130] R. F. Voss and J. Clarke, Phys. Rev. B **13**, 556 (1976).

[131] M. A. Mikulinsky, Phys. Lett. A **66**, 440 (1978).

[132] A.-M. S. Tremblay and M. Nelkin, Phys. Rev. B **24**, 2551 (1981).

[133] Yu. E. Kuzovlev and G. N. Bochkov, Radiophys. Quantum Electron. **26**, 228 (1983).

[134] T. M. Niewenhuizen and M. H. Ernst, J. Stat. Phys. **41**, 773 (1985).

[135] W. Bernard and H. B. Callen, Rev. Mod. Phys. **31**, 1017 (1959).

[136] D. J. Evans and G. P. Morriss, *Statistical Mechanics of Nonequilibrium Liquids* (Academic, London, 1990).

[137] D. J. Evans and G. P. Morriss, Comp. Phys. Rep. **1**, 300 (1984).

[138] E. T. Jaynes, Phys. Rev. **106**, 620 (1957); **108**, 171 (1957).

[139] *The Maximum Entropy Formalism*, edited by R. Levine and M. Tribus (MIT, Cambridge, MA, 1979).

[140] R. L. Stratonovich, Vestn. Mosk. Univ. Fiz. Astronomiya **5**, 16 (1962) [not available in English].

[141] R. L. Peterson, Rev. Mod. Phys. **39**, 69 (1967).

[142] L. Onsager and S. Machlup, Phys. Rev. **91**, 1505 (1953).

[143] H. Furukawa, Prog. Theor. Phys. **54**, 370 (1975).

[144] J. C. Dyre, *Five Requirements for an Approximate Nonlinear Response Theory* (IMFUFA tekst nr 190, Roskilde, 1990).

[145] R. B. Bird, R. C. Armstrong, and O. Hassager, *Dynamics of Polymeric Liquids*, 2nd ed. (Wiley, New York, 1987).

[146] J. D. Ferry, *Viscoelastic Properties of Polymers*, 3rd ed. (Wiley, New York, 1981).

[147] A. Tobolsky and H. Eyring, J. Chem. Phys. **11**, 125 (1942).

[148] W. P. Cox and E. H. Merz, J. Polym. Sci. **28**, 619 (1958).

[149] J. F. Kincaid, H. Eyring, and A. E. Stearn, Chem. Rev. **28**, 301 (1941).

[150] M. H. Wagner, Rheol. Acta **18**, 33 (1979).

[151] M. H. Wagner and S. E. Stephenson, J. Rheol. **23**, 489 (1979).

[152] XIth International Congress on Rheology (Brussels, 17-21 August, 1992).

[153] R. I. Tanner, AIChE. J. **15**, 177 (1969).

[154] M. Doi, J. Chem. Phys. **79**, 5080 (1983).

[155] R. D. Andrews, N. Hofman-Bang, and A. V. Tobolsky, J. Chem. Phys. **13**, 3 (1948).

[156] J. C. Dyre, poster presented at the XIth International Congress on Rheology (Brussels, 17-21 August, 1992).

[157] D. Jou, J. Casas-Vázquez, and G. Lebon, Rep. Progr. Phys. **51**, 1105 (1988).

[158] J. C. Phillips, Rep. Prog. Phys. **59**, 1133 (1996).

[159] S. W. Haan, Phys. Rev. A **20**, 2516 (1979).

PUBLICATIONS

The 15 publications of the thesis are reprinted below with permission from the publishers.

Paper 1 *The Random Free-Energy Barrier Model for AC Conduction in Disordered Solids (1988).*

Paper 2 *Some Remarks on AC Conduction in Disordered Solids (1991).*

Paper 3 *Universal AC Conductivity of Nonmetallic Disordered Solids at Low Temperatures (1993).*

Paper 4 *Universal Low-Temperature AC Conductivity of Macroscopically Disordered Nonmetals (1993).*

Paper 5 *Studies of AC Hopping Conduction at Low Temperatures (1994).*

Paper 6 *Universal Time Dependence of the Mean-Square Displacement in Extremely Rugged Energy Landscapes with Equal Minima (1995).*

Paper 7 *Effective One-Dimensionality of Universal AC Hopping Conduction in the Extreme Disorder Limit (1996).*

Paper 8 *Master-Equation Approach to the Glass Transition (1987).*

Paper 9 *Energy Master Equation: A Low-Temperature Approximation to Bässler's Random-Walk Model (1995).*

Paper 10 *Local Elastic Expansion Model for Viscous-Flow Activation Energies of Glass-Forming Molecular Liquids (1996).*

Paper 11 *Unified Formalism for Excess Current Noise in Random-Walk Models (1988).*

Paper 12 *Maximum Entropy Ansatz for Nonlinear Response Theory (1989).*

Paper 13 *A 'Zero-Parameter' Constitutive Relation for Pure Shear Viscoelasticity (1990).*

Paper 14 *Langevin Models for Shear-Stress Fluctuations in Flows of Viscoelastic Liquids (1993).*

Paper 15 *A Statistical Mechanical Approximation for the Calculation of Time Autocorrelation Functions (1994).*

The random free-energy barrier model for ac conduction in disordered solids

Jeppe C. Dyre

IMFUFA, Roskilde Universitetscenter, Postbox 260, DK-4000 Roskilde, Denmark

A brief review of the history of ac ionic and electronic conduction in disordered solids is given, followed by a detailed discussion of the simplest possible realistic model: the random free-energy barrier model. This model assumes conduction takes place by hopping, where the hopping charge carriers are subject to spatially randomly varying energy barriers. The model is solved in the continuous time random walk and in the effective medium approximation, and it is shown that the two solutions are almost indistinguishable. In the random free-energy barrier model, the frequency-dependent conductivity is completely determined by the dc conductivity and the dielectric loss strength. The model correctly predicts all qualitative features of ac conduction in disordered solids, and a comparison to experiment on a large number of solids shows that the model is also quantitatively satisfactory.

I. INTRODUCTION

One of the most characteristic properties of electrical conduction in disordered solids is a strong dispersion of the conductivity. At low frequencies one observes a constant conductivity while at higher frequencies the conductivity becomes strongly frequency dependent, varying approximately as a power of the frequency. The increase in conductivity usually continues up to phonon frequencies. This behavior is seen in a wide variety of nonmetallic disordered solids and has been studied extensively during the last 30 years. The classes of disordered solids investigated include amorphous semiconductors,[1-5,75] ionic conductive glasses,[6-9] ionic or electronic conducting polymers,[4,10,11] organic semiconductors,[12] nonstoichiometric or highly defective crystals,[13] or doped semiconductor single crystals at helium temperatures.[14] Even highly viscous liquids behave as typical disordered solids as regards ac ionic conductivity.

All disordered solids show similar behavior with respect to their ac properties. This is true not only for the frequency dependence of the conductivity but also for the temperature dependence. Here one observes a strongly temperature-dependent (usually Arrhenius) dc conductivity, while the ac conductivity depends much less on temperature and becomes almost temperature independent as $T \rightarrow 0$. This uniform behavior of $\sigma(\omega, T)$ for quite different solids has been pointed out a number of years ago,[2,3,5,15] but is still not generally appreciated. And indeed, the fact that ionic and electronic conducting solids show similar behavior is quite surprising. Apparently, it means that we cannot expect to learn much about details of the conduction mechanism from measuring the frequency or temperature dependence of the conductivity.

As witnessed by the large number of publications and the continued interest in the field, ac conduction in disordered solids is a subject of interest on its own. More often, however, the focus is on dc transport only. Even then, a proper understanding of ac conduction is important in order to arrive at a correct picture of the dc transport. This is because dc and ac conduction are both due to the same mechanism, as shown in Sec. II. In particular, this implies that a new interpretation of the dc conductivity activation energy is necessary. The dc conductivity activation energy is, it turns out, the *maximum* of a whole range of activation energies needed to account for the frequency dispersion (Sec. IV). We believe this fact is important for a genuine understanding of dc transport in disordered solids. It implies that most present models for dc conduction, thermopower, Hall effect, etc., in disordered solids, are probably too simple to be realistic.

The simplest and indeed the most common explanation for a conductivity which increases with frequency is the existence of one or the other kind of inhomogeneities in the solid. This assumption is consistent with the fact that a strong frequency dispersion of the conductivity is observed only in disordered solids. The inhomogeneities may be of a microscopic or a more macroscopic nature, a question which is not yet settled. In this paper, hopping models will be discussed. In hopping models one makes the assumption of inhomogeneity on the atomic scale by assuming randomly varying jump frequencies for the charge carriers. It is the purpose of the paper to show that a simple hopping model is able to give a qualitatively correct picture of ac conduction in disordered solids. By taking some care in deriving the model, it is hoped that the paper may contribute to make hopping models more popular among experimentalists. The paper, which summarizes, clarifies, and extends recent work by the author,[16-19] has the following outline: Sec. II briefly reviews the history of ac conduction in disordered solids. In Sec. III a general discussion of hopping models is given. It is argued that in order to arrive at realistic hopping models, any effect of a cutoff at large jump frequencies should be eliminated. In Sec. IV we discuss what is probably the simplest possible model consistent with observations, a model based on the assumption of randomly varying free-energy barriers for jumps. The model is solved in the continuous time random walk approximation and in the effective-medium approximation, and it is shown that the two solutions are almost identical. Also, the model is compared to experiments on a number of quite different disordered solids. Finally, in Sec. V a discussion is given.

II. ac CONDUCTION IN DISORDERED SOLIDS: A BRIEF REVIEW

Frequency-dependent conduction in disordered solids is a very broad field and probably nobody has a full general view of it. Different schools have emerged within the field. Though using different terminology, these schools discuss quite similar experimental facts. In reviewing the field, however, it is convenient to ignore this and follow the terminology of the different schools.

Historically one can distinguish two schools depending on the preferred way of presenting data.[5] The "dielectric" school uses the dielectric constant, $\epsilon(\omega) = \epsilon'(\omega) - i\epsilon''(\omega)$, while the "semiconductor" school prefers to speak about the conductivity, $\sigma(\omega) = \sigma'(\omega) + i\sigma''(\omega)$. These two quantities are related by

$$\epsilon_0\epsilon(\omega) = [\sigma(\omega) - \sigma(0)]/i\omega, \tag{1}$$

where ϵ_0 is the vacuum permittivity. More recently it has become popular, in particular in the field of ionic conduction, to present data in terms of the electric modulus, $M(\omega) = M'(\omega) + iM''(\omega)$, defined[20] by

$$M(\omega) = i\omega/\sigma(\omega). \tag{2}$$

The use of $M(\omega)$ has the advantage that there is no contribution to $M''(\omega)$ from electrode capacitances. Also, it is not necessary as in Eq. (1) to subtract $\sigma(0)$ from $\sigma(\omega)$ in order to get peaks in the imaginary part ("loss peaks"). Finally, the impedance, $Z(\omega) = Z'(\omega) - iZ''(\omega)$, is sometimes used for presenting data, usually plotted in a so-called complex impedance diagram where $x = Z'(\omega)$ and $y = Z''(\omega)$.[7]

The first systematic studies of ac conduction in disordered solids were carried out by workers within the dielectric school about 30 years ago. The systems considered were ionic conductive oxide glasses.[6,21] These solids were studied much because of technological interest; an understanding of the dielectric loss in glass as a function of frequency and temperature became important for the electrics industry in the 1950s when one started to construct large transmitting valves, x-ray tubes, and similar products.[22] Since dielectric loss in liquids had already been studied for many years, it was natural to report observations in terms of the dielectric loss. In glasses, however, it is necessary to subtract the non-zero dc conductivity in order to get proper dielectric loss peaks [Eq. (1)]. This was done without further justification, although it was soon discovered that there is a close correlation between dc conduction and dielectric loss.[23]

The main features of dielectric loss in ionic conductive glasses, as established by the end of the 1950s,[6,21,23,24] are (1) very broad dielectric loss peaks with a temperature-independent shape and an almost frequency-independent loss at high frequencies, and (2) an Arrhenius temperature-dependent dielectric loss peak frequency ω_m with the same activation energy as the dc conductivity. Point (2) means that ω_m and $\sigma(0)$ are proportional. As pointed out by Isard, the constant of proportionality is almost universal, varying only weakly with temperature and glass composition.[24] A closer analysis of the proportionality was carried out by Barton, Nakajima, and Namikawa[25-27] who found the following equation to be valid for most glasses:

$$\sigma(0) = p\Delta\epsilon\epsilon_0\omega_m. \tag{3}$$

Here $\Delta\epsilon$ is the dielectric loss strength, i.e., $\Delta\epsilon = \epsilon(0) - \epsilon(\infty)$, and p is a temperature-independent numerical constant close to one. At ordinary temperatures $\Delta\epsilon$ is usually not very much different from one, thereby explaining the approximate universality of $\sigma(0)/\omega_m$. Equation (3), which applies also for electronic conducting disordered solids,[28,29] will be referred to as the BNN relation.[19] It carries very important information, implying that ac and dc conduction are closely correlated and must be due to the same mechanism. A number of models have been proposed to explain the BNN relation but none of these models can explain at the same time the observed very broad dielectric loss peaks.[19] The random free-energy barrier model, to be discussed below, is consistent with both these experimental facts.

Perhaps the earliest model for ac conduction of ionic glasses is Stevels' and Taylor's random potential energy model.[21,23,30] This model was only qualitative and did not discuss the BNN relation. In the model, it is assumed the ions feel a more or less randomly varying potential energy deriving from the random network structure of the glass. For dc conduction the largest energy barriers have to be overcome, while lower barriers are involved for ac conduction since only a limited distance has to be traveled. Though quite attractive, it was generally believed this model is inconsistent with the experiment. It was thought that, since ω_m is determined from ac properties, the model predicts a lower activation energy for ω_m than for $\sigma(0)$. Also, it was believed that a distribution of activation energies implies a temperature-dependent shape of the loss peak.[3,15] Both things are wrong as becomes evident in Secs. IV and V where the random free-energy barrier model is discussed; this model is essentially nothing but Stevels' and Taylor's old random potential energy model.

Work within the semiconductor school started in 1961 when Pollak and Geballe measured the ac properties of n-type doped crystalline silicon at very low temperatures.[14] They observed an approximate power law for the ac conductivity,

$$\sigma'(\omega) \propto \omega^s, \tag{4}$$

with an exponent s close to 0.8. Since then it has been customary to speak about power-law frequency dependencies, inferred from straight lines in log-log plots. However, even almost perfectly straight lines does not mean that $\sigma'(\omega)$ is an exact power law; log-log plots may be deceptive. This is not always remembered and equations like (4) have created some confusion in the field by being taken literally. To avoid this, one should preferably only speak about *approximate* power laws.

During the 1960s, the study of amorphous semiconductors emerged as a new and exciting field within semiconductor physics. As regards ac properties it was soon found that all amorphous semiconductors obey Eq. (4), and for most systems studied, one found values of s close to 0.8.[4] A simple model for this is the pair approximation which was advanced by Austin and Mott in 1969,[31] generalizing an idea of Pollak and Geballe.[14] The pair approximation assumes that ac

losses are due to tunneling between pairs of localized states. For a random distribution of tunneling distances one finds an approximate power-law ac conductivity with an exponent given by[31]

$$s = 1 + 4/\ln(\omega \tau_{ph}) \qquad (5)$$

where τ_{ph} is a typical phonon time. For ordinary laboratory frequencies Eq. (5) gives $s \cong 0.8$. Despite this success, it turns out that the pair approximation has a number of problems, and this approach cannot be regarded as a serious candidate for explaining experiments: Eq. (5) predicts s is a weakly decreasing function of frequency whereas experimentally s is, if it varies at all, weakly increasing.[32] Also, the pair approximation cannot explain the transition to frequency-independent conduction at low frequencies; an expression of the form $\sigma'(\omega) = \sigma(0) + A\omega^s$ does not fit data at low frequencies where a loss peak appears, showing that ac and dc conduction are due to the same mechanism.[5,29] Finally, it has been found that $s \cong 0.8$ is not universally valid, for instance, s always converges to one as the temperature goes to zero.[32,33]

More refined models were suggested in the 1970s and early 1980s when hopping models, i.e., random walks in systems with spatially randomly varying jump frequencies, became popular. This approach was developed by Scher and Lax in 1973,[34] building on earlier ideas of Miller and Abrahams.[35] Scher and Lax suggested calculating $\sigma(\omega)$ in a hopping model by approximating the spatially inhomogeneous markovian random walk by a homogeneous nonmarkovian Montroll–Weiss-type continuous time random walk (CTRW).[36] Today the CTRW approximation is recognized as the simplest possible nontrivial mean-field approximation for calculating $\sigma(\omega)$ in random media, although the original derivation is inconsistent (Sec. III). Around 1980 the coherent potential approximation[37,38] was introduced into the field independently by several workers, where it became known as the effective-medium approximation (EMA).[39-42] Attempts were also made to improve the pair approximation. The correlated barrier hopping model is a version of the pair approximation which predicts $s \to 1$ as $T \to 0$.[33,43] Alternatively, by returning to the original Miller–Abrahams equivalent circuit, Summerfield and Butcher in the extended pair approximation (EPA) succeeded in joining the pair approximation smoothly to the dc conduction.[44] In practical applications the EPA is very similar to the EMA and both approximations lead to self-consistency equations for $\sigma(\omega)$.

Hopping models are markovian, i.e., the charge carrier jump probabilities are assumed to be time independent. This leads to simple exponential decays of the probability for a charge carrier to stay at a given site in the solid. The observed pronounced frequency dispersion of the conductivity is then attributed to spatial disorder in the solid, resulting in a broad distribution of relaxation times (waiting times). A completely different approach to the problem is possible, however, namely to assume the fundamental hopping process is itself nonexponential.[45,46] Models along these lines have not yet come up with useful predictions about $\sigma(\omega)$. It is important to note that the assumption of nonmarkovian jumps does not in itself imply the conductivity is frequency dependent. Correlations in the directions of subsequent jumps are needed to ensure $\sigma(\omega) \neq \sigma(0)$ (see Sec. III). At present there seems to be no reason to assume nonmarkovian processes to lie behind the ac conduction, and only models based on simple exponential decays will be considered in this paper.

The dielectric and the semiconductor schools not only present data in terms of different quantities but they also have different emphasis.[5] Workers from the dielectric school were always mainly interested in the loss peaks and did not put much effort into an investigation of the region of frequencies much larger than the loss peak frequency where the dielectric loss is almost constant. In contrast, this region has always been regarded as of main interest by the semiconductor school. This is because no frequency dependence analogous to Eq. (4) is found in single-crystal semiconductors where $\sigma(\omega) = \sigma(0)$ up to microwave frequencies. Also, experimentalists within the semiconductor school traditionally assumed the ac conduction to take place by a mechanism completely different from that behind the dc conduction, thereby making irrelevant any detailed investigation of the frequency region where the transition to dc conduction occurs.

As regards the question of the best way of presenting data, we suggest $\sigma(\omega)$ is to be preferred compared to $\epsilon(\omega)$ or $M(\omega)$. The use of $M(\omega)$ may have serious problems (see Sec. V). The conductivity is the more fundamental quantity, being directly related to equilibrium current-current fluctuations via the Kubo formula[47]

$$\sigma(\omega) = \frac{1}{3k_B T V} \int_0^\infty \langle \mathbf{J}(0) \cdot \mathbf{J}(t) \rangle e^{-i\omega t} \, dt, \qquad (6)$$

where $\mathbf{J}$ is the total current in volume V, and k and T have their usual meaning. Reflecting also the fundamental nature of the conductivity is the fact that the dissipation per unit time and unit volume is $\sigma'(\omega)/2$ times the absolute square of the current density. Finally, because of the nonzero dc conductivity there is no simple interpretation of $\epsilon(\omega)$ in terms of fluctuating dipole moments. A focus on the dielectric loss does have some merit, though. The very fact that peaks in $\epsilon''(\omega)$ are seen at all is very important since this, in conjunction with the BNN relation, demonstrates that dc and ac conduction are both due to the same mechanism. Thus, the early discovery of the BNN relation for ionic glasses was due to the dielectric school while the analog for amorphous semiconductors only much more recently has been firmly established.[28,29,48]

We end this section by listing the general features of ac conduction in disordered solids which are observed almost without exception and which a satisfactory model should explain[1-6,29,32,75]: (1) For $\sigma'(\omega)$ one observes at high frequencies an approximate power law with an exponent s less than or equal to one, and usually close to one. If any deviation from a power law is seen, it corresponds to a weakly increasing $s(\omega)$. (2) At lower frequencies there is a gradual transition to a frequency-independent conductivity. The transition takes place around the loss peak frequency. (3) Whenever the dc conductivity is measurable there is always a dielectric loss peak. The loss peak frequency satisfies the

BNN relation [Eq. (3)]. When there is no measurable dc conductivity the exponent s is very close to one. (4) As regards their temperature dependence, $\sigma(0)$ and ω_m are usually Arrhenius with the same activation energy although more complicated temperature dependencies are occasionally observed, e.g., in group-IV amorphous semiconductors. (5) The shape of the loss peak is temperature independent. (6) The ac conductivity is much less temperature dependent than the dc conductivity (when considered in the usual log-log plot of Fig. 1). For s very close to one the ac conductivity is practically independent of temperature. (7) The exponent s increases as the temperature decreases, and for $T \to 0$ one finds $s \to 1$. Thus, the ac conductivity becomes almost temperature independent as $T \to 0$. (8) Even though $\sigma(0)$ may vary by many orders of magnitude, the ac conductivity varies only relatively little (one or two orders of magnitude) for different solids and different temperatures. In Sec. IV a simple hopping model will be considered which can explain these facts, but first a general discussion of hopping models is given.

III. HOPPING MODELS

Though a complete model for glass ionic conductivity does not exist today, it is seldom questioned that the basic transport mechanism is thermally activated hopping across an energy barrier, a process described by Eyring's rate theory.[49] Being a stochastic theory, rate theory leads to a simple exponential decay for the probability for an ion to stay at an energy minimum. Conductivity described by rate theory is usually referred to as hopping conductivity. While ionic conductivity is a classical thermally activated process, electronic conductivity is of quantum-mechanical nature. The fact that the two kinds of conduction in disordered solids are quite similar in their frequency and temperature dependence, is surprising and must provide an important piece of information. The simplest explanation is that even electronic conduction in disordered solids is to be described by hopping models. Actually, hopping between pairs of localized states has always been assumed to account for ac conduction in amorphous semiconductors, while dc transport, with the important exceptions of impurity conduction and Mott's variable range hopping model,[4] traditionally is assumed to take place via extended state conduction. But since dc and ac conduction are due to the same mechanism (Sec. II), it seems that this approach must be abandoned and one has to assume dc conduction is due to hopping as well. The transport mechanism is probably quantum-mechanical tunneling between localized states. To ensure energy conservation the tunneling must be phonon assisted, thus destroying any quantum coherence effects. Accordingly, electronic hopping is of a stochastic nature just as ionic hopping.

Electrons are fermions, of course, but even ions behave as fermions as regards their hopping properties. This is because the Coulomb repulsion between ions and the finite ion size imply there is only room for one ion in each potential energy minimum in the solid. In the equation describing hopping fermions, it is usually assumed that transitions involve only hops of a single fermion. Even then, the equation is very complicated and further simplifications must be introduced to arrive at a tractable model. By assuming the site occupation numbers do not fluctuate in time it is possible to "project" the equation into three dimensions, in effect getting rid of all interactions between the particles, including that induced by fermistatistics.[50] The resulting equation, to be discussed below [Eq. (7)], describes hopping of noninteracting "quasi-particles" and this is what is usually meant by a hopping model. It is important to remember, however, that hopping models are built on mean-field assumptions which are far from obvious and cannot be justified in general.[51] Hopping models have recently been reviewed by Niklasson in a paper emphasizing fractal aspects of conduction in disordered solids.[52]

The very basic fact about ac conduction in disordered solids is that $\sigma'(\omega)$ is an increasing function of frequency. Any hopping model has this feature.[53] This is not surprising, since by hopping backwards and forwards at places with high jump probability a quasi-particle may sizably contribute to the ac conductivity, while the dc conductivity is determined by overcoming of unfavorable places in the solid for the formation of a continuous "percolation" path between the electrodes. The higher the frequency of the electric field, the larger is the ac conductivity because better use is made of the places with very large jump probability. As illustrated in Fig. 2, the increase in conductivity continues as long as the frequency of the field is lower than the maximum quasi-particle jump frequency (jump probability per unit time) in the solid. For larger field frequencies the conductivity stabilizes and becomes constant.

In order to arrive at a conductivity which increases for many decades of frequency, one must assume the jump frequency distribution also covers many decades. In comparison, the jump distances vary only relatively little. For nearest-neighbor hopping, for instance, the jump distance typically varies a factor of 2 or 3. It is commonly believed

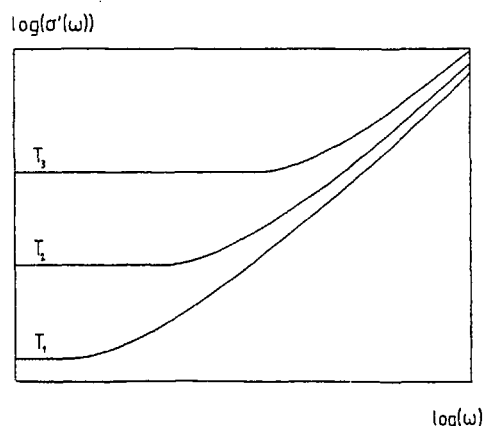$\log(\sigma'(\omega))$

$\log(\omega)$

FIG. 1. Sketch of the real part of the frequency-dependent conductivity in a disordered solid at three different temperatures $T_1 < T_2 < T_3$. At low frequencies the conductivity is constant and equal to the dc conductivity, while at higher frequencies the conductivity obeys an approximate power law. The characteristic frequency marking the onset of ac conduction, the dielectric loss peak frequency ω_m, increases with increasing temperature. Note that in this logarithmic plot, the ac conductivity is less temperature dependent than the dc conductivity.

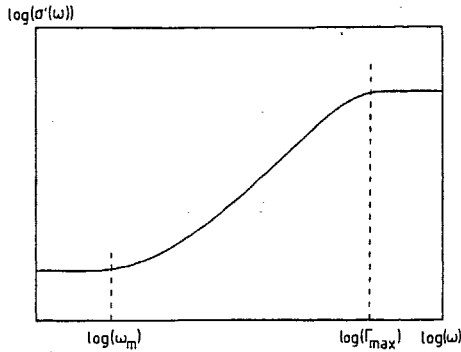log(σ'(ω))

log(ω_m)   log(Γ_max) log(ω)

FIG. 2. Typical behavior of $\sigma'(\omega)$ in a hopping model. In hopping models $\sigma'(\omega)$ is always an increasing function of frequency (Ref. 53), just as in experiment. The saturation of $\sigma'(\omega)$ at high frequencies takes place when ω is close to the maximum jump frequency Γ_{max}. Only in this region, typically close to 10^{12} Hz, is the pair approximation valid. The onset of ac conduction at low frequencies takes place around the loss peak frequency ω_m, which is the lowest effective jump frequency of the system, corresponding to the longest waiting time at a lattice site.

that this variation is insignificant. Following this, all jump distances may be assumed to be equal by considering the quasi-particle random walk to take place on a simple cubic lattice. The stochastic "equation of motion" for a quasi-particle is now the following master equation:

$$\frac{\partial P(s,t)}{\partial t} = -\gamma_s P(s,t) + \sum_{s'} \Gamma(s' \to s) P(s',t), \qquad (7)$$

where $P(s,t)$ is the probability to find the particle at the lattice site s at time t, $\Gamma(s' \to s)$ is the jump frequency for jumps from site s' to s (Γ is usually assumed to be nonzero only when s' and s are nearest neighbors), and

$$\gamma_s = \sum_{s'} \Gamma(s \to s'). \qquad (8)$$

To mimic the disorder of the solid, the Γ's are assumed to vary randomly according to some probability distribution $p(\Gamma)$. The problem of calculating $\sigma(\omega)$ from $p(\Gamma)$ is not easy and suitable approximations have to be done. Below, the derivation of the CTRW and the EMA approximations is briefly sketched.

Adopting the bra and ket notation of quantum mechanics, Eq. (7) can be rewritten as

$$\frac{\partial}{\partial t} |\psi\rangle = H |\psi\rangle, \qquad (9)$$

where $|\psi\rangle = \Sigma_s P(s) |s\rangle$ is the state with probability $P(s)$ of finding the particle at site s, and the "Hamiltonian" H is given by

$$H = -\sum_s \gamma_s |s\rangle \langle s| + \sum_{s,s'} \Gamma(s' \to s)|s\rangle \langle s'|. \qquad (10)$$

The formal solution of Eq. (9) is $|\psi(t)\rangle = \exp(Ht)|\psi(t=0)\rangle$. By two partial integrations, the Kubo formula for $\sigma(\omega)$ [Eq. (6)] reduces to

$$\sigma(\omega) = -\frac{nq^2\omega^2}{6k_BT} \int_0^\infty \langle \Delta R^2(t)\rangle e^{-i\omega t}\, dt, \qquad (11)$$

where q and n are charge respective density of the quasi-particles and $\langle \Delta R^2(t)\rangle$ is the mean-square displacement of a particle in time t. A convergence factor $\lim_{\epsilon \to 0} \exp(-\epsilon t)$ is implicitly understood in the integral. If all sites are equally populated in thermal equilibrium, i.e., have the same free energy, Eq. (9) in conjunction with Eq. (11) implies

$$\sigma(\omega) = -\frac{nq^2\omega^2}{6k_BT}\frac{1}{N}\sum_{s,s'}(s-s')^2\langle s|G(i\omega)|s'\rangle, \qquad (12)$$

where N is the number of lattice sites and G is the resolvent or Green's function operator for H:

$$G = 1/(i\omega - H). \qquad (13)$$

The Green's function depends on the actual values of the Γ's. Hopping systems in three dimensions are believed to be self-averaging, implying that different samples with different H's have the same bulk $\sigma(\omega)$. This property simplifies matters considerably since only the average of G over all possible H's, $\langle G \rangle$, needs to be evaluated in order to find $\sigma(\omega)$. $\langle G \rangle$ is translationally invariant and we now make the ansatz

$$\langle G \rangle = 1/(i\omega - H_c), \qquad (14)$$

where $H_c = H_c(\omega)$ is a "coherent" Hamiltonian determined by a coherent jump rate $\Gamma_c(\omega)$ in the following way:

$$H_c(\omega) = \Gamma_c(\omega)\left(-6\sum_s |s\rangle \langle s| + \sum_{s,s'}|s\rangle \langle s'|\right),$$

where the double sum is over nearest neighbors only. It is not hard to show from Eqs. (12) and (14), and is indeed intuitively obvious, that $\sigma(\omega)$ is proportional to $\Gamma_c(\omega)$.[54] For simplicity from now on we adopt the unit system in which the constant of proportionality is one, i.e., where $\sigma(\omega) = \Gamma_c(\omega)$.

To derive the CTRW approximation we write $H = H_0 + V$ where H_0 is the diagonal part and V the off-diagonal part of H. If G_0 is the Green's function for H_0, the standard perturbation expansion is[37]

$$G = G_0 + G_0 V G_0 + G_0 V G_0 V G_0 + \cdots. \qquad (15)$$

The CTRW approximation is now to assume that all averages of products in G are equal to products of averages, i.e.,

$$\langle G \rangle = \langle G_0 \rangle + \langle G_0 \rangle \langle V \rangle \langle G_0 \rangle + \cdots, \qquad (16)$$

which implies $\langle G_0\rangle \langle G\rangle^{-1} + \langle G_0\rangle \langle V\rangle = 1$. Taking a diagonal element of this operator identity we get the CTRW approximation for $\sigma(\omega)$ in our rationalized unit system[34,42,54,55]

$$\frac{1}{6\sigma(\omega) + i\omega} = \left\langle \frac{1}{\gamma + i\omega}\right\rangle. \qquad (17)$$

The original derivation of the CTRW approximation was made for a nonmarkovian random walk in a homogeneous medium characterized by a so-called waiting time distribution function.[34] This derivation is inconsistent, however, since the assumption of spatial homogeneity implies the current autocorrelation function is a delta function, and thus $\sigma(\omega) = \sigma(0)$ from Eq. (6).[56,57] Note that this criticism applies to any nonmarkovian hopping in a homogeneous medium; a nontrivial frequency dependence of the conductivity only comes about if there are correlations in the directions of subsequent jumps. The derivation of Eq. (17) given above is

due to Odagaki and Lax[42,54]; here the CTRW approximation appears as the simplest possible nontrivial mean-field approximation which is also referred to as the Hartree approximation.

The magnitude of the dc conductivity is usually quite wrong in the CTRW approximation, throwing doubt on this approach.[58] A more reliable way of evaluating $\sigma(\omega)$ is the EMA.[39–42] Here the idea is to focus on a particular link of the lattice, say the link between site s and s'. Assuming, as above, that all site free energies are equal, the principle of detailed balance implies $\Gamma(s \rightarrow s') = \Gamma(s' \rightarrow s)$. The link is considered to be embedded in an average medium described by the $\langle G \rangle$ of Eq. (14) and one now requires self-consistency so that, on the average, the system of link plus average medium is described by $\langle G \rangle$: Writing the effective Hamiltonian for the system, H_{eff}, as $H_{\text{eff}} = H_c + V$ where $V = [\sigma(\omega) - \Gamma(s \rightarrow s')] |a\rangle\langle a|$ with $|a\rangle = |s\rangle - |s'\rangle$, the standard perturbation expansion Eq. (15) yields for the Green's function for H_{eff}

$$G_{\text{eff}} = \langle G \rangle + \langle G \rangle T \langle G \rangle, \tag{18}$$

where

$$T = V + V\langle G \rangle V + \cdots = V(1 - \langle G \rangle V)^{-1}. \tag{19}$$

The self-consistency requirement, $\langle G_{\text{eff}} \rangle = \langle G \rangle$, now leads to $\langle T \rangle = 0$. A straightforward calculation with 2×2 matrices referring to site s and s' shows that $\langle T \rangle = 0$ is equivalent to[40,42]

$$\left\langle \frac{\Gamma - \sigma(\omega)}{1 - 2(\langle s|\langle G \rangle|s\rangle - \langle s|\langle G \rangle|s'\rangle)(\sigma(\omega) - \Gamma)} \right\rangle = 0. \tag{20}$$

This is the EMA equation for $\sigma(\omega)$; it can be simplified somewhat by noting that

$$\langle s|\langle G \rangle|s\rangle - \langle s|\langle G \rangle|s'\rangle = \frac{1 - i\omega\langle s|\langle G \rangle|s\rangle}{6\sigma(\omega)}, \tag{21}$$

which follows from evaluating the diagonal element of Eq. (14) written as $(i\omega - H_c)\langle G \rangle = 1$.

As mentioned already, the real part of the conductivity is always an increasing function of frequency. The increase continues until one reaches the region of frequencies around the maximum jump frequency of the model, where the conductivity stabilizes (Fig. 2). In experiments the conductivity usually increases until $\omega \cong 10^{12}$ Hz. At these high frequencies the stochastic assumption of hopping models cease to be valid and one enters a region characterized by various resonance effects. At even higher frequencies the conductivity starts decreasing. The stabilization of Fig. 2 predicted by hopping models is thus seldomly observed in experiment which suggests that, for the construction of realistic hopping models, one should try to eliminate completely all effects of the maximum jump frequency. This philosophy is followed below.

IV. THE RANDOM FREE-ENERGY BARRIER MODEL

Equipped with the tools of Sec. III we now address the problem of formulating the simplest possible realistic model for ac conduction in disordered solids. For most solids the dc conductivity is thermally activated: $\sigma(0) \propto \exp(-\Delta E_{\text{dc}}/$

$k_B T)$. As illustrated in Fig. 1, the ac conductivity is less temperature dependent than $\sigma(0)$, suggesting that ac conduction is dominated by processes with activation energies smaller than ΔE_{dc}. A closer analysis shows that the ac conductivity activation energy depends on frequency and temperature so it is natural to assume that, consistent with the disorder of the solid, a whole range of activation energies is involved. This idea goes back in time at least to 1946 (Refs. 30 and 59) and it is the basic ingredient in Stevels' and Taylor's model from 1957.[21,23] It should be emphasized that, even without any microscopic picture of the transport mechanism, results like Fig. 1 strongly suggest that any model for ac conduction should somehow be built on the assumption of a distribution of energy barriers. Hopping models, of course, fit nicely into this since it is realistic to assume the quasiparticle jumps are thermally activated over an energy barrier. More generally, one speaks about free-energy barriers[49] and writes

$$\Gamma = \Gamma_0 \exp\left(-\frac{\Delta F}{k_B T}\right), \tag{22}$$

where Γ_0 is the so-called attempt frequency, and the free-energy barrier, $\Delta F = \Delta E - T\Delta S$, is composed of an energy barrier ΔE and an entropy barrier ΔS. Quantum-mechanical tunneling may be thought of as providing a negative entropy barrier proportional to the tunneling distance. In this terminology it is possible to speak about ionic and electronic conduction in a unified language which, incidently, also covers the possibility of thermally activated electron or polaron jumps *over* energy barriers.

In modeling a disordered solid, the simplest possible assumption is that all free-energy barriers are equally likely. Since $p(\Gamma) = p(\Delta F)(d\Delta F/d\Gamma)$ this implies

$$p(\Gamma) \propto \Gamma^{-1}. \tag{23}$$

The model defined by Eq. (23) will be referred to as the random free-energy barrier model. To solve this model within the CTRW approximation [Eq. (17)], the distribution of γ's needs to be calculated. Since γ is a sum of Γ's [Eq. (8)], $p(\gamma)$ is a convolution of $p(\Gamma)$ with itself a number of times. The result is a complicated function, equal to γ^{-1} times some logarithmic terms. These terms are not very important compared to the γ^{-1} term, so we approximate $p(\gamma)$ simply by γ^{-1}. Substituting this now into Eq. (17) leads to

$$\sigma(\omega) = \frac{1}{6}\left(-i\omega + \frac{i\omega \ln \lambda}{\ln[(1 + i\omega/\gamma_{\text{min}})/(1 + i\omega/\gamma_{\text{max}})]}\right), \tag{24}$$

where two cutoff's have been introduced, and $\lambda = \gamma_{\text{max}}/\gamma_{\text{min}}$. According to the philosophy of Sec. III any influence of the high-frequency cutoff should be eliminated. For $\gamma_{\text{max}} \rightarrow \infty$ the second term of Eq. (24) dominates, and for frequencies $\omega \ll \gamma_{\text{max}}$ we thus have

$$\sigma(\omega) = \frac{1}{6}[i\omega \ln \lambda / \ln(1 + i\omega\tau)], \quad \tau = \gamma_{\text{min}}^{-1}. \tag{25}$$

From this we get

$$\sigma(0) = \ln \lambda / 6\tau, \tag{26}$$

which substituted into Eq. (25) finally gives[16]

$$\sigma(\omega) = \sigma(0)[i\omega\tau/\ln(1 + i\omega\tau)]. \tag{27}$$

By regarding this expression as a formula for $\sigma(\omega)$ with two free parameters, $\sigma(0)$ and τ, any influence of γ_{max} has now been formally eliminated.

The random free-energy barrier model predicts a universal shape of the conductivity curve plotted in the usual log-log plot.[16] In Fig. 3 the model is compared to experiments on a number of different solids.[65-71] Though exact universality is not observed, the model is in rough agreement with experiment. The model implies a high-frequency behavior which is very close to a power law, reminding us of the danger of deducing fundamental power laws from log-log plots. For $10^3 < \omega\tau < 10^6$ one finds $s \cong 0.8$, which offers a possible explanation for the frequently observed exponents around 0.8.[4] For $\omega\tau \gg 1$ the exponent s is given by the expression

$$s = 1 - 2/\ln(\omega\tau). \tag{28}$$

This can be easily proved from $\sigma'(\omega) \propto \omega\tau/\ln^2(\omega\tau)$, which is valid whenever $\omega\tau \gg 1$. In general, the model predicts ex-

ponents between 0.7 and 1.0, which is exactly the interval in which one finds the vast majority of reported exponents.[32] Also in agreement with experiments is the fact that $s(\omega)$ is a weakly increasing function of ω.

For the dielectric loss one finds by substituting Eq. (27) into Eq. (1),

$$\epsilon''(\omega) = 2\Delta\epsilon\left(\frac{\arctan(\omega\tau)}{[\ln\sqrt{1 + (\omega\tau)^2}]^2 + [\arctan(\omega\tau)]^2} - \frac{1}{\omega\tau}\right), \tag{29}$$

where $\Delta\epsilon$ is the dielectric loss strength given by

$$\epsilon_0\Delta\epsilon = \tfrac{1}{2}\sigma(0)\tau. \tag{30}$$

Equation (29) implies a very broad loss peak with a temperature independent shape. The loss peak is shown in Fig. 4 together with data for a typical sodium silicate glass. There is a qualitative, but not exact, agreement between theory and experiment. The BNN relation is satisfied by the model. A numerical analysis of Eq. (29) shows that the loss peak frequency is given by $\omega_m\tau = 4.71$.[19] Combining this with Eq. (30) and the definition of the BNN p parameter in Eq. (3) we get

$$p_{CTRW} = 0.42. \tag{31}$$

This number is not as close to one as required by experiment, but in comparison to the many orders of magnitude variations in $\sigma(0)$ and ω_m for the solids where the BNN relation has been found,[27] this is not a serious objection to the model.

Writing Eq. (30) in the form

$$\tau = 2\epsilon_0\Delta\epsilon/\sigma(0), \tag{32}$$

implies an interesting scaling principle which has recently been discussed by Summerfield[48] and which was also used by Scher and Lax in their 1973 papers.[4] The scaling principle, which is just the BNN relation in conjunction with the time-temperature superposition principle (i.e., the existence of a universal conductivity curve), allows one to plot different experiments onto a master curve. To make use of the scaling principle, one may use, e.g., experiments on one solid at different temperatures, as illustrated by Pollak and Geballe's original experiments replotted in Fig. 5(a)[14] and a similar

FIG. 3. CTRW solution of the random free-energy barrier model [Eq. (27)] compared to experiment on a number of solids [(a) is reproduced from Ref. 16]. The data represent conduction in (a) n-doped crystalline silicon ($\times$), sputtered films of arsenic ($\bullet$), sodium silicate glasses ($\odot$), glow-discharge silicon ($\triangle$), silicon monoxide ($+$), amorphous germanium ($\square$), $Mn_{1-x}Ni_{0.6}Co_{0.6}O_4$ (∇), monolayer of stearic acid (O); and (b) $a - As_2Se_3$ at 370 K ($\times$) (Ref. 65), viscous $0.4Ca(NO_3)_2$-$0.6KNO_3$ at 338.5 K ($\bullet$) (Ref. 66), viscous $HZnCl_3\cdot4H_2O$ at 154.5 K ($\odot$) (Ref. 67), illuminated polycrystalline zinc oxide ($\triangle$) (Ref. 63), vanadium phosphate glass at 167 K ($+$) (Ref. 68), AsF_5-doped polyphenylacetate at 271 K ($\square$) (Ref. 69), flux-grown single-crystal alumina in c direction at 873 K (∇) (Ref. 70), 81% tungsten phosphate glass at room temperature (O) (Ref. 71). For all data the characteristic time τ has been adjusted to fit the theory as well as possible; τ varies between 10^{-7} and 10^3 s.
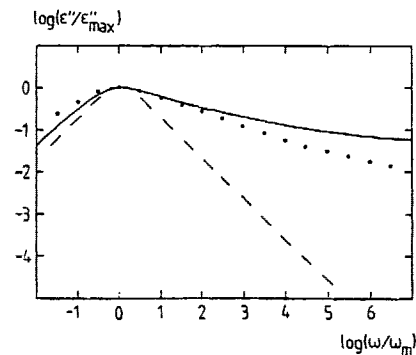

FIG. 4. Dielectric loss of the random free-energy barrier model according to Eq. (27) and data for a typical sodium-silicate glass (reproduced from Ref. 19). The dashed curve is the Debye dielectric loss peak. There is a qualitative, but not exact, agreement between theory and experiment.
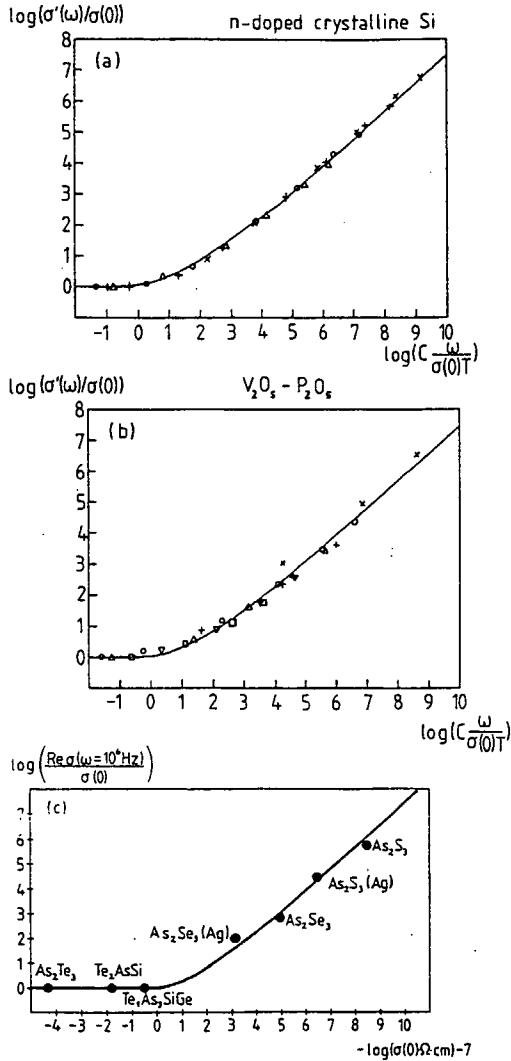
FIG. 5. Applications of the scaling principle, i.e., the BNN relation in conjunction with the time-temperature superposition principle. In the model, the scaling principle is expressed by Eq. (32) and the fact that the conductivity relative to $\sigma(0)$ is a function only of $\omega\tau$. In (a) and (b) data for a single sample at different frequencies and temperatures are plotted, making use of Eq. (32) and the Curie law equation (33). The data are compared to the CTRW solution of the random free-energy barrier model [Eq. (27)]. (a) considers the original data by Pollak and Geballe on heavily n-doped crystalline silicon at low temperatures, taken from Fig. 5 of Ref. 14. The data were obtained at the following temperatures: 2, 2.5, 3, 3.5, 4.5, 5.5 K at 0.1 kHz ($\triangle$), 1 kHz (O), 10 kHz (+), 100 kHz ($\times$). (b) considers data on a vanadium phosphate glass taken from Fig. 2 of Ref. 72. The data was obtained at 83, 100, 125, 167, and 250 K at 0.1 kHz ($\square$), 1 kHz ($\triangledown$), 10 kHz ($\triangle$), 100 kHz (O), 8 MHz (+), 3.6 GHz ($\times$). The gigahertz data deviates from the master curve, signaling a breakdown of the theory at very high frequencies. In both (a) and (b) the constant C is a fitting parameter, $C = 1.9\times10^{-12}$ for (a) and $C = 2.1\times10^{-10}$ for (b) in units of $(\Omega\,\text{cm})^{-1}\,\text{K/Hz}$. In (c) data for different chalcogenide glasses at a fixed frequency are compared to Eq. (27). It is assumed that the different samples have the same dielectric loss strength $\Delta\epsilon$ which becomes a fitting parameter ($\Delta\epsilon = 0.6$). The data were obtained at 300 K by several workers [see the references in the paper by Davis and Mott who compiled the data (Ref. 73)].

figure for measurements by Mansingh and co-workers [Fig. 5(b)].[72] Alternatively, measurements at the same frequency on different solids assumed to have the same $\Delta\epsilon$[Fig. 5(c)] may be used.[73]

In connection with the scaling principle we remind that $\Delta\epsilon$ experimentally varies with temperature according to the Curie law

$$\Delta\epsilon \propto T^{-1}, \tag{33}$$

a fact which is also predicted by the CTRW treatment though here, it has been hidden by the rationalized unit system. Figure 6 illustrates the use of the scaling principle in conjunction with Eq. (33) for measurements by Long and Balkan on amorphous germanium.[74] Except for the weak temperature dependence of $\Delta\epsilon$, Eq. (32) predicts the universal conductivity curve of Eq. (27) to be displaced in the direction 45° to the $\log(\omega)$ axis when the temperature is changed. As the temperature is lowered, $\sigma(0)\to0$, which implies that measurements at a fixed frequency in effect probes larger and larger $\omega\tau$ on the universal conductivity curve. Since $s\to1$ as $\omega\tau\to\infty$, the model thus predicts $s\to1$ as $T\to0$, which is in agreement with experiment. Substituting $\sigma(0)\propto\exp\times(-\Delta F_{\text{dc}}/k_BT)$ via Eq. (32) into Eq. (28) we find as $T\to0$ for the exponent s, measured in a fixed range of frequencies,

$$s = 1 - T/T_0, \quad k_BT_0 = \tfrac{1}{2}\Delta E_{\text{dc}} . \tag{34}$$

According to the theory, the temperature dependence of the ac conductivity is much weaker than that of the dc conductivity. Note that the temperature dependence almost vanishes whenever s approaches one. This is predicted and observed for all systems at low temperatures, but $\sigma'(\omega)$ may also become almost temperature independent at room tem-
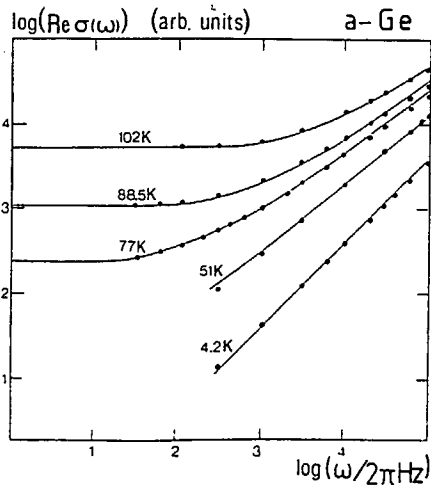

FIG. 6. Comparison between the prediction of Eq. (27) and measurements on amorphous germanium at various temperatures by Long and Balkan (Ref. 74) (reproduced from Ref. 16). The data were fitted by Eq. (27) at 77 K and then displaced according to the scaling law [Eq. (32)] taking into account Eq. (33). At the two lowest temperatures the dc conductivity is unknown and was treated as a fitting parameter.

perature for solids with a very low, perhaps unmeasurable, dc conductivity.

In experiment one finds that, while $\sigma(0)$ may vary many orders of magnitude between different solids, the ac conductivity varies only relatively little (one or two orders of magnitude).[2] This can be understood from the model: For two different solids, (1) and (2), we find from Eqs. (27) and (30)

$$\lim_{\omega \to \infty} \frac{\sigma'^{(1)}(\omega)}{\sigma'^{(2)}(\omega)} = \frac{\sigma^{(1)}(0)\tau^{(1)}}{\sigma^{(2)}(0)\tau^{(2)}} = \frac{\Delta\epsilon^{(1)}}{\Delta\epsilon^{(2)}}. \tag{35}$$

Since the dielectric loss strength varies only relatively little between different solids, Eq. (35) explains the small spread in ac conductivity.

Turning now to the problem of solving the random free-energy barrier model by the effective-medium approximation, we first substitute Eq. (21) into Eq. (20) and get

$$\langle (\Gamma - \sigma)/(\Gamma + \chi\sigma) \rangle = 0 \tag{36}$$

where

$$\chi = 3/(1 - i\omega\langle s|\langle G \rangle|s\rangle) - 1. \tag{37}$$

It is straightforward to calculate the average appearing in Eq. (36) when the distribution of Γ's is given by Eq. (23); the result is

$$(1 + \chi)\ln\left(\frac{\Gamma_{\max} + \chi\sigma}{\Gamma_{\min} + \chi\sigma}\right) = \ln\left(\frac{\Gamma_{\max}}{\Gamma_{\min}}\right), \tag{38}$$

which is a rather complicated equation for $\sigma(\omega)$. However, according to the philosophy of Sec. III we are only interested in the limit of very large $\Gamma_{\max}$. In this limit an important simplification occurs, as pointed out by Bryksin.[39] In the whole range of frequencies much smaller than $\Gamma_{\max}$ we have $\omega \ll |\sigma(\omega)|$. In this region one may therefore expand χ to first order in $\omega/\sigma(\omega)$:

$$\chi = 2 + \xi[i\omega/\sigma(\omega)] + \cdots, \tag{39}$$

where ξ is a numerical constant given by[39,60]

$$\xi = \frac{1}{6\pi^3}\int_0^\pi\int_0^\pi\int_0^\pi$$
$$\times\frac{dx\,dy\,dz}{1 - \frac{1}{3}[\cos(x) + \cos(y) + \cos(z)]} = 0.253. \tag{40}$$

The expansion in Eq. (39) is only possible in three or more dimensions where the Green's function for diffusion is well behaved as $\omega \to 0$. By putting $\chi = 2$ in Eq. (38) it is easy to see that in the frequency region of interest $\Gamma_{\min} \ll |\sigma(\omega)| \ll \Gamma_{\max}$. Thus, the ln term on the left-hand side of Eq. (38) may be replaced by $\ln(\Gamma_{\max}/\chi\sigma)$. Equation (38) now becomes, by equating the $\omega = \omega$ and the $\omega = 0$ on the left-hand side,

$$\left(3 + \xi\frac{i\omega}{\sigma(\omega)}\right)\ln\left(\frac{\Gamma_{\max}/2\sigma(\omega)}{1 + \frac{1}{2}\xi[i\omega/\sigma(\omega)]}\right) = 3\ln\left(\frac{\Gamma_{\max}}{2\sigma(0)}\right), \tag{41}$$

which expanded to first order in $\omega/\sigma(\omega)$ reduces to

$$3\ln\left(\frac{\sigma(0)}{\sigma(\omega)}\right) + \xi\frac{i\omega}{\sigma(\omega)}\ln\left(\frac{\sigma(0)}{\sigma(\omega)}\right)$$
$$+ \xi\frac{i\omega}{\sigma(\omega)}\ln\left(\frac{\Gamma_{\max}}{2\sigma(0)}\right) - \frac{3}{2}\xi\frac{i\omega}{\sigma(\omega)} = 0. \tag{42}$$

The second term is unimportant compared to the first term and may be ignored, leading to

$$\frac{\sigma(\omega)}{\sigma(0)}\ln\left(\frac{\sigma(\omega)}{\sigma(0)}\right) = i\omega\tau, \tag{43}$$

where

$$\tau = \frac{\xi}{3\sigma(0)}\left[\ln\left(\frac{\Gamma_{\max}}{2\sigma(0)}\right) - \frac{3}{2}\right]. \tag{44}$$

Equation (43) was first derived by Bryksin for electrons tunneling between nearest neighbors in a solid with electron sites randomly located in space.[39] The jump frequency probability distribution of this model is more complicated than Γ^{-1}, but in the limit $\Gamma_{\max} \to \infty$ the frequency-dependent conductivity is the same in the two models. It is quite unusual that the EMA leads to such a simple equation. This equation will henceforth be referred to as Bryksin's equation.

In Fig. 7 the solution to Bryksin's equation is compared to the CTRW solution of the random free-energy barrier model [Eq. (27)]. The two are quite similar, lending some credit to the simple CTRW expression for $\sigma(\omega)$. All features of the CTRW solution are shared by the solution of Bryksin's equation. In particular, the BNN relation is satisfied by the EMA solution, although Eq. (30) is now replaced by

$$\epsilon_0\Delta\epsilon = \sigma(0)\tau. \tag{45}$$

The loss peak frequency is given by $\omega_m\tau = 1.709$ and for the BNN p parameter one finds

$$p_{\text{EMA}} = 0.59. \tag{46}$$

This value is in better agreement with the experimentally found $p \cong 1$ than the $p_{\text{CTRW}} = 0.42$. But for other purposes the two solutions are practically identical and one may use

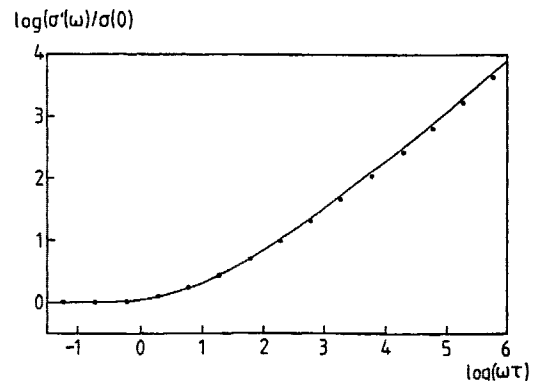$\log(\sigma'(\omega)/\sigma(0))$

FIG. 7. Comparison between the CTRW and the EMA solution of the random free-energy barrier model. The full curve is the CTRW solution [Eq. (27)] and the dots mark the EMA solution [Eq. (43)]. The two solutions are shown for the same value of $\sigma(0)$ and $\Delta\epsilon$ which, according to Eqs. (30) and (45), implies $\tau_{\text{EMA}} = 2\tau_{\text{CTRW}}$. The CTRW and EMA solutions are almost indistinguishable, lending credit to the simpler CTRW approach from the more reliable but also more involved EMA.

Eq. (27) just as well as Bryksin's equation, which has to be solved numerically before it can be compared to experiment.

V. DISCUSSION

Looking back on the history of ac conduction in disordered solids, it strikes one that a handful of glass technologists established very early the general features of glass ionic conductivity, while only much more recently the same features have been established also for electronic conductive disordered semiconductors. A likely explanation for this is the fact that electronic conductivity was always thought to be much more complicated than transport in ionic conductive solids, which obviously proceeds via thermally activated charge carrier jumps over barriers. The pair approximation, which seems to have delayed a proper understanding of electronic transport, was never really applied to ionic glasses, where one also needs a mechanism for the dc conduction which very early was known to be closely related to the ac conduction. On the other hand, the traditional ion glass researchers never managed to explain both the BNN relation and the broad dielectric loss peaks,[19] and the more successful random walk models were first solved by workers within the semiconductor school. Despite extensive theoretical work, these models have not yet become popular among experimentalists. This is perhaps because the models usually end up with complex equations which have to be solved numerically and which are far from transparent in their interpretation. But this is not necessarily the case, and one purpose of this paper has been to show that simple random walk models do exist and to encourage their use.

The justification of hopping models comes from the fact that dc and ac conduction are both due to the same mechanism. This is the message of the BNN relation which is central to the whole subject. It is of crucial importance that genuine loss peaks are observed. Otherwise, even when ac and dc conduction are totally unrelated, one may find a BNN-like relation of the form $\sigma(0) \propto \omega_m$ where ω_m is the characteristic frequency for the onset of ac conduction; this is the case, e.g., if $\sigma'(\omega) = \sigma(0) + A\omega$. In experiments one does indeed find loss peaks in all disordered solids, though this is not always as carefully checked as one might wish.

Given that conduction in disordered solids is to be described by hopping models, the only possible explanation for the ion-electron analogy is that the same jump frequency distribution applies for both cases. The simplest guess for the common distribution is that corresponding to randomly varying free-energy barriers for jumps, Eq. (23). One may argue for this distribution directly from experiments[18]: Since the shape of the $\sigma'(\omega)$ curve is temperature independent and $s \to 1$ as $T \to 0$, it can be concluded that $s \to 1$ as $\omega \to \infty$ on the master curve; the simplest jump frequency distribution consistent with this is $p(\Gamma) \propto \Gamma^{-1}$.[18] At low frequencies, when the cutoff at ω_m starts to play a role, one expects it to decrease the frequency dependence of the conductivity slightly, i.e., to push s below one. This is exactly what happens in the random free-energy barrier model [Eq. (28)]. While the assumption of completely randomly varying free-energy barriers is probably the simplest realistic choice, other barrier distributions may also be useful. This has been discussed

in detail by Macdonald in recent papers.[61] He adopts a more macroscopic point of view to ac conduction but the mathematics developed by him is quite similar to that of hopping models.

In hopping models it is possible to distinguish different characteristic regions of frequency.[39,50] At low frequencies the conductivity is constant. Here transport takes place on infinite "percolation" paths. Then comes a region of frequencies where the conductivity increases strongly with frequency (compare Fig. 2); here transport is dominated by contributions from hopping in finite clusters. Finally one encounters the region where the high-frequency cutoff starts to play a role and $s(\omega)$ decreases to zero with increasing frequency. This is where the pair approximation gradually becomes valid, i.e., where the conductivity is made up of contributions from independent pairs of sites connected by a link with a particularly large jump rate. The division into three regions of frequency is suggestive but not really based on exact theory. The validity of the pair approximation at high frequencies is an exact result, though.[50] To estimate where the pair approximation sets in, let us use the jump frequency distribution of Sec. IV [Eq. (23)] which gives equal weight to each decade of jump frequencies. In order for a link to be "isolated" from its surroundings, its jump rate must be larger than those of the 10 other links which it is directly connected to on the cubic lattice. Since the random free-energy barrier model weighs all decades of jump frequency equally, on the logarithmic frequency axis the pair approximation will be valid in the final 10% of the interval between Γ_{min} and Γ_{max}. Equation (38) implies for the dc conductivity $\sigma(0) \propto \Gamma_{min}^{1/3} \Gamma_{max}^{2/3}$ which via the BNN relation implies $\omega_m \propto \Gamma_{min}^{1/3} \Gamma_{max}^{2/3}$. Thus the pair approximation is valid only in the final third of the (logarithmic) interval between ω_m and Γ_{max}. In order to fit experiment Γ_{max} must be at least 10^{12} Hz, so the pair approximation is seldom of relevance at typical laboratory frequencies (unless at very low temperatures), and we may safely follow the philosophy of Sec. III and eliminate any influence of Γ_{max}. In the resulting "renormalized" hopping models, the physics is a consequence of the *low*-frequency cutoff at Γ_{min}. This is complementary to the pair approximation where the physics is a consequence of the *high*-frequency cutoff [Eq. (5)].[18]

When applying the renormalization philosophy to the random free-energy barrier model, one finds in the CTRW approximation a simple formula for $\sigma(\omega)$ [Eq. (27)] and in the EMA a simple transcendental equation for $\sigma(\omega)$ [Eq. (43)]. As illustrated in Fig. 7, these two solutions are almost identical. Since the dc conductivity in the CTRW approximation generally may be wrong by several orders of magnitude,[58] while the EMA value is probably much more accurate, the similarity between the two solutions is far from obvious and must be regarded as an empirical fact. Apparently, the CTRW is saved by our prescription of eliminating Γ_{max}, which leaves $\sigma(0)$ as a free parameter in the model.

Recently, it has been shown by Summerfield that several different models solved in the EPA have almost the same frequency dependence in the region of frequencies where the high-frequency cutoff is irrelevant.[48] He refers to this phenomenon as "quasi-universality." The solutions of the mod-

els discussed by Summerfield are quite close to the solution of the random free-energy barrier model. This supports a hypothesis of "quasi-universality" among all models and not only among EPA models as originally suggested. Though further investigation of this hypothesis is necessary, a preliminary conclusion is that all realistic models in the $\Gamma_{max} \to \infty$ limit gives more or less the same frequency-dependent conductivity. Equation (27) provides a simple analytical representation of the quasi-universal conductivity.

In the limit $\Gamma_{max} \to \infty$, the CTRW approximation is represented by the electrical equivalent circuit shown in Fig. 8(a).[17] In the circuit all capacitances are equal while the resistances vary. The impedance $Z(\omega)$ is given by

$$Z(\omega) = \langle 1/(R^{-1} + i\omega C)\rangle, \qquad (47)$$

where the average is over the distribution of resistances. Corresponding to randomly varying free-energy barriers, the resistance probability distribution varies as R^{-1}, the analog of Eq. (23), and thus, the characteristic time $t = RC$ is distributed according to t^{-1}. If the maximum value of t is denoted by τ and the minimum value is zero, we now get
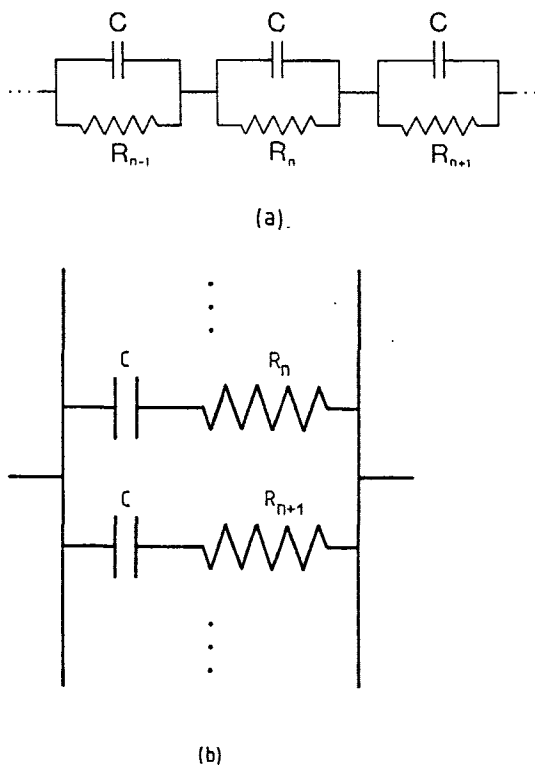

(a)

(b)

FIG. 8. Electrical equivalent circuits for (a) the CTRW approximation in the $\Gamma_{max} \to \infty$ limit and (b) the pair approximation. Note that the pair approximation does not have any dc conduction. This figure shows that the two approaches are, in a sense, complementary. This is also reflected by the fact that the exponent s in the pair approximation is a function of the logarithmic distance from ω to the high-frequency cutoff [Eq. (5)], while s in the CTRW case is a function of the logarithmic distance to the effective low-frequency cutoff at ω_m [Eq. (28)].

$$Z(\omega) = \frac{K}{C} \int_0^\tau \frac{1}{t^{-1} + i\omega} \frac{dt}{t} = \frac{K}{C} \int_0^\tau \frac{1}{1 + i\omega t} dt. \qquad (48)$$

Since t^{-1} is not normalizable, the constant K is unknown and must be determined self-consistently. When this is done after the integration has been carried out, Eq. (48) reduces to Eq. (27). Note that it is straightforward to actually build the equivalent circuit in the laboratory, since the ordinary resistance scale is logarithmic just as the distribution used in Eq. (48).

The physical interpretation of the circuit is not quite obvious. Intuitively, one may argue that the one-dimensional circuit gives a satisfactory representation of conduction in three dimensions because the broad distribution of jump rates implies that conduction is dominated by contributions from certain optimal paths, the "percolation" paths.[18] Usually, the circuit of Fig. 8(a) is not related to hopping models but applied to conduction in a solid with macroscopic inhomogeneities with different dc resistances.[20,62,63] In such models the frequency dispersion of the conductivity is described by a generalization of the Maxwell–Wagner theory of inhomogeneous dielectrics, as first suggested by Isard.[24] The reduction from three to one dimension has never really been justified.

The equivalent circuit of the renormalized CTRW approximation is complementary to the equivalent circuit of the pair approximation shown in Fig. 8(b). In the pair approximation conduction takes place in parallel channels corresponding to additive admittances, while in the CTRW case the impedances are additive, intuitively expressing the fact that charge carriers on the percolation paths have to overcome a sequence of barriers.

The random free-energy barrier model is essentially identical to Stevels' and Taylor's 1957 "random potential energy model" for glass ionic conductivity.[21,23] This model was never generally accepted because it was thought to contradict experiment on two important points[7,8,15]: It was believed that a model based on a distribution of energy barriers can never give temperature-independent loss peaks, and also that the BNN relation implies the ac conducting ions to have the same activation energy as those behind dc conduction. These objections are incorrect, however.[19] If all barriers are equally likely, the jump frequency distribution is proportional to Γ^{-1} at all temperatures, yielding a temperature-independent loss peak, and there is certainly no problem in having a whole range of activation energies involved in the conduction process. Actually, from figures like Figs. 1 and 6 one can conclude that ac conduction must have a smaller activation energy than dc conduction. Thus, the experimental facts seem to more or less force one to base the theory for ac conduction on a distribution of energy barriers, where the dc conductivity activation energy is the maximum activation energy involved in the conduction process. Correspondingly, the loss peak frequency, which marks the onset of ac conduction, must be essentially the minimum jump rate in the solid: On a time scale larger than ω_m^{-1} the conductivity is frequency independent so the solid "looks" homogeneous to the quasi-particles. This can only come about if ω_m is the effective minimum jump frequency so that many jumps necessarily are involved for times $\gg \omega_m^{-1}$. Note that, since both

dc conduction and loss peak frequency are determined by the maximum energy barriers, the proportionality between $\sigma(0)$ and ω_m in the BNN relation becomes obvious from this analysis of experimental facts, without any calculation.

The random free-energy barrier model predicts a frequency dependence of $\sigma'(\omega)$ that is very close to a power law (Fig. 3). This may seem surprising since there is no power law hidden in Eq. (27), but it is just another illustration of the old truth that "anything is a straight line in a log-log plot." Because of this, care must be taken in deducing power laws from apparently straight lines in log-log plots, though it may still be convenient to discuss measurement and theory in terms of the "exponent" s.

At the end of Sec. II was listed in eight points the universally found experimental facts on ac conduction in disordered solids, and in Sec. IV it was shown that the random free-energy barrier model explains all eight points. Here we want to point out that these facts are not independent but closely interrelated, as becomes evident when they are discussed in light of the model. The fact that $\sigma'(\omega)$ has a temperature-independent shape implies that, at lowering the temperature, one measures further and further out on the master curve which is known to exist. Consequently, since $s(\omega) \rightarrow 1$ as $\omega\tau \rightarrow \infty$, the exponent s measured in a fixed range of frequencies converges to one as $T \rightarrow 0$. The BNN relation implies that $\sigma(0)$ and ω_m are proportional [apart from the factor of T^{-1} in $\Delta\epsilon$ (Eq. (33))]. Thus, if the temperature is lowered, the conductivity curve is displaced in direction 45° to the x axis in the log-log plot. It is now obvious that the ac conductivity is less temperature dependent than the dc conductivity and that, for exponents very close to one, the ac conductivity must be practically temperature independent. In particular, this is always the case at low temperatures.

The BNN relation implies a convenient scaling principle which allows one to construct a master curve from measurements at different temperatures at a fixed frequency. In the random free-energy barrier model, the scaling principle is reflected by the fact that the whole of $\sigma(\omega)$ is determined from a knowledge of the two numbers $\sigma(0)$ and $\Delta\epsilon$. Note that, experimentally, $\Delta\epsilon$ is usually not very far from one so it is possible to get a rough idea of the magnitude of $\sigma'(\omega)$ just from a knowledge of the dc conductivity: Putting $\Delta\epsilon \approx 1$ in Eq. (30) we get $\tau \approx \epsilon_0/\sigma(0)$ which, when substituted into Eq. (27), determines $\sigma'(\omega)$. In particular, at large frequencies Eq. (27) implies $\sigma'(\omega) \approx \sigma(0)[\omega\tau/\ln^2(\omega\tau)]$ so a rough estimate of $\sigma'(\omega)$ here is

$$\sigma'(\omega) \approx \epsilon_0\omega/\ln^2(\omega\epsilon_0/\sigma(0)) . \tag{49}$$

To summarize the paper, an important point is the irrelevance of Γ_{max} for $\sigma(\omega)$ in realistic situations. Letting Γ_{max} go to infinity, one arrives at "renormalized" hopping models for which the pair approximation never becomes valid at high frequencies. In a sense the pair approximation is complementary to the renormalized CTRW approximation, as illustrated in Fig. 8. The frequency-dependent conductivity of the random free-energy barrier model is quite similar to that of a number of models discussed by Summerfield.[48] This supports the hypothesis of quasi-universality: All models based on a broad jump frequency distribution yield almost

identical $\sigma(\omega)$ in the $\Gamma_{max} \rightarrow \infty$ limit. Thus, Eq. (27) is representative for many models. This equation is in reasonably good agreement with experiment. It seems, however, that the spread among experiments is larger than among theories and one cannot really say quasi-universality applies to experiments. More work has to be done to explain this. Since quasi-universality seems to apply among the hopping models described by Eq. (7), it is possible that these linearized models are too simple and that interactions have to be taken into account, including that due to Fermi statistics, to explain experimental deviations from quasi-universality.

The fact that all disordered solids have similar ac properties means that only little can be learned about a solid from measuring its frequency-dependent conductivity.[32,48,64] Pollak and Pike have suggested that details of any particular conduction mechanism should be contained in deviations from linearity in the frequency dependence, i.e., from $s = 1$.[64] But as is clear from the model discussed in this paper, there are significant deviations from linearity 10 or more decades above the loss peak frequency, deviations that are solely a consequence of the low-frequency cutoff and which provide no important microscopic information. Tentatively, we instead suggest that details of any particular conduction mechanism in principle could be inferred from deviations from Eq. (27), which may be regarded as a zero-order approximation to reality, but more theoretical work is needed before microscopic details about the conduction mechanism can be inferred from the measured $\sigma'(\omega)$.

As regards the question of the best way to present data we recommend the use of $\sigma'(\omega)$. This quantity is fundamental, being directly related to the equilibrium current-current fluctuations.[61] The use of the frequency-dependent dielectric constant has one virtue, though: namely, that it reveals loss peaks, the existence of which is crucial to prove that dc and ac conduction are indeed due to the same mechanism. The electric modulus is not recommended because this quantity mixes in effects of ϵ_∞ which, if the ideas advanced here are correct, are independent of and unrelated to the ac conductivity. In the present approach, the total admittance is a sum of a hopping contribution and a purely imaginary dielectric contribution from the atomic polarizability (Fig. 9).
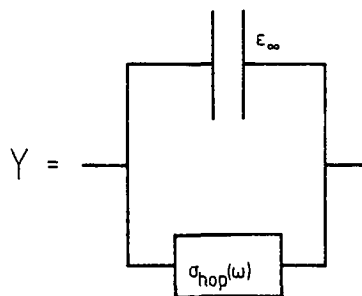

FIG. 9. Total admittance Y for a semiconducting disordered solid according to hopping models. The admittance is a sum of the hopping contribution discussed in the present paper, and a totally unrelated purely imaginary contribution from the atomic polarizability given by the high-frequency dielectric constant ϵ_∞. If this picture is correct, the use of the electric modulus in representing data is inconvenient since it mixes in effects of ϵ_∞ that are independent of, and unrelated to, the hopping admittance.

Finally, it should be emphasized again that an understanding of ac conduction and its relation to dc conduction is important, even if one is only interested in steady-state transport properties like dc conductivity, Hall resistance, thermopower, etc. From the present paper it seems it can be concluded that a whole distribution of energy barriers is involved in dc transport in disordered solids. Theories which do not take this into account are incomplete.

ACKNOWLEDGMENTS

[1] A. R. Long, Adv. Phys. 31, 553 (1982).

[2] A. K. Jonscher, Nature 267, 673 (1977).

[3] A. E. Owen, J. Non-Cryst. Solids 25, 372 (1977).

[4] N. F. Mott and E. A. Davis, *Electronic Processes in Noncrystalline Materials*, 2nd ed. (Clarendon, Oxford, 1979).

[5] A. Mansingh, Bull. Mater. Sci. (India) 2, 325 (1980).

[6] A. E. Owen, in *Progress in Ceramic Science*, edited by J. E. Burke (Macmillan, New York, 1963), Vol. 3, p. 77.

[7] D. Ravaine and J. L. Souquet, in *Solid Electrolytes*, edited by P. Hagenmuller and W. Van Gool (Academic, New York, 1978), p. 277.

[8] M. Tomozawa, in *Treatise on Materials Science*, edited by M. Tomozawa (Academic, New York, 1977), Vol. 12, p. 283.

[9] M. D. Ingram, Phys. Chem. Glasses 28, 215 (1987).

[10] A. J. Epstein, H. Rommelmann, M. Abkowitz, and H. W. Gibson, Polym. Prepr. 23, 88 (1982).

[11] C. A. Vincent, Prog. Solid State Chem. 17, 145 (1987).

[12] M. A. Careem and A. K. Jonscher, Philos. Mag. 35, 1489 (1977).

[13] M. Suzuki, J. Phys. Chem. Solids 41, 1253 (1980).

[14] M. Pollak and T. H. Geballe, Phys. Rev. 122, 1742 (1961).

[15] J. O. Isard, J. Non-Cryst. Solids 4, 357 (1970).

[16] J. C. Dyre, Phys. Lett. 108A, 457 (1985).

[17] J. C. Dyre, J. Phys. (Paris) Colloq. 46, C8-343 (1985).

[18] J. C. Dyre, IMFUFA text No. 97 (University of Roskilde, 1985).

[19] J. C. Dyre, J. Non-Cryst. Solids 88, 271 (1986).

[20] P. B. Macedo, C. T. Moynihan, and R. Bose, Phys. Chem. Glasses 13, 171 (1972).

[21] J. M. Stevels, in *Handbuch der Physik*, edited by S. Flügge (Springer, Berlin, 1957), Vol. 20, p. 350.

[22] J. M. Stevels, J. Phys. (Paris) Colloq. 46, C8-613 (1985).

[23] H. E. Taylor, J. Soc. Glass Technol. 41, 350T (1957); *ibid.* 43, 124T (1959).

[24] J. O. Isard, Proc. Inst. Elec. Eng. 109B, Suppl. No. 22 (1962), p. 440.

[25] J. L. Barton, Verres Réfr. 20, 328 (1966).

[26] T. Nakajima, in *1971 Annual Report, Conference on Electric Insulation and Dielectric Phenomena* (National Academy of Sciences, Washington, DC, 1972), p. 168.

[27] H. Namikawa, J. Non-Cryst. Solids 18, 173 (1975).

[28] A. Mansingh, J. M. Reyes, and M. Sayer, J. Non-Cryst. Solids 7, 12 (1972).

[29] A. R. Long, J. McMillan, N. Balkan, and S. Summerfield, Philos. Mag. B (to be published).

[30] C. G. Garton, "General Discussion on Dielectrics" Trans. Faraday Soc. 42, 56 (1946).

[31] I. G. Austin and N. F. Mott, Adv. Phys. 18, 41 (1969).

[32] R. M. Hill and A. K. Jonscher, J. Non-Cryst. Solids 32, 53 (1979).

[33] S. R. Elliott, Philos. Mag. 36, 1291 (1977).

[34] H. Scher and M. Lax, Phys. Rev. B 7, 4491 (1973); *ibid.* 7, 4502 (1973).

[35] A. Miller and E. Abrahams, Phys. Rev. 120, 745 (1960).

[36] E. W. Montroll and G. H. Weiss, J. Math. Phys. 6, 167 (1965).

[37] J. M. Ziman, *Models of Disorder* (Cambridge University, Cambridge, 1979).

[38] F. Yonezawa, in *The Structure and Properties of Matter*, edited by T. Matsubara (Springer, Berlin, 1982), p. 383.

[39] V. V. Bryksin, Sov. Phys. Solid State 22, 1421 (1980).

[40] S. Summerfield, Solid State Commun. 39, 401 (1981).

[41] B. Movaghar and W. Schirmacher, J. Phys. C 14, 859 (1981).

[42] T. Odagaki and M. Lax, Phys. Rev. B 24, 5284 (1981).

[43] G. E. Pike, Phys. Rev. B 6, 1572 (1972).

[44] S. Summerfield and P. N. Butcher, J. Phys. C 15, 7003 (1982).

[45] R. M. Hill and A. K. Jonscher, Cont. Phys. 24, 75 (1983).

[46] K. L. Ngai and C. T. White, Phys. Rev. B 20, 2475 (1979).

[47] R. Kubo, J. Phys. Soc. Jpn. 12, 570 (1957).

[48] S. Summerfield, Philos. Mag. B 52, 9 (1985).

[49] S. Glasstone, K. J. Laidler, and H. Eyring, *The Theory of Rate Processes* (McGraw-Hill, New York, 1941).

[50] H. Böttger and V. V. Bryksin, *Hopping Conduction in Solids* (Akademie, Berlin, 1985).

[51] B. I. Shklovskii and A. L. Efros, *Electronic Properties of Doped Semiconductors* (Springer, Berlin, 1984).

[52] G. A. Niklasson, J. Appl. Phys. 62, R1 (1987).

[53] J. C. Kimball and L. W. Adams, Phys. Rev. B 18, 5851 (1978).

[54] M. Lax and T. Odagaki, in *Macroscopic Properties of Disordered Media*, edited by R. Burridge (Springer, Berlin, 1982), p. 148.

[55] J. Klafter and R. Silbey, Surf. Sci. 92, 393 (1980).

[56] J. K. E. Tunaley, Phys. Rev. Lett. 33, 1037 (1974).

[57] J. C. Dyre, J. Phys. C 21, 2431 (1988).

[58] P. N. Butcher, J. Phys. C 7, 2645 (1974).

[59] M. Gevers and F. K. Du Pré, "General Discussion on Dielectrics" Trans. Faraday Soc. 42, 47 (1946).

[60] M. Lax, Phys. Rev. 97, 629 (1955).

[61] J. R. Macdonald, J. Appl. Phys. 58, 1955 (1985); *ibid.* 58, 1971 (1985); *ibid.* 62, R51 (1987).

[62] R. Stumpe, Phys. Status Solidi A 88, 315 (1985).

[63] A. Y. Vinnikov and A. M. Meshkov, Sov. Phys. Solid State 27, 1159 (1985).

[64] M. Pollak and G. E. Pike, Phys. Rev. Lett. 28, 1449 (1972).

[65] E. B. Ivkin and B. T. Kolomiets, J. Non-Cryst. Solids 3, 41 (1970).

[66] F. S. Howell, R. A. Bose, P. B. Macedo, and C. T. Moynihan, J. Phys. Chem. 78, 639 (1974).

[67] I. M. Hodge and C. A. Angell, J. Chem. Phys. 67, 1647 (1977).

[68] L. Murawski, J. Non-Cryst. Solids 90, 629 (1987).

[69] A. P. Bhatt, W. A. Anderson, and P. Ehrlich, Solid State Commun. 47, 997 (1983).

[70] H. M. Kizilyalli and P. R. Mason, Phys. Status Solidi A 36, 499 (1976).

[71] A. Mansingh, R. P. Tandon, and J. K. Vaid, Phys. Rev. B 21, 4829 (1980).

[72] M. Sayer, A. Mansingh, J. M. Reyes, and G. Rosenblatt, J. Appl. Phys. 42, 2857 (1971).

[73] E. A. Davis and N. F. Mott, Philos. Mag. 22, 903 (1970).

[74] A. R. Long and N. B. Balkan, J. Non-Cryst. Solids 35-36, 415 (1980).

[75] S. R. Elliott, Adv. Phys. 36, 135 (1987).

Some remarks on ac conduction in disordered solids

Jeppe C. Dyre

IMFUFA, Roskilde Universitetscenter, Postbox 260, DK-4000 Roskilde, Denmark

Alternating current conduction in disordered solids is discussed, from a general point of view. As regards experiment, it is argued that the observed power-law behavior of the frequency-dependent conductivity, $\sigma(\omega)$, is probably not fundamental, that the Ngai relation between dc and ac conductivity activation energies follows from independent experimental facts, that the shape of the modulus peak has no fundamental significance, and that there are interesting mechanical analogies to the observed ac electrical behavior. As regards hopping models for ac conduction, it is shown that three commonly used arguments against the existence of a distribution of activation energies are all incorrect. Also, it is shown that $\sigma(\omega) \neq \sigma(0)$ only if there are correlations in the directions of different charge carrier jumps; in particular this result implies $\sigma(\omega) = \sigma(0)$ for all frequencies in the continuous time random walk (CTRW) model. In the final section a number of open problems are listed, and suggestions are made for future work.

1. Introduction

This paper discusses ac conduction in non-metallic disordered solids. A number of remarks are made, most of which are not new but are still not generally appreciated. The class of disordered solids with interesting ac behavior is very large, including amorphous semiconductors [1,2], ionic conductive glasses [3,4], conducting polymers [5,6], various defective or doped crystals [7–9], and many polycrystals [10,11].

Several different representations of ac data are used. One possibility is the complex frequency-dependent conductivity, $\sigma(\omega) = \sigma'(\omega) + i\sigma''(\omega)$. A common alternative is the complex electric modulus, $M(\omega) = M'(\omega) + iM''(\omega)$, defined [12] by

$$M(\omega) = \frac{i\omega}{\sigma(\omega)}.$$ (1)

Data may also be presented in terms of the complex impedance [13,14], or in terms of the complex dielectric constant which is defined by

$$\epsilon_0\epsilon(\omega) = \frac{\sigma(\omega) - \sigma(0)}{i\omega}.$$ (2)

Here, ϵ_0 is the vacuum permittivity. The negative imaginary part of $\epsilon(\omega)$, $\epsilon''(\omega)$, is referred to as the dielectric loss.

AC conduction in quite different disordered solids shows a number of common features, a surprising fact which is often overlooked. For each of the above listed classes of glassy solids one observes, almost without exception [15–19], that at high frequencies $\sigma'(\omega)$ follows a power-law with an exponent s in the range 0.7–1.0; s goes to 1 as the temperature goes to zero. Around the dielectric loss peak frequency, ω_m, there is a transition to a frequency-independent conductivity below ω_m. The Barton–Nakajima–Namikawa (BNN) relation [20–22] is satisfied:

$$\sigma(0) = p\,\Delta\epsilon\epsilon_0\omega_m,$$ (3)

where $\Delta\epsilon = \epsilon(0) - \epsilon(\infty)$ and p is a numerical constant of order one. Finally, the time–temperature

J.C. Dyre / ac conduction in disordered solids

superposition principle is usually obeyed, i.e., the fact that the shape of the $\sigma'(\omega)$ curve is temperature-independent when plotted in a log–log plot.

The BNN relation signals an important correlation between dc and ac properties. It applies to most disordered solids with a large charge carrier concentration, the solids which are of interest here. If the loss is not due to migrating charge carriers but is dipolar in origin, one does not expect the BNN relation to be obeyed; clearly in such solids any dc conduction would have nothing to do with the dielectric loss due to the dipoles.

The outline of the paper is the following. In section 2, some points relating to experiment are discussed. Section 3 is devoted to hopping models for ac conduction. Section 4 deals with a number of open problems and gives suggestions for future work. Finally, section 5 is the conclusion.

2. Remarks relating to experiment

2.1. The observed power–law frequency dependence of the conductivity is hardly fundamental

The commonly observed large-frequency power–law

$$\sigma'(\omega) \propto \omega^s \tag{4}$$

is deduced from [log $\sigma'(\omega)$] having a linear dependence on log ω. Since both frequency and conductivity usually vary several decades, it is reasonable to plot data in a log–log plot. However, log–log plots are dangerous; an old saying [23] warns: "Almost anything is a straight line in a log–log plot". The term "anything" refers to any function $f(x)$ which changes several decades when x changes several decades. To illustrate this point, fig. 1 shows a log–log plot of $\sigma'(\omega)$ where $\sigma(\omega)$ is given by

$$\sigma(\omega) = \sigma(0) \frac{i\omega\tau}{\ln(1 + i\omega\tau)}. \tag{5}$$

This function gives a reasonably good fit to many data [19]. (There is, of course, always an additional purely imaginary contribution to the conductivity from the infinite frequency dielectric
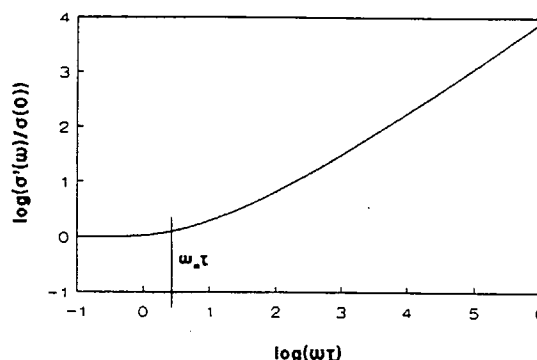

Fig. 1. Log–log plot of the real part of the function $\sigma(\omega)$ given by eq. (5). Although there is no power–law in this function, it follows closely a power–law at high frequencies. The function gives a good fit to many data [19]; this illustrates that one cannot conclude from experiment that a power–law frequency dependence of the ac conductivity of disordered solids is fundamental. The vertical line marks the dielectric loss peak frequency which is always found where the conductivity starts increasing.

constant.) At high frequencies, $\sigma'(\omega)$ follows closely a straight line in the log–log plot, although there is no power–law hidden in eq. (5). Most workers would report an exponent around 0.8 for data following fig. 1. There is no problem with this as long as one speaks only about *approximate* power–laws. However, there is no basis for concluding from $\sigma'(\omega)$ measurements that power–laws are *fundamental*, as is sometimes done [24–26]. If one wants to look into the existence of exact power–laws in data, a much more sensitive method is to study the inverse loss tangent, as shown recently by Niklasson [27].

2.2. The Ngai relation is a consequence of the BNN relation and the time–temperature superposition principle

The Ngai relation [28] correlates three quantities, the activation energy of the dielectric loss peak frequency, ΔE_m, the ac conductivity activation energy, ΔE_{ac}, and the exponent s of eq. (4), as follows:

$$\Delta E_{ac} = (1 - s)\Delta E_m. \tag{6}$$

The quantity ΔE_{ac} is defined as minus the slope of the tangent in the plot of $\log(\sigma'(\omega))$ versus T^{-1}. In general, this quantity, as well as the exponent s, depend on temperature. Equation (6) is confirmed by experiment [28] (ΔE_{ac} is sometimes derived from NMR experiments which, however, give the same activation energy as that of ac conduction [4,29]). As illustrated in fig. 1, the loss peak frequency, ω_m, is the characteristic frequency for the onset of ac conduction. Since the dielectric loss strength, $\Delta\epsilon$, is only weakly temperature-dependent, the essence of the BNN relation is an approximate proportionality between $\sigma(0)$ and ω_m. Remember that the time–temperature superposition principle is the fact that, at different temperatures, one observes in the log–log plot parallel displacements of the same $\sigma'(\omega)$ curve. Because of the proportionality between $\sigma(0)$ and ω_m, as the temperature changes, the $\sigma'(\omega)$ curve is displaced in a direction $45°$ to the x-and y-axis. Since activation energies are given as derivatives of the logarithm, it is now straightforward to show that eq. (6) is automatically obeyed whenever $\sigma'(\omega)$ follows an approximate power–law with exponent s.

2.3. The shape of the modulus peak has no fundamental significance

For all disordered solids the imaginary part of the electric modulus, $M''(\omega)$, has a peak at a frequency which is usually of the same order of magnitude as ω_m. The shape of the modulus peak is often attributed to a spectrum of relaxation times [12,30]. This spectrum, however, has no significance relative to the motion of the mobile charge carriers. This is because there is always, in parallel to the charge transport due to the mobile charge carriers, the current due to the infinitely fast dielectric displacement. The strength of the latter current is given by the infinite frequency dielectric constant, ϵ_x. If ϵ_x is changed, the shape of $M''(\omega)$ is affected [31]. This dependence is illustrated in fig. 2 where the loss modulus is plotted in a log–log plot for hypothetical solids with charge carrier contribution to the conductivity given by eq. (5) but with different values of ϵ_x.
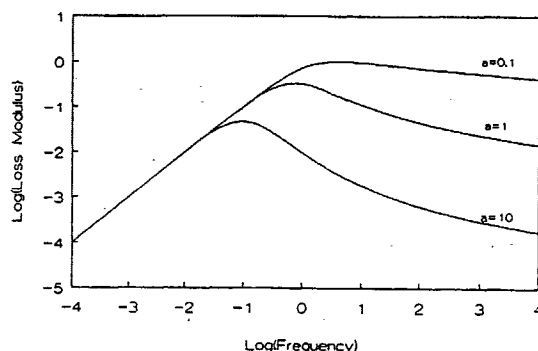

Fig. 2. Log–log plot of $M''(\omega)$ for hypothetical solids with the same hopping contribution to the conductivity but with different high frequency dielectric constant. The conductivity is given as a sum of eq. (5) and the purely imaginary contribution $i\omega\epsilon_x\epsilon_0$. The figure shows the dimensionless quantity $M''(\omega)\sigma(0)\tau$ as function of $\omega\tau$ for three different values of
$$a = \epsilon_0\epsilon_x/\sigma(0)\tau.$$

2.4. There are close mechanical analogies to the observed ac behavior

(a) Many ionic conductive glasses have an internal friction loss peak at the dielectric loss peak frequency [4,32,33]. This mechanical loss must be due to ionic motion and thus mechanical and electrical properties of ionic glasses are strongly correlated.

(b) The frequency-dependent viscosity, $\eta(\omega)$, of a typical highly viscous liquid, e.g., a polymeric liquid, looks very much like $1/\sigma(\omega)$ for a typical disordered solid. Thus, at low frequencies $|\eta(\omega)|$ is constant whereas at higher frequencies $|\eta(\omega)|$ decreases like an approximate power–law [34]. Now, suppose a foreign microscopic particle is introduced into a viscous liquid. If the particle is described by hydrodynamics, its frequency-dependent mobility (velocity/force) varies as $1/\eta(\omega)$. Thus, the particle moves about in the liquid much as a charge carrier moves about in a disordered solid. Conductivity measurements on ions dissolved in viscous liquids, where the observed conductivity is indeed like that of a disordered solid, confirms this picture [35,36].

3. Remarks relating to hopping models

In hopping models, dc and ac conduction are both due to hopping charge carriers [37]. The solid disorder is usually incorporated by assuming randomly varying transition rates $\Gamma(s' \to s)$ for transitions from site s' to site s. If $P(s, t)$ is the probability for a particle to be at site s at time t, a hopping model is described by the master equation [37,38]

$$\frac{\partial P(s, t)}{\partial t} = -\gamma_s P(s, t) + \sum_{s'} \Gamma(s' \to s) P(s', t),$$

(7)

where

$$\gamma_s = \sum_{s'} \Gamma(s \to s').$$

(8)

Equation (7) applies to the most commonly studied case of a system of non-interacting charge carriers. It refers to the zero external field situation. More generally, Γ depends on the external field, but the fluctuation–dissipation theorem allows one to calculate $\sigma(\omega)$ purely from a knowledge of the zero field jump frequencies. It can be shown that in hopping models $\sigma'(\omega)$ is always an increasing function of ω [39]. No exact analytical methods are available for evaluating $\sigma(\omega)$, but various approximate methods exist [37,38,40,41].

3.1. Three common arguments against hopping models are all incorrect

In most hopping models the variation in hopping rates is assumed to derive from a spread in activation free energies, $P(\Delta F)$. The following three arguments have traditionally been put forward against the existence of any $P(\Delta F)$.

(a) *"Any distribution of activation energies implies the dc conductivity is non-Arrhenius."* This is not necessarily true; in some models $\sigma(0)$ *is* indeed Arrhenius with an activation energy which is simply the maximum barrier encountered on any 'percolation' path between the electrodes. In one dimension, exact results are available [42,43]. Here, $p(\Delta F) = \text{constant}$, or more generally $P(\Delta F)$ proportional to $\exp(-\Delta F/\Delta F_0)$, give an

exactly Arrhenius $\sigma(0)$ if a sharp cut-off at a maximum activation energy is assumed. Similar results are obtained from the approximate analytical methods available in three dimensions [37,38,40,41].

(b) *"The BNN relation implies that ac conduction is due to processes with activation energy equal to that of $\sigma(0)$."* The BNN relation implies that the dielectric loss peak frequency has the same activation energy as $\sigma(0)$. However, this does not rule out the possibility of a distribution of activation energies being responsible for the frequency dispersion. Thus, in most hopping models ω_m corresponds to the *lowest* effective jump frequency and this quantity is determined by the *maximum* energy barrier, just as $\sigma(0)$ is itself [44].

(c) *"The time–temperature superposition principle contradicts the existence of a distribution of energy barriers."* In some cases it can be clearly excluded that a distribution of activation energies is responsible for the observed frequency dispersion [45]. In general, however, this possibility cannot be ruled out. In particular, it is incorrect to claim, as is often done, that the existence of a distribution of activation energies necessarily implies a broadening of the distribution of relaxation times as the temperature is decreased, thereby violating the time–temperature superposition principle. First, for experimental reasons, the time–temperature superposition principle is usually checked only over a relatively narrow range of temperatures and frequencies; here any sufficiently broad distribution of activation energies will obey the time–temperature superposition principle rather accurately. Second, for the flat distribution of activation energies, $p(\Delta F) = \text{constant}$, the time–temperature superposition principle is obeyed exactly. In this case, the distribution of jump frequencies varies as Γ^{-1} at all temperatures. Thus, as long as one assumes a sufficiently broad distribution of activation energies, approaching the flat distribution, there is no contradiction with experiment.

Traditionally, points (a), (b) and (c) have been thought to imply at most a quite *narrow* $p(\Delta F)$, which obviously cannot account for the observed very *broad* loss peaks. This is why an early model like Stevels' and Taylor's random potential en-

ergy model from 1957 [46,47] was never considered a serious candidate for explaining experiments.

3.2. The conductivity is frequency-dependent only if there are correlations between the directions of charge carrier jumps

Thus, if each jump occurs in a random direction one has $\sigma(\omega) = \sigma(0)$ at all frequencies [38]. To prove this result, we first recall the fluctuation–dissipation theorem which expresses $\sigma(\omega)$ in terms of the zero-field auto-correlation function of the total current in volume V, $J(t)$, in the following way [48]:

$$\sigma(\omega) = \frac{1}{3k_B TV} \int_0^\infty \langle J(0)J(t)\rangle e^{-i\omega t}\, dt. \qquad (9)$$

Here k_B is the Boltzmann constant and T is the temperature. In hopping models the jumps are instantaneous and $J(t)$ is a sum of delta functions. If the ith jump occurs at time, τ_i, and displaces a particle by Δr_i, one has

$$J(t) = q\sum_i \Delta r_i \delta(t - \tau_i), \qquad (10)$$

where q is the charge of the carrier. For $\langle J(0)J(t)\rangle$ to be non-zero at any $t > 0$, one must have $\langle \Delta r_i \Delta r_j \rangle \neq 0$ for at least one pair of $i < j$. However, whenever the direction of the latter jump, Δr_j, is random, one has necessarily $\langle \Delta r_i \Delta r_j \rangle = 0$. Consequently, $\langle J(0)J(t)\rangle$ is proportional to $\delta(t)$ and the conductivity is frequency-independent according to eq. (9). This result has two important consequences.

(a) *Any random walk in a spatially homogeneous medium has $\sigma(\omega) = \sigma(0)$*. This is true even for non-Markovian random walks. An important example is the continuous time random walk model (CTRW) of Montroll and Weiss [49]. This model is characterized by the so-called waiting-time distribution function, $\psi(t)$, which is the probability for a particle to jump at time, t, given the particle last jumped at $t = 0$. In 1973, Scher and Lax erroneously calculated $\sigma(\omega)$ in terms of $\psi(t)$ [50]; the error was pointed out by Tunaley who proved by direct calculation that there is no frequency dispersion of the conductivity in the
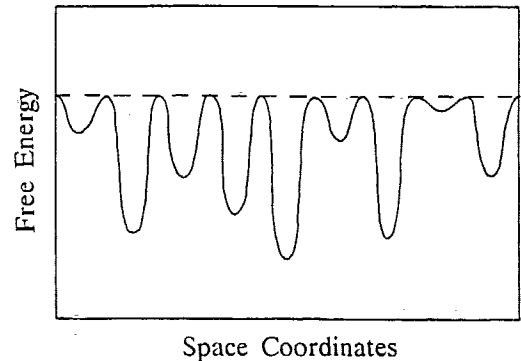

Space Coordinates

Fig. 3. Free energy surface of a hopping model which, because the direction of each charge carrier jump is random, has no frequency dependence of the conductivity. This example shows that a distribution of waiting times is not enough to ensure frequency dependence of the conductivity. Also, since the model has non-trivial transient behavior [55], the example shows that there is no correlation between ac conduction and transient behavior.

CTRW model [51,52]. While the CTRW model is itself of no use as a model for ac conduction, the formalism developed by Scher and Lax gives rise to a very useful approximation, usually referred to as the CTRW approximation or the Hartree approximation [40].

(b) *The existence of a distribution of relaxation times in a hopping model is not enough to ensure frequency dependence of the conductivity.* Consider hopping in a potential where all maxima are equal but the minima vary (fig. 3). Obviously, in this model there is a distribution of waiting times. However, the direction of each charge carrier jump is random, so $\sigma(\omega) = \sigma(0)$. This has also been shown by explicit calculation [53,54]. In passing, we note that the model of fig. 3 is a useful model for the transient behavior of photo-excited charge carriers in amorphous semiconductors [55]. Here, a brief laser pulse excites the electrons to random states at $t = 0$, and the current in an external field subsequently monitors the thermalization of the charge carriers. This example shows that, in general, transient currents cannot be calculated from $\sigma(\omega)$, as has been predicted from the study of specific models [56,57].

224 *J.C. Dyre / ac conduction in disordered solids*

4. Open problems and suggestions for future work

4.1. Are reported data always reliable and not due to contact effects?

Electrode effects may cause serious problems for the interpretation of measurements. One might think it could easily be checked, by simply varying the sample size, whether or not the bulk response is measured. This is sometimes possible [58]; more often, however, it is quite difficult to prepare two samples with identical physical properties. The contacts are usually modeled as simple RC elements, implying the bulk response is measured at sufficiently high frequencies. It has never been proved that this procedure is correct. In fact, it has been suggested that contacts and interfaces play a dominant role in the whole range of frequencies measured [59]. While this is probably too drastic a statement, even a quite simple model of the electrode/sample interface predicts a non-trivial frequency dependence of the measured conductivity, varying like $\omega^{1/2}$ [32,60]. In conclusion, it is not obvious that all reported data are bulk, and more work is needed to clarify the role of contacts.

4.2. Are dc and ac conduction always due to the same mechanism?

The BNN relation shows that dc and ac conduction in disordered solids are strongly correlated. The simplest possibility is that dc and ac conduction are both due to the same mechanism, as is the case in hopping models. The existence of a loss peak supports this; loss peaks are very hard to explain otherwise. It should be noted that, when there is no dielectric loss peak, a BNN-like relation may still exist between $\sigma(0)$ and the characteristic frequency ω'_m defined by

$$\sigma'(\omega'_m) = 2\sigma(0).\tag{11}$$

(If a loss peak does exist, ω'_m is close to ω_m.) Suppose $\sigma'(\omega) = \sigma(0) + A\omega$. Then clearly ω'_m is proportional to $\sigma(0)$ although this does not reflect any relation between dc and ac conduction. Thus, the existence of a genuine loss peak is

necessary to ensure ac and dc conduction are due to the same mechanism. The existence of loss peaks should always be carefully checked in experiments.

4.3. There are theoretical reasons to expect $\epsilon''(\omega)$ is proportional to $\omega^{1/2}$ on the low-frequency side of the dielectric loss peak

In hopping models, one has always $\sigma(\omega) = \sigma(0) + C(i\omega)^{3/2}$ as $\omega \to 0$ [38,61], an example of the celebrated 'long time tails'. However, there seems to be no experimental evidence for this prediction. As one of the few general predictions in the field, it should be tested carefully on a number of disordered solids. Unfortunately electrode effects cause very serious problems for measuring accurately the low frequency side of the loss peak, and the prediction may be very difficult to verify.

4.4. Does any solid exist which has $\sigma'(\omega) \ll \epsilon_0\omega$?

A puzzling phenomenon is the fact that, apparently, any solid has a conductivity $\sigma'(\omega)$ which is at least of order $\epsilon_0\omega$ [16]. Thus, at 1 MHz the conductivity is never much less than 10^{-6} $(\Omega$ cm$)^{-1}$. This rule seems to apply without exception, even to single crystal insulators. It could be a spurious effect due to contact effects [59], or due to experimental problems in distinguishing properly between $\sigma'(\omega)$ and $\sigma''(\omega)$ ($\sigma''(\omega)$ has always a sizable contribution from the infinite frequency dielectric constant). If the effect is real, an explanation is very much needed. Is it possible that even the most 'perfect' single crystal contains enough defects to account for this observation?

4.5. What kind of measurements could supplement the measurement of $\sigma(\omega)$?

The ac conductivity is the $k = 0$ component of the more general quantity $\sigma(k, \omega)$ (which, by the fluctuation–dissipation theorem, is related to equilibrium fluctuations of the kth Fourier component of $J(r, \omega)$). It would be interesting to have measurements of $\sigma(k, \omega)$. For electronic

systems, it is not obvious how to do these measurements but for ionic conductors neutron scattering can be applied, at least in principle. Other important measurements to supplement $\sigma(\omega)$ are transient current experiments (available only for electronic conductors) [62], excess current noise measurements [63], and large field experiments [17,32,64,65].

4.6. Is the observed ac behavior due to microscopic or macroscopic inhomogeneities?

The mathematical description of, and predictions for, inhomogeneous conductors are quite similar to that of hopping models [11,14]. Therefore, ac measurements alone do not reveal whether macroscopic or microscopic inhomogeneities are responsible for the observed frequency dispersion. It is not unlikely that, in some amorphous systems, there are inhomogeneities with dimensions of several hundred ångstroms. One way to distinguish between macroscopic and microscopic inhomogeneities is to measure the large field response; for macroscopic inhomogeneities, one expects non-linearities to set in at much lower fields than for microscopic inhomogeneities [17,32,66,67]. Unfortunately, electrode problems are a serious obstacle for reliable measurements of the non-linear conductivity.

4.7. There are two important open problems relating to hopping models:

4.7.1. How accurate are the presently available approximate analytical solutions of hopping models?

Perhaps the simplest hopping model is the random free energy barrier model which, when solved in the CTRW approximation, yields eq. (5) [19]. Numerical solutions of this model should be undertaken to assess the validity of eq. (5). Preliminary work shows that, in one dimension, eq. (5) works very well [68]. In general, the question 4.7.1. remains unanswered.

4.7.2. What is the cause of the quasi-universality among different models?

As noticed by Summerfield in 1985 [69], different models solved in the extended pair approxi-

mation (EPA) yield almost identical predictions for $\sigma(\omega)$, apart from an overall scaling of σ and ω. In fact, 'quasi-universality' applies not only to EPA models, but to most models studied so far. The cause of quasi-universality is not clear. The agreement between different hopping models is generally much better than the agreement between theory and experiment, where quasi-universality does not really apply. This indicates that the hopping models described by eq. (7) are perhaps too simple. It seems likely that interactions between the charge carriers have to be taken into account to arrive at a realistic model [70,71]. (Contrary to what is sometimes claimed, eq. (7) cannot describe interacting particles [72].)

The most important question relating to hopping models, of course, is as follows.

4.8. Are hopping models the correct framework for describing experiment?

Hopping models are simple and give reasonably good fits to experiments. However, it is possible that other types of models are more appropriate. Thus, the ω^s behavior of the dielectric loss in insulating dielectrics cannot be explained by any hopping model that allows a dc conduction, and the correct model for this phenomenon could be applicable also to describe loss in conducting dielectrics [24,25].

5. Conclusion

There are a number of important unsolved problems in the field of ac conduction. Because of this, measurements of $\sigma(\omega)$ do not yet provide unambiguous insight into the conduction process. More work, for instance along the lines of section 4, is needed before this goal is reached. In this sense, ac conduction is still a field in its infancy.

Niklasson, and A.S. Nowick is gratefully acknowledged.

References

[1] A.R. Long, Adv. Phys. 31 (1982) 553.

[2] S.R. Elliott, Adv. Phys. 36 (1987) 135.

[3] M.D. Ingram, Phys. Chem. Glasses 28 (1987) 215.

[4] C.A. Angell, Chem. Rev. 90 (1990) 523.

[5] W. Rehwald, H. Kiess and B. Binggeli, Z. Phys. B68 (1987) 143.

[6] C.A. Vincent. Prog. Solid State Chem. 17 (1987) 145.

[7] M. Pollak and T.H. Geballe. Phys. Rev. 122 (1961) 1742.

[8] M. Suzuki. J. Phys. Chem. Solids 41 (1980) 1253.

[9] D.P. Almond, A.R. West and R.J. Grant, Solid State Commun. 44 (1982) 1277.

[10] I.M. Hodge. M.D. Ingram and A.R. West. J. Electroanal. Chem. 74 (1976) 125.

[11] A.Y. Vinnikov and A.M. Meshkov. Sov. Phys. Solid State 27 (1985) 1159.

[12] P.B. Macedo, C.T. Moynihan and R. Bose, Phys. Chem. Glasses 13 (1972) 171.

[13] D. Ravaine and J.L. Souquet, in: Solid Electrolytes, eds. P. Hagenmuller and W. van Gool (Academic, New York, 1978) p. 277.

[14] J.R. Macdonald, ed., Impedance Spectroscopy (Wiley, New York, 1987).

[15] J.O. Isard. J. Non-Cryst. Solids 4 (1970) 357.

[16] A.K. Jonscher. Nature 267 (1977) 673.

[17] A.E. Owen. J. Non-Cryst. Solids 25 (1977) 372.

[18] A. Mansingh. Bull. Mater. Sci. (India) 2 (1980) 325.

[19] J.C. Dyre, J. Appl. Phys. 64 (1988) 2456.

[20] J.L. Barton, Verres Refr. 20 (1966) 328.

[21] T. Nakajima, in: 1971 Annual Report, Conference on Electric Insulation and Dielectric Phenomena (National Academy of Sciences, Washington. DC, 1972) p. 168.

[22] H. Namikawa. J. Non-Cryst. Solids 18 (1975) 173.

[23] A.S. Nowick, personal communication.

[24] K.L. Ngai, in: Non-Debye Relaxation in Condensed Matter, eds. T.V. Ramakrishnan and M. Raj Lakshmi (World Scientific, Singapore, 1987) p. 23.

[25] A.K. Jonscher, Dielectric Relaxation in Solids (Chelsea Dielectric, London, 1983).

[26] G.A. Niklasson, J. Appl. Phys. 62 (1987) R1.

[27] G.A. Niklasson, J. Appl. Phys. 66 (1989) 4350.

[28] K.L. Ngai, Solid State Ionics 5 (1982) 27.

[29] S.W. Martin, Mater. Chem. Phys. 23 (1989) 225.

[30] J.H. Ambrus, C.T. Moynihan and P.B. Macedo, J. Phys. Chem. 76 (1972) 3287.

[31] D.P. Almond and A.R. West, Solid State Ionics 11 (1983) 57.

[32] R.H. Doremus, Glass Science (Wiley, New York, 1973).

[33] W. Chomka, O. Gzowski, L. Murawski and D. Samatowicz, J. Phys. C11 (1978) 3081.

[34] R.B. Bird, R.C. Armstrong and O. Hassager, Dynamics of Polymeric Liquids, Vol. 1, 2nd Ed. (Wiley, New York, 1987).

[35] I.M. Hodge and C.A. Angell, J. Chem. Phys. 67 (1977) 1647.

[36] F.S. Howell, C.T. Moynihan and P.B. Macedo, Bull. Chem. Soc. Jpn. 57 (1984) 652.

[37] H. Böttger and V.V. Bryksin, Hopping Conduction in Solids (Akademie Verlag, Berlin, 1985).

[38] J.W. Haus and K.W. Kehr, Phys. Rep. 150 (1987) 263.

[39] J.C. Kimball and L.W. Adams, Phys. Rev. B18 (1978) 5851.

[40] T. Odagaki and M. Lax, Phys. Rev. B24 (1981) 5284.

[41] B. Movaghar, M. Grünewald, B. Pohlmann, D. Würtz and W. Schirmacher, J. Stat. Phys. 30 (1983) 315.

[42] S. Alexander, J. Bernasconi, W.R. Schneider and R. Orbach. Rev. Mod. Phys. 53 (1981) 175.

[43] B. Derrida, J. Stat. Phys. 31 (1983) 433.

[44] J.C. Dyre, J. Non-Cryst. Solids 88 (1986) 271.

[45] G. Tomandl, J. Non-Cryst. Solids 14 (1974) 101.

[46] J.M. Stevels, in: Handbuch der Physik, ed. S. Flügge, Vol. 20 (Springer, Berlin, 1957) p. 350.

[47] H.E. Taylor, J. Soc. Glass Technol. 41 (1957) 350T; and 43 (1959) 124T.

[48] R. Kubo, J. Phys. Soc. Jpn. 12 (1957) 570.

[49] E.W. Montroll and G.H. Weiss, J. Math. Phys. 6 (1965) 167.

[50] H. Scher and M. Lax, Phys. Rev. B7 (1973) 4491.

[51] J.K.E. Tunaley, Phys. Rev. Lett. 33 (1974) 1037.

[52] M. Lax and H. Scher, Phys. Rev. Lett. 39 (1977) 781.

[53] J.W. Haus, K.W.Kehr and L.W. Lyklema, Phys. Rev. B25 (1982) 2905.

[54] T. Ishii, Progr. Theor. Phys. 73 (1985) 1084.

[55] M. Grünewald, B. Movaghar, B. Pohlmann and D. Würtz, Phys. Rev. B32 (1985) 8191.

[56] P.N. Butcher, Philos. Mag. B37 (1978) 653.

[57] V.V. Bryksin, Sov. Phys. Solid State 25 (1983) 1395.

[58] J.M. Hyde, M. Tomozawa and M. Yoshiyagawa, Phys. Chem. Glasses 28 (1987) 174.

[59] A.K. Jonscher, J. Phys. C6 (1973) L235.

[60] J.R. Macdonald, J. Chem. Phys. 61 (1974) 3977.

[61] V.V. Bryksin, Sov. Phys. Solid State 26 (1984) 827.

[62] J.M. Marshall, Rep. Prog. Phys. 46 (1983) 1253.

[63] M.B. Weissman, Rev. Mod. Phys. 60 (1988) 537.

[64] N.F. Mott and E.A. Davis, Electronic Processes in Non-crystalline Materials, 2nd Ed. (Clarendon, Oxford, 1979).

[65] M.H. Nathoo and A.K. Jonscher, J. Phys. C4 (1971) L301.

[66] J.L. Barton, J. Non-Cryst. Solids 4 (1970) 220.

[67] J.P. Lacharme and J.O. Isard, J. Non-Cryst. Solids 27 (1978) 381.

[68] J.C. Dyre, unpublished.

[69] S. Summerfield, Philos. Mag. B52 (1985) 9.

[70] J.O. Isard, Philos. Mag. B62 (1990) 139.

[71] P. Maass, J. Petersen, A. Bunde, W. Dieterich and H.E. Roman, Phys. Rev. Lett. 66 (1991) 52.

[72] B.I. Shklovskii and A.L. Efros, Electronic Properties of Doped Semiconductors (Springer, Berlin, 1984).

PUBLICATIONS

Rapid Communications

Rapid Communications are intended for the accelerated publication of important new results and are therefore given priority treatment both in the editorial office and in production. A Rapid Communication in **Physical Review B** *should be no longer than four printed pages and must be accompanied by an abstract. Page proofs are sent to authors.*

Universal ac conductivity of nonmetallic disordered solids at low temperatures

Jeppe C. Dyre

Institute of Mathematics and Physics, Roskilde Universitetscenter, Postbox 260, DK-4000 Roskilde, Denmark

(Received 11 January 1993)

It is shown that, in the low-temperature limit, the effective-medium approximation predicts a universal frequency dependence of the conductivity of nonmetallic disordered solids. The calculation is based on a macroscopic approach to ac conduction and is valid in more than one dimension. The universality prediction is confirmed by simulations in two dimensions.

For many years ac conduction has been studied in disordered solids such as amorphous semiconductors, glasses, polymers, nonstoichiometric solids, or metal-cluster compounds.[1-8] All disordered solids show similar ac behavior, whether the conduction is electronic, polaronic, or ionic. The frequency-dependent conductivity follows an approximate power law with an exponent between 0.7 and 1.0. At lower frequencies there is a gradual transition to constant conductivity. The standard models for this are hopping models which deal with the random walk of noninteracting charge carriers in a random environment.[9-13] While hopping models are rather successful, the importance of Coulomb interactions has recently come into focus.[14,15] Unfortunately, hopping models with interactions are not amenable to simple analytic treatment. One way to include the effect of Coulomb interactions between charge carriers, instead of using hopping models, is to adopt a macroscopic point of view.[16-20] This is done here where conduction in inhomogeneous media is discussed by exploring Maxwell's equations.

Consider a disordered solid with spatially varying thermally activated conductivity $g(E(\mathbf{r}))=g_0 e^{-\beta E(\mathbf{r})}$. Here β is the inverse temperature and the activation energy $E(\mathbf{r})$ is assumed to vary randomly in space with a finite correlation length. In some cases the activation energy probability distribution is quite narrow; however, we are concerned here with the low-temperature case where the distribution of conductivities becomes very broad. If ϵ denotes the dielectric constant and ω the angular frequency, the continuity equation and Gauss' law imply for the electrostatic potential ϕ

$$\nabla\cdot[(i\omega\epsilon+g)\nabla\phi]=0 . \tag{1}$$

This equation is discretized[21,22] by regarding the potential ϕ as defined on the points of a simple cubic lattice and the quantity $i\omega\epsilon+g$ as defined on nearest-neighbor links. In this way Eq. (1) becomes the Kirchhoff current conservation law for a lattice where each link is a resistor

in parallel with a capacitor. If a is the lattice constant and D the dimension, the correct continuum limit is ensured if each link admittance y is given by

$$y=a^{D-2}(i\omega\epsilon+g) . \tag{2}$$

The electrical circuit is not to be interpreted literally as a physical model of the solid because the free charge currents run through the resistors only; the capacitor currents are the well-known displacement currents. However, the circuit is useful for calculating the macroscopic frequency-dependent free charge conductivity $\sigma(\omega)$, i.e., the ratio between average free charge current and average electrical field. If L is the linear circuit dimension and $G(\omega)$ is the admittance measured between opposing short-circuited faces, it is straightforward to show that, whenever ϵ is space independent, $\sigma(\omega)$ is given[23] by

$$\sigma(\omega)=\frac{G(\omega)}{L^{D-2}}-i\omega\epsilon . \tag{3}$$

If the discretization length a is chosen to be the correlation length for $E(\mathbf{r})$ and correlations beyond a are ignored,[21,24] the effective-medium approximation (EMA) may be applied to calculate G.[16,21] The EMA equation for the effective-link admittance, y_m, is $\langle(y-y_m)/[y+(D-1)y_m]\rangle_y=0$ where the bracket denotes an average over the admittance probability distribution. Since $G=N^{D-2}y_m$ where $N=L/a$, the EMA equation and Eqs. (2) and (3) imply (where $s\equiv i\omega\epsilon$)

$$\frac{1}{D(\sigma+s)}=\left\langle\frac{1}{g(E)+(D-1)\sigma+Ds}\right\rangle_E . \tag{4}$$

This equation has a simple solution in the limit $\beta\to\infty$. The root $E=E_g(s)$ of $g(E)=(D-1)\sigma+Ds$ is given by

$$E_g(s)=-\frac{1}{\beta}\ln\left[\frac{(D-1)\sigma+Ds}{g_0}\right] . \tag{5}$$

If $p(E)$ is the activation-energy probability distribution, Eq. (4) at low temperatures becomes

$$\frac{1}{D(\sigma+s)}=\frac{1}{(D-1)\sigma+Ds}\int_{E_g(s)}^{\infty}p(E)dE \qquad (6)$$

or

$$\frac{D-1}{D}+\frac{s}{D(\sigma+s)}=\int_{E_g(s)}^{\infty}p(E)dE \ . \qquad (7)$$

For large β subtracting the $s=0$ case of Eq. (7) from Eq. (7) itself leads to

$$\frac{s}{D(\sigma+s)}=\int_{E_g(s)}^{E_g(0)}p(E)dE$$

$$=p(E_g(0))\frac{1}{\beta}\ln\left[\frac{\sigma}{\sigma(0)}+\frac{D}{D-1}\frac{s}{\sigma(0)}\right] \ . \qquad (8)$$

Introducing the dimensionless variables

$$\tilde{\sigma}=\frac{\sigma}{\sigma(0)}, \quad \tilde{s}=\frac{\beta}{Dp(E_g(0))\sigma(0)}s \ , \qquad (9)$$

Eq. (8) for $\beta\to\infty$ reduces to

$$\tilde{\sigma}\ln(\tilde{\sigma})=\tilde{s} \ . \qquad (10)$$

Equation (10) was derived by Fishchuk for the uniform energy barrier distribution with cutoffs where the average in Eq. (4) can be calculated explicitly.[20] Here it has been shown that, in the low-temperature limit, the EMA predicts a *universal* frequency dependence of the conductivity (in any dimension $D>1$). There is, however, some doubt whether the EMA is reliable for systems with extremely broad distributions of admittances.[25,26] Therefore, computer simulations were carried out to test Eq. (10). At low temperatures large lattices are needed to obtain reasonable statistics, and the simulations are quite demanding. Only the two-dimensional case was studied where the highly efficient Frank-Lobb algorithm is available.[27] For simplicity the simulations were carried out for real $\tilde{s}$; by analytic continuation this is possible when the purpose is to compare the simulation results to an analytic function. Bonds were defined via Eq. (2) where g is given by a randomly chosen activation energy. Several different activation-energy distributions were used. The conductivity was evaluated from Eq. (3). Averages of 20 simulations of a 100×100 square lattice are shown in Fig. 1. The results confirm the EMA prediction of universality as the temperature is lowered. The universality represents a new type of regularity, appearing gradually as the "relaxation time distribution" becomes extremely broad. The universality is not a consequence of a diverging correlation length, as for a second-order phase transition, and there are no critical exponents. While Eq. (10) and the simulations are concerned with the *free* charge contribution to the conductivity only, it is easy to show[23] that the dipolar contribution to the total conductivity is insignificant at low temperatures in the frequency range of interest. Thus, both prediction and simulations may be thought of as concerned with the total conductivity.

The observed universality reflects the fact that for $T\to0$ all energy distributions effectively tend to the uniform distribution so the conductance distribution be-
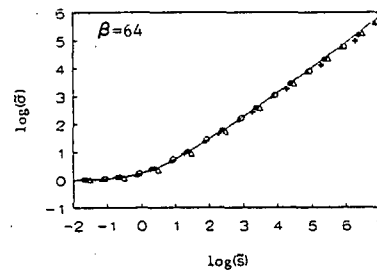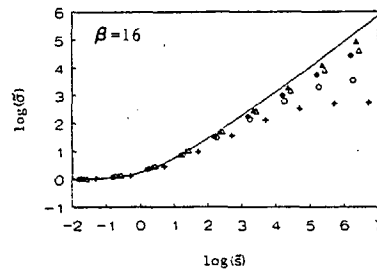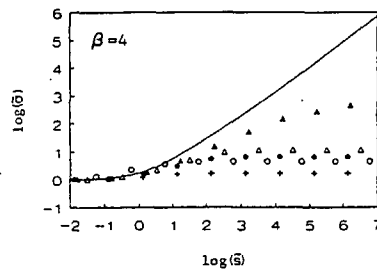

FIG. 1. Log-log plot (base 10) of the dimensionless conductivity $\tilde{\sigma}$ as function of the real dimensionless Laplace frequency $\tilde{s}$ [both quantities defined in Eq. (9)] at different temperatures. The full curve is the EMA prediction for the low-temperature limit of $\tilde{\sigma}$ ($\tilde{s}$) [Eq. (10)], while the symbols represent simulations in two dimensions for different activation energy probability distributions. β is the inverse dimensionless temperature. Each point represents the average of 20 simulations of a 100×100 lattice. The total admittance was determined by the Frank-Lobb algorithm (Ref. 27) and $\tilde{\sigma}$ subsequently found from Eq. (3). Results are shown for the following activation energy probability distributions: ($\blacktriangle$), $p(E)=(1/\sqrt{2\pi})e^{-E^2/2}$ ($-\infty<E<\infty$); ($\bullet$), $p(E)=\frac{1}{2}$ ($-1<E<1$); ($\triangle$), $p(E)=(2/\pi)(1+E^2)^{-1}$ ($0<E<\infty$); ($\circ$), $p(E)=e^{-E}$ ($0<E<\infty$); ($+$), $p(E)=2E$ ($0<E<1$). In each case the distribution should be thought of as centered around an energy E_0; this gives an extra factor $e^{-\beta E_0}$ to both conductivity and frequency without changing $\tilde{\sigma}$ or $\tilde{s}$. The quantity $E_g(0)$ in Eq. (9) is the dc conductivity activation energy [Eq. (5)] which is easily determined from the fact that the percolation threshold is $\frac{1}{2}$ in two dimensions (Refs. 21, 23, 35, and 36).

comes $P(g) \sim 1/g$. However, it is noteworthy that even at low temperatures there is a sharp cutoff in the "relaxation time distribution." This is due to the existence of a percolation threshold.

The asymptotic behavior $\sigma \sim \tilde{s}$ found for $\tilde{s} \rightarrow \infty$ is a subtle effect which is not directly due to the capacitors [since the capacitor currents do not contribute to the conductivity in Eq. (3)]. *Indirectly*, however, the capacitors do give rise to the observed frequency dispersion via their influence on the node potentials that in turn determine the resistor currents.

The EMA equation (10) was first derived by Bryksin for a model of noninteracting electrons tunneling between positionally disordered sites;[28] it has also been shown to apply for a hopping model with a box-type distribution of energy barriers.[5] Hopping models are neither physically nor mathematically equivalent to the macroscopic approach taken here. But both types of models lead to large sparse matrix equations expressing local current conservation. In view of the present findings it seems likely that, in the limit of severe disorder, the EMA for any problem of this type leads to Eq. (10) for the frequency-dependent conductivity (or diffusion constant).

An important and well-established experimental fact is the Barton-Nakajima-Namikawa (BNN) relation,[29-31] i.e., the rule that the characteristic frequency for onset of ac conduction has the same activation energy as $\sigma(0)$.[32] This follows directly from Eqs. (9) and (10) [a reduced frequency definition similar to Eq. (9) was used for hopping models by Scher and Lax[33] and by Summerfield[34]]. It is easy to understand qualitatively why the BNN relation is valid here. In the dc limit the current follows the "critical" percolation paths giving the easiest ways between the electrodes.[35] As the frequency increases there is little effect until, for $s \sim s_c$, s is of order the lowest conductivity σ_{min} met on a critical path. On the other hand, the dc conductivity is also determined by σ_{min},[35,36] and thus one expects $\sigma(0) \sim s_c$ which is the essence of the BNN relation.

In three dimensions the EMA has the percolation threshold somewhat wrong,[21] so the predicted dc conductivity activation energy is also wrong. However, Eq. (10) may still be valid in three dimensions at low temperatures. Summerfield has conjectured a "quasiuniversality" for the frequency dependence of the conductivity.[34] This idea fits nicely into the present work that predicts true universality only in the zero temperature limit. Comparing to experiments, it has been shown elsewhere[5] that all qualitative features of experiment follow the equation

$$\tilde{\sigma} = \tilde{s}/\ln(1+\tilde{s}) . \qquad (11)$$

Equation (11), which clearly is an approximate solution of Eq. (10), represents the admittance of a single critical path.[23] Both equations predict an approximate power-law frequency dependence of the real part of the conductivity where the exponent at the real frequency $\tilde{\omega} = -i\tilde{s}$ is equal to $1 - 2/\ln(\tilde{\omega})$.[5,28] A few decades above the onset of ac conduction, the exponent is predicted to be 0.8, in agreement with most experiments. Thus, there are certainly no experimental reasons to reject Eq. (10) as a low-temperature limiting universal frequency dependence of the conductivity in three dimensions.

Some time ago Pollak and Pike suggested that details of the conduction mechanism should be contained in deviations from linear frequency dependence of the conductivity.[37] While Eq. (10) approaches proportionality $\tilde{\sigma} \propto \tilde{s}$ for $\tilde{s} \rightarrow \infty$, there is a significant nontrivial frequency dependence in a very large frequency range. If the predicted universality is indeed valid also in three dimensions, there is little information in a conductivity that follows Eq. (10). It seems therefore that experiments could naturally be interpreted in terms of deviations from Eq. (10), representing the low-temperature fix point, rather than in terms of deviations from linear frequency dependence.

The EMA assumes admittances that are uncorrelated above the lattice spacing, the discretization length a. The present results may be compared to recent simulations of interacting charged particle hopping on a disordered lattice, where it was found that the dispersive regime is due to the blocking effect on very short distances.[15] Possibly, the length a may be identified with this range of length scales.

In conclusion, it has been shown that the EMA predicts a universal frequency dependence of the conductivity for disordered nonmetals at low temperatures. Simulations in two dimensions have confirmed not only the qualitative universality prediction, but the quantitative EMA prediction as well. Finally, we note that since hopping models often follow Eq. (10), one cannot distinguish, from ac measurements alone, between these two approaches to the modeling of ac conduction in disordered solids.

[1] A. E. Owen, J. Non-Cryst. Solids 25, 372 (1977).

[2] A. Mansingh, Bull. Mater. Sci. (India) 2, 325 (1980).

[3] A. K. Jonscher, *Dielectric Relaxation in Solids* (Chelsea Dielectric Press, London, 1983).

[4] M. D. Ingram, Phys. Chem. Glasses 28, 215 (1987).

[5] J. C. Dyre, J. Appl. Phys. 64, 2456 (1988).

[6] C. A. Angell, Chem. Rev. 90, 523 (1990).

[7] S. R. Elliott, *Physics of Amorphous Materials*, 2nd ed. (Longman, London, 1990).

[8] M. P. J. van Staveren, H. B. Brom, and L. J. de Jongh, Phys. Rep. 208, 1 (1991).

[9] M. Lax and T. Odagaki, in *Macroscopic Properties of Disordered Media*, edited by R. Burridge (Springer, Berlin, 1982), p. 148.

[10] H. Böttger and V. V. Bryksin, *Hopping Conduction in Solids* (Akademie Verlag, Berlin, 1985).

[11] J. W. Haus and K. W. Kehr, Phys. Rep. 150, 263 (1987).

[12] G. A. Niklasson, J. Appl. Phys. 62, R1 (1987).

[13] J.-P. Bouchaud and A. Georges, Phys. Rep. 195, 127 (1990).

[14]J. O. Isard, Philos. Mag. B **62**, 139 (1990).

[15]P. Maass, J. Petersen, A. Bunde, W. Dieterich, and H. E. Roman, Phys. Rev. Lett. **66**, 52 (1991).

[16]R. Landauer, in *Electrical Transport and Optical Properties of Inhomogeneous Media*, edited by J. C. Garland and D. B. Tanner, AIP Conf. Proc. No. 40 (AIP, New York, 1978), p. 2.

[17]A. H. Clark, Thin Solid Films **108**, 285 (1983).

[18]T. Nagatani, J. Appl. Phys. **54**, 5132 (1983).

[19]*Impedance Spectroscopy*, edited by J. R. Macdonald (Wiley, New York, 1987).

[20]I. I. Fishchuk, Phys. Status Solidi A **93**, 675 (1986).

[21]S. Kirkpatrick, Rev. Mod. Phys. **45**, 574 (1973).

[22]I. Webman, J. Jortner, and M. H. Cohen, Phys. Rev. B **11**, 2885 (1975).

[23]J. C. Dyre and T. Riedel (unpublished).

[24]I. Webman, J. Jortner, and M. H. Cohen, Phys. Rev. B **15**, 5712 (1977).

[25]J. Koplik, J. Phys. C **14**, 4821 (1981).

[26]S. Tyc and B. I. Halperin, Physica A **157**, 210 (1989).

[27]D. J. Frank and C. J. Lobb, Phys. Rev. B **37**, 302 (1988).

[28]V. V. Bryksin, Fiz. Tverd. Tela **22**, 2441 (1980) [Sov. Phys. Solid State **22**, 1421 (1980)].

[29]J. L. Barton, Verres Réfr. **20**, 328 (1966).

[30]T. Nakajima, in *1971 Annual Report, Conference on Electric Insulation and Dielectric Phenomena* (National Academy of Sciences, Washington, DC, 1972). p. 168.

[31]H. Namikawa, J. Non-Cryst. Solids **18**, 173 (1975).

[32]J. C. Dyre, J. Non-Cryst. Solids **88**, 271 (1986).

[33]H. Scher and M. Lax, Phys. Rev. B **7**, 4502 (1973).

[34]S. Summerfield, Philos. Mag. B **52**, 9 (1985).

[35]V. Ambegaokar, B. I. Halperin, and J. S. Langer, Phys. Rev. B **4**, 2612 (1971).

[36]D. Berman, B. G. Orr, H. M. Jaeger, and A. M. Goldman, Phys. Rev. B **33**, 4301 (1986).

[37]M. Pollak and G. E. Pike, Phys. Rev. Lett. **28**, 1449 (1972).

Universal low-temperature ac conductivity of macroscopically disordered nonmetals

Jeppe C. Dyre

Institute of Mathematics and Physics, Roskilde University, P.O. Box 260, DK-4000 Roskilde, Denmark

(Received 27 April 1993)

This paper discusses a macroscopic model for ac conduction in electronically or ionically conducting disordered solids. The model considers ac conduction in an inhomogeneous solid that is characterized by a spatially randomly varying thermally activated (frequency-independent) conductivity. Discretizing Maxwell's equations leads to an equivalent electrical circuit that is a simple-cubic lattice where each pair of nodes are linked by a resistor and a capacitor in parallel. The values of the resistors are determined by the local resistivity while the capacitors are all equal, given by the infinite-frequency dielectric constant. It is shown that the capacitor currents are Maxwell's displacement currents. Assuming uncorrelated resistances, the model is solved analytically at low temperatures in the effective-medium approximation (EMA) and in a naive percolation-path approximation. Both approximations predict similar universal ac responses as $T \rightarrow 0$, where the macroscopic frequency-dependent conductivity becomes independent of the activation-energy probability distribution. The universality represents an unusual type of regularity appearing in the extreme disorder limit. The universality prediction is tested by computer simulations of 200×200 lattices in two dimensions and of $50 \times 50 \times 50$ lattices in three dimensions. The computer simulations show that the EMA works very well in two dimensions in the whole temperature range studied; in particular, the low-temperature universality prediction is confirmed. In three dimensions the universality prediction is confirmed as well.

I. INTRODUCTION

Alternating current conduction in disordered solids has been studied during the last 40 years.[1-7] Numerous papers have appeared, especially after 1970, reporting the frequency and temperature dependence of the electrical conductivity in electronically or ionically conducting disordered solids like glasses or various forms of imperfect crystals. With modern frequency analyzers the measurements are fast and fairly straightforward. A considerable amount of work has gone into developing theories of ac conduction, with the main focus on hopping models.[8-10] Despite this, it is still not clear what the correct model is for ac conduction (in particular, whether macroscopic or microscopic inhomogeneities are responsible for the frequency dispersion), and it is unknown when and if Coulomb interactions are important.[11,12] Consequently, the interpretation of data is highly subjective and few examples exist of ac measurements yielding unambiguous information about charge carrier motion in a bulk disordered solid.

Besides the lack of understanding of ac phenomena, there is another problem with the application of impedance spectroscopy to disordered solids: These solids show remarkably similar behavior in regard to their frequency-dependent conductivity and its temperature dependence.[1-3,13] Thus, all disordered solids have an ac conductivity which depends on frequency as an approximate power law where the exponent is less than but close to one and goes to one as the temperature goes to zero. Furthermore, one observes in all cases a much less pronounced temperature dependence of the ac conductivity than that of the dc conductivity.

The present paper discusses a macroscopic model for ac conduction. The model, which is conceptually simpler than the popular hopping models, investigates the ac consequences of a spatially varying electrical conductivity. The model is based on the well-known Maxwell-Wagner effect, i.e., the fact that inhomogeneities give rise to a frequency dependence of the conductivity because charge carriers accumulate at the boundaries to less conducting regions, thereby creating dipolar polarization. While a number of papers have discussed the dc conductivity of disordered solids with macroscopic inhomogeneities, little work has gone into studying the ac aspects. In this paper, that extends and details a recent paper,[14] the model is derived from Maxwell's equations, assuming the local conductivity is thermally activated. It is shown how to discretize the model and two approximations are applied, focusing on the low-temperature limit of the model. Both approximations predict a universality of the ac response as T goes to zero. This prediction is confirmed by computer simulations in two and three dimensions.

The paper is organized as follows. In Sec. II, a brief review is given of the experimental observations and of the models hitherto studied. In Sec. III, the macroscopic model is formulated and discretized, and in Sec. IV, two analytical approximations are applied to the model, the effective-medium approximation (EMA) as well as a naive percolation path analysis. In Sec. V, the results from extensive computer simulations are reported, and finally Sec. VI contains a discussion.

II. THE PHYSICS OF ac CONDUCTION IN DISORDERED SOLIDS

The first systematic works on ac conduction in disordered solids were the "dielectric" studies of ionic conduc-

tive oxide glasses.[15-17] Soon after, in 1961, Pollak and Geballe[18] reported ac measurements on n-type doped crystalline silicon at helium temperatures (where the disorder due to the random substitution of the dopants becomes important). Only much later was the similarity between the ac response of ionic glasses and of electronically conducting disordered solids noted.[1-3,13] During the last 20 years a large number of publications have reported ac measurements on disordered solids like amorphous semiconductors,[3,4,19] fast ionic conductors,[5,7] nonstoichiometric or polycrystals,[20,21] ionic or electronically conducting polymers,[22,23] metal-cluster compounds,[24] polaronically conducting transition-metal oxides,[3,25] organic semiconductors,[26] or high-temperature superconductors above T_c.[27]

Experimental data are usually reported in terms of the real part $\sigma'(\omega)$ of the frequency-dependent conductivity, $\sigma(\omega)=\sigma'(\omega)+i\sigma''(\omega)$. There are, however, alternatives to this means of representation. Early publications on ionic glasses presented data in terms of the negative imaginary part $\epsilon''(\omega)$ of the complex dielectric constant $\epsilon(\omega)=\epsilon'(\omega)-i\epsilon''(\omega)$ defined by

$$\epsilon(\omega)=\frac{\sigma(\omega)-\sigma(0)}{i\omega} . \qquad (1)$$

Presently, data for ionic systems are often given in terms of the electric modulus $M(\omega)$ defined[28] by $M(\omega)=i\omega/\sigma(\omega)$ (though it has been argued that this is not a good means of presenting data).[29,30] Finally, there is also the possibility of using the complex resistivity $\rho(\omega)=1/\sigma(\omega)$.[31]

As mentioned above, all disordered solids exhibit the same qualitative ac behavior: Around the dielectric loss peak frequency marking the maximum of $\epsilon''(\omega)$, ω_m, $\sigma'(\omega)$ starts to increase, and for $\omega\gg\omega_m$, $\sigma'(\omega)$ follows an approximate power law: $\sigma'(\omega)\propto\omega^{n'}$. This behavior continues right up to phonon frequencies where the conductivity around $\omega=10^{12}$ Hz is of order 1 $(\Omega\,\mathrm{cm})^{-1}$.[32] The signature of a power law is a straight line in a log-log plot. There is some controversy as to whether the observed power laws are truly fundamental[1,33-35] or just an approximate description.[8,30] In any case, the exponent n' is always between 0.7 and 1.0 (the only exception seems to be one-dimensional conductors),[36,37] and one always finds that n' goes to one as the temperature goes to zero. The ac conductivity is always less temperature dependent than the dc conductivity (when viewed in the usual log-log plot), and for $T\to0$ the ac conductivity becomes almost temperature independent. The dc conductivity usually follows an Arrhenius law. An important universal observation is the Barton-Nakajima-Namikawa (BNN) relation,[38-42]

$$\sigma(0)=p\Delta\epsilon\omega_m , \qquad (2)$$

where $\Delta\epsilon$ is the dielectric loss strength, $\Delta\epsilon=\epsilon'(0)-\epsilon'(\infty)$, and p is a numerical constant of order 1. Since $\Delta\epsilon$ depends only weakly on temperature, the BNN relation implies that the activation energy of $\sigma(0)$ is equal to that of ω_m.[17] In the majority of disordered solids $\sigma'(\omega)$ obeys the time-temperature superposition principle, i.e.,

the fact that at different temperatures one observes the same function $\sigma'(\omega)$ just scaled (i.e., displaced in the log-log plot). This, in conjunction with the BNN relation and the Debye law $\Delta\epsilon\propto T^{-1}$, shows that the dimensionless conductivity $\bar{\sigma}=\sigma(\omega)/\sigma(0)$ is a function of $\omega/[T\sigma(0)]$.[43-45] A convenient name for the fact that all disordered solids show the same qualitative ac behavior is to refer to it as "quasiuniversality."[44]

The early experiments on ac properties of ionic glasses were interpreted in terms of a distribution of relaxation times for associated Debye processes, as is common for dielectric relaxation in liquids.[46] Workers in semiconductor physics in the 1960s proposed the pair approximation as a model for the ac loss.[47,48] This model assumes the loss is due to independent pairs of sites in the solid, where each pair provides two possible positions for a localized electron. Mathematically, this corresponds to the description in terms of Debye processes in parallel that was used in the early work on ionic glasses.

In the pair approximation there is no dc conduction. This has to be assumed to be derived from a completely different process, whereby the BNN relation becomes very hard to understand. Furthermore, the pair approximation cannot explain the fact that the exponent n' goes to one as $T\to0$. A version of the pair approximation, the correlated barrier hopping model, has been proposed by Elliott.[6,49] This model explains the low-temperature behavior of n' as a consequence of Coulomb force controlled variable range hopping and the model has a nonzero dc conductivity because the pairs are not isolated from each other.

A number of authors have considered phenomenological and intuitive models based on networks composed of resistors and capacitors.[11,21,28,34,50-55] In the present paper, following Springett, Webmann et al., Sinkkonen, and Fishchuk,[56-59] a resistor-capacitor network is also arrived at, but here it is derived directly from Maxwell's equations.

In the last 15 years a number of models have appeared[1,33-35,60-62] emphasizing the power-law behavior of $\sigma'(\omega)$ which is regarded as fundamental, much like the power laws for second-order phase transitions found close to T_c. Thereby, fractal aspects of the conduction process are emphasized.[35,63] Power laws also result if it is assumed that the phase difference between field and current is frequency independent.[64]

The most thoroughly studied models for ac conduction in disordered solids are probably the so-called hopping models.[8-10] A hopping model considers the random walk of (usually) independent charge carriers in a disordered structure. If the charge carrier sites are marked s and $\Gamma(s\to s')$ denotes the rate for jumps from site s to site s', a hopping model is characterized by the following master equation for the probability of finding a charge carrier at site s, $P(s,t)$,

$$\frac{\partial P(s,t)}{\partial t}=-\sum_{s'}\Gamma(s\to s')P(s,t)+\sum_{s'}\Gamma(s'\to s)P(s',t) .$$

$$(3)$$

The jump rates that are commonly taken to be an ex-

ponential function of an activation energy and/or a tunneling distance, are usually assumed to vary randomly and to be nonzero only for nearest-neighbor jumps. The frequency-dependent conductivity is calculated from the Kubo formula[65,66] that in D dimensions is

$$\sigma(\omega) = \lim_{V \to \infty} \frac{1}{D k_B T V} \int_0^\infty \langle \mathbf{J}(0) \cdot \mathbf{J}(t) \rangle e^{-i\omega t} dt , \quad (4)$$

where $\mathbf{J}$ is the total current in the volume V.

Hopping models are complex and cannot be solved analytically. To evaluate $\sigma(\omega)$ either one has to computer simulate, or to use some analytical approximation. An early approximation was the continuous time random walk (CTRW) approximation of Scher and Lax.[43] Today the CTRW is regarded as the simplest available approximation, a mean-field Hartree-type approximation[67] (note that the original derivation that converted the disordered Markovian hopping model to a non-Markovian random walk in a homogeneous medium was inconsistent).[30,68] The standard approximation for disordered systems, which is often also used for hopping models, is the effective-medium approximation (EMA).[9,67,69−71] A related approach is the extended pair approximation (EPA) of Summerfield and Butcher.[72]

Hopping models usually assume noninteracting charge carriers. Thus, the self-exclusion effect (allowing at most one particle at each site[73]) is ignored, as well as are Coulomb interactions between the charge carriers. Recent work includes these effects,[12] but at the price that the model becomes very complex and can only be studied by means of computer simulations. The macroscopic model considered in the next section includes Coulomb interactions via Gauss' law, without becoming extremely complex.

III. THE MACROSCOPIC MODEL AND ITS DISCRETIZATION

This section deals with setting up the equations governing ac conduction in a solid with a spatially varying (frequency-independent) conductivity.[14,56−59] It is assumed that the solid has free charge carriers characterized by a local conductivity denoted by $g(\mathbf{r})$, as well as bound charges described by the spatially constant dielectric constant ϵ_∞, equal to the $\omega \to \infty$ limit of $\epsilon(\omega)$ in Eq. (1). It is not entirely unproblematic to assume distinguishability between free and bound charge carriers in ac fields,[74] but the assumption will be made here without

further justification.

The quantity of interest is the macroscopic free charge carrier conductivity, defined as the ratio between the spatially averaged free charge current density and the spatially averaged electric field. If D denotes the displacement vector, $\mathbf{J}$ the free charge carrier current density, and ϕ the electrostatic potential, the basic constitutive equations are

$$\mathbf{D}(\mathbf{r},t) = -\epsilon_\infty \nabla \phi(\mathbf{r},t)$$
$$\mathbf{J}(\mathbf{r},t) = -g(\mathbf{r}) \nabla \phi(\mathbf{r},t) . \quad (5)$$

These equations should be combined with Gauss' law

$$\nabla \cdot \mathbf{D}(\mathbf{r},t) = \rho(\mathbf{r},t) \quad (6)$$

(where ρ is the free charge carrier density) and the continuity equation

$$\dot{\rho}(\mathbf{r},t) + \nabla \cdot \mathbf{J}(\mathbf{r},t) = 0 . \quad (7)$$

In a periodically varying field all quantities are written as a factor $e^{i\omega t}$ times a function of space. Thus, the continuity equation becomes $i\omega\rho + \nabla \cdot \mathbf{J} = 0$. Substituting Eqs. (5) and (6) into this expression and introducing the "Laplace frequency"

$$s = i\omega\epsilon_\infty , \quad (8)$$

one arrives at the following equation for the electrostatic potential:

$$\nabla \cdot \{[s + g(\mathbf{r})] \nabla \phi(\mathbf{r},s)\} = 0 . \quad (9)$$

In terms of ϕ the average current density is given by

$$\mathbf{J}(s) = \frac{1}{V} \int_V g(\mathbf{r})[-\nabla \phi(\mathbf{r},s)] d\mathbf{r} . \quad (10)$$

We now turn to the discretization of Eq. (9).[14,59] A discretization is necessary for solving the equation numerically, but it is also useful for developing an intuition about the problem and arriving at approximate analytical solutions. The discretization will be performed in D dimensions. It is assumed that the function $\phi(\mathbf{r},s)$ is known only at the points of a simple-cubic lattice with lattice constant a. If Eq. (9) is considered at the lattice point with coordinates $(n_1 a, \ldots, n_D a)$, the first of the D terms on the left-hand side becomes upon discretization (for simplicity only the first coordinate is written out explicitly, the remaining unchanged coordinates are $n_2 a, \ldots, n_D a$):

$$\frac{\partial}{\partial x_1} \left[(s+g) \frac{\partial \phi}{\partial x_1} \right] (n_1 a, s) = a^{-2} \left[\{s + g[(n_1 + \tfrac{1}{2})a]\} \{\phi[(n_1+1)a, s] - \phi(n_1 a, s)\} \right.$$
$$\left. - \{s + g[(n_1 - \tfrac{1}{2})a]\} \{\phi(n_1 a, s) - \phi[(n_1-1)a, s]\} \right] . \quad (11)$$

There are $D-1$ other similar terms, and Eq. (9) becomes the condition that the sum of all D terms is zero. Remembering the definition of s [Eq. (8)], this zero sum requirement is recognized as the Kirchhoff current conservation law for a lattice where each link is a resistor

and a capacitor in parallel (Fig. 1). Each link admittance y is given by $y = K(s+g)$, where K is a constant that is determined from requiring the correct continuum limit of the free charge current density $\mathbf{J}$: If the resistor current is I_R, $\mathbf{J}$ is numerically given by $J = I_R / a^{D-1}$. On the

other hand, if the potential drop across a link is denoted by $\Delta\phi$ one has $I_R = Kg\,\Delta\phi$ and $J = g\,\Delta\phi/a$. Combining these equations we find $K = a^{D-2}$, so the link admittance is given by

$$y = a^{D-2}(s+g) . \qquad (12)$$

The circuit of Fig. 1 is *not* a direct physical representation of the solid. This is because, while the resistor currents are indeed the true free charge currents, the capacitor currents are "ghost" currents that are not just the currents due to the actual displacement of the bound charge carriers. For instance, if $\epsilon_\infty = \epsilon_0$ (the vacuum permittivity), there are no bound charges but the capacitors are still important in the circuit. The correct interpretation of Fig. 1 is the following: In an external ac field the circuit determines the electrostatic potential. This potential in turn determines the free charge currents as those running through the resistors. Clearly, the capacitors give rise to a frequency dependence of the overall circuit admittance, but this is not the effect we are looking for. The frequency dependence of the free charge currents comes about only as an *indirect* effect of the capacitors because of their influence on the node potentials.

In the real solid the free charges accumulate at certain places. In Fig. 1, the role of the capacitors is to exactly
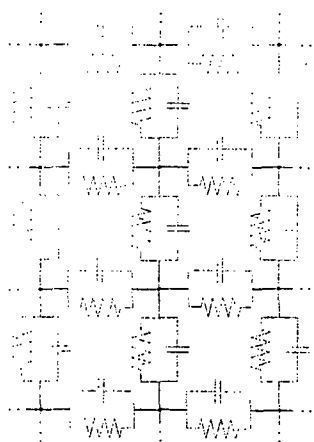

FIG. 1. Electrical equivalent circuit of Maxwell's equations discretized in 2D for an inhomogeneous conductor. Similar circuits exist in higher dimensions. All capacitors are equal while the resistors vary, reflecting the spatially varying conductivity of the solid. In the model studied here the resistors are assumed to be thermally activated and vary randomly and uncorrelated from link to link. In any external field the electrostatic potential is found from Kirchhoff's equations. The currents through the resistors are the free charge currents. The capacitor currents are Maxwell's displacement currents (parts of which are due to the bound charges and parts of which are "ghost" currents). The capacitor currents are nonzero in an ac field, thus allowing bound and free charge accumulation (the Maxwell-Wagner effect) without violating the Kirchhoff equation expressing the fact that there is no "total charge" (bound charge + free charge + "ghost" charge) accumulation at a node.

compensate the free charge accumulation, so that there is no "total charge" accumulation at any node. It follows from Eq. (12) that the continuous analogue of the capacitor current is nothing but the well-known Maxwell displacement current $\mathbf{J}_D = \dot{\mathbf{D}}$. At first sight this may seem surprising since the displacement current is usually introduced in connection with completing Maxwell's equations to ensure that $\nabla\cdot(\nabla\times\mathbf{H}) = 0$. But this is done by adding to the free charge current $\mathbf{J}$ the term $\mathbf{J}_D = \dot{\mathbf{D}}$ so constructed that the divergence of $\mathbf{J} + \mathbf{J}_D$ is zero. The equation $\nabla\cdot(\mathbf{J} + \mathbf{J}_D) = 0$ follows from Eqs. (6) and (7); in an ac field this condition is nothing but Eq. (9).

The macroscopic frequency-dependent free charge conductivity may be calculated from the overall circuit admittance $Y(s)$. Here and henceforth the macroscopic free charge conductivity will be denoted by $\sigma(s)$, despite the risk of confusing it with the total conductivity appearing in Eq. (1). The latter quantity differs from the former by the factor $i\omega(\epsilon_\infty - \epsilon_0)$. In most experiments one looks for the real part of the conductivity only, and in any case it turns out that the $i\omega(\epsilon_\infty - \epsilon_0)$ term is insignificant in the present model at low temperatures and moderately low frequencies, which is the area of focus below.

Working in D dimensions, the solid is discretized into N^D points of a cubic lattice with sidelength $L = (N-1)a$. Two opposing faces of the cube are identified with the electrodes and short circuited. If the electrodes are subjected to a potential drop $\Delta\phi(s)$, the resulting current between the electrodes is given by $I(s) = Y(s)\Delta\phi(s)$. In order to calculate the macroscopic free charge conductivity from $Y(s)$ one has to subtract from $Y(s)$ the contribution due to the capacitor currents. Between the electrodes there are $N-1$ "layers" of parallel RC elements. The total current $I(s)$ is the same in each layer. Therefore, the sum of the resistor currents and the capacitor currents in the direction perpendicular to the electrodes is given by (with obvious notation)

$$\sum I_C(s) + \sum I_R(s) = (N-1)I(s) . \qquad (13)$$

The sum of the capacitor currents is rewritten as a sum of N^{D-1} terms where each term is the "one-dimensional" sum in the field direction (with obvious notation)

$$\sum a^{D-2}s\,\Delta\phi(i \to i+1, s) = a^{D-2}s\,\Delta\phi(s) .$$

Thus, Eq. (13) becomes

$$\sum I_R(s) = (N-1)I(s) - N^{D-1}a^{D-2}s\,\Delta\phi(s)$$

$$= [(N-1)Y(s) - N^{D-1}a^{D-2}s]\Delta\phi(s) . \qquad (14)$$

The macroscopic free charge conductivity is defined as the ratio between average free charge current density and average electric field. The former quantity is

$$\sum I_R(s)/[a^{D-1}N^{D-1}(N-1)]$$

and the latter is $\Delta\phi(s)/[(N-1)a]$. Using Eq. (14) we finally find

$$\sigma(s) = \frac{N-1}{N^{D-1}a^{D-2}}Y(s) - s . \qquad (15)$$

For $N \to \infty$, Eq. (15) reduces to

$$\sigma(s) = \frac{Y(s)}{L^{D-2}} - s \ . \tag{16}$$

For a given continuously varying local conductivity, $g(\mathbf{r})$, the discretization becomes exact for $a \to 0$. A few further assumptions are now made. First, it is assumed that the local conductivity is thermally activated and that the spatial variation in conductivity is due to the activation energy varying in space:

$$g(\mathbf{r}) = g_0 e^{-\beta E(\mathbf{r})} \ . \tag{17}$$

Here $\beta = 1/(k_B T)$. The activation energy is expected to vary because the local structure of the solid varies, leading to a varying mobility or perhaps to a varying internal electrostatic potential.[59,75,76] In most cases one expects the activation energy to vary relatively little; however, our main focus here and below is the low-temperature limit where the local conductivity eventually varies several orders of magnitude.

It is realistic to assume a finite correlation length, ξ, for $E(\mathbf{r})$, where ξ as usual is defined by

$$\langle E(\mathbf{r}) E(\mathbf{r}') \rangle \simeq E_0^2 \, e^{-|\mathbf{r}-\mathbf{r}'|/\xi} \ , \quad |\mathbf{r}-\mathbf{r}'| \to \infty \ . \tag{18}$$

We now make an assumption which is very useful both from an analytical point of view (Sec. IV) and a numerical point of view (Sec. V): It is assumed that, by putting the lattice constant a equal to ξ, correlations beyond a may be ignored.[57,77] The values of g are thus assumed to be uncorrelated from link to link. In this approximation the problem is fully specified by the local activation energy probability distribution, $p(E)$, while details regarding how the activation energy varies in space are ignored.

Let us consider the low- and high-frequency limits of $\sigma(s)$ in the model. For $s \to 0$ the capacitors play no role and all circuit currents are free charge currents. Effectively, the circuit reduces to an ordinary resistor circuit. Such resistor circuits have been investigated extensively in the low-temperature limit.[78-80] In this limit the current mainly follows the percolation paths giving the "easiest" ways between the electrodes. This picture is arrived at as follows. Imagine the resistors being removed from the lattice and then reintroduced in order of decreasing admittance. At a certain filling rate, the so-called link percolation threshold, infinitely large connected clusters appear, creating a connection between the electrodes. (In two dimensions the link percolation threshold is given by $p_c = \frac{1}{2}$ exactly[81] while simulations in three dimensions have shown that $p_c = 0.2488$.[82]) At low temperatures, adding further admittances beyond the percolation threshold does not change the overall circuit admittance significantly since the added admittances are much smaller than the admittances of the percolation cluster. Therefore, the total circuit admittance is dominated by the admittance of the percolation cluster that, in turn, is dominated by the smallest admittance on the cluster. This idea, which is now more than 20 years old,[78-82] was later proved rigorously.[83] At low temperatures one thus finds

$$\sigma(0) \propto e^{-\beta E_c} \ , \tag{19}$$

where the percolation energy E_c is defined by

$$\int_{-\infty}^{E_c} p(E) dE = p_c \ . \tag{20}$$

The high-frequency limit of the conductivity is straightforward to evaluate. For $s \to \infty$ the capacitors completely dominate the circuit. As a result the potential drop perpendicular to the electrodes is everywhere the same, corresponding to a uniform electric field, so the macroscopic conductivity is given by

$$\sigma(\infty) = \langle g \rangle \ . \tag{21}$$

In one dimension the circuit becomes particularly simple. Since the total circuit impedance is a sum of the impedances of RC elements, one finds if $g(E) = g_0 e^{-\beta E}$

$$\frac{1}{Y(s)} = (N-1) \int_{-\infty}^{\infty} \frac{p(E)}{a^{-1}[g(E)+s]} dE \ . \tag{22}$$

Substituted into Eq. (15) this implies for $N \to \infty$ the following equation for $\sigma(s)$:

$$\frac{1}{\sigma(s)+s} = \int_{-\infty}^{\infty} \frac{p(E)}{g(E)+s} dE = \int_0^{\infty} \frac{p(g)}{g+s} dg \ . \tag{23}$$

As a simple example consider the "box model," i.e., the case where $p(E) = 1/E_0 \ (0 < E < E_0)$. In that case the distribution of local admittances is (compare Appendix B)

$$p(g) = p(E) \left| \frac{dE}{dg} \right| = \frac{1}{\beta E_0} \frac{1}{g} \quad (g_0 e^{-\beta E_0} < g < g_0) \ . \tag{24}$$

Equation (23) thus becomes

$$\frac{1}{\sigma(s)+s} = \frac{1}{\beta E_0} \int_{g_0 e^{-\beta E_0}}^{g_0} \frac{1}{g(g+s)} dg$$

$$= \frac{1}{\beta E_0} \frac{1}{s} \ln \left[\frac{1+s/(g_0 e^{-\beta E_0})}{1+s/g_0} \right] \ . \tag{25}$$

For large β and low Laplace frequencies $(s \ll g_0)$ this reduces to

$$\sigma(s) + s = \beta E_0 \frac{s}{\ln[1+s/(g_0 e^{-\beta E_0})]} \ . \tag{26}$$

Letting s go to zero one finds that the dc conductivity is given by

$$\sigma(0) = \beta E_0 g_0 e^{-\beta E_0} \ . \tag{27}$$

Thus, the dc conductivity activation energy is equal to the largest activation energy met on the one-dimensional (1D) path between the electrodes. This is the 1D analogue of Eq. (19).

According to Eq. (26) the conductivity becomes frequency dependent when s is of order $s_0 = g_0 e^{-\beta E_0} = \sigma(0)/(\beta E_0)$. Thus, at low temperatures the frequency dependence sets in already for $s \ll \sigma(0)$. At these low temperatures and moderate frequencies s may be ignored in $\sigma(s) + s$, reflecting the fact that the capacitor currents are very small. Equation (26) may thus be written

$$\sigma(s)=\sigma(0)\frac{s/s_0}{\ln(1+s/s_0)}\ .\tag{28}$$

In terms of the real frequency ω and the characteristic time $\tau=\epsilon_\infty/s_0$, Eq. (28) becomes

$$\sigma(\omega)=\sigma(0)\frac{i\omega\tau}{\ln(1+i\omega\tau)}\ .\tag{29}$$

This equation was first derived for a hopping model.[45] Note that, even though the capacitor currents for $\beta\rightarrow\infty$ are very small for a range of low frequencies, the capacitors may not be ignored from the circuit. If the capacitors are removed, there is no frequency dependence left. Thus, while the free charge currents run through the resistors and the capacitor currents are extremely small, the latter still have a very important effect on the magnitude of the average free charge currents, resulting in the dramatic frequency dependence of Eq. (29). In the numerical simulations reported below in two and three dimensions the same effect was found at low temperatures.

IV. TWO APPROXIMATE ANALYTICAL SOLUTIONS

This section develops two analytical approximations for calculating $\sigma(s)$, focusing on the low-temperature region. In the $T\rightarrow0$ limit a universality appears and (except for a scaling) $\sigma(s)$ becomes independent of the activation energy probability distribution $p(E)$.

The standard approximation for treating disordered systems analytically is the effective-medium approximation.[77,84] In some contexts this approach is referred to as the coherent potential approximation (CPA).[85,86] It has a number of desirable analyticity properties and seems to offer the best available compromise between being simple and being realistic. Here, the problem is to calculate the overall admittance of a large network whose admittances are independent random variables. The basic idea of the EMA is to focus on one particular admittance of the network, regarding it as placed in an "effective medium" with equal admittances y_m. The effective medium is constructed to best possibly mimic the average surroundings of the particular admittance. This is done by requiring that the electric field around the particular admittance on the average is equal to the distant homogeneous field of the surrounding effective medium, leading to the following equation for determining y_m in D dimensions[77,87] (where sub y implies an average over the admittance probability distribution)

$$\left\langle\frac{y-y_m}{y+(D-1)y_m}\right\rangle_y=0\ .\tag{30}$$

The total network admittance Y is found from y_m (for $N\rightarrow\infty$) via the obvious identity

$$Y=N^{D-2}y_m\ .\tag{31}$$

The EMA is exact in one dimension and it becomes exact for $D\rightarrow\infty$.[88] In the high-frequency limit the EMA is correct in all dimensions for the circuit of Fig. 1. In two dimensions the EMA is believed to be quite reliable;[89] here it gives the correct percolation threshold $p_c=\frac{1}{2}$ and

in a recent weak disorder perturbation calculation it was shown that the EMA is correct up to and including the fourth-order terms.[90] These results in two dimensions are both consequences of the EMA satisfying the duality symmetry of the square lattice.[91] In three dimensions the EMA is less reliable;[84,90] thus the EMA predicts $p_c=\frac{1}{3}$, whereas simulations yield $p_c=0.2488$.[82] Various improvements of the EMA exist[92] but they are rather involved and will not be used here.

Combining Eqs. (12), (16), and (31) yields $y_m=a^{D-2}(\sigma+s)$. When this is substituted into Eq. (30) the EMA equation for the conductivity becomes[59] [using Eq. (12)]

$$\left\langle\frac{g-\sigma}{g+(D-1)\sigma+Ds}\right\rangle_g=0\ .\tag{32}$$

For $s\rightarrow\infty$, Eq. (32) correctly gives $\sigma=\langle g\rangle$ [Eq. (21)] because the denominator becomes almost constant and may be ignored. Equation (32) may be solved numerically (Appendix A). In the next section the predictions of Eq. (32) at finite temperatures are compared to the results of simulations in 2D. Here we proceed to investigate the $T\rightarrow0$ limit[14] where Eq. (32) implies a universal frequency dependence given as the solution of a simple transcendental equation.

Since $g-\sigma=g+(D-1)\sigma+Ds-D(\sigma+s)$, Eq. (32) may be rewritten as

$$\frac{1}{D(\sigma+s)}=\left\langle\frac{1}{g(E)+(D-1)\sigma+Ds}\right\rangle_E\ ,\tag{33}$$

where the average is now over the activation energy distribution and $g(E)=g_0\exp(-\beta E)$. In the limit $\beta\rightarrow\infty$, $g(E)$ varies rapidly and for given σ and s there are essentially just two extreme possibilities, depending on E, either $g(E)\ll(D-1)\sigma+Ds$ or $g(E)\gg(D-1)\sigma+Ds$. In the former case $g(E)$ may be ignored while in the latter case the denominator becomes very large and there is little contribution to the right-hand side. The energy separating the two cases, $E_g(s)$, is given by

$$E_g(s)=-\frac{1}{\beta}\ln\left[\frac{(D-1)\sigma+Ds}{g_0}\right]\ .\tag{34}$$

For large β, Eq. (33) thus becomes

$$\frac{1}{D(\sigma+s)}=\frac{1}{(D-1)\sigma+Ds}\int_{E_g(s)}^{\infty}p(E)dE\tag{35}$$

or

$$\frac{D-1}{D}+\frac{s}{D(\sigma+s)}=\int_{E_g(s)}^{\infty}p(E)dE\ .\tag{36}$$

Subtracting from Eq. (36) the $s=0$ case of Eq. (36) itself leads to

$$\frac{s}{D(\sigma+s)}=\int_{E_g(s)}^{E_g(0)}p(E)dE\ .\tag{37}$$

For large β, $E_g(s)$ is close to $E_g(0)$ and the integral may be replaced by $p[E_g(0)][E_g(0)-E_g(s)]$; thus,

$$\frac{s}{D(\sigma+s)} = -\frac{p[E_g(0)]}{\beta}\left[\ln\left|\frac{(D-1)\sigma(0)}{g_0}\right|\right.$$
$$\left. -\ln\left|\frac{(D-1)\sigma+Ds}{g_0}\right|\right]$$
$$= \frac{p[E_g(0)]}{\beta}\ln\left|\frac{\sigma}{\sigma(0)}+\frac{Ds}{(D-1)\sigma(0)}\right| . \quad (38)$$

Introducing the dimensionless variables

$$\bar{\sigma}=\frac{\sigma}{\sigma(0)}, \quad \bar{s}=\frac{\beta}{Dp[E_g(0)]\sigma(0)}s , \quad (39)$$

Eq. (38) for $\beta\to\infty$ reduces[14] to

$$\bar{\sigma}\ln(\bar{\sigma})=\bar{s} . \quad (40)$$

Equation (40) was previously derived for specific hopping models[69,45] and, in the context of macroscopically inhomogeneous solids, it was derived by Fishchuk for the box distribution of activation energies.[59] The importance of Eq. (40), however, as appears from the above derivation, lies in the fact that the equation is *universal*, completely independent of the activation energy probability distribution [an implicit assumption made above is that $p(E)$ is smooth around E_c]. Note that Eq. (40) is only valid for $D>1$; for $D=1$ one has $E_g(0)=\infty$ and the step leading from Eq. (37) to Eq. (38) is invalid.

Figure 2(a) shows the dimensionless conductivity of Eq. (40) (solid curve) in a log-log plot for real dimensionless Laplace frequencies [the solution of Eq. (40) is discussed in Appendix A that also gives an analytical approximation to $\bar{\sigma}(\bar{s})$]. For large and real $\bar{s}$ the conductivity follows an approximate power law $\bar{\sigma}\propto\bar{s}^u$, where u is about 0.9 in a large region. For large Laplace frequencies Eq. (40) roughly implies

$$\bar{\sigma}_{EMA}=\frac{\bar{s}}{\ln(\bar{\sigma}_{EMA})}\simeq\frac{\bar{s}}{\ln(\bar{s})} , \quad (41)$$

which, in turn, implies

$$u=\frac{d\ln(\bar{\sigma})}{d\ln(\bar{s})}\simeq 1-\frac{1}{\ln(\bar{s})} \quad (EMA, \bar{s}\gg 1) . \quad (42)$$

At real frequencies $\bar{s}$ is imaginary. Writing $\bar{s}=i\bar{\omega}$, Fig. 2(b) shows the real part $\bar{\sigma}'_{EMA}(\bar{\omega})$ (solid curve) and the imaginary part $\bar{\sigma}''_{EMA}(\bar{\omega})$ (dashed curve) of the conductivity. At large frequencies these functions both follow approximate power laws. From the approximate expression

$$\bar{\sigma}_{EMA}\simeq\frac{i\bar{\omega}}{\ln(i\bar{\omega})}=\frac{i\bar{\omega}}{\ln(\bar{\omega})+i(\pi/2)} \quad (\bar{\omega}\gg 1) \quad (43)$$

one finds

$$\bar{\sigma}'_{EMA}\simeq\frac{\pi}{2}\frac{\bar{\omega}}{\ln^2(\bar{\omega})}, \quad \bar{\sigma}''_{EMA}\simeq\frac{\bar{\omega}}{\ln(\bar{\omega})} \quad (\bar{\omega}\gg 1) . \quad (44)$$

This implies, for the approximate exponents defined by $\bar{\sigma}'\sim\bar{\omega}^{n'}$ and $\bar{\sigma}''\sim\bar{\omega}^{n''}$,

$$n'=1-\frac{2}{\ln(\bar{\omega})}, \quad n''=1-\frac{1}{\ln(\bar{\omega})} \quad (EMA, \bar{\omega}\gg 1) . \quad (45)$$

The conductivity at real Laplace frequencies, as well as both its real and imaginary parts taken at real frequencies, all become almost proportional to frequency as it goes to infinity. Note that this is not just a trivial effect reflecting conduction in the capacitors, since the capacitor currents do not contribute to the free charge conductivity. In fact, at any given temperature $\bar{\sigma}$ stabilizes and becomes frequency independent at sufficiently large frequencies [the frequency range where Eq. (40) is valid is
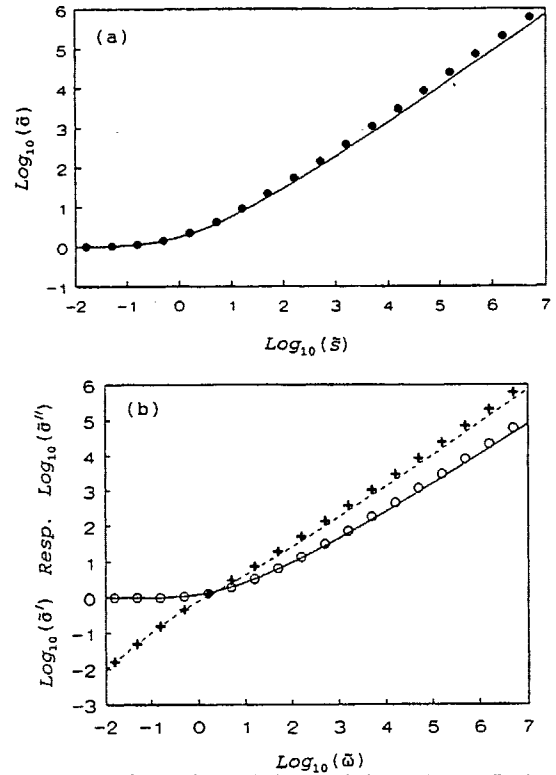

FIG. 2. Comparison of the predictions of the effective-medium approximation (EMA) and the percolation-path approximation (PPA) (see the next page) for the low-temperature universal frequency-dependent conductivity which is independent of the activation energy probability distribution. (a) shows a log-log plot of the function $\bar{\sigma}_{EMA}(\bar{s})$ at real dimensionless Laplace frequencies $\bar{s}$ [Eq. (40), solid curve] and the function $\bar{\sigma}_{PPA}(\bar{s}')$ [Eq. (47), dots], where $\bar{s}'=2\bar{s}$ scales the Laplace frequency so that the Taylor expansion of the two functions agree to first order at $\bar{s}=0$ (Ref. 45). (b) compares the real and imaginary parts of the two functions at real frequencies $\bar{\omega}=\bar{s}/i$, where $\bar{\sigma}'_{EMA}(\bar{\omega})$ is the solid curve, $\bar{\sigma}''_{EMA}(\bar{\omega})$ is the dashed curve, $\bar{\sigma}'_{PPA}(\bar{\omega}')$ is given by the circles, and $\bar{\sigma}''_{PPA}(\bar{\omega}')$ is given by crosses $(\bar{\omega}'=2\bar{\omega})$. The two approximations yield very similar predictions for the universal conductivity. In particular, one finds that their asymptotic behavior is identical as the frequency goes to infinity [Eqs. (42) vs (43) and (45) vs (50)].

only finite but becomes very large at low temperatures].

It is possible to throw light on the EMA solution by adopting a phenomenological point of view that makes sense in any dimension $D > 1$ at sufficiently low temperatures. In this regime, the admittances of the network vary many orders of magnitude and the currents primarily follow the paths of least resistance, the "critical" or "percolation" paths.[78,79] This is the idea leading to Eq. (19). We now propose an approximation referred to as the "percolation-path approximation" (PPA) that assumes that not only the dc currents but also the low-frequency ac currents mainly follow the percolation paths. The solid is regarded as having several independently conducting "channels," each channel corresponding to a percolation path. This approximation ignores the complicated fractal nature of the percolation cluster.[93] The problem of calculating the conductivity now becomes one-dimensional and one finds, as in Sec. III (where K is an unknown numerical constant),

$$\frac{1}{\sigma(s)+s} = K \int_{-\infty}^{E_c} \frac{p(E)}{g(E)+s} dE \ . \tag{46}$$

For a fixed range of frequencies around the transition frequency, the dominant contribution to Eq. (46) at low temperatures comes from energies close to E_c. Therefore, $p(E)$ may be replaced by $p(E_c)$ and the conductivity is the same as that of the one-dimensional box model already solved in Sec. III. Defining the dimensionless Laplace frequency $\tilde{s}=s/s_0$, the PPA thus predicts [compare Eq. (28)]

$$\tilde{\sigma}_{PPA}(\tilde{s}) = \frac{\tilde{s}}{\ln(1+\tilde{s})} \ . \tag{47}$$

This function is plotted in Fig. 2(a) for real $\tilde{s}$. The two solutions are very similar. As for the EMA solution one finds from Eq. (47) at real Laplace frequencies $\tilde{\sigma} \sim \tilde{s}^u$, where

$$u = 1 - \frac{1}{\ln(\tilde{s})} \quad \text{(PPA, } \tilde{s} \gg 1) \ . \tag{48}$$

At real frequencies $\tilde{\omega}=\tilde{s}/i$ one finds, since $\ln(1+i\tilde{\omega}) = \ln(1+\tilde{\omega}^2)/2 + i \arctan(\tilde{\omega})$,

$$\tilde{\sigma}'_{PPA}(\tilde{\omega}) = \frac{\tilde{\omega} \arctan(\tilde{\omega})}{\ln^2(1+\tilde{\omega}^2)/4+\arctan^2(\tilde{\omega})} \ ,$$

$$\tilde{\sigma}''_{PPA}(\tilde{\omega}) = \frac{\tilde{\omega} \ln(1+\tilde{\omega}^2)}{\ln^2(1+\tilde{\omega}^2)/2+2\arctan^2(\tilde{\omega})} \ . \tag{49}$$

For $\tilde{\omega} \rightarrow \infty$ one has $\tilde{\sigma}'_{PPA} \sim (\pi/2)\tilde{\omega}/\ln^2(\tilde{\omega})$ and $\tilde{\sigma}''_{PPA} \sim \tilde{\omega}/\ln(\tilde{\omega})$ leading to the exponents

$$n' = 1 - \frac{2}{\ln(\tilde{\omega})}, \quad n'' = 1 - \frac{1}{\ln(\tilde{\omega})} \quad \text{(PPA, } \tilde{\omega} \gg 1) \ . \tag{50}$$

These exponents are identical to those of the EMA [Eq. (45)].

Both the EMA and the PPA predict a universal frequency dependence of the low-temperature conductivity, independent of the activation energy probability distribution [assuming $p(E)$ is smooth around E_c]. Note that

the two approximations yield similar predictions (Fig. 2), despite being derived from completely different points of view. The EMA, which is usually believed to be best for systems with *weak* disorder,[88,90,94] has here been applied in the limit of extreme disorder. The PPA, on the other hand, only makes sense for the extreme disorder found at low temperatures. The similarity between the two approximations indicates that the EMA may be reliable even for systems of extreme disorder. On the other hand, the quantitative EMA prediction for the dc conductivity is known to be wrong in 3D because the percolation threshold is wrongly predicted, and thus one can, at most, expect the *shape* of the conductivity curve to be correct in the EMA. Only computer simulations can give reliable information as to whether universality really exists and, if it exists, whether it is well described by the two approximate theories.

V. COMPUTER SIMULATIONS

This section reports the results of computer simulations of the model in two and three dimensions. A lattice of admittances like in Fig. 1 is generated where each impedance is determined by an activation energy randomly chosen according to a probability distribution $p(E)$. Several different probability distributions were used; in Appendix B is explained how the activation energies were generated. At low temperatures large lattices are needed to obtain reasonable statistics. Even for relatively large lattices the system is not self-averaging at low temperatures and it is necessary to average over several lattices to obtain reproducible results. As a rule of thumb this procedure works well for $\beta < N$ whereas for larger β the fluctuations become too large to be averaged out in a reasonable number of simulations. For simplicity all simulations are carried out at *real* Laplace frequencies only; by analytic continuation this is enough when one wants to compare the simulations to an analytical expression for the conductivity.

The calculation of the frequency-dependent conductivity may be performed by several methods. One possibility, the "brute force method," is to solve Kirchhoff's equations for the potential via some sparse matrix algorithm. Another possibility is to use Eq. (15) and calculate the overall circuit admittance between short-circuited electrodes by "elimination methods." These methods eliminate nodes of the lattice one by one by introducing new admittances without changing the overall circuit admittance, a process that is continued until one is left with only one admittance. The most general elimination method was introduced into the field by Fogelholm in 1980;[95] it works as follows. Whenever a node is eliminated that has n neighbors and the admittances $Y_1, \ldots, Y_n$ to its neighbors, all possible connections between the neighbors are introduced such that the ith and the jth neighbors are given the [additional] admittance $Y_i Y_j/(Y_1 + \cdots + Y_n)$. For a full lattice the algorithm becomes very inefficient, but it works very well for calculations close to the percolation threshold where many admittances are zero.[a] In two dimensions Frank and Lobb have developed a useful algorithm that eliminates nodes

by working each of them towards the lower right via con-
secutive star-triangle transformations.[96] By means of this
algorithm it is possible to calculate the admittance of a
200×200 lattice in a few minutes on a modern PC.

Unfortunately no similarly efficient algorithm is avail-
able in 3D. Here it was found most efficient to use brute
force methods. It is a rather complex numerical problem
to solve large sparse systems of linear equations when the
coefficients vary several decades. The standard Gauss-
Seidel, as well as overrelaxation methods,[97] converge too
slowly. Fortunately, an algorithm has been developed,
the algebraic multigrid (AMG),[98,99] that was made pre-
cisely for problems of this type. The algorithm is an alge-
braic generalization of the standard geometric multigrid
method used for solving elliptic differential equations.
An excellent introduction to the multigrid idea, in gen-
eral, has been given by Goodman and Sokal.[100] The
AMG solves a problem in a time only proportional to the
number of equations. For an $N \times N$ lattice in 2D the
computing time thus varies as N^2, for an $N \times N \times N$ lat-

tice in 3D the time varies as N^3. The Frank-Lobb algo-
rithm in 2D has a computing time varying as N^3; howev-
er, in practical applications it is still superior to the
AMG because it avoids overflow problems and because
the prefactors are clearly in its favor. It should be men-
tioned that other methods are also available. The
transfer matrix method[101] is an elimination method that
works in all dimensions, and the Fourier acceleration
brute force method[102] is an alternative to the AMG for
speeding up the Gauss-Seidel relaxation scheme.

Results of simulations in 2D of 100×100 lattices have
been reported elsewhere[14] for five activation energy prob-
ability distributions at the dimensionless inverse tempera-
tures $\beta = 4, 16, 64$. In Fig. 3, these results are supplement-
ed by simulations of 200×200 lattices at
$\beta = 5, 10, 20, 40, 80, 160$ for the following activation energy
distributions (see Appendix B): (a) asymmetric Gaussian,
(b) symmetric exponential, (c) power law with exponent
-4, (d) triangle. For each temperature and activation
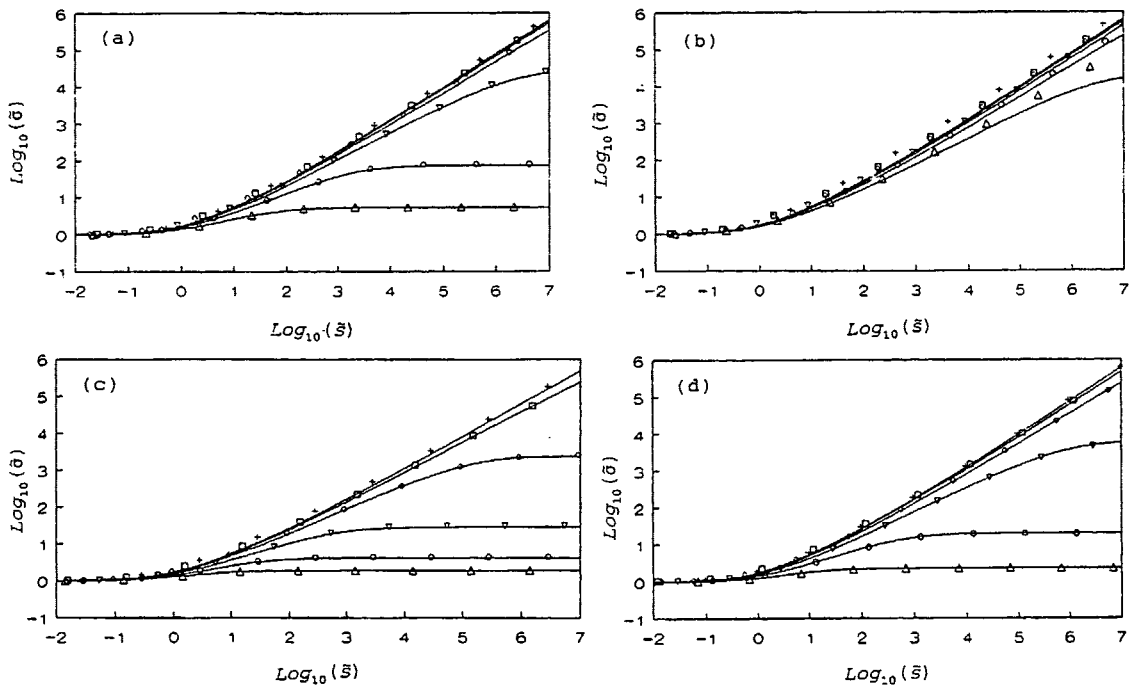energy distribution the figure shows the average of 10

FIG. 3. Log-log plots of results of computer simulations in 2D for the dimensionless conductivity $\tilde{\sigma}$ (points) compared to the EMA
predictions (solid curves) at real dimensionless Laplace frequencies $\tilde{s}$ [$\tilde{s}$ and $\tilde{\sigma}$ are defined in Eqs. (8) and (39)]. Each figure shows the
results of averaging 10 simulations of a 200×200 lattice solved by the Frank-Lobb algorithm (Ref. 96) and Eq. (15). Results for the
following dimensionless inverse temperatures are shown: $\beta = 5$ ($\triangle$), $\beta = 10$ ($\bigcirc$), $\beta = 20$ (∇), $\beta = 40$ ($\Diamond$), $\beta = 80$ ($\square$), $\beta = 160$ ($+$), for
the following activation energy probability distributions (Appendix B): (a) Asymmetric Gaussian, (b) symmetric exponential, (c)
power law with exponent -4, (d) triangle. In each case the distribution should be thought of as centered around an energy $\bar{E}$; this
gives an extra factor $e^{-\beta \bar{E}}$ to the conductivity and scales the frequencies by the same amount, leaving both $\tilde{\sigma}$ and $\tilde{s}$ unchanged. The
EMA predictions were found by solving Eq. (32) numerically (Appendix A). Given the fact that the EMA has no fitting parameters
and that $\tilde{s}$ is defined by scaling s by a factor which is in some cases larger than 10^{30}, the EMA provides a very good fit to the simula-
tions. In particular, at low temperatures the frequency-dependent conductivity becomes universal both in the EMA and in the simu-
lations.

JEPPE C. DYRE

simulations. The solid curves are the EMA predictions found by solving Eq. (32) numerically (Appendix A). The EMA works well in 2D at all temperatures. In particular, one finds that universality is approached as $T \rightarrow 0$. Some of the low-temperature results deviate from the EMA prediction. However, given the fact that the frequency in some cases (at low temperatures) has been shifted more than 50 decades according in Eq. (39), the fit must be said to be satisfactory. The *shape* of the simulated frequency dependent conductivity at low temperatures is studied in Fig. 4 where the $\beta = 80, 160$ results from Fig. 3 have been replotted and supplemented by simulations of the Cauchy and the Box distribution. In Fig. 4, an empirical scaling of the Laplace frequency was allowed to fit the EMA universality prediction [Eq. (40)] in the best possible way.

In three dimensions results for averages of five $50 \times 50 \times 50$ lattices are shown in Fig. 5 for the values $\beta = 10, 30, 60$ for the Cauchy and box activation energy
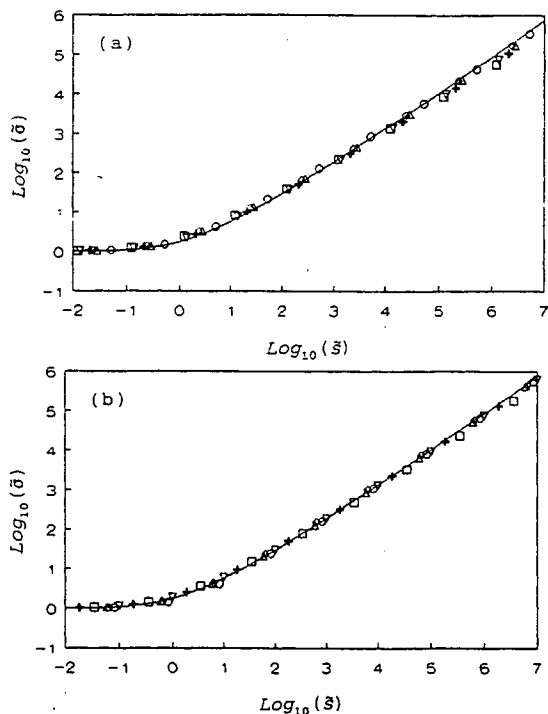
distributions. The conductivity was found by solving Kirchhoff's equations to determine the potential at each node and subsequently averaging all resistor currents. A potential $\phi = 0$ was imposed at one electrode and $\phi = 1$ at the other electrode; the remaining four faces of the cube were joined by imposing periodic boundary conditions. The 120 000 equations for the node potentials were solved by means of the AMG1R5 FORTRAN algebraic multigrid subroutine available from the Yale multigrid library.[103] This subroutine was found to be efficient, well documented, and providing useful error statements and warnings. The subroutine was previously successfully used for large
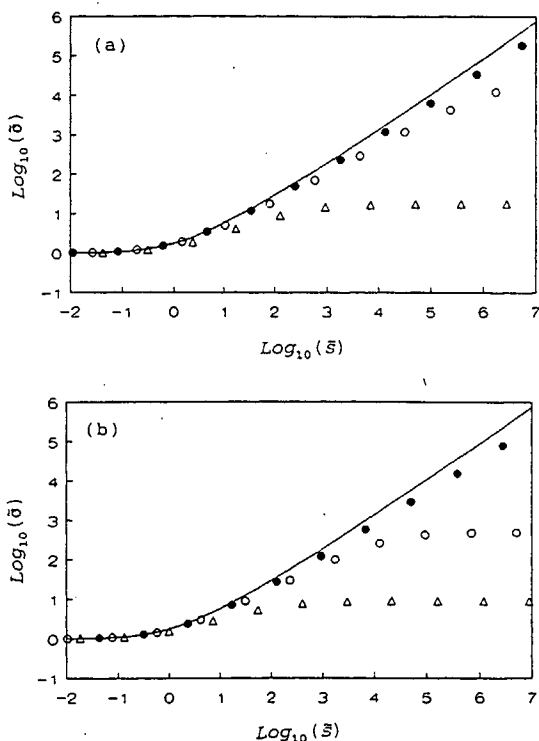

FIG. 4. Test of the EMA prediction at real dimensionless Laplace frequencies $\tilde{s}$ for the low-temperature universal conductivity [solid curve, Eq. (40)] in log-log plots. An empirical rescaling of $\tilde{s}$ has been allowed here to facilitate a comparison to the EMA prediction focusing only on the *shape* of $\tilde{\sigma}(\tilde{s})$. The figure shows results for $\beta = 80$ (a) and $\beta = 160$ (b) for asymmetric Gaussian ($\triangle$), Cauchy ($\bigcirc$), symmetric exponential ($\lozenge$), power law with exponent -4 ($\square$), box ($+$), triangle (∇). As in Fig. 3 the results were obtained by averaging over 10 simulations of a 200×200 lattice in 2D solved by means of the Frank-Lobb algorithm (Ref. 96) and Eq. (15).

FIG. 5. Approach towards universality at low temperatures in three dimensions plotted in log-log plots. The figures show results for $\tilde{\sigma}$ at real dimensionless Laplace frequencies $\tilde{s}$ [both quantities are defined in Eqs. (8) and (39)] at $\beta = 10$ ($\triangle$), $\beta = 30$ ($\bigcirc$), and $\beta = 60$ ($\bullet$), for (a) the Cauchy and (b) the box distributions. Similar results were found for other distributions. Each point represents the average of five simulations of a $50 \times 50 \times 50$ lattice where Kirchhoff's equations were solved by the algebraic multigrid algorithm using the AMG1R5 Fortran subroutine (Ref. 103). The solid curve is the EMA prediction for the low-temperature universal conductivity [Eq. (40)]. As in Fig. 4, an empirical rescaling of $\tilde{s}$ was allowed, to focus on the *shape* of the conductivity curve only. Universality is approached at low temperatures, but unfortunately it was not possible to go to low enough temperatures to allow a detailed study of the exact shape of the universal conductivity in 3D.

resistor network calculations by Edwards, Goodman, and Sokal.[104] Still, the present problem is very complex because at low temperatures the coefficients of the linear equations vary several orders of magnitude. To avoid overflow and "division by zero" problems, the equations must be "massaged" somewhat. This was done by increasing the lowest g's to a standard low value, a procedure that is easily justified since these weak links carry little current anyway. The highest g's were also changed to a standard value by lowering them; this is allowed because they more or less short circuit their nodes anyway: they are not "bottlenecks" for the conduction process. In both cases, it was carefully checked that the calculated conductivity is independent of the cutoff's introduced, proving that the procedure it permissible. The calculations are rather demanding; the present work was carried out on a modern workstation with 128 MB of memory (the AMG1R5 is quite memory consuming). The results are shown in Fig. 5 where they are compared to the EMA prediction (solid curve) as regards the predicted *shape* of the conductivity curve allowing an empirical frequency rescaling as in Fig. 4. Again one finds at low temperatures that the universal conductivity curve is approached. Similar results were found for four other activation energy probability distributions.[4] Unfortunately, it was not possible to go to lower temperatures without serious overflow problems. At present it is therefore not possible to determine whether the universal conductivity curve in 3D is slightly less steep than in 2D.

Finally, it should be mentioned that in both the 2D and the 3D simulations it was found that the capacitor currents at low temperatures are very small compared to the resistor currents in a wide range of frequencies around the transition frequency, thus confirming the analytical result for the 1D box model reported at the end of Sec. III.

VI. DISCUSSION

This paper has investigated the ac consequences of having a spatially varying electrical conductivity, focusing on the low-temperature limit in the case when the local conductivity is thermally activated. The fact that spatial inhomogeneities give rise to polarization phenomena and therefore to a frequency dependence of the macroscopic conductivity has been known for many years. Despite this, little work has gone into studying ac aspects of the "macroscopic" model involving a range of local conductivities. For instance, no papers were given dealing with ac properties in this model of inhomogeneous media at the two "Conferences on Electrical Transport and Optical Properties of Inhomogeneous Media" held in 1978 and 1988.[105] Alternating current properties are instead usually modeled by means of hopping models where the disorder is assumed to be on the atomic scale.[8−10,35,43−45] Hopping models usually do not include Coulomb interactions, a problem of recent concern,[12] whereas the macroscopic model does include the effect of Coulomb interactions via Gauss' law.

The idea of a spatially randomly varying activation energy for the conductivity has been discussed for some time in connection with particular systems like heavily

doped or compensated semiconductors[59,75] or granular materials.[76] For any disordered system one expects the various forms of inhomogeneities to influence the exact value of the activation energy of the local conductivity. The question is not whether or not this effect is present, but whether it is so pronounced that the concept of a local conductivity stops making sense, in which case the relevant model to use is a hopping model. At present it is not clear which disordered solids are best described by the macroscopic model and for which hopping models are best.

For a solid with a spatially varying conductivity, the relevant Maxwell's equations in a periodic external field boils down to the single equation (9) for the electrostatic potential. This equation is discretized by putting it on a cubic lattice. If the lattice constant a is taken to zero, the discretization becomes exact. In Sec. III, however, the model was simplified further by choosing a equal to the activation energy correlation length and by ignoring correlations beyond a. Thereby one ignores details of how the conductivity varies in space and the model becomes uniquely defined by the local activation energy probability distribution.

The discretization of Eq. (9) corresponds to the electric network of Fig. 1. Similar networks have been used many times before as models for the ac properties of disordered solids[11,21,28,34,50−55] and the one-dimensional version of the network lies behind the electric modulus formalism.[28] However, the network is traditionally used just as a suggestive picture of the solid and not justified from basic principles. When this is done (Sec. III) it turns out that the interpretation of the circuit is rather subtle. The network is *not* to be thought of as a straightforward representation of the solid. This is because the capacitor currents are Maxwell's displacement currents, parts of which do not involve real charge transport. In the model the *free charge* contribution to the conductivity depends on frequency only as an *indirect* effect of the capacitors: They influence the electrostatic potential that determines the resistor currents.

A simple model which may be solved exactly is the one-dimensional box model. In this model, as $\beta \rightarrow \infty$, there is a strongly frequency-dependent conductivity. It follows from Eq. (29) [compare Eq. (44)] that well above the transition frequency, the phase difference between the average field and the average *resistor* current is close to $\pi/2$ [for any nonzero temperature Eq. (29) is only valid in a finite range of frequencies, but this range becomes very large at low temperatures]. This happens while at the same time the capacitor currents are very small compared to the resistor currents. The same peculiar effect of a strong frequency dependence of the average resistor currents simultaneously with very small capacitor currents was also observed in the computer simulations in 2D and 3D.

The model was studied by computer simulations in 2D and 3D. In 2D, the results were fitted to the EMA prediction of Eq. (32). In 3D it is necessary to regard the scaling involved in the definition of the dimensionless Laplace frequency as a fitting parameter to obtain a reasonable fit. This is because the EMA has the percolation

threshold wrong in 3D.

There are two conclusions to be drawn from the simulations. First, the simulations show that the frequency dependence of the conductivity indeed *is* universal at low temperatures. As far as is known to the author, the present work is the first time universality has been derived analytically and the first time universality has been seen in computer simulations of any model for ac conduction. The universality represents a new type of regularity valid for systems with extreme disorder. It should be noted, however, that, by letting the temperature go to zero, one actually moves into an unphysical domain since at temperatures of the order 10–30 K other processes such as tunneling would usually be expected to dominate the conduction. This has been ignored here.

In 1985, Summerfield[44] reported that several hopping models involving tunneling electrons solved in the extended pair approximation yield almost identical predictions for the frequency dependence of the conductivity. This phenomenon was referred to as "quasiuniversality." Since no simulations were reported it was not clear whether the effect is real or due to the approximation used, and there was no study of the temperature dependence of the conductivity for activated jump rates indicating an approach to true universality as $T \rightarrow 0$. Still, Ref. 44 gives the first hint to the existence of universality.

The second conclusion to be drawn from the simulations is that the EMA works very well in 2D at all temperatures. In 3D as $T \rightarrow 0$ the EMA also works well if a phenomenological rescaling is allowed to compensate for the fact that the EMA has the percolation threshold wrong. These results are highly nontrivial since doubt has often been expressed as to how reliable the EMA is for systems with a broad distribution of admittances.[88,90,94] In one dimension the EMA universality prediction is not valid. But otherwise, since the EMA becomes exact for $D \rightarrow \infty$,[88] there is reason to believe in Eq. (40) for all $D > 1$ as a good approximation to the universal conductivity.

The percolation-path approximation is based on the fact that the percolation paths are preferred at low temperatures. These paths contain activation energies ranging up to a sharp cutoff at E_c given by Eq. (20). Furthermore, in a fixed frequency range around the transition frequency it is clear that, at sufficiently low temperatures, only a narrow interval of activation energies are important (namely, those around the percolation energy determining the smallest admittances on the percolation paths). Therefore, the circuit admittance is expected to correspond to that of a one-dimensional solid with a sharp activation energy cutoff; this is why the PPA predicts the same frequency response as the one-dimensional box model. The fact that the PPA solution is very similar to the EMA solution shows that at sufficiently low temperatures a disordered solid, as a consequence of the underlying percolation, looks like a one-dimensional solid with a sharp cutoff in the activation energy distribution.

The PPA is not quite as straightforward as it seems at first sight. For very small s the currents do follow the percolation paths, and as long as $s \ll g_c$, where g_c is the smallest admittance on a percolation path, the conduc-

tivity is clearly frequency independent. The conductivity starts to increase only for $s = s_0$, where $s_0 \sim g_c$. But this is exactly the regime where the percolation picture starts to break down because all surrounding admittances also become of order g_c. In this range of frequencies the currents still mainly follow the percolation paths; however, when the current meets one of the poorest admittances on a percolation path, it may as well pass through the surrounding admittances. But since this happens seldomly, one expects the percolation-path calculation to be roughly valid, as confirmed by the simulations.

Since the dc conductivity is determined by the poorest admittances on a percolation path (of order g_c), the Laplace frequency for onset of ac conduction, s_0, is of order $\sigma(0)$. In particular, one expects $\sigma(0)$ and s_0 to have the same temperature dependence. This is consistent with the BNN relation [Eq. (2)]. The EMA and the PPA both predict that s_0 scales with $T\sigma(0)$ rather than with just $\sigma(0)$. This is sometimes referred to as "Summerfield scaling"[44] though it was first discussed by Scher and Lax in their papers on the continuous time random walk approximation.[43] It is interesting to note that the extra factor T in the Summerfield scaling of *hopping models*[43–45] is derived from the $1/(k_B T)$ factor of the fluctuation-dissipation theorem Eq. (4) that is not applied in the macroscopic model.

What are the consequences of the presently reported results for the interpretation of experiments? First, it is to be noted that the EMA (or the PPA) $T \rightarrow 0$ universality prediction gives a rather good fit to many experiments. This has been shown in detail elsewhere[45] where a box-type hopping model yielding the same frequency-dependent conductivity [Eqs. (40) and (47)] was discussed in detail. Thus, as in experiments[45] Eq. (40) or (47) imply, (1) $\sigma'(\omega)$ follows an approximate power law with an exponent n' less that but close to one, where $n'(\omega)$ is weakly increasing and $n' \rightarrow 1$ as $T \rightarrow 0$ (the latter is because, in a fixed frequency range, as the temperature goes to zero, one in effect measures further and further out on the universal conductivity curve); (2) when there is no detectable dc conductivity, the exponent is very close to one; (3) the BNN relation [Eq. (2)] is satisfied with $p = 0.59$ in the EMA and $p = 0.42$ in the PPA; (4) the time-temperature superposition principle is satisfied; (5) the ac conductivity is less temperature dependent than the dc conductivity and for n' very close to one the ac conductivity becomes almost temperature independent, in particular, this always happens as $T \rightarrow 0$; (6) while $\sigma(0)$ may vary several orders of magnitude for different solids at different temperatures, the ac conductivity varies only relatively little [points (5) and (6) follow from the fact that $\Delta\epsilon$ is usually of order ϵ_0]. While the universal conductivity of Eqs. (40) or (47) reproduce many observations surprisingly well, the use of log-log plot comparisons alone has rightly been warned against by Macdonald.[106]

Whenever the universal conductivity gives a good fit to experiments it seems that little can be learned from ac measurements. For instance, observing a power-law dependence for the real part of the conductivity with an exponent of 0.8 a few decades above the transition frequency provides no useful information about the solid un-

der study. This is contrary to ones intuition. In 1972, Pollak and Pike[107] suggested that the microscopic details of a solid are reflected in deviations from $n'=1$. But it now appears that the situation is more complex: Details about the microscopic conduction mechanism are to be deduced from deviations from the *universal conductivity curve*, that itself has a nontrivial structure.

The universality seen in the macroscopic model at low temperatures is also present at low temperatures in hopping models, with an identical predicted universal frequency dependence.[108] At first sight this is surprising, since hopping models are in many respects complementary to the macroscopic model: (1) hopping models are microscopic, not macroscopic; (2) they usually involve noninteracting charge carriers and ignore Coulomb interactions; (3) in hopping models one controls the local electric field while in the macroscopic model the overall potential difference is controlled; and finally (4) hopping models are stochastic while the macroscopic model is deterministic. Still, both types of models lead to large systems of sparse linear equations with coefficients that at low temperatures vary several orders of magnitude. Apparently this is enough to produce the same universality for the conductivity. Several mathematical connections exist between hopping models and resistor networks,[10,109] but it is not possible to transform a hopping model into the network of Fig. 1. The Miller-Abrahams equivalent circuit for a hopping model has capacitors from each node to a voltage generator that is connected to the ground.[47,72] In conclusion, ac measurements alone cannot determine what the relevant model is for conduction in a given disordered solid. To this end other measurements have to be performed[30] like, e.g., transient current experiments monitoring the current after a brief laser pulse excitation,[30,110,111] nonlinear conductivity measurements (the macroscopic model becomes nonlinear much earlier than hopping models), $1/f$ noise measurements,[112] or possibly Hall effect measurements.[113]

Some open questions remain. Is the universality seen in computer simulations as $T \rightarrow 0$ a mathematically exact fact (as believed by the author) or is there just "quasi-universality"? It is clear that the universality is closely linked to the percolation phenomenon, but around the percolation threshold it has recently been shown[114,115] (albeit in a different context than the present) that there are *nonuniversal* critical exponents when a broad distribution of admittances is involved. If the universality is confirmed, what is the exact form of the universal frequency dependence? Is it truly independent of the dimension? From the existence of long-time tails one expects the universal conductivity curve to be nonanalytic at $\tilde{s}=0$. However, since the universal conductivity exists as a limit only, it is actually possible that the function *is* analytic and that one of Eqs. (40) or (47) is exact.

APPENDIX A: SOLVING THE EMA EQUATION

Equation (32) may easily be solved at any temperature and real Laplace frequency. The solid curves of Fig. 3 were obtained by discretizing the equation into 3000 terms using regularly spaced energies; the conductivity was then determined at fixed s and β by the bisection method.[97] Before this is done, it is convenient to rewrite Eq. (32) in terms of the variables $\tilde{\sigma}$ and $\tilde{s}$ defined in Eq. (39).

The universal conductivity given by Eq. (40) may be determined by means of the Newton-Raphson method. Consider first the case of real dimensionless Laplace frequencies $\tilde{s}$. Introducing $\lambda = \ln(\tilde{\sigma})$, Eq. (40) is rewritten by taking ln on both sides:

$$\lambda + \ln(\lambda) = \ln(\tilde{s}) . \tag{A1}$$

The Newton-Raphson method[97] for solving the equation $f(\lambda)=0$ consists of iterating after the recipe

$$\lambda_{n+1} = \lambda_n - \frac{f(\lambda_n)}{f'(\lambda_n)} . \tag{A2}$$

In the case $f(\lambda) = \lambda + \ln(\lambda) - \ln(\tilde{s})$, Eq. (A2) becomes

$$\lambda_{n+1} = \lambda_n \frac{1 - \ln(\lambda_n) + \ln(\tilde{s})}{1 + \lambda_n} . \tag{A3}$$

Equation (A3) is iterated until convergence by starting with, e.g., $\lambda_1 = \tilde{s}$ if $0 < \tilde{s} < 1$ [utilizing the fact that $\lambda = \ln(\tilde{\sigma}) \cong \tilde{s}$ for small frequencies] and starting with, e.g., $\lambda_1 = 1$ if $\tilde{s} > 1$.

An analytic fit to $\tilde{\sigma}(\tilde{s})$ is the following expression:

$$\tilde{\sigma}(\tilde{s}) = \frac{\tilde{s}}{\mathcal{L}_1(\tilde{s}) + b\mathcal{L}_2(\tilde{s}) + c\mathcal{L}_3(\tilde{s}) - (b+c)\mathcal{L}_4(\tilde{s})} , \tag{A4}$$

where $\mathcal{L}_1(\tilde{s}) = \ln(1+\tilde{s})$ and one recursively defines $\mathcal{L}_{i+1}(\tilde{s}) = \ln[1 + \mathcal{L}_i(\tilde{s})]$. The case $b = c = 0$ corresponds to the PPA solution Eq. (47). For $b = -2.2$ and $c = 3.5$, Eq. (A4) provides a fit whose logarithm (base 10) for all $\tilde{s}$ is within 0.01 of the logarithm of the true solution.

At real frequencies $\tilde{\omega} = \tilde{s}/i$, the EMA equation becomes complex, but it can still be solved by the Newton-Raphson method. Writing $\lambda = x + iy$, Eq. (A2) becomes

$$x_{n+1} = x_n - \frac{A_1(n)B_1(n) - A_2(n)B_2(n)}{\mathcal{D}(n)} , \tag{A5}$$

$$y_{n+1} = y_n - \frac{A_1(n)B_2(n) + A_2(n)B_1(n)}{\mathcal{D}(n)} ,$$

where, if $L_1(n) = \ln(x_n^2 + y_n^2)/2$ and $L_2(n) = \arctan(y_n/x_n)$, the following abbreviations have been introduced:

$$A_1(n) = x_n^2 - y_n^2 + x_n[L_1(n) - \ln(\tilde{\omega})] + y_n\left[\frac{\pi}{2} - L_2(n)\right] ,$$

$$A_2(n) = 2x_n y_n + x_n\left[L_2(n) - \frac{\pi}{2}\right] + y_n[L_1(n) - \ln(\tilde{\omega})] ,$$

$$\text{(A6)}$$

$$B_1(n) = 1 + x_n ,$$

$$B_2(n) = y_n ,$$

$$\mathcal{D}(n) = B_1{}^2(n) + B_2{}^2(n) .$$

Equation (A5) is iterated until convergence starting with, e.g., $x_1 = 0.01$ and $y_1 = \tilde{\omega}$ if $0 < \tilde{\omega} < 1$ [reflecting $\lambda = \ln(\tilde{\sigma}) \cong i\tilde{\omega}$ at low frequencies] and with, e.g., $x_1 = 1$ and $y_1 = 0$ if $\tilde{\omega} > 1$.

Substituting $\tilde{s} = i\tilde{\omega}$ into Eq. (A4) provides an analytic approximation of both $\tilde{\sigma}'(\tilde{\omega})$ and $\tilde{\sigma}''(\tilde{\omega})$. For the real part the fit (again with $b = -2.2$ and $c = 3.5$) has a logarithm (base 10) within 0.03 of the exact solution; for the imaginary part the logarithm of the fit is within 0.05 of the exact value for $\tilde{\omega} > 10^{-2}$ (for smaller frequencies the fit becomes poor).

APPENDIX B: ACTIVATION ENERGY PROBABILITY DISTRIBUTIONS

In the computer simulations of Ref. 14 and the present paper dimensionless activation energies were used. With the exceptions of the two Gaussian distributions the activation energies for a given probability distribution $p(E)$ were generated by utilizing the following well-known fact. If x is a uniformly distributed random number between 0 and 1 and $E(x)$ is some function of x, E is distributed according to the $p(E)$ given by $dp = p(E)|dE| = p(x)|dx|$. Since $p(x) = 1$ one thus finds

$$p(E) = \frac{1}{|dE/dx|} . \tag{B1}$$

To avoid spurious effects due to subtle correlations in system-supplied random numbers, the random numbers were generated using the function RAN0.[97] This function starts by setting up an array RAN[i] of 97 system-supplied random numbers. Reliable random numbers x are supplied by RAN0 by using the given random pointer to an index i_y between 1 and 97: RAN0 then returns $x = $RAN[$i_y$] and a new system-supplied random number is filled into the RAN array to replace x. Finally, x is used to generate the new pointer index i_y which is used to point out the next random number, etc.

The percolation threshold p_c is given by $p_c = 0.5000$ (exactly) in 2D and $p_c = 0.2488$ in 3D.[81,82] The percolation energy E_c that determines the dc conductivity activation energy [Eq. (19)] is found from Eq. (20):

$$\int_{-\infty}^{E_c} p(E)dE = p_c . \tag{B2}$$

A knowledge of E_c helps one to locate the frequency range of interest in the simulations; in 2D one also has $E_g(0) = E_c$ [Eq. (34)]. If $E(x)$ is an increasing function of

x one finds from Eqs. (B1) and (B2)

$$E_c = E(x = p_c) . \tag{B3}$$

The following activation energy distributions were used in the simulations of Ref. 14 and this paper.

(1) Gaussian. From 12 random numbers x_i (between 0 and 1), $E = \sum_{i=1}^{12} x_i - 6$ gives a nice Gaussian distribution of E with variance 1:[97]

$$p(E) = \frac{1}{\sqrt{2\pi}} \exp\left[-\frac{E^2}{2}\right] \quad (-\infty < E < \infty) . \tag{B4}$$

The percolation energies are determined from Eq. (B2) that implies $\text{erf}(-E_c/\sqrt{2}) = 1 - 2p_c$. Denoting the percolation energy in 2D by $E_c^{(2)}$ and in 3D by $E_c^{(3)}$ one finds

$$E_c^{(2)} = 0, \quad E_c^{(3)} = -0.678 . \tag{B5}$$

(2) Asymmetric Gaussian. For 12 random numbers one calculates $E = |\sum_{i=1}^{12} x_i - 6|$; this generates the distribution

$$p(E) = \sqrt{2/\pi} \exp\left[-\frac{E^2}{2}\right] \quad (0 < E < \infty) . \tag{B6}$$

Equation (B2) implies $\text{erf}(E_c/\sqrt{2}) = p_c$; thus,

$$E_c^{(2)} = 0.674, \quad E_c^{(3)} = 0.317 . \tag{B7}$$

(3) Cauchy. Writing $E = \tan[(\pi/2)x]$, where x is random, produces, according to Eq. (B1),

$$p(E) = \frac{2}{\pi}\frac{1}{1+E^2} \quad (0 < E < \infty) . \tag{B8}$$

Equation (B3) implies $E_c = \tan[(\pi/2)p_c]$; thus,

$$E_c^{(2)} = 1, \quad E_c^{(3)} = 0.412 . \tag{B9}$$

(4) Exponential. If $E = -\ln(1-x)$ one finds

$$p(E) = e^{-E} \quad (0 < E < \infty) . \tag{B10}$$

Equation (B3) implies $E_c = -\ln(1-p_c)$; thus,

$$E_c^{(2)} = 0.693, \quad E_c^{(3)} = 0.286 . \tag{B11}$$

(5) Symmetric exponential. If $E = \pm\ln(1-x)$ with a random sign one finds

$$p(E) = \tfrac{1}{2}e^{-|E|} \quad (-\infty < E < \infty) . \tag{B12}$$

Equation (B2) implies $E_c = \ln(2p_c)$; thus,

$$E_c^{(2)} = 0, \quad E_c^{(3)} = -0.698 . \tag{B13}$$

(6) Power law with exponent -4. If $E = x^{-1/3} - 1$ one finds

$$p(E) = 3(1+E)^{-4} \quad (0 < E < \infty) . \tag{B14}$$

Equation (B2) implies $E_c = (1 - p_c)^{-1/3} - 1$; thus,

$$E_c^{(2)} = 0.260, \quad E_c^{(3)} = 0.100 . \tag{B15}$$

(7) Box. If $E = x$ one finds

$$p(E) = 1 \quad (0 < E < 1) \tag{B16}$$

and

$$E_c^{(2)} = 0.500, \quad E_c^{(3)} = 0.249 . \tag{B17}$$

(8) Triangle. If $E = x^{1/2}$ one finds

$$p(E) = 2E \quad (0 < E < 1) . \tag{B18}$$

Equation (B3) implies $E_c = p_c^{1/2}$; thus,

$$E_c^{(2)} = 0.707, \quad E_c^{(3)} = 0.499 . \tag{B19}$$

[1] A. K. Jonscher, Nature 267, 673 (1977); *Dielectric Relaxation in Solids* (Chelsea Dielectric, London, 1983).

[2] A. E. Owen, J. Non-Cryst. Solids 25, 372 (1977).

[3] A. Mansingh, Bull. Mater. Sci. (India) 2, 325 (1980).

[4] A. R. Long, Adv. Phys. 31, 553 (1982).

[5] M. D. Ingram, Phys. Chem. Glasses 28, 215 (1987).

[6] S. R. Elliott, *Physics of Amorphous Materials*, 2nd ed. (Longman Scientific, London, 1990).

[7] C. A. Angell, Chem. Rev. 90, 523 (1990).

[8] H. Böttger and V. V. Bryksin, *Hopping Conduction in Solids* (Akademie-Verlag, Berlin, 1985).

[9] J. W. Haus and K. W. Kehr, Phys. Rep. 150, 263 (1987).

[10] J.-P. Bouchaud and A. Georges, Phys. Rep. 195, 127 (1990).

[11] J. O. Isard, Philos. Mag. B 62, 139 (1990); Philos. Mag. A 66, 213 (1992).

[12] P. Maass, J. Petersen, A. Bunde, W. Dieterich, and H. E. Roman, Phys. Rev. Lett. 66, 52 (1991).

[13] J. O. Isard, J. Non-Cryst. Solids 4, 357 (1970).

[14] J. C. Dyre, Phys. Rev. B 47, 9128 (1993).

[15] J. M. Stevels, in *Handbuch der Physik*, edited by S. Flügge (Springer-Verlag, Berlin, 1957), Vol. 20, p. 350.

[16] H. E. Taylor, J. Soc. Glass Tech. 41, 350T (1957); 43, 124T (1959).

[17] J. O. Isard, Proc. Inst. Elec. Eng. 109B, 440 (1962).

[18] M. Pollak and T. H. Geballe, Phys. Rev. 122, 1742 (1961).

[19] S. R. Elliott, Adv. Phys. 36, 135 (1987).

[20] M. Suzuki, J. Phys. Chem. Solids 41, 1253 (1980).

[21] A. Ya. Vinnikov and A. M. Meshkov, Fiz. Tverd Tela (Leningrad) 27, 1929 (1985) [Sov. Phys. Solid State 27, 1159 (1985)].

[22] A. R. Blythe, *Electrical Properties of Polymers* (Cambridge University Press, London, 1979).

[23] F. Kremer, J. Ruhe, and W. H. Meyer, Makromol. Chem., Macromol. Symp. 37, 115 (1990).

[24] M. P. J. van Staveren, H. B. Brom, and L. J. de Jongh, Phys. Rep. 208, 1 (1991).

[25] M. Sayer, A. Mansingh, J. M. Reyes, and G. Rosenblatt, J. Appl. Phys. 42, 2857 (1971).

[26] M. A. Careem and A. K. Jonscher, Philos. Mag. 35, 1489 (1977).

[27] S. Mollah, K. K. Som, K. Bose, and B. K. Chaudhuri, J. Appl. Phys. 74, 931 (1993).

[28] P. B. Macedo, C. T. Moynihan, and R. Bose, Phys. Chem. Glasses 13, 171 (1972).

[29] D. P. Almond and A. R. West, Solid State Ion. 11, 57 (1983).

[30] J. C. Dyre, J. Non-Cryst. Solids 135, 219 (1991).

[31] *Impedance Spectroscopy*, edited by J. R. Macdonald (Wiley, New York, 1987).

[32] C. A. Angell, Solid State Ion. 18-19, 72 (1986).

[33] K. L. Ngai, in *Non-Debye Relaxation in Condensed Matter*, edited by T. V. Ramakrishnan and M. R. Lakshmi (World Scientific, Singapore, 1987), p. 23.

[34] L. A. Dissado and R. M. Hill, Phys. Rev. B 37, 3434 (1988).

[35] G. A. Niklasson, J. Appl. Phys. 62, R1 (1987).

[36] S. Yoshikado, T. Ohachi, I. Taniguchi, Y. Onodo, M. Watanabe, and Y. Fujiki, Solid State Ion. 7, 335 (1982).

[37] A. J. Epstein, in *Handbook of Conjugated Electrically Conducting Polymers*, edited by T. A. Skotheim (Marcel Dekker, New York, 1986), Vol. 2, p. 1041.

[38] J. L. Barton, Verres Réfr. 20, 328 (1966).

[39] T. Nakajima, *1971 Annual Report, Conference on Electric Insulation and Dielectric Phenomena* (National Academy of Sciences, Washington, D.C., 1972), p. 168.

[40] H. Namikawa, J. Non-Cryst. Solids 18, 173 (1975).

[41] M. Tomozawa, in *Treatise on Materials Science*, edited by M. Tomozawa (Academic, New York, 1977), Vol. 12, p. 283.

[42] J. C. Dyre, J. Non-Cryst. Solids 88, 271 (1986).

[43] H. Scher and M. Lax, Phys. Rev. B 7, 4491 (1973); 7, 4502 (1973).

[44] S. Summerfield, Philos. Mag. B 52, 9 (1985).

[45] J. C. Dyre, J. Appl. Phys. 64, 2456 (1988).

[46] C. J. F. Bottcher, O. C. Van Belle, P. Bordewijk, and A. Rip, *Theory of Electric Polarisation* (Elsevier, Amsterdam, 1990), Vol. 2.

[47] A. Miller and E. Abrahams, Phys. Rev. 120, 745 (1960).

[48] I. G. Austin and N. F. Mott, Adv. Phys. 18, 41 (1969).

[49] S. R. Elliott, Philos. Mag. 36, 1291 (1977).

[50] I. M. Hodge, M. D. Ingram, and A. R. West, J. Electroanal. Chem. 74, 125 (1976).

[51] J. R. Macdonald, J. Appl. Phys. 62, R51 (1987).

[52] R. Stumpe, Phys. Status Solidi A 88, 315 (1985).

[53] R. Blender and W. Dieterich, J. Phys. C 20, 6113 (1987).

[54] A. Coniglio, M. Daoud, and H. J. Herrmann, J. Phys. A 22, 4189 (1989).

[55] P. Smilauer, Thin Solid Films 203, 1 (1991).

[56] B. E. Springett, Phys. Rev. Lett. 31, 1463 (1973).

[57] I. Webman, J. Jortner, and M. H. Cohen, Phys. Rev. B 15, 5712 (1977).

[58] J. Sinkkonen, Phys. Status Solidi B 103, 231 (1981).

[59] I. I. Fishchuk, Phys. Status Solidi A 93, 675 (1986).

[60] L. A. Dissado and R. M. Hill, Proc. R. Soc. London, Ser. A 390, 131 (1983).

[61] K. L. Ngai and F.-S. Liu, Phys. Rev. B 24, 1049 (1981).

[62] K. Weron, J. Phys.: Condens. Matter. 3, 9151 (1991).

[63] S. Havlin and D. Ben-Avraham, Adv. Phys. 36, 695 (1987).

[64] A. K. Jonscher, Appl. Phys. A 55, 135 (1992).

[65] R. Kubo, J. Phys. Soc. Jpn. 12, 570 (1957).

[66] J. C. Kimball and L. W. Adams, Phys. Rev. B 18, 5851 (1978).

[67] T. Odagaki and M. Lax, Phys. Rev. B 24, 5284 (1981).

[68] J. K. E. Tunaley, Phys. Rev. Lett. 33, 1037 (1974).

[69] V. V. Bryksin, Fiz. Tverd. Tela (Leningrad) 22, 2441 (1980) [Sov. Phys. Solid State 22, 1421 (1980)].

[70]S. Summerfield, Solid State Commun. **39**, 401 (1981).

[71]B. Movaghar and W. Schirmacher, J. Phys. C **14**, 859 (1981).

[72]S. Summerfield and P. N. Butcher, J. Phys. C **15**, 7003 (1982).

[73]B. I. Shklovskii and A. L. Efros, *Electronic Properties of Doped Semiconductors* (Springer-Verlag, Berlin, 1984).

[74]N. W. Ashcroft and N. D. Mermin, *Solid State Physics* (Holt, Rinehart, and Winston, New York, 1976), Appendix K.

[75]B. Pistoulet, F. M. Roche, and S. Abdalla, Phys. Rev. B **30**, 5987 (1984).

[76]C. J. Adkins, J. Phys. C **20**, 235 (1987).

[77]S. Kirkpatrick, Rev. Mod. Phys. **45**, 574 (1973).

[78]V. Ambegaokar, B. I. Halperin, and J. S. Langer, Phys. Rev. B **4**, 2612 (1971).

[79]B. I. Shklovskii and A. L. Efros, Zh. Eksp. Teor. Fiz. **60**, 867 (1971) [Sov. Phys. JETP **33**, 468 (1971)].

[80]D. Berman, B. G. Orr, H. M. Jaeger, and A. M. Goldman, Phys. Rev. B **33**, 4301 (1986).

[81]H. Kesten, *Percolation Theory for Mathematicians* (Birkhauser, Boston, 1982).

[82]D. B. Gingold and C. J. Lobb, Phys. Rev. B **42**, 8220 (1990).

[83]S. Tyc and B. I. Halperin, Phys. Rev. B **39**, 877 (1989).

[84]R. Landauer, in *Electrical Transport and Optical Properties of Inhomogenous Media* (Ohio State University, 1977), Proceedings of the First Conference on the Electrical Transport and Optical Properties of Inhomogeneous Materials, AIP Conf. Proc. No. 40, edited by J. C. Garland and D. B. Tanner (AIP, New York, 1978), p. 2.

[85]J. A. Krumhansl, in *Amorphous Magnetism*, edited by H. O. Hooper and A. M. de Graaf (Plenum, New York, 1973), p. 15.

[86]F. Yonezawa, in *The Structure and Properties of Matter*, edited by T. Matsubara (Springer-Verlag, Berlin, 1982), p. 383.

[87]B. D. Hughes, M. Sahimi, L. E. Scriven, and H. T. Davis, Int. J. Eng. Sci. **22**, 1083 (1984).

[88]J. Koplik, J. Phys. C **14**, 4821 (1981).

[89]M. Hori and F. Yonezawa, J. Phys. C **10**, 229 (1977).

[90]J. M. Luck, Phys. Rev. B **43**, 3933 (1991).

[91] J. Bernasconi, W. R. Schneider, and H. J. Wiesmann, Phys. Rev. B **16**, 5250 (1977).

[92]M. Sahimi, Chem. Eng. Commun. **64**, 177 (1988).

[93]D. Stauffer and A. Aharoni, *Introduction to Percolation Theory*, 2nd ed. (Taylor and Francis, London, 1992); M. B. Isichenko, Rev. Mod. Phys. **64**, 961 (1992).

[94]S. Tyc and B. I. Halperin, Physica A **157**, 210 (1989).

[95]R. Fogelholm, J. Phys. C **13**, L571 (1980).

[96]D. J. Frank and C. J. Lobb, Phys. Rev. B **37**, 302 (1988).

[97]W. H. Press, B. P. Flannery, S. A. Teukolsky, and W. T. Vetterling, *Numerical Recipes* (Cambridge University Press, Cambridge, 1986).

[98]K. Stuben, Appl. Math. Computation **13**, 419 (1983).

[99]A. Brandt, Appl. Math. Computation **19**, 23 (1986).

[100]J. Goodman and A. D. Sokal, Phys. Rev. D **40**, 2035 (1989).

[101]B. Derrida and J. Vannimenus, J. Phys. A **15**, L557 (1982).

[102]G. G. Batrouni, A. Hansen, and M. Nelkin, Phys. Rev. Lett. **57**, 1336 (1986).

[103]The AMGIRS FORTRAN subroutine is available from "casper.na.cs.yale.edu" (128.36.12.1); log in as anonymous ftp, then look for the file "amg.tar.Z" in the "gmd" directory under the "mgnet" directory.

[104]R. G. Edwards, J. Goodman, and A. D. Sokal, Phys. Rev. Lett. **61**, 1333 (1988).

[105]*Electrical Transport and Optical Properties of Inhomogeneous Media* (Ref. 84); Physica A **157**, 1 (1989).

[106]J. R. Macdonald, J. Appl. Phys. **65**, 4845 (1989).

[107]M. Pollak and G. E. Pike, Phys. Rev. Lett. **28**, 1449 (1972).

[108]J. C. Dyre (unpublished).

[109]P. G. Doyle and J. L. Snell, *Random Walks and Electric Networks* (The Mathematical Association of America, Washington, D.C., 1984).

[110]P. N. Butcher, Philos. Mag. B **37**, 653 (1978).

[111]V. V. Bryksin, Fiz. Tverd. Tela (Leningrad) **25**, 2431 (1983) [Sov. Phys. Solid State **25**, 1395 (1983)].

[112]R. Rammal, C. Tannous, and A.-M. S. Tremblay, Phys. Rev. A **31**, 2662 (1985).

[113]I. I. Fishchuk, J. Phys.: Condens. Matter **4**, 8045 (1992).

[114]W. Dieterich, Philos. Mag. B **59**, 97 (1989).

[115]M. Octavio and C. J. Lobb, Phys. Rev. B **43**, 8233 (1991).

Studies of ac hopping conduction at low temperatures

Jeppe C. Dyre

Institute of Mathematics and Physics (IMFUFA), Roskilde Universitetscenter, Postbox 260, DK-4000 Roskilde, Denmark
(Received 4 October 1993; revised manuscript received 13 December 1993)

A method is presented that makes computer simulations of hopping conduction in symmetric hopping models with thermally activated jump rates possible at arbitrarily low temperatures. The method utilizes the ac Miller-Abrahams electrical equivalent circuit which is systematically reduced by the general star-mesh transformation until one ends up with an admittance matrix referring to the voltage generators. From this matrix the conductivity is easily calculated. Results from simulations of hopping in two dimensions are presented and compared to the predictions of the effective-medium approximation (EMA). Generally there is good agreement, with some deviation at the lowest temperatures. It is shown that, as the temperature goes to zero, the frequency-dependent conductivity in the EMA becomes universal, i.e., independent of the activation energy probability distribution. The computer simulations confirm the existence of universality, although there is no exact agreement between the simulations and the EMA universality prediction.

I. INTRODUCTION

ac conduction in disordered solids like amorphous semiconductors, ionic conductive glasses, polymers, or metal-cluster compounds show a number of common features.[1-8] Above a characteristic frequency ω_m, the conductivity becomes strongly frequency dependent, varying as an approximate power law with an exponent between 0.7 and 1.0. The ac conductivity is always less temperature dependent than the dc conductivity, and at low temperatures the ac conductivity becomes almost temperature independent. A final ubiquitous observation is the Barton, Nakajima, and Namikawa (BNN) relation[9-13] which essentially expresses the fact that the characteristic frequency ω_m is proportional to the dc conductivity $\sigma(0)$. In particular, these two quantities always have the same activation energy.

The most thoroughly studied models for ac conduction in disordered solids are the so-called hopping models.[14-16] A hopping model describes jumps of charge carriers in a stochastic framework. The disorder is usually mimicked by assuming that the transition rates vary randomly according to some probability distribution. Linearized hopping models are amenable to simple analytic treatment. Linearized hopping models, henceforth just referred to as hopping models, describe the motion of *noninteracting* charge carriers. Thus, one ignores self-exclusion as well as Coulomb interactions.

Recently, the role of Coulomb interactions has come into focus.[17,18] To include the effects of Coulomb repulsion, a "macroscopic" model was studied by the present author,[19,20] following previous work by Springett,[21] Webman *et al.*,[22] Sinkkonen,[23] and Fishchuk.[24] When Maxwell's equations for an inhomogeneous semiconductor are discretized, one arrives at an electrical equivalent circuit with nodes placed on a cubic lattice and links between neighboring nodes consisting of a resistor and a capacitor in parallel.[20,22,24] The capacitor currents are Maxwell's displacement currents while the resistor

currents are the free charge currents.[20] Computer simulations of this model have shown[20] that the effective medium approximation (EMA) for random admittance networks[25] works very well, even at low temperatures where the spread in conductances is very large. In particular, the simulations confirmed the EMA prediction[19,20] of a *universal* frequency dependence of the conductivity at low temperatures, independent of the probability distribution of the local conductivity activation energy. If one defines $\tilde{\sigma} = \sigma(\omega)/\sigma(0)$ and $\tilde{s} = i\tilde{\omega}$ where $\tilde{\omega}$ is a suitable dimensionless frequency, the EMA equation for the universal frequency-dependent conductivity in the macroscopic model is

$$\tilde{\sigma} \ln(\tilde{\sigma}) = \tilde{s} . \tag{1}$$

Reference 19 gave the first general derivation of Eq. (1) and presented the first computer simulations confirming it. Equation (1), however, appeared in the literature already in 1980 in a study of the *hopping model* with electrons tunneling between positionally disordered sites.[26] The recent results for the *macroscopic model* therefore raise a number of questions. Is the EMA for hopping models as reliable as it is for the macroscopic model? In particular, as the temperature goes to zero, does the EMA predict Eq. (1) as the *universal* low-temperature frequency dependence of the conductivity even for hopping models with thermally activated jump rates? If this is the case, is the universality confirmed by computer simulations? To answer the last question, a new numerical method must be developed since neither the standard Monte Carlo type method nor, e.g., the Gauss-Seidel relaxation method makes it possible to go to low temperatures where the jump rates vary over several decades (often more than 50 decades).

The present paper introduces a new method for computer simulation of hopping models. The method allows one to go to arbitrarily low temperatures without any computational "slowing down." The method utilizes the Miller-Abrahams equivalent circuit which is systemati-

cally reduced by eliminating nodes according to a transformation well known from electrical engineering. Before this method is presented in Sec. III, Sec. II briefly reviews the basic equations of symmetric hopping models and the EMA equation for the frequency-dependent conductivity in hopping models. Section IV reports the results of computer simulations in 2D and compares the simulations to the EMA predictions. In Sec. V, the low-temperature limit of the EMA is studied. It is shown that Eq. (1) is predicted to be the universal low-temperature conductivity even for hopping models. Also, Eq. (1) is compared to the results of computer simulations. Finally, Sec. VI contains a discussion.

II. SYMMETRIC LINEAR HOPPING MODELS

This section briefly reviews symmetric linear hopping models and their approximate solution in the EMA. Since several reviews have been written on this subject,[14-16,27-30] only the most necessary background is given here.

For simplicity we consider first hopping in one dimension in thermal equilibrium, i.e., with no external electric field. A model solid is regarded in which the charge carriers can be only at regularly spaced discrete sites. Let N_i denote the average number of charge carriers at site i. This number changes in time because some charge carriers leave site i and others arrive from the neighboring sites $i-1$ and $i+1$ (only nearest-neighbor jumps are allowed). If $\Gamma(i \rightarrow j)$ denotes the probability per unit time of a jump from site i to site $j=i\pm1$, the basic equation for the average N_i's is

$$\frac{dN_i}{dt} = -[\Gamma(i \rightarrow i+1) + \Gamma(i \rightarrow i-1)]N_i$$
$$+ \Gamma(i-1 \rightarrow i)N_{i-1} + \Gamma(i+1 \rightarrow i)N_{i+1} . \quad (2)$$

This equation is a simple example of a master equation.[31,32]

In *symmetric* hopping models one has symmetric equilibrium jump probabilities,

$$\Gamma(i \rightarrow j) = \Gamma(j \rightarrow i) \equiv \Gamma_0(i,j) \quad (j=i\pm1) . \quad (3)$$

Introducing the probability of finding a charge carrier at site i, $P_i = N_i/N$ where N is the total number of charge carriers, and, when Eq. (3) is taken into account, Eq. (2) becomes

$$\frac{dP_i}{dt} = \Gamma_0(i-1,i)(P_{i-1}-P_i) - \Gamma_0(i,i+1)(P_i-P_{i+1}) .$$
$$(4)$$

The stationary solution of Eq. (4) corresponds to all sites being equally probable. Any initial nonhomogeneous distribution of charge carriers will eventually equilibrate through "diffusion" of charge carriers away from densely populated sites.

Equation (4) is *linear*. This is the mathematical expression of the fact that the equation deals with *noninteracting* charge carriers. The charge carriers cannot feel each other: neither is Coulomb repulsion taken into account

nor is "self-exclusion" (i.e., that there is room for only one charge carrier at each site). In some papers dealing with hopping models, more general nonlinear hopping models are formulated, attempting to take these effects into account. Equation (4) is then arrived at by *linearizing* the general hopping equation. However, as pointed out by Shklovskii and Efros, this linearization is not exact, but involves uncontrolled approximations.[33]

For systems of tunneling electrons, the transition rates depend exponentially on the tunneling distance (as well as on the difference of the site energies). In the present paper we are concerned with the "classical" case where the jump rates are *thermally activated*, i.e., where one has

$$\Gamma_0(i,j) = \Gamma_0 e^{-\beta E_{i,j}} \quad (j=i\pm1) . \quad (5)$$

Here $\beta = 1/(k_B T)$, while $E_{i,j}$ is the so-called activation energy—the barrier to be overcome. The prefactor Γ_0 is the "attack frequency" which is usually of order 10^{12} Hz (a typical phonon frequency). Equation (5) is relevant for ionic conduction and for certain cases of polaronic conduction.

In symmetric hopping models one usually assumes that the jump rates vary randomly, so the model is completely characterized by the activation energy probability distribution $p(E)$. Figure 1 shows an example of the potential for a symmetric hopping model in 1D with thermally activated jumps. At low temperatures the jump rates vary several orders of magnitude, and a charge carrier makes many jumps between pairs of sites separated by low barriers. Via the fluctuation-dissipation theorem this implies that the conductivity depends strongly on frequency.

Before considering the effect of an electric field, we briefly discuss the boundary conditions. The *bulk* behavior of the model is calculated by letting the volume go to infinity. In any computer simulation, however, only a finite sample is present and one has to specify the boundary conditions. The case of *periodic boundary conditions* is characterized by requiring $P_0 = P_N$ if the sites are numbered from 0 to N. An alternative is the case of *blocking electrodes*, i.e., to modify Eq. (4) at the end points so that no charge carriers may pass beyond these.
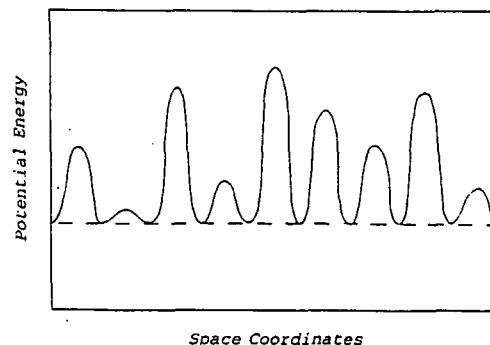

Space Coordinates

FIG. 1. Potential felt by a charge carrier in a one-dimensional symmetric hopping model with thermally activated jump rates. If β denotes $1/(k_B T)$ and E is the energy barrier height, the rate for jumps between two sites is $\Gamma_0 e^{-\beta E}$.

A third possible boundary condition is the case of *perfectly conducting electrodes*. This is arrived at by imposing a fixed probability at the end points:

$$P_0 = P_N = \text{const} . \tag{6}$$

Equation (6) corresponds to having no accumulation at the electrodes, allowing completely free passage for the charge carriers. This boundary condition is used below in the computer simulations.

In an external electric field the symmetry of the jump rates is broken, since it becomes more favorable to jump in the direction of the field than opposite to it (assuming the charge $q > 0$). If the energy barrier is placed symmetrically between the two charge-carrier sites and a denotes the distance between neighboring sites, the jump rates are modified[14] according to [note that E in Eqs. (7)–(9) below is the electric field and not an energy barrier]

$$\Gamma(i \rightarrow i+1, E) = \Gamma_0(i, i+1) e^{\beta q a E / 2} ,$$
$$\Gamma(i+1 \rightarrow i, E) = \Gamma_0(i, i+1) e^{-\beta q a E / 2} . \tag{7}$$

In the linear limit (which defines the ordinary conductivity) Eq. (7) is expanded to first order in the electric field:

$$\Gamma(i \rightarrow i+1, E) = \Gamma_0(i, i+1) \left[1 + E \frac{\beta q a}{2} \right] ,$$
$$\Gamma(i+1 \rightarrow i, E) = \Gamma_0(i, i+1) \left[1 - E \frac{\beta q a}{2} \right] . \tag{8}$$

Consequently, Eq. (2) in terms of the P_i's becomes

$$\frac{dP_i}{dt} = \Gamma_0(i-1, i)(P_{i-1} - P_i) - \Gamma_0(i, i+1)(P_i - P_{i+1})$$
$$+ E \frac{\beta q a}{2} [\Gamma_0(i-1, i)(P_{i-1} + P_i)$$
$$- \Gamma_0(i, i+1)(P_i + P_{i+1})] . \tag{9}$$

In this equation the electric field may depend on time in any arbitrary way.

The complex frequency-dependent conductivity $\sigma(\omega)$ is defined as the ratio between the spatially averaged current density and the electric field in a steady state, where the electric field varies periodically as $e^{i\omega t}$. The Kubo formula[34] expresses the frequency-dependent conductivity in terms of the current-current time autocorrelation function. For hopping models it is convenient to rewrite the Kubo formula by performing two partial integrations. This leads[35] to the following expression

$$\sigma(\omega) = -\frac{nq^2 \omega^2}{2k_B T} \int_0^\infty \langle \Delta x^2(t) \rangle_0 e^{-i\omega t} dt . \tag{10}$$

Here, n is the average charge carrier density, $\langle \Delta x^2(t) \rangle_0$ denotes the equilibrium mean-square displacement of a charge carrier in time t, and a convergence factor $\lim_{\epsilon \rightarrow 0} e^{-\epsilon t}$ is implicitly understood in the integral.

For a homogeneous system (i.e., with all jump rates equal) the mean-square displacement is determined from the diffusion constant D_0 via Einstein's equation

$\langle \Delta x^2(t) \rangle_0 = 2D_0 t$. As is easy to see, Eq. (10) then gives the frequency-independent conductivity $\sigma = nq^2 \mu$ where μ is the mobility which is given by the Nernst-Einstein relation $\mu = D_0 / (k_B T)$. In the time t a charge carrier in a homogeneous system with equilibrium jump rate Γ performs on the average $N = 2\Gamma t$ jumps. Therefore, one has

$$\langle \Delta x^2(t) \rangle_0 = Na^2 = 2\Gamma a^2 t ,$$

which implies $D_0 = \Gamma a^2$. Combining these equations, one finds for the frequency-independent conductivity of a homogeneous system

$$\sigma = \frac{nq^2 a^2}{k_B T} \Gamma . \tag{11}$$

For any inhomogeneous system, the high-frequency limit of the conductivity is given by a similar expression. It can be shown[36] that $\sigma(\infty)$ is given simply by the average jump frequency:

$$\sigma(\infty) = \frac{nq^2 a^2}{k_B T} \langle \Gamma \rangle . \tag{12}$$

It is convenient to redefine the conductivity and absorb the prefactor $nq^2 a^2 / (k_B T)$. In this "rationalized" unit system, which will be used henceforth, Eq. (12) simply becomes $\sigma(\infty) = \langle \Gamma \rangle$.

It is also possible to calculate the dc conductivity exactly in one dimension.[36] Thus, in 1D the high and low frequency limits are in the "rationalized" unit system given by

$$\sigma_{1-D}(0) = \langle \Gamma^{-1} \rangle^{-1} ,$$
$$\sigma_{1-D}(\infty) = \langle \Gamma \rangle . \tag{13}$$

The inequality $1 \leq \langle \Gamma \rangle \langle \Gamma^{-1} \rangle$ may be derived from the Cauchy-Schwartz inequality; it implies that $\sigma_{1-D}(0) \leq \sigma_{1-D}(\infty)$. In fact, it can be shown[37] for any hopping model in any number of dimensions that the real part of the conductivity is an increasing function of the frequency.

Hopping models in D dimensions for $D > 1$ are straightforward generalizations of the one-dimensional case. If P_s denotes the probability of finding a charge carrier at site s, Eq. (4) is replaced by (for symmetric hopping models)

$$\frac{d}{dt} P_s = \sum_{s'} \Gamma_0(s, s')(P_{s'} - P_s) . \tag{14}$$

In the present paper the sites s are assumed to lie on a simple cubic lattice and the sum is restricted to nearest neighbors. The Kubo formula Eq. (10) is also valid for $D > 1$ where the mean-square displacement $\langle \Delta x^2(t) \rangle_0$ is in any of the D axis directions. The three above-mentioned boundary conditions may also be applied for $D > 1$. In an external field, the concepts of blocking or perfectly conducting electrodes make sense only for sample faces *perpendicular* to the field; it is natural to apply periodic boundary conditions to all remaining faces.

Even for $D > 1$ it is convenient to use the "rationalized" unit system representing the conductivity in terms of an equivalent jump frequency. In this unit system the

high-frequency limit of the conductivity is for any D given[28,37] by

$$\sigma(\infty) = \langle \Gamma \rangle . \tag{15}$$

For the dc conductivity, on the other hand, there is no general analytical expression similar to Eq. (13) in one dimension. However, the temperature dependence of $\sigma(0)$ is known; it is given[38-40] by

$$\sigma(0) \propto e^{-\beta E_c} \quad (D > 1) , \tag{16}$$

where the so-called percolation energy E_c in terms of the activation energy probability distribution $p(E)$ and the link percolation threshold p_c is given by

$$\int_{-\infty}^{E_c} p(E)dE = p_c . \tag{17}$$

For $D = 2$ one has $p_c = \frac{1}{2}$ exactly[41] while for $D = 3$ simulations have shown that $p_c = 0.2488$.[42]

The calculation of the frequency-dependent conductivity in hopping models is a complicated problem. The standard approximation for disordered systems is the coherent potential approximation (CPA).[43,44] The CPA is a mean-field approximation that gives an estimate of the relevant Green's function that has a number of attractive analyticity properties. For hopping models, the CPA is known as the effective medium approximation (EMA) because it is derived by considering one "link" (i.e., jump frequency) of the lattice as embedded in an "effective medium" mimicking the average surroundings. Several papers[15,26,30,45-48] derive the EMA equation. If the complex frequency $s = i\omega$ is introduced—referred to below as the "Laplace frequency"—the conductivity $\sigma = \sigma(s)$ in the "rationalized" unit system introduced above is in the EMA given[15] as the solution of the equation

$$\left\langle \frac{\Gamma - \sigma}{D\sigma + [1 - s\tilde{G}](\Gamma - \sigma)} \right\rangle_\Gamma = 0 . \tag{18}$$

In Eq. (18) the average is over the jump frequency probability distribution and $s\tilde{G}$ is defined by

$$s\tilde{G} = \int_{1-BZ} \frac{d^D k}{(2\pi)^D} \frac{s}{s + 2D\sigma[1 - p(\mathbf{k})]} , \tag{19}$$

where the integral is over the first Brillouin zone $(-\pi < k_i < \pi)$ and

$$p(\mathbf{k}) = \frac{1}{D} \sum_{i=1}^{D} \cos(k_i) . \tag{20}$$

For $s \to \infty$ one has $s\tilde{G} \to 1$. Thus, Eq. (18) implies the correct high-frequency limit Eq. (15). In the limit $s \to 0$ one has $s\tilde{G} \to 0$. Thus, the EMA equation for the dc conductivity is

$$\left\langle \frac{\Gamma - \sigma(0)}{\Gamma + (D-1)\sigma(0)} \right\rangle_\Gamma = 0 . \tag{21}$$

For $D = 1$ Eq. (21) gives the correct result Eq. (13).

To solve Eq. (18) numerically one needs to calculate the quantity $s\tilde{G}$ of Eq. (19). This is a standard exercise in calculating the diagonal element of the Green's function for a random walk on a cubic lattice or, equivalently, for

the quantum-mechanical tight-binding model.[49] In 1D one finds[49,50]

$$s\tilde{G}_{1D} = \left[1 + \frac{4}{x} \right]^{-1/2} \quad (x = s/\sigma) . \tag{22}$$

In two dimensions one finds[49,50]

$$s\tilde{G}_{2D} = \frac{2}{\pi} \frac{x}{4+x} K\left[\frac{4}{4+x} \right] \quad (x = s/\sigma) , \tag{23}$$

where K is the complete elliptic integral of the first kind. In three dimensions one finds[49]

$$s\tilde{G}_{3D} = \frac{x}{2\pi^2} \int_0^\pi t(\phi) K[t(\phi)]d\phi$$

$$\left[t(\phi) = \frac{4}{x + 6 - 2\cos(\phi)}, \quad x = s/\sigma \right] . \tag{24}$$

Note that Eqs. (22)–(24) all imply $s\tilde{G} \to 1$ as $s \to \infty$, as required by Eq. (19). A rough analytical approximation to Eq. (24) is Hubbard's Green's function[49]

$$s\tilde{G}_{3D} \cong \frac{2}{1 + 6/x + \sqrt{1 + 12/x}} \quad (x = s/\sigma) . \tag{25}$$

III. A METHOD FOR THE NUMERICAL EVALUATION OF THE FREQUENCY-DEPENDENT CONDUCTIVITY IN HOPPING MODELS

The frequency-dependent conductivity may be evaluated numerically in several ways. In principle, the problem is the straightforward one to solve a large system of linear equations with complex coefficients; from the solution, the conductivity is easily calculated. The Gauss-Seidel or the Jacobi relaxation methods[51] are usually applied to such a problem. Unfortunately, they converge much too slowly if the coefficients vary over several orders of magnitude, as is the case when one wants to study hopping at low temperatures. Overrelaxation methods[51] may be faster, but are still too slow.

An obvious way of evaluating the frequency-dependent conductivity in hopping models is to use an equivalent of a Monte Carlo simulation, simulating the charge-carrier jumps in "real" time. This method works fine at high temperatures, but for β larger than about 10 the charge carriers get caught and tend to jump backwards and forwards between two sites without moving away until after thousands or millions of Monte Carlo steps. While this behavior reflects the real physics of low-temperature hopping, the method is clearly very inefficient.

We now proceed to describe an alternative method for evaluating $\sigma(s)$, where a systematic reduction is applied to the ac Miller-Abrahams (ACMA) equivalent circuit. The reduction ends up with a frequency-dependent admittance matrix from which the conductivity is easily calculated. To describe the method we first review the one-dimensional ACMA equivalent circuit, and then show how to reduce the circuit. Finally, the generalization of the method to higher dimensions is discussed.

To solve Eq. (9) one notes that for small electrical fields the probabilities P_i are only slightly different from the average probability $\langle P \rangle$: $P_i = \langle P \rangle + \delta P_i$. When substituted into Eq. (9) this gives to first order in ϵ and δP_i where $\epsilon = \beta q a \langle P \rangle E$ is a dimensionless measure of the electric field

$$\frac{d}{dt} \delta P_i = \Gamma_0(i-1,i)(\delta P_{i-1} - \delta P_i)$$

$$- \Gamma_0(i,i+1)(\delta P_i - \delta P_{i+1})$$

$$+ \epsilon[\Gamma_0(i-1,i) - \Gamma_0(i,i+1)] . \quad (26)$$

Consider now the ACMA electrical circuit shown in Fig. 2(a). The capacitors all have capacity equal to one while the (real) conductance between site i and $i+1$ is $\Gamma_0(i,i+1)$. The voltage generators impose the potential drop $-i\epsilon$ from the capacitors to the ground. If the voltage at site i is denoted by U_i, the Kirchhoff law expressing charge conservation is

$$\frac{d}{dt}(U_i + i\epsilon) = \Gamma_0(i-1,i)(U_{i-1} - U_i)$$

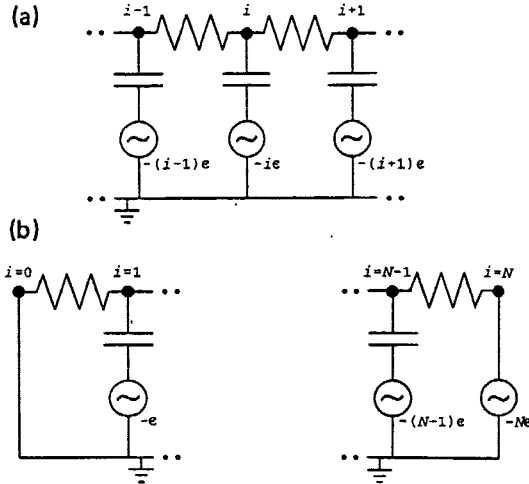$$- \Gamma_0(i,i+1)(U_i - U_{i+1}) . \quad (27)$$

(a)

(b)

FIG. 2. (a) ac Miller-Abrahams (ACMA) electrical equivalent circuit of a symmetric hopping model in one dimension. All capacitors have unit capacitance while the conductance of the resistor between site i and site $i+1$ is equal to the equilibrium jump frequency $\Gamma_0(i,i+1)$. The electric field in the sample, for which ϵ is a dimensionless measure, is reflected in the voltage generators. The currents in the resistors are equal to the currents in the hopping model [Eq. (30)]. Similar electrical equivalent circuits exist in higher dimensions. Here, the voltage depends only on the coordinate in the direction of the electric field, and thus the capacitors in a plane perpendicular to the field are all connected to the same voltage generator. This fact is crucial for the numerical method for calculating the frequency-dependent conductivity derived in Sec. III. (b) Boundary conditions to the ACMA circuit in one dimension. These boundary conditions correspond to *perfectly conducting electrodes* [Eq. (6)].

This equation transforms into Eq. (26) if one makes the identification

$$U_i = \delta P_i - i\epsilon . \quad (28)$$

Solving Eq. (26) therefore becomes equivalent to solving the ACMA circuit.[27,52–54] To completely specify the problem the boundaries must be considered.[14] We use perfectly conducting electrodes for which the boundary conditions are $\delta P_0 = \delta P_N = 0$ [Eq. (6)]. For $i=0$ this implies $U_0 = 0$ while for $i=N$ the condition is $U_N = -N\epsilon$. These two boundary conditions correspond to the circuit endings without capacitors shown in Fig. 2(b).

Before the ACMA circuit is "solved," let us consider the calculation of the frequency-dependent conductivity from the solution. By definition, $\sigma(s)$ is the ratio between the spatially averaged current and the electric field in a steady periodic situation. If $\langle J \rangle_\epsilon$ denotes the spatially averaged current in the field ϵ, we have (where K is a proportionality constant depending on the unit system)

$$\langle J \rangle_\epsilon = K \sum_{i=0}^{N-1} [\Gamma(i \to i+1)P_i - \Gamma(i+1 \to i)P_{i+1}] . \quad (29)$$

To first order in $\epsilon = \beta q a \langle P \rangle E$ this expression via Eqs. (8) and (28) reduces to

$$\langle J \rangle_\epsilon = K \sum_{i=0}^{N-1} \Gamma_0(i,i+1) \left[2\frac{\epsilon}{2\langle P \rangle} \langle P \rangle + \delta P_i - \delta P_{i+1} \right]$$

$$= K \sum_{i=0}^{N-1} \Gamma_0(i,i+1)(U_i - U_{i+1}) . \quad (30)$$

At very high frequencies the capacitors may be ignored and the potential drop across each resistor simply becomes ϵ. In order to reproduce Eq. (13) for the high-frequency conductivity, the general expression for the conductivity in the "rationalized" unit system must therefore be

$$\sigma = \frac{1}{N} \sum_{i=0}^{N-1} \Gamma_0(i,i+1)(U_i - U_{i+1}) \quad (\epsilon = 1) . \quad (31)$$

If $I_R(i \to i+1)$ denotes the current in the resistor from site i to site $i+1$ when $\epsilon = 1$, one has

$$\sigma = \frac{1}{N} \sum_{i=0}^{N-1} I_R(i \to i+1) \quad (\epsilon = 1) . \quad (32)$$

In the dc limit the capacitors are completely blocking and only the voltage generator at the site $i=N$ matters [since here there is no capacitor, compare Fig. 2(b)]. The ACMA circuit then effectively reduces to resistances in series and the current is the same in each resistor. This current is determined by the total resistance from $i=0$ to $i=N$. Each resistor has the value $1/\Gamma_0(i,i+1)$ and the total resistance is the sum of all resistors. When the current thus determined is substituted into Eq. (32), one finds the expression given in Eq. (13) for the dc conductivity of a 1D hopping model.

Returning now to the case of an arbitrary frequency (but still in 1D), it is convenient to rewrite Eq. (32) in terms of the current through each voltage generator. If $I_V(i)$ denotes the current "upwards" through the ith

voltage generator towards site i, charge conservation implies

$$I_R(0 \to 1) = I_V(0) ,$$

$$I_R(1 \to 2) = I_R(0 \to 1) + I_V(1) = I_V(0) + I_V(1) ; \tag{33}$$

in general,

$$I_R(i \to i+1) = I_V(0) + \cdots + I_V(i) . \tag{34}$$

When substituted into Eq. (32) this gives

$$\sigma = \frac{1}{N} \sum_{i=0}^{N} (N-i) I_V(i) \quad (\epsilon = 1) . \tag{35}$$

Equation (35) suggests regarding the ACMA circuit as an N port consisting of all the capacitors and the resistors as "internal" elements with "external" nodes that are to be subjected to the potentials $-\epsilon, \ldots, -N\epsilon$ relative to the ground defined by site 0. Such a circuit is characterized by a (frequency-dependent) symmetric matrix of admittances. This matrix is here defined by

$$I_V(i) = \sum_{j=0}^{N} Y[i,j](U_i - U_j) , \tag{36}$$

where $Y[i,i]$ may be any number. In particular, it is possible from $Y[i,j]$ to calculate the generator currents for $\epsilon = 1$,

$$I_V(i) = \sum_{j=0}^{N} (j-i) Y[i,j] . \tag{37}$$

Substituting this into Eq. (35) one finally arrives at

$$\sigma = \frac{1}{N} \sum_{i=0}^{N} \sum_{j=0}^{N} (N-i)(j-i) Y[i,j] . \tag{38}$$

The problem is now reduced to calculating the admittance matrix. This is done by utilizing the general star-mesh transformation well known from electrical engineering.[55] This transformation, which was first used for random resistor networks by Fogelholm,[56,57] is a prescription of how to remove nodes from a circuit without changing the "external" properties of the circuit. Consider any node in an electrical circuit connected to m other nodes by the admittances $Y_1, \ldots, Y_m$. This is illustrated in Fig. 3 for the case $m = 5$. The central node may be removed by introducing new admittances between all possible pairs of the m neighbor nodes. The new admittance between the neighbor nodes i and j, Y_{ij}, is given[55] by

$$Y_{ij} = \frac{Y_i Y_j}{Y_1 + \cdots + Y_m} . \tag{39}$$

If some of the m neighbor nodes were already connected by an admittance before the transformation, this admittance is increased by the amount given by Eq. (39). What does it actually mean *physically* that the new circuit is "equivalent" to the old? This means that, for all possible choices of potentials applied to the m neighbor nodes, the same currents run from each of these nodes into the circuit. In this sense, the m neighbor nodes cannot detect any difference before and after the transformation. Once this condition has been specified, it is straightforward to
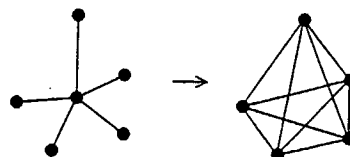

FIG. 3. General star-mesh transformation of an electrical circuit (Ref. 55). In this example the central node is removed. This node is connected to five neighboring nodes by the admittances $Y_1, \ldots, Y_5$. After the transformation, all possible connections between the five "external" nodes are created by, between the ith and the jth node, introducing the admittance $Y_i Y_j / (Y_1 + \cdots + Y_5)$. Physically, the fact that the new circuit is equivalent to the old means that, for any "external" potentials applied to the five nodes, the same currents run into the circuit before and after the transformation. The general star-mesh transformation may be applied to the ACMA circuit of Fig. 2 and its higher-dimensional analogs. When all nodes have been removed one is left with an admittance matrix $Y[i,j]$ which directly determines the frequency-dependent conductivity [Eq. (38) in 1D or Eq. (40) in 2D].

derive Eq. (39).

When this transformation is applied to the ACMA circuit each of the "internal" nodes indexed $i = 0, 1, \ldots, N$ is removed. Eventually, one is left with all possible connections between the "external" nodes. Each connection has an admittance which specifies the corresponding matrix element in the admittance matrix $Y[i,j]$. With this method for evaluating $\sigma(s)$ for a hopping model, the number of calculations that are to be performed is independent of the temperature. A further advantage is that the present method, by proceeding through a number of simple algebraic operations on the circuit admittances without any subtractions, introduces virtually no numerical inaccuracies. Thus, the conductivity is evaluated with a very high precision.

The method is easily generalized to higher dimensions. Considering the case $D = 2$, the ACMA circuit is a square lattice here whose nodes are indexed by (i,k) where $i = 0, \ldots, N$ and $k = 1, \ldots, N$. As in Fig. 2(a) each node on the lattice is connected to the ground via a capacitor and a voltage generator.[14,54] Neighboring nodes are connected by a resistor whose conductance is the equilibrium jump frequency. The external electric field is assumed to be in the direction of the x axis (indexed by i). This means that the voltage generators have a voltage equal to $-i\epsilon$, independent of k. In effect, there is thus just one voltage generator for each i. In the y direction we use *periodic boundary* conditions so that the point $(i, N+1)$ is identified with the point $(i, 1)$. In the x direction the *perfect electrode* boundary condition is used. For calculating the conductivity, all nodes (i,k) with $i = 1, \ldots, N-1$ are removed according to the recipe of Eq. (39). After the reduction has been performed one ends up with an $(N+1) \times (N+1)$ symmetric admittance matrix $Y[i,j]$, where both indexes refer to the x coordinates. The calculation of the conductivity from the matrix proceeds as in

Eq. (38), except that a further division by N is necessary to compensate for the fact that each "layer" perpendicular to the x axis has N parallel channels. Introducing an s to remind of the fact that the conductivity is frequency dependent, we thus get

$$\sigma(s) = \frac{1}{N^2} \sum_{i=0}^{N} \sum_{j=0}^{N} (N-i)(j-i)Y[i,j;s] . \qquad (40)$$

It is not clear in which order the nodes should be removed to have the fastest algorithm. This point is important because the removal of one node introduces several new connections. And the more connections there are to a given node, the more calculations are required for removing it. The nodes should therefore be removed so that as few new connections as possible are created. In the original Fogelholm algorithm in each step one removes the node with fewest connections to its surroundings.[57] This works well for a system where most neighboring nodes are not connected, as is the case close to the link percolation threshold. In the present case, however, where all neighbors are connected, this procedure becomes very inefficient, because the last nodes to be removed become excessively costly. We found it better to

"contain the damage" by removing one column at time (i.e., the nodes with the same index i). After the first p columns have been removed, one has a situation where the $p+1$ "electrodes" connected to the voltages $0, -1, \ldots, -p$ are all connected to each other. Furthermore, all possible connections exist from these $p+1$ "electrodes" to the N nodes of the $(p+1)$th column, and all nodes in the $(p+1)$th column are connected to each other. A further optimization of the algorithm is obtained by, after removing the first $N/2$ columns, starting from the other end of the circuit by removing columns in decreasing order of the i index.

IV. COMPUTER SIMULATIONS

The algorithm derived in Sec. III was applied to a study of hopping in two dimensions. At low temperatures large lattices are needed to obtain reasonable statistics. We chose to simulate hopping on a 100×100 lattice. For this system a standard workstation calculates the conductivity accurately (at one particular frequency) in about 1 min. However, even a 100×100 lattice is not self-averaging at low temperatures, and it was necessary
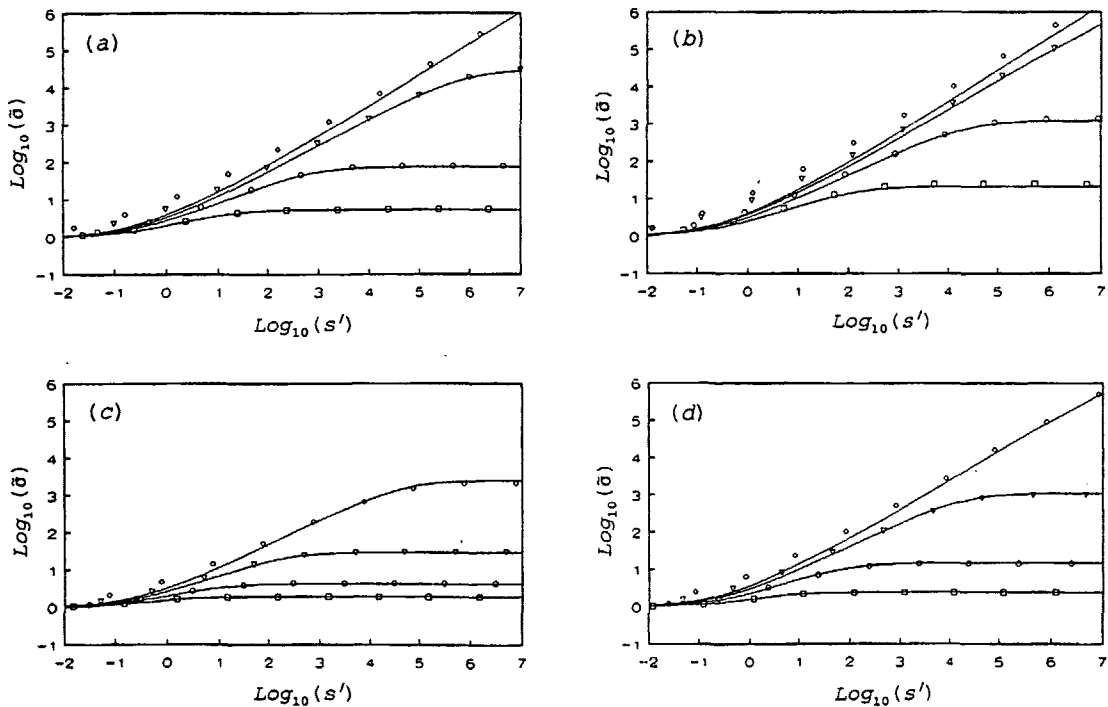

FIG. 4. Log-log plots of the results of computer simulations in two dimensions (points) compared to the EMA predictions (full curves) for symmetric hopping on a 100×100 lattice. The figures show the conductivity as function of the real Laplace frequency (i.e., at imaginary frequencies). The computer simulations were carried out using the algorithm developed in Sec. III. The points represent averages over 20 different 100×100 lattices, where the jump frequency activation energy varies according to the following distributions (compare Appendix B of Ref. 20): (a) asymmetric Gaussian; (b) Cauchy; (c) power law with exponent -4; and (d) box. Each figure shows the following dimensionless inverse temperatures: $\beta = 5$ ($\square$), $\beta = 10$ ($\circ$), $\beta = 20$ (∇), and $\beta = 40$ ($\diamond$). The "reduced" Laplace frequency s' as well as $\bar{\sigma}$ are defined in Eq. (42). The EMA predictions were found by solving Eq. (18) where $s\bar{G}$ is given by Eq. (23).

to average over several simulations to obtain reproducible results.

In each simulation a 100×100 lattice was generated by, for each link, choosing a random activation energy according to the probability distribution under study. Four different probability distributions were used: The asymmetric Gaussian, the Cauchy, the power law with exponent -4, and the box. The details of how the energies were generated are described in Appendix B of Ref. 20; to avoid spurious correlations the random numbers were generated according to the RANO algorithm of Ref. 51.

For each lattice the frequency-dependent conductivity was evaluated from Eq. (40) at a number of frequencies, where the admittance matrix $Y[i,j;s]$ results from the reduction of the ACMA circuit. For simplicity, the simulations were carried out at *real* Laplace frequencies, corresponding to purely imaginary frequencies. This trick simplifies the computations and, since $\sigma(s)$ is real for real s, makes it possible to present the frequency-dependent conductivity in one single curve.

Figure 4 shows a log-log plot of the averages of 20 simulations for the four activation energy distributions at the dimensionless inverse temperatures $\beta = 5$, 10, 20, and 40. If $p(E)$ is the normalized energy probability distribution and one introduces (compare Sec. V)

$$\tilde{\beta} = \frac{\beta}{8\pi p(E_c)} , \qquad (41)$$

the quantities s' and $\bar{\sigma}$ in Fig. 4 are defined by

$$s' = \frac{\tilde{\beta}}{\sigma(0)} s, \quad \bar{\sigma} = \frac{\sigma}{\sigma(0)} . \qquad (42)$$

In Fig. 4 the full curves are the EMA predictions found by solving Eq. (18) numerically. In two dimensions the quantity $s\tilde{G}$ is given by Eq. (23). A numerical approximation to the elliptic function was used.[58] Equation (18) was discretized into 10.000 terms and then solved by the bisection method.[51]

The EMA is usually derived from a perturbation expansion around the homogeneous state. As such, there is no *a priori* reason to believe in the EMA predictions in severely disordered cases like low-temperature hopping, which is really quite extreme: It involves jump frequencies that for $\beta = 40$ vary 20–60 *decades*. This enormous variation implies that the scaling of the frequency introduced in Eq. (42) shifts the frequency by in some cases more than 15 decades. In this light it must be said that the EMA works rather well in Fig. 4.

V. THE LOW-TEMPERATURE LIMIT OF THE EMA: THE APPEARANCE OF UNIVERSALITY

This section studies the EMA prediction for the $T \to 0$ limit of the frequency-dependent conductivity in symmetric hopping models in more than one dimension. The derivation starts by noting that, as $\beta \to \infty$,

$$x = s/\sigma \ll 1 \qquad (43)$$

for all frequencies in an increasingly large range around the frequency marking the onset of ac conduction. This observation was first made by Bryksin in a paper from

1980 (Ref. 26) dealing with electrons tunneling between random positions. In the derivation given below, Eq. (43) will be assumed first and subsequently shown to be consistent with the result derived.

Equation (18) is rewritten

$$0 = \left\langle \frac{\Gamma - \sigma}{\Gamma - \sigma + D\sigma/(1 - s\tilde{G})} \right\rangle_\Gamma . \qquad (44)$$

When x is small, $s\tilde{G}$ is small. Expanding to first order in $s\tilde{G}$ leads to (where the numerator is rewritten for convenience below)

$$0 = \left\langle \frac{\Gamma + [(D-1) + Ds\tilde{G}]\sigma - D(1 + s\tilde{G})\sigma}{\Gamma + [(D-1) + Ds\tilde{G}]\sigma} \right\rangle_\Gamma . \qquad (45)$$

If we introduce the notation $\Gamma(E) = \Gamma_0 e^{-\beta E}$ to emphasize the activation energy dependence of the jump frequency and if the average is converted into an average over the activation energy probability distribution, Eq. (45) becomes

$$\frac{1}{D(1 + s\tilde{G})\sigma} = \left\langle \frac{1}{\Gamma(E) + [(D-1) + Ds\tilde{G}]\sigma} \right\rangle_E . \qquad (46)$$

For large β the jump frequency $\Gamma(E)$ varies extremely rapidly and, for given σ and s, there are essentially just two extreme possibilities: Either one has

$$\Gamma(E) \ll [(D-1) + Ds\tilde{G}]\sigma$$

or the opposite extreme. In the former case $\Gamma(E)$ may be ignored altogether from the denominator in Eq. (46), while in the latter case the denominator becomes very large and there is little contribution to the right-hand side. The energy separating the two cases, $E_g(s)$, is given as the solution of

$$\Gamma(E) = [(D-1) + Ds\tilde{G}]\sigma ;$$

thus

$$E_g(s) = \frac{-1}{\beta} \ln \left[\frac{[(D-1) + Ds\tilde{G}]\sigma}{\Gamma_0} \right] . \qquad (47)$$

Accordingly, the right-hand side of Eq. (46) becomes

$$\left\langle \frac{1}{\Gamma(E) + [(D-1) + Ds\tilde{G}]\sigma} \right\rangle_E$$
$$= \frac{1}{[(D-1) + Ds\tilde{G}]\sigma} \int_{E_g(s)}^\infty p(E) dE \qquad (48)$$

and Eq. (46) reduces to

$$\frac{D-1}{D} + \frac{s\tilde{G}}{D(1 + s\tilde{G})} = \int_{E_g(s)}^\infty p(E) dE . \qquad (49)$$

Evaluating Eq. (49) at $s = 0$ gives an expression for $(D-1)/D$. When this expression is subtracted from Eq. (49), one gets

$$\frac{s\tilde{G}}{D(1 + s\tilde{G})} = \int_{E_g(s)}^{E_g(0)} p(E) dE . \qquad (50)$$

For large β, $E_g(0)$ is close to $E_g(s)$ and therefore the integral on the right-hand side can easily be evaluated. If $p[E_g(0)]$ is denoted by p_0, the integral is simply

$p_0[E_g(0) - E_g(s)]$. Introducing the symbol $\tilde{\sigma} = \sigma/\sigma(0)$ into Eq. (50) and using Eq. (47) one gets

$$\frac{s\tilde{G}}{D(1 + s\tilde{G})} = \frac{p_0}{\beta} \ln\left[\left(1 + \frac{D}{D-1}s\tilde{G}\right)\tilde{\sigma}\right] .$$ (51)

To leading order in the small quantity $s\tilde{G}$, Eq. (51) reduces to

$$\frac{\beta}{Dp_0}s\tilde{G} = \ln[\tilde{\sigma}] .$$ (52)

Since for $D = 1$ one has $E_g(0) = \infty$, the derivation assumes $D > 1$. As $\beta \to \infty$, $E_g(0)$ approaches the dc conductivity activation energy which is equal to the percolation energy defined by Eq. (17); thus

$$p_0 = p(E_c) .$$ (53)

In further development one has to distinguish between the cases $D = 2$ and $D > 2$. In the latter case, which is the simplest, the quantity $s\tilde{G}$ as a function of $x = s/\sigma$ contains a regular first-order term. Writing

$$D > 2: \quad s\tilde{G} = \alpha_D x \quad (x \to 0) ,$$ (54)

Eq. (19) implies

$$\alpha_D = \tfrac{1}{2} \int_{1-BZ} \frac{d^D k}{(2\pi)^D} \frac{1}{D - (\cos k_1 + \cdots + \cos k_D)} .$$ (55)

For $D = 3$ one has $\alpha_3 = 0.253$.[59] Substituting the expansion Eq. (54) into Eq. (52) leads to Eq. (1), $\tilde{\sigma}\ln(\tilde{\sigma}) = \tilde{s}$, where

$$D > 2: \quad \tilde{s} = \frac{\beta \alpha_D}{Dp_0 \sigma(0)}s .$$ (56)

Finally, the consistency of the derivation is checked: The assumption Eq. (43) is indeed satisfied, since for $\beta \to \infty$ one has $x = s/\sigma \propto \tilde{s}/(\tilde{\sigma}\beta) \to 0$ for fixed $\tilde{\sigma}$ and $\tilde{s}$.

Turning now to the two-dimensional case [where the integral in Eq. (55) diverges] we use the asymptotic expansion of the complete elliptic integral of the first kind:[60] For $k \to 1$ one has $K(k) = \ln(4/k')$ where $k^2 + k'^2 = 1$. This implies that

$$K(k) = \frac{-1}{2}\ln(1 - k)$$

for $k \to 1$. Thus,

$$K\left(\frac{4}{4+x}\right) = \frac{-1}{2}\ln(x)$$

for $x \to 0$. When this is substituted into Eq. (23) one finds asymptotically

$$s\tilde{G}_{2-D} = \frac{-1}{4\pi}x \ln(x) \quad (x \to 0) .$$ (57)

In terms of the $\tilde{\beta}$ defined in Eq. (41), Eq. (52) thus becomes

$$\ln(\tilde{\sigma}) = \tilde{\beta}\frac{s}{\sigma}\ln\left[\frac{\sigma}{s}\right] .$$ (58)

Defining now

$$D = 2: \quad \tilde{s} = \frac{\tilde{\beta}\ln(\tilde{\beta})}{\sigma(0)}s ,$$ (59)

Eq. (58) becomes

$$\ln(\tilde{\sigma}) = \tilde{\beta}\frac{1}{\tilde{\sigma}}\frac{\tilde{s}}{\tilde{\beta}\ln(\tilde{\beta})}\{\ln(\tilde{\sigma}) - \ln(\tilde{s}) + \ln(\tilde{\beta}) + \ln[\ln(\tilde{\beta})]\} .$$

(60)

For fixed $\tilde{\sigma}$ and $\tilde{s}$ as $\tilde{\beta} \to \infty$, Eq. (60) reduces to Eq. (1), $\tilde{\sigma}\ln(\tilde{\sigma}) = \tilde{s}$. Note that the assumption $x = s/\sigma \ll 1$ is also satisfied for $D = 2$ for fixed $\tilde{\sigma}$ and $\tilde{s}$ when $\tilde{\beta}$ is sufficiently large.

The numerical solution of Eq. (1) was discussed in Appendix A in Ref. 20 where an analytical approximation to the function $\tilde{\sigma}(\tilde{s})$ was also given.

Figure 5 tests the EMA universality prediction against computer simulations. The four different activation energy distributions of Fig. 4 were used, supplemented by results for the exponential distribution.[20] For each distribution the temperature was chosen so that $\tilde{\beta} = 4$. Each point in the figure represents the average of 50 simulations of a 100×100 lattice. The figure clearly shows that there is universality at low temperatures, but there is not a quantitative agreement with the EMA universality prediction. A further discussion of this result is given in the next section.

VI. DISCUSSION

In this paper a method for the numerical solution of symmetric hopping models has been derived. The method, which makes use of the ac Miller Abrahams
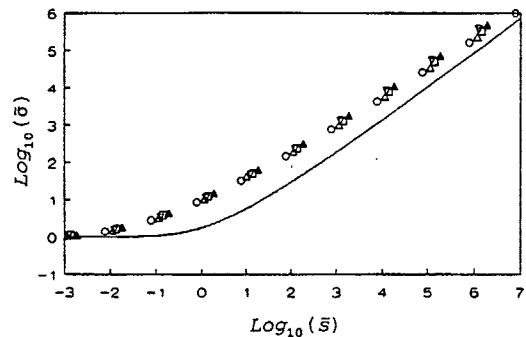

FIG. 5. Log-lot plot comparing the EMA universality prediction [full curve; Eq. (1)] to computer simulations (points) of a 100×100 lattice for five different activation energy probability distributions. Each point represents the average of 50 simulations taken at the "reduced" inverse dimensionless temperature $\tilde{\beta} = 4$ where $\tilde{\beta}$ is defined in Eq. (41); this corresponds to (the relevant E_c's are given in Appendix B of Ref. 20) $\beta = 63.91$ for the asymmetric Gaussian, $\beta = 32.00$ for the Cauchy, $\beta = 50.27$ for the exponential, $\beta = 119.66$ for the power law with exponent -4, and $\beta = 100.53$ for the box distribution. The "reduced" Laplace frequency $\tilde{s}$ is defined in Eq. (59) and $\tilde{\sigma} = \sigma/\sigma(0)$. The figure shows results for the following distributions: asymmetric Gaussian (▲); Cauchy (○); exponential (□); power law with exponent -4 (△); and box (▽).

electrical equivalent circuit, may be generalized immediately to deal with nonsymmetric hopping models; the only change is that in the ACMA circuit the capacitors then vary from site to site.[14,54] The method allows a faster and more accurate calculation of $\sigma(s)$ in hopping models for larger lattices and at lower temperatures than previous methods. Thus, the standard Monte Carlo type method is useless if one wants to study low temperatures as in Fig. 4. The standard relaxation methods for solving linear equations are also too slow in this regime where the coefficients vary many orders of magnitude.

There exists a clever algorithm for solving linear equations with coefficients that vary many orders of magnitude. This is the algebraic multigrid algorithm (AMG)[61,62] which is available from the Yale multigrid library in a well-documented and carefully debugged FORTRAN version.[63] The AMG is an algebraic generalization of the multigrid method for solving elliptic partial differential equations. The AMG has been tested successfully for large random admittance networks with admittances varying many orders of magnitude.[20,64] It solves the Kirchhoff equations in a time proportional to the number of equations. For the present problem, the AMG solves the problem in D dimensions in a time $\propto N^D$. At first sight, this is much better than the method presented in Sec. III, which, as is easy to show for $D > 1$, calculates the conductivity in a time $\propto N^{3D-2}$. However, in the practical use of the AMG it is not presently superior to the method of Sec. III. Thus, when applied to a hopping problem at low temperatures, the AMG easily runs into overflow problems, whereas the method of Sec. III avoids such problems. At low temperatures, if one wants to calculate the conductivity by solving Eq. (26) or the higher-dimensional analogs, the solution must be extremely accurate. The standard double precision real number representation is not enough, since the equations should be solved with an accuracy of 50–100 digits (depending on how low the temperature is). Unfortunately, higher precisions are not hardware implemented today and are therefore quite slow. The method presented in Sec. III seems to be the best available at present. On a longer time span it is likely that the AMG will eventually become the best choice.

The results of extensive computer simulations of a 100×100 lattice in 2D was reported in Sec. IV. In order to obtain reproducible results at low temperatures, it was necessary to average over several simulations of different lattices generated for the same activation energy probability distribution. The main problem in the reproducibility lies at low frequencies; thus, at frequencies where $\log_{10}(\bar{\sigma}) > 1$ the results (i.e., $\bar{\sigma}$ as function of s') are generally quite reproducible.

The results of the computer simulations were compared to the predictions of the EMA at real Laplace frequencies at a number of temperatures in Fig. 4. The use of real Laplace frequencies not only simplifies the calculations, but also makes it possible to represent the results in one curve (instead of two, one for the real part and one for the imaginary part of the conductivity). This curve contains all information about the frequency dependence of the conductivity. This is because the function $\sigma(s)$ is

analytic in the upper half s plane so, by analytic continuation, the behavior on the real s axis determines the function uniquely. A further virtue of this representation is that deviations from the EMA are somewhat magnified here compared to the use of real frequencies. The "reduced" frequency used in Fig. 4 is not the $\bar{s}$ of Eq. (59) simply because, for some of the highest temperatures studied, $\tilde{\beta}$ becomes less than one, so that Eq. (59) does not make sense. Instead, the related "reduced" frequency $s' = \tilde{\beta}s / \sigma(0)$ [Eq. (42)] was used in Fig. 4.

As far as is known to the author, these results are the first simulations of a hopping model at low temperatures where the jump frequencies Γ vary over several decades (here up to about 50–60 decades). In general, there is a rather good agreement between the simulations and the EMA, with some deviations in the transition region where the EMA at low temperatures consistently underestimates the conductivity.

At low temperatures the EMA predicts a universal frequency dependence of the conductivity, independent of the activation energy probability distribution (Sec. V). A particular case of the equation governing the universal conductivity, Eq. (1) was derived by Bryksin in 1980 (Ref. 26) for a system of tunneling electrons. The equation was later derived by Fishchuk[24] for the box distribution of activation energies in the macroscopic model, and by the present author for a hopping model with the box distribution.[30] Recently, it was shown by means of the EMA for random admittance networks that Eq. (1) is *universal* in the low-temperature limit of the macroscopic model.[19,20] In Sec. V it was shown that the equation is also the universal EMA prediction for symmetric hopping models. Physically what happens is that, at low temperatures, the conduction mainly follows the percolation paths, and the only "signature" of the activation energy distribution left is the number $p(E_c)$.

The universality prediction was tested in Fig. 5, which studies five different activation energy probability distributions at the same "reduced" temperature $\tilde{\beta}=4$. There is clearly a universality in the sense that the function $\bar{\sigma}(\bar{s})$ is independent of the activation energy distribution. However, the results deviate from the EMA prediction Eq. (1). One reason for the discrepancy may be that the temperature is simply not low enough in Fig. 5. Unfortunately, it is not possible to go to lower temperatures for a 100×100 lattice without loosing reproducibility.

There are interesting differences between the macroscopic model[20] and hopping models. Figures 4 and 5 indicate a systematic deviation of the simulations from the EMA predictions at low temperatures in the transition region. Here the data give a less sharp transition to frequency dependence than the EMA predicts. In the macroscopic model, on the other hand, there is a very good agreement between the EMA predictions and the simulations at all temperatures and frequencies. It is not clear what the origin of these differences is. Apparently, the hopping model is more complex than the macroscopic model. Thus, in the derivation of universality for hopping models, one has to distinguish between the cases $D=2$ and $D > 2$, which is not necessary for the derivation of Eq. (1) for the macroscopic model.[20]

In the simplest realistic approximation to hopping models, the continuous time random walk (CTRW) approximation,[35] the conductivity for the box distribution of energy barriers[30] is

$$\tilde{\sigma} = \frac{\tilde{s}}{\ln(1+\tilde{s})} .$$
(61)

As has been shown elsewhere,[20] this expression is close to that given by Eq. (1); in particular, the two functions $\tilde{\sigma}(\tilde{s})$ have the same asymptotic expressions for the exponents of the real and imaginary parts of the conductivity. These exponents converge slowly to one as the frequency goes to infinity.[20] (A convincing experimental demonstration of this phenomenon has recently been given for metal-cluster compounds.[8])

There has been relatively little discussion of universality for ac conduction in the literature.[1-3,8] In experiments, a number of authors pointed out early that quite different systems like ionic conductive glasses and amorphous semiconductors have surprisingly similar ac responses.[1-3] In a theoretical paper, Summerfield[65] in 1985 termed the phrase "quasi-universality" for the fact that a number of different models, when solved in the EPA,[54] give almost the same frequency dependence of the conductivity.

The macroscopic model based on Maxwell's equations for an inhomogeneous solid leads to an electrical equivalent circuit, where the nodes on a cubic lattice are joined by a capacitor and a resistor in parallel.[20,24] The resistors carry the free charge currents while the capacitor currents are Maxwell's displacement currents.[20] In contrast to the circuit of Fig. 2, there are no connections to the ground and no voltage generators; the "solid" is simply subjected to a macroscopic potential drop at the electrodes (equal to two opposing end faces). In the dc limit the macroscopic model and hopping models both give simple resistance circuits. Thus, the dc limit of the EMA hopping equation, Eq. (21), is identical to the EMA equation for a random resistance circuit.

An interesting connection between the symmetric hopping model and the macroscopic model is that the CTRW approximation[28,35] to hopping models corre-

sponds to the one-dimensional version of the macroscopic model. As has been discussed in detail elsewhere,[20] this version becomes realistic at low temperatures where conduction mainly follows the percolation paths. Along these lines, an approximation to the macroscopic model referred to as the "percolation path approximation" (PPA) was proposed in Ref. 20, leading to Eq. (61).

Throughout this paper the limit of extreme disorder (where the jump frequencies Γ vary several decades) was arrived at by going to low temperatures for a system with thermally activated hopping. The same limit is also arrived at in a system of localized electrons tunneling between nearest-neighbor sites, when the density of electrons becomes very small. The system of tunneling electrons has been studied extensively in the past.[26,54,66] Though it was not spelled out in detail in Sec. V, in the extreme disorder limit, the EMA universality prediction [Eq. (1)] applies to this system as well.[26]

There are a number of open problems and work that remains to be done. The symmetric hopping model should be studied numerically at low temperatures also in three dimensions. Regarding the numerical method, it is not clear what the optimal strategy for removing nodes is. From the theoretical point of view the main question is: Is there true universality in the extreme disorder limit, or is there only "quasi-universality?" If true universality does exist, as believed by the author, is the universal function $\tilde{\sigma}(\tilde{s})$ the same in all dimensions? If this is not the case, analytical methods more accurate than the EMA should be developed to calculate the universal conductivity. A further question is: What is the cause of the difference between the hopping model and the macroscopic model, where the EMA works better than for hopping?

ACKNOWLEDGMENTS

[1]A. K. Jonscher, Nature 267, 673 (1977); *Dielectric Relaxation in Solids* (Chelsea Dielectric, London, 1983).

[2]A. E. Owen, J. Non-Cryst. Solids 25, 372 (1977).

[3]A. Mansingh, Bull. Mater. Sci. (India) 2, 325 (1980).

[4]A. R. Long, Adv. Phys. 31, 553 (1982).

[5]M. D. Ingram, Phys. Chem. Glasses 28, 215 (1987).

[6] S. R. Elliott, *Physics of Amorphous Materials*, 2nd ed. (Longman Scientific, London, 1990).

[7]C. A. Angell, Chem. Rev. 90, 523 (1990).

[8]M. P. J. van Staveren, H. B. Brom, and L. J. de Jongh, Phys. Rep. 208, 1 (1991).

[9]J. L. Barton, Verres Réfract. 20, 328 (1966).

[10]T. Nakajima, in *1971 Annual Report, Conference on Electric Insulation and Dielectric Phenomena* (National Academy of Sciences, Washington, DC, 1972), p. 168.

[11]H. Namikawa, J. Non-Cryst. Solids 18, 173 (1975).

[12]M. Tomozawa, in *Treatise on Materials Science*, Vol. 12, edited by M. Tomozawa (Academic, New York, 1977), p. 283.

[13]J. C. Dyre, J. Non-Cryst. Solids 88, 271 (1986).

[14]H. Böttger and V. V. Bryksin, *Hopping Conduction in Solids* (Akademie-Verlag, Berlin, 1985).

[15]J. W. Haus and K. W. Kehr, Phys. Rep. 150, 263 (1987).

[16]J.-P. Bouchaud and A. Georges, Phys. Rep. 195, 127 (1990).

[17]J. O. Isard, Philos. Mag. B 62, 139 (1990); Philos. Mag. A 66, 213 (1992).

[18]P. Maass, J. Petersen, A. Bunde, W. Dieterich, and H. E. Roman, Phys. Rev. Lett. 66, 52 (1991).

[19]J. C. Dyre, Phys. Rev. B 47, 9128 (1993).

[20]J. C. Dyre, Phys. Rev. B 48, 12 511 (1993).

[21]B. E. Springett, Phys. Rev. Lett. 31, 1463 (1973).

[22]I. Webman, J. Jortner, and M. H. Cohen, Phys. Rev. B 15, 5712 (1977).

[23]J. Sinkkonen, Phys. Status Solidi B 103, 231 (1981).

[24]I. I. Fishchuk, Phys. Status Solidi A 93, 675 (1986).

[25]S. Kirkpatrick, Rev. Mod. Phys. 45, 574 (1973).

[26]V. V. Bryksin, Fiz. Tverd. Tela (Leningrad) 22, 2441 (1980) [Sov. Phys. Solid State 22, 1421 (1980)].

[27]P. N. Butcher, in *Linear and Nonlinear Electronic Transport in Solids,* edited by J. T. de Vreese and V. E. van Doren (Plenum, New York, 1976), p. 341.

[28]M. Lax and T. Odagaki, in *Macroscopic Properties of Disordered Media,* edited by R. Burridge (Springer-Verlag, Berlin, 1982), p. 148.

[29]G. A. Niklasson, J. Appl. Phys. 62, R1 (1987).

[30]J. C. Dyre, J. Appl. Phys. 64, 2456 (1988).

[31]H. Haken, *Synergetics* (Springer, Berlin, 1983).

[32]N. G. van Kampen, *Stochastic Processes in Physics and Chemistry* (North-Holland, Amsterdam, 1981).

[33]B. I. Shklovskii and A. L. Efros, *Electronic Properties of Doped Semiconductors* (Springer-Verlag, Berlin, 1984).

[34]R. Kubo, J. Phys. Soc. Jpn. 12, 570 (1957).

[35]H. Scher and M. Lax, Phys. Rev. B 7, 4491 (1973); 7, 4502 (1973).

[36]S. Alexander, J. Bernasconi, W. R. Schneider, and R. Orbach, Rev. Mod. Phys. 53, 175 (1981).

[37]J. C. Kimball and L. W. Adams, Phys. Rev. B 18, 5851 (1978).

[38]V. Ambegaokar, B. I. Halperin, and J. S. Langer, Phys. Rev. B 4, 2612 (1971).

[39]B. I. Shklovskii and A. L. Efros, Zh. Eksp. Teor. Fiz. 60, 867 (1971) [Sov. Phys. JETP 33, 468 (1971)].

[40]S. Tyc and B. I. Halperin, Phys. Rev. B 39, 877 (1989).

[41]H. Kesten, *Percolation Theory for Mathematicians* (Birkhauser, Boston, 1982).

[42]D. B. Gingold and C. J. Lobb, Phys. Rev. B 42, 8220 (1990).

[43]J. A. Krumhansl, in *Amorphous Magnetism,* edited by H. O. Hooper and A. M. de Graaf (Plenum, New York, 1973), p. 15.

[44]F. Yonezawa, in *The Structure and Properties of Matter,* edited by T. Matsubara (Springer-Verlag, Berlin, 1982), p. 383.

[45]S. Summerfield, Solid State Commun. 39, 401 (1981).

[46]B. Movaghar and W. Schirmacher, J. Phys. C 14, 859 (1981).

[47]T. Odagaki and M. Lax, Phys. Rev. B 24, 5284 (1981).

[48]W. Schirmacher, Ber. Bunsenges. Phys. Chem. 95, 368 (1991).

[49]E. N. Economou, *Green's Functions in Quantum Physics* (Springer, Berlin, 1983).

[50]M. Sahimi, B. D. Hughes, L. E. Scriven, and H. T. Davis, J. Chem. Phys. 78, 6849 (1983).

[51]W. H. Press, B. P. Flannery, S. A. Teukolsky, and W. T. Vetterling, *Numerical Recipes* (Cambridge University Press, Cambridge, 1986).

[52]A. Miller and B. Abrahams, Phys. Rev. 120, 745 (1960).

[53]M. Pollak, in *Proceedings of the Fifth International Conference on Amorphous and Liquid Semiconductors,* Garmisch-Partenkirchen 1973, Vol. 1 (Taylor and Francis, London, 1974), p. 127.

[54]S. Summerfield and P. N. Butcher, J. Phys. C 15, 7003 (1982).

[55]N. M. Morris, *Electrical Circuit Analysis and Design* (Macmillan, London, 1993).

[56]R. Fogelholm, J. Phys. C 13, L571 (1980).

[57]R. Fogelholm, Report No. TRITA-FYS-5075, Royal Institute of Technology, Stockholm, 1980 (unpublished).

[58]*Handbook of Mathematical Functions,* edited by M. Abramowitz and I. A. Stegun (Dover, New York, 1965).

[59]M. Lax, Phys. Rev. 97, 629 (1955).

[60]H. B. Dwight, *Tables of Integrals and Other Mathematical Data* (Macmillan, New York, 1961).

[61]K. Stuben, Appl. Math. Comput. 13, 419 (1983).

[62]A. Brandt, Appl. Math. Comput. 19, 23 (1986).

[63]The AMG1R5 FORTRAN subroutine is available from "casper.na.cs.yale.edu" (128.36.12.1); ftp as anonymous, then look for the file "amg.tar.Z" in the "gmd" directory under the "mgnet" directory.

[64]R. G. Edwards, J. Goodman, and A. D. Sokal, Phys. Rev. Lett. 61, 1333 (1988).

[65]S. Summerfield, Philos. Mag. B 52, 9 (1985).

[66]B. Movaghar and W. Schirmacher, J. Phys. C 14, 859 (1981).

Universal time dependence of the mean-square displacement in extremely rugged energy landscapes with equal minima

Jeppe C. Dyre and Jacob M. Jacobsen

Institute of Mathematics and Physics (IMFUFA), Roskilde University, P.O. Box 260, DK-4000 Roskilde, Denmark

(Received 18 January 1995)

This paper presents a calculation of the time dependence of the mean-square displacement for symmetric random energy barrier hopping models at low temperatures, where the frequency dependence of the normalized diffusion constant $\tilde{D}$ becomes universal, i.e., independent of the energy barrier probability distribution [J. C. Dyre, Phys. Rev. B **49**, 11 709 (1994)]. The universal time dependence of the mean-square displacement is calculated from the effective medium approximation (EMA) universality equation, $\tilde{D} \ln \tilde{D} = \tilde{s}$, where $\tilde{s}$ is the dimensionless imaginary frequency, as well as for the approximation to the EMA universality equation $\tilde{D} \cong \tilde{s}/\ln(1 + \tilde{s})$. At long times the universal mean-square displacement is linear in time, corresponding to ordinary diffusion, whereas the mean-square displacement at short times t in dimensionless units varies as $2/\ln(t^{-1})$.

PACS number(s): 05.40.+j, 05.60.+w

I. INTRODUCTION

The study of stochastic motion in a rugged energy landscape is relevant in a number of contexts [1]. Examples include models for ac conduction in disordered solids [2–5], protein dynamics [6], viscous flow in liquids close to the glass transition [7,8], diffusion in random flows [9], or plasma heat conduction in stochastic magnetic fields [9]. To be specific, consider the Langevin equation of motion [10] for a system with d degrees of freedom subject to the potential $U(X_1, ..., X_d)$,

$$\dot{X}_i = -\mu \frac{\partial U}{\partial X_i} + \xi_i(t), \tag{1}$$

where μ is a constant and $\xi_i(t)$ is a Gaussian white noise term with variance given by $\langle \xi_i(t)\xi_j(t')\rangle = 2\mu k_B T \delta_{i,j} \delta(t - t')$ (k_B is Boltzmann's constant and T is the temperature). In the study of motion in a complex energy landscape the potential is usually assumed to be random in some specific sense. For instance, the potential could be chosen according to a Gaussian functional probability distribution with a specified spatial correlation.

For the dynamics defined by Eq. (1) it is possible to monitor the average energy as a function of time, as well as the average displacement as a function of time. As an example relating to energy relaxation, the temperature may be an arbitrarily varying function of time and one may calculate how the average energy varies in time. Thus, energy relaxations in viscous liquids close to the glass transition may be modeled [7,8]. Also, the equilibrium energy time autocorrelation function may be calculated, giving the frequency-dependent linear specific heat [11,12]. In both cases, it is convenient in numerical simulations to use the Smoluchowski equation [10,13] for the probability instead of the noisy Langevin equations.

When the quantity of interest is the displacement as a function of time, the focus is usually on the average

mean-square displacement in some fixed axis direction i, $\langle \Delta X_i^2(t)\rangle$. In terms of the canonical equilibrium probability, $P_o(X) \propto \exp[-\beta U(X)]$, and the Green's function, $G(X \to X'; t)$, the mean-square displacement is given by the $2d$-dimensional integral (assuming isotropy)

$$\langle \Delta X_i^2(t)\rangle = \frac{1}{d} \int P_o(X)\, G(X \to X'; t)$$
$$\times (X - X')^2\, dX\, dX' . \tag{2}$$

The mean-square displacement increases linearly with time asymptotically as $t \to \infty$. In disordered systems at shorter times the mean-square displacement varies more rapidly, leading to a negative curvature of $\langle \Delta X_i^2(t)\rangle$,

$$\frac{d^2}{dt^2} \langle \Delta X_i^2(t)\rangle \le 0 . \tag{3}$$

The fast average displacement at short times is easy to understand. The particle spends most of its time in a potential energy minimum. The most likely displacement is to overcome a low energy barrier to another energy minimum, which is a relatively fast process. From this new position the most likely jump is often to go back to the starting point. Thus, at longer times the displacement is smaller than expected from an extrapolation of the short time displacement.

If s denotes the imaginary (Laplace) frequency, $s = i\omega$, the frequency-dependent diffusion constant, $D(s)$, is defined [2] by

$$D(s) = \frac{s^2}{2} \int_0^\infty \langle \Delta X_i^2(t)\rangle\, e^{-st}\, dt . \tag{4}$$

It is understood that there is a convergence factor $\lim_{\epsilon \to 0} e^{-\epsilon t}$ ($\epsilon > 0$) in the integral. For ordinary diffusion, where $\langle \Delta X_i^2(t)\rangle = 2Dt$, one has $D(s) = D$. It is convenient to regard $D(s)$ as an analytic function of s that may be studied also for nonimaginary Laplace frequencies. For real s it is straightforward to show that

Eq. (3) implies that $D(s)$ is an increasing function of s . Writing for real frequencies ω, $D(i\omega) = D'(\omega) + iD''(\omega)$, it can also be shown [14] that $D'(\omega)$ is always an increasing function of ω.

If the particle moves in three dimensions and carries a charge, the system is characterized by a frequency-dependent conductivity, $\sigma(\omega)$. By the fluctuation-dissipation theorem $\sigma(\omega)$ is proportional to the frequency-dependent diffusion constant. In fact, Eq. (4) may be derived from the Kubo formula for $\sigma(\omega)$ by two partial integrations [2], utilizing the fact that the second time derivative of the mean-square displacement is twice the velocity time autocorrelation function.

One way to simplify Eq. (1) is to put it on a lattice. In this way one arrives at a hopping model [3,8,15–18]. A particularly simple case is when all energy minima are equal. If the minima correspond to the sites of the lattice, the problem is reduced to the study of a hopping model with symmetric transition rates for nearest-neighbor jumps. Each transition rate is proportional to $\exp(-\beta E)$ where E is the energy barrier. A further simplification is to assume that the transition rates are uncorrelated from link to link; the model is then completely specified by the energy barrier probability distribution.

Symmetric hopping models have been studied extensively, particularly with respect to evaluating their frequency-dependent conductivity. These models are quite complex and cannot be solved analytically, even in one dimension. However, a useful approximation exists for evaluating $D(s)$ [or equivalently $\sigma(s)$]: the effective medium approximation (EMA) [3,15,18,19]. The EMA is based on an approximation similar to that used in the derivation of the Clausius-Mossotti formula for the dielectric constant of a mixture [20]; in the solid state physics of disordered media the same idea is used in the coherent potential approximation (CPA) [21]. The EMA equation is simplest in the unit system where the diffusion constant on a homogeneous lattice with link jump rate Γ is given by $D = \Gamma$. If the dimension is d, and if one defines

$$p(\mathbf{k}) = \frac{1}{d}\sum_{i=1}^{d}\cos(k_i)$$ and the following integral over the first Brillouin zone $(-\pi < k_i < \pi)$

$$s\bar{G} = \int_{1\text{-BZ}} \frac{s}{s + 2\,d\,D[1 - p(\mathbf{k})]}\frac{d\mathbf{k}}{(2\pi)^d}\,, \qquad (5)$$

the EMA equation for $D(s)$ is expressed as an average over the jump rate probability distribution,

$$\left\langle \frac{\Gamma - D}{d\,D + [1 - s\bar{G}(\Gamma - D)]} \right\rangle_{\Gamma} = 0. \qquad (6)$$

The EMA is a mean-field theory. As recently shown [17], the EMA equation becomes rather simple in the extreme disorder limit, i.e., where the temperature goes to zero and the jump frequencies consequently cover more and more decades. In this limit, the EMA equation for $D(s)$ becomes universal in more than one dimension, i.e., independent of the energy barrier probability distribution. Introducing the normalized dimensionless diffusion constant $\tilde{D} = D(s)/D(0)$ and the dimensionless Laplace

frequency $\tilde{s} = s\tau$, where τ is a characteristic time marking the onset of frequency dispersion (the precise value of which is of little interest here), the EMA universality equation [17] is

$$\tilde{D}\,\ln\tilde{D} = \tilde{s}. \qquad (7)$$

At any nonzero temperature this expression is valid only for a finite range of Laplace frequencies, since $\tilde{D}(\tilde{s})$ becomes independent of $\tilde{s}$ for sufficiently large $\tilde{s}$. However, as the temperature goes to zero, the range of validity of the EMA universality equation extends to infinity, and therefore the existence of the high frequency plateau for $\tilde{D}(\tilde{s})$ at nonzero temperatures is ignored below.

The numerical solution of Eq. (7) was discussed in Ref. [22] that also gave an accurate analytical approximation to $\tilde{D}(\tilde{s})$. Equation (7) implies that

$$\tilde{D} = \frac{\tilde{s}}{\ln\tilde{D}} \cong \frac{\tilde{s}}{\ln\tilde{s}} \quad (|\tilde{s}| \to \infty). \qquad (8)$$

An approximate solution of the EMA universality equation is provided by the following expression [first derived [4,23] as the continuous time random walk (CTRW) solution of the symmetric hopping model with a box distribution of energy barriers]:

$$\tilde{D} = \frac{\tilde{s}}{\ln(1 + \tilde{s})}. \qquad (9)$$

Equations (7) and (9) both imply that $\tilde{D}(\tilde{s})$ follows an approximate power law as $|\tilde{s}| \to \infty$. For real Laplace frequencies as $\tilde{s} \to \infty$ one has $\tilde{D} \propto \tilde{s}^u$, where $u = 1 - 1/\ln\tilde{s}$. For real frequencies $\tilde{\omega} = \tilde{s}/i$, one finds for $\tilde{\omega} \to \infty$ [22] $\tilde{D}' \propto \tilde{\omega}^v$, where $v = 1 - 2/\ln\tilde{\omega}$.

II. CALCULATION OF THE UNIVERSAL TIME DEPENDENCE OF THE MEAN-SQUARE DISPLACEMENT

The mean-square displacement is given by the inverse Laplace transform of Eq. (4), where the integration contour as usual stretches from $-i\infty$ to $i\infty$ to the right of all poles and branch cuts,

$$\langle \Delta X_i^2(t) \rangle = \frac{1}{2\pi i}\oint \frac{2\,D(s)}{s^2}\,e^{st}\,ds. \qquad (10)$$

It is convenient to adopt the "rationalized" unit system where $D(0) = 1$ and the time unit is chosen so that $\tilde{s} = s$; this is done by writing $\tilde{D} = D$ and $\tilde{s} = s$. In the "rationalized" unit system the quantities D, s, and t are all dimensionless and the EMA universality equation (7) becomes $D\ln D = s$. Note that the boundary condition

$$\langle \Delta X_i^2(0) \rangle = 0 \qquad (11)$$

is ensured by Eq. (10) for $D(s)$ given by Eq. (7) as well as by Eq. (9) because both equations imply that $D/s \to 0$ for $|s| \to \infty$.

The calculation of the universal mean-square displace-

ment is complicated by the fact that $D(s)$ is given only indirectly. We first evaluate the inverse Laplace transform of the approximate expression Eq. (9), which is simpler (using again the "rationalized" unit system). Substitution of Eq. (9) into Eq. (10) gives

$$\langle \Delta X_i^2(t) \rangle = \frac{1}{2\pi i} \oint \frac{2}{s \ln(1+s)} e^{st} \, ds. \qquad (12)$$

The integrand has a pole at $s = 0$ and a branch cut along the negative real s axis from $s = -1$ to $s = -\infty$. The integration contour is displaced to run slightly below the real axis from $s = -\infty$ to 0 and back to $-\infty$ slightly above the axis. The residue at the pole $s = 0$ is found by expanding

$$\frac{2e^{st}}{s \ln(1+s)} = 2 \frac{1 + st + \cdots}{s(s - \frac{s^2}{2} + \cdots)}$$

$$= \frac{2}{s^2}(1 + st + \cdots)\left(1 + \frac{s}{2} + \cdots\right)$$

$$= \frac{2}{s^2}\left(1 + (t + \frac{1}{2})s + \cdots\right). \qquad (13)$$

The contribution to the integral from this pole is $2t + 1$. If one defines $f(x) = 2\, e^{xt}/[x \ln(1 + x)]$ the remaining part of the integral equals (where $\epsilon > 0$ is infinitesimal)

$$\frac{1}{2\pi i} \int_1^\infty [f(-u - i\epsilon) - f(-u + i\epsilon)] du. \qquad (14)$$

Since $f(-u + i\epsilon)$ is the complex conjugate of $f(-u - i\epsilon)$ expression (14) becomes

$$\frac{2}{\pi} \int_1^\infty \text{Im} \frac{e^{-ut}}{(-u)[\ln(u - 1) - i\pi]} \, du$$

$$= -2 \int_1^\infty \frac{e^{-ut}}{\ln^2(u - 1) + \pi^2} \frac{du}{u}. \qquad (15)$$

Summarizing, the mean-square displacement is in the approximation Eq. (9) given by

$$\langle \Delta X_i^2(t) \rangle = 2t + 1 - 2 \int_1^\infty \frac{e^{-ut}}{\ln^2(u - 1) + \pi^2} \frac{du}{u}. \qquad (16)$$

By means of Eq. (11) this may be rewritten [24] as

$$\langle \Delta X_i^2(t) \rangle = 2t + 2 \int_1^\infty \frac{1 - e^{-ut}}{\ln^2(u - 1) + \pi^2} \frac{du}{u}. \qquad (17)$$

Equation (17) makes it possible to estimate the asymptotic behavior of the mean-square displacement at short times ($t \ll 1$): The term $2t$ is insignificant compared to the integral, which is separated into two terms: one integral from 1 to t^{-1} and one from t^{-1} to ∞. In the first integral the term $1 - e^{-ut}$ is smaller than ut and the denominator may be replaced by $\ln^2(t^{-1})$. Thus this integral is of order $2/\ln^2(t^{-1})$, which is small compared to the value of the second integral: Here the term $1 - e^{-ut}$ may be replaced by 1 and the denominator may be re-

placed by $\ln^2(u)$. Thus, for $t \ll 1$ one has

$$\langle \Delta X_i^2(t) \rangle \cong \int_{t^{-1}}^\infty \frac{2}{\ln^2(u)} \frac{du}{u} = \frac{2}{\ln(t^{-1})}. \qquad (18)$$

This asymptotic behavior suggests the following analytical approximation to Eq. (17);

$$\langle \Delta X_i^2(t) \rangle \cong \frac{2}{\ln(1 + t^{-1})}. \qquad (19)$$

In fact, this expression has the correct short time behavior given by Eq. (18) as well as the correct long time behavior, $\langle \Delta X_i^2(t) \rangle \cong 2t + 1$. Equation (19) gives an approximation to Eq. (17) which for any t deviates less than 7%.

We now turn to the Laplace inversion of the EMA universality equation. It is possible to show that $D \ln D = s$ defines $D(s)$ for all complex s, except the negative real numbers between $-\infty$ and $-1/e$ [compare Eqs. (24), (25), and (34) below]. We again choose the integration contour going from $s = -\infty$ slightly below the real s axis returning to $s = -\infty$ slightly above the axis, encircling all poles and branch cuts. Just as above, there is a pole at $s = 0$, but the branch cut this time stretches from $s = -1/e$ to $s = -\infty$. The residue at $s = 0$ for the integrand of Eq. (10) is by standard rules equal to

$$\frac{d}{ds}\left[2\, D(s)e^{st}\right]\Big|_{s=0} = 2(D'(0) + D(0)t). \qquad (20)$$

The normalization condition is $D(0) = 1$ and the EMA universality equation $D \ln D = s$ implies that $D'(0)[\ln D(0) + 1] = 1$ or $D'(0) = 1$. Thus, the residue is equal to $2t + 2$. For the remainder of Eq. (10) it is convenient to change to D as integration variable; $s = D \ln D$ implies $ds = (1 + \ln D)dD$ and thus

$$\langle \Delta X_i^2(t) \rangle = 2t + 2$$
$$+ \frac{1}{2\pi i} \oint 2 \frac{D + D \ln D}{(D \ln D)^2} e^{D \ln D t} \, dD, \qquad (21)$$

where the integration contour in the D plane is defined by $D \ln D$ being real and $\leq -1/e$. Writing $D = re^{i\theta}$, the equation defining the integration contour is [25] $\text{Im}(D \ln D) = 0$ which, since $\ln D = \ln r + i\theta$, implies that $\theta \cos \theta + \ln r \sin \theta = 0$, or

$$r = e^{-\theta \cot \theta} \qquad (-\pi < \theta < \pi). \qquad (22)$$

Equation (22) implies that the real number $D \ln D$ on the integration contour is given by

$$D \ln D = re^{i\theta}(\ln r + i\theta)$$
$$= e^{-\theta \cot \theta} \theta (-\cos \theta \cot \theta - \sin \theta) \qquad (23)$$

or

$$D \ln D = -E(\theta), \qquad (24)$$

where

$$E(\theta) = \frac{\theta}{\sin \theta} e^{-\theta \cot \theta}. \qquad (25)$$

The function $E(\theta)$ varies monotonically from $1/e$ to ∞ as $|\theta|$ varies from 0 to π. Next, the integration variable is changed to θ. The differential of D is given by $dD = e^{i\theta}(dr + ir\,d\theta)$. From Eq. (22) one finds $dr = r(-\cot\theta + \frac{\theta}{\sin^2\theta})d\theta$, and thus

$$dD = D\left(-\cot\theta + \frac{\theta}{\sin^2\theta} + i\right)d\theta. \qquad (26)$$

Substituting Eqs. (24) and (26) into Eq. (21) one obtains

$$\langle \Delta X_i^2(t)\rangle = 2t + 2 + \frac{1}{2\pi i}\int_{-\pi}^{\pi} 2\,\frac{re^{i\theta} - E(\theta)}{E^2(\theta)} e^{-E(\theta)t} re^{i\theta}\left(-\cot\theta + \frac{\theta}{\sin^2\theta} + i\right)d\theta. \qquad (27)$$

Since $r = \frac{\sin\theta}{\theta}E(\theta)$ [Eqs. (22) and (25)] the factor $E^2(\theta)$ cancels. The integrand is the real number $e^{-E(\theta)t}$ times the quantity

$$2\left(\frac{\sin\theta}{\theta}(\cos\theta + i\sin\theta) - 1\right)\frac{\sin\theta}{\theta}(\cos\theta + i\sin\theta)\left(-\cot\theta + \frac{\theta}{\sin^2\theta} + i\right). \qquad (28)$$

This function of θ has an antisymmetric real part and a symmetric imaginary part equal to $-2F(\theta)$ where

$$F(\theta) = \left(\cos\theta - \frac{\sin\theta}{\theta}\right)^2 + \sin^2\theta. \qquad (29)$$

Since expression (28) is to be multiplied with the symmetric factor $e^{-E(\theta)t}$ and integrated from $-\pi$ to π, only the symmetric imaginary part of Eq. (28) gives a contribution. We thus finally arrive at

$$\langle \Delta X_i^2(t)\rangle = 2t + 2 - \frac{2}{\pi}\int_0^{\pi} F(\theta)\,e^{-tE(\theta)}\,d\theta. \qquad (30)$$

Utilizing Eq. (11) we may rewrite Eq. (30) as

$$\langle \Delta X_i^2(t)\rangle = 2t + \frac{2}{\pi}\int_0^{\pi} F(\theta)\left(1 - e^{-tE(\theta)}\right)d\theta. \qquad (31)$$

Figure 1 shows a log-log plot of the universal mean-square displacement (full curve) as well as the mean-square displacement according to the rough analytical approximation given by Eq. (19) (dashed curve). At long times one has ordinary diffusion and a mean-square displacement that grows linearly with time. At short times, the mean-square displacement is much larger than expected by extrapolation from the long time behavior. A detailed analysis of the asymptotic behavior of Eq. (31) for $t \to 0$ is somewhat involved. However, the short time behavior of $\langle \Delta X_i^2(t)\rangle$ is determined by the behavior of $D(s)$ for large Laplace frequencies. A detailed analysis is unnecessary since we can refer directly to Eq. (18) which, because of the asymptotic behavior Eq. (8), must be valid also for the mean-square displacement given by Eq. (31). An analytic approximation to Eq. (31) that is considerably more accurate than Eq. (19) is given by the following expression (which for any t is more accurate that 3.3%):

$$\langle \Delta X_i^2(t)\rangle \cong \frac{2}{\ln(1+t^{-1}) - \ln[\ln(e+t^{-1})]} - \frac{2t}{e-1}. \qquad (32)$$

Finally, we note that Eq. (30), when substituted into

Eq. (4), gives rise to an explicit integral expression for the EMA universal $D(s)$. The term $2t + 2$ in Eq. (30) is transformed into $1 + s$ and thus

$$D(s) = 1 + s - \frac{1}{\pi}\int_0^{\pi} F(\theta)\frac{s^2}{s + E(\theta)}d\theta. \qquad (33)$$

Since $\int_0^{\pi} F(\theta)d\theta = \pi$ [which follows from Eqs. (11) and (30)], Eq. (33) may be rewritten

$$D(s) = 1 + \frac{1}{\pi}\int_0^{\pi} F(\theta)\frac{sE(\theta)}{s + E(\theta)}d\theta. \qquad (34)$$

Equation (34) confirms that $D(s)$ is defined for all complex s except the negative real numbers from $-1/e$ to $-\infty$.
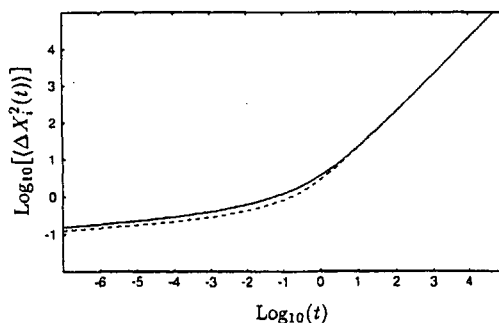

FIG. 1. The universal mean-square displacement in a fixed axis direction in dimensionless units in a log-log plot according to the EMA [Eq. (31), full curve] and to the rough analytical approximation given by $\langle\Delta X_i^2(t)\rangle \cong 2/\ln(1+t^{-1})$ [Eq. (19); dashed curve, deviating less than 33% from the full curve]. At short times the mean-square displacement varies as $2/\ln(t^{-1})$ which implies a considerably faster motion than expected from an extrapolation of the long time diffusive behavior, $\langle\Delta X_i^2(t)\rangle \propto t$. Physically, this effect arises because at short times it is mainly small barriers that are overcome, which is a fast process, while at longer times the largest barrier on a "percolation path" will have to be overcome in order to extend the diffusion to infinity.

III. CONCLUSION

An analytic expression for the time dependence of the mean-square displacement for low-temperature hopping has been derived from the EMA universality equation. At short times the mean-square displacement varies as $2/\ln(t^{-1})$, indicating a considerably faster motion than expected from the long time diffusive behavior $\propto t$. The expression derived for the mean-square displacement Eq. (31) is valid asymptotically as the temperature goes to zero. At any finite temperature the mean-square displacement actually returns to diffusive behavior $\propto t$ at *very* short times, corresponding to the fact that at very high Laplace frequencies $D(s)$ becomes constant. This effect has been ignored here because the range of validity of Eq. (31) becomes larger and larger as the temperature is lowered.

The transition from "logarithmic" diffusion to ordinary diffusion defines a characteristic time, which in the above used dimensionless units is of order 1. In real units this characteristic time is thermally activated with an activation energy equal to the percolation energy, the lowest energy barrier met on a long optimal path. It follows from the EMA [17], that the dc diffusion constant in real units, $D(0)$, is exponentially activated with the same activation energy, a result which is probably rigorously valid. This fact—the Barton-Namikawa-Nakajima (BNN) relation [17,26] — has been known for many years from experiments on ac conduction in ionically and electronically disordered solids and was recently confirmed by computer simulations in two dimensions [17].

[1] P. G. Wolynes, Acc. Chem. Res. **25**, 513 (1992).

[2] H. Scher and M. Lax, Phys. Rev. B **7**, 4491 (1973).

[3] J. W. Haus and K. W. Kehr, Phys. Rep. **150**, 263 (1987).

[4] J. C. Dyre, J. Appl. Phys. **64**, 2456 (1988).

[5] P. Maass, J. Petersen, A. Bunde, W. Dieterich, and H. E. Roman, Phys. Rev. Lett **66**, 52 (1991).

[6] H. Frauenfelder, S. G. Sligar, and P. G. Wolynes, Science **254**, 1598 (1991).

[7] R. Richert and H. Bässler, J. Phys. Condens. Matter **2**, 2273 (1990).

[8] J. C. Dyre, Phys. Rev. B **51**, 12 276 (1995).

[9] M. B. Isichenko, Rev. Mod. Phys. **64**, 961 (1992).

[10] N. G. van Kampen, *Stochastic Processes in Physics and Chemistry* (North-Holland, Amsterdam, 1981).

[11] T. Christensen, J. Phys. (Paris) Colloq. **46**, C8-635 (1985).

[12] N. O. Birge and S. R. Nagel, Phys. Rev. Lett. **54**, 2674 (1985).

[13] M. Doi and S. F. Edwards, *The Theory of Polymer Dynamics* (Clarendon, Oxford, 1986).

[14] J. C. Kimball and L. W. Adams, Phys. Rev. B **18**, 5851

(1978).

[15] H. Böttger and V. V. Bryksin, *Hopping Conduction in Solids* (Akademie Verlag, Berlin, 1985).

[16] J.-P. Bouchaud and A. Georges, Phys. Rep. **195**, 127 (1990).

[17] J. C. Dyre, Phys. Rev. B **49**, 11709 (1994).

[18] B. D. Hughes, *Random Walks and Random Environments* (Clarendon, Oxford, 1995), Vols. 1 and 2.

[19] T. Odagaki and M. Lax, Phys. Rev. B **24**, 5284 (1981).

[20] J. A. Krumhansl, in *Amorphous Magnetism*, edited by H. O. Hooper and A. M. de Graaf (Plenum, New York, 1973), p. 15.

[21] F. Yonezawa, in *The Structure and Properties of Matter*, edited by T. Matsubara (Springer, Berlin, 1982), p. 383.

[22] J. C. Dyre, Phys. Rev. B **48**, 12511 (1993).

[23] J. C. Dyre, Phys. Lett. **108A**, 457 (1985).

[24] J. C. Dyre, Rheol. Acta **29**, 145 (1990).

[25] V. V. Bryksin and P. Kleinert, J. Phys. Condens. Matter **6**, 7879 (1994).

[26] J. C. Dyre, J. Non-Cryst. Solids **88**, 271 (1986).

Effective one-dimensionality of universal ac hopping conduction in the extreme disorder limit

Jeppe C. Dyre and Thomas B. Schrøder

Department of Mathematics and Physics, Roskilde University, Postbox 260, DK-4000 Roskilde, Denmark

(Received 23 February 1996; revised manuscript received 23 August 1996)

A phenomenological picture of ac hopping in the symmetric hopping model (regular lattice, equal site energies, random energy barriers) is proposed according to which conduction in the extreme disorder limit is dominated by essentially one-dimensional "percolation paths." Modeling a percolation path as strictly one dimensional with a sharp jump rate cutoff leads to an expression for the universal ac conductivity that fits computer simulations in two and three dimensions better than the effective medium approximation. [S0163-1829(96)06745-8]

While ordered solids show no frequency dependence of their conductivity at frequencies below phonon frequencies, disordered solids are characterized by ac conductivity that varies as an approximate power law of frequency.[1-6] The exponent is usually less than, but often close to, 1. As the frequency goes to zero the conductivity becomes frequency independent. These features are observed universally for electronically conducting disordered solids like amorphous semiconductors,[1,2,4,7] polymers,[8,9] doped-crystalline semiconductors at helium temperatures[10] (where the random positions of the dopant atoms become important), or high-temperature superconductors above T_c,[11] as well as for ionically conducting disordered solids like glasses or polymers.[2,3,5,6]

This paper deals with ac hopping conduction in disordered solids, but before proceeding we note that the study of stochastic motion in disordered systems ("rugged energy landscapes") is relevant in a number of other contexts.[12-14] Examples include models for protein dynamics,[15-18] flow of viscous liquids close to the glass transition,[19,20] diffusion in random flows,[21] or rate processes controlled by the anomalous diffusion of reactants.[22-24] Diffusion in a disordered system is characterized by a mean-square displacement that at short times varies more rapidly than expected from extrapolating the long-time linear "Einsteinian" time dependence. If the mean-square displacement in an axis direction i as a function of time is denoted by $\langle \Delta X_i^2(t) \rangle$, the frequency-dependent diffusion constant is defined[25] by [where s denotes the "Laplace" (imaginary) frequency, $s = i\omega$]

$$D(s) = \frac{s^2}{2} \int_0^\infty \langle \Delta X_i^2(t) \rangle e^{-st} dt. \tag{1}$$

For diffusion in an ordered structure, where $\langle \Delta X_i^2(t) \rangle = 2Dt$, one has $D(s) = D$. According to the fluctuation-dissipation theorem, if the diffusing particle carries a charge, $D(s)$ is proportional to the frequency-dependent conductivity $\sigma(s)$.[26] Consequently, all results derived below for the normalized frequency-dependent conductivity $\tilde{\sigma} = \sigma(s)/\sigma(0)$ are valid for the normalized frequency-dependent diffusion constant $\tilde{D} = D(s)/D(0)$.

We consider hopping of charge carriers on a regular lattice with equal site energies and random nearest-neighbor jump rates (model A of Ref. 14). This model for ac conduction in disordered solids has been studied extensively during the last 15 years.[26-33] If the jump rates are taken to be thermally activated with randomly varying activation energies, the limit of extreme disorder may be studied by letting the temperature go to zero. It has recently been shown[34] that in this limit the ac conductivity in suitably scaled units becomes universal in more than one dimension, i.e., independent of temperature and of the activation energy probability distribution $p(E)$. The existence of universality was predicted by the effective medium approximation (EMA) and confirmed by computer simulations in two dimensions. If $\tilde{s}$ is the scaled dimensionless Laplace frequency, the EMA universality equation[34] is

$$\tilde{\sigma} \ln \tilde{\sigma} = \tilde{s}. \tag{2}$$

This equation[35] was originally derived by Bryksin for the model of electrons tunneling between randomly localized positions.[28,36]

While the existence of universality was confirmed by computer simulations in two dimensions, the onset of ac conduction turned out to be smoother than predicted by Eq. (2).[34] The EMA is thus *qualitatively* correct by predicting universality in the extreme disorder limit, but *quantitatively* inaccurate. This is perhaps not surprising. After all, the EMA replaces the disordered solid by an "effective" homogeneous solid with characteristics determined by a self-consistency condition. Such an ordered medium cannot *a priori* be expected to accurately represent conduction in the extreme disorder limit.[37]

It is well known that dc and low-frequency ac hopping at extreme disorder is dominated by percolation effects, i.e., mainly take place on the percolation cluster.[28,37-39] The percolation cluster is a complicated object with fractal dimension equal to 1.9 and 2.5 in two and three dimensions, respectively.[21] Removing "dead ends" (contributing little to the low-frequency conductivity) from the percolation cluster leaves us with the "backbone," which has fractal dimension equal to 1.6 and 1.7 in two and three dimensions, respectively.[21] The backbone contains loops, but at low tem-
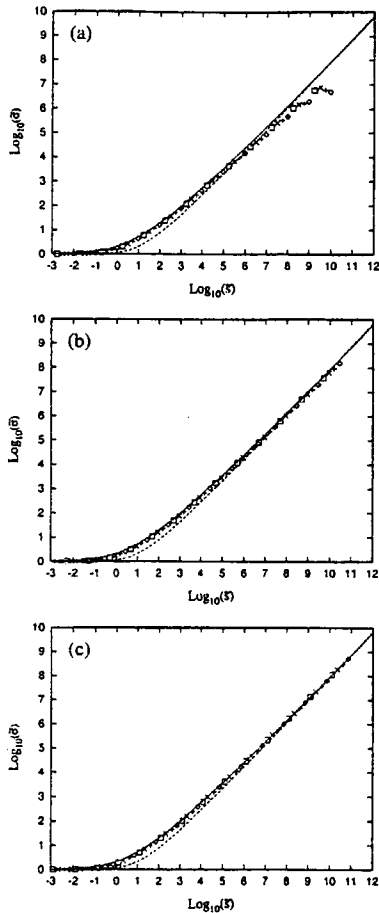
FIG. 1. log-log plot of computer simulations (symbols) of low-temperature ac conductivity in three dimensions at real Laplace frequencies s ($s = i\omega$) for four different activation energy probability distributions, compared to the PPA [Eq. (11), solid curve] and to the zero-temperature limit of the EMA universality equation (2), dashed curve. The dimensionless Laplace frequency $\tilde{s}$ is defined by Eq. (10)—however, a further (minor) empirical rescaling was applied to focus exclusively on the *shape* of the conductivity curve; $\tilde{\sigma}$ is defined by $\tilde{\sigma} = \sigma(\tilde{s})/\sigma(0)$. The jump rates are given by $\Gamma = \Gamma_0 \exp(-\beta E)$, where β is the inverse temperature and the activation energy E is chosen randomly according to the following probability distributions (Ref. 40): asymmetric Gaussian [$p(E) \propto \exp(-E^2/2)$, $0 < E < \infty$] (×), Cauchy [$p(E) \propto 1/(1 + E^2)$, $0 < E < \infty$] (+), exponential [$p(E) = \exp(-E)$, $0 < E < \infty$] (◊), and box [$p(E) = 1$, $0 < E < 1$] (□). To speed up the calculations all jump rates with activation energy larger than $E_c + K/\beta$ were set to zero, where E_c is defined from the bond percolation threshold in Eq. (3). By varying the factor K the maximum errors introduced by this approximation were estimated to be below 1% for both $\sigma(0)$ and $\tilde{\sigma}(\tilde{s})$ for the $K = 6.4$ used for the data presented here. In terms of the dimensionless inverse temperature $\tilde{\beta} = \beta/p(E_c)$ the figure shows data for 100 averages of simulations of cubic lattices with linear dimension N where (a) $\tilde{\beta} = 80$ ($N=29$), (b) $\tilde{\beta} = 160$ ($N=54$), and (c) $\tilde{\beta} = 320$ ($N=100$) [by varying N, the maximum errors introduced by using finite lattices are estimated to be below 30% and 5% for $\sigma(0)$ and $\tilde{\sigma}(\tilde{s})$, respectively]. This figure shows that the ac conductivity becomes universal at low temperatures and that the PPA gives a better fit to data than the EMA universality equation.

peratures one branch of a loop usually has a much higher conductivity than others. The dimension of the actual conduction paths must thus be lower than the dimension of the backbone. Given these arguments, we now make the simplest possible assumption by regarding the conducting paths as one dimensional. This approach, which works well for impedance networks in the extreme disorder limit,[40] is referred to as the "percolation path approximation" (PPA).

It should be stressed that the PPA is an approximation that builds on a highly phenomenological picture of conduction in the extreme disorder limit. In a sense, the PPA may be viewed as being complementary to the EMA: In the EMA the disordered medium is replaced by a homogeneous medium of the same dimension (determined by a self-consistency condition), while in the PPA the disordered medium is replaced by one dimensional conduction paths (determined by percolation arguments).

To summarize, in the PPA conduction takes place via "percolation" paths that have two characteristics: They are strictly one dimensional and they only involve activation energies up to the "percolation energy" E_c. This quantity, which is known to be the activation energy of the dc conductivity,[41,42] is defined from the bond percolation threshold p_c by

$$p_c = \int_0^{E_c} p(E)\,dE. \qquad (3)$$

The purpose of this paper is to show that the PPA approach to ac conduction in the extreme disorder limit, reminiscent of the "conducting path model,"[43,44] gives a good representation of computer simulations. We thereby indirectly confirm the recent findings of Brown and Esser,[45] according to which the actual paths of particles in disordered systems become predominantly one dimensional when the disorder is strong.

Unfortunately, the one-dimensional hopping model behind the PPA is not analytically solvable. Below we derive an approximation to the PPA utilizing the *one-dimensional* EMA, which is known to work very well[46] [this is confirmed below in Fig. 2(a)]. We then show by computer simulations that this one-dimensional EMA, henceforth identified with the PPA, gives a better representation of the universal low-temperature ac hopping conductivity in two and three dimensions than Eq. (2) does.

To arrive at the PPA, hopping in one dimension with a sharp activation energy cutoff is addressed [i.e., $p(E) = 0$ for $E > E_c$ and $p(E_c) > 0$]. In the "rationalized" unit system where the conductivity for a homogeneous system is equal to the jump rate,[29] the EMA equation for the ac conductivity $\sigma(s)$ in one dimension[26,29,33,34,46–50] is (where Γ is the jump rate and the brackets denote an average over the jump rate probability distribution)

$$\langle (\Gamma - \sigma)/[\sigma + (1 - s\tilde{G})(\Gamma - \sigma)] \rangle = 0. \qquad (4)$$

Here, $\tilde{G}$ is the diagonal element of the Green's function for a random walk on a one-dimensional lattice with uniform jump rate σ (the "effective medium"); $s\tilde{G}$ is given[34,46,50] by

$$s\tilde{G} = (1 + 4\sigma/s)^{-1/2}. \qquad (5)$$

We are only concerned with relatively low frequencies where $s\widetilde{G} \ll 1$. To lowest order in $s\widetilde{G}$, Eq. (4) implies[51]

$$1/\sigma = \langle 1/(\Gamma + s\widetilde{G}\sigma) \rangle. \tag{6}$$

The right-hand side may be expanded as a power series in $s\widetilde{G}\sigma$, leading to

$$\frac{1}{\sigma} = \sum_{n=0}^{\infty} (-s\widetilde{G}\sigma)^n \langle \Gamma^{-(n+1)} \rangle. \tag{7}$$

Since $\Gamma = \Gamma_0 \exp(-\beta E)$, where β is the inverse temperature, the average $\langle \Gamma^{-(n+1)} \rangle$ is easily evaluated in the low-temperature limit: If $\widetilde{\beta} = \beta/p(E_c)$, one finds to leading order in $1/\widetilde{\beta}$

$$\langle \Gamma^{-(n+1)} \rangle = \int_0^{E_c} \Gamma_0^{-(n+1)} e^{(n+1)\beta E} p(E) dE = \frac{\Gamma(E_c)^{-(n+1)}}{(n+1)\widetilde{\beta}}. \tag{8}$$

When this is substituted into Eq. (7) the following is obtained:

$$\frac{1}{\sigma} = \sum_{n=0}^{\infty} (-s\widetilde{G}\sigma)^n \frac{\Gamma(E_c)^{-(n+1)}}{(n+1)\widetilde{\beta}} = \frac{1}{\widetilde{\beta}s\widetilde{G}\sigma} \ln\left[1 + \frac{s\widetilde{G}\sigma}{\Gamma(E_c)}\right]. \tag{9}$$

Letting s go to zero we find $\sigma(0) = \widetilde{\beta}\Gamma(E_c)$. Introducing the dimensionless Laplace frequency

$$\widetilde{s} = [\widetilde{\beta}^2/4\sigma(0)]s, \tag{10}$$

one finds that, whenever $s\widetilde{G} \ll 1$, Eq. (5) implies $\widetilde{\beta}s\widetilde{G} = \sqrt{\widetilde{s}/\widetilde{\sigma}}$ [where as in Eq. (2) $\widetilde{\sigma} = \sigma/\sigma(0)$]. Substituting this and $\Gamma(E_c) = \sigma(0)/\widetilde{\beta}$ into Eq. (9) finally leads to the PPA expression

$$\sqrt{\widetilde{\sigma}}\ln[1 + \sqrt{\widetilde{s}\widetilde{\sigma}}] = \sqrt{\widetilde{s}}. \tag{11}$$

Due to the factor $\widetilde{\beta}$ in $\widetilde{\beta}s\widetilde{G} = \sqrt{\widetilde{s}/\widetilde{\sigma}}$, as the temperature is lowered towards zero the condition $s\widetilde{G} \ll 1$ is obeyed in a wider and wider range of dimensionless frequencies. Note that Eqs. (10) and (11) imply that the frequency marking the onset of ac conduction in real units has roughly the same activation energy as the dc conductivity.[31] We also note that Eq. (11) implies that the equilibrium mean-square displacement at short times varies proportionally to $1/\ln^2(t^{-1})$.[52]

We have carried out computer simulations of low-temperature ac hopping in one, two, and three dimensions using the Fogelholm algorithm[53] to reduce the ac Miller-Abrahams electrical equivalent circuit of hopping[54-56] according to a recently proposed scheme.[34] While standard Monte Carlo techniques can hardly be used for simulations at inverse temperatures above $\widetilde{\beta} = 20$,[45,57] the new scheme can be used at much lower temperatures (in our simulations up to inverse temperatures of $\widetilde{\beta} = 320$). Figure 1 shows the results of our simulations of low-temperature ac hopping in three dimensions at real Laplace frequencies. Results are shown for averages of 100 simulations of the ac conductivity for four different activation energy probability distributions at the following inverse temperatures: (a) $\widetilde{\beta} = 80$, (b) $\widetilde{\beta} = 160$, and (c) $\widetilde{\beta} = 320$. The solid curve is the PPA [Eq. (11)] and
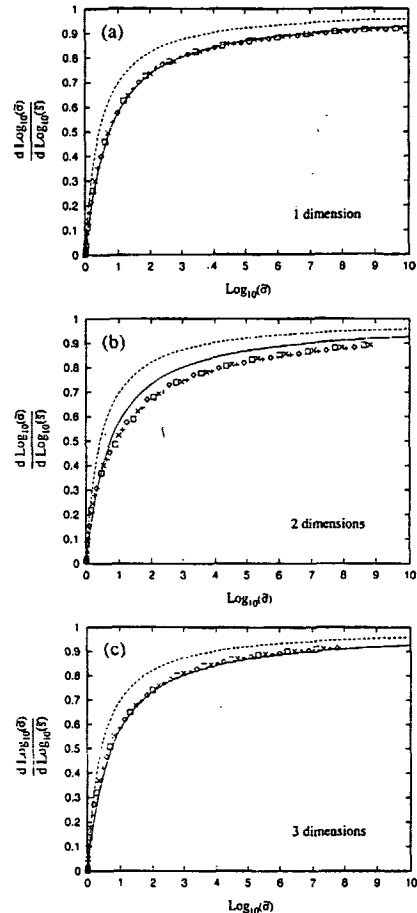
FIG. 2. The slope of the log-log plot of $\widetilde{\sigma}(\widetilde{s})$ at real Laplace frequencies, $d\log_{10}(\widetilde{\sigma})/d\log_{10}(\widetilde{s})$, as function of $\log_{10}(\widetilde{\sigma})$ for simulations at the dimensionless inverse temperature $\widetilde{\beta} = 320$ in (a) one dimension (100 averages of 8192 point lattices), (b) two dimensions (30 averages of 880×880 lattices), and (c) three dimensions (100 averages of 100×100×100 lattices) for the four activation energy probability distributions of Fig. 1. The simulations in one dimension were carried out with a sharp activation energy cutoff at $E = 1$ in order to show the validity of the one-dimensional EMA used in deriving Eq. (11). In two and three dimensions, as in Fig. 1, the smallest jump rates were set to zero to speed up the simulations. The simulations are compared to the predictions of the PPA [solid curve, Eq. (11)] and to the EMA universality equation [dashed curve, Eq. (2)]. Both the EMA and the PPA predict that the slope of the log-log plot goes to 1 as $\widetilde{s} \to \infty$, as seen in experiment (Ref. 1). However, the PPA works better than the EMA in two dimensions and much better than the EMA in three dimensions.

the dashed curve is the EMA universality equation (2). Empirical rescalings of the frequency were allowed in order to focus only on the *shape* of the conductivity curves. Figure 1 shows that universality is approached as the temperature goes to zero and that the PPA gives a quite good fit to the universal ac conductivity in three dimensions.

The universality may be studied without use of empirical rescalings by plotting the slope of the log-log plot, $d\log_{10}(\widetilde{\sigma})/d\log_{10}(\widetilde{s})$, as a function of $\log_{10}(\widetilde{\sigma})$. This is done in Fig. 2 for the same activation energy probability distributions as in Fig. 1 for $\widetilde{\beta} = 320$ data from computer simulations

in one, two, and three dimensions. The solid curve is the PPA prediction and the dashed curve is the EMA universality equation. The simulations in one dimension were for systems with a sharp activation energy cutoff; these simulations were carried out to ensure that Eq. (11) does indeed give an accurate representation of this situation. The real subject of interest is ac conduction in two and three dimensions without any activation energy cutoff [Figs. 2(b) and 2(c)]. In both dimensions the PPA works better than the EMA universality equation.

Considering the simplicity of the phenomenological picture behind the PPA, the agreement with computer simulations in three dimensions is striking. We take our results as an indication that, at least in three dimensions, low-frequency conduction at extreme disorder in fact *is* dominated by essentially one-dimensional conduction paths. This makes sense in light of the "nodes-links" model[58,59] for the infinite network just above the percolation threshold (dc and low-frequency ac conduction are known to take place on this network[28]): According to this model, the backbone of the percolation cluster comprises links (quasi-one-dimensional strings) and nodes (intersection of links). Possibly, the PPA

works well because it models the ac response of a single link. Note that "blobs" on the percolation cluster, as in the more realistic "nodes-links-blobs" model,[58,59] are expected to be unimportant in the extreme disorder limit, since usually one branch of the blob has a much higher conductivity than others.

The problem of ac hopping in the extreme disorder limit is still far from fully understood. This is indicated by the deviation between the PPA and computer simulations in two dimensions, where the PPA according to the arguments involving the fractal dimension of the backbone should work slightly better than in three dimensions and not much worse.[60] Clearly, more work is needed before a genuine understanding of universal ac hopping in the extreme disorder limit is arrived at. Thus, ac hopping in more than three dimensions should be simulated. Also, the actual paths of the particles should be traced out to see whether they are indeed almost one dimensional. Finally, a closer investigation of the analyticity properties of the universal ac conductivity is needed to throw light on whether the prediction of the PPA (that $\tilde{\sigma} - 1 \propto \tilde{s}^{1/2}$ for $\tilde{s} \rightarrow 0$) is really obeyed.

[1] A. K. Jonscher, Nature **267**, 673 (1977); *Universal Relaxation Law* (Chelsea Dielectric, London, 1996).

[2] A. E. Owen, J. Non-Cryst. Solids **25**, 372 (1977).

[3] M. D. Ingram, Phys. Chem. Glasses **28**, 215 (1987).

[4] S. R. Elliott, *Physics of Amorphous Materials*, 2nd ed. (Longman Scientific, London, 1990).

[5] C. A. Angell, Chem. Rev. **90**, 523 (1990).

[6] K. Funke, Prog. Solid State Chem. **22**, 111 (1993).

[7] A. R. Long, Adv. Phys. **31**, 553 (1982).

[8] A. R. Blythe, *Electrical Properties of Polymers* (Cambridge University Press, London, 1979).

[9] F. Kremer *et al.*, Makromol. Chem. Macromol. Symp. **37**, 115 (1990).

[10] M. Pollak and T. H. Geballe, Phys. Rev. **122**, 1742 (1961).

[11] S. Mollah *et al.*, J. Appl. Phys. **74**, 931 (1993).

[12] P. G. Wolynes, Acc. Chem. Res. **25**, 513 (1992).

[13] S. A. Kauffman, *The Origins of Order* (Oxford University Press, Oxford, 1993).

[14] D. L. Stein and C. M. Newman, Phys. Rev. E **51**, 5228 (1995).

[15] H. Frauenfelder *et al.*, Science **254**, 1598 (1991).

[16] H. Frauenfelder and P. G. Wolynes, Phys. Today **47**(2), 58 (1994).

[17] J. D. Bryngelson *et al.*, Proteins Struct. Funct. Genet. **21**, 167 (1995).

[18] Yu. A. Berlin *et al.*, Chem. Phys. **200**, 369 (1995).

[19] R. Richert and H. Bässler, J. Phys. Condens. Matter **2**, 2273 (1990).

[20] J. C. Dyre, Phys. Rev. B **51**, 12 276 (1995).

[21] M. B. Isichenko, Rev. Mod. Phys. **64**, 961 (1992).

[22] A. Plonka, *Time-Dependent Reactivity of Species in Condensed Media*, Lecture Notes in Chemistry (Springer, Berlin, 1986).

[23] Yu. A. Berlin, Mol. Cryst. Liq. Cryst. **228**, 93 (1993).

[24] A. Plonka, Annu. Rep. Prog. Chem. Sec. C **91**, 107 (1994).

[25] H. Scher and M. Lax, Phys. Rev. B **7**, 4491 (1973).

[26] T. Odagaki and M. Lax, Phys. Rev. B **24**, 5284 (1981).

[27] S. Alexander *et al.*, Rev. Mod. Phys. **53**, 175 (1981).

[28] H. Böttger and V. V. Bryksin, *Hopping Conduction in Solids* (Akademie-Verlag, Berlin, 1985).

[29] J. W. Haus and K. W. Kehr, Phys. Rep. **150**, 263 (1987).

[30] G. A. Niklasson, J. Appl. Phys. **62**, R1 (1987).

[31] J. C. Dyre, J. Appl. Phys. **64**, 2456 (1988).

[32] J.-P. Bouchaud and A. Georges, Phys. Rep. **195**, 127 (1990).

[33] B. D. Hughes, *Random Walks and Random Environments* (Clarendon, Oxford, 1995).

[34] J. C. Dyre, Phys. Rev. B **49**, 11 709 (1994); **50**, 9692(E) (1994).

[35] Equation (2) predicts that $\tilde{\sigma}(\tilde{s})$ is an analytic function. This may seem surprising since at any finite temperature it is well known that $\tilde{\sigma}(\tilde{s})$ has nonanalyticities reflecting the long-time tails of the velocity autocorrelation function, nonanalyticities which are also present in the EMA at

finite temperatures. However, the EMA universality equation (2) arises in the zero-temperature limit and is thus an example of the fact that a limit of non-analytical functions may very well be analytic.

[36] V. V. Bryksin, Fiz. Tverd. Tela **22**, 2441 (1980) [Sov. Phys. Solid State **22**, 1421 (1980)].

[37] A. Hunt, J. Non-Cryst. Solids **183**, 109 (1995).

[38] I. P. Zvyagin, Phys. Status Solidi B **95**, 227 (1979).

[39] B. I. Shklovskii and A. L. Efros, *Electronic Properties of Doped Semiconductors* (Springer, Berlin, 1984).

[40] J. C. Dyre, Phys. Rev. B **48**, 12 511 (1993).

[41] V. Ambegaokar *et al.*, Phys. Rev. B **4**, 2612 (1971).

[42] B. I. Shklovskii and A. L. Efros, Zh. Eksp. Teor. Fiz. **60**, 867 (1971) [Sov. Phys. JETP **33**, 468 (1971)].

[43] H. Namikawa, J. Non-Cryst. Solids **18**, 173 (1975).

[44] M. Tomozawa, in *Treatise on Materials Science and Technology*, edited by M. Tomozawa (Academic Press, New York, 1977), Vol. 12, p. 283.

[45] R. Brown and B. Esser, Philos. Mag. B **72**, 125 (1995).

[46] V. V. Bryksin, Fiz. Tverd. Tela **22**, 2048 (1980) [Sov. Phys. Solid State **22**, 1194 (1980)].

[47] S. Summerfield, Solid State Commun. **39**, 401 (1981).

[48] I. Webman, Phys. Rev. Lett. **47**, 1496 (1981).

[49] B. Movaghar and W. Schirmacher, J. Phys. C **14**, 859 (1981).

[50] M. Sahimi *et al.*, J. Chem. Phys. **78**, 6849 (1983).

[51] Obtained by putting the dimension equal to one and ignoring the unimportant factor $s\tilde{G}$ in the denominator on the left-hand side of Eq. (46) in Ref. 34.

[52] J. C. Dyre and J. M. Jacobsen, Chem. Phys. **112** (to be published).

[53] R. Fogelholm, J. Phys. C **13**, L571 (1980).

[54] A. Miller and E. A. Abrahams, Phys. Rev. **120**, 745 (1960).

[55] M. Pollak, in *Proceedings of the Fifth International Conference on Amorphous and Liquid Semiconductors*, edited by J. Stuke and W. Brenig Garmisch-Partenkirchen, 1973, (Taylor & Francis, London, 1974), Vol. 1, p. 127.

[56] S. Summerfield and P. N. Butcher, J. Phys. C **15**, 7003 (1982).

[57] I. Avramov *et al.*, Phys. Rev. E **47**, 2303 (1993).

[58] D. Stauffer and A. Aharony, *Introduction to Percolation Theory*, 2nd ed. (Taylor & Francis, London, 1992).

[59] T. Nakayama *et al.*, Rev. Mod. Phys. **66**, 381 (1994).

[60] In view of the "nodes-links-blobs" model, one may speculate that the PPA works relatively poorly in two dimensions because the "blobs" here are much more important than in higher dimensions. In this line of reasoning, there are too many branches of a "blob" in two dimensions that one can argue, as above, that one branch of the blob dominates conduction.

Master-Equation Approach to the Glass Transition

Jeppe C. Dyre

Institute of Mathematics and Physics IMFUFA, University of Roskilde, DK-4000 Roskilde, Denmark
(Received 13 November 1986)

From a simple master-equation description of viscous liquids it is shown that there exist two different kinds of glass transitions. Slow glass transitions lead to a Gaussian, while fast glass transitions lead to an exponential, distribution of frozen-in energies in the glass. It is argued that amorphous semiconductors prepared by a fast glass transition have exponential band tails of localized states.

By sufficiently rapid cooling, glasses may be formed from any liquid, whether bonded by covalent, ionic, metallic, or molecular forces. The glass transition is thus a universal phenomenon.[1-6] It continues to attract attention both from a purely scientific and from a practical point of view. As a fundamental physical problem, the glass transition is interesting because it somehow involves a breakdown of ergodicity.[7] Technologically, an understanding of the glass transition is important because glass properties depend on exactly how the liquid structure is frozen at the glass transition.

Since glasses are formed from viscous liquids, a better understanding of glasses and the glass transition must derive from a better understanding of viscous liquids. The properties of simple liquids can be calculated from first principles today,[8,9] but this is not the case for viscous liquids. Though recently there have been interesting attempts to extrapolate the theory of simple liquids into the viscous and glassy regime,[10,11] we here take the different point of view in which viscous liquids are regarded as *qualitatively* different from nonviscous liquids. The idea is the following. A high viscosity implies a small diffusion constant. This means that most molecular motion goes into vibrations so that a viscous liquid spends most time in potential-energy minima.[12] Occasionally, effective displacements of the molecules do take place, however. Since one molecule cannot move without having its neighbors move too, these "flow events" must be highly cooperative. This is an old idea; the small parts of the viscous liquid in which the flow events take place have been referred to as "cooperatively rearranging regions,"[13] "quasi-independent units,"[14] "thermokinetic structures,"[15] or just "regions."[16] This picture of viscous flow is simple and attractive. There is evidence in favor of it from extensive computer simulations.[5] Also, from a comparison of dielectric relaxation and Kerr-effect measurements it can be shown that dipolar reorientation in viscous liquids occurs cooperatively via large-angle jumps and does not take place by rotational diffusion.[17,18]

The cooperatively rearranging regions are believed to be fairly small but large enough to be considered as mutually noninteracting. The viscous liquid may therefore be regarded as an ensemble of regions, each of which

spends most time in a potential-energy minimum. Henceforth, potential energy is referred to as energy and energy minima as states. Now, to describe the dynamics of the regions, it is natural to use transition-state theory.[14,19] Goldstein has suggested that the transition state corresponds to the high-temperature, more-fluid, liquid.[14] If we denote the energy of this "fluid" state by E_0, the relaxation time, $\tau(E)$, for transitions from a state with energy E is given by

$$\tau(E) = \tau_0 e^{(E_0 - E)/T} \quad (E < E_0), \qquad (1)$$

where τ_0 is a microscopic time and Boltzmann's constant is put equal to unity. In a recent very interesting paper Brawer has shown that Eq. (1) in the region picture is able to explain all observed features of relaxation in viscous liquids and glasses.[16] These features include the nonlinearity, the broad distributions of relaxation times, and the fact that glassy relaxation proceeds with a smaller activation energy than relaxation in viscous liquids.

The "fluid" state must have a structure much different from the lower-lying states. It is reasonable to assume that, once excited into this state, a region has forgotten which state it came from and may end up in any other state. This is consistent with the observed large-angle dipolar reorientations.[18] Under this assumption, a simple master equation describes the time evolution of the energy probability density, $P(E,t)$:

$$\frac{\partial P(E,t)}{\partial t} = -\frac{P(E,t)}{\tau(E)} + n(E) \int_0^{E_0} \frac{P(E',t)}{\tau(E')} dE', \quad (2)$$

where τ is given by Eq. (1), $n(E)$ is the normalized density of states, and the lowest possible region energy is zero. Equation (2) is equivalent to Brawer's kinetic equation.[16]

Since each region consists of many molecules, thermodynamic concepts may be applied.[3] In thermal equilibrium, $P(E,t)$ is approximately a Gaussian, centered around the mean energy $\bar{E}(T)$. If the temperature is lowered, the Gaussian is displaced towards lower energies. For a finite cooling rate, however, the system will fall out of equilibrium sooner or later for continued cooling. This is, of course, the glass transition; it takes place around the temperature where the time to relax to equi-

librium is comparable to the cooling time. Suppose the system is cooled at a constant rate to zero temperature in time t_0, from a state of thermal equilibrium at high temperature where the liquid relaxation time is small compared to t_0. At any temperature during the cooling the equation $\tau(E) = t_0$ defines a characteristic energy, E_d, given by

$$E_d = E_0 - T \ln(t_0/\tau_0). \tag{3}$$

Regions with energy less than E_d are frozen. E_d, the so-called demarcation energy, was originally introduced in the theory for excited charge-carrier thermalization in amorphous semiconductors.[20,21] As the temperature is lowered, E_d increases while at the same time the equilibrium Gaussian is displaced towards lower energies. When the Gaussian meets E_d the glass transition takes place.

We have studied the glass transition for systems with

$$P_0(E) \cong [2\pi\langle(\Delta E)^2\rangle]^{-1/2} \exp\left[-\frac{(E - E_g)^2}{2\langle(\Delta E)^2\rangle} \right] \quad \text{(slow cooling)}, \tag{4}$$

where $E_g = cT_g$, $\langle(\Delta E)^2\rangle = cT_g^2$, and T_g is determined from $E_d(T_g) = cT_g$, i.e.,

$$T_g = E_0/[c + \ln(t_0/\tau_0)]. \tag{5}$$

In the case of fast cooling rates, $\ln(t_0/\tau_0) \ll c$, something different happens. Then E_d moves only very slowly compared to the Gaussian, so that E_d is almost constant during the glass transition. Approaching the glass transition, the regions jump in energy according to Eq. (2) until they, with probability $\propto n(E)$, happen to hit an energy E below E_d. There will be only a few states left above $E_g = cT_g$ in the glassy state, where the glass transition temperature is again given by Eq. (5). Since $n(E)$ is approximately exponential around E_g with a slope of $1/T_g$, we find

$$P_0(E) \cong \begin{cases} T_g^{-1}\exp[(E - E_g)/T_g], & E < E_g, \\ 0, & E > E_g \quad \text{(fast cooling)}. \end{cases} \tag{6}$$

An illustration of this result is provided by the inset of the $c = 81$ case in Fig. 1. There will, of course, always be some states left above E_g; note also that $E_g \to E_0$ as $c \to \infty$.

We conclude that, insofar as Eq. (2) does describe viscous liquids, there exist two different kinds of glass transitions: slow and fast glass transitions. Since glasses are thermally arrested liquids, it is generally believed that the glass structure is nearly the same as the structure of the equilibrium liquid at temperatures just above T_g. According to the present theory, however, this is true only if the glass is prepared by a slow glass transition. Curiously enough, a slow glass transition freezes the equilibrium structure because E_d moves *fast* across the equilibrium Gaussian.

constant specific heat c. The solution of Eq. (2) is plotted in Fig. 1 for $c = 3, 9, 27, 81$ at a cooling rate given by $\ln(t_0/\tau_0) = 9$. The full curve is $P(E, t)$, the dotted curve is the equilibrium $P(E)$, and the vertical line marks E_d. For each value of c four snapshots are given, starting at almost thermal equilibrium and ending showing the frozen-in energy distribution which will be denoted by $P_0(E)$. Figure 1 gives an idea of the physics of the glass transition according to Eq. (2). The figure shows that $P_0(E)$ is essentially a Gaussian for small c's while it is asymmetric for large c values.

It is not hard to understand what happens at the glass transition in two limiting cases. Consider first small cooling rates: $\ln(t_0/\tau_0) \gg c$. In this case E_d moves fast towards higher energies while the equilibrium Gaussian almost does not move at all. When E_d sweeps past the Gaussian it simply freezes it, so that $P_0(E)$ is just the equilibrium Gaussian at the glass transition temperature, T_g:

The relevant parameter characterizing the glass transition is the ratio $K = \ln(t_0/\tau_0)/c_g$. Here c_g is the region specific heat at T_g, allowing for the more general case of a temperature-dependent specific heat. The region energies are distributed according to a Gaussian or an exponential, depending on whether $K \gg 1$ or $K \ll 1$. This has important consequences for the properties of glasses. By expanding to first order, one finds that any physical property which is a function of E will be Gaussian or exponentially distributed depending on the value of K. This may explain the ubiquitous appearance of Gaussian and exponential energy-barrier distributions for linearly and nonlinearly relaxing degrees of freedom in glassy solids.[22-25] For instance, amorphous semiconductors prepared by a fast glass transition are likely to have exponential band tails: It is reasonable to assume that the region energy is a function of density, where low densities correspond to large energies.[16] The transfer integral, t, for electron jumps depends exponentially on the distance between neighboring atoms, but for sufficiently small distance fluctuations t may be expanded to first order. Expanding also the region energy E to first order in $\bar{r}$, the average atom-atom distance within a region, one finds from Eq. (6) for the distribution of average transfer integrals within a region $p(\bar{r}) \propto \exp(-\bar{t}/T_0)$, where $T_0 = T_g(d\bar{r}/dE)|d\bar{t}/d\bar{r}|$. This implies an exponentially decreasing distribution of band widths for the bands of electron states within each region. With allowance for electron jumps between the regions, the midband states will delocalize but the tail states will probably remain localized within each region. It is not hard to show then that the bulk solid will have exponential band tails of localized states.
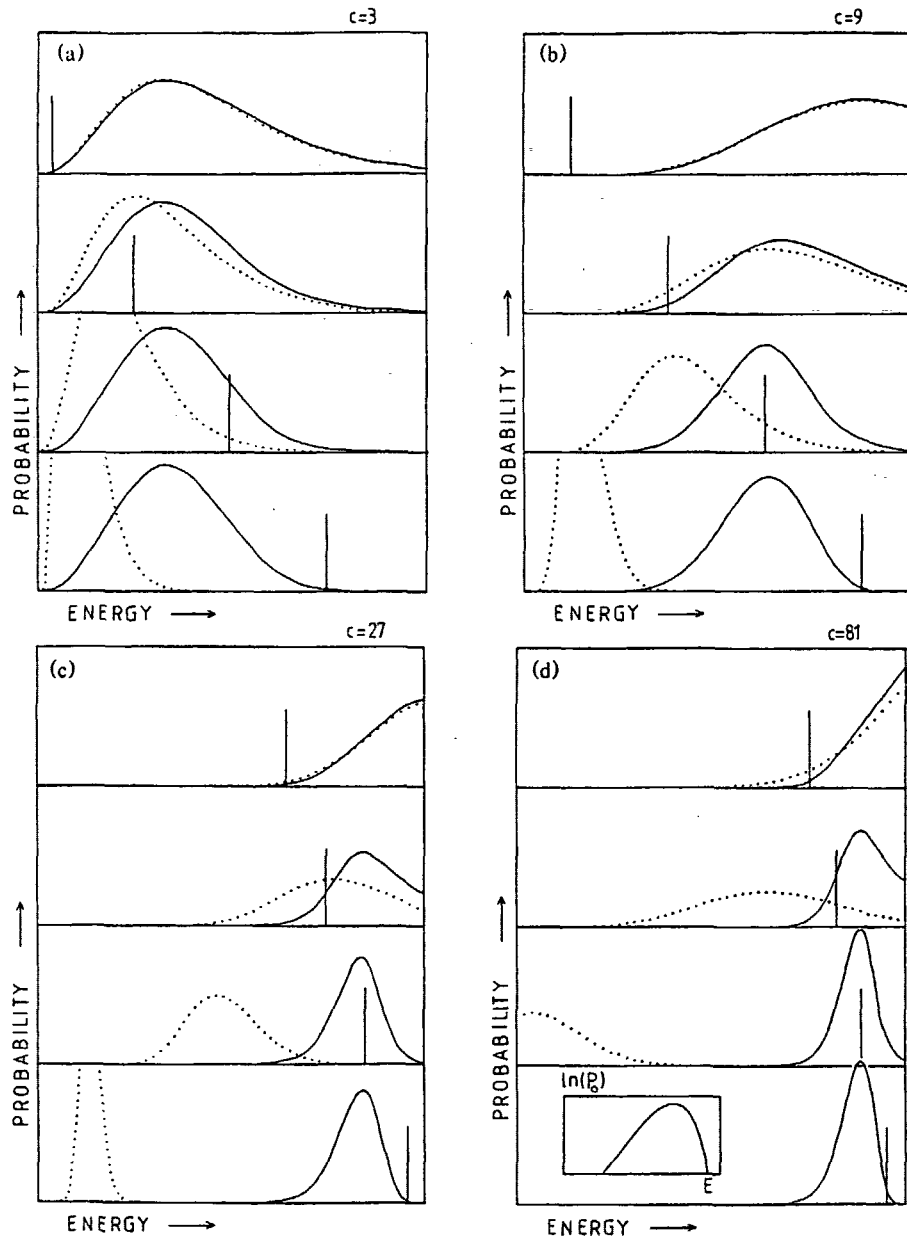
FIG. 1. Solution of Eq. (2) showing the glass transition for various values of the specific heat of the cooperatively rearranging regions in the viscous liquid. The cooling time, t_0, is given by $\ln(t_0/\tau_0) = 9$. The full curve is $P(E,t)$, the dotted curve is the thermal equilibrium energy probability density which is approximately Gaussian, and the line shows the demarcation energy E_d. All states below E_d are frozen. The glass transition takes place when, upon cooling, E_d meets the equilibrium Gaussian. For each value of c, four snapshots of the cooling are shown, the lowest subfigure showing the frozen-in energy distribution, $P_0(E)$. Figure 1 is meant to illustrate Eqs. (4) and (6) according to which $P_0(E)$ is a Gaussian for slow cooling $[c \ll \ln(t_0/\tau_0)]$ and an exponential for fast cooling $[c \gg \ln(t_0/\tau_0)]$. If T_s denotes the starting temperature for the cooling process, the parameters for the figure are, for $c = 3$, $T_s = 0.111E_0$, $0 < E < E_0$; for $c = 9$, $T_s = 0.097E_0$, $0 < E < E_0$; for $c = 27$, $T_s = 0.045E_0$, $0 < E < E_0$; for $c = 81$, $T_s = 0.020E_0$, $E_0/2 < E < E_0$.

The present approach to the glass transition differs in important respects from that of Adam and Gibbs.[13] In their model, the size of the regions is temperature dependent and this is ultimately the cause of the slow relaxation near the glass transition. Also, it is assumed that each region only contains a few states, while here a region has many available states. Despite these differences, the present theory is not necessarily inconsistent with the beautiful idea of an underlying second-order phase transition to a state of zero configurational entropy at a finite temperature.[26] As shown by Goldstein, even a finite region may have a rather sharp transition to a state of almost zero entropy.[14] There will be a transition at $T = T_0$ if $n(E) \propto \exp(E/T_0)$ as $E \to 0$.[14,27] The state of zero configurational entropy of the bulk equilibrium viscous liquid simply corresponds to having each region in its "ground state."

Throughout this Letter, by a glass transition is meant cooling from a temperature so high that the liquid relaxation time, τ_s, is small compared to the cooling time. But another scenario is also possible, namely the cooling in a short time compared to τ_s, e.g., by sudden cooling of a well-annealed very viscous liquid. This is a true quench; obviously it leads to a Gaussian $P_0(E)$. The glassy state may thus be reached in three different ways: by slow glass transitions, by fast glass transitions, and by quenches. Slow glass transitions and quenches lead to a Gaussian $P_0(E)$, while fast glass transitions lead to an exponentially increasing, abruptly decaying $P_0(E)$.

[1]W. Kauzmann, Chem. Rev. 43, 219 (1948).
[2]R. O. Davies and G. O. Jones, Adv. Phys. 2, 370 (1953).
[3]E. Donth, *Glasübergang* (Akademie-Verlag, Berlin, 1981).
[4]R. Parthasarathy, K. J. Rao, and C. N. R. Rao, Chem. Soc. Rev. 12, 361 (1983).
[5]S. Brawer, *Relaxation in Viscous Liquids and Glasses* (American Ceramic Society, Columbus, Ohio, 1985).
[6]J. Jäckle, Rep. Prog. Phys., to be published.
[7]R. G. Palmer, Adv. Phys. 31, 669 (1982).
[8]J. P. Hansen and I. R. McDonald, *Theory of Simple Liquids* (Academic, London, 1976).
[9]J. P. Boon and S. Yip, *Molecular Hydrodynamics* (McGraw-Hill, New York, 1980).
[10]E. Leutheusser, Phys. Rev. A 29, 2765 (1984).
[11]U. Bengtzelius, W. Götze, and A. Sjölander, J. Phys. C 17, 5915 (1984).
[12]M. Goldstein, J. Chem. Phys. 51, 3728 (1969).
[13]G. Adam and J. H. Gibbs, J. Chem. Phys. 43, 139 (1965).
[14]M. Goldstein, Faraday Symp. Chem. Soc. 6, 7 (1972).
[15]E. Donth, J. Non-Cryst. Solids 53, 325 (1982).
[16]S. A. Brawer, J. Chem. Phys. 81, 954 (1984).
[17]G. Williams, in *Dielectric and Related Molecular Processes*, edited by M. Davies (The Chemical Society, London, 1975), Vol. 2, p. 151.
[18]M. S. Beevers, J. Crossley, D. C. Garrington, and G. Williams, Faraday Symp. Chem. Soc. 11, 38 (1977).
[19]W. Kauzmann, Rev. Mod. Phys. 14, 12 (1942).
[20]V. I. Arkhipov, M. S. Iovu, A. I. Rudenko, and S. D. Shutov, Phys. Status Solidi (a) 54, 67 (1979).
[21]J. Orenstein, M. A. Kastner, and V. Vaninov, Philos. Mag. B 46, 23 (1982).
[22]A. S. Nowick and B. S. Berry, IBM J. Res. Dev. 5, 297 (1961).
[23]W. Chambron and A. Chamberod, Solid State Commun. 33, 157 (1980).
[24]J. R. Macdonald, J. Appl. Phys. 58, 1955, 1971 (1985).
[25]J. C. Dyre, J. Phys. C 19, 5655 (1986).
[26]J. H. Gibbs and E. A. DiMarzio, J. Chem. Phys. 28, 373 (1958).
[27]B. Derrida, Phys. Rev. Lett. 45, 79 (1980).

Energy master equation: A low-temperature approximation to Bässler's random-walk model

Jeppe C. Dyre

Institute of Mathematics and Physics (IMFUFA), Roskilde University, P.O. Box 260, DK-4000 Roskilde, Denmark

(Received 20 October 1994)

The first part of this paper deals with the justification of Bässler's phenomenological random-walk model for viscous liquids [Phys. Rev. Lett. **58**, 767 (1987)], which considers the random walk of a "particle" representing the liquid state on a d-dimensional infinite cubic lattice with site energies chosen randomly according to a Gaussian. The random-walk model is here derived from Newton's laws by making a number of simplifying assumptions. In the second part of the paper an approximate low-temperature description of energy fluctuations in the random-walk model—the energy master equation (EME)—is arrived at. The EME is one dimensional and involves only energy; it is derived by arguing that percolation dominates the relaxational properties of the random-walk model at low temperatures. The approximate EME description of the random-walk model is expected to be valid at low temperatures at long times in high dimensions. However, computer simulations show that the EME works well already in two dimensions and at only moderately low temperatures. The EME has no randomness and no fitting parameters. The EME is completely specified from the density of states and the attempt frequency of the random-walk model. The EME allows a calculation of the energy probability distribution at realistic laboratory time scales for an arbitrarily varying temperature as function of time. The EME is probably the only realistic equation available today with this property that is also explicitly consistent with statistical mechanics. The final part of the paper gives a comprehensive discussion, comparing the EME to related work and listing the EME's qualitatively correct predictions, its new predictions, and some "wrong" predictions, most of which go against the common picture of viscous liquids and the glass transition without violating experiments.

I. INTRODUCTION

The glass transition takes place when a liquid upon cooling becomes more and more viscous and finally solidifies to form a glassy solid.[1-14] Most, or perhaps all, liquids are able to form glasses when cooled sufficiently fast to avoid crystallization. Examples of glasses include the classical oxide glasses,[15] ionic glasses,[16] polymers,[6,17,18] metallic glasses,[19] and glasses made by cooling organic liquids to low temperatures.[20,21] Even simple liquids form glasses in computer experiments, where extremely high cooling rates are possible.[12,22,23] Spin glasses are examples of nonliquid systems that exhibit glassy features.[24,25]

The glass transition is still far from well understood, but the kinetic nature of the transition is not in doubt. The glass transition is not a phase transition, though it is thermodynamically similar to a second-order phase transition. This is evidenced by several facts universally observed: The transition is not sharp, the transition temperature depends on the cooling rate, and the transition is irreversible and exhibits various hysteresis phenomena.

Despite large chemical differences, viscous liquids close to the glass transition have common features, notably a broad distribution of relaxation times and a stronger than Arrhenius temperature dependence of the viscosity. Around the glass transition there are further common characteristics like the overshoot of the specific heat upon reheating,[8,14] the crossover effect,[8] or the prepeak upon the melting of a well-annealed glass.[11] The universal properties of viscous liquids and the glass transition

motivates a search for a phenomenological model valid for any viscous liquid.

While phenomenological models of viscous liquids and the glass transition have been studied for many years, the 1980's brought an interesting first-principles theory, the mode-coupling theory.[26,27] Extensive work has gone into studying the mode-coupling theory and comparing it to experiment. At present there seems to be a growing consensus[28] that mode-coupling theory gives an accurate description of the onset of viscous behavior, the temperature region where the relaxation times are shorter than about 1 ns. However, the theory does not seem to be able to explain the highly viscous regime and the laboratory glass transition. This is because the activated "hopping" type processes that dominate this regime are not accounted for in the simplest version of mode-coupling theory,[26-30] but have to be postulated as an extra assumption. Thus, the focus is now once again on attempts to formulate a phenomenological model that captures the essentials of viscous liquids and the glass transition. Nevertheless, mode-coupling theory has served to emphasize the different physical bases of the low- and high-temperature regimes.

Since the glass transition is a kinetic "freezing" of the viscous liquid, a phenomenological model should first of all incorporate the basic physics of viscous liquids in thermal equilibrium. An important characteristic here is the *average relaxation time* of the viscous liquid τ, which is a direct measure of the time needed for molecular rearrangements. The average relaxation time may be determined, e.g., as the inverse dielectric, mechanical or

specific-heat loss-peak frequency. Alternatively, it may be calculated from the viscosity η and the infinite frequency shear modulus G_∞ by means of the expression

$$\tau = \frac{\eta}{G_\infty} \ . \tag{1}$$

These definitions do not give exactly identical τ's,[13] but the difference is insignificant for the present discussion. Typical values of τ for glass-forming liquids lie in the millisecond, second or even hour range. These times are to be compared to a typical microscopic time, the average vibration time, which is less than 1 psec.

The basic thing one would like to understand about the average relaxation time is its non-Arrhenius temperature dependence. For almost all viscous liquids τ has an apparent activation energy that increases as the temperature decreases. Naive models assuming some distribution of energy barriers usually lead to the opposite behavior. Therefore, explaining $\tau(T)$ is a real challenge, but also a likely key to understanding viscous liquids.

The phenomenological models may be classified into two types (an alternative to the below classification has been given by Scherer in an excellent review of relaxation in viscous liquids[29]). One type of models, "type-I," are models that have a non-Arrhenius average relaxation time, but otherwise do not attempt to model the liquid. These models are so simple that they can be analyzed in detail.[31] Examples of type-I models are Derrida's random energy model,[32] the kinetic Ising model,[33] or the tiling model of Weber, Fredrickson, and Stillinger.[34] The other type of models, "type-II," do attempt to realistically model the physics of real viscous liquids. In all type-II models the elementary flow process occurs within a "cooperatively rearranging region." The type-II models can be further classified according to which thermodynamical quantity controls τ, *entropy, volume*, or *energy*.

A well-known entropy-controlled model is the theory of Gibbs and co-workers.[35,36] According to this model the average relaxation time is expressed in terms of the excess configurational entropy S_c as $\tau \propto \exp[C/(TS_c)]$. The model correlates the non-Arrhenius behavior with the Kauzmann paradox,[2,11] the fact that the configurational entropy extrapolates to zero at a finite temperature, T_K: Expanding S_c to first order close to T_K, the average relaxation time follows the Vogel-Fulcher-Tammann (VFT) law[11,29] (where A is a constant and the characteristic temperature T_0 is predicted to be equal to T_K):

$$\tau = \tau_0 e^{A/(T-T_0)} \ . \tag{2}$$

The VFT law gives a good fit to $\tau(T)$ for many viscous liquids and in most experiments one also finds that T_0 is indeed close to T_K.[11]

Gibbs' model predicts that underlying the laboratory glass transition there is a genuine second-order phase transition at $T = T_K$ to a state of zero configurational entropy. However, there are a number of problems with this approach. The original Gibbs-DiMarzio model[35] was based on a mean-field theory for polymers that later

was shown to be incorrect.[37] Also, the VFT law seldom applies in the whole temperature range of interest; usually deviations occur close to the glass transition where the average relaxation time is less temperature dependent than predicted.[8,20,29] [If the physics of the high and low viscosity regimes are different, as predicted by mode-coupling theory, there is no motivation to choose a phenomenological representation of $\tau(T)$ which can cross the boundary between the two regimes.] Finally, it should be noted that the Kauzmann paradox does not have to be a paradox. As shown by Angell and Rao in 1972,[38] even a system with only two energy levels has an entropy which, if only known at high temperatures, extrapolates to zero at a positive temperature. Though this model does not fit experiment, the excess entropy data may be fitted with a model with only a finite number of energy levels and thus a positive entropy at any positive temperature.[39]

The standard example of a volume-controlled model is the "free volume model."[40] In this model, the average relaxation time is determined by the volume freely available for cooperative rearrangements of the molecules, V_f, according to the expression $\tau \propto \exp(C/V_f)$. In the simplest version of the model the free volume decreases linearly with decreasing temperature, leading if $V_f = 0$ at $T = T_0$ to a non-Arrhenius $\tau(T)$ of the VFT type [Eq. (2)].

In energy-controlled models one formulates a master equation[41] governing the dynamics of the cooperatively rearranging regions. The relevance of potential energy was previously emphasized in 1969 in a classic paper by Goldstein.[42] More recently, Brawer proposed a model where transitions between different states occur via excitations to a common high-lying energy level.[8,43] This picture goes back to Goldstein.[39] Brawer's model was later simplified.[44]

Bässler's random-walk model[45,46] is an energy-controlled model, which is similar to those used in the description of ac conduction in disordered solids[47,48] and of energetic relaxation and diffusion of electronic excitations in random organic solids.[49] The model considers the random walk of a "particle" on a cubic lattice in d dimensions, where each site has an energy chosen randomly according to a Gaussian. The particle represents the state of a cooperatively rearranging region. For the random-walk model $\tau(T)$ is predicted[45,46] to follow

$$\tau = \tau_0 \exp\left[\frac{C}{T^2}\right] \ . \tag{3}$$

This simple expression fits experiments well.[45,46,50,51] An even better fit is obtained by using the following generalization of Eq. (3): $\tau = \tau_0 \exp(C/T^n)$.[20,21,52]

In a recent paper by Arkhipov and Bässler[53] the random-walk model was extended to a model that reduces to the original model at high temperatures—the "real liquid" regime—while at low temperatures—the "supercooled melt" regime—the system is described by a simple master equation. The idea[53] is that, at high temperatures direct jumps between metastable states are possible because the energy landscape itself fluctuates; these jumps correspond to an elementary step on the d-

dimensional lattice of the original random-walk model. At low temperatures, on the other hand, the landscape fluctuations are frozen on the relevant time scale and each jump leads to a totally new configuration, the dynamics here being described by a simple master equation.[44]

The purpose of the present paper is to show that the master equation, assumed by Arkhipov and Bässler to describe the different physics going on at low temperatures, in fact gives a good description of the low-temperature behavior of the *original* random-walk model. Thus, in a sense the Arkhipov-Bässler model is contained in Bässler's original and simpler random-walk model. The low-temperature approximate master equation, the "energy master equation" is arrived at by arguing that *percolation* in the random-walk model becomes important at low temperatures. The transition state energy of the energy master equation is identified with the highest energy met on a percolation path. In effect, one arrives at a picture which is similar to that recently proposed by Hunt,[13,54] according to which the low-temperature properties of viscous liquids are dominated by percolation. However, in his works effects of cooperativity are treated separately in relaxation and in thermodynamics.

The paper has the following outline. In Sec. II a justification of the random-walk model is given where the model is traced back to Newton's laws for the molecules of a cooperatively rearranging region. This section supplements the original arguments for the model given by Bässler and co-workers.[45,46] In Sec. III the approximate energy master equation is derived. In Sec. IV computer simulations are presented, comparing the random walk model and the energy master equation. Section V discusses what to expect at the glass transition according to the energy master equation. Section VI gives a comprehensive discussion which includes a qualitative comparison to experiment. Finally, Sec. VII gives the conclusions.

II. THE RANDOM-WALK MODEL AND ITS "DERIVATION" FROM NEWTON'S SECOND LAW

The purpose of this section is to "derive" the random-walk model[45,46] from the equations of motion for the molecules of the viscous liquid. The "derivation," which proceeds in five steps, is not rigorous, but rather an attempt to make explicit the assumptions that need to be made in order to justify the model from basic principles. The viewpoints presented below are similar to those of Bässler, but there are also some differences as will be discussed at the end of this section.

Before presenting the "derivation" of the random-walk model, we recall the exact definition of the model. The model considers the random walk of a particle on an infinite d-dimensional cubic lattice. The particle represents the state of the region, which is thus completely specified by d integer coordinates. Each state has an energy E, which is chosen randomly according to a Gaussian with variance σ:

$$n(E) = \frac{1}{\sqrt{2\pi\sigma^2}} \exp\left[-\frac{E^2}{2\sigma^2}\right] . \tag{4}$$

The energies of adjacent states are uncorrelated. The dynamics of the system is described by a master equation,[41] specifying the time development of the probability that the particle is in state i, P_i. If $\Gamma(i \rightarrow j)$ is the transition rate for jumps from state i to state j, the general master equation[41] is

$$\frac{dP_i}{dt} = -\sum_j \Gamma(i \rightarrow j)P_i + \sum_j \Gamma(j \rightarrow i)P_j . \tag{5}$$

The first term describes particles jumping away from state i and the second term describes particles jumping into state i. The jump rates must satisfy the principle of detailed balance,[41] which ensures consistency with statistical mechanics [$\beta = 1/(k_B T)$],

$$\frac{\Gamma(i \rightarrow j)}{\Gamma(j \rightarrow i)} = \exp[\beta(E_i - E_j)] . \tag{6}$$

In random-walk models the transition rates are usually chosen to be zero except for nearest-neighbor jumps (i.e., where a single coordinate changes plus or minus one). If Γ_0 is the "attempt frequency," the transition rate for a nearest-neighbor jump is in Bässler's random-walk model given by Metropolis dynamics,

$$\Gamma(i \rightarrow j) = \begin{cases} \Gamma_0 , & E_i > E_j \\ \Gamma_0 e^{-\beta(E_j - E_i)}, & E_i < E_j. \end{cases} \tag{7}$$

It is realistic to take Γ_0 to be of order 10^{13} Hz, corresponding to a typical phonon frequency. Note that Eq. (7) satisfies the principle of detailed balance Eq. (6).

What kind of predictions can be made from the random-walk model? The model predicts how the average energy changes in time for any externally controlled time-dependent temperature. This includes monitoring how the energy relaxes to equilibrium from a nonequilibrium state, or how the dynamic specific heat changes through the glass transition. In particular, the average relaxation time for energy relaxations close to equilibrium can be calculated as a function of temperature, and the equilibrium frequency-dependent specific heat may be obtained.

We now proceed to justify the random-walk model from basic principles in five steps, assuming that the molecules of the viscous liquid are described by classical mechanics.

Step 1: The Region Assumption. All type-II models for the dynamics of viscous liquids assume cooperative "flow events" that are localized to small "regions" of the liquid.[6,8,36,39,42–44,55–60] These regions have been called "cooperatively rearranging subsystems"[29] or "cooperatively rearranging regions,"[36] "quasi-independent units,"[39] "thermokinetic structures,"[58] "molecular domains,"[59] or "dynamically correlated domains."[60] This picture of viscous flow, proceeding via strongly cooperative motion of particles confined to small regions of the liquid, has been confirmed by computer simulations.[61,62] The "region assumption," however, is not just the quite reasonable idea that flow events are localized. The assumption is the much stronger one that the liquid

may be regarded as an ensemble of noninteracting regions. There are two potential problems with this assumption. It ignores region-region interactions that may be important because the regions are expected to be relatively small [some 10–20 Å (Ref. 58)]. Also, the picture is static and not easy to relate to an actual flow that will deform the regions. Nevertheless, the region assumption seems to be necessary to arrive at a simple phenomenological model.

Step 2: Replacing Newton's laws with Langevin dynamics. From now on the attention is confined to a single region, the molecules of which move according to Newton's laws. The motion depends on the potential energy as function of the molecular coordinates, $U(Q_1, \ldots, Q_d)$ (for simplicity only rectangular coordinates are considered). The importance of the potential energy "surface" for understanding viscous liquids and the glass transition has been emphasized in a number of papers.[11,30,39,42,63,64] Following the tradition in polymer physics,[65] we now replace Newton's deterministic equations of motion by stochastic Langevin equations (similar nondeterministic equations are used for the description of Brownian particles suspended in liquids[66]). The Langevin equations of motion[41,65] are

$$\dot{Q}_i = -\mu \frac{\partial U}{\partial Q_i} + \xi_i(t) \quad (i = 1, \ldots, d) , \qquad (8)$$

where μ is the "mobility" [velocity/force] and $\xi_i(t)$ is a Gaussian white-noise term obeying

$$\langle \xi_i(t)\xi_j(t') \rangle = 2\mu k_B T \delta_{i,j} \delta(t - t') . \qquad (9)$$

The crucial property of the Langevin equations of motion[41,65] is that each state is visited with the correct canonical probability P_0 of statistical mechanics,

$$P_0(Q_1, \ldots, Q_d) \propto e^{-\beta U(Q_1, \ldots, Q_d)} . \qquad (10)$$

Physically, the assumption of Langevin dynamics is reasonable for viscous liquids,[67] because the molecules collectively vibrate in potential energy minima for long times before occasionally "jumping" to another potential energy minimum. And the rate of jumps between two energy minima is, for both Newtonian and Langevin dynamics, dominated by a factor $\propto \exp(-\beta \Delta U)$,[68] where ΔU is the energy barrier to be overcome.

Step 3: From Langevin dynamics to a hopping model. We now proceed to discretize the spatial variables of the Langevin equations. The resulting state space is a d-dimensional cubic lattice. It is reasonable to assume that, since the underlying Langevin dynamics has a continuous trajectory, only nearest-neighbor jumps are allowed on the lattice. For the jump rates those given by Eq. (7) are an obvious choice: Unless infinitely steep potentials are allowed, the Langevin equation implies that it takes some definite (but very small) time to travel the discretization length downhill; in the discrete version this means there should be a maximum jump rate. If the discretization is to be self-consistent, the jump rates must be uniquely determined from the state energies. The simplest jump rates satisfying these conditions are the Metropolis rates [Eq. (7)]. These jump rates ignore the possible existence

of a barrier to be overcome between two nearest-neighbor discrete states. The discretization does not allow continuous vibrational motion. The term "energy" E is henceforth to be thought of as the potential energy U at a minimum or a saddle point, the "configurational part" of the potential energy. Similarly, the term "specific heat" refers to the configurational part of the measured specific heat, the so-called "excess specific heat" (in excess of the phonon contribution to the specific heat).

Step 4: Replacing complexity with randomness. The potential energy is a very complex function with numerous minima.[30,42,63] Therefore, it is reasonable to replace the function E defined on the lattice with a function that is in some sense random. The basic idea of replacing complexity with randomness[69] is that some phenomena occurring in a specific complex system are typical of those that occur in most systems chosen randomly out of an ensemble of possible systems. If this is so, the study of random systems tells us what to expect for particular complex systems. Motion in random potentials has been studied extensively in various contexts.[47,48,70,71] In discretizing such a model one often chooses a discretization length a equal to the correlation length of the random function and assumes that correlations beyond a may be ignored.[71] When this is done for the hopping model arrived at above, the values of the potential are assumed to be uncorrelated from point to point on the d-dimensional cubic lattice. In this approximation the model is completely specified by the energy probability distribution, the "density of states" $n(E)$.

Step 5: The assumption of cooperativity. A region contains many molecules and thus $d \gg 1$. Any system with many degrees of freedom has a density of states for which the entropy as function of energy, $S(E) = \ln[n(E)]$, at relevant energies[72] obeys

$$\frac{\partial S}{\partial E} > 0; \quad \frac{\partial^2 S}{\partial E^2} < 0 . \qquad (11)$$

The Gaussian Eq. (4) obeys Eq. (11), but only for negative energies. However, at any temperature negative energies are most likely for the Gaussian, and therefore this density of states is permissible as representing a system with many degrees of freedom.

The assumption of a Gaussian density of states concludes the "derivation" of Bässler's random-walk model. The model is completely specified by the parameters Γ_0, σ, and d. The first two are scaling parameters, so from a qualitative point of view only the dimension d is of interest.

In thermal equilibrium the probability of visiting any given site is given by the Boltzmann factor $\exp(-\beta E)$. Combining this with the Gaussian probability Eq. (4), one finds for the equilibrium energy probability distribution $P_0(E) \propto \exp[-\beta E - E^2/(2\sigma^2)]$. By "completing the square" and normalizing, one finds

$$P_0(E) = \frac{1}{\sqrt{2\pi\sigma^2}} \exp\left[-\frac{(E - \bar{E})^2}{2\sigma^2}\right], \quad \bar{E} = -\sigma^2\beta . \qquad (12)$$

Clearly $\bar{E}$ is the average energy. Note that $\bar{E}$ is also the most likely energy (in fact, for any system with many de-

grees of freedom the average energy is close to the most likely energy). The equilibrium specific heat c_0 is given by

$$c_0 \equiv \frac{d\bar{E}}{dT} = \frac{\sigma^2}{k_B T^2} . \tag{13}$$

Equation (13) may be derived directly from Einstein's expression, $c_0 = \langle (\Delta E)^2 \rangle / (k_B T^2)$, since the Gaussian distribution Eq. (12) implies $\langle (\Delta E)^2 \rangle = \sigma^2$. The equilibrium specific heat increases towards infinity as the temperature goes to zero. While this cannot be the case down to zero temperature in experiment, there is actually a tendency for most supercooled liquids for the excess specific heat to increase as the temperature decreases.[2,38]

The random-walk model was originally proposed by analogy to transport and relaxation of charge excitations in random organic solids,[49] where the jump rates Eq. (7) are the well-known Miller-Abrahams jump rates for electronic hopping.[73] There are some differences between the above "derivation" of the random-walk model and Bässler's justification of the model. In Bässler's picture, the experimental dependence of the glass transition temperature on the sample history was understood as an effect due to the density of states depending on the preparation conditions.[45] In contrast, the above picture is static; the density of states arises from the discretization of the potential energy and does not depend on the conditions of sample preparation. A further difference is that here cooperativity is emphasized, implying $d \gg 1$, while the original Bässler model considered elementary jump processes on a "molecular or weakly cooperative level,"[49] implying that d is not *much* larger than one.

III. THE ENERGY MASTER EQUATION: AN APPROXIMATION TO THE RANDOM-WALK MODEL

In order to monitor the average energy during a cooling and subsequent glass transition in the random-walk model, there is no other simple method than to solve the master equation numerically by taking time steps of order $1/\Gamma_0 < 1$ ps. Clearly, this procedure cannot be used for simulating realistic laboratory time scales of order minutes or hours. In this section an approximation to the random-walk model is derived, which makes it possible to investigate the model on realistic time scales. The approximate equation, termed the "energy master equation," is an equation for the time evolution of the energy probability distribution $P(E,t)$, which ignores the spatial d-dimensional structure of the random-walk model.

Consider the random-walk model in many dimensions ($d \gg 1$) at low temperatures ($k_B T \ll \sigma$) and long times ($t \gg \tau_0$). Whenever $k_B T \ll \sigma$ the most likely energies are close to $\bar{E} = -\sigma^2 \beta \ll -\sigma$ [Eq. (12)], i.e., deep into the negative tail of the Gaussian. States with these low energies are very rare; nevertheless, at low temperatures the relaxation properties of the random-walk model are dominated by transitions between them. The distance between two low-energy states is large, and a transition between two such states consists of a long and complex path joining neighboring states. It is very hard to calculate the actual transition rate, but it is obvious that the

transition rate depends crucially on the maximum energy encountered on the path. Thus, of all possible paths between two low-energy states, the most likely paths are those that have the lowest maximum energy. The value of this maximum energy is identified by *percolation theory*:[70,74–76] Imagine the sites of the lattice gradually being filled in order of increasing energy. At a certain filling rate, the site percolation threshold p_c, the infinite "percolation cluster" of marked sites appears. In two dimensions $p_c = 0.593$, while in three dimensions $p_c = 0.312$.[70] In high dimensions one finds[76] $p_c \cong 1/(2d-1)$. The highest energy on the percolation cluster, the "percolation energy" E_c, is given by

$$\int_{-\infty}^{E_c} n(E)dE = p_c . \tag{14}$$

The percolation energy E_c gives a good estimate of the largest energy met on an "optimal" path between two low-energy sites. This is because just above p_c a large fraction of the marked sites belongs to the percolation cluster. We thus surmise that the effective transition rate from a low-energy site with energy E_i to another low energy site with energy E_j is given by the barrier $\Delta E = E_c - E_i$: $\Gamma(i \rightarrow j) \propto \exp[-\beta \Delta E]$. This expression satisfies the principle of detailed balance Eq. (6). There are many possible final states, but since each jump rate is given by the above expression, the total rate for jumps away from a site with energy E, $\Gamma(E)$, is given by

$$\Gamma(E) = \Gamma_0^* e^{-\beta(E_c - E)} . \tag{15}$$

To determine Γ_0^* we evaluate $\Gamma(E_c)$ by viewing the percolation cluster as a one-dimensional path, where each site on the average has two neighbors belonging to the cluster. This naive point of view ignores the complicated fractal nature of the cluster, but it does become realistic in high dimensions where it leads[76] to the correct percolation threshold. Since E_c is the largest energy on the percolation cluster, sites with energy E_c have on the average two neighbors with lower energy. Thus, the total rate for jumps away from such a site is on the average $2\Gamma_0$, plus some terms for jumps to the higher-energy neighbors. These terms are unimportant at low temperatures, and thus the prefactor of Eq. (15) is given by

$$\Gamma_0^* = 2\Gamma_0 . \tag{16}$$

To arrive at the simplest possible approximate description, the spatial structure of the lattice is now completely ignored. Consequently, all final states are regarded as equally likely, and one arrives at the picture of Fig. 1 which was proposed by Goldstein[39] in a different context and later discussed in more detail by Brawer.[8,43]

The approximate master equation considers only one variable, the energy. Let $P(E,t)$ denote the energy probability distribution as function of time. Since all final states are regarded as equally likely, the probability of jumping into an energy around E is proportional to the density of states, $n(E)$. The relaxation rate for jumps from states with energy E is $\Gamma(E)$, so the equation for $P(E,t)$ is for some constant $K(t)$
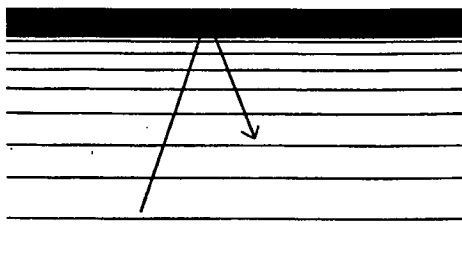
FIG. 1. The Goldstein-Brawer picture of a "flow event" in a viscous liquid (Refs. 8, 39, and 43). The figure illustrates the excitation from one "state," i.e., a potential energy minimum for the molecules in a region of the liquid, to another state—the vertical axis being the energy axis. In Goldstein's model the transition state (black) is identified with the high-temperature, more-fluid, liquid (Ref. 39); Brawer identifies it with a low-density state giving room for the molecules to rearrange (Refs. 8 and 43). In the approximate energy master equation (EME) description of Bässler's random-walk model leading to the same picture of a transition, the energy of the transition state is identified with the energy at the percolation threshold [Eq. (14)]. Conversely, the Goldstein-Brawer picture leads to the EME [Eq. (20)] if it is assumed that, once excited into the transition state, the region has forgotten which state it came from and ends up in a randomly chosen state.

$$\frac{\partial P(E,t)}{\partial t} = -\Gamma(E)P(E,t)+K(t)n(E) \ . \tag{17}$$

The constant is determined by requiring conservation of probability:

$$0 = \frac{d}{dt}\int_{-\infty}^{\infty} P(E',t)dE' = \int_{-\infty}^{\infty}\frac{\partial P(E',t)}{\partial t}dE' \tag{18}$$

implies, since $n(E)$ is normalized, that

$$K(t) = \int_{-\infty}^{\infty}\Gamma(E')P(E',t)dE' \ . \tag{19}$$

In this reasoning all energies were counted, despite the fact that the picture breaks down for $E > E_c$. However, including the energies above E_c gives the simplest description and causes little change because high-energy states are very unlikely, anyway. Using Eq. (19), Eq. (17) becomes an integrodifferential equation,[44] the "energy master equation" (EME),

$$\frac{\partial P(E,t)}{\partial t} = -\Gamma(E)P(E,t)$$
$$+ n(E)\int_{-\infty}^{\infty}\Gamma(E')P(E',t)dE' \ . \tag{20}$$

We remind the reader that in this equation the jump rate $\Gamma(E)$ depends on the temperature, which may be an arbitrary function of time.

The EME was first discussed as a model for the thermalization of photoexcited charge carriers in amorphous semiconductors.[77,78] In this case $n(E)$ is the density of trapping levels in the band gap and E_c is the mobility edge of the conduction band. For viscous liquids a similar, but somewhat more complicated master equation

was proposed by Brawer in 1984.[43] Brawer's equation contains an extra entropy factor enumerating the different paths from a particular state to the transition state. A related approach towards relaxation in viscous liquids was advocated by Robertson, Simha, and Curro.[79] Towards the end of the 1980's Eq. (20) was studied[80,81] as a model for the relaxation properties of Derrida's random energy model,[32] and Eq. (20) was proposed as a model for the dynamics of viscous liquids and studied numerically through the glass transition.[44] Recently, Eq. (20) was used by Arkhipov and Bässler to describe the low-temperature regime of viscous liquids, assuming that the high-temperature regime is described by the random-walk model.[53]

The static solution of the EME, $P_0(E)$, is given by

$$P_0(E) = \text{const}\frac{n(E)}{\Gamma(E)} \ . \tag{21}$$

This is the canonical probability distribution required by statistical mechanics. In the course of time, the canonical ensemble is realized in a very simple way: All states are visited equally often, but the average time spent in a state with energy E, $1/\Gamma(E)$, is proportional to the Boltzmann factor $\exp(-\beta E)$, thus giving the canonical probabilities.

At any fixed temperature an initial nonequilibrium energy probability distribution will approach the equilibrium distribution. This is also the case if the temperature changes in time: At any given time the distribution approaches the equilibrium distribution corresponding to the temperature at that time. Upon continued cooling the system freezes[44] at the temperature where the time it takes to reach equilibrium becomes larger than the cooling time.

The numerical solution of the EME (detailed in the Appendix) is based on a calculation using the Laplace transformation,[82,83] resulting in an analytical expression for the relaxation of $P(E,t)$ towards the equilibrium solution $P_0(E)$ at a fixed temperature. An arbitrary thermal history is solved by taking small time steps changing the temperature at each step.

IV. COMPUTER SIMULATIONS

This section reports computer simulations of the random-walk model and compares them to the EME predictions. Results for a continuous cooling and reheating are given, as well as a study of the time evolution of the energy probability distribution for relaxation towards equilibrium at a fixed temperature. Unfortunately, it is impossible to check the validity of the EME description where it is expected to apply best: at low temperatures and long times in many dimensions. This would require enormous computer capacity. All simulations were performed in two dimensions utilizing periodic boundary conditions, and in experiments monitoring relaxation towards equilibrium the lowest temperature studied was $0.25\sigma/k_B$.

A numerical solution of the random-walk model may be obtained by following the motion of a single "particle" in time, the analog of a Monte Carlo simulation. However, this introduces considerable noise and it is much more efficient to solve the master equation Eq. (5) directly. At

any given time the state of the system is represented by the probabilities, P_i. In two dimensions any site has four neighbors so the maximum transition rate is $4\Gamma_0$ [Eq. (7)]. In the simulations a time step of length $1/(4\Gamma_0)$ was chosen. For each pair of neighboring sites, A and B, the new probabilities were found as follows: If $\Delta E = E_A - E_B > 0$, the probabilities are changed according to

$$\Delta P_A = -\tfrac{1}{4}P_A + \tfrac{1}{4}e^{-\beta \Delta E}P_B \ ,$$
$$\Delta P_B = -\Delta P_A \ . \tag{22}$$

For one time step each site is upgraded four times according to Eq. (22) (each time, of course, the nonupgraded probabilities from the previous time step are used as P_A and P_B). This time-discretization of the master equation is quite crude, but at long times it is sufficiently accurate. The important thing is to ensure exact probability conservation in each time step.

Figure 2 shows the glass transition monitored via the "dynamic" specific heat during a cooling to zero temperature at a constant rate and a subsequent reheating at the same rate. The dynamic specific heat c is defined by

$$c = \frac{dE/dt}{dT/dt} \ . \tag{23}$$

The full curves give the results of the simulations of the random-walk model, the dashed curves the EME predictions, and the dots indicate the thermal equilibrium specific heat [Eq. (13)]. Figure 2(a) and 2(b) show $c(t)$ for cooling and reheating from $T = 2\sigma/k_B$ to $T = 0$ in the time $100/\Gamma_0$, while 2(c) and 2(d) show the same but in the time $10\,000/\Gamma_0$. As expected, the EME predictions work better in the latter case.

Figure 3 shows the frozen-in energy for the cooling, i.e., the energy at zero temperature, as function of the cooling rate. The full curve gives the results of the simulations and the dashed curve the EME prediction.

Figures 4 and 5 show thermalization of the energy probability distribution, starting in equilibrium at one temperature and suddenly changing the temperature. In Fig. 4 the temperature was suddenly lowered. Four snapshots are shown giving the simulation results (full curves) and the EME predictions (dashed curves). The dots indicate the equilibrium energy probability distribution which is approached as $t \to \infty$. There is a sliding ap-
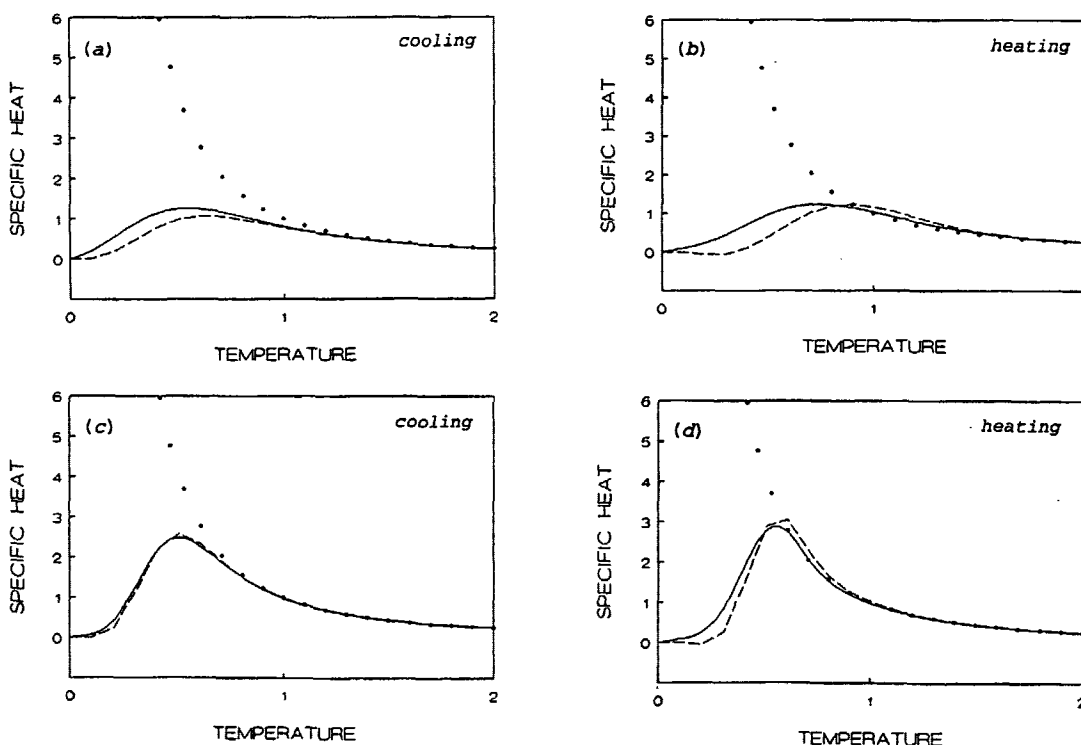

FIG. 2. The glass transition in the random-walk model in two dimensions monitored via the dynamic specific heat (full curves) during a cooling at constant rate to zero temperature and subsequent reheating at the same rate. The dashed curves give the EME predictions, and the dots mark the thermal equilibrium specific heat [Eq. (13)]. (a) shows the specific heat $[k_B]$ as function of temperature $T[\sigma/k_B]$ for cooling in the time $t = 100$ $[1/\Gamma_0]$ starting from equilibrium at $T = 2.0$; (b) gives the reheating data. (c) and (d) are similar but with cooling and reheating time $t = 10\,000$. The random-walk model data were obtained by averaging ten simulations of a 50×50 lattice. The EME was solved by the method detailed in the Appendix. Clearly, the EME works better for the slower cooling rate.
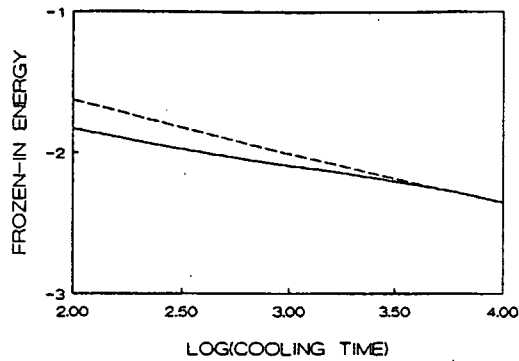
FIG. 3. The average frozen-in energy $[\sigma]$ at zero tempera-
ture as function of the logarithm (base 10) of the cooling time
$[1/\Gamma_0]$ for coolings starting from equilibrium at $T=2.0$
$[\sigma/k_B]$. The full curve gives the results based on simulations
for each half decade of the random-walk model (each simulation
consists of ten averages of a 50×50 lattice), and the dashed
curve gives the EME predictions which are best at long cooling
times. The approximate linear relation between the frozen-in
energy and the cooling time reflects what is sometimes called
"ln(t) kinetics" (Refs. 107 and 108).

proach towards the equilibrium distribution. This is not
the case for a sudden change from a low temperature to a
higher temperature (Fig. 5). Here a two-bump distribu-
tion occurs (see Sec. VI), a phenomenon that was predict-
ed within the EME.[82]

In Figs. 4 and 5 what happens is that most states with
energy E below a characteristic energy E_d are frozen,
while above E_d there is almost thermal equilibrium. The
energy E_d, which is marked by the vertical lines, is the
"demarcation energy" that was introduced by Arkhipov
et al. in the theory for excited charge-carrier thermaliza-
tion in amorphous semiconductors.[77] At any time t,
$E_d(t)$ is found by putting $\Gamma(E_d)$ [Eq. (15)] equal to $1/t$
(where T is the temperature during the relaxation pro-
cess):

$$E_d(t)=E_c-k_BT\ln(\Gamma_0^*t) .\tag{24}$$

V. THE GLASS TRANSITION ACCORDING TO THE ENERGY MASTER EQUATION

The previous section showed that the EME gives a
good fit to the random-walk model. The glass transition
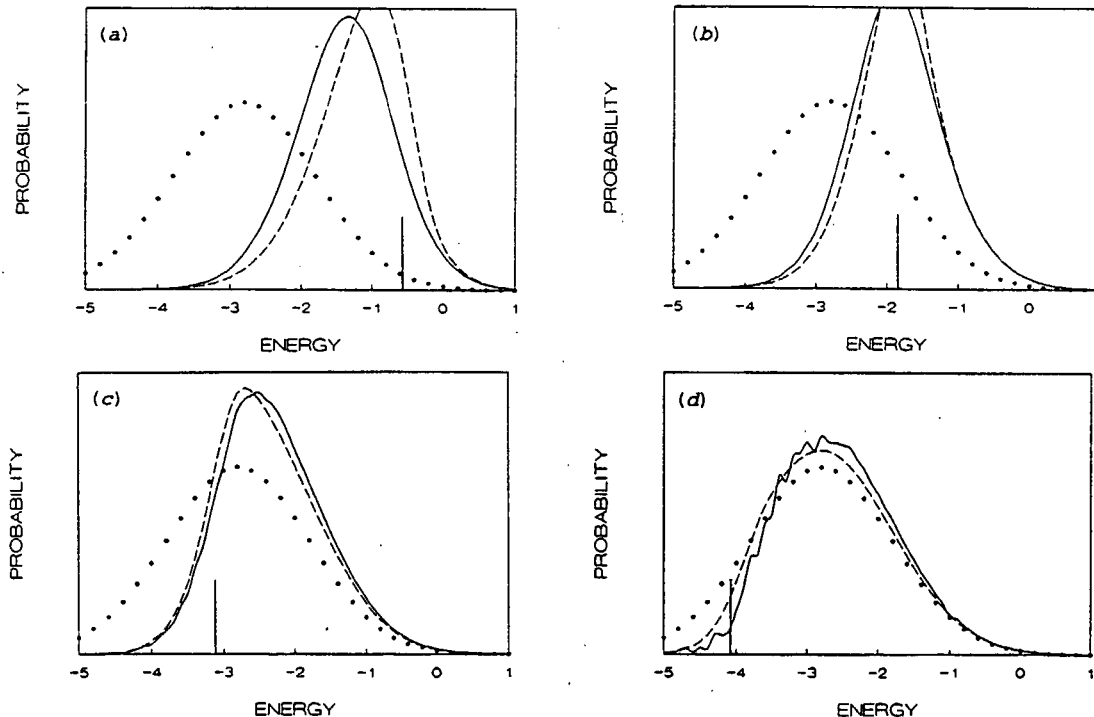was studied by the EME some time ago,[44] and this sec-

FIG. 4. Relaxation of the energy probability distribution in the random-walk model, $P(E,t)$, towards thermal equilibrium upon a
sudden lowering of the temperature starting at equilibrium. The figure shows four snapshots of $P(E,t)$ (full curves) and the EME
predictions (dashed curves) starting at $T=2.0$ $[\sigma/k_B]$ lowering the temperature at $t=0$ to $T=0.357$ at the following times $[1/\Gamma_0]$:
(a) $t=5$, (b) $t=184$, (c) $t=5953$, (d) $t=80\,752$. The vertical lines mark the demarcation energy E_d defined at time t by Eq. (24). In
the approximate EME description most states with $E<E_d$ have not jumped since $t=0$. As $t\to\infty$, $E_d\to-\infty$ and thermal equilibri-
um is reached. For (a)–(c) the full curves give results for averages of ten simulations of a 1000×1000 lattice, while for (d) only three
simulations were possible for this large lattice (thus, giving rise to more noise).

tion reviews the findings of Ref. 44 to discuss what to expect at the glass transition in the random-walk model.

In the EME the system is completely characterized by the energy probability distribution $P(E,t)$. At the glass transition temperature T_g, $P(E,t)$ freezes and stops changing upon further cooling. Only in some cases is the frozen-in energy distribution equal to the equilibrium energy probability distribution at T_g.[44] To understand this phenomenon it is convenient again to refer to the demarcation energy E_d, which however now acquires a meaning slightly different from that of Sec. IV: Suppose the liquid is cooled at a constant rate to zero temperature in a time t_c, starting at equilibrium at some high temperature where the average relaxation time is much smaller

than t_c. At any time during the cooling, the demarcation energy is defined as the energy separating nonfrozen states from the states that are frozen *from that time on.* If t_L is the time left before zero temperature is reached, E_d is given by $E_d(t)=E_c-k_B T(t)\ln(\Gamma_0^* t_L)$. In realistic cases, the glass transition takes place at a t_L which is of the same order of magnitude as t_c and much larger than $1/\Gamma_0^*$. Since $\Gamma_0^* t_L$ in the expression for $E_d(t)$ enters only in a logarithm, t_L may to a good approximation be replaced by the cooling time t_c:

$$E_d(t)=E_c-k_B T(t)\ln(\Gamma_0^* t_c) . \qquad (25)$$

Note that $E_d(t)$ increases with time during the cooling,

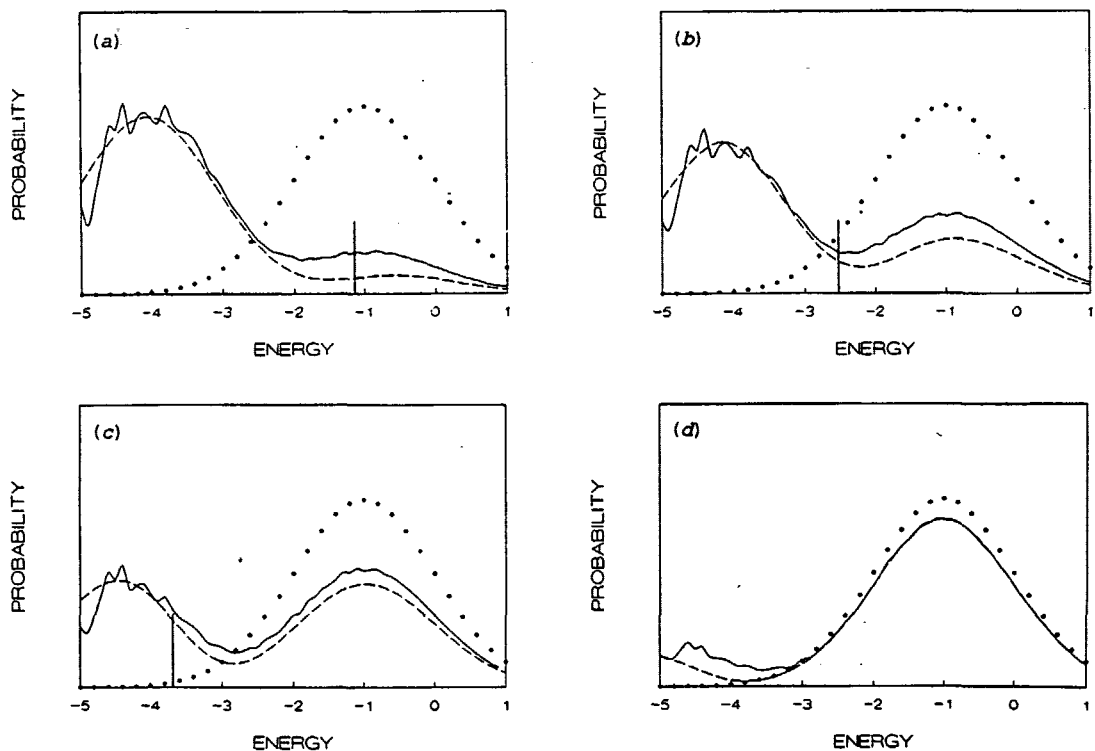FIG. 5. Relaxation of the energy probability distribution in the random-walk model, $P(E,t)$, towards thermal equilibrium upon a sudden raising of the temperature starting at equilibrium. The figure shows four snapshots of $P(E,t)$ (full curves) and the EME predictions (dashed curves) starting at $T=0.25$ $[\sigma/k_B]$ at time $t=0$ and subsequently annealing at the temperature $T=1.0$. The snapshots are taken at the following times $[1/\Gamma_0]$: (a) $t=2$, (b) $t=8$, (c) $t=25$, (d) $t=126$. The vertical lines mark the demarcation energy E_d defined at time t by Eq. (24). In the approximate EME description most states with $E<E_d$ have not jumped since $t=0$. As $t\rightarrow\infty$, $E_d\rightarrow-\infty$ and thermal equilibrium is reached. The full curves give results for averages of 20 simulations of a 1000×1000 lattice. (In both Figs. 4 and 5 very large lattices are needed to minimize the statistical fluctuations and to be able to move deep into the Gaussian tail.) The noise seen at low energies is statistical noise due to the fact that there are very few states in the deep Gaussian tail. The two-bump distribution appearing at intermediate times during the annealing reflects that, once a populated state has jumped away from its low energy, it almost immediately thermalizes. This is because there are many high-energy states which are easy to find. Since the region energy must correlate with the volume (because the liquid has a thermal-expansion coefficient which is larger than that of the glass), the model predicts that there is an anomalously large x-ray scattering at intermediate times during the annealing.

whereas in Sec. IV it decreased with time. In thermal equilibrium the energy probability distribution is a Gaussian centered around $\bar{E}(T)$ [Eq. (12)]. As the temperature is lowered, the equilibrium Gaussian is displaced towards lower energies while at the same time $E_d(t)$ increases. When the Gaussian meets $E_d(t)$, the glass transition takes place.[44] This happens when $\bar{E}[T(t)]=E_d(t)$. For the system with constant specific heat ck_B studied in Ref. 44, corresponding to $n(E) \propto E^{c-1}, 0 < E < E_c$ (where E_c now plays the additional role of a cutoff), one has at low temperatures $\bar{E}(T)=ck_BT$. From $\bar{E}=E_d$ one finds that the glass transition temperature is given by

$$k_BT_g = \frac{E_c}{c + \ln(\Gamma_0^* t_c)} . \qquad (26)$$

A linear relationship between $1/T_g$ and the logarithm of the cooling time is often observed in experiment.[84]

For the freezing of the energy probability distribution there are two different limiting scenarios, depending on the rate of change with temperature of E_d and $\bar{E}$, respectively. In the model studied in Ref. 44, $d\bar{E}/dT=ck_B$ and $dE_d/dT=-k_B\ln(\Gamma_0^*t_c)$. The case when E_d changes much faster with temperature than $\bar{E}$ was referred to as a "slow" glass transition, since it requires long cooling times: $\ln(\Gamma_0^* t_c)\gg c$. In this case the equilibrium Gaussian almost does not move at all when the demarcation energy passes it and freezes in the energies. Thus, the frozen-in energy distribution, $P_f(E)$, is close to that corresponding to thermal equilibrium at $T=T_g$:

$$P_f(E) \cong \frac{1}{\sqrt{2\pi\langle(\Delta E)^2\rangle}} \exp\left[-\frac{(E-E_g)^2}{2\langle(\Delta E)^2\rangle}\right] , \qquad (27)$$

where $E_g=ck_BT_g$ and $\langle(\Delta E)^2\rangle=c(k_BT_g)^2$. The other limiting case is that of a "fast" glass transition: $\ln(\Gamma_0^*t_c)\ll c$. Here, the demarcation energy moves very slowly compared to the Gaussian and is almost constant during the glass transition. To determine $P_f(E)$ consider the energy fluctuations of a single region. As long as its energy is above the demarcation energy, the region "jumps" many times between the high-energy common states. Sooner or later, however, the region ends up in a state below E_d, or just above E_d, being subsequently frozen when E_d passes. As for all other jumps, this last jump hits an energy with a probability proportional to the density of states. Around E_g the density of states is proportional to $\exp[E/(k_BT_g)]$,[72] so the normalized $P_f(E)$ is roughly given by (where again $E_g=ck_BT_g$)

$$P_f(E) \cong \begin{cases} \dfrac{1}{k_BT_g}\exp\left[\dfrac{(E-E_g)}{k_BT_g}\right], & E < E_g \\ 0, & E > E_g. \end{cases} \qquad (28)$$

In Ref. 44 the predicted exponential increase of $P_f(E)$ below E_g was confirmed in the numerical solution of the master equation; above E_g, however, $P_f(E)$ did not drop discontinuously to zero, but followed a Gaussian decay.

The conclusion from the above is that, in general, one cannot expect a glass merely to have the structure of the

equilibrium liquid at $T=T_g$. Certainly, the average frozen-in energy is equal to the average energy of the equilibrium liquid at T_g, but the *distribution* of frozen-in energies in the glass may be different from that corresponding to the equilibrium liquid. This has consequences for the glass properties. In the glass, any physical property which is a function of the region energy (if it depends linearly on E for the relevant energies) is, depending on the cooling rate, distributed according to a Gaussian or an exponential. Along these lines it has been argued that amorphous semiconductors prepared by a fast glass transition have exponential band tails.[85]

It is convenient to define a number that distinguishes between the two types of glass transitions. This number, denoted by ι, is the absolute value of the ratio between the change in the average energy and the change in the demarcation energy at the glass transition:

$$\iota = \left|\frac{d\bar{E}}{dE_d}\right|(T_g) . \qquad (29)$$

"Slow" glass transitions arise whenever $\iota \ll 1$, while "fast" glass transitions correspond to $\iota \gg 1$.

We now proceed to calculate the ι parameter for the random-walk model from the approximate EME description. The average energy is given by Eq. (12), $\bar{E}=-\sigma^2/(k_BT)$. Thus, the equation determining T_g, $\bar{E}=E_d$ is

$$-\sigma^2/(k_BT_g)=E_c-k_BT_g\ln(\Gamma_0^* t_c) ,$$

or

$$\ln(\Gamma_0^* t_c)(k_BT_g)^2-E_c(k_BT_g)-\sigma^2=0 . \qquad (30)$$

The positive solution of this equation is

$$k_BT_g = \frac{E_c+\sqrt{E_c^2+4\sigma^2\ln(\Gamma_0^* t_c)}}{2\ln(\Gamma_0^* t_c)} . \qquad (31)$$

Since $d\bar{E}/dT=\sigma^2/(k_BT^2)$ and $dE_d/dT=-k_B\ln(\Gamma_0^* t_c)$ the ι parameter is via Eqs. (29) and (30) given by

$$\iota = \frac{\sigma^2}{(k_BT_g)^2\ln(\Gamma_0^* t_c)}$$

$$= 1 - \frac{E_c}{(k_BT_g)\ln(\Gamma_0^* t_c)} . \qquad (32)$$

If the dimension $d > 2$, the percolation energy E_c is negative and Eq. (31) implies

$$d > 2: \quad \frac{E_c}{k_BT_g} = -\frac{2\ln(\Gamma_0^* t_c)}{\sqrt{1+4(\sigma^2/E_c^2)\ln(\Gamma_0^* t_c)}-1} . \qquad (33)$$

When Eq. (33) is substituted into Eq. (32) one gets

$$d > 2: \quad \iota = 1 + \frac{2}{\sqrt{1+4(\sigma^2/E_c^2)\ln(\Gamma_0^* t_c)}-1} . \qquad (34)$$

In the case $d=2$, E_c is positive and, as is easy to show, the ι parameter is given by

$$d = 2: \quad \iota = 1 - \frac{2}{\sqrt{1+4(\sigma^2/E_c^2)\ln(\Gamma_0^* t_c)}+1} . \qquad (35)$$
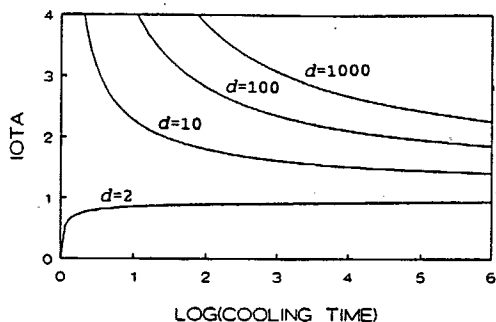
FIG. 6. The parameter ι [Eqs. (29), (34), and (35)] characterizing the glass transition in the random-walk model for different dimensions ($d = 2$, 10, 100, 1000) as function of cooling time [$1/\Gamma_0^*$] according to the EME. The difference between $d = 2$ and $d > 2$ arises from the fact that only in two dimensions is the percolation energy positive. If $\iota \ll 1$ the transition is a "simple freezing" glass transition, where the energy probability distribution of the glass is the equilibrium distribution at T_g, frozen-in almost unmodified. In the other limit, $\iota \gg 1$, the transition is a "relaxational" glass transition, where relaxations at the glass transition considerably deform the equilibrium energy probability. As a result, the glass does *not* acquire a structure corresponding to the equilibrium liquid at T_g. For very long cooling times one ends up in the mixed case $\iota = 1$ where there is some relaxation at T_g.

Figure 6 gives the ι parameter as function of the cooling time for $d = 2$, 10, 100, 1000.

The terminology of Ref. 44 referring to "slow" and "fast" glass transitions is not appropriate for the random-walk model. For this model, as the cooling time goes to infinity, one finds $\iota \to 1$ in all dimensions (Fig. 6); thus there are no "slow" glass transitions for slow cooling rates. On the other hand, whenever $d > 2$ the glass transition is "fast" for sufficiently small cooling times; the case $d = 2$ is peculiar in that the glass transition is "slow" for fast coolings. In view of this it is better to refer to glass transitions with $\iota \gg 1$ [previously: "fast"] as "relaxational" glass transitions: These are the interesting cases where relaxation processes right at the glass transition result in a frozen-in energy distribution different from the equilibrium distribution at T_g. The cases when $\iota \ll 1$ [previously: "slow"] may be referred to as "simple freezing" glass transitions; here the equilibrium energy distribution is simply frozen-in at T_g.

VI. DISCUSSION

In this paper Bässler's random-walk model for viscous liquids and the glass transition was "derived" in Sec. II. In Secs. III and IV, it was argued physically and illustrated by computer simulations that the energy master equation (EME) gives a good fit to the random-walk model. Thereby, two at first sight quite different approaches to the glass transition problem[44,45] are unified. The EME is an equation for the energy probability distribution, which even for an arbitrarily varying temperature and for very long times makes it possible to calculate this quantity. However, it should be remembered that the EME only deals with *energy;* there are a number of interesting properties of the random-walk model that relate to the displacement of the "particle," which are not dealt with by the EME.

The below discussion is sectioned into eight parts, the first four (A)–(D) discuss the random-walk model and its connection to the EME, while the last four (E)–(H) deal with the EME itself as a model for viscous liquids and the glass transition.

A. The random-walk model in the present paper

The physical justification of the random energy model was discussed in detail in Sec. II. The most drastic approximation[29] is the partitioning of the liquid into noninteracting regions, an approximation that must be made to arrive at a tractable model. Replacing the deterministic equations of classical physics with stochastic equations seems more acceptable, though not without pitfalls.[67,86] A further approximation is the replacing of "complexity" by "randomness."[69] This, in conjunction with the discretization of state space lead to the model of a random walk on a lattice with random energies. Models involving random walks in random environments ("rugged" energy landscapes) have been used in many contexts.[48,70,75,86–91] In formulating a model of this type one is led to ask whether the energy minima or the energy maxima should vary randomly, or both. The random-walk model gives a simple and beautiful answer to this question: No states are appointed "maxima" or "minima." All states are equal, but the higher-energy states *behave as maxima*, being part of the paths between the populated, but rare, low-energy states. The assumption of Gaussianly random energies is the simplest choice. Fortunately, it leads to an equilibrium specific heat which increases with decreasing temperature, as seen in experiment.

Following the ideas of Derrida's "random energy model"[32] it is possible to discuss the Kauzmann paradox within the model: Since there is only a finite "excess" entropy of the supercooled liquid, a truncation of the Gaussian at some low energy is forced on the model to avoid the Kauzmann paradox.[92,93] This truncation implies that the thermodynamics of the model becomes almost indistinguishable from that of Derrida's "random energy model." The truncation has not been discussed here, because the truncated random-walk model does not reproduce the experimental correlation between the Kauzmann temperature and the T_0 of the VFT law Eq. (2).

The random-walk model contains three parameters. There are two scaling parameters, the width of the Gaussian σ and the attempt frequency Γ_0, while the third parameter is the dimensionless state space dimension d. For a qualitative discussion of the model there is thus only one relevant parameter d.

B. A comparison to the original approach of Bässler and co-workers

Bässler and co-workers[45,46] justified the Gaussian density of states by reference to the central-limit theorem, assuming that the region energy is a sum of a large number of independent contributions. However, one might similarly argue that *any* macroscopic system has a Gaussian density of states, implying that any such system has a specific heat varying with temperature as T^{-2}, which is clearly incorrect. In the present paper the Gaussian is an *ad hoc* assumption, only justified from the fact that it gives a "thermodynamic" density of states [Eq. (11)]. A further difference is that Bässler and co-workers assumed that the density of states fluctuates in time. This justified their use of Metropolis dynamics, since the "particle" awaits a favorable time for jumping where the barrier to be overcome is negligible. Here, the density of states is assumed constant and time independent. This difference in the two approaches means that the present work cannot maintain the original interpretation of the fact that T_g depends on sample history. This was explained[45] as a logical consequence of the fact that the density of states depends on preparation conditions. However, even for a constant density of states does the glass transition temperature depend on sample history.

The most elaborate version of the Bässler model was given in a recent paper by Arkhipov and Bässler.[53] They distinguish between a high-temperature regime described by the random-walk model and a low-temperature regime described by the EME. The present work fully confirms this picture. Here, however, the random-walk model is assumed to be the underlying model at all temperatures, and the parameters of the low-temperature approximate EME are uniquely determined from the random-walk model.

C. From the random-walk model to the EME

At low temperatures the populated states of the random-walk model are rare low-energy states, and the transitions between these far apart states follow the optimal paths, the ones that have the lowest maximum energy. The distance between two low-energy states is large and the maximum energy of an optimal path is close to the percolation energy defined from the site percolation threshold by Eq. (14). A number of authors have previously emphasized the importance of percolation at the glass transition,[13,40,94-96] but in contexts different from the present.

The importance of percolation at low temperatures means that the random-walk model here is regarded as consisting of states (=the deep minima) separated by barriers of the same height. Effectively, the model reduces to a model of the "trapping" type used, e.g., for describing trapping of electrons in amorphous semiconductors. Interestingly, it has previously been noted that the predictions of trapping models are almost indistinguishable from the predictions of the EME.[97,98]

The existence of the percolation energy makes it possible to distinguish two temperature regimes for the random-walk model, a high-temperature regime opposed

to the low-temperature regime where $|\bar{E}(T)| \gg |E_c|$. In the high-temperature regime, the most likely states usually have one or more neighbors with a lower energy and these states consequently have a very short "lifetime." In the low-temperature regime, typical populated states are surrounded by states all of which have a higher energy. Only well into the low-temperature regime does the approximate EME description apply. This picture, which is valid whenever $d > 2$ (for $d = 2$ there is no high-temperature regime), is close to that recently advocated in general terms by Hunt.[13,95] He predicts that viscous liquids have a high-temperature regime described by effective-medium type theories and a low-temperature regime where percolation effects dominate. A two regime picture also results from the mode-coupling theory,[26] but in a different context.

The low-energy states could be thought of as effectively including a number of their relatively low-energy neighboring states, thus forming rather complex low energy "basins", in agreement with the ideas of Stillinger and Weber[63,64] and Angell.[11,30] The complexity of the basins implies that considerable entropy resides inside each basin.[11,99] Note that this picture of complex minima derives from a model where neighboring energies are completely uncorrelated.

A transition between two low-energy states is a complex sequence of steps. Such a transition involves an element of *cooperativity*[8,29] in the sense that a long sequence of jumps is undertaken in order to have a successful transition. Thus, at low temperatures the random-walk model contains both cooperativity and heterogeneity, the two factors identified by Scherer[29] as being important for any realistic model of viscous liquids. The random-walk model also conforms to the thoughts of Goldstein in 1969, expressing a firm belief that, "when all is said and done, the existence of potential energy barriers large compared to the thermal energy are intrinsic to the occurrence of the glassy state, and dominate flow, at least at low temperatures."[42]

The approximate EME description of the random-walk model ignores the spatial structure of the state space (the only trace left being the d dependence of the percolation energy). In the limit of large d this is not unrealistic, since there are many deep energy minima available not too far from a given minimum. Consequently, transitions to all states should be allowed with equal probability, as in the EME.

D. Computer simulations: Comparing the random-walk model to the EME predictions

The approximate EME description makes it possible to study the random-walk model for realistic long times. This involves a numerical implementation of the analytic EME solution valid for the approach to thermal equilibrium at a fixed temperature (Appendix). In order to check the validity of the EME approximation, computer simulations were carried out (Sec. IV). The EME is expected only to be valid in many dimensions at low temperatures and long times, a regime that cannot be studied by even the fastest computers available today because of two problems: At low temperatures the most likely states are

very rare so enormous lattices are needed; also, the relaxation times are extremely long. Instead, the simulations were carried out in two dimensions and at moderate temperatures. Despite this, the computer simulations revealed a rather good agreement with the EME predictions. A numerical study of thermalization in the random-walk model was previously performed by Bässler and co-workers, starting in equilibrium at infinite temperature.[100] In Figs. 4 and 5 of the present paper, the thermalization was studied going from one finite to another finite temperature. A surprising thing happens in the more exotic case going from a low to a high temperature (Fig. 5) where a two-bump structure appears at intermediate times, a phenomenon that is reproduced by the EME. Thus, if the random-walk model is realistic, one may induce a "dynamically generated phase separation" in a glass by the following procedure: Anneal the glass for a very long time at a relatively low temperature, then increase the temperature and finally quench the glass at the right time in order to catch it in a state corresponding to Fig. 5(c). The dynamically generated phase separation results in a glass consisting of low-energy regions and high-energy regions, but only few of intermediate energy. Such a glass has a well-defined correlation length, equal to the region size.

The rest of Sec. VI deals with the EME independently of its connection to the random-walk model.

E. The EME as the simplest possible truly cooperative master equation, "derived" from the non-Arrhenius temperature dependence of the average relaxation time

Since most naive phenomenological models involving a distribution of energy barriers give an average relaxation time $\tau(T)$ with an apparent activation energy that *decreases* with decreasing temperature, the observed non-Arrhenius $\tau(T)$ must contain an important clue to the construction of a phenomenological model. Assuming that the activation entropy plays little role we write

$$\tau(T) = \tau_0 e^{\Delta E(T)/(k_B T)} . \tag{36}$$

Experiments imply that $\Delta E(T)$ increases as the temperature decreases. The simplest way to explain this is as follows: $\Delta E(T)$ is the difference between the barrier to be overcome and the most likely region energy. If a region contains many molecules ("cooperativity"), the most likely energy is by general thermodynamic principles close to the average energy $\bar{E}(T)$. If furthermore the maximum to be overcome is assumed to be constant, $=E_c$, one has

$$\Delta E(T) = E_c - \bar{E}(T) . \tag{37}$$

Since $\bar{E}(T)$ decreases with decreasing temperature, the barrier increases. This simple idea is the basis for the EME as a model for viscous liquids (independent of the random-walk model): Equation (37) motivates Eq. (15) and to derive the EME one just needs the further assumption—again the simplest possible—that, once excited into the transition state, a region ends up in a randomly chosen other state. This assumption means that

an excitation must be a complete reordering of the region molecules. Thus, the EME is *truly cooperative*.

F. The EME as the simplest master equation conforming to the Goldstein-Brawer picture (Fig. 1)

In an interesting paper from 1972, Goldstein[39] proposed a picture of viscous flow where the transition state is the "high-temperature, more-fluid, liquid usually studied by theorists." Once excited into this common transition state—being totally different from the potential energy minimum which the region was excited from—the only reasonable assumption is that any other (low energy) state can be reached. In the EME these other states are reached with equal probability. Thus, from Goldstein's ideas[39,42] one is led almost automatically to the EME. However, Goldstein did not discuss any master equation; a master equation in the spirit of his ideas was set up by Brawer in 1984.[8,43] Brawer's model is more detailed than Goldstein's and his master equation is more complex than the EME. In the 1985 version of Brawer's model[8] a region has K volume elements, each of which has two states: a low-density (high-energy) state and a high-density (low-energy) state. If a certain fraction of the K volume elements are excited into the low-density state, a transition is allowed. The jump thus involves a number of the volume elements forming a complex sequence of density changes, somewhat like a transition between two low-energy states in the random-walk model.

G. The EME interpretation versus the naive interpretation of the activation energy

Figure 7 sketches typical experimental results for the average relaxation time using an Arrhenius plot (full curves): There is a non-Arrhenius high-temperature regime for the equilibrium viscous liquid and an Arrhenius low-temperature regime (the glass). The naive interpretation of this [Fig. 7(a)] is based on writing $\tau(T) = \tau_0 \exp[\Delta F(T)/(k_B T)]$ and using the standard thermodynamic relations $\Delta F = \Delta E - T\Delta S$ and $d\Delta F/dT = -\Delta S$; from this it is easy to show that the activation energy ΔE is the slope of the tangent (dashed line). This slope changes abruptly at the glass transition, which is sometimes explained as being due to the fact that below T_g relaxation takes place in an essentially fixed structure, while above T_g the activation energy has an additional contribution from structural changes. Figure 7(b) gives the EME interpretation of data which follows from Eq. (15) [or Eqs. (36) and (37)]. Here, the activation energy ΔE is the slope of the *secant* from $\tau(T)$ to τ_0. Thus, at $T = T_g$ the activation energy simply *stops changing*, because glassy relaxation takes place in an essentially fixed structure.

H. A qualitative comparison of the EME to experiments

The random-walk model has been quantitatively successfully compared to experiments on a number of glass-forming liquids.[45,46,53] We here proceed to argue that the
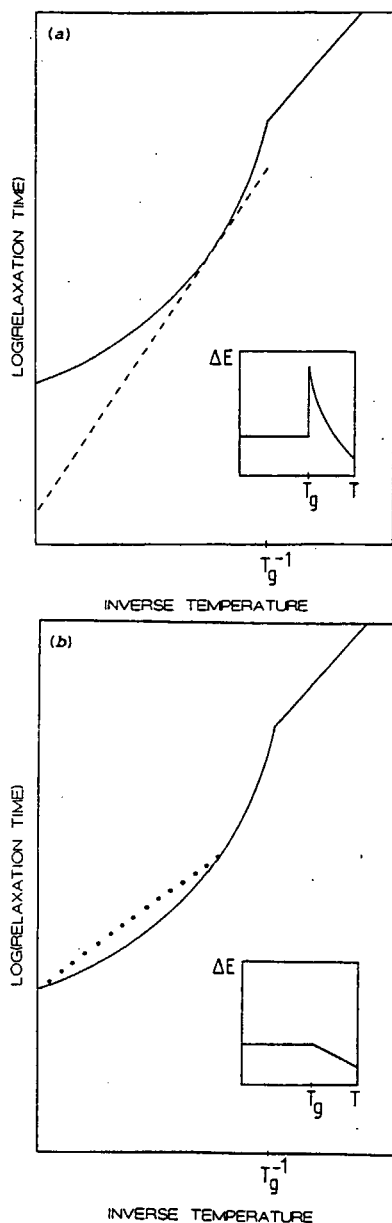
FIG. 7. Naive interpretation of the activation energy (a) compared to the interpretation underlying the EME (b). Both figures show an Arrhenius plot of the same typical average relaxation time data for the supercooled liquid (non-Arrhenius part, $T > T_g$) and for the glass (Arrhenius part, $T < T_g$). In (a) the activation energy is interpreted as the slope of the *tangent*, which changes discontinuously at T_g. In (b) the activation energy is interpreted as the slope of the *secant* drawn to the microscopic time. In both cases one finds that the activation energy increases as the temperature decreases. In (b), at the glass transition the activation energy stops increasing and becomes constant. In the naive interpretation (a), the activation energy changes discontinuously at the glass transition.

EME itself, despite being very simple, qualitatively reproduces a large number of experimental observations, yields some new predictions, and also some "wrong" predictions. Most of the properties of the EME listed below will not be detailed here, but are straightforward to derive.[82]

1. Qualitatively correct predictions of the EME

(a) The EME gives a qualitatively correct temperature dependence of the average relaxation time above and below T_g (Fig. 7);

(b) The preexponential of $\tau(T)$ for glassy relaxation is predicted to be close to τ_0, i.e., a phonon time;[8,43]

(c) A true Arrhenius behavior of $\tau(T)$ implies a zero region specific heat and thus no distribution of relaxation times.[7,51,101] If the region size is universal, as conjectured by Nemilov,[102,103] there is a correlation between the magnitude of the "excess" specific heat (the configurational specific heat), the degree of non-Arrhenius behavior of $\tau(T)$, and the relaxation time distribution width;[7,104,105]

(d) If the region specific heat is regarded as roughly constant close to T_g, the EME predicts a proportionality between $1/T_g$ and the logarithm of the cooling time;[84,106]

(e) In the glassy state, energy relaxation proceeds according to the EME with a logarithmic time dependence [compare Eq. (24)], "$\ln(t)$ kinetics,"[81,107,108] with a slower than logarithmic time dependence at both the initial and final stages. The logarithmic relaxation law is conventionally explained as being due to a "relaxation" of the relaxation rate itself.[8,29,43,81,82,109] The EME conforms to this picture in a particularly simple way;

(f) For relaxation upon a sudden change in temperature an asymmetry is predicted between the two possible cases, a well-known phenomenon referred to as "nonlinearity";[8,29]

(g) If one assumes a correlation between the region energy and its volume (which is necessary because the viscous liquid has a larger thermal-expansion coefficient than the glass or crystal), the EME also gives predictions regarding the pressure dependence of the average relaxation time. Writing $\tau(p) \propto \exp[p\Delta V(p)]$, experiments imply that the activation volume increases as the pressure increases.[110] If $\Delta V(p) = V_c - \bar{V}(p)$ just as for the activation energy this observation is explained, since the region average volume decreases with increasing pressure. A further possibility is to assume a linear relation between region volume and energy. In that case the normalized frequency-dependent isothermal compressibility is equal to the normalized frequency-dependent specific heat, as proposed by Zwanzig;[111] there are some indications that this is the case in experiment.[112] Also, for quantities uncorrelated with the region energy, it can be shown that the EME predicts a slight "decoupling" of their average relaxation time from that of the frequency-dependent specific heat, where the average relaxation time for the latter becomes somewhat larger (Fig. 8). This is also the case experimentally.[112]
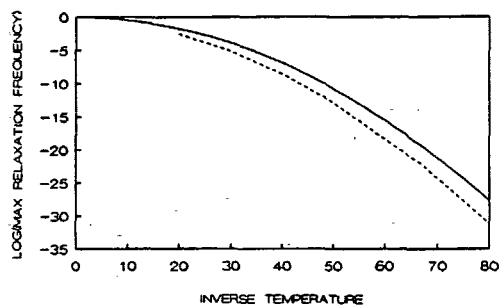
FIG. 8. Decoupling of thermal relaxation times from other relaxation times according to the EME for a Gaussian density of states with $E_c = 0$. The maximum relaxation frequency is given in units of Γ_0^* and the temperature in units of σ/k_B. The full curve gives the loss peak frequency for a quantity that is uncorrelated to the energy (calculated from its time autocorrelation function). The dashed curve is the specific-heat loss peak frequency (Ref. 117). The figure shows that there is a slight slowing down of thermal relaxations compared to other relaxations, an effect that has been seen in experiments (Ref. 112).

2. New predictions of the EME

(a) At low temperatures the average relaxation time of the equilibrium viscous liquid is predicted to become Arrhenius with a pre-exponential equal to τ_0. Thus, a change in sign of the curvature of the Arrhenius-plot, $d^2\ln[\tau(T)]/d(T^{-1})^2$, is predicted. Similarly, a change in sign of $d^2\ln[\tau(p)]/dp^2$ at large pressure is predicted. This follows from the fact that a region must have a lowest energy state or a minimum volume;

(b) The EME gives detailed predictions regarding the nature of the asymmetry of relaxation upon sudden changes in temperature: For a sudden cooling from thermal equilibrium relaxation is predicted to proceed continuously (Fig. 4), while relaxation upon a sudden increase in temperature is peculiar, resulting in a two-bump energy probability distribution at intermediate times (Fig. 5). In the latter case, if the relaxation is interrupted by quenching to low temperatures, one ends up with a strange glass in which some regions have low energy and some have high energy, a "dynamically generated phase separation." The energy correlates with the volume [compare H 1 g]. Therefore, a dynamically generated phase separated glass will give an anomalous x-ray scattering signal. Nemilov has predicted a similar phenomenon on purely thermodynamic grounds;[113]

(c) The EME predicts that there are two different limiting cases of the glass transition (Sec. V), "relaxational" (previously called "fast") glass transitions and "simple freezing" (previously called "slow") glass transitions. The latter type freezes-in the region energy probability distribution at T_g and the glass simply inherits the structure of the equilibrium liquid at this temperature. At a relaxational glass transition, relaxation processes right at T_g result in a frozen-in region energy distribution different from the equilibrium distribution. (Of course,

glasses may be produced by a third kind of process, a quench to low temperatures in a time much shorter than the average relaxation time at the starting temperature—this process clearly results in a frozen-in region energy distribution that is equal to the equilibrium distribution at the starting temperature.)

3. "Wrong" predictions of the EME

(a) The VFT law Eq. (2) is inconsistent with the EME which predicts a finite average relaxation time at all temperatures. Experimentally, however, deviations from this law seem to occur for large viscosities, where the data exhibit a less dramatic temperature-dependence than predicted;[20,29,51]

(b) The Kauzmann paradox is also inconsistent with the EME (without a low-energy cutoff in the density of states), which at all temperatures predicts a positive specific heat. However, a suitably chosen region density of states (e.g., a truncated Gaussian[32,92,93]) easily reproduces the experimental configurational entropy;

(c) The Kohlrausch-Williams-Watts law (stretched exponentials) for the time dependence of the energy relaxation is not reproduced by the model. However, the EME does predict broad distributions of relaxation times.

These three points are places where the EME on the one hand does not reproduce the conventional picture of viscous liquids and glassy relaxation, but on the other hand is not inconsistent with experiment. The final point to be mentioned here is a more serious objection to the EME:

(d) If the correct non-Arrhenius behavior of $\tau(T)$ is to be reproduced by choosing a suitable $n(E)$ (possibly a non-Gaussian), the model predicts a peak of the imaginary part of the frequency-dependent linear specific heat[114] that is too broad. This conclusion seems to hold, despite the fact that only few measurements of this quantity have been published and that there is a considerable discrepancy between the results of Christensen[115] and those of Birge and Nagel.[116] This disagreement between the EME and experiment means that the EME is too simple to be realistic. Preliminary work[117] indicates that it is possible to solve this problem and still retain the region assumption and the assumption that the only important parameter is the region energy. This is done by the following extension of the EME. One introduces two densities of states, one numbering the minima and another essentially giving the entropy of each minimum. Thus, each minimum is a cluster of states that may be reached from each other by not exciting all the way to the energy E_c.[118] Besides giving greater flexibility to the EME model, making it able to fit the frequency-dependent specific-heat experiments, this approach also allows for the existence of β relaxation as the process associated with intraminima transitions.[118]

VII. CONCLUSIONS

A derivation of Bässler's random-walk model has been sketched, which emphasizes the potential importance of this model as a "canonical" or prototype phenomenologi-

cal model for viscous liquids and the glass transition. The random-walk model views relaxation as a consequence of activated transport in a multidimensional rugged energy landscape. It is probably the simplest model of this type. The "derivation" of Sec. II traces the random-walk model back to Newton's equations for the molecules of one region. However, the derivation is in no way exact, which is clear just from the fact that the crystalline state of much lower energy than the supercooled liquid state is absent from the model.

It has been shown that the EME gives a good approximate description of the energy fluctuations of the random-walk model. The EME is solvable by a combination of analytical and numerical techniques (Appendix). This makes it possible to predict the behavior of the random-walk model for an arbitrary temperature time variation at very long times. Independently of its justification from the random-walk model, the EME may have a value of its own as a phenomenological model for viscous liquids and the glass transition. It incorporates true cooperativity and is consistent with statistical mechanics, while still being simple and solvable for realistic laboratory time scales. It is noteworthy that such a simple model leads to new predictions, like that there are two different types of glass transitions and that a well-annealed glass upon heating gives an anomalously large x-ray scattering at intermediate times before equilibrium is reached.

ACKNOWLEDGMENTS

APPENDIX: SOLVING THE ENERGY MASTER EQUATION

We first calculate how an initial nonequilibrium energy probability distribution at a fixed temperature converges to the canonical equilibrium distribution.[43,79-82] To solve the EME numerically, it must be discretized. The energy axis is discretized into N evenly spaced energies, $E_1 < \cdots < E_N$. At low temperatures it is important to include large negative energies into the set of discrete energies, despite these lying far into the Gaussian tail. If one defines $\Gamma_i \equiv \Gamma(E_i)$, $P_i \equiv P(E_i, t)/C_p$, and $n_i \equiv n(E_i)/C_n$, where the normalization constants C_p and C_n are determined so that

$$\sum_{j=1}^{N} P_j = 1; \quad \sum_{j=1}^{N} n_j = 1 , \tag{A1}$$

the EME Eq. (20) becomes upon discretization

$$\frac{dP_i}{dt} = -\Gamma_i P_i + n_i \sum_{j=1}^{N} \Gamma_j P_j \quad (i = 1, \ldots, N) . \tag{A2}$$

The normalization condition for the n_j's [Eq. (A1)] ensures probability conservation at all times.

At any temperature this equation may be solved by Laplace transformation.[43,80-83] The Laplace transform of the function $P_i(t)$ in Eq. (A2), $\tilde{P}_i(s)$, is as usual defined[83] by

$$\tilde{P}_i(s) = \int_0^\infty P_i(t) e^{-st} dt . \tag{A3}$$

Since the Laplace transform of the time derivative of a function $f(t)$ is $s\tilde{f}(s) - f(0)$, Eq. (A2) becomes upon Laplace transforming

$$s\tilde{P}_i(s) - P_i(0) = -\Gamma_i \tilde{P}_i(s) + n_i X(s) , \tag{A4}$$

where $X(s) = \sum_{j=1}^{N} \Gamma_j \tilde{P}_j(s)$. This equation determines $\tilde{P}_i(s)$ from a knowledge of the initial probabilities $P_i(0)$. The probabilities $P_i(t)$ are calculated by the inverse Laplace transformation,[83]

$$P_i(t) = \frac{1}{2\pi i} \int_{-i\infty}^{+i\infty} \tilde{P}_i(s) e^{st} ds . \tag{A5}$$

Isolating $\tilde{P}_i(s)$ from Eq. (A4) leads to

$$\tilde{P}_i(s) = \frac{P_i(0)}{s + \Gamma_i} + \frac{n_i}{s + \Gamma_i} X(s) . \tag{A6}$$

From this expression an equation for $X(s)$ is found by multiplying with Γ_i on each side and summing:

$$X(s) = \sum_{i=1}^{N} \frac{\Gamma_i P_i(0)}{s + \Gamma_i} + X(s) \sum_{i=1}^{N} \frac{n_i \Gamma_i}{s + \Gamma_i} , \tag{A7}$$

or

$$X(s) = \frac{\sum_{i=1}^{N} [\Gamma_i P_i(0)/(s + \Gamma_i)]}{1 - \sum_{i=1}^{N} [n_i \Gamma_i/(s + \Gamma_i)]} . \tag{A8}$$

Using Eq. (A1) the denominator may be rewritten

$$1 - \sum_{i=1}^{N} \frac{n_i(\Gamma_i + s - s)}{s + \Gamma_i} = s \sum_{i=1}^{N} \frac{n_i}{s + \Gamma_i} . \tag{A9}$$

When this is substituted into Eq. (A8), Eq. (A6) becomes (changing the summation index from i to j)

$$\tilde{P}_i(s) = \frac{P_i(0)}{s + \Gamma_i} + \frac{n_i}{s(s + \Gamma_i)} \frac{\sum_{j=1}^{N} [\Gamma_j P_j(0)/(s + \Gamma_j)]}{\sum_{j=1}^{N} [n_j/(s + \Gamma_j)]} . \tag{A10}$$

From Eq. (A10) $P_i(t)$ may be calculated via Eq. (A5), where the integration contour in the complex plane lies to the right of all poles of $\tilde{P}_i(s)$. The integral is evaluated by including an infinitely large semicircle surrounding the left half of the complex plane. This closes the integration contour and the residue theorem may be applied. For each i there are N poles which, due to the structure of the energy master equation, are the same for all $\tilde{P}_i(s)$. There is one pole at $s = 0$. The apparent singularities at $s = -\Gamma_j$, are all "removable", i.e., not real singularities. If $j = i$ this follows from the fact that

$$\lim_{s \to -\Gamma_i} (s + \Gamma_i)\tilde{P}_i(s) = P_i(0) + \frac{n_i}{(-\Gamma_i)}\frac{\Gamma_i P_i(0)}{n_i} = 0 \; ,$$

$$(A11)$$

while for $j \neq i$ it follows from

$$\lim_{s \to -\Gamma_j} (s + \Gamma_j)\tilde{P}_i(s) = 0 + 0\frac{\Gamma_j P_j(0)}{n_j} = 0 \; . \qquad (A12)$$

Besides the $s = 0$ pole there are poles whenever s obeys

$$\sum_{j=1}^{N} \frac{n_j}{s + \Gamma_j} = 0 \; . \qquad (A13)$$

This equation has $N - 1$ solutions, each of which is a negative real number. The solutions are conveniently denoted by $s = -\omega_k$ and numbered such that

$$\Gamma_k < \omega_k < \Gamma_{k+1} \quad (k = 1, \ldots, N-1) \; . \qquad (A14)$$

The ω's are thus defined by

$$\sum_{j=1}^{N} \frac{n_j}{\Gamma_j - \omega_k} = 0 \quad (k = 1, \ldots, N-1) \; . \qquad (A15)$$

We next proceed to find the residues. At the pole $s = 0$ the residue is given by

$$\lim_{s \to 0} s\tilde{P}_i(s) = 0 + \frac{n_i}{\Gamma_i}\frac{\sum_{j=1}^{N} P_j(0)}{\sum_{j=1}^{N} (n_j/\Gamma_j)} = \frac{n_i/\Gamma_i}{\sum_{j=1}^{N} (n_j/\Gamma_j)} \; . \qquad (A16)$$

Since the quantity $n_i/\Gamma_i \propto n_i \exp(-\beta E_i)$ is proportional to the canonical equilibrium probability for the system having energy E_i, the residue at $s = 0$ is simply the normalized equilibrium probability $P_{0,i}$:

$$\lim_{s \to 0} s\tilde{P}_i(s) = P_{0,i} \; . \qquad (A17)$$

Using the rule that the residue of a function of the form $f(z)/g(z)$ at a simple zero for $g(z)$ at $z = z_0$ is equal to $f(z_0)/g'(z_0)$, one finds for the residues at $s = -\omega_k$

$$\lim_{s \to -\omega_k} (s + \omega_k)\tilde{P}_i(s)$$

$$= 0\frac{P_i(0)}{\Gamma_i - \omega_k} + \frac{n_i}{(-\omega_k)(\Gamma_i - \omega_k)}$$

$$\times \frac{\sum_{j=1}^{N} [\Gamma_j P_j(0)/(\Gamma_j - \omega_k)]}{\sum_{j=1}^{N} [(-n_j)/(\Gamma_j - \omega_k)^2]}$$

$$= \frac{n_i}{\omega_k(\Gamma_i - \omega_k)} A_k \; , \qquad (A18)$$

where

$$A_k = \frac{\sum_{j=1}^{N} [\Gamma_j P_j(0)/(\Gamma_j - \omega_k)]}{\sum_{j=1}^{N} [n_j/(\Gamma_j - \omega_k)^2]} \quad (k = 1, \ldots, N-1) \; .$$

$$(A19)$$

Having determined the residues, the integral Eq. (A5) is now easily calculated by the residue theorem:

$$P_i(t) = P_{0,i} + \sum_{k=1}^{N-1} \frac{n_i}{\omega_k(\Gamma_i - \omega_k)} A_k e^{-\omega_k t} \; . \qquad (A20)$$

The equations (A15), (A19), and (A20) give the solution of the energy master equation at a fixed temperature. As expected, the solution converges to the equilibrium solution as $t \to \infty$. The ω_k's play the role of characteristic relaxation rates. Note that conservation of probability is ensured by virtue of Eq. (A15).

In the numerical implementation, the ω_k's are determined from Eq. (A15) by the bisection method. Depending on the numerical precision large numerical errors may arise from the term $1/(\Gamma_k - \omega_k)$ in Eqs. (A19) and (A20) at low energies where ω_k is extremely close to Γ_k; in this case one may use Eq. (A15) to approximate as follows:

$$\frac{1}{\Gamma_k - \omega_k} \approx -\frac{1}{n_k} \sum_{j=1, j \neq k}^{N} \frac{n_j}{\Gamma_j - \omega_k} \; . \qquad (A21)$$

Another problem that may arise is overflow. In the present work both these numerical problems were avoided by using the 80 bit floating point "extended" data type of Turbo Pascal. Alternatively, overflow problems may be avoided by the following procedure: The numbers $P_j, P_j(0), n_j, \Gamma_k, \omega_k$ are each represented by their logarithm. Each sum appearing in Eqs. (A15), (A19), and (A20) is evaluated by first identifying the leading term and then factorizing it. There remains a sum of terms less than one, each term being a product which is evaluated as, e.g., $ab = \exp[\ln(a) + \ln(b)]$.

By means of Eq. (A20) the master equation may be solved numerically at arbitrary long times at a fixed temperature with great accuracy. If the temperature changes in time, the above method is applied for time steps small enough that the temperature may be regarded as constant. In the solutions of the master equation plotted in Figs. 2-5 the energy axis was discretized into energies spaced 0.1σ apart spanning an energy interval of 10 σ, suitably placed on the energy axis depending on the problem. The solutions plotted in Fig. 2 were obtained from 2×100 time steps where the temperature is changed in each step. In two dimensions the percolation energy [Eq. (14)] is given by $E_c = 0.235\sigma$.

---

[1]G. Tammann, *Der Glaszustand* (Voss, Leipzig, 1933).
[2]W. Kauzmann, Chem. Rev. **43**, 219 (1948).
[3]R. O. Davies and G. O. Jones, Adv. Phys. **2**, 370 (1953).
[4]M. Goldstein, in *Modern Aspects of the Vitreous State*, edited by J. D. Mackenzie (Butterworths Scientific, London, 1964), p. 90.
[5]C. A. Angell and W. Sichina, Ann. N.Y. Acad. Sci. **279**, 53 (1976).

[6]E. Donth, *Glasübergang* (Akademie-Verlag, Berlin, 1981).

[7]C. A. Angell, in *Relaxations in Complex Systems*, edited by K. L. Ngai and G. B. Wright (Government Printing Office, Washington, DC, 1985), p. 3.

[8]S. Brawer, *Relaxation in Viscous Liquids and Glasses* (American Ceramic Society, Columbus, OH, 1985).

[9]G. W. Scherer, *Relaxation in Glass and Composites* (Wiley, New York, 1986).

[10]J. Jäckle, Rep. Prog. Phys. 49, 171 (1986).

[11]C. A. Angell, J. Non-Cryst. Solids 131-133, 13 (1991).

[12]F. Yonezawa, in *Solid State Physics: Advances in Research and Applications*, edited by H. Ehrenreich and D. Turnbull (Academic, New York, 1991), Vol. 45, p. 179.

[13]A. Hunt, J. Non-Cryst. Solids 160, 183 (1993).

[14]I. M. Hodge, J. Non-Cryst. Solids 169, 211 (1994).

[15]H. Rawson, *Properties and Applications of Glass* (Elsevier, Amsterdam, 1980).

[16]C. A. Angell, J. Phys. Chem. 70, 2793 (1966).

[17]A. J. Kovacs, Fortschr. Hochpoly.-Forsch. 3, 394 (1963).

[18]J. D. Ferry, *Viscoelastic Properties of Polymers*, 3rd ed. (Wiley, New York, 1980).

[19]H. S. Chen, Rep. Prog. Phys. 43, 353 (1980).

[20]A. J. Barlow, J. Lamb, and A. J. Matheson, Proc. R. Soc. London, Ser. A 292, 322 (1966).

[21]G. Harrison, *The Dynamic Properties of Supercooled Liquids* (Academic, New York, 1976).

[22]C. A. Angell, J. H. R. Clarke, and L. V. Woodcock, Adv. Chem. Phys. 48, 397 (1981).

[23]J.-P. Hansen, Physica A 201, 138 (1993).

[24]K. Binder and A. P. Young, Rev. Mod. Phys. 58, 801 (1986).

[25]V. S. Dotsenko, Usp. Fiz. Nauk 163, 1 (1993) [Phys. Usp. 36, 455 (1993)].

[26]W. Götze and L. Sjögren, Rep. Prog. Phys. 55, 241 (1992).

[27]S. P. Das and G. F. Mazenko, Phys. Rev. A 34, 2265 (1986).

[28]Second International Discussion Meeting on Relaxations in Complex Systems, Alicante, Spain, 1993, edited by K. L. Ngai, E. Riande, and G. B. Wright [J. Non-Cryst. Solids 172-174, 1–1457 (1994)].

[29]G. W. Scherer, J. Non-Cryst. Solids 123, 75 (1990).

[30]C. A. Angell, J. Phys. Chem. Solids 49, 863 (1988).

[31]J. Jäckle, in *Structure, Relaxation, and Physical Aging of Glassy Polymers*, edited by R. J. Roe and J. M. O'Reilly, MRS Symposia Proceedings No. 215 (Materials Research Society, Pittsburgh, 1991), p. 151.

[32]B. Derrida, Phys. Rev. Lett. 45, 79 (1980).

[33]G. H. Fredrickson, Ann. Rev. Phys. Chem. 39, 149 (1988).

[34]T. A. Weber, G. H. Fredrickson, and F. H. Stillinger, Phys. Rev. B 34, 7641 (1986).

[35]J. H. Gibbs and E. A. DiMarzio, J. Chem. Phys. 28, 373 (1958).

[36]G. Adam and J. H. Gibbs, J. Chem. Phys. 43, 139 (1965).

[37]P. D. Gujrati and M. Goldstein, J. Chem. Phys. 74, 2596 (1981).

[38]C. A. Angell and K. J. Rao, J. Chem. Phys. 57, 470 (1972).

[39]M. Goldstein, Faraday Symp. Chem. Soc. 6, 7 (1972).

[40]G. S. Grest and M. H. Cohen, Adv. Chem. Phys. 48, 455 (1981).

[41]N. G. van Kampen, *Stochastic Processes in Physics and Chemistry* (North-Holland, Amsterdam, 1981).

[42]M. Goldstein, J. Chem. Phys. 51, 3728 (1969).

[43]S. A. Brawer, J. Chem. Phys. 81, 954 (1984).

[44]J. C. Dyre, Phys. Rev. Lett. 58, 792 (1987).

[45]H. Bässler, Phys. Rev. Lett. 58, 767 (1987).

[46]R. Richert and H. Bässler, J. Phys.: Condens. Matter 2, 2273

(1990).

[47]J. W. Haus and K. W. Kehr, Phys. Rep. 150, 263 (1987).

[48]J. C. Dyre, Phys. Rev. B 49, 11 709 (1994).

[49]H. Bässler, in *Advances in Disordered Semiconductors*, edited by H. Fritzsche and M. Pollak (World Scientific, Singapore, 1990), p. 491.

[50]J. H. Simmons and P. B. Macedo, J. Res. Nat. Bureau Stand. 75A, 175 (1971).

[51]H. Tweer, J. H. Simmons, and P. B. Macedo, J. Chem. Phys. 54, 1952 (1971).

[52]T. A. Litovitz, J. Chem. Phys. 20, 1088 (1952).

[53]V. I. Arkhipov and H. Bässler, J. Phys. Chem. 98, 662 (1994).

[54]A. Hunt, Int. J. Theor. Phys. B 8, 855 (1994).

[55]W. Kauzmann, Rev. Mod. Phys. 14, 12 (1942).

[56]T. Alfrey, *Mechanical Properties of High Polymers* (Interscience, New York, 1948).

[57]G. Williams, in *Dielectric and Related Molecular Processes*, edited by M. Davies (Chemical Society, London, 1975), p. 151.

[58]E. Donth, J. Non-Cryst. Solids 53, 325 (1982).

[59]F. H. Stillinger, J. Chem. Phys. 89, 6461 (1988).

[60]R. V. Chamberlin, Phys. Rev. B 48, 15 638 (1993).

[61]G. Wahnström, Phys. Rev. A 44, 3752 (1991).

[62]R. D. Mountain and D. Thirumalai, Phys. Rev. A 45, R3380 (1992).

[63]F. H. Stillinger and T. A. Weber, Science 225, 983 (1984).

[64]F. H. Stillinger, Phys. Rev. B 41, 2409 (1990).

[65]M. Doi and S. F. Edwards, *The Theory of Polymer Dynamics* (Clarendon, Oxford, 1986).

[66]W. Hess and R. Klein, Adv. Phys. 32, 173 (1983).

[67]H. Löwen, J.-P. Hansen, and J.-N. Roux, Phys. Rev. A 44, 1169 (1991).

[68]H. Eyring, J. Chem. Phys. 4, 283 (1936).

[69]P. G. Wolynes, Acc. Chem. Res. 25, 513 (1992).

[70]M. B. Isichenko, Rev. Mod. Phys. 64, 961 (1992).

[71]S. Kirkpatrick, Rev. Mod. Phys. 45, 574 (1973).

[72]K. Huang, *Statistical Mechanics* (Wiley, New York, 1963).

[73]A. Miller and E. Abrahams, Phys. Rev. 120, 745 (1960).

[74]V. Ambegaokar, B. I. Halperin, and J. S. Langer, Phys. Rev. B 4, 2612 (1971).

[75]B. I. Shklovskii and A. L. Efros, Zh. Eksp. Teor. Fiz. 60, 867 (1971) [Sov. Phys. JETP 33, 468 (1971)].

[76]D. Stauffer and A. Aharony, *Introduction to Percolation Theory*, 2nd ed. (Taylor and Francis, London, 1992).

[77]V. I. Arkhipov, M. S. Iovu, A. I. Rudenko, and S. D. Shutov, Phys. Status Solidi A 54, 67 (1979).

[78]J. Orenstein, M. A. Kastner, and V. Vaninov, Philos. Mag. B 46, 23 (1982).

[79]R. E. Robertson, R. Simha, and J. G. Curro, Macromolecules 17, 911 (1984).

[80]G. J. M. Koper and H. J. Hilhorst, Europhys. Lett. 3, 1213 (1987).

[81]E. I. Shakhnovich and A. M. Gutin, Europhys. Lett. 9, 569 (1989).

[82]J. C. Dyre (unpublished).

[83]G. Arfken, *Mathematical Methods for Physicists* (Academic, New York, 1985).

[84]C. T. Moynihan, A. J. Easteal, M. A. DeBolt, and J. Tucker, J. Am. Ceram. Soc. 59, 12 (1976).

[85]J. C. Dyre, Key Eng. Mater. 13-15, 501 (1987).

[86]W. Tschöp and R. Schilling, Phys. Rev. E 48, 4221 (1993).

[87]J. C. Dyre, J. Appl. Phys. 64, 2456 (1988).

[88]H. Frauenfelder, S. G. Sligar, and P. G. Wolynes, Science 254, 1598 (1991).

[89]C. Aslangul, N. Pottier, and D. Saint-James, Physica A **164**, 52 (1990).

[90]R. Tao, Phys. Rev. A **43**, 5284 (1991).

[91]A. B. Kolomeisky and E. B. Kolomeisky, Phys. Rev. A **45**, R5327 (1992).

[92]M. D. Bal'makov, Fiz. Khim. Stekla **12**, 527 (1986) [Sov. J. Glass Phys. Chem. **12**, 279 (1986)].

[93]R. D. Young, J. Chem. Phys. **98**, 2488 (1993).

[94]Y. Hiwatari, J. Chem. Phys. **76**, 5502 (1982).

[95]A. Hunt, Solid State Commun. **84**, 701 (1992).

[96]M. F. Thorpe, J. Non-Cryst. Solids **57**, 355 (1983).

[97]M. Silver, G. Schönherr, and H. Bässler, Phys. Rev. Lett. **48**, 352 (1982).

[98]H. Bässler, Prog. Colloid Polym. Sci. **80**, 35 (1989).

[99]M. Goldstein, J. Chem. Phys. **64**, 4767 (1976).

[100]B. Ries, H. Bässler, M. Grünewald, and B. Movaghar, Phys. Rev. B **37**, 5508 (1988).

[101]A. R. Dexter and A. J. Matheson, Adv. Mol. Relaxation Processes **2**, 251 (1972).

[102]S. V. Nemilov, Fiz. Khim. Stekla **2**, 193 (1976) [Sov. J. Glass Phys. Chem. **2**, 187 (1976)].

[103]S. V. Nemilov, Fiz. Khim. Stekla **4**, 129 (1978) [Sov. J. Glass Phys. Chem. **4**, 113 (1978)].

[104]T. A. Vilgis, Phys. Rev. B **47**, 2882 (1993).

[105]R. Böhmer, J. Non-Cryst. Solids **172-174**, 628 (1994).

[106]G. M. Bartenev, *The Structure and Mechanical Properties of Inorganic Glasses* (Wolters-Noordhoff, Groningen, 1970).

[107]M. R. J. Gibbs, J. E. Evetts, and J. A. Leake, J. Mater. Sci. **18**, 278 (1983).

[108]A. van den Beukel, S. van der Zwaag, and A. L. Mulder, Acta Metall. **32**, 1895 (1984).

[109]O. V. Mazurin, J. Non-Cryst. Solids **25**, 130 (1977).

[110]G. P. Johari and E. Whalley, Faraday Symp. Chem. Soc. **6**, 23 (1972).

[111]R. Zwanzig, J. Chem. Phys. **88**, 5831 (1988).

[112]T. Christensen and N. B. Olsen, Phys. Rev. B **49**, 15396 (1994); (unpublished).

[113]S. V. Nemilov, Fiz. Khim. Stekla **11**, 146 (1985) [Sov. J. Glass Phys. Chem **11**, 97 (1985)].

[114]K. D. Jensen and J. Nielsen (unpublished).

[115]T. Christensen, J. Phys. (Paris) Colloq. **46**, C8-635 (1985).

[116]N. O. Birge and S. R. Nagel, Phys. Rev. Lett. **54**, 2674 (1985).

[117]J. C. Dyre (unpublished).

[118]V. Rosato and G. Williams, Adv. Mol. Relaxation Processes **20**, 233 (1981).

Local elastic expansion model for viscous-flow activation energies of glass-forming molecular liquids

Jeppe C. Dyre, Niels Boye Olsen, and Tage Christensen

Department of Mathematics and Physics (IMFUFA), Roskilde University, P.O. Box 260, DK-4000 Roskilde, Denmark

(Received 27 June 1995; revised manuscript received 15 August 1995)

A model for the viscosity of glass-forming molecular liquids is proposed in which a "flow event" requires a local volume increase. The activation energy for a flow event is identified with the work done in shoving aside the surrounding liquid; this work is proportional to the high-frequency shear modulus, which increases as the temperature decreases. The model is confirmed by experiments on a number of molecular liquids.

Glass formation is a universal property of supercooled liquids.[1-9] For simple liquids rapid cooling is required to avoid crystallization. For most complex liquids supercooling causes no problems; in fact, many complex liquids are difficult to crystallize. The glass transition takes place when the viscosity of the supercooled liquid becomes so large that molecular motion is arrested. The laboratory glass transition is dynamic and not a phase transition, although many workers in the field believe it to be a manifestation of an underlying equilibrium second-order phase transition. For cooling rates of order Kelvin per minute, the glass transition takes place when the viscosity, η, is around 10^{13} poise (P). In the following, the glass transition temperature, T_g, is defined as the temperature at which $\eta = 10^{13}$ P.

The linear shear mechanical properties of a liquid are determined by the shear modulus as function of frequency, $G(\omega) = G'(\omega) + iG''(\omega)$. At low frequencies $G(\omega) = i\omega\eta$. At high frequencies liquid becomes solidlike and $G(\omega)$ approaches a limiting value, $\lim_{\omega\to\infty} G(\omega) = G_\infty$. In terms of η and G_∞, the average shear relaxation time, τ, is given[3] by Maxwell's expression

$$\tau = \frac{\eta}{G_\infty}. \qquad (1)$$

For all viscous liquids τ and η depend dramatically on temperature, varying often more than ten decades over a temperature range quite narrow compared to T_g. G_∞ depends much less on temperature, usually increasing less than a factor of 4 upon cooling in the same temperature range. This variation, on the other hand, is considerably larger than that found in simple nonviscous liquids or in crystals and glasses.

Intimately linked to the problem of understanding the glass transition is the problem of the temperature dependence of viscosity: Upon cooling the viscosity increases more than expected from a simple Arrhenius law (exceptions to this are SiO_2 and GeO_2). There is still no consensus regarding what causes the non-Arrhenius temperature dependence of viscosity. The two most important phenomenological models are the free volume model of Grest and Cohen,[10] and the entropy model of Gibbs and co-workers.[11,12] In the free volume model, the viscosity is controlled by the volume available for molecular rearrangements, which decreases with decreasing temperature. In the entropy model, the increase in viscosity upon cooling is caused by the decrease in the configurational

entropy.[13] In the less viscous regime, the non-Arrhenius viscosity is explained by mode-coupling theories.[14,15]

It is generally believed that flow in viscous liquids proceeds via sudden flow events involving several molecules.[3,10,12,16-21] In terms of the free energy barrier to be overcome, $\Delta F(T)$, the temperature dependence of the viscosity is given by

$$\eta = \eta_0 \exp\left[\frac{\Delta F(T)}{k_B T}\right]. \qquad (2)$$

According to Eq. (2) the non-Arrhenius temperature dependence of the viscosity arises because $\Delta F(T)$ increases as the temperature decreases. The problem is to explain why.

In molecular liquids van der Waals forces (and possibly hydrogen bonding) are present between the molecules. The starting point for the present model is the fact that the repulsions between the molecules are strong, while the attractions are only weak. Many properties of simple liquids derive from this fact.[22] In a viscous liquid a flow event involves a significant rearrangement of a number of densely packed molecules. If the flow event takes place at a constant volume, the molecules are forced into close contact. Because of the strong repulsions between the molecules, this is energetically very costly. Alternatively, the molecules may shove aside the surrounding liquid to increase the volume available for rearranging. This must be less costly than rearranging at a constant volume; consequently, the new model is based on "shoving" flow events.

The barrier height has two contributions, one from shoving aside the surrounding liquid and one from separating the flow event molecules. In a harmonic solid, as is easy to show, the two contributions are of the same order of magnitude, but the relative distance changes between the flow event molecules are too large for using the harmonic approximation. Since the attractive forces are only weak, the energy cost for separating the flow event molecules is considerably lower than estimated from the harmonic approximation. We ignore this contribution and identify $\Delta F(T)$ with the shoving work done on the surrounding liquid.

Like any thermally activated transition, a flow event is a rapid process. During the shoving the surrounding liquid behaves like a solid, and the shoving work depends linearly on the infinite-frequency bulk and shear moduli, K_∞ and G_∞. To
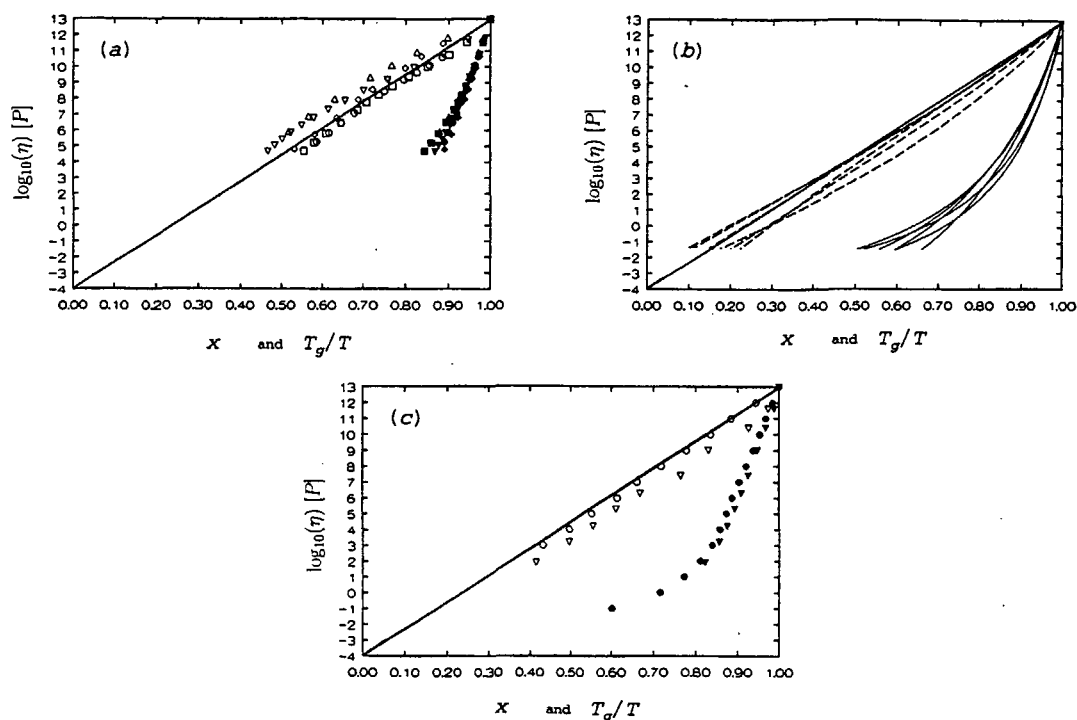
FIG. 1. Logarithm of the viscosity in Poise as function of T_g/T and as function of the variable $x \approx G_\infty(T)/T$ normalized to one at $T = T_g$: $x = [G_\infty(T)T_g]/[G_\infty(T_g)T]$. According to the model the logarithm of the viscosity depends linearly on x [Eqs. (2) and (3)]. In each subfigure the diagonal line joins the point $x = 1$ and $\log_{10}(\eta) = 13$ with the point $x = 0$ and $\log_{10}(\eta) = -4$. The former point defines the glass transition and the latter corresponds to the viscosity prefactor of Eq. (2), η_0, equal to 10^{-4} P (a typical prefactor, corresponding to the shear relaxation time close to an average period of vibration) [Ref. 24]. The subfigures give data where $G_\infty(T)$ was obtained from extrapolations of measurements in different frequency ranges (a) mHz–kHz; (b) MHz; (c) GHz. (a) shows our data for five molecular liquids. These liquids all accurately obey the time-temperature superposition principle for the shear modulus (except for a β component with a magnitude less than 10%). Consequently, the Kramers-Kronig sum rule $G_\infty = (2/\pi) \int_{-\infty}^{\infty} G''(\omega) d \ln\omega$ implies that G_∞ is proportional to the maximum loss, G''_{max}, which makes it possible to evaluate the variable x directly from data without any analytical extrapolation: $x = [G''_{max}(T)T_g]/[G''_{max}(T_g)T]$. In (a) the full symbols give the viscosity as function of T_g/T and the open symbols give the viscosity as function of x. The figure shows data for 4-methylpentan-2-ol ($\triangle$), dioctyl phthalate ($\square$), phenyl salicylate (salol) (O), dibutyl phthalate (∇), and the silicone oil MS704 ($\Diamond$). (b) gives the data of Barlow et al. (Ref. 28), where G_∞ was obtained from extrapolations of ultrasonic measurements (Ref. 2). The full curves give the viscosities as function of T_g/T and the dashed curves give the viscosities as function of x for the following six molecular liquids: isopropyl benzene, n-propyl benzene, sec.-butyl benzene, di(isobutyl)phthalate, di(n-butyl)phthalate, di(2-ethyl hexyl)phthalate. (c) gives data where G_∞ was obtained from depolarized Brillouin scattering. As in (a) the full symbols give the viscosity as function of T_g/T and the open symbols give the viscosity as function of x. The figure shows data for 5-phenyl-4-ether (O) (Ref. 42) and for α-phenyl-o-cresol (∇) (Refs. 43 and 44).

be specific, we assume that shoving increases the volume of the flow event molecules from a sphere to a larger sphere. According to elasticity theory[23] this induces a radial displacement in the surroundings, u_r, varying as $u_r \propto r^{-2}$. This is a pure shear displacement ($\nabla \cdot u = 0$ as for the Coulomb field) and therefore the shoving work is independent of K_∞ and proportional to G_∞. The constant of proportionality will be referred to as the characteristic volume, V_c. For simplicity V_c is assumed to be temperature independent, and thus

$$\Delta F(T) = G_\infty(T) V_c. \qquad (3)$$

The characteristic volume is not equal to the volume change during shoving, the activation volume, ΔV. For small acti-

vation volume it is easy to show that V_c is given by (where V is the volume before the shoving)

$$V_c = \frac{2}{3} \frac{(\Delta V)^2}{V}. \qquad (4)$$

Since $G_\infty(T)$ increases upon cooling, the model predicts a non-Arrhenius viscosity with an activation energy that increases as the glass transition is approached. This is what is observed in experiments. On the other hand, the model is inconsistent with the popular Vogel-Fulcher-Tammann expression,[6,7] where the viscosity diverges at a finite temperature (unless one accepts that G_∞ may become infinite which seems unphysical).

According to the new model the logarithm of the viscosity depends linearly on $G_\infty(T)/T$. Figure 1 compares this prediction to experiments in Angell's fragility plots[24] where the logarithm of the viscosity (in poise) is plotted as function of $x \propto 1/T$, and as function of $x \propto G_\infty(T)/T$ (both x coordinates are normalized to one at $T = T_g$). We have measured $G(\omega)$ for five molecular liquids using the piezoelectric shear modulus gauge transducer (PSG) consisting of three piezoceramic discs,[25] a device based on principles similar to those of the bulk modulus transducer.[26] With recent improvements[27] the PSG is now able to provide shear modulus data in the frequency range 1 mHz–50 kHz. Figure 1(a) shows our results for the viscosity as function of T_g/T (full symbols) and as function of x (open symbols). The line connects the point $x=1$ and $\log_{10}\eta = 10^{13}$ (defining the glass transition) with the point $x=0$ and $\log_{10}\eta = 10^{-4}$ [a typical viscosity prefactor, corresponding to the average shear relaxation time of Eq. (1) close to an average period of vibration[24]]. The results of Fig. 1(a), while favorable for the model, ignore possible additional high-frequency relaxations outside the frequency range covered by the PSG. To investigate whether high-frequency methods for measuring G_∞ confirm our findings, we plot data taken from the literature in Figs. 1(b) and 1(c). Figure 1(b) presents the data of Barlow et al.[28] for G_∞ obtained from ultrasonic measurements working in the MHz range. Figure 1(c) presents data where G_∞ was obtained from depolarized Brillouin scattering, a technique that operates in the GHz range.

Given the uncertainties in evaluating G_∞ and the crudeness of the new model, Fig. 1 shows a satisfactory agreement between the model and experiment for molecular liquids. We have also compared the model to Brillouin data for two nonmolecular liquids,[29] B_2O_3 and $Ca_{0.4}K_{0.6}(NO_3)_{1.4}$ (CKN). For B_2O_3, G_∞ is too dependent on temperature to account for the rather weak non-Arrhenius viscosity. However, viscous flow of B_2O_3 involves the breaking of covalent bonds, which goes beyond the present model. For CKN the model works well for the temperature dependence of the conductivity relaxation time [which decouples from the viscosity close to T_g (Ref. 30)], but the model is not able to fully explain the dramatic non-Arrhenius viscosity.

We now briefly discuss related work. The idea that volume is needed for a flow event to take place is old; this is the basic idea behind the free volume model.[10] Here, however, the problematic concept of a "free" volume is extraneous. The present picture is more closely related to that of Brawer, who assumed that the transition state for a flow event is a low-density state with room for the molecules to rearrange.[3] In his approach, the activation energy was taken to be a function of the energy of the flow event molecules, and the shoving work is ignored.[3,19] The model proposed here is very similar to that used by Fourkas, Benigno, and Berg[31,32] for explaining the hole-burning spectra and the time-dependent Stokes' shift of a nonpolar solute molecule in a glass-forming solvent. These authors argued that an electronic excitation increases the effective size of the solute molecule, and showed that the viscoelastic response of the surrounding solvent changes the transition energy and causes a time-dependent Stokes' shift. Equation (3) appeared in 1968 in two papers by Nemilov[33,34] in a version where $V_c = V$. Nemilov used Eq. (3) for calculating the rate of flow of optical silicate glasses. He justified Eq. (3) by substituting Eyring's expression for η (Ref. 35) and Dushman's expression for τ (Ref. 36) into Eq. (1). Buchenau and Zorn[37,38] found empirically that the viscosity of selenium follows the expression $\eta = \eta_0 \exp[u_0^2/\langle u^2 \rangle_{loc}]$, where $\langle u^2 \rangle_{loc}$ is the atomic mean-square displacement for the vibrational motions in the liquid minus the same quantity for the crystal (at the same temperature). This result is related to, but not identical to, that of the present model: If the high-frequency bulk and shear moduli are identical (denoted by M_∞) and the interatomic harmonic potential is denoted by $(1/2)m\omega^2 u^2$, the equipartition theorem implies that $\omega^2 \langle u^2 \rangle \propto T$. The sound velocity is proportional to ω and to $M_\infty^{1/2}$. Combining these facts: $M_\infty \langle u^2 \rangle \propto T$ and thus Eqs. (2) and (3) imply $\eta \propto \exp[C/\langle u^2 \rangle]$. If the difference between $\langle u^2 \rangle_{loc}$ and $\langle u^2 \rangle$ is ignored, this is the result of Buchenau and Zorn. As shown by Hall and Wolynes[39] the relation $\eta \propto \exp[C/\langle u^2 \rangle]$ may be derived by assuming a fixed distance between two minima for harmonic potentials: The energy difference between one minimum and the intersection of the two harmonic potentials varies as ω^2, which is proportional to $T/\langle u^2 \rangle$. A convincing example of this relation between an activation energy and a phonon frequency was given by Köhler and Herzig,[40] who were able to explain a number of anomalies in self-diffusion in bcc metals. In their model, the fact that the activation energy for self-diffusion in bcc metals decreases as the temperature decreases, is due to softening of the 111 phonon. Finally, Miles, Le, and Kivelson in a study of the pressure dependence of the sound velocity in triphenylphosphite found that the transverse sound velocity is solely a function of the viscosity.[41] While their measurements were performed in the less viscous regime, this result is what is expected from the present model (although here viscosity is a function of the transverse sound velocity instead of vice versa), ignoring an insignificant factor T.

[1] W. Kauzmann, Chem. Rev. 43, 219 (1948).
[2] G. Harrison, The Dynamic Properties of Supercooled Liquids (Academic, New York, 1976).
[3] S. Brawer, Relaxation in Viscous Liquids and Glasses (American Ceramic Society, Columbus, Ohio, 1985).
[4] J. Jäckle, Rep. Progr. Phys. 49, 171 (1986).
[5] C. A. Angell, J. Phys. Chem. Solids 49, 863 (1988).
[6] G. W. Scherer, J. Non-Cryst. Solids 123, 75 (1990).
[7] C. A. Angell, J. Non-Cryst. Solids 131-133, 13 (1991).
[8] A. Hunt, J. Non-Cryst. Solids 160, 183 (1993).
[9] I. M. Hodge, J. Non-Cryst. Solids 169, 211 (1994).
[10] G. S. Grest and M. H. Cohen, Adv. Chem. Phys. 48, 455 (1981).
[11] J. H. Gibbs and E. A. DiMarzio, J. Chem. Phys. 28, 373 (1958).
[12] G. Adam and J. H. Gibbs, J. Chem. Phys. 43, 139 (1965).
[13] E. A. DiMarzio, Ann. N.Y. Acad. Sci. 371, 1 (1981).
[14] S. P. Das and G. F. Mazenko, Phys. Rev. A 34, 2265 (1986).

[15] W. Götze and L. Sjögren, Rep. Progr. Phys. 55, 241 (1992).

[16] M. Goldstein, J. Chem. Phys. 51, 3728 (1969).

[17] G. Williams, in *Dielectric and Related Molecular Processes, Specialist Periodical Report, Vol. 2*, edited by M. Davies (Chemical Society, London, 1975), p. 151.

[18] E. Donth, *Glasübergang* (Akademie-Verlag, Berlin, 1981).

[19] J. C. Dyre, Phys. Rev. Lett. 58, 792 (1987).

[20] F. H. Stillinger, J. Chem. Phys. 89, 6461 (1988).

[21] R. V. Chamberlin, Phys. Rev. B 48, 15 638 (1993).

[22] D. Chandler, J. D. Weeks, and H. C. Andersen, Science 220, 787 (1983).

[23] L. D. Landau and E. M. Lifshitz, *Theory of Elasticity*, 2nd ed. (Pergamon, London, 1970).

[24] C. A. Angell, in *Relaxations in Complex Systems*, edited by K. L. Ngai and G. B. Wright (U.S. G.P.O., Washington, DC, 1985), p. 3.

[25] T. Christensen and N. B. Olsen, J. Non-Cryst. Solids 172-174, 357 and 362 (1994).

[26] T. Christensen and N. B. Olsen, Phys. Rev. B 49, 15 396 (1994).

[27] T. Christensen and N. B. Olsen, Rev. Sci. Instrum. 66, 5019 (1995).

[28] A. J. Barlow, J. Lamb, A. J. Matheson, P. R. K. L. Padmini, and J. Richter, Proc. R. Soc. London Ser. A 298, 467 (1967).

[29] M. Grimsditch, R. Bhadra, and L. M. Torell, Phys. Rev. Lett. 62, 2616 (1989).

[30] F. S. Howell, R. A. Bose, P. B. Macedo, and C. T. Moynihan, J. Phys. Chem. 78, 639 (1974).

[31] J. T. Fourkas, A. Benigno, and M. Berg, J. Chem. Phys. 99, 8552 (1993).

[32] J. T. Fourkas, A. Benigno, and M. Berg, J. Non-Cryst. Solids 172-174, 234 (1994).

[33] S. V. Nemilov, Dokl. Akad. Nauk SSSR 181, 1427 (1968).

[34] S. V. Nemilov, Zh. Fiz. Khim. 42, 1391 (1968) [Russ. J. Phys. Chem. 42, 726 (1968)].

[35] H. Eyring, J. Chem. Phys. 4, 283 (1936).

[36] S. Dushman, J. Franklin Inst. 184, 515 (1920).

[37] U. Buchenau and R. Zorn, Europhys. Lett. 18, 523 (1992).

[38] U. Buchenau, Philos. Mag. B 65, 303 (1992).

[39] R. W. Hall and P. G. Wolynes, J. Chem. Phys. 86, 2943 (1987).

[40] U. Köhler and C. Herzig, Philos. Mag. A 58, 769 (1988).

[41] D. G. Miles, Jr., N. Le, and D. Kivelson, J. Chem. Phys. 90, 5327 (1989).

[42] C. T. Moynihan, P. B. Macedo, C. J. Montrose, P. K. Gupta, M. A. DeBolt, J. F. Dill, B. E. Dom, P. W. Drake, A. J. Easteal, P. B. Elterman, R. P. Moeller, H. Sasabe, and J. A. Wilder, Ann. N.Y. Acad. Sci. 279, 15 (1976).

[43] C. H. Wang, R.-J. Ma, and Q.-L. Liu, J. Chem. Phys. 80, 617 (1984).

[44] W. T. Laughlin and D. R. Uhlmann, J. Phys. Chem. 76, 2317 (1972).

Unified formalism for excess current noise in random-walk models

Jeppe C. Dyre

Institute of Mathematics and Physics (IMFUFA), Roskilde University, Postbox 260, DK-4000 Roskilde, Denmark
(Received 23 September 1987; revised manuscript received 27 January 1988)

Excess current noise in random-walk models with a frequency-independent conductivity is studied from a general point of view. By introducing a "dynamical" diffusion constant, it is shown that the current autocorrelation function in an external field probes the equilibrium dynamical diffusion-constant autocorrelation function. From this a number of results, previously shown for particular models, are derived. Also, it is shown that the external-field current autocorrelation function is proportional to the equilibrium autocorrelation function for the absolute value of the current. Thus, the excess-noise spectrum probes the equilibrium-speed autocorrelation function. In the treatment advanced here, the study of excess current noise in random-walk models reduces to a study of the stochastic point process constituted by the particle-jump times. This point process contains all information about the noise. As an illustration of the general theory, the continuous-time random-walk model is briefly reviewed and a simple derivation of the excess noise in the model is given. Finally, the role of Fermi statistics in models for $1/f$ noise is discussed. It is argued that number-fluctuation models, i.e., models with long trapping times, are incompatible with Fermi statistics. On the other hand, it is shown there is a peculiar "single-particle" $1/f$ noise which is due to Fermi statistics but has nothing to do with the observed $1/f$ current noise.

I. INTRODUCTION

Electrical $1/f$ noise has been a major puzzle in solid-state physics for many years and is still far from being understood.[1-11] This noise is found at low frequencies in apparently any conducting solid in an external electric field. $1/f$ noise is always observed together with white noise, the origin of which is well understood, and therefore $1/f$ noise is often referred to as excess noise. One may speak of excess current noise in a constant-voltage circuit or excess voltage noise in a constant-current circuit. The spectra of the two are always identical and only excess current noise will be discussed here.

Experimentally, the spectrum of excess current noise is given by

$$S_{\text{exc},J}(\omega) = K \frac{\langle J \rangle_E^2}{V} \omega^{-\alpha} , \tag{1}$$

where $\langle J \rangle_E$ is the average current in the electric field E, V is the volume of the sample, K is a constant, and the exponent α is close to 1. The case $\alpha = 1$ has given the name to the subject: $1/f$ noise, where f is the frequency. The fact that the noise is proportional to $\langle J \rangle_E^2$ suggests it is the resistance that fluctuates and consequently one often speaks about $1/f$ resistance fluctuations. If the resistance really fluctuates, however, there should be $1/f$ fluctuations in the magnitude of the Nyquist noise in zero external field. This was shown actually to be the case by Voss and Clarke in 1976.[12] Their work was a major breakthrough because it showed that $1/f$ noise is an equilibrium phenomenon and is not created by the rather strong electric fields usually applied when measuring $1/f$ excess noise. The Voss and Clarke experiment raised the obvious question: How can noise fluctuate, being itself

due to fluctuations? It was soon shown that fluctuations in the magnitude of the Nyquist noise are due to nontrivial *fourth*-order correlations in the equilibrium current or voltage fluctuations,[13,14] implying these fluctuations are non-Gaussian.

During the 1980's there has been considerable interest in random-walk models for $1/f$ noise. These models are probably the simplest one can think of as a means of getting a better understanding of the purely statistical properties of the noise. In particular, the appearance of non-Gaussian equilibrium current fluctuations can be studied in detail. In Sec. II of the present paper we study general features of the current noise in random-walk models. The treatment is centered around the concept of a "dynamical" diffusion constant. In Sec. III the continuous-time random-walk (CTRW) model for $1/f$ noise is briefly reviewed as an illustration of the general theory. Finally, Sec. IV contains a discussion where the role of Fermi statistics for the application of random-walk models is emphasized. It is argued that any model for $1/f$ noise based on long trapping times, including the CTRW model in its multiple trapping realization, is incompatible with Fermi statistics and is therefore unrealistic.

II. EXCESS CURRENT NOISE
IN RANDOM-WALK MODELS

To simplify the discussion we consider just one particle which performs a random walk in one dimension on a lattice with lattice constant a. No assumption is made about the underlying dynamics which does not have to be Markovian. It is assumed that the direction of any single jump is random; via the fluctuation-dissipation theorem this ensures a frequency-independent conductivity. If the

particle jumps at times τ_i we assign to it a dynamical diffusion constant $D(t)$ defined by

$$D(t)=\frac{a^2}{2}\sum_i \delta(t-\tau_i) . \tag{2}$$

$D(t)$ is characterized by

$$\langle v(t)v(t')\rangle_{re}=2D(t)\delta(t-t') , \tag{3}$$

where v is the velocity, or

$$D(t)=\int_0^{\infty}\langle v(t)v(t+\tau)\rangle_{re}d\tau . \tag{4}$$

Here, $\langle\ \rangle_{re}$ denotes a "restricted ensemble average" by which is meant an average over all trajectories with the same $D(t)$, i.e., with the same jump times. The time average of $D(t)$ is the ordinary diffusion constant D:

$$D=\langle D(t)\rangle=\lim_{T_0\to\infty}\frac{1}{T_0}\int_0^{T_0}D(t)dt . \tag{5}$$

The relevance of $D(t)$ to the excess current noise becomes clear when the current in an external electric field is evaluated. In a weak field it is slightly more probable for the particle to jump to one side than to the other. To lowest order in E the total jump probability does not change, however, and the particle still jumps at times τ_i. The restricted ensemble average current is thus proportional to the equilibrium $D(t)$:

$$\langle J(t)\rangle_{E,re}=\frac{q^2E}{kT}D(t) , \tag{6}$$

where q is the particle charge, and k and T have their usual meaning. The constant of proportionality follows from requiring the time average of Eq. (6) to obey the Nernst-Einstein relation. The measured current noise is the cosine transform of the current autocorrelation function. Since the currents at different times within the restricted ensemble are uncorrelated, one has

$$\langle J(t)J(0)\rangle_{E,re}=\langle J(t)\rangle_{E,re}\langle J(0)\rangle_{E,re}$$
$$=\left[\frac{q^2E}{kT}\right]^2 D(t)D(0)\quad (t>0) . \tag{7}$$

When averaged over the whole ensemble of possible jump times this leads to

$$\langle J(t)J(0)\rangle_E=\left[\frac{q^2E}{kT}\right]^2\langle D(t)D(0)\rangle\quad (t>0) , \tag{8}$$

where $\langle\ \rangle$ on the right-hand side denotes an equilibrium average. To obtain the total current autocorrelation function one should add to this expression a white-noise term proportional to $\delta(t)$. This term is not of interest here. According to Eq. (8) the excess noise measures the spectrum of dynamical diffusion constant fluctuations in equilibrium.

The autocorrelation function $\langle D(t)D(0)\rangle$ has a simple physical interpretation. From Eq. (2) it follows immediately that

$$\langle D(t)D(0)\rangle=\frac{Da^2}{2}p(t\mid 0)\quad (t>0) , \tag{9}$$

where $p(t\mid 0)$ denotes the probability density for a jump at time t given the particle jumped at $t=0$. Except for a numerical constant, low-frequency excess noise is thus the cosine transform of $p(t\mid 0)$.[15] $1/f$ noise implies long-time correlations in this probability. The particle or the medium in which it jumps somehow has a long-term memory. For an ordinary random walk, on the other hand, $p(t\mid 0)$ is constant and there is no excess noise.

Generalizing the above results to more than one particle is straightforward. Assuming the particles are independent and noninteracting, one just lets τ_i denote the collection of jump times for all the particles. In generalizing to d dimensions the factor 2 in Eq. (2), etc., should be replaced by $2d$. Equations like (6) and (8) apply unchanged where J is now, of course, the component of the current in the direction of the field. No new features appear and in the rest of the paper only the one-dimensional case will be considered. The important thing, which is independent of the dimension and number of particles, is that all information about the noise lies in the statistical properties of the collection of jump times τ_i. In statistics a stochastic collection of times is referred to as a "point process." The study of point processes is a mature branch of the theory of stochastic processes.[16–18] Point processes have been applied in the study of photoelectron statistics, cosmic-ray showers, kinetic theory, population growth, telephone traffic, etc. An important class of point processes is the class of so-called doubly stochastic Poisson processes. An example is the jump times τ_i for a particle performing a random walk where the jump probability at time t, $\gamma(t)$, is itself a stochastic process. Here one may define a second kind of time-dependent diffusion constant $\tilde{D}(t)$ by

$$\tilde{D}(t)=\frac{a^2}{2}\gamma(t) . \tag{10}$$

While $\tilde{D}(t)$ is of course different from $D(t)$, their statistical properties are identical: For the average over a particular realization of $\gamma(t)$ it is easy to see that $\langle D(t_1)\cdots D(t_n)\rangle_{\gamma(t)}=\tilde{D}(t_1)\cdots\tilde{D}(t_n)$. Averaging this expression over all possible $\gamma(t)$'s leads to

$$\langle D(t_1)\cdots D(t_n)\rangle=\langle\tilde{D}(t_1)\cdots\tilde{D}(t_n)\rangle . \tag{11}$$

Thus, our definition of $D(t)$ in Eq. (2) is consistent in the case where the ordinary diffusion constant really does fluctuate in time via a time-dependent jump probability.

We now turn to the problem of expressing the current autocorrelation function in an external field in terms of equilibrium current fluctuations. Focusing attention on diffusion-constant fluctuations according to Eq. (8), we note that the integrated dynamical diffusion constant counts the number of jumps N in time t:

$$N=\frac{2}{a^2}\int_0^t D(t')dt' . \tag{12}$$

For the variance of N one has

$$\langle (\Delta N)^2 \rangle_t = \frac{4}{a^4} \left[\int_0^t \int_0^t \langle D(t')D(t'') \rangle dt' dt'' \right.$$

$$\left. - \left[\int_0^t \langle D(t') \rangle dt' \right]^2 \right]$$

$$= \frac{8}{a^4} \int_0^t (t-\tau) C_D(\tau) d\tau , \qquad (13)$$

where $C_D(\tau)$ is the autocorrelation function for the dynamical diffusion constant,

$$C_D(\tau) \equiv \langle D(\tau)D(0) \rangle - D^2 . \qquad (14)$$

Equation (13) leads to

$$C_D(t) = \frac{a^4}{8} \frac{d^2}{dt^2} \langle (\Delta N)^2 \rangle_t . \qquad (15)$$

The next step is to relate the right-hand side to averages of the displacement in time t, $\Delta x(t)$. The quantity $\langle e^{ik \Delta x(t)} \rangle$ is an average of a product of independent factors $e^{\pm ika}$ and thus

$$\langle e^{ik \Delta x(t)} \rangle = \langle \cos^N(ka) \rangle_t . \qquad (16)$$

From this equation averages of all powers of $\Delta x(t)$ can be found. For the first two nonzero averages one finds

$$\langle (\Delta x)^2(t) \rangle = -\frac{d^2}{dk^2} \langle \cos^N(ka) \rangle_t |_{k=0} = a^2 \langle N \rangle_t , \qquad (17)$$

$$\langle (\Delta x)^4(t) \rangle = \frac{d^4}{dk^4} \langle \cos^N(ka) \rangle_t |_{k=0}$$

$$= a^4 (3\langle N^2 \rangle_t - 2\langle N \rangle_t) .$$

In particular, the fourth-order cumulant of $\Delta x(t)$, $\langle \Delta x^{(4)}(t) \rangle \equiv \langle (\Delta x)^4(t) \rangle - 3\langle (\Delta x)^2(t) \rangle^2$, is given by

$$\langle \Delta x^{(4)}(t) \rangle = a^4 [3\langle (\Delta N)^2 \rangle_t - 2\langle N \rangle_t] . \qquad (18)$$

Since $\langle N \rangle_t$ is always proportional to t, Eq. (18) in conjunction with Eq. (15) implies[19-22]

$$C_D(t) = \frac{1}{24} \frac{d^2}{dt^2} \langle \Delta x^{(4)}(t) \rangle . \qquad (19)$$

Equation (19) was first derived by Kuzovlev and Bochkov as a consequence of

$$\langle e^{ik \Delta x(t)} \rangle = \left\langle \exp \left[-k^2 \int_0^t D(t') dt' \right] \right\rangle , \qquad (20)$$

derived for "slowly fluctuating" $D(t)$.[20] Their definition of $D(t)$ is not obvious, but Eq. (20) is not valid for any reasonable definition of $D(t)$ as long as $a > 0$, since it does not apply even in the case of an ordinary random walk with a constant $D(t)$: For $D(t)=D$ Eq. (20) reduces to $\ln \langle e^{ik \Delta x(t)} \rangle = -k^2 Dt$ which implies $\langle \Delta x^{(4)}(t) \rangle = 0$. In reality $\langle \Delta x^{(4)}(t) \rangle \propto t$ in this case since cumulants are additive and $\Delta x(t)$ is a sum of independent increments. Instead, Eq. (20) must be replaced by

$$\langle e^{ik \Delta x(t)} \rangle = \left\langle \exp \left[\frac{2 \ln[\cos(ka)]}{a^2} \int_0^t D(t') dt' \right] \right\rangle \qquad (21)$$

which just combines Eqs. (12) and (16). For $a \to 0$ Eq. (21) reduces to Eq. (20). This limit, however, is only permissible in certain models. From Eq. (21) it is possible to derive Eq. (19) directly by expanding the logarithm of the equation to fourth order in k, but we found it more instructive and also useful below to arrive at Eq. (19) via averages of N and its fluctuations.

Defining as usual the fourth-order cumulant of the velocity by

$$\langle v(t_1),v(t_2),v(t_3),v(t_4) \rangle \equiv \langle v(t_1)v(t_2)v(t_3)v(t_4) \rangle - \langle v(t_1)v(t_2) \rangle \langle v(t_3)v(t_4) \rangle$$

$$- \langle v(t_1)v(t_3) \rangle \langle v(t_2)v(t_4) \rangle - \langle v(t_1)v(t_4) \rangle \langle v(t_2)v(t_3) \rangle , \qquad (22)$$

Eq. (19) can be rewritten as

$$C_D(t) = \int_0^t d\tau' \int_0^{\tau'} d\tau'' \langle v(t),v(\tau'),v(\tau''),v(0) \rangle . \qquad (23)$$

The right-hand side is the Burnett coefficient.[21,22] Equation (23) was derived by Kuzovlev and Bochkov[20] from Eq. (20), and also by Nieuwenhuizen and Ernst from a different point of view.[22] The latter authors define a "fluctuating diffusion coefficient," $D(t,\tau)$, by

$$D(t,\tau) = \frac{1}{2} \frac{\partial}{\partial t} \{ [x(t)-x(\tau)]^2 \} . \qquad (24)$$

They then proceed to show that for the Markovian random-walk model under study $C_D \equiv \langle D(t,\tau)D(t',\tau') \rangle - D^2$ is actually a function of $t - t'$ only which obeys Eq. (23).

Combining Eqs. (8), (14), and (23) we finally arrive at

$$\langle J(t)J(0) \rangle_E = \langle J \rangle_E^2 + \left[\frac{E}{kT} \right]^2 \int_0^t d\tau' \int_0^{\tau'} d\tau'' \langle J(t),J(\tau'),J(\tau''),J(0) \rangle \quad (t > 0) . \qquad (25)$$

Since cumulants are additive, this equation implies the excess current noise is proportional to $\langle J \rangle^2_E / V$ as in experiment [Eq. (1)]. Actually, this follows also directly from Eq. (8). It was first shown for a random-walk model by Tunaley.[23] Equations like Eq. (25) have been derived by a number of authors,[13,14,20–22,24] thereby greatly clarifying and simplifying the subject by reducing the current noise in an external field to equilibrium current fluctuations. We note here that it is actually possible to express $\langle J(t)J(0)\rangle_E$ in terms of equilibrium *two*-point correlation functions. Since

$$|J(t)| = qa \sum_i \delta(t - \tau_i) = \frac{2q}{a} D(t) ,$$
(26)

Eq. (8) can be rewritten as

$$\langle J(t)J(0)\rangle_E = \left| \frac{qaE}{2kT} \right|^2 \langle |J(t)| \, |J(0)| \rangle \quad (t > 0) ,$$
(27)

where the right-hand side is, as usual, an equilibrium average. This result is simpler than Eq. (25) and, perhaps, more aesthetically pleasing. But it is less general than Eq. (25) since it explicitly involves the lattice constant and thus depends on the existence of a lattice.

For the generation of $1/f$ noise one needs long-time correlations in the fluctuations of $D(t)$. Actually, noise that varies approximately as $1/f$ is obtained only if $C_D(t)$ is almost constant, typically varying as $\log(t)$ to some negative power. One may imagine two different ways of generating $1/f$ noise. The one case is that of "genuine" mobility fluctuations, i.e., when the random walk is a doubly stochastic Poisson point process with $1/f$ noise in the $\tilde{D}(t)$ fluctuations of Eq. (10). The other case is when long-time correlations in $D(t)$ arise because of occasional long trapping times of the particles. Here one must assume the existence of a broad spectrum of trapping times exceeding the longest experimental times. This may be regarded as the case of number fluctuations since a charge carrier trapped for the whole period of observation for all practical purposes is nonexistent.

We close this section by showing that only $1/f$ noise with strong fluctuations in the number of jumps is observable. By strong noise we mean noise obeying

$$\langle (\Delta N)^2 \rangle_t \gg \langle N \rangle_t$$
(28)

on the relevant time scale. This is the criterion for N fluctuations much larger than for an ordinary random walk, where there is equality in Eq. (28) on account of the Poisson statistics. Both the mobility and the trapping mechanism may satisfy Eq. (28) which rules out only the case of very weak mobility fluctuations. To show Eq. (28) we calculate first the white noise in equilibrium. From $J = qa \sum_i \pm \delta(t - \tau_i)$ we get immediately

$$S_{\text{white},J}(\omega) = 2q^2 a^2 \frac{\langle N \rangle_t}{t}, \quad t = \omega^{-1}$$
(29)

where the number of jumps per unit time, $\langle N \rangle_t / t$, is of

course independent of t. In a weak external field there is a slight increase in the white noise which, however, is insignificant for the present calculation.[22,23] Since $C_D(t)$ varies only very slowly one has $S_D(\omega) \lesssim 4tC_D(t)$ and Eq. (13) implies $C_D(t) \simeq (a^4/4)[\langle (\Delta N)^2 \rangle_t / t^2]$, where $t = \omega^{-1}$. Combining these results we get for the excess current noise

$$S_{\text{exc},J}(\omega) \lesssim q^2 a^2 \left| \frac{qaE}{kT} \right|^2 \frac{\langle (\Delta N)^2 \rangle_t}{t}, \quad t = \omega^{-1} .$$
(30)

In linear-response theory $qaE/kT \ll 1$ and the criterion for measurable excess noise reduces to Eq. (28). This condition is independent of the size of the system since both sides of Eq. (28) are additive.

III. EXAMPLE: EXCESS NOISE IN THE CONTINUOUS-TIME RANDOM-WALK MODEL

One way or the other $1/f$ noise arises from long-time correlations in the diffusion constant fluctuations. This may occur, for instance, via occasional very long trapping times for the change carriers. The simplest example of this is the CTRW model of Montroll and Weiss.[25] Here the jump probability at any time is a function only of the time elapsed since the preceding jump. The CTRW model was first applied to the $1/f$ noise problem by Tunaley[23] and later by Nelkin and co-workers.[24,26] The central quantity in this model is the waiting time distribution function, $\psi(t)$, which is the probability density for jumps the time t after the latest jump. In the language of stochastic point processes, the sequence of waiting times is a so-called renewal process.[16,27] In this section we calculate the excess noise from $\psi(t)$. This was done by Tunaley[23] but is repeated here as an illustration of the general theory of Sec. II and also because the below derivation is simpler than that of Tunaley.

If the particle jumps at $t = 0$ we let $\psi_n(t)$ denote the probability density for the nth jump hereafter occurring at time t. Obviously one has

$$\psi_{n+1}(t) = \int_0^t \psi_n(t - \tau)\psi(\tau)d\tau .$$
(31)

For the function $f(t)$ defined by

$$f(t) = \sum_{n=1}^\infty \psi_n(t)$$
(32)

Eq. (31) implies

$$f(t) - \psi(t) = \int_0^t f(t - \tau)\psi(\tau)d\tau .$$
(33)

Taking the Laplace transform of this equation one gets $\tilde{f}(s) - \tilde{\psi}(s) = \tilde{f}(s)\tilde{\psi}(s)$, or

$$\tilde{f}(s) = \frac{\tilde{\psi}(s)}{1 - \tilde{\psi}(s)} .$$
(34)

The quantity $p(t \mid 0)$ occurring in Eq. (9) is just $f(t)$ and thus

$$S_{exc}(\omega) \equiv \frac{S_{exc,D}(\omega)}{D^2} = \frac{a^2}{2D} 4 \int_0^\infty f(t)\cos(\omega t)dt ,$$

$$= \frac{2a^2}{D} \mathrm{Re}\,\tilde{f}(i\omega)$$

$$= \frac{2a^2}{D} \left[\mathrm{Re}\frac{1}{1-\tilde{\psi}(i\omega)} - 1 \right] . \tag{35}$$

This is Tunaley's result for the excess noise.[23] It is convenient to write $\psi(t)$ as a sum of exponential decays, $\psi(t) = \langle \gamma e^{-\gamma t} \rangle$, where the average is over a distribution of jump rates.[24,26] From this $\tilde{\psi}(s) = \langle \gamma/(\gamma+s) \rangle$ and $D = \frac{1}{2}a^2 \langle \gamma^{-1} \rangle^{-1}$ which substituted into Eq. (35) yields

$$S_{exc}(\omega) = \frac{2a^2}{D} \left[\mathrm{Re}\frac{1}{i\omega \left\langle \frac{1}{\gamma+i\omega} \right\rangle} - 1 \right]$$

$$= \frac{2a^2}{D\omega} \left[\mathrm{Im}\left\langle \frac{1}{\gamma+i\omega} \right\rangle^{-1} - \omega \right] , \tag{36}$$

i.e.,

$$S_{exc}(\omega) = \frac{4\langle \gamma^{-1} \rangle}{\omega} \left[\mathrm{Im}\left\langle \frac{1}{\gamma+i\omega} \right\rangle^{-1} - \omega \right] . \tag{37}$$

A simple example yielding $1/f$ noise is the case of all γ's equally likely:

$$p(\gamma) = \frac{1}{\gamma_0}, \quad \gamma_{min} < \gamma < \gamma_0 \tag{38}$$

where $\gamma_{min} \ll \gamma_0$ is assumed. One may think of γ_0 as a phonon frequency and γ_{min} as corresponding to long waiting times, e.g., one day or one year. For the whole range of intermediate frequencies $\langle (\gamma+i\omega)^{-1} \rangle \simeq \gamma_0^{-1}\ln(\gamma_0/i\omega)$ and

$$S_{exc}(\omega) \simeq \frac{4}{\omega}\ln\lambda \, \mathrm{Im}\frac{1}{\ln(\gamma_0/i\omega)} \simeq \frac{2\pi\ln\lambda}{\ln^2(\gamma_0/\omega)}\frac{1}{\omega} , \tag{39}$$

where $\lambda = \gamma_0/\gamma_{min}$. We thus find $S_{exc}(\omega) \propto \omega^{-\alpha}$, where

$$\alpha = 1 - \frac{2}{\ln(\gamma_0/\omega)} . \tag{40}$$

At ordinary laboratory frequencies one has $\alpha \simeq 0.9$. This model may be termed the "standard model of $1/f$ noise" since it is probably the simplest exact soluble random-walk model giving $1/f$ excess noise. Of course $1/f$ noise is built into the model via Eq. (38). This is equivalent to a waiting time distribution function $\psi(t) \propto t^{-2}$ (Ref. 28)

above γ_{min}, which implies a logarithmically divergent average waiting time. The excess noise of the standard model is identical in functional form to the expression derived by Kuzovlev and Bochkov for a scale-invariant random walk.[10,20] Their derivation is based on Eq. (20) which has been criticized above. The derivation is not quite transparent; also, the factor $\ln\lambda$ in Eq. (39) is absent in their calculation of the excess noise.

IV. DISCUSSION

Random-walk models provide a simple framework for understanding the fluctuation-dissipation theorem. It is therefore an obvious idea also to use these models for getting a better understanding of low-frequency resistance fluctuations. Various random-walk models have been studied with this purpose.[19–24,26,28–30] In this paper a general framework for discussing excess noise in random-walk models has been proposed. Following previous work, in Sec. II we focused on the concept of a fluctuating diffusion constant, the dynamical diffusion constant $D(t)$. While the exact definition of $D(t)$ hitherto has not been clear, we here use a definition of $D(t)$ which is simpler than previous implicit definitions. For all practical purposes, however, it is identical to these since the expressions for $\langle D(t)D(0) \rangle$ in Eqs. (19) and (23) are identical to those given by Kuzovlev and Bochkov,[19,20] and Machta, Nelkin, Nieuwenhuizen, and Ernst.[21,22] The relevance of $D(t)$ to excess current noise is shown by Eq. (8) according to which the current fluctuations in an external field directly probes the equilibrium $\langle D(t)D(0) \rangle$. An important general property of random-walk models is the fact that the noise is proportional to $\langle J \rangle_E^2$ and inversely proportional to the volume or any other extensive property like the number of charge carriers. This follows immediately from Eq. (8) since $D(t)$ and autocorrelation functions are additive.

As an application of the general formalism, note that Eq. (6) is valid also in a time-dependent external field. From this it is straightforward to show that in a sinusoidal field one finds the so-called $1/\Delta f$ noise[31–33] which is directly proportional to the magnitude of the $1/f$ noise in a constant field. A weakness of the formalism of Sec. II should be mentioned, namely, that it does not easily allow for an exact calculation of the white noise in an external field. Though insignificant in the linear regime, there is an interesting small increase in the white noise when the field is turned on.[22,23]

The dynamical diffusion constant is proportional to the absolute value of the current. This leads to a simple expression for the current fluctuations in an external field in terms of equilibrium fluctuations [Eq. (27)], a result which can be rewritten in terms of autocorrelation functions as

$$\langle [J(t) - \langle J \rangle_E][J(0) - \langle J \rangle_E] \rangle_E = \left| \frac{qaE}{2kT} \right|^2 \langle [|J(t)| - \langle |J| \rangle][|J(0)| - \langle |J| \rangle] \rangle \quad (t > 0) . \tag{41}$$

Analogous to the frequency-dependent conductivity which probes the equilibrium *velocity* autocorrelation function, the excess-noise spectrum thus probes the equilibrium *speed* autocorrelation function. But it should be remembered that a frequency-independent conductivity must be assumed to derive Eq. (41), and also that the random walk takes place on a lattice. Equation (41) cannot be expected to apply more generally. For this to be the case, one should be able to define a characteristic length to play the role of the lattice constant a in Eq. (41). The only possibility for this seems to be to let a be the length for which $qaE \simeq kT$ at fields marking the onset of non-linearities. Since, however, nonlinearities involve new physics which is in general uncorrelated to linear-response phenomena, there is little hope that this approach can be generally valid. Thus, Eq. (41) must be limited to lattice models.

The unified formalism for excess current noise in random-walk models developed above provides a convenient starting point for a discussion of general properties of $1/f$ noise. In particular, the point process approach makes it possible to throw some light on the old controversy as to whether $1/f$ noise is due to mobility or to number fluctuations.[6,9] We end this paper by giving a general argument to the effect that Fermi statistics rules out the number-fluctuation mechanism. Mobility fluctuations correspond to noise *in* the effective charge-carrier Hamiltonian, whereas number fluctuations due to occasional deep trapping is noise generated *by* the Hamiltonian itself. In the language of point processes, the standard example of mobility fluctuations is the case when the jump times τ_i constitute a doubly stochastic Poisson process, while the standard example of trapping noise is the case when τ_i is a renewal process, i.e., when we have a continuous-time random-walk. This case is non-Markovian and therefore in a sense unphysical, admittedly, but the CTRW model is equivalent to a Markovian multistate trapping model where the noise then is indeed generated *by* the Hamiltonian.[26]

In Sec. III the excess noise in the CTRW model was calculated. A simple example termed the standard model was worked out in detail. This model is one out of the class of CTRW models discussed by Nelkin and Harrison.[26] In the multistate trapping realization of the CTRW, the standard model corresponds to a density of energies, ε, given by

$$p(\varepsilon) \propto \exp(\varepsilon/kT) . \qquad (42)$$

Though this implies only very few deep trapping states, in the course of time all energies are equally likely to be occupied because of the Boltzmann factor to be multiplied with Eq. (42) to get the probability. Thus, the standard model is just another example of the old idea of $1/f$ noise arising when all activation energies are equally likely. At the same time the standard model satisfies the requirement for $1/f$ noise given by Nieuwenhuizen and Ernst, namely, an exponential density of states.[22,28]

A temperature-dependent density of states as in Eq. (42) arises in a system of fermions. Here a single particle senses, in a mean-field approximation, a density of *avail-*

able states below the Fermi energy, $p_{\text{eff}}(\varepsilon)$, which is given by

$$p_{\text{eff}}(\varepsilon) \simeq n(\varepsilon)e^{(\varepsilon-\varepsilon_F)/kT} \quad (\varepsilon < \varepsilon_F) , \qquad (43)$$

where $n(\varepsilon)$ is the ordinary density of states. For a constant $n(\varepsilon)$ Eq. (42) is obtained. Equation (43) implies $1/f$ noise in the motion of the single particles, a point we will return to below. While interesting on its own, this has nothing to do with the observed $1/f$ resistance fluctuations, however. This is because the mean-field approximation does not apply due to strong interparticle correlations: Below the Fermi level the particle number fluctuations (in one energy level) are exponentially small, $\langle(\Delta n)^2\rangle = \langle n \rangle \langle 1-n \rangle \ll \langle n \rangle$ (Ref. 34), while for independent particles one would have $\langle(\Delta n)^2\rangle = \langle n \rangle$ because of the Poisson statistics, i.e., much larger fluctuations.

We now extend the above and argue that Fermi statistics actually rules out *any* $1/f$ noise model based on the trapping mechanism. Basically, one may imagine two different ways of producing long trapping times. The first case involves hopping between localized states of similar energy separated by various long tunneling distances or large energy barriers. In this case, inevitably, there is a strong frequency dependence of the conductivity and models of this kind cannot explain the usual case of $1/f$ fluctuations of a frequency-independent conductivity. (Note that McWhorter's model based on tunneling to surface states[9] is not ruled out by this argument which is only concerned with bulk and isotropic $1/f$ noise.) The second way of having long trapping times is that of trapping into deep energies. This only works for independent particles with the peculiar density-of-states of Eq. (42). For fermions, the density-of-states above the Fermi energy is not temperature dependent, and below the Fermi level, where Eq. (43) does apply in a mean-field sense, the particles are not independent as discussed already.

To summarize the effect of Fermi statistics, it has been argued that for Fermi systems $1/f$ resistance fluctuations cannot be due to occasional deep trapping of the charge carriers. The number-fluctuation mechanism thus can be ruled out on general grounds, and, e.g., the CTRW model in the multiple trapping realization is not realistic. Thus, the noise must be caused by mobility fluctuations. The central problem, which until today remains largely unsolved, is to identify the origin of the mobility fluctuations.

While Fermi statistics rules out number fluctuations, it implies on the other hand a peculiar kind of "single-particle" $1/f$ noise: The motion of a single localized fermion exhibits $1/f$ noise as a consequence of Eq. (43). In principle this is observable, since, for a system of fermions described by a master equation (an implicit assumption in the argument), there are no quantum coherence effects and, in effect, the particles are classical and distinguishable. Similarly, atoms or ions diffusing in a disordered medium with a distribution of available potential minima also exhibit single-particle $1/f$ noise, since they behave as fermions because of their strong repulsion. This should be observable by monitoring the motion of tracer atoms or ions in time.

Except for the above arguments ruling out number fluctuations, the cause of $1/f$ noise has not been discussed in the present paper. We feel there is no simple and generally valid mechanism explaining $1/f$ noise. Rather, $1/f$ noise may arise from a number of different mechanisms which probably, one way or the other, involve lattice defects overcoming or tunneling through barriers. Following this line of thought, $1/f$ noise and its dependence on temperature, etc., provide important information about the solid under study. Note that while $S_{exc}(\omega)$ probes only $\langle D(t)D(0)\rangle$ there is an enormous amount of information hidden in the higher-order correlations of $D(t)$. This is illustrated by the fact that the total amount of information in the noise is contained in a function of *two* variables

$$P(u,t)=\langle e^{uN}\rangle_t , \qquad (44)$$

while $S_{exc}(\omega)$ is only a function of one variable. The fact that there is more to the noise than just the spectrum was emphasized already ten years ago by Voss in a discussion of linearity of the $1/f$ noise mechanism.[35] The higher-order correlations of $J(t)$ and thereby $D(t)$ are accessible today by digital techniques and their determination should provide a means of distinguishing between various models for $1/f$ noise. Other promising lines of research is the measurement of $1/f$ noise anisotropy,[11] and the problem of stationarity of the noise and the dependence of the noise on the annealing state (in any system with long relaxation times the possibility of "glass transitions" should not be forgotten); $1/f$ noise is still mainly an experimental field and it seems that a lot of work remains to be done here before reliable theories can be proposed.

[1] H. Bittel, Ergeb. Exakten Naturwiss. **31**, 84 (1959).

[2] F. N. Hooge, Physica B + C **83B**, 14 (1976).

[3] D. Wolf, in *Noise in Physical Systems*, edited by D. Wolf (Springer-Verlag, Berlin, 1978), p. 122.

[4] W. H. Press, Comments Astrophys. Space Phys. **7**, 103 (1978).

[5] A. van der Ziel, Adv. Electron. Electron Phys. **49**, 225 (1979).

[6] D. A. Bell, J. Phys. C **13**, 4425 (1980).

[7] P. Dutta and P. M. Horn, Rev. Mod. Phys. **53**, 497 (1981).

[8] K. M. van Vliet and H. Menta, Phys. Status Solidi B **106**, 11 (1981).

[9] F. N. Hooge, T. G. M. Kleinpenning, and L. K. J. Vandamme, Rep. Prog. Phys. **44**, 479 (1981).

[10] G. N. Bochkov and Y. E. Kuzovlev, Usp. Fiz. Nauk **141**, 151 (1983) [Sov. Phys.—Usp. **26**, 829 (1983)].

[11] S. M. Kogan Usp. Fiz. Nauk **145**, 285 (1985) [Sov. Phys.—Usp. **28**, 170 (1985)].

[12] R. F. Voss and J. Clarke, Phys. Rev. B **13**, 556 (1976).

[13] M. A. Mikulinsky, Phys. Lett. **66A**, 440 (1978).

[14] A.-M.S. Tremblay and M. Nelkin, Phys. Rev. B **24**, 2551 (1981).

[15] J. K. E. Tunaley, J. Appl. Phys. **43**, 3851 (1972).

[16] S. K. Srinivasan, *Stochastic Point Processes* (Griffin, London, 1974).

[17] D. L. Snyder, *Random Point Processes* (Wiley, New York, 1975).

[18] B. Saleh, *Photoelectron Statistics* (Springer-Verlag, Berlin, 1978).

[19] Y. E. Kuzovlev and G. N. Bochkov, Pis'ma Zh. Tekh. Fiz. **8**, 1260 (1982) [Sov. Tech. Phys. Lett. **8**, 542 (1982)].

[20] Y. E. Kuzovlev and G. N. Bochkov, Radiophys. Quantum Electron. **26**, 228 (1983).

[21] J. Machta, M. Nelkin, T. M. Nieuwenhuizen, and M. H. Ernst, Phys. Rev. B **31**, 7636 (1985).

[22] T. M. Nieuwenhuizen and M. H. Ernst, J. Stat. Phys. **41**, 773 (1985).

[23] J. K. E. Tunaley, J. Stat. Phys. **15**, 149 (1976).

[24] C. J. Stanton and M. Nelkin, J. Stat. Phys. **37**, 1 (1984).

[25] E. W. Montroll and G. H. Weiss, J. Math. Phys. **6**, 167 (1965).

[26] M. Nelkin and A. K. Harrison, Phys. Rev. B **26**, 6696 (1982).

[27] D. R. Cox, *Renewal Theory* (Methuen, London, 1962).

[28] T. M. Nieuwenhuizen and M. H. Ernst, Phys. Rev. B **33**, 2824 (1986).

[29] H. Spohn, Z. Phys. B **57**, 255 (1984).

[30] W. Lehr, J. Machta, and M. Nelkin, J. Stat. Phys. **36**, 15 (1984).

[31] B. K. Jones and J. D. Francis, J. Phys. D **8**, 1172 (1975).

[32] R. F. Voss and J. Clarke, Phys. Rev. Lett. **36**, 42 (1976).

[33] M. A. Mikulinsky, Phys. Lett. **71A**, 473 (1979).

[34] L. D. Landau and E. M. Lifshitz, *Statistical Physics* (Pergamon, Oxford, 1969).

[35] R. F. Voss, Phys. Rev. Lett. **40**, 903 (1978).

Maximum-entropy ansatz for nonlinear-response theory

Jeppe C. Dyre*
Noyes Laboratory, University of Illinois at Urbana-Champaign, Urbana, Illinois 61801
(Received 13 February 1989)

An approximate nonlinear-response theory is derived by maximizing the information theoretic entropy in the space of fluctuations $J(t)$ of the degree of freedom of interest, subject to constant-energy dissipation in the external field. The resulting formalism expresses all cumulant averages of $J(t)$ in an external field in terms of equilibrium cumulants.

Linear-response theory[1-7] is fundamental to much present-day work in solid-state physics, chemical physics, plasma physics, etc. Its usefulness rests in the fact that the response to an external field to first order is determined by an equilibrium autocorrelation function. The extension of linear-response theory to include higher-order terms had been discussed already in the 1950s.[6,8] In contrast to the linear case, the higher-order terms cannot be expressed in terms of equilibrium correlation functions of the degree of freedom under consideration.[9] The exact nonlinear-response theory is complex and has found little application. There is also the question of the convergence of the formal expansion in the external field. Strong fields may induce, e.g., phase transitions or self-organization, information about which one does not expect to be hidden in the equilibrium fluctuations. Despite these reservations, one may ask whether a theory that predicts the nonlinear response from equilibrium fluctuations does exist, at least as a reasonable approximation applicable not too far from equilibrium. In an attempt to answer this question, this paper discusses an ansatz for nonlinear-response theory which generalizes a little-known theory due to Stratonovich.[10] The ansatz is derived from the maximum-entropy principle. Some simple examples are given and the validity of the ansatz is discussed. Finally, it is argued that the ansatz represents the simplest way a system may become nonlinear.

The degree of freedom of interest is denoted by Q; it may be microscopic or macroscopic. The underlying dynamics is assumed to be classical and Q is assumed to be invariant under time reversal. Q couples to an external field E via a term $-EQ$ in the Hamiltonian. Only the case of a time-independent external field will be considered. It is convenient to discuss response and fluctuations in terms of $J(t) \equiv \dot{Q}(t)$. In general, one is interested in not only the average $\langle J \rangle_E$ but also in the autocorrelation function and perhaps higher-order averages of $J(t)$ in the external field. To calculate these quantities one needs to know the probability of any $J(t)$ fluctuation in the external field $P_E[J(t)]$. As mentioned above, even a complete knowledge of the equilibrium fluctuations $P_0[J(t)]$ in general is not enough to determine $P_E[J(t)]$. The task of finding $P_E[J(t)]$ may be viewed as a missing-information problem. In an external field there is a certain rate of energy dissipation. Suppose no more than

this and $P_0[J(t)]$ are known. The maximum-entropy formalism is a general method that, based on the insufficient information available, gives a least-biased estimate of probabilities.[11,12] In applications to a continuous problem a reference measure is needed. In the present case, in order to have a smooth transition to the zero-field case this measure must be $P_0[J(t)]$. The maximum-entropy requirement leads to[11,12]

$$P_E[J(t)] = N^{-1} P_0[J(t)] \exp\left[-\lambda E \int_{-\infty}^{\infty} J(t) dt \right], \quad (1)$$

where N is a normalization constant and $\lambda = \lambda(E)$ is a Lagrangian multiplier. Normally, one would now proceed to determine λ from the constraint, i.e., the energy dissipation rate. In this case, however, λ is determined by fundamental requirements of statistical mechanics. As shown by Bochkov and Kuzovlev,[13,14] the time-reversal invariance of the microscopic equations of motion implies

$$\frac{P_E[J(t)]}{P_E[-J(-t)]} = \exp\left[\beta E \int_{-\infty}^{\infty} J(t) dt \right], \quad (2)$$

where β is the inverse temperature. Equation (2) is derived by assuming thermal equilibrium at $t = -\infty$ followed by a decoupling of the heat bath and evolution according to the canonical equations of motion for the system interacting with the external field. This assumption is identical to that used by Kubo in deriving linear-response theory.[6] Equation (2) is also valid for any system that is described by a master equation; in this case, Eq. (2) expresses the principle of detailed balance. Since $P_0[J(t)]$ is time-reversal invariant, Eqs. (1) and (2) imply $\lambda = -\beta/2$ for all E, i.e.,

$$P_E[J(t)] = N^{-1} P_0[J(t)] \exp\left[\frac{\beta}{2} E \int_{-\infty}^{\infty} J(t) dt \right]. \quad (3)$$

Equation (3) allows one to calculate all higher-order cumulant averages of J in the external field, in terms of equilibrium cumulants. The cumulants are defined by the generating functional

$$D[u(t);E] = \ln\left\langle \exp\left[\int_{-\infty}^{\infty} u(t)J(t)d\tau\right]\right\rangle_E$$

$$= \sum_{n=1}^{\infty} \frac{1}{n!}\int_{-\infty}^{\infty} dt_1 \cdots dt_n \langle J(t_1),\ldots,J(t_n)\rangle_E$$

$$\times u(t_1)\cdots u(t_n) , \qquad (4)$$

and Eq. (3) implies

$$D[u(t);E] = D[u(t)+(\beta/2)E;0] - D[(\beta/2)E;0] . \qquad (5)$$

From Eq. (5) the nonequilibrium cumulants may be found as derivatives with respect to $u(t)$ at $u \equiv 0$.

For the average of J one finds from Eq. (5)

$$\langle J\rangle_E = \sum_{n=0}^{\infty} \frac{1}{n!}\left[\frac{\beta E}{2}\right]^n \int_{-\infty}^{\infty} dt_1 \cdots dt_n$$

$$\times \langle J(0),J(t_1),\ldots,J(t_n)\rangle_0 . \qquad (6)$$

The first-order term is that predicted by linear-response theory. Note that, for a macroscopic Q, Eq. (6) is consistent also in the thermodynamic limit since cumulants are additive for independently fluctuating quantities. An identity for the $(n+1)$th cumulant average of $\Delta Q(t)=Q(t)-Q(0)$,

$$\lim_{t\to\infty} t^{-1}\langle \Delta Q^{(n+1)}(t)\rangle_0$$

$$= \int_{-\infty}^{\infty} dt_1 \cdots dt_n \langle J(0),J(t_1),\ldots,J(t_n)\rangle_0 ,$$

allows one to rewrite Eq. (6) as

$$\langle J\rangle_E = \lim_{t\to\infty} t^{-1}\frac{d}{du}\ln\langle e^{u\Delta Q(t)}\rangle_0\bigg|_{u=(\beta/2)E} . \qquad (7)$$

As a simple example of Eq. (7), consider a particle performing a random walk in one dimension on a lattice with lattice constant a. Q is the coordinate and J the ve-

locity of the particle. If there are N jumps in time t, it is easy to see that $\langle e^{u\Delta Q(t)}\rangle_0 = \cosh^N(ua)$. Since N is Poisson-distributed around a mean $\overline{N} = \Gamma t$, one has

$$\langle e^{u\Delta Q(t)}\rangle_0 = e^{-\overline{N}}\sum_{N=0}^{\infty} \frac{\overline{N}^N}{N!}\cosh^N(ua)$$

$$= \exp\{\overline{N}[\cosh(ua)-1]\} , \qquad (8)$$

which implies

$$\langle v\rangle_E = \Gamma a \sinh[(\beta/2)Ea] . \qquad (9)$$

This is the correct result if the random walk is realized as the low-temperature limit of a particle in a symmetric periodic potential obeying a Langevin equation; the well-known Eq. (9) follows from the fact that the field lowers the barrier for jumps in the direction of E and increases the barrier for jumps opposite E. As another example of Eq. (7), consider the case when Q is the x coordinate of an atom in a liquid. Then Eq. (7) expresses the velocity of the atom in a field in the x direction acting only on the atom, in terms of the equilibrium incoherent intermediate scattering function $F_s(k,t)$:

$$\langle v\rangle_E = \lim_{t\to\infty}(it)^{-1}\frac{\partial}{\partial k}\ln F_s(k,t)\bigg|_{k=\beta E/2i} . \qquad (10)$$

For simple Gaussian diffusion, $F_s(k,t) = \exp(-Dk^2t)$.[15] In this case, the response is exactly linear and Eq. (10) reduces to the Nernst-Einstein relation between mobility and diffusion constant. A more realistic fit to experiment is the prediction of the jump-diffusion model[15,16]

$$F_s(k,t) = \exp[-Dk^2t/(1+Dk^2\tau_0)] .$$

From this, Eq. (10) predicts the onset of nonlinearity at fields for which $E l \beta \approx 1$, where the length $l = \sqrt{D\tau_0}$ in fits to data is of order-1 interatomic spacing.

For the external field autocorrelation function, Eq. (5) implies

$$\langle J(0),J(t)\rangle_E = \langle J(0),J(t)\rangle_0 + \frac{\beta E}{2}\int_{-\infty}^{\infty} dt_1 \langle J(0),J(t),J(t_1)\rangle_0$$

$$+ \frac{1}{2}\left[\frac{\beta E}{2}\right]^2 \int_{-\infty}^{\infty} dt_1 dt_2 \langle J(0),J(t),J(t_1),J(t_2)\rangle_0 + \cdots . \qquad (11)$$

An example is the case when J is the electric current. For a system with frequency-independent conductivity the zeroth-order term is a δ function, giving rise to white noise. In most cases the next term is zero by symmetry and the so-called excess current noise is given by the second-order term. Excess current noise is ubiquitous and usually has a $1/f$ spectrum.[17-19] A number of random-walk models have been studied to gain a better understanding of the phenomenon. In these models one finds[20-23]

$$\langle J(0),J(t)\rangle_E$$

$$= (\beta E)^2 \int_0^t dt_2 \int_0^{t_2} dt_1 \langle J(0),J(t),J(t_1),J(t_2)\rangle_0 + \cdots$$

$$(t>0) , \qquad (12)$$

which is equivalent to Eq. (11) because in random-walk models $\langle J(t_1),J(t_2),J(t_3),J(t_4)\rangle$ is nonzero only if $t_1\approx t_2$ and $t_3\approx t_4$ (or permutations thereof) where $t_1\approx t_2$ means that t_1-t_2 is a microscopic time.[20,21]

The similarity between the right-hand sides of Eqs. (6) and (11) suggests that a relation exists between $\langle J \rangle_E$ and $\langle J(0), J(t) \rangle_E$. As a matter of fact, it is easy to show that Eqs. (6) and (11) imply

$$\frac{d}{dE}\langle J \rangle_E = \frac{\beta}{2} \int_{-\infty}^{\infty} \langle J(0), J(t) \rangle_E dt \ . \tag{13}$$

This result is not approximate but a special case of an exact theorem due to Peterson.[24]

Since higher than second-order cumulants are zero for a Gaussian system, the maximum-entropy ansatz implies that the response is exactly linear whenever the equilibrium J fluctuations are Gaussian. This is analogous to what happens in equilibrium statistical mechanics. A magnetic system, for instance, has a field-independent susceptibility if the free energy is quadratic in the magnetization. Note that non-Gaussian fluctuations survive in the thermodynamic limit, the central limit theorem notwithstanding. A simple example of this in statistical mechanics is energy fluctuations in the canonical ensemble. If the energy fluctuations are strictly Gaussian, the average energy is linear in β so the specific heat varies as T^{-2}. Whenever this is not the case, the energy fluctuations are non-Gaussian.

The maximum-entropy formalism has a long history of applications to the problem of estimating the density matrix for a nonequilibrium system. This leads to a general-ization of equilibrium statistical mechanics, which takes into account the limited amount of information available about the system.[25-29] Some applications of the formal-ism characterize the nonequilibrium system by its energy dissipation rate.[30,31] As shown above, when applied to the external-field-induced "nonequilibrium" in the $J(t)$ space, this idea leads to definite predictions of the non-linear response in terms of equilibrium fluctuations. An equivalent of Eq. (5) was discussed briefly by Bochkov and Kuzovlev,[13] building on earlier work by Stratono-vich.[10] Only the case $u(t) = $const was considered and the discussion was limited to Markovian systems. The Stratonovich theory is based on the assumption that, for jumps between two minima, the barrier to overcome is placed halfway between the two minima (in the direction of Q).

The maximum-entropy property of the ansatz shows that it is the most reasonable, given only a knowledge of the equilibrium fluctuations. This does not guarantee that the ansatz is correct, however. To look into this question, we first discuss the consequences of a phenome-nological Langevin equation for Q and then an exact re-sult.

Suppose Q obeys a Langevin equation $\dot{Q} = CF(Q) + \xi(t)$ where $F(Q) = F_0(Q) + E$ is the general-ized force and $\xi(t)$ is a Gaussian white-noise term. Then the path probability is given by[32,33]

$$P[Q(t)] = N^{-1}\exp\left[-\beta/(4C)\int_{-\infty}^{\infty}[\dot{Q}(t) - CF(Q(t))]^2 dt\right] \ ,$$

or

$$P_E[Q(t)] = N^{-1}P_0[Q(t)]\exp\left[\frac{\beta}{2}E\int_{-\infty}^{\infty}J(t)dt\right]\exp\left[-\frac{\beta}{2}EC\int_{-\infty}^{\infty}F_0[Q(t)]dt\right] \ . \tag{14}$$

The transformation from $Q(t)$ to $\dot{Q}(t)$ is linear. There-fore, Eq. (14) implies that the maximum-entropy ansatz leads to correct results whenever the last term is unim-portant. As an example, consider again a particle in one dimension in a symmetric periodic potential at low tem-perature. Because of the $P_0[Q(t)]$ factor, the important paths fluctuate for some time around a potential-energy minimum before suddenly "jumping" to a new minimum. For these paths, the last term of Eq. (14) is almost in-dependent of the number of minima traversed and may be ignored for the calculation of $\langle \Delta Q(t) \rangle_E$ for large t. Thus, the maximum-entropy ansatz leads to correct re-sults in this case, as already shown in Eq. (9).

A result due to Furukawa sheds more light on the maximum-entropy ansatz. He showed that, for slowly fluctuating $J(t)$, the exact microscopic equation of motion implies[34]

$$P_E[J(t)] = N^{-1}P_0[J(t)]\exp\left[\frac{\beta}{2}E\int_{-\infty}^{\infty}J(t)dt + O(E^2)\right] \ . \tag{15}$$

Equation (15) suggests that there are two different ways a system may become nonlinear: either (i) as an interplay between non-Gaussian equilibrium J fluctuations and the first-order term, or (ii) as a result of the higher-order terms becoming important. The first case is when the maximum-entropy ansatz gives correct results; this may be referred to as a "simple" nonlinearity since it results from the very same term in Eq. (15) that gives rise to the linear response. Upon increasing the external field, a sys-tem may pass from linear through simple nonlinear response to finally the "complex" nonlinear response due to the higher-order terms, or it may go directly from linear to complex nonlinear response. The maximum-entropy ansatz is never correct for the latter systems, and in the former case it should only be trusted at not-too-large external fields.

To summarize, it has been shown that the maximum-entropy formalism in conjunction with statistical mechanics leads to unique predictions for the external-field cumulant averages of $J(t)$ in terms of equilibrium averages. The ansatz Eq. (3) may be justified in other ways. It corresponds to keeping only the first-order term

in Eq. (15) which is exact for slowly fluctuating $J(t)$. This term is responsible for the linear response, so the ansatz is clearly the simplest way to extrapolate linear-response theory into the nonlinear regime. The extrapolation has the property that the response is exactly linear if the equilibrium J fluctuations are Gaussian. If Q obeys a Langevin equation, the ansatz is correct whenever the last term of Eq. (14) is unimportant; for slowly fluctuating $J(t)$, the requirement of consistency between Eqs. (14) and (15) implies that the extra terms of both equations must be insignificant and the maximum-entropy ansatz must be correct.

The maximum-entropy ansatz solves a conceptual problem, but open questions remain regarding the validity and the practical value of the ansatz. One obvious problem is that the ansatz predicts a universal form of the nonlinear response while one expects the response to depend on the way heat generated by the external field is removed. However, because the temperature enters into Eq. (5), the ansatz only makes sense in situations where the temperature is almost constant throughout the sample. In many cases, this requirement may be satisfied for a given external field by working with a sufficiently small sample; in this limit the problem of heating often becomes insignificant.

Equation (15) implies that the ansatz may be applied only at not-too-large external fields. Also, Eq. (15) implies that a system may become nonlinear either by first exhibiting the simple nonlinearity predicted by the ansatz before becoming complex nonlinear, or by going directly from the linear to the complex nonlinear regime. In this connection it should be noted that all formulas given above may be generalized to several degrees of freedom. One may speculate that, by including the "mode-coupling" terms to other relevant degrees of freedom (e.g., the energy density), a complex nonlinearity may be converted to a simple nonlinearity, thus extending the validity of the ansatz. Even when the maximum-entropy ansatz is valid, the practical value of it is not clear at present. It is possible that the calculation of the equilibrium higher-order cumulant averages requires at least as much effort as a direct calculation of the nonlinear response. Certainly, this is the case for the previously discussed simple random walk in one dimension. On the other hand, Eq. (12) has provided insight into the problem of $1/f$ noise in conductors. And, for instance, Eq. (10) gives explicit predictions for the response of a single atom to an external force, based on a knowledge of the equilibrium intermediate incoherent scattering function, a quantity which has been studied extensively.[15]

*Present and permanent address: IMFUFA, Roskilde Universitetscenter, P.O. Box 260, DK-4000 Roskilde, Denmark.

[1]H. Nyquist, Phys. Rev. **32**, 110 (1928).

[2]L. Onsager, Phys. Rev. **37**, 405 (1931); **38**, 2265 (1931).

[3]J. G. Kirkwood, J. Chem. Phys. **14**, 180 (1946).

[4]H. B. Callen and T. A. Welton, Phys. Rev. **83**, 34 (1951).

[5]M. S. Green, J. Chem. Phys. **20**, 1281 (1952).

[6]R. Kubo, J. Phys. Soc. Jpn. **12**, 570 (1957).

[7]L. P. Kadanoff and P. C. Martin, Ann. Phys. (N.Y.) **24**, 419 (1963).

[8]W. Bernard and H. B. Callen, Rev. Mod. Phys. **31**, 1017 (1959).

[9]R. L. Stratonovich, Zh. Eksp. Teor. Fiz. **58**, 1612 (1970) [Sov. Phys.—JETP **31**, 864 (1970)].

[10]R. L. Stratonovich, Vestn. Mosk. Univ. Fiz. Astronomiya **5**, 16 (1962).

[11]E. T. Jaynes, Phys. Rev. **106**, 620 (1957); **108**, 171 (1957).

[12]*The Maximum Entropy Formalism*, edited by R. Levine and M. Tribus (MIT, Cambridge, MA, 1979).

[13]G. N. Bochkov and Yu. E. Kuzovlev, Zh. Eksp. Teor. Fiz. **72**, 238 (1977) [Sov. Phys.—JETP **45**, 125 (1977)].

[14]G. N. Bochkov and Yu. E. Kuzovlev, Physica **106A**, 443 (1981); **106A**, 480 (1981).

[15]J. P. Boon and S. Yip, *Molecular Hydrodynamics* (McGraw-Hill, New York, 1980).

[16]K. S. Singwi and A. Sjölander, Phys. Rev. **119**, 863 (1960).

[17]D. A. Bell, J. Phys. C **13**, 4425 (1980).

[18]P. Dutta and P. M. Horn, Rev. Mod. Phys. **53**, 497 (1981).

[19]M. B. Weissman, Rev. Mod. Phys. **60**, 537 (1988).

[20]C. J. Stanton and M. Nelkin, J. Stat. Phys. **37**, 1 (1984).

[21]Th. M. Nieuwenhuizen and M. H. Ernst, J. Stat. Phys. **41**, 773 (1985).

[22]J. Machta, M. Nelkin, Th. M. Nieuwenhuizen, and M. H. Ernst, Phys. Rev. B **31**, 7636 (1985).

[23]J. C. Dyre, Phys. Rev. B **37**, 10 143 (1988).

[24]R. L. Peterson, Rev. Mod. Phys. **39**, 69 (1967).

[25]E. T. Jaynes, in *Statistical Physics* Vol. 3 of *1963 Brandeis Lectures*, edited by W. K. Ford (Benjamin, New York, 1963), p. 181.

[26]H. Schwegler, Z. Naturforsch. **20A**, 1543 (1965).

[27]B. Robertson, Phys. Rev. **144**, 151 (1966).

[28]D. N. Zubarev and V. P. Kalashnikov, Physica **46**, 550 (1970).

[29]W. T. Grandy, Jr., Phys. Rep. **62**, 175 (1980).

[30]H. Sato, Prog. Theor. Phys. **57**, 1115 (1977).

[31]T. M. Brown, J. Phys. A **15**, 2285 (1982).

[32]L. Onsager and S. Machlup, Phys. Rev. **91**, 1505 (1953).

[33]H. Risken, *The Fokker-Planck Equation* (Springer, Berlin, 1984).

[34]H. Furukawa, Prog. Theor. Phys. **54**, 370 (1975).

A "zero-parameter" constitutive relation for simple shear viscoelasticity

J.C. Dyre

IMFUFA, Roskilde Universitetscenter, Denmark

Abstract: Based on the Cox-Merz rule and Eyring's expression for the nonlinear shear viscosity, a Wagner-type constitutive relation with no nontrivial adjustable parameters is proposed for simple shear viscoelasticity. The predictions for a number of non-steady shear flows are worked out analytically. It is shown that most features of shear viscoelasticity are reproduced by the model.

Key words: Shear flow; shear thinning; viscoelasticity; Cox-Merz rule

1. Introduction

After several years of research a number of useful constitutive relations are now available [1]. In order to reproduce experiments accurately these relations all contain a number of fitting parameters. In this paper the following question is asked: What is the simplest possible constitutive relation which still reproduces important features of viscoelasticity? To limit the discussion, only simple shear viscoelasticity is considered, and normal stresses are ignored all together. Starting from the Cox-Merz rule, a Wagner-type constitutive relation with no nontrivial adjustable parameters is arrived at. The nonlinear steady state shear viscosity is, by construction, close to that predicted by Eyring's phenomenological theory of liquid flow [2]. Various non-steady shear flows are then considered and worked out analytically. It is shown that the constitutive relation reproduces most qualitative features of shear viscoelasticity, with the notable exception of the overshoot usually observed in the shear stress growth upon inception of a steady shear flow.

2. The model

The well-known Cox-Merz rule [3] states that

$$\eta(\dot{\gamma}) = \left| \eta_0^*(\omega) \right|\Big|_{\omega = \dot{\gamma}} , \tag{1}$$

where $\eta(\dot{\gamma})$ is the nonlinear shear viscosity as function of shear rate and $\eta_0^*(\omega)$ is the frequency-dependent viscosity in the linear response regime. The Cox-Merz rule is a useful empiricism obeyed by many polymeric liquids. The quantity $\eta_0^*(\omega)$ is obtained [1] from the equation

$$\eta_0^*(\omega) = \int_0^\infty dt'\, G(t') e^{-i\omega t'} , \tag{2}$$

where $G(t')$ is the shear relaxation modulus. By definition, $G(t')$ determines the stress τ in the linear limit from the shear rate history by means of

$$\tau(t) = \int_0^\infty dt'\, G(t') \dot{\gamma}(t - t') . \tag{3}$$

From Eqs. (1) and (2) one expects the Cox-Merz rule to be satisfied if

$$\eta(\dot{\gamma}) = \int_0^\infty dt'\, G(t') e^{-\dot{\gamma} t'} \quad (\dot{\gamma} > 0) . \tag{4}$$

A straightforward generalization of Eq. (3) to include Eq. (4) for the stationary case is the following constitutive relation

$$\tau(t) = \int_0^\infty dt'\, G(t') \dot{\gamma}(t - t')$$

$$\cdot \exp\left\{ - \int_{t-t'}^t |\dot{\gamma}(t'')|\, dt'' \right\} . \tag{5}$$

Equation (5) is similar to Wagner's constitutive relation [1, 4]. The difference is that, in the "linear" part of the relation, y in Wagner's model is here replaced by $\dot{y}$. Also, the "damping function" is here $\exp\{-\int_{t-t'}^{}|\dot{y}|\}$ instead of Wagner's $\exp\{-|\int_{t-t'}^{}\dot{y}|\}$. The present choice of damping function is suggested because this damping function sums over all shear displacement taking place between time $t-t'$ and t, independent of the direction of the displacement.

Next, a specific form of $G(t')$ is chosen, namely $G(t') = E_1(t')$ where $E_1(t')$ is the exponential integral [5]

$$E_1(t') = \int_{t'}^{\infty} \frac{e^{-u}}{u}\,du \ . \tag{6}$$

For convenience we here and henceforth work with dimensionless time, stress, and viscosity, the latter quantity normalized so that $\eta_0^*(\omega = 0) = 1$. The final constitutive relation is

$$\tau(t) = \int_0^{\infty} dt'\,E_1(t')\dot{y}(t-t')$$

$$\cdot \exp\left\{-\int_{t-t'}^{t}|\dot{y}(t'')|\,dt''\right\} \ . \tag{7}$$

The use of $E_1(t')$ as the relaxation modulus is motivated by the fact that this choice leads to a nonlinear viscosity which is close to that predicted by Eyring's phenomenological theory of liquid flow [2] which fits many experiments:

$$\eta(\dot{y}) = \frac{\sinh^{-1}(\dot{y})}{\dot{y}} \ . \tag{8}$$

To see this, note that the Laplace transform of E_1 is [5]

$$\bar{E}_1(s) = \frac{\ln(1+s)}{s} \ , \tag{9}$$

so the nonlinear viscosity is given by

$$\eta(\dot{y}) = \frac{\ln(1+\dot{y})}{\dot{y}} \ . \tag{10}$$

From the identity $\sinh^{-1}(x) = \ln(x+\sqrt{1+x^2})$ it follows that Eyring's nonlinear shear viscosity for large $\dot{y}$ is close to that predicted in Eq. (10). This is illustrated in Fig. 1. Note that the present model com-
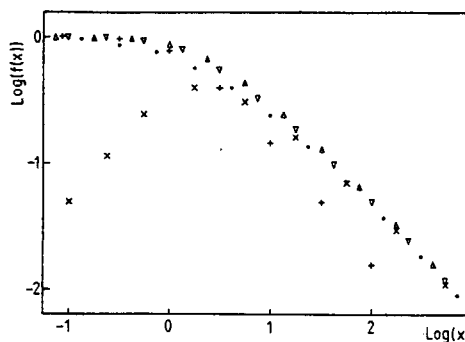

Fig. 1. Log-log plot of various quantities characterizing the model. In this figure, and throughout, dimensionless time, stress, and viscosity are used, the latter quantity normalized so that $\eta_0^*(\omega = 0) = 1$. The figure shows: (1) The predicted nonlinear viscosity as function of $x = \dot{y}$ (●) [Eq. (10)], (2) Eyring's nonlinear viscosity as function of $x = \dot{y}$ (△) [Eq. (8)], (3) $|\eta_0^*(\omega = x)|$ (▽) [Eq. (11)], and (4) the real (+) and the imaginary (×) part of $\eta_0^*(\omega = x)$ [Eq. (12)]. A comparison of the ● and △ points shows that Eyring's viscosity, which is known to give a good fit to many experiments, is reproduced reasonably well by the model. Comparing the ● and the ▽ points shows that the Cox-Merz rule is obeyed, though not quite accurately in the transition region. The real and imaginary parts of $\eta_0^*(\omega)$ looks much like in experiment

pared to Eyring's has a less sharp transition to nonlinear behavior. Figure 1 also shows that the Cox-Merz rule, as expected, is obeyed approximately by the constitutive relation. This observation is based on the fact that the frequency-dependent linear viscosity is given by

$$\eta_0^*(\omega) = \int_0^{\infty} dt'\,E_1(t')e^{-i\omega t'} = \frac{\ln(1+i\omega)}{i\omega} \ , \tag{11}$$

which implies for the real part and for the negative imaginary part

$$\eta'(\omega) = \text{Arctan}(\omega)/\omega$$

$$\eta''(\omega) = \ln\left[\sqrt{1+\omega^2}\right]/\omega \ . \tag{12}$$

We now proceed to calculate the time-dependent nonlinear response in various situations (following Chapter 3.4 in [1]). Consider first the stress growth upon inception of a steady shear flow, i.e., the case when the shear rate is given by

$$\dot{y}(t) = \begin{cases} 0 \ , & t<0 \\ \dot{y}_0 \ , & t>0 \ . \end{cases} \tag{13}$$
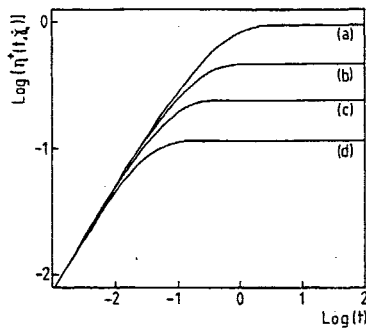
Fig. 2. Stress growth upon inception of a steady shear flow with shear rate $\dot{y}_0$. The quantity $\eta^+(t,\dot{y}_0)$, given by Eq. (16), is plotted as a function of time for: (a) $\dot{y}_0 = 0.1$ (reflecting the linear limit), (b) $\dot{y}_0 = 3$, (c) $\dot{y}_0 = 10$, and (d) $\dot{y}_0 = 30$. Like in experiment, $\eta^+(t,\dot{y}_0)$ follows the linear $\eta^+(t)$ for short times while it stabilizes for large t at the nonlinear viscosity, a stabilization which takes place sooner the larger is $\dot{y}_0$. The overshoot of $\eta^+(t,\dot{y}_0)$ often seen in experiment is not reproduced by the model

In this case Eq. (7) implies for the stress τ^+:

$$\tau^+(t) = \dot{y}_0 \int_0^t dt' E_1(t') e^{-\dot{y}_0 t'} \tag{14}$$

or, for the quantity $\eta^+(t,\dot{y}_0) = \tau^+(t)/\dot{y}_0$,

$$\eta^+(t,\dot{y}_0) = \int_0^t dt' E_1(t') e^{-\dot{y}_0 t'} . \tag{15}$$

After a partial integration Eq. (15) reduces to

$$\eta^+(t,\dot{y}_0) =$$
$$\{E_1[(1+\dot{y}_0)t] - E_1(t)e^{-\dot{y}_0 t} + \ln(1+\dot{y}_0)\}/\dot{y}_0 , \tag{16}$$

where use has been made of the fact that $E_1(t)$ varies as $-\ln(t)$ for $t \to 0$. In Fig. 2 $\eta^+(t,\dot{y}_0)$ is plotted in a logarithmic plot for different values of $\dot{y}_0$. The figure shows that η^+ is always monotonously increasing. This is not quite like in experiment where there is usually a characteristic "overshoot" of η^+ as function of time before the steady state value is reached [1].

Consider now stress relaxation after cessation of a steady shear flow, i.e., when

$$\dot{y}(t) = \begin{cases} \dot{y}_0 , & t < 0 \\ 0 , & t > 0 . \end{cases} \tag{17}$$

Then Eq. (7) implies for the stress τ^-:

$$\tau^-(t) = \dot{y}_0 \int_t^\infty dt' E_1(t') e^{-\dot{y}_0(t'-t)} . \tag{18}$$

Equations (10), (15), and (18) imply

$$\eta^+(t,\dot{y}_0) + e^{-\dot{y}_0 t} \eta^-(t,\dot{y}_0) = \frac{\ln(1+\dot{y}_0)}{\dot{y}_0} , \tag{19}$$

where $\eta^-(t,\dot{y}_0) = \tau^-(t)/\dot{y}_0$. By means of Eq. (16) we thus find

$$\eta^-(t,\dot{y}_0) = \{E_1(t) - E_1[(1+\dot{y}_0)t]e^{\dot{y}_0 t}\}/\dot{y}_0 . \tag{20}$$

Figure 3 shows η^- for various values of $\dot{y}_0$. As in experiment, one finds that $\eta^-(t,\dot{y}_0)$ is a monotonously decreasing function of time for all $\dot{y}_0$, and that η^- reaches zero faster the larger is $\dot{y}_0$.

We now turn to the calculation of stress relaxation after a sudden shearing displacement y_0. The shear rate is given by $\dot{y}(t) = y_0 \delta(t)$. Substituted into Eq. (7), this gives

$$\tau(t) = (1 - e^{-y_0}) E_1(t) , \tag{21}$$

which is easily shown by rewriting Eq. (7) as

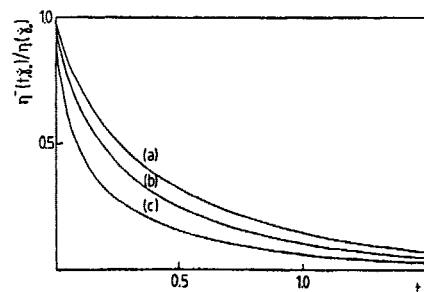$$\tau(t) = \int_0^\infty dt' E_1(t') \left[-\frac{d}{dt'} \right] e^{-\int_{t-t'}^t \dot{y}(t'')dt''} , \tag{22}$$

Fig. 3. Stress relaxation after cessation of a steady shear flow with shear rate $\dot{y}_0$. The figure shows the quantity $\eta^-(t,\dot{y}_0)/\eta(\dot{y}_0)$ as a function of time, where η^- is given by Eq. (20), for: (a) $\dot{y}_0 = 0.1$ (reflecting the linear limit), (b) $\dot{y}_0 = 3$, and (c) $\dot{y}_0 = 30$. As in experiment, $\eta^-(t,\dot{y}_0)$ decreases to zero as $t \to \infty$ faster the larger is $\dot{y}_0$

which is valid whenever $\dot\gamma \geq 0$. For the relaxation modulus $G(t,\gamma_0) = \tau(t)/\gamma_0$, one thus finds

$$G(t,\gamma_0) = E_1(t)\,\frac{1-e^{-\gamma_0}}{\gamma_0}\;. \tag{23}$$

For $\gamma_0 \to 0$, $G(t,\gamma_0)$ reduces to the linear shear relaxation modulus $E_1(t)$. Equation (23) shows that $G(t,\gamma_0)$ factorizes into a function of time multiplied by a function of γ_0, as expected for a Wagner type model [1, 4].

Next we consider the calculation of the nonlinear creep compliance $J(t,\tau_0)$, defined as $\gamma(t)/\tau_0$, where $\gamma(t)$ is the total shear displacement in time t when a constant stress τ_0 is applied at $t = 0$. The calculation of J from a constitutive relation is usually complicated by the fact that $y(t)$ is only given indirectly. For the present constitutive relation, however, $y(t)$ may be found analytically in the following way. First, Eq. (7) is rewritten for the case under consideration as

$$\tau_0 e^{\gamma(t)} = \int_0^t dt'\,E_1(t')\,\dot\gamma(t-t')e^{\gamma(t-t')}\quad (t>0)\;. \tag{24}$$

Equation (24) is linear in the variable $C(t) = \exp[\gamma(t)]$:

$$\tau_0 C(t) = \int_0^t dt'\,E_1(t')\dot C(t-t')\;. \tag{25}$$

This equation is now Laplace transformed into

$$\tau_0 \bar C(s) = \bar E_1(s)\dot{\bar C}(s) \tag{26}$$

or

$$\bar C(s) = \frac{\tau_0}{\ln(1+s)-\tau_0}\;. \tag{27}$$

Here, use has been made of Eq. (9) and the identity $\dot{\bar C}(s) = s\bar C(s) - C(0) = s\bar C(s) - 1$. $\bar C(s)$ has a branch cut on the negative real axis from $s = -1$ to $s = -\infty$ and a pole at $s = \dot\gamma_0$, where

$$\dot\gamma_0 = e^{\tau_0} - 1 \tag{28}$$

is the steady state shear rate [Eq. (10)]. The Laplace inversion of Eq. (27) is performed by deforming the integration contour to run from $-\infty$ slightly below the negative real axis, rounding the pole at $s = \dot\gamma_0$, and returning to $-\infty$ above the negative real axis.

After standard manipulations one thus finds

$$\dot C(t) = \tau_0(1+\dot\gamma_0)e^{\dot\gamma_0 t}$$

$$+ \tau_0 \int_1^\infty du\,e^{-ut}\,\frac{1}{[\ln(u-1)-\tau_0]^2+\pi^2} \tag{29}$$

or finally, by integration with respect to time,

$$e^{J(t,\tau_0)\tau_0} = 1 + \tau_0\,\frac{1+\dot\gamma_0}{\dot\gamma_0}\,(e^{\dot\gamma_0 t}-1)$$

$$+ \tau_0 \int_1^\infty du\,\frac{1-e^{-ut}}{u}\,\frac{1}{[\ln(u-1)-\tau_0]^2+\pi^2}\;. \tag{30}$$

In the linear limit Eq. (30) reduces to

$$J = t + \int_1^\infty du\,\frac{1-e^{-ut}}{u}\,\frac{1}{\ln^2(u-1)+\pi^2}\;. \tag{31}$$

The creep complicance $J(t,\tau_0)$ of Eq. (30) is plotted in Fig. 4 in a log-log plot for different values of $\dot\gamma_0$.

As a final example of the use of Eq. (7) consider the constrained recoil after a steady shear flow is interrupted at $t = 0$ by suddenly removing the shear stress. We wish to calculate the so-called recoverable shear γ_∞. Writing

$$\dot\gamma(t) = \begin{cases} \dot\gamma_0\,, & t<0 \\ -f(t)\,, & t>0\,, \end{cases} \tag{32}$$
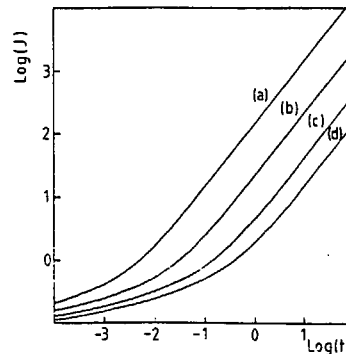

Fig. 4. Creep compliance $J = \gamma(t)/\tau_0$, where J is given by Eq. (30), plotted as function of time for: (a) $\dot\gamma_0 = 1000$, (b) $\dot\gamma_0 = 100$, (c) $\dot\gamma_0 = 10$, and (d) $\dot\gamma_0 = 1$, where $\dot\gamma_0$ is related to τ_0 by Eq. (28)

where $f(t) > 0$, Eq. (7) implies for $t > 0$

$$0 = -\int_0^t dt' E_1(t') f(t-t') e^{-\int_{t-t'}^t f(t'')dt''}$$

$$+ \int_t^\infty dt' E_1(t') \dot{\gamma}_0 e^{-\dot{\gamma}_0(t'-t) - \int_0^t f(t'')dt''}$$ (33)

or

$$\int_0^t dt' E_1(t') f(t-t') e^{\int_0^{t-t'} f(t'')dt''}$$

$$= \dot{\gamma}_0 e^{\dot{\gamma}_0 t} \int_t^\infty dt' E_1(t') e^{-\dot{\gamma}_0 t'} .$$ (34)

Defining $F(t) = \exp\left(\int_0^t f(t'')dt''\right)$, Eq. (34) becomes

$$\int_0^t dt' E_1(t') \dot{F}(t-t')$$

$$= \dot{\gamma}_0 e^{\dot{\gamma}_0 t} \int_t^\infty dt' E_1(t') e^{-\dot{\gamma}_0 t'} .$$ (35)

The Laplace transform of Eq. (35) is

$$\bar{E}_1(s)[s\bar{F}(s) - 1] = \frac{\dot{\gamma}_0}{\dot{\gamma}_0 - s} [\bar{E}_1(s) - \bar{E}_1(\dot{\gamma}_0)]$$ (36)

or

$$\bar{F}(s) = \frac{1}{s}\left[1 + \frac{\dot{\gamma}_0}{\dot{\gamma}_0 - s} \frac{\bar{E}_1(s) - \bar{E}_1(\dot{\gamma}_0)}{\bar{E}_1(s)}\right] .$$ (37)

The recoverable shear is determined from $e^{\gamma_\infty} = \lim_{t \to \infty} F(t)$. This limit is given by the residue of the pole at $s = 0$ of Eq. (37), and one finds $\gamma_\infty = \ln [2 - \bar{E}_1(\dot{\gamma}_0)]$, or

$$\gamma_\infty = \ln [2 - \eta(\dot{\gamma}_0)] .$$ (38)

In the two limits one has

$$\gamma_\infty = \begin{cases} \frac{1}{2} \dot{\gamma}_0 , & \dot{\gamma}_0 \ll 1 \\ \ln 2 , & \dot{\gamma}_0 \gg 1 . \end{cases}$$ (39)

$\gamma_\infty(\dot{\gamma}_0)$ is monotonously increasing which is also the case in experiment. Also like in experiment, γ_∞ stabilizes on a recoverable shear of order one at high $\dot{\gamma}_0$.

3. Discussion

In this paper it has been argued that a simple constitutive relation exists which has no adjustable parameters (except the overall scaling of time and viscosity) and which gives a qualitatively correct picture of shear viscoelasticity. The relation Eq. (7) was arrived at by requiring the Cox-Merz rule to be satisfied and that Eyring's nonlinear viscosity Eq. (8) is to be reproduced approximately. This ensures a nonlinear viscosity and a frequency-dependent linear viscosity which are both close to those observed in many experiments. Figure 5 shows the nonlinear steady state viscosity of the model compared to experiments on four polymeric liquids. In Fig. 6 the absolute value of the complex frequency-dependent viscosity of the model is compared to experiments on three of the systems of Fig. 5. In both figures there is a qualitative agreement between model and experiment. From studies of the literature it is estimated that $25 - 50\%$ of the published rheological data on polymeric systems may be fitted similarly by the model. A quantitatively satisfactory fit is only possible for few systems, however. To obtain this, one or more fitting parameters must be introduced into the model, which will not be attempted here.

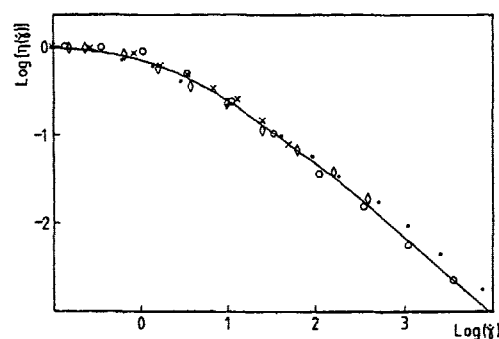The choice of the linear relaxation modulus to be $E_1(t')$ may be justified from the box model, i.e., the

Fig. 5. Nonlinear viscosity of the model [full curve, Eq. (10)] compared to experiments on four different polymeric liquids. As throughout this work, both the viscosity and the shear rate are reported in dimensionless units, the scaling parameters being, respectively, the linear shear viscosity and $1/T$ where T is a characteristic time. The figure shows data for (a) linear, monodisperse polystyrene in 1-CN ($\bigcirc$, Fig. 15 of [6]), (b) Poly-1-olefins ($\bullet$, Fig. 1 of [7] based on data from [8]), (c) poly (methyl methacrylate) ($\times$, Fig. 15a of [9]), and (d) 0.75% polyacrylamide ($\Diamond$, Fig. 3 of [10] based on data from [11])
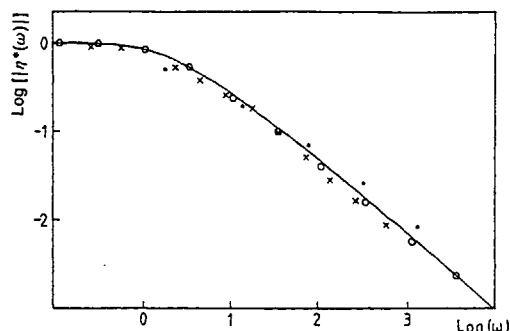
Fig. 6. Modulus of the complex linear frequency-dependent viscosity in the model [full curve, based on Eq. (12)] compared to experiments on three different polymeric liquids quoted in Fig. 5. For each set of data the dimensionless viscosity is shown as a function of the dimensionless frequency defined by the same characteristic time as used in Fig. 5. The figure shows data for (a) linear, monodisperse polystyrene in 1-CN (○), (b) poly-1-olefins (●), and (c) poly (methyl methacrylate) (×)

postulate of a uniform distribution of activation energies for microscopic motion. Consider the motion of a foreign microscopic particle in the liquid. Suppose the particle feels a spatially randomly varying potential energy, and that it moves by thermally activated hopping between the various potential energy minima. Then the linear mobility of the particle (the velocity divided by an external force acting on the particle), is to a good approximation given by [12]

$$\mu^*(\omega) = \mu(0) \frac{i\omega}{\ln(1+i\omega)} . \tag{40}$$

Assuming the Stokes law is valid for the particle, one has $\mu^* \propto 1/\eta^*$ which shows that the linear shear relaxation modulus of the liquid is $E_1(t')$ in this approximation.

Because the Cox-Merz rule is obeyed by the model it is not surprising that the Gleissele mirror relation [1] is also satisfied: The linear limit of η^+ from Eq. (16) is

$$\lim_{\dot{\gamma}_0 \to 0} \eta^+(t,\dot{\gamma}_0) = tE_1(t) - e^{-t} + 1 . \tag{41}$$

Gleissele's mirror relation states that $\eta(\dot{\gamma})$ is equal to this limit evaluated at $t = 1/\dot{\gamma}$, thus

$$\eta(\dot{\gamma}) = \begin{cases} 1 , & \dot{\gamma} \ll 1 \\ (1 - C + \ln \dot{\gamma})/\dot{\gamma} , & \dot{\gamma} \gg 1 , \end{cases} \tag{42}$$

where $C = 0.577\ldots$ is Euler's constant. A comparison of Eqs. (10) and (42) shows that the mirror relation is indeed satisfied to a good approximation.

The constitutive relation Eq. (7) reproduces most qualitative features of shear viscoelasticity. (An exception is the overshoot usually observed in η^+ as a function of time, where the model predicts η^+ to increase monotonously to the steady state value.) The fact that qualitative features of experiment are generally reproduced is not surprising, given the similarity between the present model and the Wagner model, which is well-known to give a satisfactory description of experiment. However, it should be noted that the present model, despite the similarity to Wagner's model in the use of an exponential damping function, does not belong to the class of single integral constitutive relations of the Boltzmann-superposition-type involving a nonlinear strain measure. This is because, in Eq. (7), $\dot{\gamma}$ appears instead of γ. As shown by Booij et al. [13], for the former type of models the Cox-Merz rule may be accurately reproduced only if one uses a specific non-monotonous strain measure. This problem is avoided here because the analysis of Booij et al. does not apply to this model; however, it should be emphasized that the Cox-Merz rule is after all obeyed only approximately in the present model (Fig. 1).

The use of an exponential damping function in the present model is inspired by Wagner's work [4]. This damping function, in effect, cuts-off relaxation processes with rates less than the shearing rate, an idea discussed by several authors [14 – 18]. An important difference from Wagner's model is that his damping function is $\exp[-|\int_{t-t'}^t \dot{\gamma}|]$, whereas we here use $\exp[-\int_{t-t'}^t |\dot{\gamma}|]$. For a monotonously increasing or decreasing $\gamma(t)$ this does not make any difference. In more general flows there may be considerable differences between the two approaches. For instance, if the net shear displacement between time $t-t'$ and t is zero there is no damping at all in Wagner's approach. In contrast, all shear displacement taking place between time $t-t'$ and t contributes to the damping in the model of Eq. (7). Thereby an irreversibility related to the network rupture hypothesis of Tanner [14, 18] is incorporated into the model. The model may be regarded as expressing a continuous version of Tanner's idea that entanglements are lost irreversibly in the process of deformation as soon as a limiting strain is exceeded; here entanglements are lost continuously during any deformation. In passing we note that Wagner's model has been extended to incorporate irreversibility using a rather complicated functional of the strain history in the memory function [19]. This

Dyre, A "zero-parameter" constitutive relation for simple shear viscoelasticity   151

gives better agreement with experiment than the original Wagner model.

A possible objection to the kind of damping term used here is that, for a periodic shear $\gamma = \gamma_0 \sin(\omega t)$, one might expect that the nonlinearity sets in at high frequencies, even at very small amplitudes (because the damping apparently is a function of $\gamma_0 \omega$, and not of γ_0), in contradiction to experiment. This, however, is not correct: Suppose the worst possible case of the non-linearity, i.e., put the damping function equal to $\exp(-\omega \gamma_0 t')$ in Eq. (7). Then the response is

$$\tau(t) = \gamma_0 \omega \int_0^\infty dt' E_1(t') \cos[\omega(t-t')] e^{-\omega \gamma_0 t'}$$

$$= \gamma_0 \omega [\cos(\omega t) \operatorname{Re} g - \sin(\omega t) \operatorname{Im} g] , \quad (43)$$

where

$$g = \int_0^\infty dt' E_1(t') e^{-(i\omega + \gamma_0 \omega)t'}$$

$$\qquad\qquad\qquad\qquad\qquad\qquad (44)$$

$$= \frac{\ln(1+x)}{x} , \quad x = i\omega + \gamma_0 \omega .$$

At a fixed ω the onset of nonlinearity may be estimated from

$$\gamma_0 \omega \simeq \left| \frac{g(x)}{g'(x)} \right| \Bigg|_{x=i\omega} , \quad (45)$$

which is the criterion for the first order term being equal to the zero-th order term in the Taylor expansion of g as function of γ_0. Equation (45) leads to

$$\gamma_0 \omega \simeq \omega \left| \frac{\ln(1+i\omega)}{i\omega/(1+i\omega) - \ln(1+i\omega)} \right| . \quad (46)$$

It is now easy to see that whenever $\omega \gtrsim 1$ the onset of nonlinearity takes place for γ_0 of order one. For $\omega \ll 1$, however, the onset of nonlinearity is at $\gamma_0 = \omega^{-1}$, corresponding to a maximum shear rate of order one in the periodic variation.

References

1. Bird RB, Armstrong RC, Hassager O (1987) Dynamics of Polymeric Liquids, Second Edition. Wiley, New York
2. Kincaid JF, Eyring H, Stearn AE (1941) Chem Rev 28:301 – 365
3. Cox WP, Merz EH (1958) J Polym Sci 28:619 – 622
4. Wagner MH (1979) Rheol Acta 18:33 – 50
5. Abramowitz M, Stegun IA (eds) (1972) Handbook of Mathematical Functions. Dover Publications, New York
6. Yasuda K, Armstrong RC, Cohen RE (1981) Rheol Acta 20:163 – 178
7. Kulicke WM, Porter RS (1980) Rheol Acta 19:601 – 605
8. Wang JS, Knox JR, Porter RS (1978) J Polym Sci, Polym Phys Ed 16:1709 – 1719
9. Martinez CB, Williams MC (1980) J Rheol 24:421 – 450
10. Wagner MH (1977) Rheol Acta 16:43 – 50
11. Marsh BD (1967) (as cited by PJ Carreau, IF Macdonald, RB Bird (1968) Chem Eng Sci 23:901)
12. Dyre JC (1988) J Appl Phys 64:2456 – 2468
13. Booij HC, Leblans P, Palmen J, Tiemersma-Thoone G (1983) J Polym Sci, Polym Phys Ed 21:1703 – 1711
14. Tanner RI, Simmons JM (1967) Chem Eng Sci 22:1803 – 1815
15. Chen I-J, Bogue DC (1972) Trans Soc Rheol 16:59 – 78
16. Bersted BH (1976) J Appl Polym Sci 20:2705 – 2714
17. Thurston GB (1981) J Non-Newtonian Fluid Mech 9:57 – 68
18. Tanner RI (1969) AIChE J 15:177
19. Wagner MH, Stephenson SE (1979) J Rheol 23: 489 – 504

Authors' address:

Dr. Jeppe C. Dyre
IMFUFA
Roskilde Universitetscenter
P.O. Box 260
4000-Roskilde, Denmark

Langevin models for shear-stress fluctuations in flows of viscoelastic liquids

Jeppe C. Dyre

Institut for Studiet af Matematik og Fysik samt deres Funktioner i Undervisning, Forskning og Anvendelser,
Roskilde Universitetscenter, Postbox 260, DK-4000 Roskilde, Denmark
(Received 1 March 1993)

From the principle of virtual work it is shown that, if equilibrium stress fluctuations are described by a Langevin equation, there is only one possible extension of this equation to describe stress fluctuations in a shear flow. It is shown that the resulting equation is consistent with linear-response theory. The formalism developed may be looked upon as a method for extending differential constitutive relations to incorporate thermal fluctuations. A few simple models are discussed as illustrations. These include a model where the stress fluctuates freely below a certain limit, and a model constructed to mimic the Tobolsky-Eyring phenomenological theory [J. Chem. Phys. **11**, 125 (1942)] of viscoelastic liquids. It is concluded that these and similar models, however, do not realistically describe real polymeric liquids. To reach this goal, models involving several stress degrees of freedom will have to be considered.

I. INTRODUCTION

Presently, the most popular models of the viscoelasticity of polymeric liquids are based on a microscopic description, where the bead coordinates are the basic degrees of freedom [1,2]. These models are rather successful but, unfortunately, also quite complicated to solve. The present paper investigates the more phenomenological approach to take as a basic degree of freedom the quantity of main interest, the shear stress. In part, this represents a return to ideas proposed by Eyring, Tobolsky, Andrews, and Hofman-Bang many years ago [3–5]. Here, however, a formalism is developed which is consistent with statistical mechanics. This is done by assuming a Langevin equation for the shear-stress dynamics in equilibrium. From this the stress fluctuations may be calculated and thereby, via the fluctuation-dissipation theorem, the linear frequency-dependent viscosity may be calculated. The main result of the paper is a proof that the nonlinear response to any shear displacement is uniquely determined by the requirement that the principle of virtual work is obeyed. It is shown that this principle ensures that linear-response theory is obeyed, a *sine qua non* requirement (Sec. II). In Sec. III a few simple models are worked out. Finally, in Sec. IV a discussion is given. It is concluded that, in order to model realistically reality, the proposed formalism must be generalized to include spatially varying stresses.

II. UNIQUE COUPLING OF DEFORMATION TO STRESS FLUCTUATIONS

Here and henceforth the term "stress" refers to the shear stress σ_{xy}, while the corresponding x-y shear rate is denoted by $\dot{\gamma}(t)$. The fluctuation-dissipation theorem [2] allows a calculation of the frequency-dependent viscosity $\eta(\omega)$ in terms of equilibrium stress fluctuations. The theorem states that the stress relaxation modulus $G(t)$, which is characterized by

$$\eta(\omega) = \int_0^\infty G(t)e^{-i\omega t}dt , \qquad (1)$$

is given by

$$G(t) = \beta \frac{\langle s(0)s(t)\rangle_0}{V} . \qquad (2)$$

Here, a sample of volume V is considered, s is the "total" stress (i.e., $\sigma_{xy} = s/V$), and $\beta = 1/k_B T$. The subscript zero on the right-hand side of Eq. (2) is introduced to remind one that the autocorrelation function refers to fluctuations in thermal equilibrium. If $\mathbf{R}_i$ is the coordinate vector of the ith bead and $\mathbf{F}_i$ is the force on the ith bead, the quantity s is given [2] by

$$s = -\sum_i R_{i,x}F_{i,y} . \qquad (3)$$

[Note that the relaxation modulus of Eq. (2) has a well-defined limit for $V \to \infty$: this is the usual macroscopic shear-stress relaxation modulus.]

From now on the following simple model is adopted. The liquid is regarded as divided into regions whose stresses fluctuate independently. A discussion of this rather severe approximation is postponed to Sec. IV. There is just one relevant degree of freedom in the model, the quantity s of Eq. (3), where the sum is now restricted to one region. The quantity s has dimension energy, but will still be referred to as the "stress." It is convenient also to redefine "viscosity" by absorbing the region volume, so that viscosity is from now on simply $\langle s \rangle / \dot{\gamma}$. With these definitions Eqs. (1) and (2) become

$$\eta(\omega) = \beta \int_0^\infty \langle s(0)s(t)\rangle_0 e^{-i\omega t}dt . \qquad (4)$$

We remind the reader that Eq. (4) is equivalent to saying that the average stress for small shear rate $\dot{\gamma}(t)$ is given by

$$\langle s(t)\rangle_\gamma = \beta \int_0^\infty \langle s(0)s(\tau)\rangle_0 \dot{\gamma}(t-\tau)d\tau . \qquad (5)$$

According to statistical mechanics, the probability of an s

fluctuation in equilibrium is given by the free energy as a function of s, $F(s)$. If Γ denotes the complete set of microscopic coordinates referring to one region, and $s(\Gamma)$ and $E(\Gamma)$ denote, respectively, the value of s and of energy in state Γ, $F(s)$ is given by

$$e^{-\beta F(s)} = \int e^{-\beta E(\Gamma)} \delta(s - s(\Gamma)) d\Gamma \ . \tag{6}$$

It is assumed that $F(s) \to \infty$ as $|s| \to \infty$, and that $F(s) = F(-s)$. Note that the free energy of one region is given by

$$e^{-\beta F} = \int_{-\infty}^{\infty} e^{-\beta F(s)} ds \ . \tag{7}$$

Now the further assumption is made that the s fluctuations in equilibrium are described by a Langevin equation,

$$\dot{s} = -\mu \frac{dF}{ds} + \xi(t) \ . \tag{8}$$

Here, μ is the "mobility" ("velocity"/"force") which determines the time scale, and $\xi(t)$ is a Gaussian white-noise term:

$$\langle \xi(t)\xi(t') \rangle = 2\mu k_B T \delta(t - t') \ . \tag{9}$$

While Eq. (8) is a completely phenomenological postulate, it has the crucial property [2,6,7] that the stationary s-probability distribution $P_0(s)$ is that required by statistical mechanics:

$$P_0(s) = N^{-1} e^{-\beta F(s)} \ . \tag{10}$$

Any initial probability distribution converges to $P_0(s)$ as $t \to \infty$; the equation governing this is the well-known Smoluchowski equation [2,6,7] (sometimes referred to as the Fokker-Planck equation or just the diffusion equation)

$$\frac{\partial P}{\partial t} = \frac{\partial}{\partial s}\left[\mu \frac{dF}{ds}P + \mu k_B T \frac{\partial P}{\partial s}\right] \ . \tag{11}$$

A substitution of Eq. (10) into Eq. (11) confirms that $P_0(s)$ is the stationary solution.

How is the s dynamics changed when the liquid flows? The simplest way to modify Eq. (8) is to add an extra term coupling to $\dot{\gamma}(t)$, writing

$$\dot{s} = -\mu \frac{dF}{ds} + \dot{\gamma}(t)J(s) + \xi(t) \ . \tag{12}$$

In Eq. (12) the shear rate plays the role of an external field. Obviously, $J(s)$ is a kind of stress-dependent infinite frequency shear modulus. The Smoluchowski equation corresponding to Eq. (12) is

$$\frac{\partial P}{\partial t} = \frac{\partial}{\partial s}\left\{\left[\mu \frac{dF}{ds} - \dot{\gamma}(t)J\right]P + \mu k_B T \frac{\partial^2 P}{\partial s^2}\right\} \ . \tag{13}$$

We now proceed to show first that $J(s)$ is uniquely determined by the principle of virtual work. Then it is shown that, with this choice of $J(s)$, linear-response theory [Eqs. (1) and (2)] is reproduced in the small shear rate limit, as is necessary to have a consistent theory.

For any probability distribution $P(s)$ the dynamical

free energy A is defined [2] by

$$A = \int_{-\infty}^{\infty} ds\, P(s)\{F(s) + k_B T \ln[P(s)]\} \ . \tag{14}$$

The principle of virtual work [2,8] says that after the virtual displacement

$$\dot{\gamma}(t) = \delta\gamma\delta(t) \ , \tag{15}$$

A is changed by

$$\delta A = \langle s \rangle \delta\gamma \ . \tag{16}$$

From Eq. (14) the variation in A is given by

$$\delta A = \int_{-\infty}^{\infty} ds\, \delta P(s)\{F(s) + k_B T \ln[P(s)]\} \ . \tag{17}$$

Substituting Eq. (15) into Eq. (13) and integrating over a small interval around 0 gives, to lowest order in $\delta\gamma$,

$$\delta P = -\delta\gamma \frac{\partial}{\partial s}(JP) \ . \tag{18}$$

By combining Eqs. (17) and (18) one finds by partial integrations

$$\begin{aligned}
\delta A &= -\delta\gamma \int_{-\infty}^{\infty} ds \left[F\frac{\partial}{\partial s}(JP) + k_B T \ln(P)\frac{\partial}{\partial s}(JP)\right] \\
&= \delta\gamma \int_{-\infty}^{\infty} ds \left[\frac{dF}{ds}JP + k_B T \frac{\partial P}{\partial s}J\right] \\
&= \delta\gamma \int_{-\infty}^{\infty} ds \left[\frac{dF}{ds}J - k_B T \frac{dJ}{ds}\right]P \ .
\end{aligned} \tag{19}$$

If this is to be consistent with Eq. (16) for all $P(s)$, $J(s)$ must obey

$$\frac{dJ}{ds} = \beta \frac{dF}{ds}J - \beta s \ . \tag{20}$$

The solution of this equation is

$$J(s) = e^{\beta F(s)} \int_{s}^{\infty} ds'\, \beta s'\, e^{-\beta F(s')} \ . \tag{21}$$

All other solutions lead to an exponentially increasing $J(s)$ and thereby an inconsistent model where s runs off to infinity in any shear flow. For $\beta \to \infty$ Eq. (21) implies $J(s) = s/(dF/ds)$.

Next it is shown that the $J(s)$ of Eq. (21) ensures that linear-response theory is reproduced. First Eq. (12) is rewritten as

$$\dot{s} = -\mu \frac{\partial}{\partial s}[F - \dot{\gamma}(t)\Phi] + \xi(t) \ , \tag{22}$$

where

$$\frac{d\Phi}{ds} = \frac{J}{\mu} \ . \tag{23}$$

Equation (22) shows that the coupling to the shear displacement "field" appears as an extra term $-\dot{\gamma}(t)\Phi(s)$ in the Hamiltonian. In the small-shear-rate limit, linear-response theory *applied to Eq. (22)* leads [2] to

$$\langle s(t) \rangle_{\dot{\gamma}} = \beta \int_{0}^{\infty} \dot{\gamma}(t - \tau)\frac{-d}{d\tau}\langle \Phi(\tau=0)s(\tau) \rangle_0 d\tau \ . \tag{24}$$

Equation (24) is consistent with Eq. (5) if

$$-\frac{d}{d\tau}\langle \Phi(\tau=0)s(\tau)\rangle_0 = \langle s(0)s(\tau)\rangle_0 \ . \tag{25}$$

To prove Eq. (25) note that the $\Phi - s$ correlation function is given by

$$\langle \Phi(\tau=0)s(\tau)\rangle_0$$
$$= \int_{-\infty}^{\infty} ds's' \int_{-\infty}^{\infty} ds\, P_0(s)\Phi(s)G_0(s,s';\tau) \ , \tag{26}$$

where $G_0(s,s';\tau)$ is the equilibrium Green's function, i.e., the probability of finding stress s' at time t if the stress

were s at $t=0$. By substituting into this expression the time-integrated version of detailed balance $P_0(s)G_0(s,s';\tau) = P_0(s')G_0(s',s;\tau)$, one finds

$$-\frac{d}{d\tau}\langle \Phi(\tau=0)s(\tau)\rangle_0$$
$$= -\int_{-\infty}^{\infty} ds's' P_0(s') \int_{-\infty}^{\infty} ds\, \Phi(s)\frac{\partial G_0}{\partial \tau}(s',s;\tau) \ . \tag{27}$$

The Green's function considered as a function of the second variable satisfies Eq. (11), of course, and therefore one gets

$$-\frac{d}{d\tau}\langle \Phi(\tau=0)s(\tau)\rangle_0 = -\int_{-\infty}^{\infty} ds's' P_0(s') \int_{-\infty}^{\infty} ds\, \Phi(s)\left[\mu\frac{\partial}{\partial s}\left[\frac{dF}{ds}G_0\right]+\frac{\mu}{\beta}\frac{\partial^2 G_0}{\partial s^2}\right]$$
$$= \int_{-\infty}^{\infty} ds's' P_0(s') \int_{-\infty}^{\infty} ds\, \left[J(s)\frac{dF}{ds}-\frac{1}{\beta}\frac{dJ}{ds}\right]G_0(s',s;\tau) \ . \tag{28}$$

Because $J(s)$ satisfies Eq. (20) it is now clear that Eq. (25) is obeyed.

III. SOME SIMPLE MODELS

A. Gaussian model

In this model the free energy is assumed to be quadratic in s:

$$F(s)=\tfrac{1}{2}\alpha s^2 \ . \tag{29}$$

The equilibrium s-probability distribution is a Gaussian

$$P_0(s)=\left[\frac{\alpha\beta}{2\pi}\right]^{1/2} e^{-(1/2)\alpha\beta s^2} \ , \tag{30}$$

which implies

$$\langle s^2\rangle_0 = \frac{1}{\alpha\beta} \ . \tag{31}$$

The "equation of motion" for s is

$$\dot{s}(t)=-\mu\alpha s(t)+\xi(t) \ . \tag{32}$$

If Eq. (32) is multiplied by $s(0)$ and averaged, one finds

$$\frac{d}{dt}\langle s(0)s(t)\rangle_0 = -\mu\alpha\langle s(0)s(t)\rangle_0 \quad (t>0) \ . \tag{33}$$

The solution of Eq. (33) which satisfies Eq. (31) is

$$\langle s(0)s(t)\rangle_0 = \frac{1}{\alpha\beta}e^{-\mu\alpha t} \quad (t>0) \ . \tag{34}$$

The calculation of $J(s)$ is straightforward; from Eq. (21) one finds

$$J(s)=e^{(1/2)\alpha\beta s^2}\int_s^{\infty}\beta s' e^{-(1/2)\alpha\beta s'^2}ds' = \frac{1}{\alpha} \ . \tag{35}$$

The Smoluchowski equation (13) thus is

$$\frac{\partial P}{\partial t}=\frac{\partial}{\partial s}\left[\left[\mu\alpha s-\frac{\dot{\gamma}(t)}{\alpha}\right]P\right]+\mu k_B T\frac{\partial^2 P}{\partial s^2} \ . \tag{36}$$

From Eq. (36) a simple equation for the average $\langle s(t)\rangle_{\dot{\gamma}}$ may be derived by application of the obvious identity

$$\frac{d}{dt}\langle s(t)\rangle_{\dot{\gamma}} = \int_{-\infty}^{\infty} s\frac{\partial P}{\partial t}(s,t)ds \ . \tag{37}$$

Substituting Eq. (36) into Eq. (37), one finds after partial integrations

$$\frac{d}{dt}\langle s(t)\rangle_{\dot{\gamma}} = -\mu\alpha\langle s(t)\rangle_{\dot{\gamma}}+\frac{\dot{\gamma}(t)}{\alpha} \ . \tag{38}$$

As usual it is assumed that the shear rate "field" $\dot{\gamma}(t)$ is introduced gradually in the distant past. The solution of Eq. (38) which vanishes as $t\rightarrow -\infty$ is

$$\langle s(t)\rangle_{\dot{\gamma}} = \int_{-\infty}^{t}\frac{\dot{\gamma}(t')}{\alpha}e^{-\mu\alpha(t-t')}dt' \ . \tag{39}$$

By means of Eq. (34) this may be rewritten as

$$\langle s(t)\rangle_{\dot{\gamma}} = \beta\int_0^{\infty}\langle s(0)s(\tau)\rangle_0\dot{\gamma}(t-\tau)d\tau \ . \tag{40}$$

Equation (40) is nothing but the prediction of linear-response theory [Eq. (5)]. Thus, the Gaussian model is linear for all displacements.

B. Box model

This model is defined by

$$F(s)=\begin{cases}0, & |s|<s_0 \\ \infty, & |s|>s_0\end{cases} \ . \tag{41}$$

The model is named after the box model in elementary quantum mechanics; it should not be confused with the box-model distribution of relaxation times sometimes used in rheology [9]. Since there is a maximum value of the stress, the box model must exhibit shear thinning at large shear rates. To find the nonlinear viscosity $\eta(\dot{\gamma})$ we need to determine $J(s)$ first. In the present case Eq. (20) reduces to $dJ/ds=-\beta s$. The solution of this equation, which satisfies the boundary conditions $J(-s_0)=J(s_0)=0$, is

$$J(s) = \frac{\beta}{2}(s_0^2 - s^2) . \tag{42}$$

The Φ function of Eq. (23) thus becomes

$$\Phi(s) = \frac{\beta}{2\mu}(s_0^2 s - \tfrac{1}{3}s^3) . \tag{43}$$

For a given shear rate $\dot{\gamma}$, the stationary solution of Eq. (13) is

$$P(s) = N^{-1} e^{\beta \dot{\gamma} \Phi(s)}, \quad (|s| < s_0) , \tag{44}$$

where N is a normalization constant, and $P(s) = 0$ for $|s| > s_0$. If the dimensionless shear rate

$$\dot{\gamma}^* = \frac{\beta^2 s_0^3}{\mu} \dot{\gamma} \tag{45}$$

is introduced, one finds from Eq. (44)

$$\langle s \rangle_{\dot{\gamma}} = s_0 \frac{\int_{-1}^{1} t e^{\dot{\gamma}^*[(t/2) - (t^3/6)]} dt}{\int_{-1}^{1} e^{\dot{\gamma}^*[(t/2) - (t^3/6)]} dt} . \tag{46}$$

From this the nonlinear viscosity $\eta = \langle s \rangle / \dot{\gamma}$ is readily evaluated. The result is shown in Fig. 1(a) and is not unlike that seen in polymeric liquids. In the linear limit one finds, by expanding Eq. (46) to first order in $\dot{\gamma}^*$, the shear rate independent viscosity η_0 given by

$$\eta_0 = \frac{2\beta^2 s_0^4}{15\mu} . \tag{47}$$

The equilibrium dynamics is governed by the simple diffusion equation [Eq. (11)]

$$\frac{\partial P}{\partial t} = \frac{\mu}{\beta} \frac{\partial^2 P}{\partial s^2} , \tag{48}$$

subject to the boundary conditions

$$\frac{\partial P}{\partial s}(s = -s_0) = \frac{\partial P}{\partial s}(s = s_0) = 0 . \tag{49}$$

The eigenfunctions of this problem are $\cos[n\pi(s_0 - s)/(2s_0)]$ $(n = 0, 1, 2, \dots)$. From this one finds by standard methods [10] that the equilibrium Green's function is given by

$$G_0(s, s'; t) = \frac{1}{2s_0} + \sum_{n=1}^{\infty} \frac{1}{s_0} e^{-\omega_n t} \cos[\lambda_n(s_0 - s)]$$

$$\times \cos[\lambda_n(s_0 - s')] , \tag{50}$$

where

$$\lambda_n = \frac{\pi}{2s_0} n, \quad \omega_n = \frac{\mu}{\beta} \lambda_n^2 \quad (n = 1, 2, \dots) . \tag{51}$$

It is now easy to derive an analytical expression for the frequency-dependent viscosity $\eta(\omega)$. Since the equilibrium probability distribution is $P_0(s) = 1/(2s_0)$, the autocorrelation function becomes

$$\langle s(0)s(t) \rangle_0 = \int_{-s_0}^{s_0} \frac{ds}{2s_0} \int_{-s_0}^{s_0} ds' ss' G_0(s, s'; t) . \tag{52}$$

From Eqs. (50) and (52) and the fluctuation-dissipation

theorem [Eq. (4)], one finds

$$\eta(\omega) = \frac{32\beta s_0^2}{\pi^4} \sum_{\text{odd } n} \frac{1}{n^4(i\omega + \omega_n)} . \tag{53}$$

In the zero-frequency limit Eq. (53) reduces to Eq. (47) via the identity [11]

$$\frac{1}{1^6} + \frac{1}{3^6} + \frac{1}{5^6} + \cdots = \frac{\pi^6}{960} . \tag{54}$$

Figure 1(b) shows the real part of $\eta(\omega)$. The spectrum contains infinitely many relaxation times but these are hardly visible, being completely dominated by the fundamental frequency ω_1. In effect, $\eta(\omega)$ is almost indistinguishable from the prediction of a simple Maxwell model where $\text{Re}\,\eta(\omega)$ is proportional to ω^{-2} for $\omega \to \infty$.

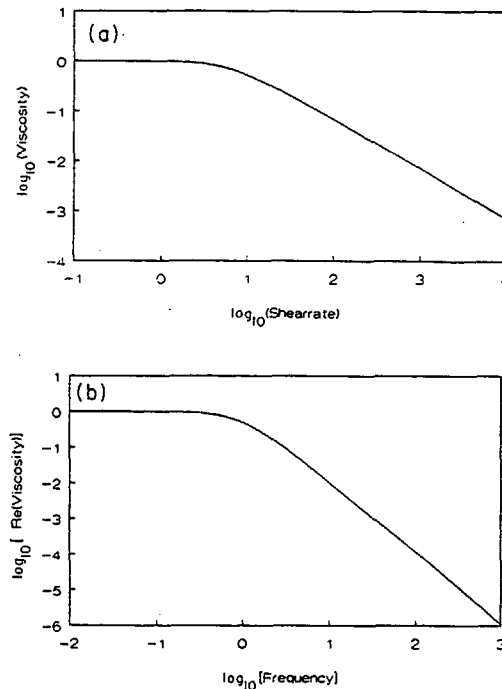Only in the relaxation towards equilibrium from a

FIG. 1. Box-model predictions for the viscosity. (a) shows a log-log plot of the steady-state viscosity relative to the linear viscosity, as a function of the dimensionless shear rate given by Eq. (45). At large shear rates the viscosity varies as the inverse of the shear rate; this is a consequence of there being a maximum possible stress in the model. (b) shows a log-log plot of the real part of the frequency-dependent viscosity relative to the zero-frequency viscosity, as a function of the dimensionless frequency ω/ω_1. Despite the fact that the model has infinitely many relaxation times, the longest relaxation time dominates the frequency dependence completely. In effect, the frequency dependence is almost indistinguishable from that of a standard Maxwell model where the real part of the viscosity varies as ω^{-2} at large frequencies.

strongly nonequilibrium state do the higher harmonics give significant contributions. If $\langle s(t)\rangle_s$ denotes the average stress, given the value s at $t=0$, one has obviously

$$\langle s(t)\rangle_s = \int_{-s_0}^{s_0} s' G_0(s,s';t)ds' .\tag{55}$$

Relaxation from a state with probability distribution $P(s)$ at $t=0$ is thus given by

$$\langle s(t)\rangle_P = \int_{-s_0}^{s_0} \langle s(t)\rangle_{s'} P(s')ds' .\tag{56}$$

Two well-known examples are stress relaxation after cessation of a steady flow, and stress relaxation after a sudden shear displacement starting from equilibrium [1]. In the first case, the probability distribution $P(s)$ is given by Eq. (44) at $t=0$. In the latter case, after the sudden shear displacement given by $\dot{\gamma}(t)=\gamma_0\delta(t)$, it is possible to show that $P(s)$ is given by

$$P(s) = \frac{2\lambda s_0}{[(1+\lambda)s_0-(1-\lambda)s]^2}, \quad \lambda = e^{-\beta\gamma_0 s_0} .\tag{57}$$

In both cases $P(s)$ is strongly peaked around $s=s_0$. From Eq. (50) we find

$$\langle s(t)\rangle_s = \frac{2}{s_0}\sum_{\text{odd } n}\frac{1}{\lambda_n^2}e^{-\omega_n t}\cos[\lambda_n(s_0-s)] .\tag{58}$$

This implies

$$s-\langle s(t)\rangle_s = \frac{2}{s_0}\sum_{\text{odd } n}\frac{1}{\lambda_n^2}(1-e^{-\omega_n t})\cos[\lambda_n(s_0-s)] .\tag{59}$$

The interpretation of Eq. (59) is as follows. Whenever t is so large that $\lambda_n(s_0-s)\ll 1$ for all n with $\omega_n t<1$, the cosine factor may be ignored altogether, and below a limiting $n=p$ given by $\omega_p t=1$, the exponential may be expanded to first order. Writing $p=at^{-1/2}$, one has

$$s-\langle s(t)\rangle_s \simeq C_1\int_1^P t\,dn+C_2\int_p^\infty\frac{dn}{n^2}\propto t^{1/2} ,\tag{60}$$

where C_1 and C_2 are constants. At very short times the quantity $s-\langle s(t)\rangle_s$ is exponentially close to zero. Then according to Eq. (60) comes a range of times where this quantity increases like $t^{1/2}$, and finally it converges to s. A similar result applies to relaxation from a state with probability distribution $P(s,t=0)$, since

$$\langle s(0)\rangle_P - \langle s(t)\rangle_P = \int_{-s_0}^{s_0}[s-\langle s(t)\rangle_s]P(s,t=0)ds .\tag{61}$$

If the width of $P(s,t=0)$, Δs, is defined by the integral of P from $s_0-\Delta s$ to $s_0+\Delta s$ being $\frac{1}{2}$, it is not hard to show that

$$\langle s(0)\rangle_P - \langle s(t)\rangle_P \begin{cases} \simeq 0, & t\ll t_1 \\ \propto t^{1/2}, & t_1\ll t\ll t_2 , \\ \simeq\langle s(0)\rangle, & t_2\ll t \end{cases}\tag{62}$$

where

$$t_1 = \frac{\beta}{\mu}(\Delta s)^2, \quad t_2 = \frac{\beta}{\mu}s_0^2 .\tag{63}$$

In the case of relaxation after a sudden cessation of a steady shear flow, Δs is given by [compare Eq. (44)]

$$(\Delta s)^2 \simeq \frac{\mu}{s_0\beta^2}\frac{1}{\dot{\gamma}} .\tag{64}$$

In the case of a sudden large shear displacement, γ_0, Δs is given by [compare Eq. (57)]

$$\Delta s \simeq 2s_0 e^{-\beta\gamma_0 s_0} .\tag{65}$$

Note that, in both cases, the non-Debye character of the relaxation is apparent only because we have considered the quantity $\langle s(0)\rangle_P - \langle s(t)\rangle_P$. If one looks at just $\langle s(t)\rangle_P$, this quantity would be hard to distinguish from a simple exponential decay in time.

C. Cosine hyperbolic model

A phenomenological model for stress relaxation was proposed by Tobolsky and co-workers in the 1940s [3–5]. The model is a Maxwell element consisting of a Hooke's law spring and a non-Newtonian dashpot in series, the viscosity of the dashpot obeying the Eyring viscosity equation. The model leads to

$$\dot{\gamma} = A\dot{s}+B\sinh\left[\frac{s}{s_0}\right] ,\tag{66}$$

where A, B, and s_0 are constants. Equation (66) reproduces Eyring's viscosity equation and predicts a logarithmic stress relaxation at constant extension: At large $s(t=0)$ one has approximately $\dot{s}=-\text{const}\times\exp(s/s_0)$, which implies at intermediate times [4]

$$s(t)\simeq\alpha-\beta\ln(t) .\tag{67}$$

Both predictions of Eq. (66) mimic experiment on typical polymeric liquids. The model, however, does not take into account thermal fluctuations. The formalism developed in Sec. II allows one to construct a model based on Eq. (66) which is consistent with statistical mechanics. Since relaxation towards equilibrium is governed by $\dot{s}=-\text{const.}\times\sinh(s/s_0)$, the obvious choice for $F(s)$ is

$$F(s) = f_0\cosh\left[\frac{s}{s_0}\right] .\tag{68}$$

The Langevin equation corresponding to Eq. (68) is then

$$\dot{s} = -\mu\frac{f_0}{s_0}\sinh\left[\frac{s}{s_0}\right]+\xi(t) .\tag{69}$$

We now proceed to investigate this model, being particularly interested in to which extent it reproduces the predictions of Eq. (66).

First the nonlinear steady-state viscosity is considered. At low temperatures it is possible to derive an analytical expression for the viscosity. The derivation is given here for a general $F(s)$. If $\langle s\rangle$ denotes the average of s during a steady shear flow, one has from Eq. (12) at low temperatures where fluctuations are small

$$\dot{\gamma} J(\langle s \rangle) = \mu \frac{dF}{ds}(\langle s \rangle) . \tag{70}$$

The quantity $\langle s \rangle$ is a function of $\dot{\gamma}$. If the derivative of this function is denoted by $\langle s \rangle'$, Eq. (70) implies by differentiation

$$J + \dot{\gamma} \frac{dJ}{ds} \langle s \rangle' = \mu \frac{d^2F}{ds^2} \langle s \rangle' . \tag{71}$$

Combining this with Eq. (20) leads to

$$J = \langle s \rangle' \left[\mu \frac{d^2F}{ds^2} - \beta \dot{\gamma} \left(\frac{dF}{ds} J - \langle s \rangle \right) \right] . \tag{72}$$

For $\beta \rightarrow \infty$ the term in the inner parentheses must vanish. In conjunction with Eq. (70) one finds

$$\langle s \rangle = \frac{\mu}{\dot{\gamma}} \left[\frac{dF}{ds}(\langle s \rangle) \right]^2 , \tag{73}$$

or for the viscosity

$$\eta = \frac{1}{\mu} \left[\frac{\langle s \rangle}{\frac{dF}{ds}(\langle s \rangle)} \right]^2 . \tag{74}$$

For the cosh model we thus have

$$\eta = \eta_0 \left[\frac{\langle s \rangle / s_0}{\sinh(\langle s \rangle / s_0)} \right]^2 , \tag{75}$$

where

$$\eta_0 = \frac{1}{\mu} \frac{s_0^4}{f_0^2} \tag{76}$$

is the linear viscosity. Perhaps surprisingly, one does not recover the Eyring viscosity expression

$$\eta = \eta_0 \frac{\langle s \rangle / s_0}{\sinh(\langle s \rangle / s_0)} , \tag{77}$$

but, as is clear from Fig. 2, the cosh model viscosity may be fitted reasonably well by Eq. (77).

Consider now relaxation towards equilibrium from a nonequilibrium state with stress s. At low temperatures $J(s)$ may be found explicitly from Eq. (21), which for $\beta \rightarrow \infty$ reduces to

$$J(s) = \frac{s_0^2}{f_0} \frac{s/s_0}{\sinh(s/s_0)} . \tag{78}$$

When substituted into Eq. (12) this leads to, in the zero noise limit,

$$\dot{\gamma} = \frac{f_0}{s_0^2} \frac{\sinh(s/s_0)}{s/s_0} \dot{s} + \mu \frac{f_0^2}{s_0^3} \frac{\sinh^2(s/s_0)}{s/s_0} . \tag{79}$$

This looks nothing like Eq. (66). But again we find the nonlinear viscosity given by Eq. (75). Furthermore, for constant elongation, s relaxes according to

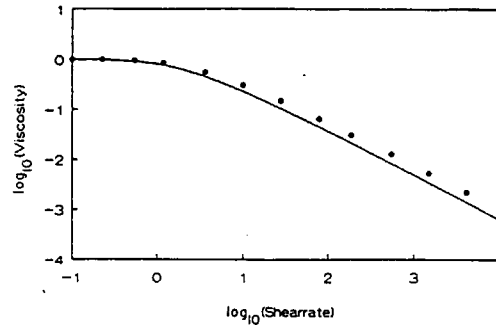$$\dot{s} = -\mu \frac{f_0}{s_0} \sinh \left[\frac{s}{s_0} \right] , \tag{80}$$

FIG. 2. Log-log plot of the steady-state nonlinear viscosity of the cosh model. The nonlinear viscosity is shown relative to the linear viscosity as a function of the dimensionless shear rate $\dot{\gamma}/(s_0/\eta_0)$. The nonlinear viscosity of the cosh model is not identical to the Eyring viscosity of Eq. (77) (marked by dots).

as expected from Eq. (69).

A final correspondence of the cosh model to Tobolsky's phenomenological model is the frequency-dependent viscosity. As is the case for any differential constitutive relation [1], Eq. (66) reduces to the Maxwell model in the linear limit. In the cosh model one might expect a more interesting frequency dependence, at least at high temperatures where the sinh factor of Eq. (69) cannot be replaced by a s^2 factor. But it turns out that even at high temperatures the autocorrelation function $\langle s(0)s(t) \rangle_0$ is actually very close to an exponential (which corresponds to the Maxwell model). What happens is that the logarithmic s relaxation of Eq. (80), even at quite short times, is killed by the s diffusion due to the noise term.

D. Power-law model

As a final example we briefly discuss the power-law model where

$$F(s) = f_0 \left| \frac{s}{s_0} \right|^n \quad (n > 0) . \tag{81}$$

The fact that $F(s)$ is nonanalytical at $s = 0$ is insignificant. The case $n = 2$ is the Gaussian model and the $n \rightarrow \infty$ limit is the box model.

The power-law model makes sense only for $n > \frac{1}{2}$. To prove this, the low-temperature limit is considered. For $\beta \rightarrow \infty$, $J(s)$ may be evaluated asymptotically from Eq. (21). Writing $s'^n - s^n = ns^{n-1}(s' - s)$, one gets

$$J(s) = \beta \int_s^\infty ds' s' e^{-\beta(f_0/s_0^n)ns^{n-1}(s'-s)}$$

$$\propto s(s^{n-1})^{-1} = s^{2-n} . \tag{82}$$

Thus, whenever $\dot{\gamma}$ is positive there is a "force" proportional to s^{2-n} working to increase s. The "restoring force" from the potential varies as s^{n-1}. This force must dominate at large s in order to avoid s running off to infinity, thus $n - 1 > 2 - n$ or $n > \frac{3}{2}$. Mathematically, there is no normalizable stationary state whenever $n < \frac{1}{2}$.

The border case $n = \frac{1}{2}$ leads to a model which is well defined up to a certain shear rate, above which s runs off to infinity. This corresponds to there being a phase transition at a definite shear rate to a state of infinitely high viscosity.

To estimate the viscosity we use Eq. (73), which implies

$$\dot{\gamma} \propto \frac{1}{s} \left[\frac{dF}{ds} \right]^2 \propto s^{2n-3} . \qquad (83)$$

This implies

$$\eta = s / \dot{\gamma} \propto \dot{\gamma}^{(4-2n)/(2n-3)} . \qquad (84)$$

For $\frac{1}{2} < n < 2$ the model exhibits shear thickening, whereas for $2 < n$ there is shear thinning. The case $n = 2$ gives a shear-rate-independent viscosity, as shown already.

IV. DISCUSSION

The model of stress fluctuations considered in the present paper involves several nontrivial assumptions. The liquid is regarded as divided into "regions," and correlations between stress fluctuations of different regions are ignored completely. These assumptions are made for simplicity, but may be unrealistic since elastic forces are long ranged. The region picture becomes even harder to justify when a shear flow is considered. Such a flow deforms the regions and the picture can only be maintained whenever the longest correlation time is smaller than the inverse shear rate.

The main result of the paper is the proof that, if equilibrium stress fluctuations follow a Langevin equation, there is only one possible stress dynamics in nonequilibrium which is consistent with the principle of virtual work. Not only is the nonlinear response uniquely determined, but this is true also for the stress fluctuations in nonequilibrium. Crucial to this theorem is the assumption of a Langevin dynamics for the stress. This is a phenomenological postulate, but it should be emphasized that Langevin dynamics is the "canonical" guess if one is to discuss dynamics purely from a knowledge of equilibrium statistical mechanics. There is no other way of estimating the dynamics from a knowledge of only the equilibrium free energy $F(s)$. But, of course, this does not guarantee that the Langevin equation leads to correct results.

The assumption of linear coupling of the shear rate "field" in Eq. (12) is not essential. In fact, it is easy to show that the principle of virtual work implies the coupling must be linear. This is because the shear rate does not occur in Eq. (16).

The formalism developed may be generalized by replacing the term "stress" (which is the transverse momentum current) by any other current. One thus has a method for predicting the nonlinear response from a knowledge of equilibrium current fluctuations. The considering of currents as independent degrees of freedom has become popular in recent years, being the basis of extended irreversible thermodynamics [12,13]. The approach of Sec. II may be regarded as a statistical-

mechanical counterpart to extended irreversible thermodynamics.

To illustrate the formalism a few simple models were studied in Sec. III. The Gaussian model leads to an exactly linear response even at large shear rates, reducing simply to the standard Maxwell model. The fact that the Gaussian model is linear is quite satisfactory, since a similar result is valid in ordinary statistical mechanics. Here, strictly Gaussian equilibrium fluctuations of, e.g., the magnetization, implies a field-independent magnetic susceptibility.

A more interesting model is the box model. It predicts a nonlinear viscosity (because there is a maximum possible stress), and a spectrum of relaxation times. In equilibrium this spectrum is not really visible, however; the autocorrelation function $\langle s(0)s(t) \rangle_0$ is approximately an exponential, leading to almost a Maxwell-type frequency dependence of the viscosity. Only in the relaxation from a strongly nonequilibrium state does the spectrum play any significant role, and even here the lowest eigenfrequency dominates the overall picture.

The cosh model was constructed to mimic Tobolsky's phenomenological model for stress relaxation. But although the zero noise relaxation equation is equal to Tobolsky's [Eq. (66)], the predictions of the model are not identical to those of Eq. (66). This is an illustration of a point made by van Kampen [7] that, by adding a noise term to a phenomenological model of the form $\dot{s} = f(s)$, some of the properties of the equation are lost because of the noise. In the case of the cosh model, the properties are retained in a qualitative sense, though. Thus, there is an Eyring-like viscosity in the model (Fig. 2), and the frequency dependence of the phenomenological model and the model of Eq. (69) are almost equal. The latter point may seem surprising, given the fact that the cosh model leads to a logarithmic relaxation towards zero in the zero noise limit (which, as is well known, corresponds to a spectrum of relaxation times varying like τ^{-1}). However, just as in the box model, the spectrum is not significant in equilibrium where the noise term completely dominates the autocorrelation function, resulting in an almost exponential decay.

The cosh model corresponds to an exponentially increasing free energy $F(s)$. The case of $F(s)$ increasing following a power law was also considered in Sec. III. [The case of a logarithmically increasing $F(s)$ leads to an inconsistent model where s runs off to infinity whenever $\dot{\gamma} \neq 0$.] The power-law model is consistent only for $n > \frac{1}{2}$, $n = \frac{1}{2}$ being a border case where the model makes sense for not too large shear rates. Whenever $\frac{1}{2} < n < 2$ the model exhibits shear thickening, whereas $2 < n$ corresponds to the experimentally more common case of shear thinning. The case $n = 2$ is the Gaussian model, and the limit $n \to \infty$ is the box model. A closer analysis than given in Sec. III reveals that the shear thickening in the case $\frac{1}{2} < n < 2$ is a consequence of one not having $J(s) \to 0$ as $|s| \to \infty$ [while for $2 < n$ $J(s) \to 0$ as $|s| \to \infty$]. Since $J(s)$ may be interpreted as an s-dependent infinite frequency shear modulus, the study of the power-law model leads to a novel view on the origin of nonlinearity: Nonlinearity may be viewed as a consequence of a stress-

dependent infinite frequency shear modulus G_∞. The case when G_∞ increases with increasing stress corresponds to shear thickening while a decreasing G_∞ (i.e., softening) corresponds to shear thinning. The Gaussian linear case $n = 2$ corresponds to a stress independent G_∞. A final thing to be noted about the power-law model is that in the zero noise limit this model has a power-law time dependence of the stress relaxation, as is easy to show.

The predictions of the models are approximately on the level of differential constitutive relations: these have realistic nonlinear steady-state viscosities but only a simple Maxwell frequency dependence of the viscosity [1]. Compared to differential constitutive relations, the presently considered models have the advantage of being consistent with statistical mechanics. Thus, the method presented may be regarded as a means of modifying differential constitutive relations to include thermal fluctuations. The modification, however, is nontrivial in the sense that the differential constitutive relation is *not* recovered exactly in the low-temperature limit, as shown in detail for the cosh model.

Several important features of polymeric liquids are not mimicked by the models of Sec. III. The predicted almost single relaxation-time frequency dependence of the viscosity is very far from that observed in polymeric liquids. Another important point which is not captured by the models is the fact that experimentally, nonlinearity sets in at a shear rate about equal to the frequency marking the onset of frequency dependence of the viscosity

[1,14]. Finally, the temperature dependence of the viscosity is weak and there is a well-defined viscosity in the zero-temperature limit. While this last point could be handled by assuming the mobility μ is temperature dependent, the two other points are quite serious, indeed. A further objection is the fact that in the present model there is time reversibility in a steady shear flow: The steady-flow Langevin equation obeys detailed balance for a suitably chosen energy function [compare Eq. (26)]. In a real flow one expects a genuine violation of time reversibility.

In conclusion, the types of models studied in Sec. III are not satisfactory as models of reality. To arrive at more realistic models one has to consider several stress coordinates interacting with each other, for instance by taking into account the spatial variation of the stress. This leads to a field theory in which the free energy is a functional of the stress field. If this function has several minima, the Langevin dynamics gives thermally activated relaxation times (just as in the description of chemical reactions), and thereby more realistic temperature and frequency dependences. Also, it may be shown that in a model with more than one degree of freedom there is genuine time irreversibility in any shear flow.

[1] R. B. Bird, R. C. Armstrong, and O. Hassager, *Dynamics of Polymeric Liquids,* 2nd ed. (Wiley, New York, 1987), Vols. 1 and 2.

[2] M. Doi and S. F. Edwards, *The Theory of Polymer Dynamics* (Clarendon, Oxford, 1986).

[3] A. Tobolsky and H. Eyring, J. Chem. Phys. **11**, 125 (1942).

[4] A. V. Tobolsky and R. D. Andrews, J. Chem. Phys. **13**, 3 (1945).

[5] R. D. Andrews, N. Hofman-Bang, and A. V. Tobolsky, J. Polym. Sci. **3**, 669 (1948).

[6] R. Becker, *Theory of Heat* (Springer, Berlin, 1967).

[7] N. G. van Kampen, *Stochastic Processes in Physics and Chemistry* (North-Holland, Amsterdam, 1981).

[8] M. Doi, J. Chem. Phys. **79**, 5080 (1983).

[9] J. D. Ferry, *Viscoelastic Properties of Polymers,* 3rd ed. (Wiley, New York, 1981).

[10] P. M. Morse and H. Feshback, *Methods of Theoretical Physics* (McGraw-Hill, New York, 1953).

[11] M. R. Speigel, *Mathematical Handbook,* Schaum's Outline Series in Mathematics (McGraw-Hill, New York, 1968).

[12] D. Jou, J. Casas-Vázquez, and G. Lebon, Rep. Prog. Phys. **51**, 1105 (1988).

[13] D. Jou, J. Casas-Vázquez, and G. Lebon, J. Non-Equilib. Thermodyn. **17**, 383 (1992).

[14] W. W. Graessley, Adv. Polym. Sci. **16**, 1 (1974).

TEKST NR 287   1994

A Statistical Mechanical Approximation for the Calculation of Time Auto-Correlation Functions

By: Jeppe C. Dyre

TEKSTER fra

ABSTRACT

This paper considers the problem of estimating the time auto-correlation function for a quantity that is defined in configuration space, given a knowledge of the mean-square displacement as function of time in this part of phase space. An approximate formula is derived which reduces the calculation of the time auto-correlation function to a "double canonical" average. In this approximation, the mean-square displacement itself may be evaluated from the "double partition function" in the case of Langevin dynamics. The scheme developed is illustrated by computer simulations of a simple one-dimensional systems, showing a good agreement between the exact time auto-correlation functions and those found by the approximation.

The calculation of a time auto-correlation function [1,2] is a straightforward matter in any computer simulation tracing the time evolution of a system [3-5]. However, computer simulations are not feasible today on time scales longer than microseconds. These time scales are relevant for viscous liquids approaching the glass transition. Therefore, one cannot by simulations calculate a number of experimentally accessible quantities in viscous liquids. Examples are the frequency-dependent viscosity [7], bulk modulus [8], dielectric constant [9], or specific heat [10,11], that all via the fluctuation-dissipation theorem [1,2,6] are given as Laplace transforms of a time auto-correlation function. In this situation one would like to have an approximate theory at hand. Focussing only on time auto-correlation functions of quantities $A(X)$ that are defined in configuration space, $X = (X_1, .., X_n)$, an approximation is proposed below, based on an ansatz for the joint probability of initial point X at $t=0$ and final point X' after time t, $P(X, X'; t)$. In terms of the joint probability the time auto-correlation function is given by

$$\langle A(0)A(t) \rangle = \int dXdX' \, A(X) A(X') \, P(X, X'; t) \quad . \tag{1}$$

If Z is the configurational partition function, given in terms of $\beta = 1/(k_B T)$ and the potential energy $U(X)$ as

$$Z(\beta) = \int dX \, e^{-\beta U(X)} \quad , \tag{2}$$

and $G(X \rightarrow X'; t)$ is the Green's function, the exact expression for

3

the joint probability is

$$P(X, X'; t) = \frac{e^{-\beta U(X)}}{Z} G(X \rightarrow X'; t) \quad . \tag{3}$$

However, Eq. (3) is not very useful unless the Green's function is known. The principle of detailed balance implies that $P(X, X'; t) = P(X', X; t)$, a requirement any approximation should also satisfy to ensure time-reversal invariance.

The exact method for calculating $\langle A(0)A(t)\rangle$ is shown in Fig. 1 illustrating the path in configurational space. At a number of times $t_1, .., t_n$ one computes the quantity $A(X(t_j))A(X(t_j+t))$, and $\langle A(0)A(t)\rangle$ is the average of this product as $n \rightarrow \infty$. Assuming here and henceforth that the X_i's are simple rectangular coordinates and that $\langle A\rangle = 0$, one always finds $\langle A(0)A(t)\rangle \rightarrow 0$ as $t \rightarrow \infty$. This loss of correlation after long time comes about because the final point X' is far away from the initial point X. A measure of the distance travelled in time t is provided by the mean-square displacement, $\langle \Delta X^2(t)\rangle$: If $X \equiv X(t_j)$, $X' \equiv X(t_j+t)$, and $\langle\rangle$ denotes an average over j, the mean-square displacement is defined by

$$\langle \Delta X^2(t)\rangle = \langle (X-X')^2\rangle \equiv \sum_{i=1}^{n} \langle (X_i-X_i')^2\rangle \quad . \tag{4}$$

Assuming that the mean-square displacement itself is a known function of time, the idea is now to estimate $\langle A(0)A(t)\rangle$ via

4

the "spatial" auto-correlation of A in configurational space evaluated at distances equal to $\sqrt{<\Delta X^2(t)>}$. Before proceeding, we briefly discuss the physics of this way of thinking about the time auto-correlation function. A simple case is when the mean-square displacement is proportional to time (for $t \to \infty$ this is, of course, always the case). In this case, if the "spatial" correlation of A has a Gaussian distance decay, the time auto-correlation function is a simple exponential, corresponding to Debye relaxation. If, however, the spatial correlation of A has an exponential distance decay, the time auto-correlation function is a stretched exponential with exponent $\frac{1}{2}$. The latter case gives a reasonable fit to many experiments on viscous liquids [12]. The above picture of decomposing the time auto-correlation function into a) a "geometric" correlation and b) the distance travelled in a given time, is in harmony with another well-known property of viscous liquids. In these systems all linear relaxation functions have roughly the same average relaxation rate, a rate which slows down dramatically upon cooling. In the "geometric" picture, this is simply a consequence of the motion slowing down in configuration space, whereas the "spatial" correlation probably only change little upon cooling in a narrow range of temperatures. The mean-square displacement acts as a "molecular clock".

We now turn to the problem of estimating the joint probability $P(X, X'; t)$. In the thermodynamic limit $n \to \infty$ the relative fluctuations in the mean-square displacement go to zero,

and therefore the distance between $X=X(t_j)$ and $X'=X(t_j+t)$ is precisely $\sqrt{\Delta X^2(t)}$. Similarly, the relative fluctuations in potential energy go to zero, so the potential energy of both points X and X' is equal to $\langle U \rangle = -\dfrac{\partial \ln Z}{\partial \beta}$. The ansatz for $P(X,X';t)$ assumes equal probability for all pair of points with the correct distance and the correct potential energy. Thus,

$$P(X,X';t) \propto$$
$$\delta[(X-X')^2 - \langle \Delta X^2(t) \rangle]\, \delta[U(X)-\langle U \rangle]\, \delta[U(X')-\langle U \rangle] \quad . \tag{5}$$

In the thermodynamic limit there is "equipartition" between $U(X)$ and $U(X')$, and the last two delta functions may be replaced by a single delta function,

$$P(X,X';t) \propto \delta[(X-X')^2 - \langle \Delta X^2(t) \rangle]\, \delta[U(X)+U(X')-2\langle U \rangle] \quad . \tag{6}$$

The next step is to convert Eq. (6) to a "canonical" form, which is computationally more convenient than the "microcanonical" form. This is done by replacing the first delta function by $\exp[-a(X-X')^2]$ where a is a Lagrangian multiplier adjusted to give the correct mean-square displacement. Similarly, the second delta function is replaced by $\exp(-b[U(X)+U(X')])$ where b is adjusted to ensure that the average of $U(X)+U(X')$ is $2\langle U \rangle$. If the "double partition function"

$$D(a,b) = \int dX dX' \ e^{-a(X-X')^2 - b[U(X) + U(X')]} \qquad (7)$$

is introduced, the final ansatz for the calculation of the time auto-correlation function is

$$\langle A(0)A(t)\rangle = \int \frac{dX dX'}{D(a,b)} \ A(X)A(X') \ e^{-a(X-X')^2 - b[U(X) + U(X')]} \quad .$$

$$(8)$$

In the thermodynamic limit Eq. (8) is equivalent to the average Eq. (1) over the distribution Eq. (5).

The two parameters a and b are determined in the following way. First, $b=b(a)$ is found from the condition that the average joint potential energy of initial and final point is $2\langle U \rangle$. Thus, $b(a)$ is determined from the condition that this average is independent of a:

$$\frac{d}{da} \frac{\partial \ln D}{\partial b} = 0 \quad . \qquad (9)$$

Since $\frac{d}{da} = \partial_a + \frac{db}{da} \partial_b$ [with the standard abbreviated notation for

partial derivatives], the expansion of Eq. (9) leads to the following first order differential equation for $b(a)$

$$\frac{db}{da} = \frac{\partial_a D \ \partial_b D - D \ \partial^2_{ab} D}{D \ \partial^2_b D - (\partial_b D)^2} \quad . \qquad (10)$$

Once the function $b(a)$ has been determined, $a=a(t)$ is found from requiring the mean-square displacement calculated from $D(a,b(a))$ to be correct:

$$- \frac{\partial \ln D}{\partial a} = \langle \Delta X^2(t) \rangle \quad . \tag{11}$$

The short and long time limits are determined as follows. For $a(t)$ one clearly has

$$a(t=0) = \infty$$
$$a(t=\infty) = 0 \tag{12}$$

In the limit of large times X and X' are far apart and $U(X)$ is uncorrelated with $U(X')$. In this limit $b=\beta$:

$$b(a=0) = \beta \quad . \tag{13}$$

In the short time limit the points X and X' are forced together. Thus, $P(X, X'; t) \propto \delta (X-X') \exp [-2bU(X)]$ for $t \to 0$ and Eq. (1) yields

$$\lim_{t \to 0} \langle A(0) A(t) \rangle = \frac{\int dX \, A^2(X) \, e^{-2bU(X)}}{\int dX \, e^{-2bU(X)}} \quad . \tag{14}$$

In order for this to give the correct canonical average one must have $b=\beta/2$, i. e.,

$$b(a=\infty) = \frac{\beta}{2} \quad . \tag{15}$$

The short time behavior of $a(t)$ may be derived directly from the equations of motion, as briefly sketched below. In the case of Newtonian dynamics, the Green's function at short times is easily found from the integrated equations of motion where the momentum is Gaussianly distributed (for simplicity it is assumed that all particles have the same mass m),

$$G(X \to X'; t) \; \propto \; \exp\left[-\frac{\beta}{2m} \sum_{i=1}^{n} \left(\frac{m}{t} \; (X_i' - X_i) \; + \; \frac{1}{2} \; \partial_i U \; t\right)^2\right] \; . \tag{16}$$

To first order in t this yields

$$G(X \to X'; t) \; \propto \; \exp\left[-a(t)(X - X')^2 \; - \; \frac{\beta}{2} \; [U(X') - U(X)]\right] \; , \tag{17}$$

where

$$a(t) \; = \; \frac{\beta m}{2 t^2} \qquad \textit{(Newtonian dynamics, } t \to o) \quad . \tag{18}$$

Note that via Eq. (3) this Green's functions confirms the form of the ansatz Eq. (8) for $t \to 0$, as well as the boundary condition Eq. (15). Next we consider the case of Langevin dynamics,

$$\dot{X}_i \; = \; -\mu \; \frac{\partial U}{\partial X_i} \; + \; \xi_i(t) \quad , \tag{19}$$

with the standard Gaussian white noise term [14] $\langle \xi_i(t)\xi_j(t')\rangle = 2 \; \mu \; k_B T \; \delta_{i,j} \; \delta(t-t')$. From the equations of motion one finds that, because the integrated noise term is Gaussianly distributed,

$$G(X \to X'; t) \; \propto \; \exp\left[-\frac{\beta}{4\mu t} \sum_{i=1}^{n} \left(X_i' - X_i \; + \; \mu \; \partial_i U \; t\right)^2\right] \; . \tag{20}$$

At short times this again leads to Eq. (17), where however now

$$a(t) \; = \; \frac{\beta}{4\mu t} \qquad \textit{(Langevin dynamics, } t \to 0) \quad . \tag{21}$$

In the case of Langevin dynamics Eq. (8) may be applied to the calculation of the force-force time auto-correlation

9

function. This leads to an equation that in principle allows a calculation of $\langle \Delta X^2(t) \rangle$ directly from the double partition function. The mean-square displacement in time t is given by (sum over i)

$$\langle \Delta X^2(t) \rangle = \int_0^t dt' \int_0^t dt'' \langle \dot{X}_i(t') \dot{X}_i(t'') \rangle \quad . \tag{22}$$

Since the noise terms are uncorrelated at different times, Eqs. (19) and (22) imply

$$\frac{d^2}{dt^2} \langle \Delta X^2(t) \rangle = 2 \langle \dot{X}_i(0) \dot{X}_i(t) \rangle = 2 \mu^2 \langle \partial_i U(0) \partial_i U(t) \rangle \quad . \tag{23}$$

From Eq. (8) the force-force time auto-correlation function is rewritten as

$$\langle \partial_i U(0) \partial_i U(t) \rangle =$$
$$\frac{1}{b^2} \int \frac{dX dX'}{D(a,b)} \left[\partial_i e^{-bU(X)} \right] \left[\partial'_i e^{-bU(X')} \right] e^{-a(X-X')^2} \tag{24}$$

By partial integrations one finds

$$\langle \partial_i U(0) \partial_i U(t) \rangle =$$
$$- 4 \frac{a^2}{b^2} \int \frac{dX dX'}{D(a,b)} (X-X')^2 e^{-a(X-X')^2 - b[U(X)+U(X')]} \tag{25}$$
$$= 4 \frac{a^2}{b^2} \frac{\partial \ln D}{\partial a}$$

Thus, the equation for $a(t)$ is from Eqs. (11), (23) and (25)

$$\left(\frac{d^2}{dt^2} + 8 \mu^2 \frac{a^2}{b^2} \right) \frac{\partial \ln D}{\partial a} = 0 \quad . \tag{26}$$

The expansion of Eq. (26) is straightforward, though tedious.

In order to check the validity of Eq. (8) a simple systems was studied numerically obeying Langevin dynamics. The system was chosen to be so simple that the integral in Eq. (8) may be evaluated "exactly", thus avoiding the noise of Monte Carlo simulations. No attempts were made to verify that Eq. (26) gives the correct $a(t)$. Instead the following procedure was followed. At a number of fixed a-values $b(a)$ was found from the requirement that the average joint potential energy is $2\langle U\rangle$. Then the mean-square displacement was evaluated for each a from Eq. (11) and also as function of time from the dynamical simulations, allowing an identification of the times corresponding to the fixed a-values. Finally, the time auto-correlation function was calculated from Eq. (8) at the fixed a-values. Figure 2 shows the results for $\langle X^3(0)X^3(t)\rangle$ for the Langevin motion of a particle in a double-well potential [14]. The full curve is the exact time auto-correlation function found by solving the Smoluchowski equation [13] and the dots give the prediction of Eq. (8). Results are shown for $\beta=2$ and for $\beta=8$ in dimensionless units.

In this paper a statistical mechanical approximation for the calculation of time auto-correlation functions was derived. The formalism assumes a knowledge of the mean-square displacement in configurational space as function of time; the mean-square displacement acts as the "molecular clock". The remaining "spatial" auto-correlation calculation is a "double canonical" average (Eq. (8)). Note that the corresponding double partition

function, $D(a,b)$, contains the ordinary configurational partition function as a special case, $Z^2(\beta)=D(0,\beta)$.

The approximation is only useful if $\langle \Delta X^2(t) \rangle$ is known. Experimentally, this quantity is accessible via the intermediate incoherent scattering function. In some cases a phenomenological estimate of the mean-square displacement may be given. Thus, for hopping in a rugged energy landscape where all minima are equal, the mean-square displacement is **universal** at low temperatures (except for trivial scalings), i.e., it is independent of the barrier height probability distribution. This has been shown recently [15] by effective medium calculations and by computer simulations of the frequency-dependent conductivity, which is simply related to the mean-square displacement [16]. Finally, there is the possibility that the mean-square displacement may be found approximately from Eq. (26) if Langevin dynamics is assumed, as is common, e. g., in polymer dynamics [17].

Equation (26) signals that Langevin dynamics plays a special role in the proposed scheme for calculation of time autocorrelation functions. A question of considerable interest is if and when Langevin dynamics can be expected to give the same time auto-correlation functions as Newtonian dynamics [18]. If the ansatz is correct, two different dynamics give the same time auto-correlation functions for any quantity defined in configuration space, if just the two dynamics give the same mean-square displacement. In this way the ansatz provides a mechanism for the consistency of any two types of dynamics.

ACKNOWLEDGEMENT

REFERENCES

1.   J. P. Boon and S. Yip, "Molecular Hydrodynamics" (McGraw Hill, New York, 1980).

2.   J.-P. Hansen and I. R. Macdonald, "Theory of Simple Liquids", 2nd Ed. (Academic Press, New York, 1986).

3.   M. P. Allen and D. J. Tildesley, "Computer Simulations of Liquids" (Clarendon Press, Oxford, 1987).

4.   "Simulations of Liquids and Solids", Eds. G. Ciccotti, D. Frenkel, and I. R. Macdonald (North-Holland, Amsterdam, 1987).

5.   "Computer Simulations in Chemical Physics", Eds. M. P. Allen and D. J. Tildesley (Kluwer Academic Publishers, Dordrecht, 1993).

6.   R. Zwanzig, Ann. Rev. Phys. Chem. **16**, 67 (1965).

7.   R. B. Bird, R. C. Armstrong, and O. Hassager, "Dynamics of Polymeric Liquids", 2nd Ed. (Wiley, New York, 1987), Vol. 1.

8.   T. Christensen and N. B. Olsen, Phys. Rev. B **49**, 15396 (1994).

9.   G. Williams, in: "Dielectric and Related Molecular Processes, Specialist Periodical Report, Vol. 2", Ed. M. Davies (Chem. Soc., London, 1975), p. 151.

10.   T. Christensen, J. Phys. (Paris) Colloq. **46**, C8-635 (1985).

11.   N. O. Birge and S. R. Nagel, Phys. Rev. Lett. **54**, 2674 (1985).

12.   R. Böhmer, K. L. Ngai, C. A. Angell, and D. J. Plazek, J. Chem. Phys. **99**, 4201 (1993).

13.   N. G. van Kampen, "Stochastic Processes in Physics and Chemistry" (Norht-Holland, Amsterdam, 1981).

14.   M. Morillo and J. Gómez-Ordónez, Phys. Rev. A **46**, 6738 (1992).

15.   J. C. Dyre, Phys. Rev. B **49**, 11709 (1994); erratum Phys. Rev. B **50**, 9692 (1994).

16.   H. Scher and M. Lax, Phys. Rev. B **7**, 4491 (1973).

17.   M. Doi and S. F. Edwards, "The Theory of Polymer Dynamics" (Clarendon Press, Oxford, 1986).

18.   H. Löwen, J.-P. Hansen, and J.-N. Roux, Phys. Rev. A **44**, 1169 (1991).

FIGURE CAPTIONS

Fig. 1:

Path in configuration space with coordinates $X=(X_1,..,X_n)$ illustrating the exact definition of the time auto-correlation function. At a number of times $t_1,..,t_n$ one computes the quantity $A(X(t_j))A(X(t_j+t))$, and the time auto-correlation function is obtained as the average of this product as $n\rightarrow\infty$. In the thermodynamic limit the distance between the points $X(t_j)$ and $X(t_j+t)$ is the same for all j, because the relative distance fluctuations go to zero as the number of degrees of freedom go to infinity. This distance is the square root of the mean-square displacement in time t. In the approximation for evaluating the time auto-correlation function proposed here, equal probability is given to all pairs of initial (t=0) and final points after time t, that have the correct distance and where each point has the correct potential energy.

Fig. 2:

Log-log plot of $\langle X^3(0)X^3(t)\rangle$ as function of time for a Langevin particle in a double-well potential given in dimensionless units as $U(X)=(1/4)X^4-(1/2)X^2$. The full curve is the exact time auto-correlation function evaluated by solving the Smoluchowski equation. The symbols give the predictions of Eq. (8); the system is so simple that no Monte Carlo simulation is necessary to evaluate Eq. (8). Results are shown for $\beta=2$ and for $\beta=8$.
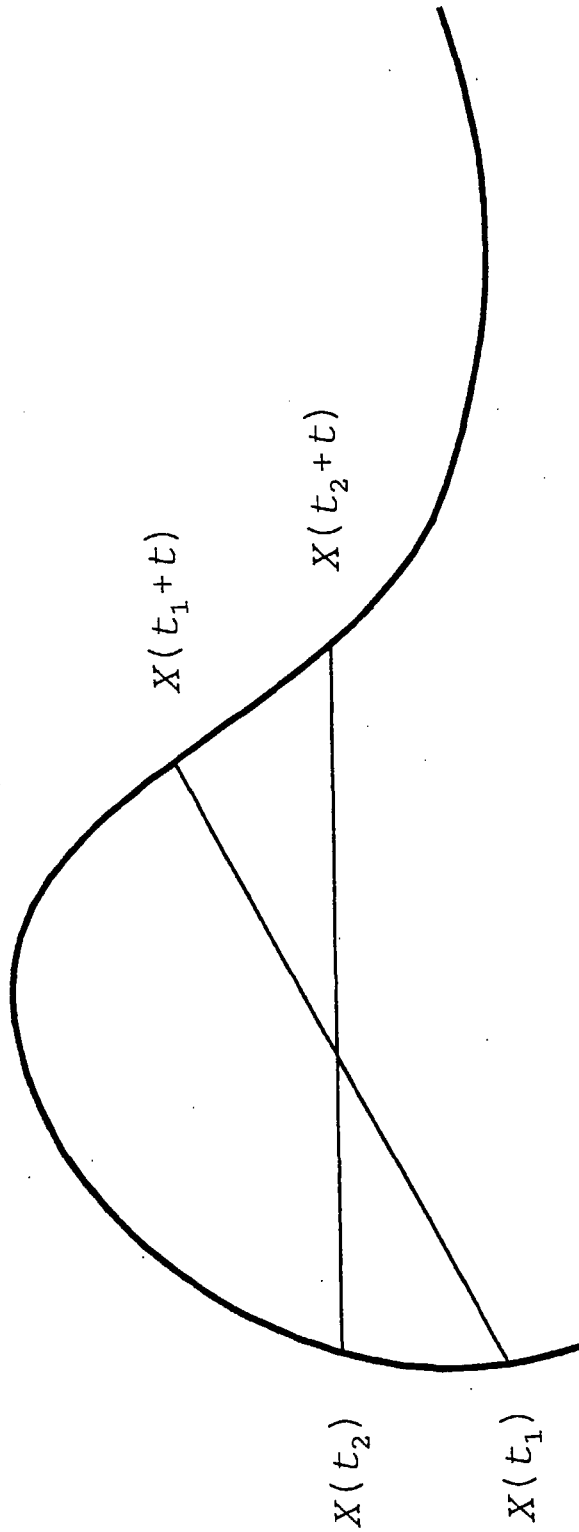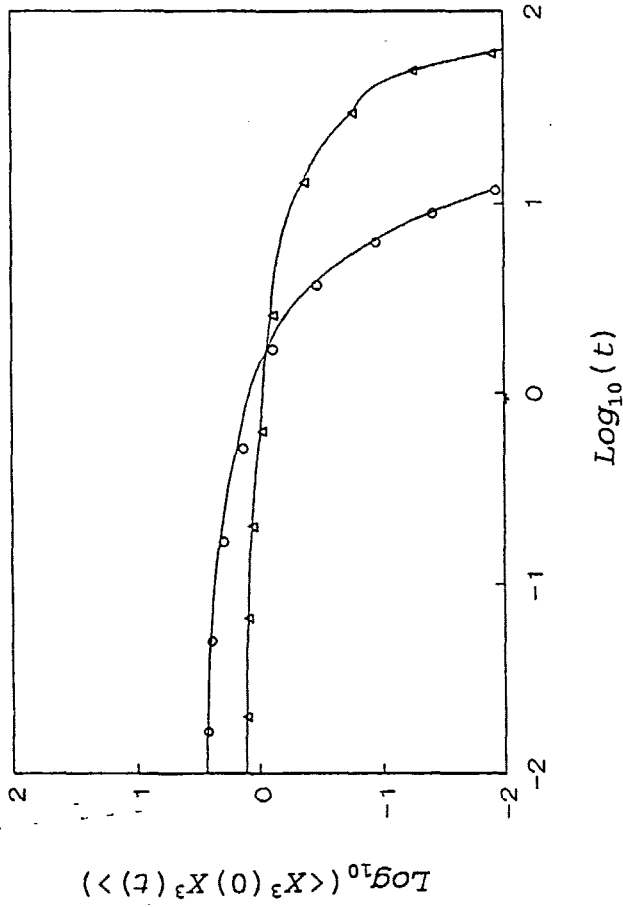
15

Fig. 1

Fig. 2

332/97 ANOMAL SWELLING AF LIPIDE DOBBELTLAG
Specialerapport af: Stine Korremann
Vejleder: Dorthe Posselt

333/97 Biodiversity Matters
an extension of methods found in the literature on monetisation of biodiversity
by: Bernd Kuemmel

334/97 LIFE-CYCLE ANALYSIS OF THE TOTAL DANISH ENERGY SYSTEM
by: Bernd Kuemmel and Bent Sørensen

335/97 Dynamics of Amorphous Solids and Viscous Liquids
by: Jeppe C. Dyre

336/97 Problem-orientated Group Project Work at Roskilde University
by: Kathrine Legge

337/97 Verdensbankens globale befolkningsprognose
- et projekt om matematisk modellering
af: Jørn Chr. Bendtsen, Kurt Jensen, Per Pauli Petersen

338/97 Kvantisering af nanolederes elektriske ledningsevne
Første modul fysikprojekt
af: Søren Dam, Esben Danielsen, Martin Niss,
Esben Friis Pedersen, Frederik Resen Steenstrup
Vejleder: Tage Christensen

339/97 Defining Discipline
by: Wolfgang Coy

340/97 Prime ends revisited - a geometric point of view -
by: Carsten Lunde Petersen

341/97 Two chapters on the teaching, learning and assessment of geometry
by: Mogens Niss

342/97 A global clean fossil scenario DISCUSSION PAPER prepared by Bernd Kuemmel
for the project LONG-TERM SCENARIOS FOR GLOBAL ENERGY DEMAND
AND SUPPLY

343/97 IMPORT/EKSPORT-POLITIK SOM REDSKAB TIL OPTIMERET UDNYTTELSE
AF EL PRODUCERET PÅ VE-ANLÆG
af: Peter Meibom, Torben Svendsen, Bent Sørensen

344/97 Puzzles and Siegel disks
by: Carsten Lunde-Petersen

345/98 Modeling the Arterial System with Reference to an Anesthesia Simulator
Ph.D. Thesis
by: Mette Sofie Olufsen

346/98 Klyngedannelse i en hulkatode-forstøvningsproces
af: Sebastian Horst
Vejledere: Jørn Borggren, NBI, Niels Boye Olsen

347/98 Verificering af Matematiske Modeller
- en analyse af Den Danske Eulerske Model
af: Jonas Blomqvist, Tom Pedersen, Karen Timmermann, Lisbet Øhlenschlæger
Vejleder: Bernhelm Booss-Bavnbek

348/98 Case study of the environmental permission procedure and the environmental impact
assessment for power plants in Denmark
by: Stefan Krüger Nielsen
project leader: Bent Sørensen

349/98 Tre rapporter fra FAGMAT - et projekt om tal og faglig matematik i
arbejdsmarkedsuddannelserne
af: Lena Lindenskov og Tine Wedege

350/98 OPGAVESAMLING - Bredde-Kursus i Fysik 1976 - 1998
Erstatter teksterne 3/78, 261/93 og 322/96

351/98 Aspects of the Nature and State of Research in Mathematics Education
by: Mogens Niss

352/98 The Herman-Swiatec Theorem with applications
by: Carsten Lunde Petersen

353/98 Problemløsning og modellering i en almendannende matematikundervisning
Specialerapport af: Per Gregersen og Tomas Højgaard Jensen

354/98 A Global Renewable Energy Scenario
by: Bent Sørensen and Peter Meibom

355/98 Convergence of rational rays in parameter spaces
by: Carsten Lunde Petersen and Gustav Ryd

356/98   Terrænmodellering
Analyse af en matematisk model til konstruktion af digitale terrænmodeller
Modelprojekt af: Thomas Frommelt, Hans Ravnkjær Larsen og Arnold Skimminge
Vejleder: Johnny Ottesen

357/98   Cayleys Problem
En historisk analyse af arbejdet med Cayleys problem fra 1870 til 1918
Et matematisk videnskabsfagsprojekt af: Rikke Degn, Bo Jakobsen, Bjarke K.W. Hansen, Jesper S. Hansen, Jesper Udesen, Peter C. Wulff
Vejleder: Jesper Larsen

358/98   Modeling of Feedback Mechanisms which Control the Heart Function in a View to an Implementation in Cardiovascular Models
Ph.D. Thesis by: Michael Danielsen

359/99   Long-Term Scenarios for Global Energy Demand and Supply
Four Global Greenhouse Mitigation Scenarios
by: Bent Sørensen (with contribution from Bernd Kuemmel and Peter Meibom)

360/99   SYMMETRI I FYSIK
En Meta-projektrapport af: Martin Niss, Bo Jakobsen & Tune Bjarke Bonné
Vejleder: Peder Voetmann Christiansen

361/99   Symplectic Functional Analysis and Spectral Invariants
by: Bernhelm Booß-Bavnbek, Kenro Furutani

362/99   Er matematik en naturvidenskab? - en udspænding af diskussionen
En videnskabsfagsprojekt-rapport af: Martin Niss
Vejleder: Mogens Nørgaard Olesen

363/99   EMERGENCE AND DOWNWARD CAUSATION
by: Donald T. Campell, Mark H. Bickhard, and Peder V. Christiansen

364/99   Illustrationens kraft - Visuel formidling af fysik
Integreret speciale i fysik og kommunikation
af Sebastian Horst
Vejledere: Karin Beyer, Søren Kjørup

365/99   To know - or not to know - mathematics, that is a question of context
by: Tine Wedege

366/99   LATEX FOR FORFATTERE - En introduktion til LATEX
og IMFUFA-LATEX
af: Jørgen Larsen

367/99   Boundary Reduction of Spectral Invariants and Unique Continuation Property
by: Bernhelm Booss-Bavnbek

368/99   Kvartvejsrapport for projektet SCENARIER FOR SAMLET UDNYTTELSE AF BRINT SOM ENERGIBÆRER I DANMARKS FREMTIDIGE ENERGISYSTEM
Projektleder: Bent Sørensen

369/99   Dynamics of Complex Quadratic Correspondences
by: Jacob S. Jalving
Supervisor: Carsten Lunde Petersen

370/99   OPGAVESAMLING - Bredde-Kursus i Fysik 1976 - 1999
Eksamensopgaver fra perioden 1976 - 1999. Denne tekst erstatter tekst nr. 350/98

371/99   Bevisets stilling - beviser og bevisførelse i en gymnasial matematik undervisning
Et matematikspeciale af: Maria Hermannsson
Vejleder: Mogens Niss

372/99   En kontekstualiseret matematikhistorisk analyse af ikke-lineær programmering:
Udviklingshistorie og multipel opdagelse
Ph.d.-afhandling af Tinne Hoff Kjeldsen

373/99   Criss-Cross Reduction of the Maslov Index and a Proof of the Yoshida-Nicolaescu Theorem
by: Bernhelm Booss-Bavnbek, Kenro Furutani and Nobukazu Otsuki

374/99   Det hydrauliske spring - Et eksperimentelt studie af polygoner og hastighedsprofiler
Specialeafhandling af: Anders Marcussen
Vejledere: Tomas Bohr, Clive Ellegaard, Bent C. Jørgensen

375/99   Begrundelser for Matematikundervisningen i den lærde skole hhv. gymnasiet 1884-1914
Historiespeciale af Henrik Andreassen, cand.mag. i Historie og Matematik

376/99   Universality of AC conduction in disordered solids
by: Jeppe C. Dyre, Thomas B. Schrøder

377/99   The Kuhn-Tucker Theorem in Nonlinear Programming: A Multiple Discovery?
by: Tinne Hoff Kjeldsen

378/00   Solar energy preprints:
1. Renewable energy sources and termal energy storage
2. Integration of photovoltaic cells into the global energy system
by: Bent Sørensen

379/00
EULERS DIFFERENTIALREGNING
Eulers indførelse af differentialregningen stillet over for den moderne
En tredjesemesters projektrapport på den naturvidenskabelige basisuddannelse
af: Uffe Thomas Volmer Jankvist, Rie Rose Møller Pedersen, Maja Bagge Pedersen
Vejleder: Jørgen Larsen

380/00
MATEMATISK MODELLERING AF HJERTEFUNKTIONEN
Isovolumetrisk ventrikulær kontraktion og udpumpning til det cardiovaskulære system
af: Gitte Andersen (3.moduls-rapport), Jakob Hilmer og Stine Weisbjerg (speciale)
Vejleder: Johnny Ottesen

381/00
Matematikviden og teknologiske kompetencer hos kortuddannede voksne
- Rekognosceringer og konstruktioner i grænselandet mellem matematikkens didaktik og forskning i voksenuddannelse
Ph. d.-afhandling af Tine Wedege

382/00
Den selvundvigende vandring
Et matematisk professionsprojekt
af: Martin Niss, Arnold Skimminge
Vejledere: Viggo Andreasen, John Villumsen

383/00
Beviser i matematik
af: Anne K.S.Jensen, Gitte M. Jensen, Jesper Thrane, Karen L.A.W. Wille, Peter Wulff
Vejleder: Mogens Niss

384/00
Hopping in Disordered Media: A Model Glass Former and A Hopping Model
Ph.D. thesis by: Thomas B. Schrøder
Supervisor: Jeppe C. Dyre

385/00
The Geometry of Cauchy Data Spaces
This report is dedicated to the memory of Jean Leray (1906-1998)
by: B. Booss-Bavnbek, K. Furutani, K. P. Wojciechowski

386/00
Neutrale mandatfordelingsmetoder – en illusion?
af: Hans Henrik Brok-Kristensen, Knud Dyrberg, Tove Oxager, Jens Sveistrup
Vejleder: Bernhelm Booss-Bavnbek

387/00
A History of the Minimax Theorem: von Neumann´s Conception of the Minimax Theorem - - a Journey Through Different Mathematical Contexts
by: Tinne Hoff Kjeldsen

388/00
Behandling af impuls ved kilder og dræn i C. S. Peskins 2D-hjertemodel
et 2. moduls matematik modelprojekt
af: Bo Jakobsen, Kristine Niss
Vejleder: Jesper Larsen

389/00
University mathematics based on problemoriented student projects: 25 years of experience with the Roskilde model
By: Mogens Niss
Do not ask what mathematics can do for modelling. Ask what modelling can do for mathematics!
by: Johnny Ottesen

390/01
SCENARIER FOR SAMLET UDNYTTELSE AF BRINT SOM ENERGIBÆRER I DANMARKS FREMTIDIGE ENERGISYSTEM Slutrapport, april 2001
Projektleder: Bent Sørensen
Projektdeltagere: DONG: Aksel Hauge Petersen, Celia Juhl, Elkraft System[#]: Thomas Engberg Pedersen[##] , Hans Ravn, Charlotte Søndergren, Energi 2[#]: Peter Simonsen, RISØ Systemanalyseafd.: Kaj Jørgensen , Lars Henrik Nielsen, Helge V. Larsen, Poul Erik Morthorst, Lotte Schleisner, RUC: Finn Sørensen[**] , Bent Sørensen
[#]Indtil 1/1-2000 Elkraft, [##] fra 1/5-2000 Cowi Consult
[*] Indtil 15/6-1999 DTU Bygninger & Energi, [**] fra 1/1-2001 Polypeptide Labs.
Projekt 1763/99-0001 under Energistyrelsens Brintprogram

391/01
Matematisk modelleringskompetence – et undervisningsforløb i gymnasiet
3. semesters Nat.Bas. projekt af: Jess Tolstrup Boye, Morten Bjørn-Mortensen, Sofie Inari Castella, Jan Lauridsen, Maria Gøtzsche, Ditte Mandøe Andreasen
Vejleder: Johnny Ottesen

392/01
"PHYSICS REVEALED" THE METHODS AND SUBJECT MATTER OF PHYSICS
an introduction to pedestrians (but not excluding cyclists)
PART III: PHYSICS IN PHILOSOPHICAL CONTEXT
by: Bent Sørensen.

393/01
Hilberts matematikfilosofi
Specialerapport af: Jesper Hasmark Andersen
Vejleder: Stig Andur Pedersen

394/01
"PHYSICS REVEALED" THE METHODS AND SUBJECT MATTER OF PHYSICS
an introduction to pedestrians (but not excluding cyclists)
PART II: PHYSICS PROPER
by: Bent Sørensen.

395/01
Menneskers forhold til matematik. Det har sine årsager!
Specialeafhandling af: Anita Stark, Agnete K. Ravnborg
Vejleder: Tine Wedege

396/01
2 bilag til tekst nr. 395: Menneskers forhold til matematik. Det har sine årsager!
Specialeafhandling af: Anita Stark, Agnete K. Ravnborg
Vejleder: Tine Wedege

408/02   Weak UCP and Perturbed Monopole Equations
          By: Bernhelm Booss-Bavnbek, Matilde Marcolli, Bai-Ling Wang

409/02   Algebraisk ligningsløsning fra Cardano til Cauchy
          - et studie af kombinationers, permutationers samt invariansbegrebets betydning for
          den algebraiske ligningsløsning før Gauss, Abel og Galois
          Videnskabsfagsprojekt af: David Heiberg Backchi, Uffe thomas Volmer Jankvist,
          Neslihan Saglanmak
          Vejleder: Bernhelm Booss-Bavnbek

410/02   2 projekter om modellering af influenzaepidemier
          Influenzaepidemier- et matematisk modelleringsprojekt
          Af: Claus Jørgensen, Christina Lohfert, Martin Mikkelsen, Anne-Louise H. Nielsen
          Vejleder: Morten Blomhøj
          Influenza A: Den tilbagevendende plage – et modelleringsprojekt
          Af: Beth Paludan Carlsen, Christian Dahmcke, Lena Petersen, Michael Wagner
          Vejleder: Morten Blomhøj

411/02   Polygonformede hydrauliske spring
          Et modelleringsprojekt af: Kåre Stokvad Hansen, Ditte Jørgensen, Johan Rømby
          Pedersen, Bjørn Toldbod
          Vejleder: Jesper Larsen

397/01   En undersøgelse af solvents og kædelængdes betydning for anomal swelling i
          phospholipiddobbeltlag
          2. modul fysikrapport af: Kristine Niss, Arnold Skimminge, Esben Thormann, Stine
          Timmermann
          Vejleder: Dorthe Posselt

398/01   Kursusmateriale til "Lineære strukturer fra algebra og analyse" (E1)
          Af: Mogens Brun Heefelt

399/01   Undergraduate Learning Difficulties and Mathematical Reasoning
          Ph.D Thesis by: Johan Lithner
          Supervisor: Mogens Niss

400/01   On Holomorphic Critical quasi circle maps
          By: Carsten Lunde Petersen

401/01   Finite Type Arithmetic
          Computable Existence Analysed by Modified Realisability and Functional
          Interpretation
          Master´s Thesis by: Klaus Frovin Jørgensen
          Supervisors: Ulrich Kohlenbach, Stig Andur Pedersen and Anders Madsen

402/01   Matematisk modellering ved den naturvidenskabelige basisuddannelse
          - udvikling af et kursus
          Af: Morten Blomhøj, Tomas Højgaard Jensen, Tinne Hoff Kjeldsen og Johnny
          Ottesen

403/01   Generaliseringer i integralteorien
          - En undersøgelse af Lebesgue-integralet, Radon-integralet og Perron-integralet
          Et 2. modul matematikprojekt udarbejdet af: Stine Timmermann og Eva Uhre
          Vejledere: Bernhelm Booss-Bavnbek og Tinne Hoff Kjeldsen

404/01   "Mere spredt fægtning"
          Af: Jens Højgaard Jensen

405/01   Real life routing
          - en strategi for et virkeligt vrp
          Et matematisk modelprojekt af: David Heiberg Backchi, Rasmus Brauner Godiksen,
          Uffe Thomas Volmer Jankvist, Jogvan Martin Poulsen og Neslihan Saglanmak
          Vejleder: Jørgen Larsen

406/01   Opgavesamling til dybdekursus i fysik
          Eksamensopgaver stillet i perioden juni 1976 til juni 2001
          Denne tekst erstatter tekst nr. 25/1980 + efterfølgende tillæg

407/01   Unbounded Fredholm Operators and Spectral Flow
          By: Bernhelm Booss-Bavnbek, Matthias Lesch, John Phillips